

THIRD EDITION

# CONDUCTIVE ELECTROACTIVE POLYMERS

*Intelligent Polymer Systems*



Gordon G. Wallace • Geoffrey M. Spinks  
Leon A. P. Kane-Maguire • Peter R. Teasdale



CRC Press  
Taylor & Francis Group

THIRD EDITION

**CONDUCTIVE  
ELECTROACTIVE  
POLYMERS**

---

Intelligent Polymer Systems

---



THIRD EDITION

# CONDUCTIVE ELECTROACTIVE POLYMERS

---

Intelligent Polymer Systems

---

Gordon G. Wallace

University of Wollongong, New South Wales, Australia

Geoffrey M. Spinks

University of Wollongong, New South Wales, Australia

Leon A. P. Kane-Maguire

University of Wollongong, New South Wales, Australia

Peter R. Teasdale

Griffith University, Queensland, Australia



CRC Press

Taylor & Francis Group

Boca Raton London New York

---

CRC Press is an imprint of the  
Taylor & Francis Group, an **informa** business

CRC Press  
Taylor & Francis Group  
6000 Broken Sound Parkway NW, Suite 300  
Boca Raton, FL 33487-2742

© 2009 by Taylor & Francis Group, LLC  
CRC Press is an imprint of Taylor & Francis Group, an Informa business

No claim to original U.S. Government works  
Printed in the United States of America on acid-free paper  
10 9 8 7 6 5 4 3 2 1

International Standard Book Number-13: 978-1-4200-6709-5 (Hardcover)

This book contains information obtained from authentic and highly regarded sources. Reasonable efforts have been made to publish reliable data and information, but the author and publisher cannot assume responsibility for the validity of all materials or the consequences of their use. The authors and publishers have attempted to trace the copyright holders of all material reproduced in this publication and apologize to copyright holders if permission to publish in this form has not been obtained. If any copyright material has not been acknowledged please write and let us know so we may rectify in any future reprint.

Except as permitted under U.S. Copyright Law, no part of this book may be reprinted, reproduced, transmitted, or utilized in any form by any electronic, mechanical, or other means, now known or hereafter invented, including photocopying, microfilming, and recording, or in any information storage or retrieval system, without written permission from the publishers.

For permission to photocopy or use material electronically from this work, please access [www.copyright.com](http://www.copyright.com) (<http://www.copyright.com/>) or contact the Copyright Clearance Center, Inc. (CCC), 222 Rosewood Drive, Danvers, MA 01923, 978-750-8400. CCC is a not-for-profit organization that provides licenses and registration for a variety of users. For organizations that have been granted a photocopy license by the CCC, a separate system of payment has been arranged.

**Trademark Notice:** Product or corporate names may be trademarks or registered trademarks, and are used only for identification and explanation without intent to infringe.

---

**Library of Congress Cataloging-in-Publication Data**

---

Conductive electroactive polymers : intelligent polymer systems / Gordon G.

Wallace ... [et al.]. -- 3rd ed.

p. cm.

Includes bibliographical references and index.

ISBN 978-1-4200-6709-5 (alk. paper)

1. Smart materials. 2. Conducting polymers. I. Wallace, Gordon G. II. Title.

TA418.9.S62C648 2009

620.1'92--dc22

2008023732

---

Visit the Taylor & Francis Web site at  
<http://www.taylorandfrancis.com>

and the CRC Press Web site at  
<http://www.crcpress.com>

---

# Contents

|   |      |
|---|------|
| Preface .....   | xi   |
| The Authors .....   | xiii |
| <b>Chapter 1</b> Introduction .....                                 | 1    |
| What Are Intelligent Material Systems and Structures? .....         | 2    |
| The Basis of the Revolution .....                                   | 4    |
| Identifying Macromolecular Building Blocks .....                    | 5    |
| Academic Research in Conducting Polymers .....                      | 5    |
| Shorter-Term Opportunities: Other Applications of CEPs .....        | 10   |
| Applications Utilizing the Polymers' Inherent Conductivity .....    | 11   |
| Electrochemical Switching/Energy Storage/Conversion .....           | 12   |
| Polymer Photovoltaics (Light-Induced Charge Separation) .....       | 14   |
| Display Technologies: Electrically Stimulated Light Emission .....  | 15   |
| Electrochromics .....   | 16   |
| Electromechanical Actuators .....                                   | 17   |
| Separation Technologies .....                                       | 18   |
| Controlled-Release Devices .....                                    | 21   |
| Corrosion Protection .....  | 22   |
| Chemical Sensors .....  | 22   |
| Biomedical Applications .....                                       | 24   |
| Cellular Communications .....                                       | 26   |
| Sensors for Biomechanics .....                                      | 27   |
| Artificial Muscles: Manipulating Movement .....                     | 27   |
| Micro-Electromechanical Systems (MEMS) and other Microdevices ..... | 31   |
| Communication and Characterization Tools .....                      | 32   |
| Electrochemical Methods .....                                       | 32   |
| Electrochemical Quartz Crystal Microbalance .....                   | 35   |
| Resistometry .....  | 35   |
| Electromechanical Analysis .....                                    | 36   |
| Chemical Analysis .....   | 37   |
| Dynamic Contact Angle Analyses .....                                | 40   |
| Scanning Probe Microscopy .....                                     | 42   |
| In Situ Spectroscopy .....  | 46   |
| UV-Visible Spectroscopy .....                                       | 46   |
| Circular Dichroism (CD) Spectroscopy .....                          | 47   |
| Raman Spectroscopy .....  | 48   |
| Electron Spin Resonance (ESR) Spectroscopy .....                    | 49   |
| Localized Electrochemical Mapping .....                             | 51   |
| Conclusions: Conducting Polymers as Intelligent Materials .....     | 51   |
| References .....  | 53   |

|  |     |
|--|-----|
| <b>Chapter 2</b> Assembly of Polypyrroles .....                                    | 59  |
| Electropolymerization—“A Complex Process Oversimplified” .....                     | 59  |
| The Polymerization Environment/Cell Design .....                                   | 63  |
| Electrochemical Conditions .....   | 66  |
| Electrode Materials .....  | 68  |
| The Solvent .....  | 70  |
| The Counterion/Cation Effect: Choice of Electrolyte .....                          | 71  |
| The Monomer .....  | 74  |
| Chemical Polymerization .....  | 75  |
| Mechanism of Chemical Polymerization .....   | 75  |
| Influence of Polymerization Conditions .....                                       | 76  |
| The Oxidant .....  | 76  |
| The Solvent .....  | 76  |
| Polymerization Temperature .....   | 76  |
| The Dopant Counterion ( $A^-$ ) .....  | 77  |
| Achieving Regioselective Coupling with Pyrrole Monomers .....                      | 77  |
| In Situ Chemical Polymerization .....  | 78  |
| Routes to More Processable PPy's .....   | 79  |
| Counterion-Induced Solubilization .....  | 79  |
| Colloidal PPy Dispersions .....  | 80  |
| Side-Chain-Induced Solubilization .....  | 81  |
| Photochemically Initiated Polymerization .....                                     | 83  |
| Enzyme- and Acid-Catalyzed Polymerizations .....                                   | 83  |
| The Quest for Extra Functionality .....  | 84  |
| Molecular Structure and Microstructure of PPy .....                                | 86  |
| Molecular Weight, Branching, and Crosslinking .....                                | 86  |
| Crystallinity and Molecular Order .....  | 88  |
| Surface Morphology and Film Density .....  | 89  |
| Nanostructured PPy's .....   | 91  |
| References .....   | 96  |
| <br>   |     |
| <b>Chapter 3</b> Properties of Polypyrroles .....                                  | 103 |
| Electrical Properties: Conductivity .....  | 103 |
| Switching Properties .....   | 105 |
| Chemical and Biochemical Properties .....  | 114 |
| Optical Properties of PPy's .....  | 119 |
| Electronic Band Structure .....  | 119 |
| UV-Visible-NIR Spectra: Dependence on Doping Level and Chain<br>Conformation ..... | 120 |
| Chiroptical Properties of Optically Active PPy's .....                             | 121 |
| Electrochemical Asymmetric Synthesis, Chiral Separations, and Sensing .....        | 122 |
| Mechanical Properties of PPy .....   | 123 |
| Dry-State Mechanical Properties .....  | 123 |
| Environmental Effects on Mechanical Properties .....                               | 128 |

|  |     |
|--|-----|
| Conclusions .....  | 132 |
| References .....   | 133 |
| <b>Chapter 4</b> Synthesis of Polyanilines .....                           | 137 |
| Electrochemical Polymerization .....                                       | 138 |
| Mechanism of Electrochemical Polymerization.....                           | 138 |
| Electrode Materials.....   | 140 |
| Concentration and Nature of the Dopant Acid (HA).....                      | 140 |
| Solvent .....  | 141 |
| Temperature .....  | 142 |
| Monomer Type.....  | 142 |
| Colloidal PAN's .....  | 142 |
| Chemical Polymerization.....   | 143 |
| Mechanism of Chemical Polymerization .....                                 | 143 |
| Polymerization Temperature.....  | 144 |
| Nature and Concentration of the Dopant Acid (HA).....                      | 144 |
| Nature of the Oxidant .....  | 145 |
| Nature of the Solvent .....  | 146 |
| Interfacial Polymerization .....   | 146 |
| Self-Stabilized Dispersion Polymerization.....                             | 146 |
| Achieving Regioselective Coupling with Aniline Monomers.....               | 147 |
| Template-Guided Synthesis .....  | 147 |
| Comparison of Chemically and Electrochemically Prepared PAN<br>Films ..... | 147 |
| Vapor-Phase Deposition.....  | 148 |
| Photochemically Initiated Polymerization.....                              | 148 |
| Enzyme-Catalyzed Polymerization .....                                      | 148 |
| Polymerization Using Electron Acceptors.....                               | 149 |
| Miscellaneous Polymerization Methods.....                                  | 150 |
| Routes to More Processable PAN's.....                                      | 150 |
| Emulsion Polymerization.....   | 150 |
| Colloidal PAN Dispersions.....   | 151 |
| Substituted PAN's .....  | 152 |
| Alkyl- and Alkoxy-Substituted PAN's.....                                   | 152 |
| Covalently Bound Chiral Substituents .....                                 | 153 |
| Sulfonic Acid Substituted PAN's.....                                       | 153 |
| Postpolymerization Modification: Enhancing Functionality.....              | 154 |
| Covalently Substituted PAN's.....  | 154 |
| Doping of EB with Brönsted Acids (HA).....                                 | 155 |
| Incorporation of Chiral Dopant Anions or Cations.....                      | 156 |
| Doping of EB with Lewis Acids.....   | 157 |
| Doping of EB with Organic Electron Acceptors.....                          | 158 |
| Ion Implantation .....   | 158 |
| Structure of PAN .....   | 158 |
| Molecular Structure and Conformation.....                                  | 158 |



|   |     |
|---|-----|
| Molecular Weight.....   | 159 |
| Chain Conformation .....  | 160 |
| Bulk Structure.....   | 160 |
| Nanoscale Heterogeneity .....   | 160 |
| Crystallinity, Molecular Order, and Conformation in Solid State.....                                    | 160 |
| Solution-Cast Emeraldine Base .....   | 161 |
| Emeraldine Salt from Protonation of EB.....   | 163 |
| Solution-Cast Emeraldine Salt.....  | 163 |
| Electropolymerized Emeraldine Salt.....   | 166 |
| Influence of Water and “Secondary Dopants” on PAn Crystallinity .....                                   | 166 |
| Morphology and Density .....  | 166 |
| Nanostructured Polyanilines.....  | 168 |
| Deposition in Nanoscale Matrices .....  | 171 |
| References .....  | 171 |
| <b>Chapter 5</b> Properties of Polyanilines .....   | 179 |
| Electrical Properties .....   | 179 |
| Conductivity.....   | 179 |
| Metallic Polyaniline .....  | 182 |
| Switching Properties.....   | 183 |
| Chemical Properties.....  | 186 |
| Mechanical Properties of Polyaniline.....   | 187 |
| Electrochemically Prepared Films .....  | 187 |
| Optical Properties of Polyanilines .....  | 189 |
| Base Forms of Polyaniline.....  | 189 |
| Circular Dichroism Spectra .....  | 191 |
| Chiral Discrimination and Asymmetric Induction with Chiral Polyanilines .....                           | 193 |
| Solvatochromism and Thermochromism.....   | 193 |
| References .....  | 194 |
| <b>Chapter 6</b> Synthesis and Properties of Polythiophenes .....                                       | 197 |
| Synthesis of Polythiophene.....   | 197 |
| Electropolymerization .....   | 197 |
| Chemical Polymerization .....   | 201 |
| Vapor-Phase Polymerization.....   | 202 |
| UV Polymerization of Oligothiophenes .....  | 203 |
| Substituted Polythiophenes .....  | 203 |
| Poly(3-alkylthiophenes) and Poly(3-alkoxythiophenes) .....  | 203 |
| Regioregular Substituted Polythiophenes .....   | 206 |
| Regioregular Poly(3-alkylthiophenes) with Low Polydispersities and<br>Controlled Molecular Weights..... | 207 |
| Polythiophenes with Special Functional Groups.....  | 208 |
| Water-Soluble Polythiophenes .....  | 208 |
| Organic-Solvent-Soluble Chiral Polythiophenes.....  | 208 |

|   |     |
|---|-----|
| Postpolymerization Modification: Enhancing Functionality.....           | 210 |
| Structure of Polythiophenes.....  | 211 |
| Molecular Structure and Conformation.....                               | 211 |
| Molecular Weight .....  | 211 |
| Electropolymerized Polythiophenes.....                                  | 212 |
| Crystallinity, Molecular Order, Conformation in Solid State .....       | 212 |
| Morphology and Density .....  | 213 |
| Solution-Cast Polythiophenes.....                                       | 213 |
| Properties of Polythiophenes .....                                      | 216 |
| Conductivity.....   | 216 |
| Mechanical Properties of Polythiophenes .....                           | 217 |
| Chemical Properties .....   | 219 |
| Switching Properties.....   | 219 |
| n-Doping of Polythiophenes .....  | 220 |
| Optical Properties of Polythiophenes.....                               | 221 |
| Electronic Band Structure and UV-Visible Spectra.....                   | 221 |
| Thermochromism and Solvatochromism in Poly(3-<br>alkylthiophenes) ..... | 221 |
| Chiroptical Properties of Optically Active Polythiophenes .....         | 222 |
| Conclusions .....   | 225 |
| References .....  | 226 |
| <br>  |     |
| <b>Chapter 7</b> Processing and Device Fabrication .....                | 231 |
| Integration/Fabrication after Polymerization .....                      | 231 |
| Solution-Processable CEPs .....   | 231 |
| Melt-Processable CEPs .....   | 233 |
| Assembly of Conducting Polymers in Host Matrices .....                  | 235 |
| Chemical Polymerization.....  | 235 |
| Deposition on Glass/Plastics.....                                       | 235 |
| Interfacial Polymerization .....  | 238 |
| Electrochemical Integration.....  | 239 |
| Device Fabrication .....  | 243 |
| Fiber-Spinning Technologies .....                                       | 243 |
| Printing Technologies .....   | 246 |
| References .....  | 249 |
| <br>  |     |
| <b>Index</b> .....  | 253 |



---

# Preface

Intelligent materials are being incorporated into many new applications/devices, and the science develops at a breakneck pace. The new approach to material design, synthesis, and system integration, as championed in this book with conducting electroactive polymers, has many adherents. The desire to have built-in sensing, processing, actuating, energy conversion, and storage functions continues to require the identification of dynamic materials with chemical and physical properties that are readily manipulated. The need to create these materials in different forms to enable integration into or interfacing with other structures, including living bodies and cells, is vital.

Natural polymers remain an inspiration and provide considerable stimulation for researchers of artificial intelligent materials and systems. For example, antibodies and enzymes provide the molecular recognition capabilities used so magnificently by nature. Macromolecules are also the basis of that most useful of actuator systems: muscles. Furthermore, it is the generation and transmission of electrical signals that regulate the processes behind the formation and operation of these biosystems.

Rapid advances in synthetic polymer science and nanotechnology have now placed us in a position to utilize the unique properties of this versatile class of materials. Our ability to design and assemble polymers from the molecular level, coupled with a better understanding of structure–property relationships enables the design of sophisticated structures. We believe that inherently conducting electroactive polymers (CEPs) will continue to play a central role in the development of intelligent material science over the following decades.

The parameters affecting the formation of important CEPs, such as polypyrroles, polyanilines and polythiophenes are discussed. How these parameters can be used to manipulate the chemical, physical, and energy parameters of these polymers is then revealed. We attempt to clarify the chemical and energy parameters that determine the structure and, hence, the chemical, electrical, and mechanical properties of these fascinating structures. We present examples wherein the ability to manipulate the structure and properties of conducting polymers is used to produce materials with useful sensing, processing, and actuating capabilities.

We've tried to include all substantial developments and advances in this new edition. Significant developments in biomedical applications, microelectromechanical systems, and electronic textiles have been included, as has synthesis of nanostructured CEPs. New methods for characterizing CEPs, such as electrochemical Raman and electron spin resonance spectroscopy, have also been described. Significant progress is also detailed in techniques for processing CEPs and the fabrication of devices.



---

# The Authors



**Gordon Wallace, Ph.D., D.Sc., FTSE**, is currently executive research director of the ARC Centre of Excellence for Electromaterials Science, Intelligent Polymer Research Institute, University of Wollongong, New South Wales, Australia. His research interests include organic conductors, nanomaterials, and electrochemical probe methods of analysis. A current focus of his involves the use of these tools and materials in developing biocommunications, from the molecular to skeletal domains, in order to improve human performance via medical bionics.

He completed his undergraduate (1979) and Ph.D. (1983) degrees at Deakin University. He was awarded a D.Sc. from Deakin in 2000. In 1990 he was appointed as professor at the University of Wollongong, and the follow-

ing year was awarded an Australian Research Council (ARC) QEII Fellowship in 1991. He was given an ARC Senior Research Fellowship in 1995. In 2002 he was appointed to an ARC Professorial Fellowship, and in 2006 was awarded an ARC Federation Fellowship.

He was elected as a fellow of the Australian Academy of Technological Sciences and Engineering in 2003 and as a fellow of the Australian Academy of Science in 2007. He was elected as a fellow of the Institute of Physics (UK) in 2004 and is a fellow of the Royal Australian Chemical Institute (RACI).

Dr. Wallace received the inaugural Polymer Science and Technology Award from the Royal Australian Chemical Institute in 1992. He was awarded an ETS Walton Fellowship by Science Foundation Ireland in 2003, and received the RACI Stokes Medal for research in electrochemistry in 2004. Professor Wallace has published more than 400 refereed publications and a monograph (two editions) on inherently conducting polymers for intelligent material systems. He has supervised 50 Ph.D. students to completion.



**Geoffrey Spinks, Ph.D.**, is currently discipline advisor for materials engineering at the University of Wollongong and a program leader in the ARC Centre of Excellence for Electromaterials Science. His research interests relate to the mechanical behavior of organic conductors and polymeric nanomaterials. A particular focus of his involves the development of actuator materials and systems, from the nano- to the macro-scale.

He completed his undergraduate (1986) and Ph.D. (1990) degrees at the University of Melbourne. He was appointed as a lecturer at the University of Wollongong in 1989, and subsequently was promoted to senior lecturer (1995), associate professor (2001), and professor (2005). He became discipline advisor for materials engineering in 2003.

He received the Australian Polymer Science and Technology Achievement Award from the Royal Australian Chemical Institute (RACI) in 1998 and the Treloar Prize from RACI in 1990. Professor Spinks has published more than 100 refereed publications and a monograph (two editions) on inherently conducting polymers for intelligent material systems. He has supervised 16 Ph.D. students to completion.



**Leon Kane-Maguire, Ph.D.**, is currently a project leader in the ARC Centre of Excellence for Electromaterials Science at the University of Wollongong. His research interests are the synthesis of conducting organic polymers and characterizing their stereochemical and photophysical properties. A strong focus of his recent work has been the synthesis of chiral conducting polymers (especially polyanilines) and their use as novel chiral electrodes for electrochemical asymmetric synthesis.

Leon Kane-Maguire completed his undergraduate (1964) and Ph.D. (1967) degrees in chemistry at the University of Queensland, where he was awarded a University Medal. After postdoctoral studies in the United States at Northwestern University, in London at University College and at Cambridge University, he was appointed as a lecturer in chemistry at University College Cardiff, Wales, in 1971. There, his research focused on synthetic and mechanistic studies of organometallic reactions.

In 1983 he returned to Australia as professor and head of the department of chemistry at the University of Wollongong. Since 1993 he has enjoyed a very fruitful collaboration with Prof. Gordon Wallace in the area of electrically conducting polymers, where his major contribution has been the development of chiral polyanilines.

He has published 175 refereed papers and book chapters as well as a monograph on conducting polymers. He has supervised 20 Ph.D. students to completion.



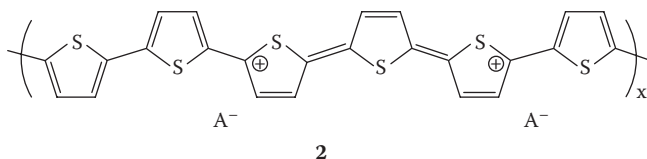
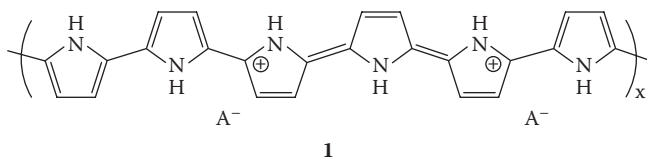
**Peter Teasdale, Ph.D.**, is a senior lecturer in environmental chemistry at Australian Rivers Institute, Griffith University Gold Coast Campus. His current research interests include in situ sensors for metals and nutrients, natural, recycled and potable water quality, microbial toxicology, and sediment biogeochemistry. Peter is the current chair of the Royal Australian Chemical Institute Environment Division. He has published over 40 refereed publications. Coauthoring this book reflects his interest in the field of conducting electroactive polymers, the area in which he completed his Ph.D. in 1993 at the University of Wollongong.



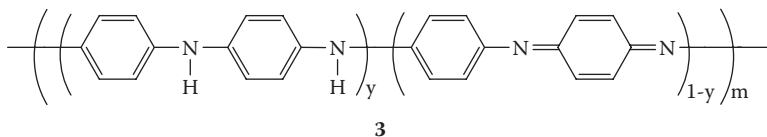


# 1 Introduction

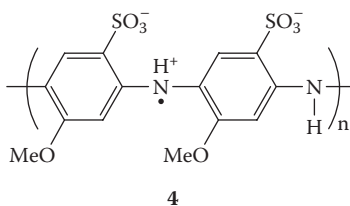
Conducting electroactive polymers (CEPs) such as polypyrrole, polythiophene, polyaniline, and sulfonated polyaniline (**1–4** shown subsequently) are complex, dynamic structures that captivate the imagination of those of us involved in intelligent material research.<sup>1,2,3,4,5</sup>



(The number of monomer units per unit positive charge is usually 3–4 for polypyrrole and polythiophene.  $A^-$  is a counterion incorporated during synthesis.)



Polyaniline: leucoemeraldine ( $y = 1$ ), emeraldine ( $y = 0.5$ ), and pernigraniline ( $y = 0$ );  $m$  determines the molecular weight.



It is possible to create conducting polymers with a diverse range of properties. For example, chemical properties can be manipulated to produce materials capable of trapping simple anions, or to render them bioactive. Electrical properties can also be manipulated to produce materials with different conductivities, capacitance, or redox properties. After synthesis, the properties of these fascinating structures can be manipulated further through electrochemical switching. The application of electrical stimuli can result in drastic changes in the chemical, electrical, and mechanical properties of CEPs. These complex properties can only be controlled if we understand, first, the nature of the processes that regulate them during the synthesis of the conducting polymers, and second, the extent to which these properties are changed by the application of an electrical stimulus. It is these dynamic properties of CEPs that are the focus of this text, because it is the ability to control them in various operational environments that should lead to the development of Intelligent Material Systems.

The state of the art is such that an understanding of these processes is now well established, and an exciting fertile field lies before intelligent material research scientists. We can, by design, control the chemical and electrical properties of conducting polymers at the point of assembly. How these properties are likely to vary as a result of application of external stimuli can also be manipulated by the synthesis process.

Of course, the molecular organization required to achieve the desired chemical and electrical properties will also determine the mechanical properties of any practical structure we are to make. These three properties (chemical, electrical, and mechanical) are inextricably linked.

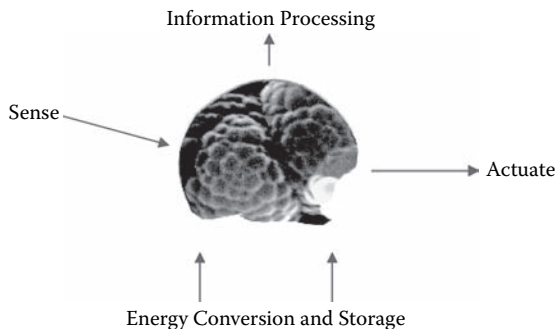
The method of assembly is also important as it determines the physical form of the materials. A wide variety of synthesis and processing methods now exist that can be manipulated to produce materials in forms that can be integrated into truly intelligent structures.

Before exploring these materials in detail, some general discussion of intelligent material science is warranted.

## WHAT ARE INTELLIGENT MATERIAL SYSTEMS AND STRUCTURES?

This question has already been addressed by numerous authors,<sup>6,7,8,9,10</sup> and many definitions are employed. For the purpose of our work, we will use the following: An *intelligent material* is capable of recognizing appropriate environmental stimuli, processing the information arising from the stimuli, and responding to it in an appropriate manner and time frame. A further desirable feature is that the material should ideally be self-powered, having energy conversion/storage functions (Figure 1.1).

What is particularly important is that the responses obtained be appropriate. That is, they must result in desirable behavior that enhances the performance of the material itself or the structure within which the material is operational. For example, the first instance might involve the material responding to stress by increasing strength. In the second instance, the material may become capable of initiating controlled release of a drug as part of an environmentally stimulated (e.g., change in temperature) biodegradation process. So, although the performance of the material itself is not enhanced, that of the overall system is.



**FIGURE 1.1** An “intelligent material”: the surface of polypyrrole (as seen with an electron microscope) in the shape of a human brain. The intelligent material, similar to our brain, processes information from sensors to actuate an appropriate response, and is supported by energy conversion/storage systems.

No matter what definition we employ, the underlying feature that differentiates intelligent materials from more conventional ones is their dynamic character. Without such character, there can be no intelligence. However, this character must be controllable, and the time frame within which it responds must be appropriate if truly intelligent behavior is to be realized. If it is too slow, it may have no practical application. If it is too fast, it may be useless, or even dangerous.

There is little doubt that intelligence is more demonstrable when physical processes such as motion (mechanical activity) are apparent. However, we should remember that in complex systems such as living entities, motion is a physical manifestation of activity at the molecular and electronic levels. Similarly, motion resulting from the application of an external force causes changes both at the molecular and electronic levels within a material.

If the stimulus and response required are chemical or biochemical in nature, involving activity only at the cellular, molecular, or even atomic level, then the use of a single intelligent material may be possible. Also, a mechanical stress of a gradual or slight nature may be recognized and responded to with a single material. However, in many applications, more than one material is required to perform the desired functions. This is when we encounter *intelligent material systems*, which in turn may be incorporated into much larger *intelligent structures* made up of a number of component systems and materials of varying kinds and functions. In intelligent material systems and structures, the individual functions of stimuli recognition, information processing, and response generation are brought about by the combination of appropriate materials. The greater the severity and variety of the stimuli, and the more demanding the requirements of the response, the more complex the intelligent material structure must be.

However, again, there is the underlying fundamental requirement that the creation of intelligent material systems must involve the identification of molecular systems whose chemical and electrical properties can be manipulated and controlled.

To continue to operate effectively, the material may be required to learn, grow, and even decay in a fashion determined by the operational environment. What is

clear is that the properties of such materials must change with time; that is, they must be dynamic. We must identify material systems in which chronological behavior can be controlled, plotted, and predicted as a function of the environmental stimuli that are likely to be encountered. Then, if the materials are to behave properly, we must develop procedures to manipulate their molecular structure, and thereby their dynamic character during the early stages of synthesis and processing.

## THE BASIS OF THE REVOLUTION

The diversity of approaches used to develop intelligent material systems and structures is a healthy symptom of the stage of development of this scientific endeavor.

At least two distinct approaches are currently obvious:

- Integration of functions at the bulk material level
- Integration of functions at the molecular level

The concept of intelligent material systems and structures emerged from the research activities of the U.S. Army Research Office. Scientists here realized that integration of appropriate materials at the bulk *material level* could produce a system capable of monitoring and responding to environmental conditions. The concept of embedding sensors and actuators within structures, coupled with localized processing, remains the shortest-term approach to gaining benefits in the intelligent material area.

However, information is much easier to process and transmit in a material integrated at the *molecular level*, and preferably integrated during processing or growth. Nature and biological systems have refined this approach and provide many examples. There is indeed great potential for diversity at this level of organization.

Nature achieves intelligent behavior by assembling appropriate molecules in a more sophisticated and timely fashion than we humans have been able to achieve artificially to date. Macromolecular structures may be integrated into systems composed of numerous other inorganic materials or, preferably as nature does, the active (organic) components may create the required mechanical structure. The molecular approach to the development of synthetic intelligent systems involves the design and assembly of appropriate molecules to produce the properties required to sense, process, and respond to information.

Progress in this approach may be accelerated by borrowing selected macromolecules, such as proteins, from nature to become active components in our synthetic structures. Nature has developed the appropriate stimuli recognition, information processing and storage, and response mechanisms to allow life, as we know it, to continue to exist. This is no mean feat, and to emulate it we must consider a macromolecular approach.

Many materials are, of course, composed of molecular building blocks. It is how we put them together, and how we integrate and spatially distribute the components required for intelligence that is important. This approach requires the identification of suitable building blocks, that is, suitable molecular components. There is a need for molecular conducting wires, molecular insulators, and molecular switches. It will take some time to develop, understand, and integrate many of the molecular

components, but much work in the field of molecular engineering and molecular electronics is already under way.

There is also a need for a more detailed chemical understanding of these material systems. Inevitably, they involve chemical processes occurring at a dynamic heterogeneous interface. The well-defined chemical rules that apply in homogeneous solutions no longer apply. Instead, we must deal with chemical (molecular) interactions in which spatial distribution of active sites occurs at the nanodimensional level, and the fact that the nature of these sites varies as a function of time and environmental stimuli is important.

Of course, not all molecular systems are suitable. It appears likely that only a handful of systems will be produced to solve our intelligent material systems needs. It is not so much that sophisticated molecules are required to produce materials capable of sophisticated behavioral patterns; simple molecules, assembled creatively, achieve this objective in nature, and this is something those of us involved in synthetic materials aspire to.

## IDENTIFYING MACROMOLECULAR BUILDING BLOCKS

CEPs have emerged as one of the champions in intelligent material research. They have all the desirable properties: they are readily engineered at the molecular level to recognize specific stimuli; they facilitate transport of electrical information as they are conductive; and they are capable of localized processing as well as actuation of response mechanisms. A wide range of CEPs are available (Table 1.1).

CEPs have a further unique and practical advantage. The fact that they conduct electricity means that we can communicate with them using electronic tools (computers and interfaces) that have become part of our scientific lives. Information on the behavior of these systems can be retrieved from real *in situ* environments using existing and emerging characterization tools (described later). In addition, their behavior can be manipulated *in situ* using appropriate electrical stimuli (Table 1.2).

In the Intelligent Polymer Research Institute (IPRI), the unique features of CEPs were identified based on pyrrole, aniline, and thiophene. Stimuli-recognition sites can be incorporated into these CEPs, for which information-processing capabilities are inherent, and various response mechanisms can be integrated into them.

There is no doubt that conducting polymers are a class of materials destined to play a major role in intelligent material science. As outlined in the remainder of this text, the properties of these materials are versatile and possess the dynamism required for intelligent behavior.

## ACADEMIC RESEARCH IN CONDUCTING POLYMERS

Since their discovery in the mid-1970s, conducting polymers have been a hot research area for many academic institutions. This research has supported the industrial development of conducting polymer products and has provided the fundamental understanding of the chemistry, physics, and materials science of these materials. The impact of the field on science, in general, was recognized in 2000 by the awarding of the Nobel Prize for Chemistry to the three discoverers of conducting polymers: Alan MacDiarmid, Alan Heeger, and Hideki Shirakawa (Figure 1.2).

**TABLE 1.1**  
**Typical Conducting Polymer Structures**  
**(in Undoped Form)**

| Name                                 | Structure |
|--------------------------------------|-----------|
| Polyacetylene (PAC)                  |           |
| Polypyrrole (PPy)                    |           |
| Polythiophene (PTh)                  |           |
| Poly(ethylenedioxythiophene) (PEDOT) |           |
| Polyseleneophene (X = Se)            |           |
| Polyfuran (X = O)                    |           |
| Poly(thienylene-vinylene) (PTV)      |           |
| Poly(furylene-vinylene) (PFV)        |           |
| Polyaniline (PAN)                    |           |
| Poly(diphenylamine)                  |           |

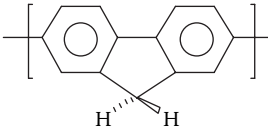
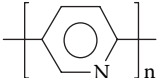
**TABLE 1.1 (Continued)**  
**Typical Conducting Polymer Structures**  
**(in Undoped Form)**

| Name                             | Structure |
|----------------------------------|-----------|
| Poly(para-phenylene) (PPP)       |           |
| Poly(phenylene-vinylene) (PPV)   |           |
| Poly(phenylenesulfide) (PPS)     |           |
| Poly(phenylene ethynylene) (PPE) |           |
| Polycarbazole                    |           |
| Poly(indole)                     |           |
| Poly(thieno[3,2-b]pyrrole)       |           |
| Poly(thieno[3,2-b]thiophene)     |           |

Continued



**TABLE 1.1 (Continued)**  
**Typical Conducting Polymer Structures**  
**(in Undoped Form)**

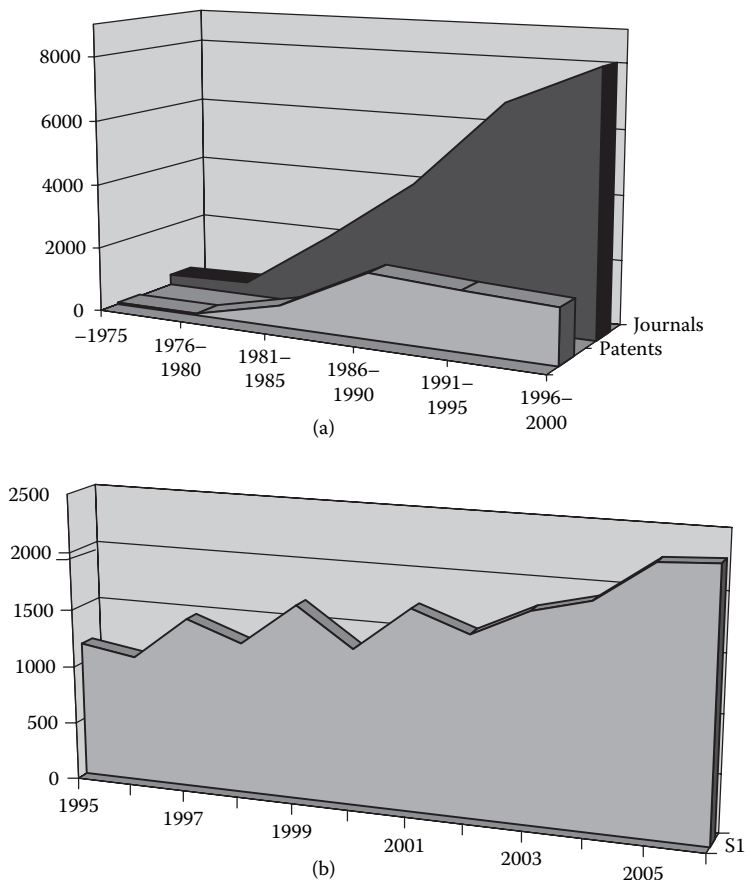
| Name           | Structure   |
|----------------|---|
| Poly(flourene) |  |
| Polypyridine   |  |

**TABLE 1.2**  
**Property Changes Typically Observed upon Electrical Stimulation**  
**to Switch CEPs between Oxidized and Reduced States**

| Property         | Typical Change   | Potential Application          |
|------------------|--|--------------------------------|
| Conductivity     | From $10^{-7}$ to $10^3$ S/cm  | Electronic components, sensors |
| Volume           | 10%  | Electromechanical actuators    |
| Color            | 300 nm shift in absorbance band                                      | Displays, smart windows        |
| Mechanical       | Ductile to brittle transition  | —                              |
| Ion permeability | From 0 to $10^{-8}$ mol $\text{cm}^{-2}$ $\text{s}^{-1}$ in solution | Membranes                      |



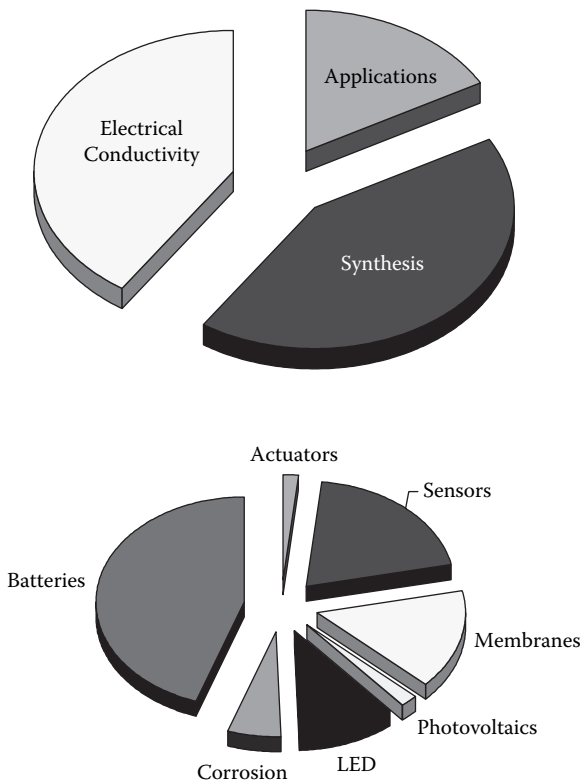
**FIGURE 1.2** The three discoverers of polyacetylene, the first inherently conducting polymer: Alan Heeger, Alan MacDiarmid, and Hideki Shirakawa.



**FIGURE 1.3** Number of journal articles published annually relating to CEPs; (a) data obtained from chemical abstracts (1975–2000); (b) data obtained from ISI Thomson Scientific Web of Science (1995–2005).

A search of chemical abstracts over the period 1975–2000 shows the level of publications increasing rapidly after 1980 (Figure 1.3a). The data suggest a peak in patenting in the late 1980s, and the rate of scientific publications increased unabated through the end of the 1990s. A similar trend is shown in journal articles tracked by ISI Thomson Scientific Web of Science, with the steady increase in journals published per year relating to CEPs continuing to the present time (Figure 1.3b).

Figure 1.4 shows the main areas of interest for papers published on CEPs, with almost half of the publications relating to synthesis of new types of CEPs or modifications to existing ones. The next largest area of research has been in the physics of the conduction mechanisms, while applications of CEPs account for less than 20% of publications. A further breakdown of the areas of application of CEPs shows a great deal of interest in batteries, followed by sensors, membranes, and polymer light-emitting diodes (PLEDs). There has been a distinct move in recent years toward biological/biomedical applications of CEPs.



**FIGURE 1.4** Scientific papers published on conducting polymers (1990–2000) categorized into various topics.

Research in CEPs remains extremely fruitful, with fundamental studies underpinning the exciting commercial developments described in the following sections.

### SHORTER-TERM OPPORTUNITIES: OTHER APPLICATIONS OF CEPS

In pursuing the development of intelligent materials, it is impossible to ignore the shorter-term opportunities that are available for applications of CEPs. The science is such that a better understanding of dynamic materials has been obtained, and this has been used to advantage in the development of new and improved products.

The potential applications of conducting polymers have been discussed at length in numerous reviews.<sup>11,12,13,14,15,16,17,18</sup> From Figure 1.3 it is evident that the patent activity relating to conducting polymers peaked in the mid-to-late 1980s. The rapid increase in patents in the early 1980s reflects the growing appreciation of the versatility of conducting polymers in many application areas. The commercialization of conducting polymers has been particularly boosted since the mid-1990s by breakthroughs in processing technologies that have given both soluble and melt-processable forms of conducting polymers. The various spin-off application areas are

described in the following sections, and processing and device fabrication technologies are described in Chapter 7.

## APPLICATIONS UTILIZING THE POLYMERS' INHERENT CONDUCTIVITY

On realizing that polymers could be made electrically conductive, the possibility of having lightweight conductors capable of replacing metals in many applications was immediately grasped. However, this promise has not been realized to date. The development of highly conducting polymers with adequate mechanical properties and stability is yet to be achieved. However, materials with lower conductivities (100–200 S/cm) that can be produced routinely are proving extremely useful in electromagnetic shielding applications.

Another area that utilizes the semiconducting nature of conducting polymers is antistatic applications. Electrostatic discharge (ESD) is particularly damaging for electronic components; a high-voltage surge can destroy componentry. Consequently, all electronic components are shipped in antistatic packaging materials. It is often desirable that the packaging material be transparent so that the contents can be viewed. The challenge for antistatic coatings (metals and polymers) is to provide both the desired levels of surface conductivity and transparency (coupled with adhesion and scratch resistance).

A number of companies seek to overcome the limitations of existing materials by using conducting polymers for ESD protection. The main materials currently in use are ionic conductors, carbon-black-filled plastics, and vacuum metallized plastics.<sup>19</sup> Ionic conductors operate by absorbing moisture from the atmosphere to form a conductive surface ( $10^{11}$ – $10^{12}$   $\Omega$ /square). They are highly transparent coatings, but are also highly sensitive to moisture and become ineffective when humidity is low. The ionic conductors are also easily removed by washing, so reuse of the container is difficult. Carbon-black-loaded polymers give lower surface resistivities ( $10^3$ – $10^5$   $\Omega$ /square), which are suitable for electromagnetic interference shielding, but are too low for ESD protection. Carbon-black-filled polymers are also intensely colored and suffer from the loss of carbon particles from friction (a serious problem in clean-room applications). Metallized plastics are only transparent for very thin coatings, and adhesion to the polymer is difficult to achieve. Further development of conducting polymers to give acceptable surface resistivity (especially over time and after repeated washing) and adhesion to the substrate will overcome many of the limitations of existing methods for ESD protection. Similarly, highly conducting CEPs are being investigated for shielding of electromagnetic interference (EMI). CEPs are strong absorbers of electromagnetic radiation over a wide frequency range and CEP-coated textile fabrics have been investigated for EMI shielding applications.<sup>20,21,22</sup>

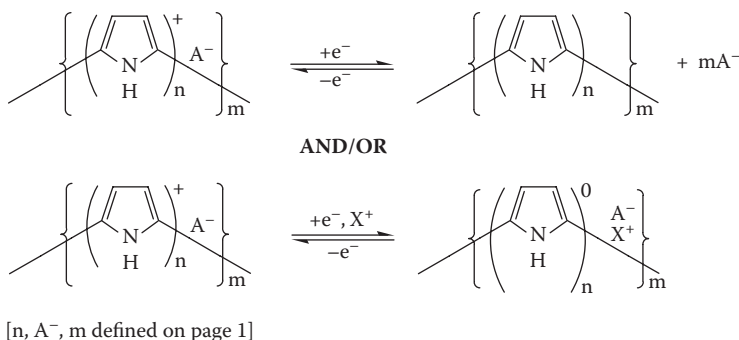
Recently, conducting polymers have been considered for microelectronics applications. Electronics company Philips is involved in the development of “plastic chip” technology using conducting polymers.<sup>23</sup> In this application, a simple processor chip is fabricated using polyaniline electrodes and a polythiénylenevinylene semiconductor layer. The layers are spin-coated onto a polyimide substrate. Patterning of the polyaniline electrodes is achieved by exposing the polymer to UV light through a

suitable mask. A photosensitizer molecule incorporated into the polyaniline absorbs the UV light and induces a photochemical reaction that leads to an increase in conductivity of 10 orders of magnitude. The end result is patterned tracks of conducting polyaniline in a nonconducting matrix. The performance of the all-plastic circuits is poor compared to silicon-based electronics. However, the devices are designed for applications where low cost and mechanical flexibility are desired. One example being pursued is the “smart label” to replace the ubiquitous barcode incorporated in virtually all packaged products. As recently reviewed,<sup>24</sup> prototype products based on printed CEP circuits are showing promise. An example is the printed transistor circuit produced by PolyIC in Germany.<sup>25</sup>

Conducting polymers also have other applications in microelectronics, as reviewed by Angelopolous.<sup>26</sup> Polyaniline layers have been shown to improve the resolution of electron-beam patterning, where the conducting polymer prevents the buildup of charge in the resist layer and so eliminates distortion. Polyaniline conductivities of  $10^{-4}$  S/cm were shown to be effective at eliminating resist layer charging. Mitsubishi Rayon in Japan has been producing a water-soluble sulfonated methoxy-aniline polymer for use in e-beam lithography. Similarly, IBM has introduced a family of water-soluble polyanilines (PanAquas) that are effective at eliminating resist layer charging when used as 200 nm-thick layers. The same polymers were also shown to be effective in reducing charging of nonconducting specimens during scanning electron microscopy. The advantage of using conducting polymers (compared with more traditional sputtered metal coatings) is that the polymer can be easily dissolved so that specimens can be nondestructively analyzed.<sup>27</sup> Other applications for conducting polymers in microelectronics fabrication include the use of polyaniline coatings for electroless deposition of copper connectors, and future applications may include interconnects and even devices such as diodes and transistors.

## ELECTROCHEMICAL SWITCHING/ENERGY STORAGE/CONVERSION

The next most obvious applications of conducting polymers utilize their conductivity and electroactivity. Conducting polymers such as polypyrrole are readily oxidized and reduced, according to the reaction in Figure 1.5, in cases where the counterion is able to freely leave the CEP matrix and is immobilized within the CEP matrix.



**FIGURE 1.5** The electrodynamic character of polypyrroles.

---

**TABLE 1.3**  
**Battery Performance Data**

| Anode   | Cathode       | Open Circuit Voltage (V) | Charge Density (Ah/kg) |
|---------|---------------|--------------------------|------------------------|
| Lithium | Polyacetylene | 3.5–3.9                  | 100–300                |
| Lithium | Polyaniline   | 3.0–4.0                  | 50–150                 |
| Lithium | Polypyrrole   | 3.0–4.0                  | 50–170                 |

*Source:* From Angelopoulos, M. *IBM J. Res. Dev.* 2001, 45(1): 57.

---

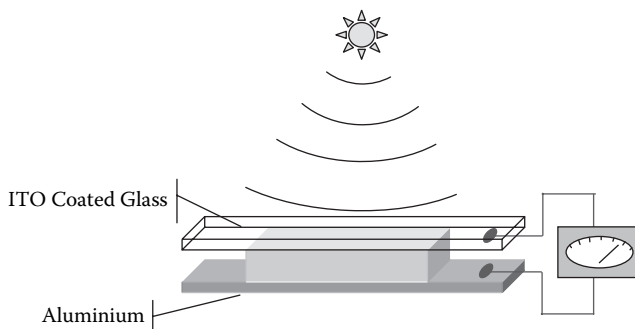
The general changes in the properties of the polymer that accompany this reaction are indicated in Table 1.2.

Anion movement predominates in cases where a small mobile dopant, e.g.,  $\text{Cl}^-$ , is used. If large anion dopants such as polyelectrolytes are employed, then cation movement will predominate.

The fact that conducting polymers can be charged and discharged has aroused much interest among those involved in developing new rechargeable battery technologies.<sup>28</sup> Conducting polymers are usually combined in a cell with lithium as the other electrode, and a usable voltage of approximately 3 V is obtained. The achievable energy densities are several times that of the nickel-cadmium and lead-acid batteries. Typical performances of several CEP-based batteries are summarized in Table 1.3.

These solid-state batteries were introduced commercially in the early 1990s by Bridgestone (Japan), Allied Signal (USA), and Volta (Germany), but the products were discontinued because of low sales. The slow sales have been attributed to the release of other competing battery technologies, such as lithium-ion batteries. A breakthrough in battery design was announced by John Hopkins University researchers in 1996.<sup>29</sup> Whereas previous battery designs used a conducting polymer as one electrode only (cathode), the new design incorporates a polymer cathode, an anode, and electrolyte. The design gives good battery performance and has the advantages of high flexibility and light weight. Such improvements may give a new impetus to polymer battery commercialization. Alternatively, novel forms of CEPs may facilitate their use as batteries in nonconventional applications. For example, a recent report describes CEP fibers as battery materials, and conducting-polymer-coated textiles have been shown to be highly effective battery electrodes.<sup>30</sup> Fully packaged CEP fiber batteries may be useful as a power source for wearable electronic systems.

Recent research has suggested that conducting polymers are also set to emerge in devices used to store energy in the form of supercapacitors and photovoltaic systems. The intense interest in these applications is driven by developments in electric-powered vehicles and alternative energy in general. Supercapacitors are those devices able to store a charge of 50 F/g (or 30 F/cm<sup>3</sup>) or higher. This high storage capacity and ability to deliver high power density can be utilized in electronic equipment and electric vehicles.<sup>31</sup> The fast discharge rate obtainable from capacitors means that high power



**FIGURE 1.6** Device design for polymer photovoltaic device (the thickness of the polymer layer is greatly exaggerated).

can be delivered for short periods. Conducting polymers are being researched for “redox supercapacitors.” In these devices, the redox chemistry of the polymer is used in the same way as described earlier for batteries. However, the design of the device is such that the conducting polymer is applied as a thin coating on a high-surface-area substrate. This design allows for very rapid charging and discharging of the polymer so that capacitor-like performance is obtained, with specific capacitances reported up to 250 F/g (based on the weight of the polymer).<sup>28</sup> All solid-state redox supercapacitors using PTh and PPy with solid polymer electrolytes have been reported<sup>32</sup> as having storage capacities of 18 F/g, and more recent reports show that supercapacitors with solid electrolytes can have capacities even higher than their liquid electrolyte counterparts.<sup>33</sup> Ionic liquid electrolytes also provide significant advantages to supercapacitor performance, such as greatly increased cycle life.<sup>34</sup>

The development of organic-inorganic hybrid materials as capacitors presents additional opportunities,<sup>35</sup> with the inherent capacity of metal oxides such as  $V_2O_5$  being used to advantage.<sup>36</sup>

## POLYMER PHOTOVOLTAICS (LIGHT-INDUCED CHARGE SEPARATION)

Polymer photovoltaic devices using conducting polymers are also being developed.<sup>37</sup> In a typical arrangement, the photosensitive polymer (such as PPV and its derivatives) is sandwiched between two electrodes (Figure 1.6). One is a transparent material, typically indium tin oxide (ITO)-coated glass, and the other electrode is a low-work-function metal, such as aluminum or calcium. Light is absorbed by the polymer, creating excitons (electron–hole pairs) that dissociate at an appropriate interface to give charge separation and, hence, current flow. The advantages of using CEPs in solar cells have been summarized recently:<sup>38</sup>

- Stable after absorption of visible light in an inert atmosphere
- Strong absorbers of visible light
- Tunable absorption spectrum
- High yield of charge generation when mixed with electron-accepting materials

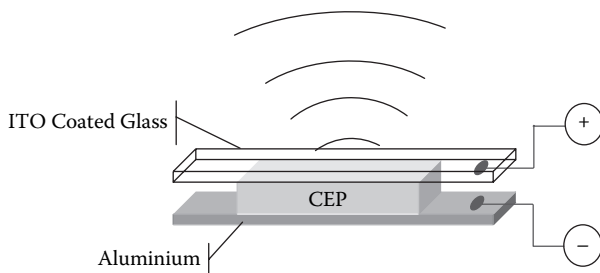
Efficiencies of polymer-based photovoltaic devices are currently low compared with silicon semiconductor materials. However, polymer photovoltaics have the potential to be manufactured very cheaply and can be applied to very large areas, such as rooftops and exterior walls of buildings. The large surface areas can compensate for the lower efficiencies to provide an adequate supply of electricity. Of course, efficiencies are being improved by chemical modification of the polymer and better design of the photovoltaic devices. One approach to polymer modification is to attach “light-harvesting” groups to the polymer chains so as to increase the amount of light absorbed. Once again, the fabrication of the device is critical in determining device performance. It has been shown that formation of interpenetrating networks of donor- and acceptor-type polymers results in marked improvements in photovoltaic efficiency, as reviewed recently.<sup>39</sup> The distance moved by the separated charge is very small in CEPs due to low carrier mobilities,<sup>38</sup> so efficient charges generation requires a large interface between the electron donor (CEP) and the electron acceptor materials. Nanostructured metal oxides and Buckminster fullerenes have been shown to be suitable acceptor materials.<sup>38</sup>

CEPs have also been used as the photoactive component in photoelectrochemical (Gratzel) cells<sup>40,41</sup> as well as catalytic counter electrodes in place of platinum.<sup>42</sup>

## DISPLAY TECHNOLOGIES: ELECTRICALLY STIMULATED LIGHT EMISSION

The process used for the photovoltaic device can be reversed to produce a light-emitting diode. When an electric field is applied to two electrodes, as shown in Figure 1.7, electrons are injected into the conduction band of the polymer layer from the cathode (usually a high-work-function metal, such as aluminum or calcium). At the ITO-glass anode, electrons are removed from the valence band of the polymer, to produce vacancies, or holes. The free electrons and holes move in opposite directions under the influence of the electric field, and when they combine, a photon of light is emitted. The color of the light emitted depends on the band gap between the valence and conduction bands in the polymer. Appropriate derivitization of PPV polymers has produced polymer light-emitting diodes (PLEDs) that emit the three primary colors: red, blue, and green.

The PLED was first demonstrated by Richard Friend and coworkers at Cambridge University in 1990. The early PLED devices from Friend’s group in Cambridge had an efficiency of only 0.01%, but this has now been improved to 4% or better, which



**FIGURE 1.7** Device design for a polymer light-emitting diode (PLED).



provides sufficient light to be seen in daylight. Early devices also suffered problems of stability, but improved lifetimes have been obtained by totally sealing the devices from oxygen and moisture. Removal of excess heat also stabilizes the polymer against degradation. A great many conjugated polymers and copolymer systems have been investigated for use in PLEDs, with significant advances made in terms of processability and color tuning. However, according to a recent review, a great deal of work still remains to be done to fully understand the complex mechanisms involved in device operation and to fully optimize device performance.<sup>43</sup>

PLEDs offer one of the most exciting prospects for conducting polymer commercialization as they offer several advantages over existing technologies for flat panel displays. Several breakthroughs in the synthesis and processing of electroluminescent PPV by the Cambridge University group have spearheaded the commercial development of flat screen displays. The first products were backlit displays for automobile instrument panels and mobile phones. The displays were being manufactured by electronics giant Philips in partnership with Cambridge Display Technologies, a company spun off from the original research at Cambridge University. Philips released an electric razor in 2002 that used a PLED display. Uniax Corporation, United States, has also entered into a partnership with Philips to commercialize conducting polymer displays based on the research work of Nobel Laureate Prof. Alan Heeger's group at the University of California, Santa Barbara. PLED development is also an interest for most major chemical companies, including DuPont, Hoechst, and Dow Chemical.

## ELECTROCHROMICS

Another interesting application that uses the dynamic properties of conducting polymers is electrochromic devices.<sup>44,45,46,47</sup> An electrochromic device based on polypyrrole is shown in Figure 1.8. The polypyrrole changes from colorless to black when it is oxidized by the application of positive potentials. Similarly, polythiophene and polyaniline undergo distinct color changes when an electrical potential is applied.



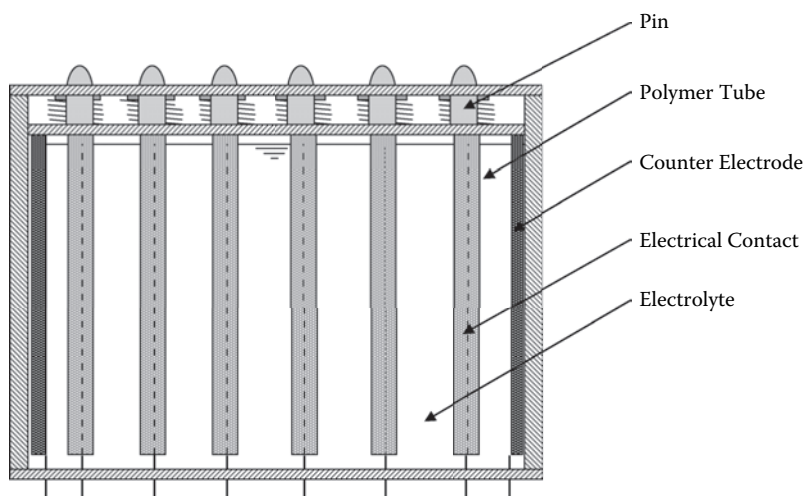
**FIGURE 1.8** Example of electrochromic device based on polypyrrole-coated glass.

Thin films of polythiophene can be switched from red (oxidized) to blue (reduced), and polyaniline displays a spectrum of colors as different potentials are applied to it. The polythiophenes are particularly interesting, given the diverse chemistries available to enable fine-tuning of the polymer band gap and, hence, the color changes observed upon electrochemical switching.<sup>48,49,50,51,52</sup> This has possible applications in advertising displays and smart windows. This bistable material can also be used as a memory storage device for information storage. All of the preceding applications use conducting polymers in the solid state in environments in which the dynamic character is readily characterized, controlled, and utilized. Recently, however, ionic liquid electrolytes have proved to be very beneficial, especially in terms of enhanced lifetime of CEP devices.<sup>53</sup> One electrochromic device was cycled  $10^6$  times without significant loss in performance.<sup>54</sup>

## ELECTROMECHANICAL ACTUATORS

More futuristic applications for conducting polymers that are receiving considerable attention include electromechanical actuators (artificial muscles).<sup>55</sup> Allied Signal (now Honeywell International) is interested in the development of lower-power/ lower-voltage moving parts for micromachined optical devices. NASA has also been involved in the development of low-power, lightweight actuators for the window wiper on the Mars Explorer. Companies dedicated to the development of artificial muscles based on conducting polymers have also emerged in recent years. Micro-Muscle based in Sweden and EAMEX from Japan are both actively pursuing actuators for biomedical and electronics applications. Academic laboratories have also developed several demonstration products, including a variable camber hydrofoil,<sup>56</sup> a gas valve,<sup>57</sup> and a micropump.<sup>58</sup>

IPRI is also currently involved in the development of actuators for an electronic Braille screen (Figure 1.9) in collaboration with Quantum Technology (Sydney, Aus-



**FIGURE 1.9** The electronic Braille screen based on conducting electroactive polymers.

tralia).<sup>59</sup> Lack of a convenient user interface is the single biggest barrier to blind people accessing information in the Internet age. The future of Braille lies in a low-cost refreshable surface, or screen, where the individual Braille dots are raised and lowered electronically by low-voltage/low-power actuator systems, allowing changing messages or decision options to be displayed.

We envisage the screen as a device consisting of multiple rows of a new type of Braille cell. The pins making up each Braille cell of the screen are driven electronically by polymer actuators in place of the piezoelectric mechanisms of existing technology. Because of its size and simple mechanical design, the proposed cell can be used to make multiple lines of Braille. These can be manufactured in modular building blocks suitable for use in a wide variety of product configurations, from a full-page screen to electronic note takers, ATMs, etc. The target performance characteristics for the actuating elements of the Braille cell are

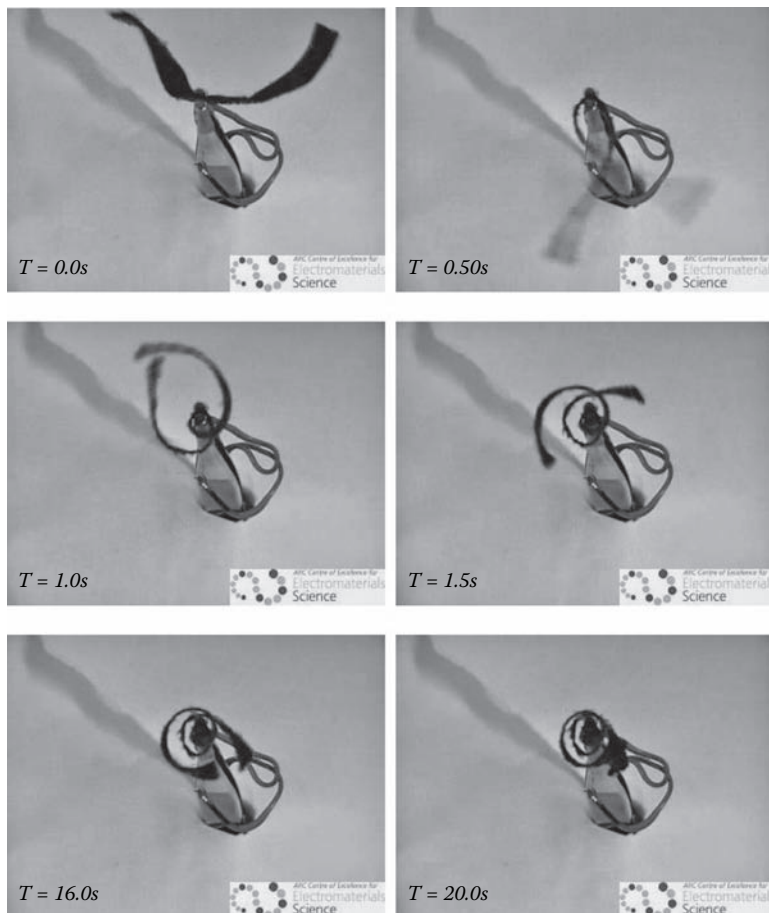
- Axial movement of 0.5 mm in 0.2 s with a tensile load of 50 mN (1% strain; 5% s<sup>-1</sup> strain rate; 0.2 MPa isotonic stress for a cell 50 mm high working against a 0.1 N/m spring)
- Operating voltage < 20 V
- Operating lifetime > 10<sup>6</sup> cycles

Electromechanical actuators are materials that can change their physical dimensions when stimulated by an electrical signal. In the case of conducting polymers, the volume change occurs as a result of ion movement into and out of the polymer during redox cycling.<sup>60</sup> The change in volume can be more than 10%; in length and thickness, changes of more than 30% have recently been reported.<sup>61,62,63</sup> When tested isometrically (at constant length), the stress generated by volume changes is on the order of 10 MPa. The performance of conducting polymer actuators compares favorably with natural muscle (10% stroke and 0.3 MPa stress) and piezoelectric polymers (0.1% stroke and 6 MPa). Piezoelectric polymers are driven by high electric fields, usually 100–200 V, whereas conducting polymers require only 1–5 V to operate. Some of the disadvantages of CEP actuators include slow response time and limited lifetime, although recent studies have shown strain rates of >10%/s<sup>59,64</sup> (natural muscle can respond at 10%/s) so that bending-type actuators can operate at close to 100 Hz.<sup>65</sup>

An important development in conducting polymer actuators has been the use of a solid polymer electrolyte (SPE),<sup>66</sup> an important advance in terms of realizing practically useful devices. Figure 1.10 shows the bending operation of a solid-state actuator consisting of five layers: gold, CEP, SPE, CEP, and gold. The SPE acts as both an ion source and ion sink, and replaces the liquid electrolyte used in previous studies. Ionic gels made by polymerizing a conventional polymer (such as polymethylmethacrylate) in an ionic liquid have also been shown to be stable solid-state electrolytes for CEP actuators.<sup>67</sup> Such gels are inherently more stable, both environmentally and electrochemically, than traditional SPEs.

## SEPARATION TECHNOLOGIES

The dynamic character of conducting polymers has been used to advantage in the development of new smart membrane technologies.<sup>68,69,70,71,72</sup> A membrane consist-

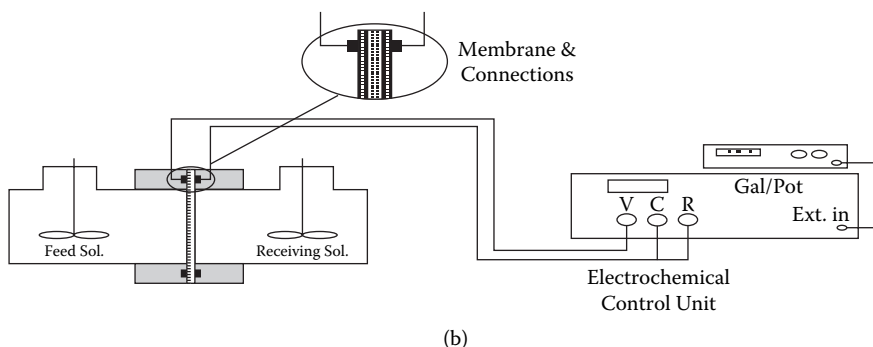
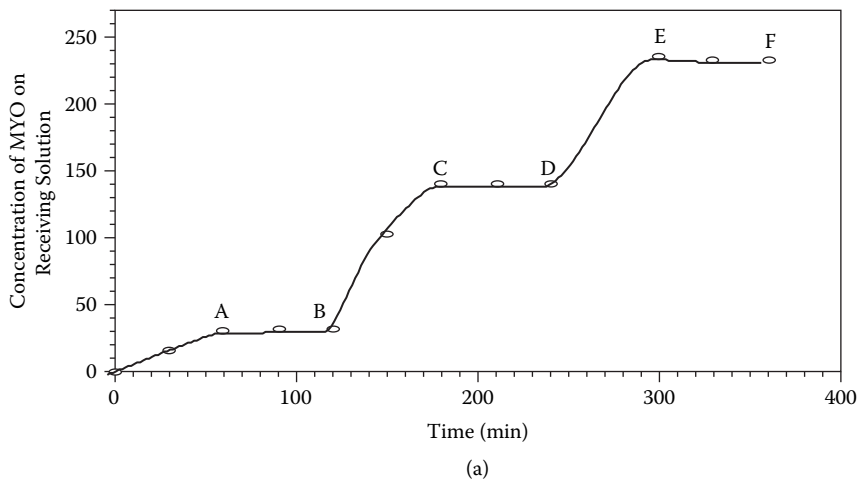


**FIGURE 1.10** Time lapse photographs showing bending movement of bimorph-type actuator (two active electrodes) made from polypyrrole and a porous membrane separator, and activated by 1.5 V potential difference between the polymer electrodes.

ing of, or coated with, a CEP can be stimulated *in situ* using small electrical pulses to trigger the transport of electroinactive ions such as  $K^+$  and  $Na^+$ , transition metal ions such as  $Cu^{2+}$  and  $Fe^{3+}$ , small organic molecules such as sulfonated aromatics, and even large macromolecular species such as proteins (see Figure 1.11). The flux and selectivity attainable are dependent on several factors:

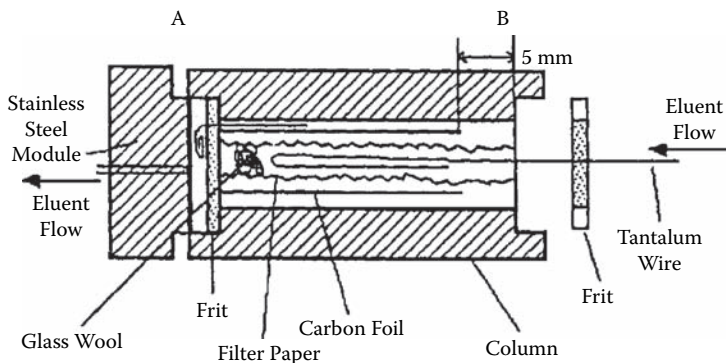
1. The composition of the membrane.
2. The porosity as determined by the CEP and/or a more porous substrate onto which the polymer may be coated.
3. The electrochemical conditions used during operation (potential pulse height and pulse width are critical).

Switching the polymer repeatedly between its available oxidation states facilitates transport of ionic/molecular species through the polymer membrane. Changes in



**FIGURE 1.11** (a) Controlled transport of myoglobin across a conducting polymer membrane. Fast transport occurs when an electrical potential is applied to the polymer (0–A, B–C, and D–E). Undetectable permeation occurs when no potential is applied (A–B, C–D, and E–F). (b) Schematic diagram of the membrane transport cell. The membrane separates the stirred feed and receiving solutions and is connected to a galvanostat/potentiostat for control of the electrical potential and current.

permeability between these different states occur due to differences in their densities and charge. Consequently, different species will diffuse through the polymer structure at different rates depending on the oxidation state of the membrane polymer. Ionic species can also be “electrochemically pumped” through the membrane by switching between oxidation states. If the polymer is synthesized using a large, immobile counterion, then reduction of the polymer causes cations from the surrounding electrolyte to be incorporated into the polymer. Subsequent reoxidation of the polymer ejects these cations. In this manner, cations can be incorporated into the polymer membrane from the feed solution and ejected into the receiving side of the membrane. Selectivity to certain ions is based on size and charge. An exciting prospect is in chiral separations, where chiral-conducting polymers can discriminate between different hands of the target molecule.



**FIGURE 1.12** Electrochemically controlled liquid chromatography column.

The full utilization of this fascinating new membrane technology is currently limited by our ability to process and fabricate large-surface-area membrane structures at a reasonable cost. Such separation technologies should have a widespread impact in chemical separations for processing and refining purposes and in controlled-release technologies.<sup>73</sup> The separation of neutral volatile organic species using pervaporation has also been achieved using conducting polymer membranes,<sup>74,75</sup> and recently, the use of CEPs for gas separation has been explored.<sup>76,77</sup>

Electrochemically controlled chemical behavior can also be used to design surfaces capable of selective molecular recognition. This has potential for the development of new chromatographic separation media.<sup>78</sup> In fact, the chemical properties of the chromatographic phase can be tuned *in situ* to effect the desired separation characteristics. Using a specially designed chromatographic column (see Figure 1.12) that allows electrical potentials to be applied during separation, the chemical affinity of the polymer can be adjusted as required.

## CONTROLLED-RELEASE DEVICES

Conducting polymer films and coatings are also ideal hosts for the controlled release of chemical substances including therapeutic drugs, pesticides, fungicides, and many others. Figure 1.5 shows that the oxidation/reduction of polymer involves the movement of ionic species into and out of the polymer material. By incorporating the target species as the dopant in the conducting polymer, the redox chemistry of the polymer can be used to release the target species at the desired time.

Both anionic and cationic species can be incorporated into the polymer and released at the desired time. Anionic species are the usual dopant ions incorporated with PPy, PAn, and PTh polymers; however, it is also possible to trap cations. The incorporation of cations involves synthesizing the polymer using a large, immobile polyanion such as poly(vinyl sulfonate). When this polymer is reduced, the large anion cannot leave the polymer, so cations from the surrounding electrolyte are incorporated into the polymer to balance the charge of the polyanion. Subsequent oxidation of this polymer releases the cation species back into the surrounding electrolyte. The possible ion flows during redox reactions of PPy are illustrated in Figure 1.5.

Initially, the ability to incorporate biomolecules during the growth of conducting polymers and to expel these molecules by electrical stimulation was seen as a means to develop novel controlled-release systems<sup>79,80</sup> for active ingredients such as anticancer drugs (flouracil)<sup>81</sup> or anti-inflammatories (dexamethasone).<sup>82</sup>

In other applications the release can also be automatically stimulated by a change in the environment. For example, it is known that the galvanic coupling of conducting polymer coatings (such as polyaniline) to metals such as steel and aluminum causes a reduction of the polymer from the emeraldine salt state to the leucoemeraldine base state, and this process involves the release of the dopant ion into the surrounding electrolyte. It has been speculated<sup>83</sup> that the dopant could be designed such that it acts as a corrosion inhibitor for the metal so that the polymer can release the inhibitor at the point when corrosive conditions first form. Indeed, a number of studies have shown that the dopant used with PAN has a large impact on the corrosion protection provided by the polyaniline, suggesting that the inhibition process may be involved in corrosion protection.

## CORROSION PROTECTION

Controlled release of corrosion inhibitors may be involved in new-generation corrosion protection coatings based on conducting polymers.<sup>84,85</sup> There is considerable evidence indicating that conducting polymers provide beneficial protection to many metals in a corrosive environment. Many studies since the mid-1980s have shown that a coating of PAN, PPy, or PTh can inhibit the corrosion rate of mild steel,<sup>86</sup> stainless steel,<sup>87</sup> aluminum,<sup>88</sup> and copper.<sup>89</sup> The conducting polymer can either be applied as a neat coating or as a dispersion in another polymer binder. In most studies, a barrier topcoat is also applied over the top of the conducting polymer “primer.” Figure 1.13 shows an example from our laboratories illustrating the corrosion resistance of mild steel coated with PAN primer/epoxy topcoat after a 3-yr immersion in saltwater. Although large blisters have formed (after approximately 2 yr), there is little sign of steel rusting.

Elucidation of the corrosion mechanism is complicated by the many testing variables involved: type of polymer used; form in which the polymer is applied to the metal; use, type, and thickness of the topcoat; preparation of the metal; and nature of the corrosive environment. All of these factors will influence corrosion performance. Elsenbaumer<sup>90</sup> has proposed the concept that the conducting polymer promotes the formation of a passive oxide at the polymer–metal interface. It is believed that the dense nature of this oxide impedes electrochemical corrosion reactions. Studies of the interface region have shown that oxide layers are present.<sup>91</sup> However, many other factors may also be involved in the overall process, such as the formation of metal ion–polymer complexes and the release of corrosion inhibitors by the polymer; simple barrier protection has also been suggested as being involved in the corrosion process. The use of conducting polymers as corrosion protection coatings has recently been reviewed.<sup>92</sup>

## CHEMICAL SENSORS

The combination of tunable chemical properties with the electronic properties of conducting polymers has also had a tremendous impact on the development



**FIGURE 1.13** Steel sample coated with a polyaniline primer and an epoxy topcoat after a 3-yr immersion in saltwater—note the absence of corrosion products in the test solution.

of new sensors. The use of conducting polymers in sensors has been reviewed recently.<sup>93,94,95,96,97,98,99,100</sup> Sensing surfaces have been designed that are capable of interacting with simple anions,<sup>101</sup> metal ions,<sup>102,103</sup> small organic molecules,<sup>104,105,106</sup> or proteins.<sup>107,108</sup> The electrical signals measured can be current flow, change in capacitance, or change in resistance. The area of biosensors has proved particularly interesting in this regard, as conducting polymer systems have been shown to be capable of *in situ* control of antibody–antigen interactions, making them reversible under selected conditions. The sensors are used in a flow-injection analysis mode enabling rapid sample throughput.

Biosensors combine a specific biorecognition process with a signal transduction process. In CEPs, biorecognition has been demonstrated through the incorporation of oligonucleotides, enzymes, or antigens/antibodies into the polymer. The incorporation of these species has been achieved either by covalent attachment to the polymer backbone or by use of the biological agent as a dopant. Once interaction has occurred between the CEP and the target analyte, a signal must be detected by the transduction system. Various means for detecting the interaction have been developed including optical, electrical (e.g., by using a field-effect transistor), electrochemical (including potentiometric, amperometric, or impedimetric approaches), and mass changes (as detected by a quartz crystal microbalance, for example). The extensive literature relating to CEP biosensors has recently been reviewed.<sup>109</sup>

Electronic nose systems that utilize conducting polymers as the sensor elements have also been developed.<sup>110,111,112,113,114</sup> These systems utilize arrays of robust CEPs, each with differing chemical selectivity, using changes in resistance as the signal generation method. The change in resistivity (or conductivity) is brought about either through a change in doping level or through a change in polymer



conformation. Vapors such as  $\text{NO}_2$  (A),  $\text{H}_2\text{S}$  (D), and  $\text{NH}_3$  (D) that are either electron donors (D) or electron acceptors (A) have a dramatic effect on conductivity. Changes in polymer chain conformation can also affect conductivity by increasing or decreasing the localization length over which electrons can move freely. Importantly, both mechanisms appear to be fully reversible in most cases, because the conductivity can be reset to the original values by exposing the polymer to a “neutral” vapor, such as dry nitrogen (Figure 1.14).

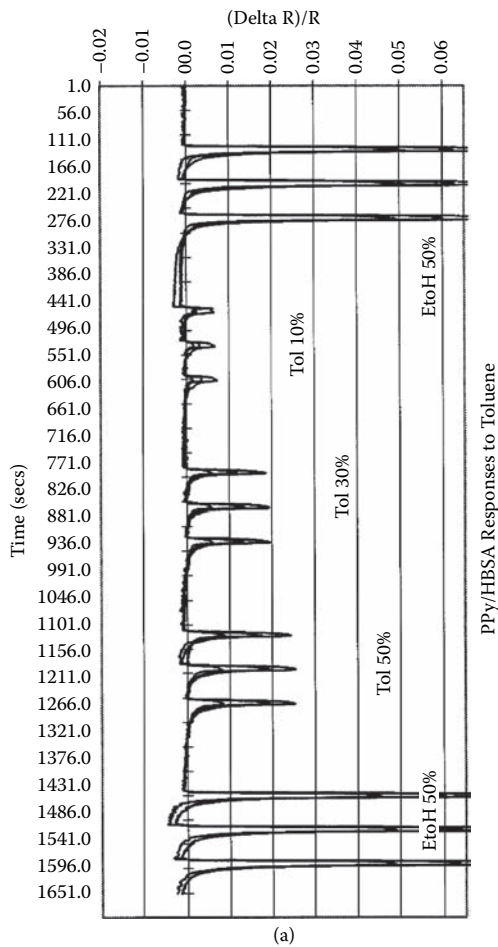
Such an approach has been used to develop customized noses (specific arrays of polymers) for classification of beers, detection and identification of microorganisms, olive oil characterization, and detection/classification of BTEX compounds (volatile organic carbons).

Conducting polymer sensors can be operated either to quantitatively measure the concentration of a target vapor species or to qualitatively analyze a complex mixture of vapors. For single vapors, the detection limits can be in the low-ppm region. Exposure to a mixture of vapors results in a unique pattern of responses, which is usually deciphered using standard chemometric techniques. The pattern can be used like a fingerprint to identify certain products, or to establish the quality of foodstuffs, wines, perfumes, etc. The electronic nose has similar components as the natural nose; this is illustrated in Figure 1.15.

The electronic nose has found the most widespread application in the food industry. Ongoing research is aimed at improving the selectivity and sensitivity both in the vapor and solution phases using resistometric and other detection systems. Particular emphasis has been placed on chemical functionalization of the polymer to increase the selectivity of the sensor to the desired species in a complex mixture. The sensitivity at present is limited primarily by the method of sensor fabrication: the detection limit is lowered by producing ultrathin and coherent layers of the conducting polymer. Screen-printing and ink-jet printing techniques provide some interesting opportunities in this regard. Improvements in device fabrication should expand applications to environmental and biomedical areas.

## BIOMEDICAL APPLICATIONS

The most striking advances in research areas concerned with the application of CEPs has in recent years been in the area of biomedical applications. The wet and soft nature of conducting polymers combined with their multifunctionality makes them immediately interesting. The separate functions of controlled surface energy, controlled release, and actuation are being exploited for many applications, both internal (implants) and external to the body. For implants, biocompatibility is a required attribute that is met by a number of CEP formulations. A number of biomedical and bioengineering applications are described in the following sections to illustrate the enormous potential of conducting polymers in the area of bionics—requiring effective interfacing of the biological and electronic worlds to improve human performance. The following examples cover bionic applications at the cellular (relevant to implantable devices) and skeletal (relevant to wearable) levels.



(a)



(b)

**FIGURE 1.14** The electronic nose. (a) Response of conducting polymer sensor to different concentrations of toluene (Tol) and ethanol (EtOH). (b) Photograph of portable electronic nose with an array of conducting polymer sensors (bottom left).

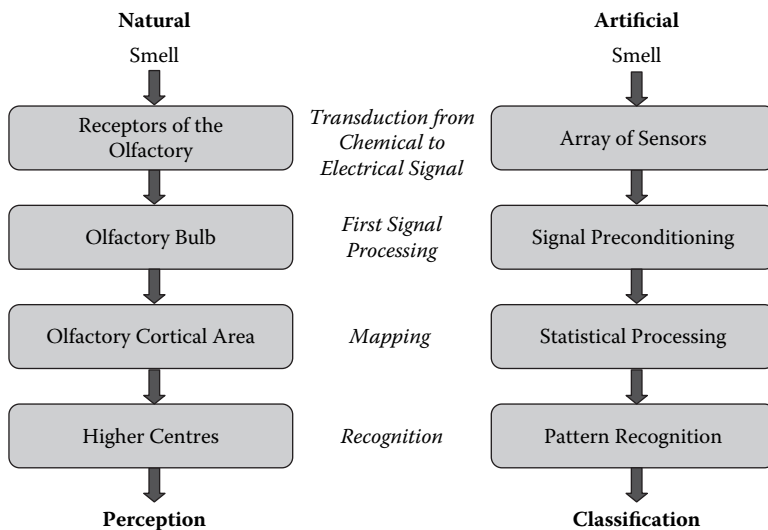


FIGURE 1.15 Similarities between natural and artificial noses.

### CELLULAR COMMUNICATIONS

The versatility in the synthesis of some CEPs (especially polypyrrole) now enables a range of bioactive surfaces to be created. For example, the incorporation of proteins<sup>115</sup> such as enzymes or antibodies is readily achieved. Combined with the chemical tuning available, this can be used in the development of biocompatible and/or new surfaces for biotechnology processing applications. Studies<sup>116,117,118</sup> involving the growth and control of biological cell cultures on conducting polymers were initiated in the early 1990s (Figure 1.16). Using this approach, it is envisaged that electrical and chemical stimuli can be used to address living cells in culture and thereby stimulate and regulate growth.

The ability to support mammalian cell growth on CEP surfaces is enhanced by the application of electrical stimuli. The majority of studies to date have focused on

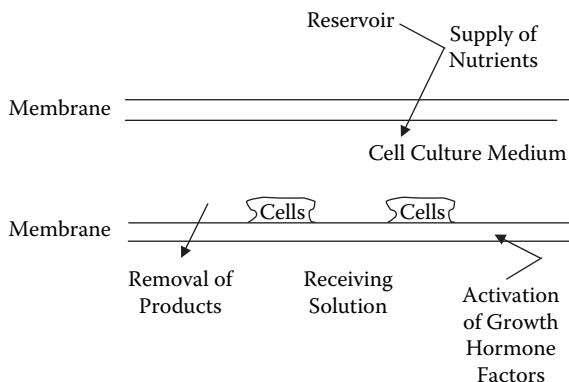


FIGURE 1.16 Schematic illustration of the use of intelligent membranes for cell culturing.

nerve cells. Given the enormous benefits to be gained from effectively interfacing nerves and conducting materials for implants such as the cochlear implant or artificial retina, this is not surprising. The possibility of using such materials for nerve repair either in the peripheral nervous system or even for spinal chord regeneration underscores the need for this ongoing research. It was shown in 1994<sup>117</sup> that the growth and differentiation of PC12 cells can be assisted by electrically controlled release of a nerve growth factor protein. Langer's group<sup>118</sup> has subsequently shown that neurite outgrowth on polypyrrole is facilitated by passage of current through the structure. It has also shown that the electrochemical effects on cell growth are fibronectin dependent,<sup>119</sup> a finding recently substantiated by Schmidt.<sup>120</sup> It has been demonstrated that neural glial cells can be attracted to and grown on PPy-coated electrodes containing the nonapeptide CDPGYIGSR.<sup>121</sup> Improved adhesion of osteoblast cells to titanium-coated PPy containing a synthetic peptide has been observed.<sup>122</sup>

Even without the release of chemical species, CEPs have also been demonstrated to be potentially very useful materials for tissue-engineering scaffolds.<sup>123</sup> Electrical stimulation of CEPs was found to promote favorable cell growth, including nerve cells, leading to the development of CEPs for a range of implant applications.

In a recent work, it was shown that a neurotrophin (NT<sub>3</sub>) can be incorporated into polypyrrole<sup>124</sup> and released using mild electrical stimulation. These materials were found to promote a significant increase in neurite extension from a cochlear explant (Figure 1.17).<sup>125</sup> At the skeletal level, materials capable of both monitoring and manipulating human movement are important.

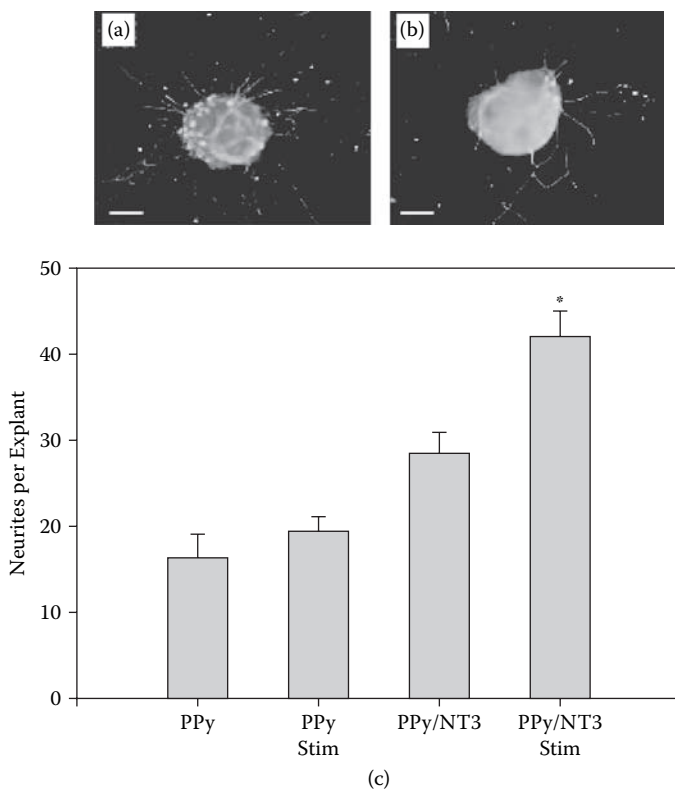
## SENSORS FOR BIOMECHANICS

Conducting polymers can also be used as sensors for the physical environment, particularly for strain or stress. Polypyrrole strain gauges have been constructed from both neat films and from coated stretch fabrics, such as Lycra®. Strain gauge materials are characterized by their gauge factor (change in resistance per change in length), dynamic range, linearity, and hysteresis. These parameters are illustrated in Figure 1.18. The use of polypyrrole to stretch fabrics to give strain gauge materials having a dynamic range up to 100% has opened up several new exciting applications. Figure 1.18 shows that an almost linear strain gauge response with low hysteresis can be obtained from polypyrrole-coated Lycra from 20 to 60% strain. These results compare with existing capacitive-based strain gauges that show a gauge factor of 2–4 and dynamic range to only 4%.

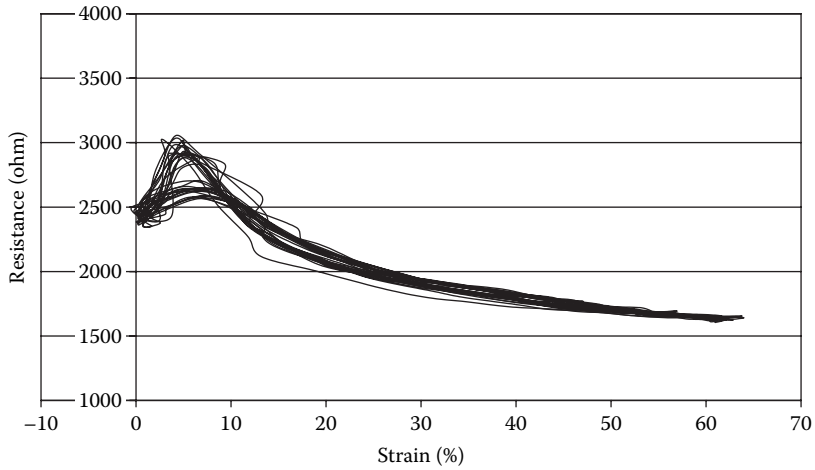
CEP materials have particular application in the field of biomechanics, where the strain gauge fabrics can be incorporated into regular sports clothing. Figure 1.19 shows an example of a patented knee sleeve using PPy and Lycra combined with a feedback device that emits an audible signal when the knee angle reaches a preset degree.

## ARTIFICIAL MUSCLES: MANIPULATING MOVEMENT

Numerous examples of developing conducting polymer actuators to operate as artificial muscles have been described in the literature. For example, a steerable cochlear implant with the CRC Cochlear Implant. (Melbourne, Australia), is under development.<sup>126</sup> The microactuator will assist surgeons during implantation of the “Bionic



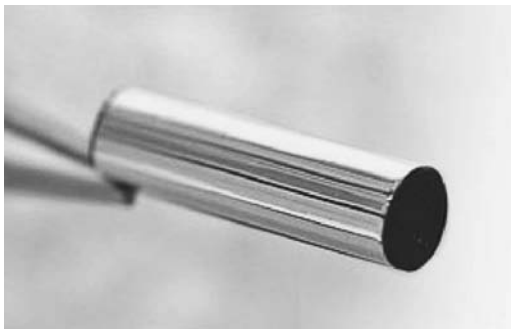
**FIGURE 1.17** Electrical stimulation of PPy for release of NT3. Explants were grown for 24 h on CAM-coated PPy/pTS or PPy/pTS/NT3 and subjected to a biphasic current pulse stimulus for 1 h. Neurite outgrowth was examined after a further 3 d in culture. A greater number of neurites per explant were observed on explants grown on (a) the stimulated PPy/pTS/NT3 compared to explants grown on (b) stimulated PPy/pTS. (c) Stimulation of PPy/pTS did not significantly alter the number of neurites per explant compared to unstimulated PPy/pTS ( $p = 1.0$ ). On the other hand, explants grown on PPy/pTS/NT3 with applied stimulation had enhanced outgrowth of neurites compared to explants grown on unstimulated PPy/pTS/NT3 and stimulated or unstimulated PPy/pTS ( $p < 0.001$ ). (R.T. Richardson et al. 2007. *Biomaterials*, 28, 513. With permission from Elsevier.)



**FIGURE 1.18** Resistance change during stretching of PPy-coated Lycra® (graph courtesy of T. Campbell).



**FIGURE 1.19** Example of fabric strain gauge for determining knee flexion; such devices can be used in sports training, biomechanics studies, and rehabilitation.



**FIGURE 1.20** The connector for blood vessels, as developed by Micromuscle AB. (Figure reproduced with permission from Micromuscle AB; <http://www.micromuscle.com>).

Ear,” a device used to assist performatly deaf patients, giving the ability to hear. The implantation process is a delicate one and the ability to steer the implant through the narrow channel will help prevent any damage, while leaving the device as close as possible to the inner ear after insertion.

Implantable devices using conducting polymer actuators are also being pursued in other areas of bioengineering, as reviewed recently.<sup>127</sup> In one concept being developed,<sup>128</sup> Micromuscle AB in Sweden has produced a clamp as shown in Figure 1.20. A hollow polymer actuator cylinder (approx. 1 mm in diameter and 3 mm in length) is used to reconnect separated blood vessels. The cylinder’s diameter expands or collapses at small electric potentials. Micromuscle is also working with medical device companies on other actuator applications. More futuristic micromuscle systems have also been proposed for bioengineering. One example shows how boxes may be opened and closed, perhaps allowing single cell capture and manipulation.<sup>129</sup> The use of electromechanical actuators based on CEPs is also being pursued in exoskeleton applications. For example, a rehabilitation glove is currently being built in collaboration with North Shore Hospital Service (Sydney, Australia) (Figure 1.21).



**FIGURE 1.21** The rehabilitation glove showing sensor strips on each finger.

Actuators will be integrated throughout the wearable glove structure to provide assisted movement during rehabilitation.

## **MICRO-ELECTROMECHANICAL SYSTEMS (MEMS) AND OTHER MICRODEVICES**

MEMS are devices that are fabricated in the 1–100  $\mu\text{m}$  range. Whereas most current MEMS applications are sensors (such as the air bag accelerometer), a growing number of actuator systems are also emerging (such as the micropumps used on ink-jet printers). Microsystems are sensor and actuator elements linked by a signal transduction or processing unit,<sup>130</sup> which has uncanny parallels to the intelligent materials system shown earlier in Figure 1.1. In both systems, the fundamental idea is the same: the sensor detects a change in the local environment (such as temperature, pressure, or chemical species), and the actuator produces an output response (such as a movement or change in color).

In many respects, conjugated polymers are well suited for microdevices. CEPs enable useful functionality in terms of actuation, sensing, and energy storage, as well as compatibility with wet biological environments. Furthermore, the speed of micro-sized CEP devices can be greatly enhanced over macroscale devices, as ion transport distances are small and surface areas are large. Finally, a wide range of patterning methods suitable for conjugated polymers enables straightforward microfabrication of these materials. The application of CEPs in microdevices and the fabrication methods used for constructing these devices have recently been reviewed.<sup>131</sup>

Perhaps the most spectacular CEP microdevice yet constructed is the microrobot arm produced by researchers at Linköping University in Sweden.<sup>132</sup> This microrobot consists of several CEP actuators that provide elbow-, wrist-, and finger-like movements. The robot has been demonstrated through a series of maneuvers where it first grasps, picks up, moves, and releases a glass sphere.

The processability of certain CEPs has been utilized in the construction of microsystems, particularly miniature sensor systems. For example, simply dip-coating connecting platinum wires with a polyaniline formulation produces a useful humidity sensor.<sup>133</sup> CEPs can also be screen-printed or ink-jet-printed to produce the complex shapes needed for various devices. Electrodeposition of CEPs is also a popular processing method, and this technique is compatible with conventional MEMS fabrication, where lithography and etching can be used to prepattern metal electrodes. Subsequent deposition of CEP by electrochemical polymerization produces the CEP microdevice.<sup>129</sup>

Microfluidics is an area that is particularly attractive for CEP-based MEMS because of the compatibility of CEPs with wet environments. Micropump systems have been developed using CEP actuators. Lee and coworkers<sup>134</sup> have presented a membrane pump using polypyrrole as a diaphragm so that the displacement in liquid electrolyte was hundreds of microns. Wu has used the thickness direction expansion of polypyrrole layers to generate a pumping action on the order of 2.5 mL/min.<sup>58</sup> Similarly, thickness direction expansion can be used as a valve to seal a fluid channel.<sup>135</sup> Other valve systems have been demonstrated using bending-type CEP actuators.<sup>136</sup>



Changes in polymer surface energy are also potentially useful in microfluidic applications.<sup>137,138</sup> In one study,<sup>139</sup> the surface energies of polyaniline and polythiophene CEPs were found to change significantly by oxidation and reduction. By producing a gradient in the doping level of a polyaniline film, a water droplet was made to move toward the reduced side. In a separate study,<sup>140</sup> polypyrrole coated on microchannels was made to move the electrolyte in the channel by reducing the polypyrrole.

## COMMUNICATION AND CHARACTERIZATION TOOLS

An important criterion in choosing intelligent material building blocks is that we be able to communicate with the assemblages produced from them. That is, we must be able to monitor behavior in the operational environment, apply stimuli, and study property (behavioral) changes in real time. This will undoubtedly be an iterative process, with the communication tools being refined as the science progresses. In fact, the intelligent materials produced may well serve as the future transducers and conduits of information that are required for us to obtain information at a molecular level. Only then can we understand, manipulate, and imprint the desired behavior characteristics into the material.

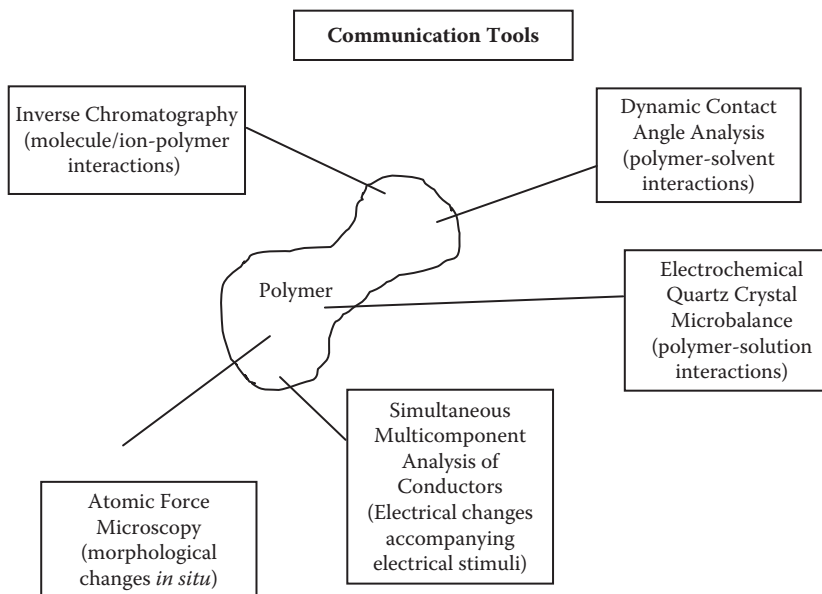
Traditionally, new material characterization is performed *ex situ* using techniques that require environments which distort the properties of the material under consideration. Consequently, they are of little use in characterizing dynamic structures. Most spectroscopic techniques, for example, are used in air or in a vacuum. For dynamic polymer systems that are used in solution, such methods do not provide all essential information. In addition, conventional techniques do not normally allow the imposition of stimuli capable of collecting information on the molecular changes brought about by these stimuli in real time.

Consequently, numerous techniques that allow dynamic materials such as conducting polymers to be studied *in situ* have been developed or newly applied over the last decade (Figure 1.22). These include

- Electrochemical methods
- Dynamic contact angle measurements
- Quartz crystal microgravimetry
- In situ spectroscopy
  - UV-visible spectroscopy
  - Circular dichroism spectroscopy
  - Raman spectroscopy
  - Electron spin resonance spectroscopy
- Inverse chromatography
- Scanning probe microscopy
- In situ mechanical testing

## ELECTROCHEMICAL METHODS

Electrochemical methods are applicable in our case due to the inherent conductivity of the polymers under investigation. As we shall show throughout this work, elec-

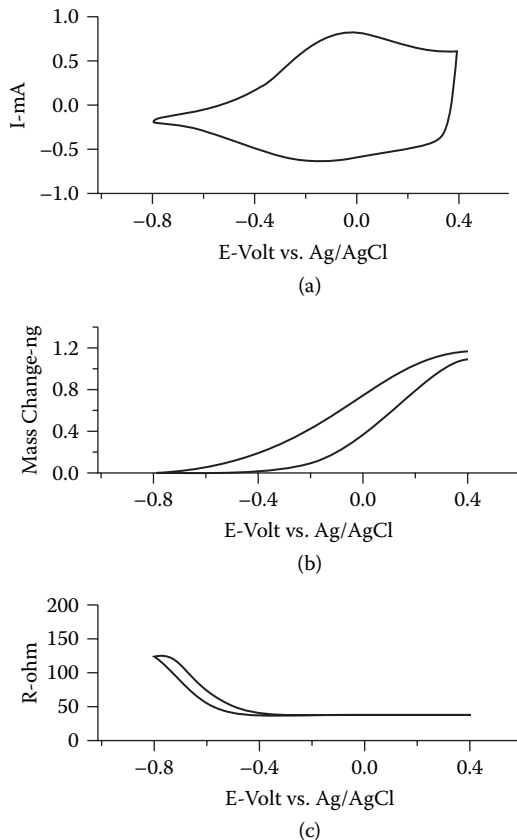


**FIGURE 1.22** Emerging tools for “communication” with dynamic polymer structures.

trochemical methods provide the major means of communicating with conducting polymer–solution interfaces. Given our current fascination with electronic communications, it is fortuitous that conducting polymers are so open to communication through this medium.

The most common electrochemical method employed for characterization is cyclic voltammetry (CV).<sup>141,142</sup> This involves application of a potential gradient in forward and backward directions to the polymer as an electrode in an electrolyte solution. The current flow as a function of this potential variation is measured, and a typical readout is shown in Figure 1.23. According to Figure 1.5, this current flow is a result of the oxidation/reduction processes and the concomitant ion flow that occurs. The readout is useful in characterizing the electroactivity of the material. The oxidation and reduction potentials under solution conditions can be estimated from the peak positions, and the peak areas allow quantification of the charge passed during oxidation and reduction. Comparing the peak areas for oxidation and reduction provides an assessment of the reversibility of the electrochemical reactions.

CVs typically obtained for conducting polymers do not fit the model expected for ideal, reversible electrochemical systems. Instead, CEP CVs often display a large separation between the oxidation and reduction peaks, often showing large, constant current flow over a range of voltages. These properties significantly depend on polymer composition and preparation conditions. The effect of polymer composition on the polymer electroactivity (switching properties) is considered in more detail in following chapters. A great deal of research has been conducted to elucidate the origin of specific features in the CVs of conducting polymers.<sup>143</sup> The current understanding is that separation of the oxidation and reduction peaks is due to the molecular reorganization that accompanies doping and dedoping of the



**FIGURE 1.23** Communicating with a conducting polymer PPy/Cl in solution: (a) cyclic voltammetry—a plot of current flow versus the electrical (potential) stimulus applied; (b) the electrochemical quartz crystal microbalance readout—mass polymer versus electrical (potential) stimulus applied; (c) the resistometry readout—resistance of the polymer versus the electrical (potential) stimulus applied. (Printed with permission from *Materials Science Forum*, Vol. 189–190, “Characterization of conducting polymer-solution interfacial processes using a new electrochemical method,” A. Talaie, G. G. Wallace, 1995, p. 188, Trans Tech Publications, Switzerland.)

polymer. In particular, the oxidized polymer is believed to adopt a more planar conformation to allow better conjugation. The constant-current region (between 0 and +0.4 V in Figure 1.23) is thought to be due to the overlap of very many redox peaks. As the polymer is a mixture of molecular weights and each has a different oxidation potential, the CV records a continuous current corresponding to the sequential oxidation (reduction) of different oligomeric/polymeric species in the sample. The practical consequence is that the oxidation and reduction potentials of the conducting polymers are ill defined, and a rather wide range of potentials have been reported (Table 1.4).

The data in Table 1.4, accepted by many scientists for the best part of a decade, belie the complexity of the controllable dynamic behavior of conducting polymers.

---

**TABLE 1.4**  
**Oxidation and Reduction Potentials**  
**(versus SCE) and Maximum Doping**  
**Levels for Selected Conducting Polymers**

| Polymer       | $E^0_{ox}$ (V) | $E^0_{red}$ (V) | Doping Level <sup>a</sup> |
|---------------|----------------|-----------------|---------------------------|
| Polyacetylene | 0.75           | -1.35           | 0.1                       |
| Polythiophene | 0.70           | +0.66           | 0.3                       |
| Polypyrrole   | -0.20          | -0.54           | 0.4                       |
| Polyaniline   | 0.60           | +0.16           | 1                         |

<sup>a</sup> Charge per monomer unit.

---

It was only the subsequent development of other *in situ* techniques that revealed the complexities that take us closer to fully understanding and controlling the behavior of CEPs.

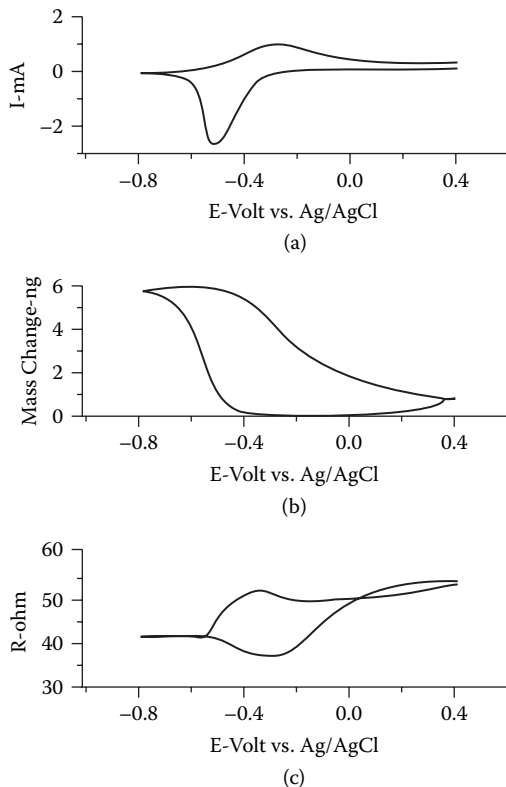
## ELECTROCHEMICAL QUARTZ CRYSTAL MICROBALANCE

A system developed recently sheds further light on these dynamic processes. The technique is the electrochemical quartz crystal microbalance (EQCM), wherein the polymer is deposited on a gold-coated quartz crystal. Changes in polymer mass, as the polymer is electrochemically reduced or oxidized, can then be monitored *in situ*.<sup>144,145</sup> For example, as the polymer is reduced, anion removal is indicated by the change in mass observed, as shown in Figure 1.23b. This technique has proved particularly useful for the study of complex systems, e.g., those containing polyelectrolytes, wherein cation movement rather than anion predominates, and this is reflected in increases in mass at negative potentials.

## RESISTOMETRY

An alternative *in situ* electrochemical method provides another piece of valuable information. Resistometry, a technique invented by Fletcher and coworkers, and first used for CEPs in our laboratories,<sup>146</sup> enables changes in the resistance of conducting polymers to be monitored *in situ*. The increase in resistance of the polymer material as it is reduced is obvious (Figure 1.23c). The definite potential/time lag between the current flow and resistance change is also apparent. This lag is due to the finite time required for the chemical processes causing the resistance change to occur.

This method indicates that the description of Figure 1.5 is an oversimplification. Although anions are expelled, it is not a simple redox process. Rather, anions are continuously expelled, starting at anodic potentials, suggesting the presence of multiple redox sites, all with different standard potential ( $E^0$ ) values. When the polymer is grown containing a different counterion, the behavior observed can be markedly different. For example, Figure 1.24 shows the response observed with a polypyrrole-dodecyl sulfate (PPy/DS) electrode when applying these same electrochemical

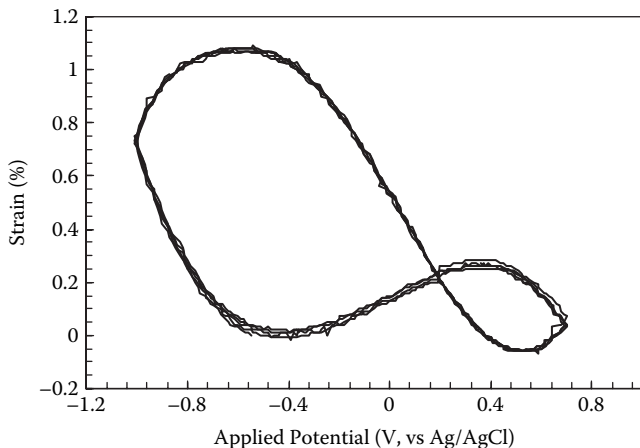


**FIGURE 1.24** Communication with the PPy/DS electrode in solution: (a) cyclic voltammetry, (b) electrochemical quartz crystal microbalance readout, (c) resistometry readout. (Printed with permission from *Materials Science Forum*, Vol. 189–190, “Characterization of conducting polymer-solution interfacial processes using a new electrochemical method.” A. Talaie, G. G. Wallace, 1995, p. 188, Trans Tech Publications, Switzerland).

potentials scanned in 1 M NaCl. In this case, mass loss (due to anion movement) as the potential is scanned to a more negative value is minimal. However, excursion to even more negative potentials results in an increase in the mass of the polymer system as cation is incorporated into the polymer (see Figure 1.5). Note also that the potential-resistance profile is markedly different from that obtained when PPy/Cl is reduced. This information is obtained using a simultaneous-analysis technique that has been developed<sup>147</sup> to allow current, mass flow, and changes in electronic properties (resistance) to be monitored simultaneously *in situ* as the polymer is stimulated by varying conditions of electrical potentials.

## ELECTROMECHANICAL ANALYSIS

A complementary technique to EQCM is to monitor volume changes during cyclic potential sweeps—electromechanical analysis (EMA). This method is based on work by Pei and Inganas<sup>148,149</sup> and has been further developed at IPRI (see Chapter 3). The



**FIGURE 1.25** Electromechanical analysis (EMA) data showing length changes (strain) during potential cycling of PPy/pTS.

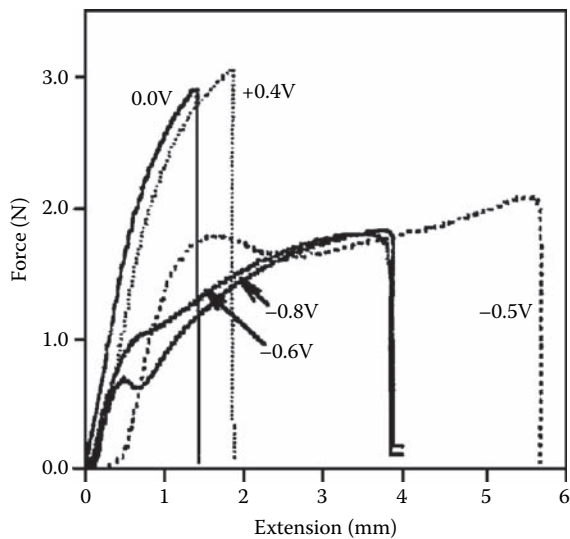
technique involves stretching a film of the conductive polymer in an electrochemical cell and monitoring the force or length changes within the film as the potential is cycled. Insertion of ions into the polymer causes swelling and stress relaxation, whereas expelling ions from the polymer causes contraction and stress generation.

An example of length changes from an EMA study is given in Figure 1.25, which show the changes in length (as percentage stretch) within a PPy/pTS film as a result of swelling and contraction during a potential cycle from  $-1.0$  to  $+0.75$  V (versus Ag/AgCl) in a  $\text{NaNO}_3$  solution. Cation incorporation occurs at negative potentials, followed by a salt-draining process in which  $\text{Na}^+\text{pTS}^-$  ion pairs diffuse from the polymer. At positive potentials, the polymer is reoxidized and anions from the electrolyte diffuse into the polymer, which again causes an increase in length.

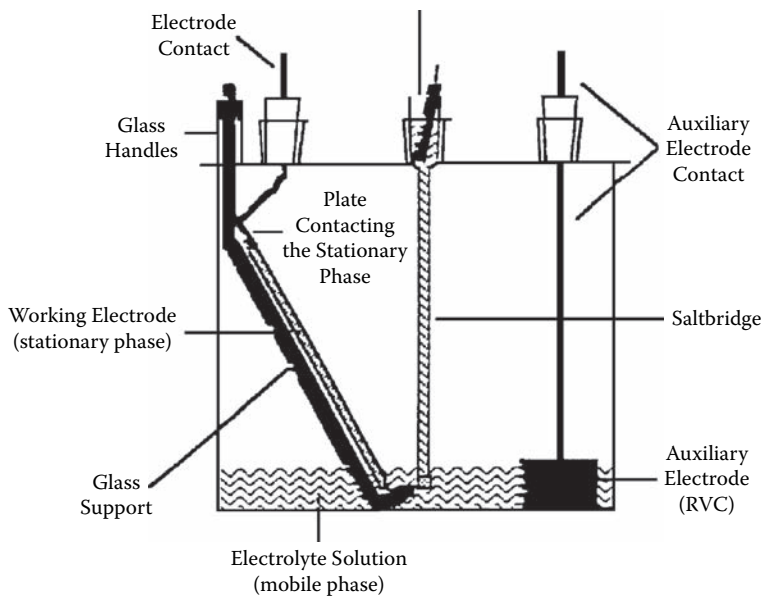
*In situ* mechanical tests have also been performed on conducting polymers. For polypyrrole, a strong ductile–brittle transition was observed when the polymer was changed from the reduced to the oxidized state (Figure 1.26). The transition is similar to that observed when polymers are cooled to below their glass transition temperature. The brittleness of the oxidized state was attributed to the greater extent of intermolecular bonding occurring as a result of dipole–dipole secondary bonds within the polymer structure. These bonds restrict molecular motion and therefore promote brittleness.

## CHEMICAL ANALYSIS

Other *in situ* techniques have also been developed in recent years that measure changes in the chemical interactions that occur.<sup>150</sup> They include inverse chromatography, in which the polymer is used as the stationary phase in a column or thin-layer mode, and a series of molecular probes is used to determine the molecular interaction capabilities of the polymer. These systems may be adopted to allow the application of electrical stimuli (as shown in Figure 1.27) to the polymer and to study


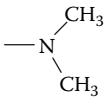


**FIGURE 1.26** Stress–strain curves generated by tensile testing immersed PPy samples at different electrochemical potentials.



**FIGURE 1.27** The inverse electrochemical TLC experimental setup (ITLC).

**TABLE 1.5**  
**A Molecular Probe Series for Inverse HPLC (Ge Series)**

| Molecular Probe             | Functional Group  | Molecular Interaction           |
|-----------------------------|---|---------------------------------|
| Benzene (principal unit)    |  | Standard                        |
| Toluene                     | -CH <sub>3</sub>  | Nonpolar                        |
| Phenol                      | -OH   | Polar, H-bonding                |
| Benzoic acid                | -COOH   | Proton donor, anion exchange    |
| Aniline                     | -NH <sub>2</sub>  | Electron donor, cation exchange |
| <i>N,N</i> -dimethylaniline |  | Nonspecific adsorption          |

the effect of these stimuli on the molecular interaction capabilities. The key to this technique lies in the identification of appropriate molecular probes. Such probes must be capable of interacting (reversibly) with the polymeric phase so that well-defined chromatograms can be obtained. To obtain pertinent information, the series of probes must vary in a logical and ordered fashion so that the effect of a particular molecular interaction parameter can be defined. Typically, the strength of the interaction with the polymer is related to the retention of the molecular probe (strong interactions produce long retention).

The Ge series allows interactions listed in Table 1.5 to be determined. Using column chromatography, a comparison of the retention of a test molecule compared to the base molecule benzene allows the presence of certain types of interactions to be assessed. Using capacity factors ( $k'$ ), a quantitative measure of the interaction parameter (IP) for a hydrophobic interaction can be obtained according to

$$IP = \frac{k' \text{ test molecule}}{k' \text{ benzene}}$$

Example of an ion exchange:

$$IP (\text{an ion exchange}) = \frac{k' \text{ benzoic acid}}{k' \text{ benzene}}$$

These parameters must be quoted for a particular solvent, as the solvent as well as the intrinsic nature of the polymer will determine what interactions occur. Selected data on conducting polymer phases obtained using this series are shown in Table 1.6, where they are compared with a conventional hydrophobic material, carbon (C<sub>18</sub> alkyl chains)-coated silica. The retention index obtained using toluene indicates that the conducting polymers are capable of nonpolar interactions. The high reten-



**TABLE 1.6**  
**Chromatographic Interactions on Polypyrrole-Coated C<sub>18</sub> (a Silica-Based Phase Coated with an Octadecyl Carbon Chain)**

| Test Compounds              | PPy-C <sub>18</sub> | PPy Chloride | PPy Dodecyl Sulfate |
|-----------------------------|---------------------|--------------|---------------------|
|                             | <i>k'/k'</i>        | <i>k'/k'</i> | <i>k'/k'</i>        |
|                             | Benzene             | Benzene      | Benzene             |
| Benzene                     | 1.00                | 1.0          | 1.00                |
| Toulene                     | 1.81                | 1.79         | 1.82                |
| Phenol                      | 0.30                | 0.38         | 0.33                |
| Benzoic acid                | 0.06                | ∞            | ∞                   |
| Aniline                     | 0.42                | 0.34         | 1.29                |
| <i>N,N</i> -dimethylaniline | 2.12                | 1.72         | 6.0                 |

tion index obtained using benzoic acid indicates that the polymers are also strong anion exchangers.

Another interesting series of molecular probes is the polyaromatic hydrocarbons (Table 1.7). These can be used to probe the ability of new polymer phases to discriminate on the basis of molecular size and shape.

In another work, the use of inverse electrochemical thin-layer chromatography (ITLC) (Figure 1.27) has been investigated. This approach was found to be complementary to inverse chromatography using high-pressure liquid chromatography (HPLC), as the physical characteristics of the polymers appropriate for each method were very different. This technique is much simpler in that it does not require expensive HPLC pumps, injectors, and detectors. The chromatographic run is carried out in a basic thin-layer chromatography (TLC) tank. The ability to electrically stimulate the polymer to obtain information on the molecular interaction capabilities as a function of potential is more easily achieved using the TLC approach. Detection of test molecules is usually carried out visually. We have used a series of amino acids as the molecular probes.

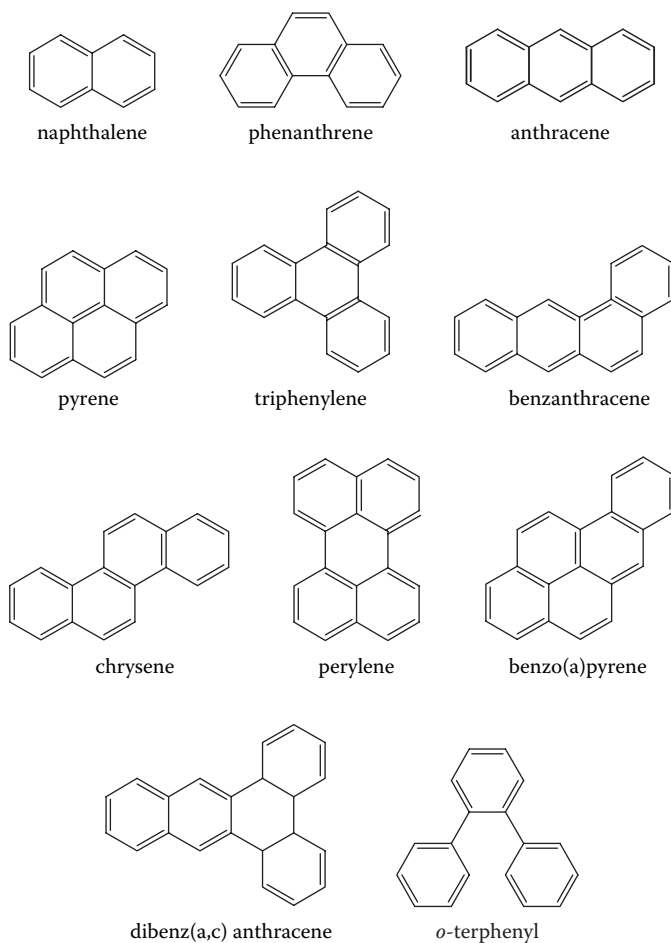
These simple groups of molecules have tremendous molecular flexibility in terms of the reactions they can undergo, and they were particularly useful for ITLC. The molecules are readily visualized after transfer onto filter paper followed by a conventional chemical derivatization with a ninhydrin reagent. This series has been used to study both polypyrrole and polyaniline materials. A typical readout is shown in Figure 1.28. Using different solvents, interactions based on either hydrophobic interactions or ion exchanges were highlighted. This ion-exchange selectivity was markedly different from that observed for conventional ion exchangers.<sup>151</sup> Other workers<sup>152,153</sup> have used a series of volatile molecular probes to characterize conducting polymers using inverse gas chromatography.

## DYNAMIC CONTACT ANGLE ANALYSES

Dynamic contact angle (DCA) analysis is a technique that allows polymer–solvent interactions to be quantified.<sup>154</sup> These are inherent for all processes occurring at

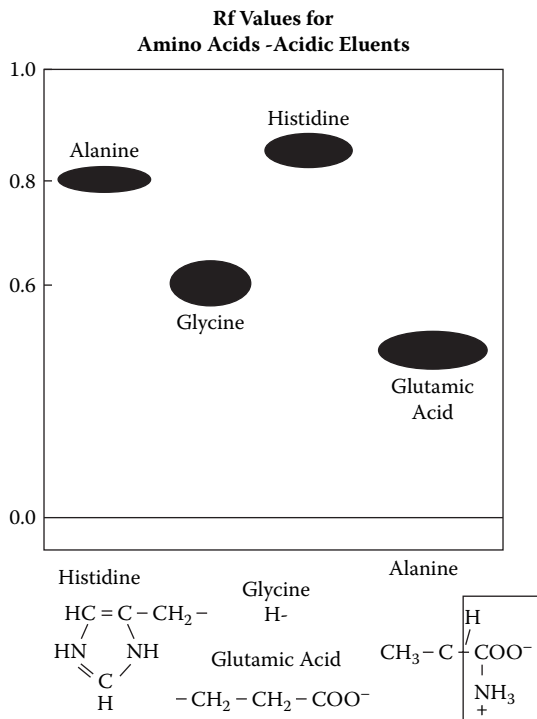
---

**TABLE 1.7**  
**The Structure of PAHs**



polymer–solution interfaces and are likely to be responsible for the dynamic behavior of conducting polymers. Information regarding these interactions is of central importance to our understanding of the properties of these materials. Also, it provides information on how exposure to different solvent environments affects the chemical properties of the material. It is also possible to apply electrical stimuli to the polymer during DCA analysis<sup>155</sup> to characterize the effect this has on the interactions between the polymer and its environment.

The method is based on Wilhelmy's plate technique for measuring DCAs. The technique involves the measurement of force as a plate is (automatically) immersed into and then emersed from a liquid at a constant rate. The forces (weight) can be plotted as a function of the immersion depth, and, from this, contact angles calculated (Figure 1.29a,b).



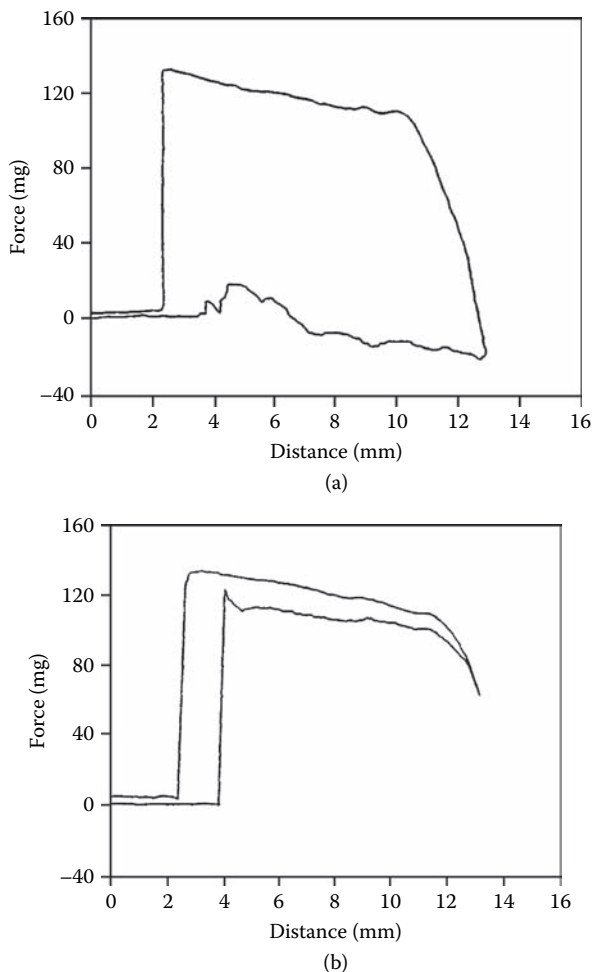
**FIGURE 1.28** Typical readout from inverse thin-layer chromatography.

This technique has been used to study the wettability of different conducting polymer systems (see Table 1.8) and how this is influenced by the counterion incorporated during synthesis and/or functionalization of the monomer.<sup>156</sup> The monomers studied are shown in Table 1.8.

These results indicate that the functional groups on poly(3-carboxy-4-methylpyrrole) (PCMP) and poly(3-carbomethoxy-4-methylpyrrole) (PCEMP) act to increase the hydrogen-bonding interactions of the conducting polymers, as the  $\theta_a$  values for each of these are less than those for polypyrrole, which is indicative of a stronger interaction between the solid and liquid phases. Also, the  $\theta_a$  value for the polypyrrole/PCMP copolymer is intermediate between the values for the constituent monomers. Furthermore, the magnitude of the trend is very close to that which could have been predicted from an analysis of the functional groups on the monomers.

## SCANNING PROBE MICROSCOPY

Since the pioneering work of Binnig<sup>157</sup> in the 1980s, the family of microscopic techniques collectively known as scanned probe microscopy (or SPM) has become widely available and is extensively used in conducting polymer research. SPM consists of a number of related techniques in which a fine probe is rastered across a sample surface. Interaction between the probe tip and the sample drives a feedback system that allows topographical mapping of the sample surface. Scanning tunnel-



**FIGURE 1.29** Force–distance plot for (a) polypyrrole ( $\text{NO}_3^-$ ) and (b) polyaniline (HCl) on carbon foil.

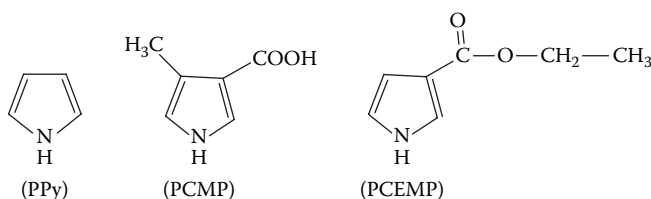
ing microscopy (STM) uses the tunneling current between the tip and the (electrically conductive) surface, whereas atomic force microscopy (AFM) uses the force of attraction (or repulsion) between the tip and the sample surface. The resolution of the piezoelectric transducers used to move the tip is such that atomic-scale resolution can be achieved (magnification  $\times 10^9$ ). AFM has been further developed such that qualitative information concerning the properties of the sample surface can also be obtained. Thus, differences in molecular friction and surface mechanical properties can be discerned. Other techniques can map the surface magnetic domains and electrical properties.

Recent applications of SPM techniques have revealed new details of the electrical properties of conducting polymers. In one example, STM images were taken of the granular structure of electrochemically prepared polyaniline films. Simultane-

**TABLE 1.8**  
**Comparison of  $\cos \theta$ ,  $\theta$ , and  $\Delta\theta$  Values for Polypyrrole, Poly(3-carboxy-4-methylpyrrole) (PCMP), and Poly(3-carbomethoxy-4-methylpyrrole) (PCEMP) on Glassy Carbon**

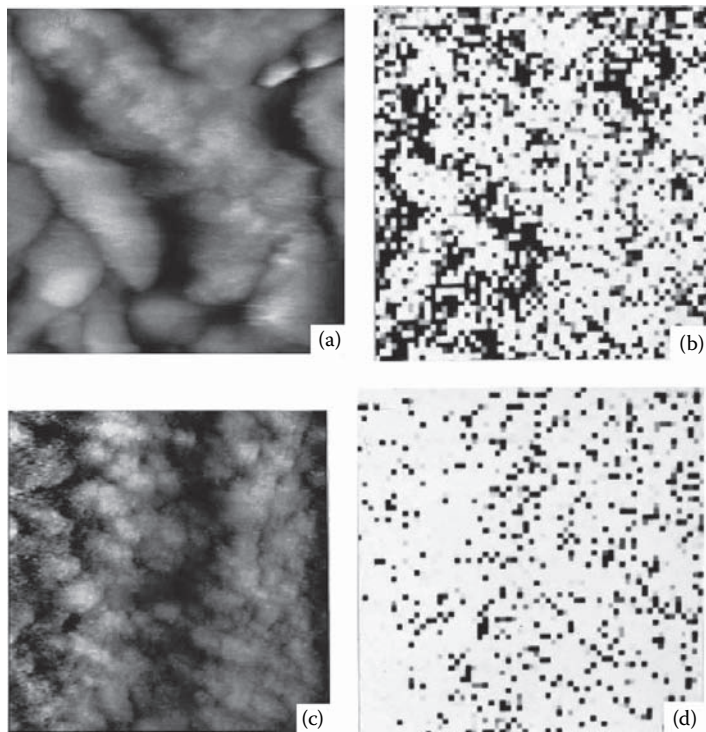
| Sample           | $\cos \theta_a$ | $\cos \theta_r$ | $\theta_a$ | $\theta_r$ | $\Delta\theta$ |
|------------------|-----------------|-----------------|------------|------------|----------------|
| Polypyrrole      | 0.09            | 1.08            | 85°        | <i>u</i>   | 85°*           |
| Polypyrrole/PCMP | 0.048           | 1.01            | 61°        | <i>u</i>   | 61°*           |
| PCMP             | 0.60            | 1.01            | 53°        | <i>u</i>   | 53°*           |
| PCEMP            | 0.39            | 1.02            | 67°        | <i>u</i>   | 67°*           |

$\theta_a$ : Advancing contact angle;  $\theta_r$ : Receding contact angle, *u* = undefined.



ously, the electrical characteristics of the surface were analyzed by scanning tunneling spectroscopy (STS). In STS, the tip remains at a constant vertical position above the surface, and the voltage difference between the tip and sample is changed. By also measuring the current flow, it is possible to obtain the current–voltage (I–V) curve of regions of the sample surface only a few nanometers in diameter. Additionally, a map of the electronic properties of the surface can be obtained by taking I–V curves at discrete points in a 2-D array across the sample surface. This technique is known as current-imaging tunneling spectroscopy (CITS); CITS images of polyaniline in the doped (emeraldine salt) and deprotonated (emeraldine base) forms are shown in Figure 1.30. These images show insulating regions as white and “metallic” regions as gray or black. The electronically conducting emeraldine salt displays a continuous pathway of metallic domains (20–80 nm in diameter). In comparison, the emeraldine base shows fewer metallic domains that are surrounded by insulating regions, and these structures account for the very low electronic conductivity of the deprotonated polyaniline.

By applying a potential difference between an oscillating tip in the so-called “tapping mode” of the AFM operation, it is possible to also investigate the electronic properties of conducting materials. The imaging method is called electrical force microscopy (EFM), and the microscope acts like a Kelvin probe, allowing the material work function to be determined. The *work function* is the energy required to remove an electron from the bulk of the material to a point just outside that phase. Although measured in different ways, the work function and oxidation potential of a material are related, because both are measures of the energy needed to remove an electron. Work function (WF) measurements of conducting polymers are therefore useful in characterizing the electrochemical properties. The EFM method offers a

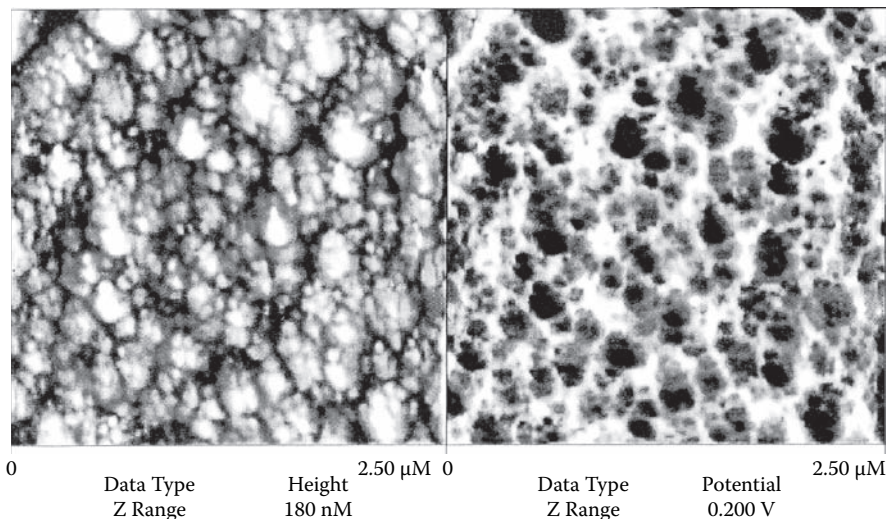


**FIGURE 1.30** Topographical and CITS images of: (a,b) doped and (c,d) undoped polyaniline.

spatial resolution of a few nanometers, so the technique provides a unique insight into the local electrical properties of a conducting surface.<sup>158,159</sup>

Figure 1.31 shows the topography image and the work function image of a sample of polypyrrole. The topography is the granular structure typical of these polymers with grain sizes in the range 50–100 nm. The EFM image shows a distinct contrast in the WF between the center of the grains and the peripheral regions, with the center showing a higher WF. The interpretation of these images is that the central regions are more highly doped and that the  $E^0$  value varies on a local scale. These results support the view that, macroscopically, conducting polymers behave as a mixture of materials having slightly different  $E^0$  values, as concluded from electrochemical studies described earlier.

In other EFM studies,<sup>158</sup> part of the sample was electrochemically oxidized by partially immersing in electrolyte and applying a positive potential. The EFM image clearly showed a distinction between the immersed (oxidized) and nonimmersed (less oxidized) parts of the sample in terms of relative work function. Similar shifts in work function had also been observed for polythiophenes when exposed *in situ* to ultraviolet (UV) radiation during EFM imaging.<sup>160</sup> An increase in the work function upon UV exposure is due to the formation of electron–hole pairs that produce photocurrent in photovoltaic devices. Thus, the EFM provides fundamental insights into the processes involved in many of the applications for CEPs.



**FIGURE 1.31** Topography image (left) and electrical force microscopy (EFM) image (right) of a polypyrrole film. Darker regions in the EFM image indicate higher work function.

The great advantage of SPM for conducting polymer research is its suitability for *in situ* imaging, giving rise to such techniques as electrochemical AFM (EC-AFM) and electrochemical STM (EC-STM). It is therefore possible to track topography changes caused by electrochemical oxidation/reduction of the polymer. Chainet and Billon<sup>161</sup> have carefully imaged the same area of a polypyrrole sample while electrochemically cycling between the oxidized and reduced states. The nodular surface features were observed to become enlarged during oxidation, demonstrating the microscopic origin of the volume changes responsible for the artificial muscles described earlier.

## IN SITU SPECTROSCOPY

In recent years, spectroscopic techniques have become invaluable tools for probing the molecular structures and interactions in CEPs. Three of the most useful are the UV-visible, circular dichroism, and Raman spectroscopy techniques. In each of these cases, absorption of the incident radiation by water (and many other electrolytes) is minimal, meaning that it is possible to obtain the spectra by reflection or transmission of light from the sample while it is immersed in an electrolyte as part of an electrochemical cell. Another valuable technique has been electron spin resonance (ESR) spectroscopy, which involves the absorption of microwaves.

## UV-VISIBLE SPECTROSCOPY

Light absorption by a CEP causes electronic transitions from its valence band to the conduction band ( $\pi$ - $\pi^*$  transitions) as well as to bands within the band gap (e.g.,  $\pi$ -polaron transitions). The resultant UV-visible spectra are very sensitive to the

oxidation state of the CEPs and to the 3-D arrangement adopted by their chains. When CEPs are switched from one oxidation state to another, their color changes dramatically (e.g., for polypyrrole, between black and pale yellow), which is reflected in their UV-visible spectra. MacDiarmid and coworkers<sup>162</sup> have, for example, used UV-visible spectroscopy as a rapid and simple technique to estimate quantitatively the proportions of each of the three oxidation states (leucoemeraldine, emeraldine, and pernigraniline) present in polyaniline samples. The specific absorption peaks observed are also indicative of the nature of the charge carriers (e.g., polarons or bipolarons) and the number of such charge carriers present.

Extension into the near-infrared (NIR) region provides new insights into molecular conformations of CEPs. Classical studies have been conducted on polyaniline emeraldine salts, where the presence or absence of a strong, broad absorbance in the NIR region (called the “free-carrier tail”) was strongly associated with molecular conformations. The presence of an intense free-carrier tail in the NIR region has been reported by MacDiarmid and coworkers<sup>163,164</sup> to be diagnostic of an emeraldine salt in an “extended coil” conformation. In contrast, this NIR band is replaced by a localized polaron band in the region 750–900 nm for emeraldine salts where the chains adopt a “compact coil” conformation. The conformation can be altered by the use of different dopants and even by exposing the doped polymer to certain solvents and vapors (a process dubbed “secondary doping” by MacDiarmid). As the polymer conformation changes from a “compact coil” to an “extended coil,” the  $\pi$ -orbitals more effectively overlap to allow greater in-chain conduction. The presence of the free-carrier tail in the UV-visible-NIR spectrum is therefore strongly correlated with the electrical conductivity in polyaniline.

For CEP films deposited on transparent electrodes such as indium tin oxide (ITO)-coated glass, *in situ* spectroelectrochemical studies are possible by insertion in an electrochemical cell constructed in a 1-cm quartz cuvette. Changes in the UV-visible spectrum of such a CEP with changes in applied potential have provided valuable information on the electrochemical redox switching of CEPs.<sup>165,166,167</sup> The technique has also been used to monitor *in situ* the electrochemical polymerization of monomers such as aniline to generate conducting CEPs on an ITO-coated glass working electrode, giving insights into the mechanism of such polymerizations.<sup>168,169</sup>

## CIRCULAR DICHROISM (CD) SPECTROSCOPY

There has been considerable recent interest in chiral CEPs in which polymer chains (or aggregates of polymer chains) adopt a one-handed helical arrangement. Circular dichroism (CD) spectroscopy provides a powerful tool to probe the chain conformation (and preferred hand) in such chiral polymers. This spectroscopic technique measures the difference in absorption of left- and right-hand circularly polarized light by a chiral sample as follows:

$$\Delta\epsilon_{l-r} = \epsilon_l - \epsilon_r$$

where  $\epsilon_l$  and  $\epsilon_r$  are the extinction coefficients measured for the absorption of the left- and right-hand circularly polarized light, respectively.



*In situ* spectroelectrochemical studies can also be carried out on chiral CEP films deposited on ITO-coated glass electrodes inserted in electrochemical cells constructed in quartz cuvettes, allowing detailed studies of the changes in the CEP structures upon redox switching between different oxidation states.

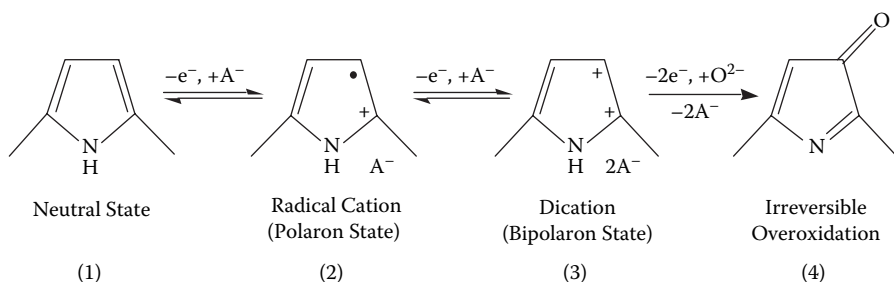
## RAMAN SPECTROSCOPY

The Raman spectrum is produced by irradiating the sample with laser light of a certain frequency and analysing the scattered radiation caused by the Stokes shift. The difference in frequency of the incident and scattered light is equal to the actual vibrational frequencies of the material. Thus, the Raman spectrum can identify and track changes in specific chemical groups. The Raman spectrum may be obtained using a light microscope so that mapping of a surface is possible to a resolution of around 1  $\mu\text{m}$ .

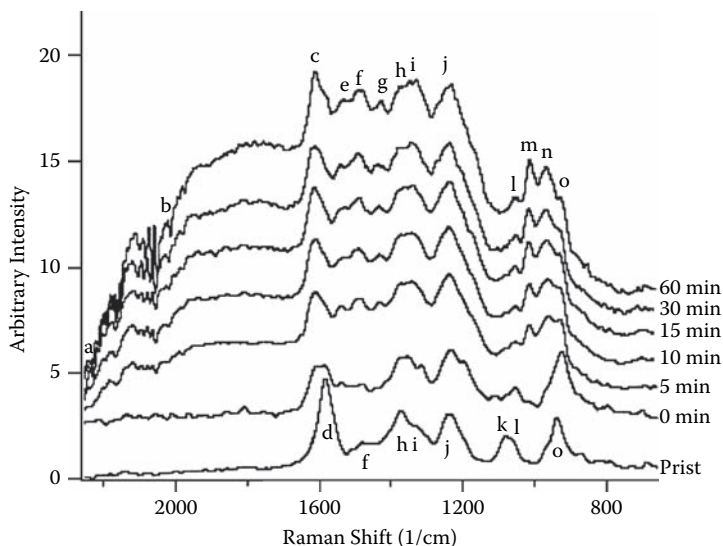
Raman spectroscopy has been used to study the chemical stability of conducting polymers. Conductivity is known to decline upon aging in ambient environments, but the process is accelerated by elevated temperatures mainly owing to the thermal loss of dopant.<sup>170</sup> In addition, high electrical potentials can also result in “over-oxidation.” Over-oxidation is the irreversible, electrochemical oxidative degradation of a conducting polymer under an anodic applied potential.<sup>171</sup> During over-oxidation, a polymer loses conductivity, charge storage ability, electrochromism, electroactivity, conjugation, mechanical properties, and adhesion to the substrate. In fact, almost all of the beneficial features of a conducting polymer are destroyed by this process.

It is important to understand the over-oxidation phenomenon to ensure long lifetimes for intelligent material systems using conducting polymer electrodes.<sup>172</sup> *In situ* Raman studies (in which an electrochemical cell is attached to a Raman spectrometer) have shown that PPy (doped with *p*-toluene sulfonate) undergoes irreversible chemical degradation when it is immersed in an aqueous electrolyte and a potential of +0.8 V (versus Ag/AgCl reference) is applied. Changes occur rather quickly (within 5 min) and can be ascribed to the formation of oxygen-containing groups in the polymer. The carbonyl groups (C=O) shown in Figure 1.32 are one possible source of the peak, indicated “c” in Figure 1.33, suggesting that the over-oxidation rapidly reduces the conjugation of the polymer, leading to a loss of conductivity.

Conducting polymer can be reversibly switched between the first three states at the electrochemical potentials shown (the exact potential depends on the nature



**FIGURE 1.32** Oxidation states of polypyrrole.



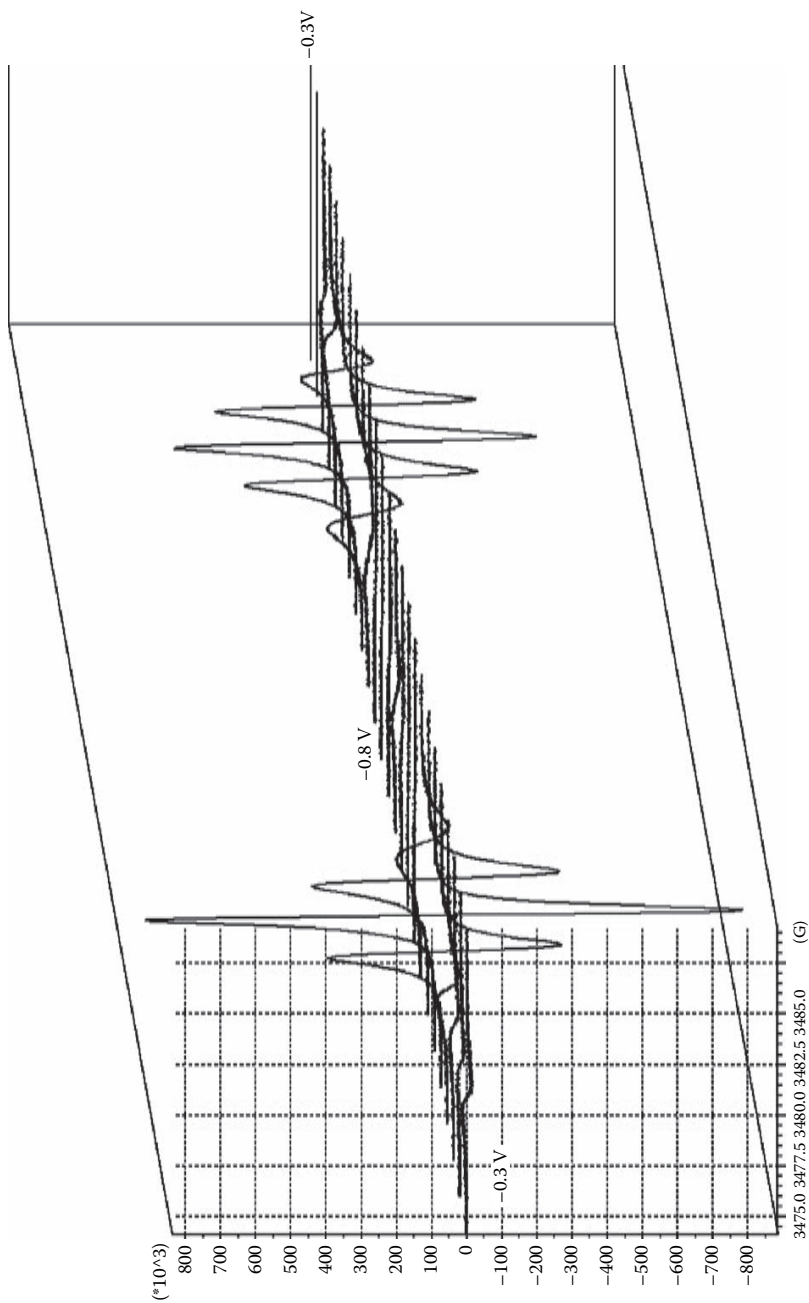
**FIGURE 1.33** Raman spectrum of PPy/pTS held at 0.8 V (versus Ag/AgCl) in 1 M NaCl with a pH of 2.25. (From T. Lewis, PhD thesis, University of Wollongong, 1998.)

of the counterion,  $A^-$ , incorporated with the polymer). The highest oxidation state is referred to as over-oxidized, because the conductivity decreases owing to loss of conjugation, and oxidation from the third to fourth state is not reversible.

*In situ* electrochemical Raman spectroscopy has also proved invaluable in identifying the neutral, radical cation and dication species formed during redox switching of polypyrroles. For example, the appearance and disappearing of Raman peaks characteristic of these during the reversible electrochemical cycling of a PPy/dodecylbenzenesulfonate film between  $-0.9$  and  $+0.5$  V (versus Ag/AgCl) in 0.10 M  $NaClO_4$ .<sup>173</sup> Raman spectroscopy also provides very useful information on the relative proportion of benzenoid and quoid rings present in polyaniline in its three oxidation states (leucoemeraldine, emeraldine, and pernigraniline),<sup>174</sup> and in establishing the species formed on heating or degradation of polyaniline samples.<sup>175</sup> Redox switching between the three oxidation states of polyaniline can be readily monitored by *in situ* electrochemical Raman spectroscopy.<sup>176</sup>

## ELECTRON SPIN RESONANCE (ESR) SPECTROSCOPY

In ESR spectroscopy, absorption of microwaves by molecules causes unpaired electrons within the structure to change spin. Consequently, it has been widely used as a tool for identifying (and quantifying) the presence of polaron charge carriers (which have spin) in CEPs, in contrast to bipolaron charge carriers, which are dications with no spin.<sup>177</sup> A typical ESR spectrum is shown in Figure 1.34, which is for fully sulfonated polyaniline, poly(2-methoxyaniline-5-sulfonic acid) (PMAS) in water. The intensity of the ESR signal is directly related to the concentration of polaronic species in the sample, and the  $g$  value obtained from the spectrum gives insights into the chemical environment of the unpaired electron. ESR spectroscopy is also a sensitive



**FIGURE 1.34** ESR spectral changes of PAN/PMAS electrodeposited on Pt wires and probed in aqueous 0.10 M HCl using applied potentials of  $-0.3$  to  $0.8$  V to  $-0.3$  V in 100 mV steps. The film was equilibrated at each potential for 3 min prior to signal acquisition. (Courtesy of Dr. Peter Immis, University of Wollongong.)

tool for identifying changes in a conducting polymer caused by environmental factors, such as when polyaniline emeraldine salt films are exposed to moisture.<sup>178</sup>

*In situ* electrochemical ESR studies, employing an ESR spectrometer to which an electrochemical cell is attached, have also proved very useful in elucidating the redox mechanisms of CEPs and their precursors.<sup>179,180</sup>

## LOCALIZED ELECTROCHEMICAL MAPPING

Recently, two new electrochemical mapping techniques have become available: the scanning vibrating electrode technique (SVET) and the localized electrochemical impedance spectroscopy (LEIS) technique. These techniques provide the capability to identify and monitor electrochemical behavior down to the micron level. These represent significant advances over traditional electrochemical methods (cyclic voltammetry, EIS, and even EQCM), which provide data that reflect only an average over the entire sample surface. Although such data are very useful, a major drawback is that no local or spatial information is obtained.

SVET detects the electrochemical potential of a sample surface (with respect to a reference electrode) with a spatial resolution of tens of microns. The technique uses a probe tip that is rastered above the sample surface and then is oscillated perpendicular to the sample surface with an amplitude of 1–60  $\mu\text{m}$ .

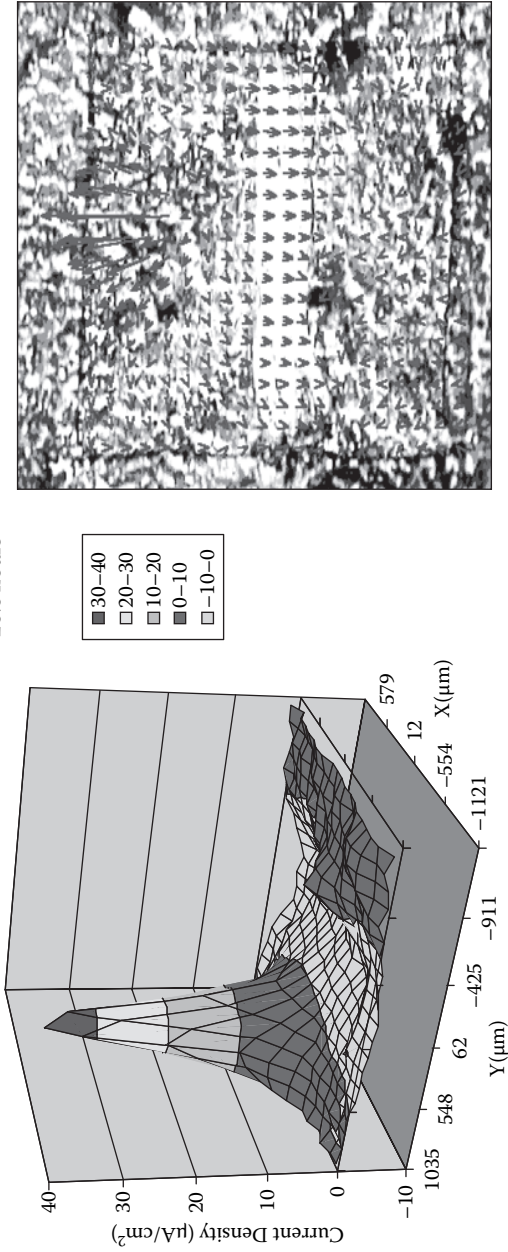
One of the first uses of SVET for conducting polymer analysis (Figure 1.35) was in the area of corrosion protection.<sup>181</sup> In these studies, the SVET probe was rastered over a pinhole defect in a conducting polymer coating on aluminum. The SVET method clearly showed that the pinhole was anodic, whereas the conducting polymer coating was cathodic. After a short period of immersion, the anodic activity at the pinhole ceased, which is believed to be due to the passivation induced by galvanic coupling with the conducting polymer coating.

In LEIS, the full electrochemical impedance spectrum of the sample/electrolyte interface can be obtained at the submillimeter level. The system works by stepping a probe tip across the sample surface (the smallest step size is 0.5  $\mu\text{m}$ ) while the sample (connected as the working electrode) is perturbed by an ac voltage waveform (usually about the open-circuit potential with an amplitude typically of 20 mV). The probe tip consists of two separated platinum electrodes, separated by a known distance. Measurement of the potential difference between the two electrodes allows the calculation of the potential gradients above the sample surface, which then give the current density. Comparison of the in-phase and out-of-phase current flow produces the impedance data, as with the regular EIS. The data can be plotted as Bode or Nyquist charts for specific points on the surface, or impedance maps of the sample surface can be obtained.

## CONCLUSIONS: CONDUCTING POLYMERS AS INTELLIGENT MATERIALS

The areas of application and the ability to characterize and communicate with conducting polymers using emerging technologies highlight the versatile, dynamic, yet controllable, nature of these materials. They undoubtedly possess properties that

Poly(3-octylpyrrole) on Al-2024 T3 Immersed in Dilute Harrison Solution  
26.6 hours



**FIGURE 1.35** SVET map showing electrochemical potential of a metal coated with conducting polymer for corrosion protection—the metal has been scribed.

make their use in the pursuit of intelligent materials systems or structures inevitable. For example, they are sensitive to numerous stimuli and can be made to respond. They can store information and energy, and are capable of performing intelligent functions. Further, we can communicate with these systems using tools now available in research laboratories.

The following chapters will describe how the design and assembly of various important polymers can be used to produce predetermined properties. (The synthesis and properties of polypyrroles, polyanilines, and polythiophenes are discussed in detail and differences between these systems emphasized.) A multitude of other CEP systems exist, and the interested reader is referred to the extensive literature now available. Furthermore, the synthesis of CEPs to produce different forms that enable integration of all the functions required for intelligent operation or that allow incorporation into a larger structure will be described.

Undoubtedly, this pursuit will result in spin-off benefits for conducting polymer research and, perhaps, polymer (macromolecular) science in general. For too long, the implications of the inherent dynamic properties of polymers have been ignored, as we have devised ingenious ways to eradicate them. A more sophisticated approach to its understanding and manipulating these dynamic properties may revolutionize polymer science in its own right.

## REFERENCES

1. Teasdale, P.R.; Wallace, G.G. *Chimi Oggi*. 1992, 10: 19.
2. Riley, P.J.; Wallace, G.G. *J. Int. Mat. Syst. Struct.* 1991, 2: 228.
3. Wallace, G.G. *Mat. Forum* 1992, 16: 111.
4. Talaie, A.; Sadik, O.; Wallace, G.G. *J. Mat. Syst. Struct.* 1993, 4: 123.
5. Mirmohseni, R.; Price, W.E.; Wallace, G.G.; Zhao, H. *J. Int. Mat. Syst. Struct.* 1993, 4: 43.
6. *US-Japan Workshop on Smart/Intelligent Materials and Systems*. Ahmad, I.; Crowson, A.; Rogers, C.A.; Aizawa, M. (Eds.). Technomic Publishing Co., Inc., Lancaster, 1990.
7. *Smart Materials, Structures and Mathematical Issues*. Rogers, C.A. (Ed.). Technomic Publishing Co., Inc., Lancaster, 1989.
8. "Matters Arising." Teasdale, P.R.; Wallace, G.G. *Proceedings of First Asia Pacific Workshop on Intelligent Materials*. University of Wollongong, 1992.
9. Ghandi, M.V.; Thompson, B.S. *Smart Materials and Structures*. Chapman and Hall. London, 1992.
10. Takgai, T.; Takahoshi, K.; Aizawa, M.; Mirata, S. *Procedures of the First International Conference on Intelligent Materials*. Technomic Publishing Co., Inc., Lancaster, 1993.
11. Honeybourne, C.L. *J. Phys. Chem. Solids* 1987, 48: 109.
12. Wirsen, A. *Electroactive Polymer Materials*. Technomic Publishing Co., Inc., Lancaster, 1990.
13. Walton, D.J. *Mater. Design* 1990, 11: 142.
14. Genies, E.M. *Proceedings of European Physical Society*. Industrial Workshop, Lofthus, Norway, 1990: 93.
15. Kaner, R.B.; MacDiarmid, A.G. *Scientific Am.* 1988: 60.
16. Reynolds, J.R. *Chem. Tech.* 1988, 18: 440.
17. Kanatzidis, M.G. *Chem. Eng. News* 1990: 36.

18. Skotheim, T.A. and Reynolds, J.R. *Handbook of Conducting Polymers: Conjugated Polymers Processing and Applications*, Eds. Skotheim, T. and Reynolds, J.R. (3rd edition), CRC Press, Boca Raton, 2007.
19. Kulkarni, V.G.; *Polym. Prepr. (Am. Chem. Soc., Div. Polym. Chem.)* 1998, 39 (1): 127.
20. Trevedi, D.C.; Dhawan, S.K. *Synth. Met.* 1993, 59: 267.
21. Dhawan, S.K.; Singh, D.; Venkatachalam, S. *Synth. Met.* 2001, 125: 389.
22. Kim, S.H.; Jang, S.H.; Byun, S.W.; Lee, J.Y.; Joo, J.S.; Jeong, S.H.; Park, M.-J. *J. Appl. Polym. Sci.* 2003, 87: 1969.
23. Ziemelis, K. *Nature* 1998, 393: 619.
24. Robinson, N.D. and Berggren, M. *Handbook of Conducting Polymers: Conjugated Polymers Processing and Applications*, Eds. Skotheim, T. and Reynolds, J.R. (3rd edition), CRC Press, Boca Raton, 2007: 4-1.
25. Krumm, J.; Eckert, E.; Glauert, W.H.; Ullmann, A.; Fix, W.; Clemens, W. *Electron Dev Lett IEEE* 2004, 25(6): 399.
26. Angelopoulos, M. *IBM J. Res. Dev.* 2001, 45(1): 57.
27. Angelopoulos, M.; Shaw, J.M.; Lecorre, M.A.; Tissier, M. *Microelectron. Eng.* 1991, 13: 515.
28. Irvin, J.A.; Irvin, D.J. and Stenger-Smith, J.D. *Handbook of Conducting Polymers: Conjugated Polymers Processing and Applications*, Eds. Skotheim, T. and Reynolds, J.R. (3rd edition), CRC Press, Boca Raton, 2007: 9-1.
29. Killian, J.G.; Coffey, B.M.; Gao, F.; Poehler, T.O.; Searson, P.C. *J. Electrochem. Soc.* 1996, 354: 1555.
30. Wang, C.Y.; Mottaghitalab, V.; Too, C.O.; Spinks, G.M.; Wallace, G.G. *J. Power Sources* 2007, 163: 1105.
31. Huggins, R.A. *Phil. Trans. R. Soc. London A* 1996, 354: 1555.
32. Hashimi, S.A.; Latham, R.J.; Lindford, R.G.; Schlindwein, W.S. *Ionics* 1997, 3: 177.
33. Prasad, K.R.; Munichandraiah, N. *Electrochem. Solid State Lett.* 2002, 5(12): A271.
34. Stenger-Smith, J.D.; Webber, C.K.; Anderson, N.; Chafin, A.P.; Zong, K.; Reynolds, J.R. *J. Electrochem. Soc.* 2002, 149(8): A973.
35. Gomez-Romero, P.; Chojak, M.; Cuentas-Gallegos, K.; Asensio, J.A.; Kulesza, P.J.; Casan-Pastor, N.; Lira-Cantu, M. *Electrochem. Commun.* 2003, 5: 149.
36. Huguenin, F.; Giroto, E.M.; Ruggeri, G.; Torresi, R.M. *J. Power Sources* 2003, 114: 133.
37. Wallace, G. G., Too, C. O., Officer, D. O., Dastoor, P. *Chem. Innovation* 2000, 15.
38. Mozer, A.J. and Sariciftci, N.S. *Handbook of Conducting Polymers: Conjugated Polymers Processing and Applications*, Eds. Skotheim, T. and Reynolds, J.R. (3rd edition), CRC Press, Boca Raton, 2007: 10-1.
39. Brabec, C.J.; Sariciftci, N.S.; Hummelen, J.C. *Adv. Functional Mater.* 2001, 11(1): 15.
40. Kim, Y.-G.; Walker, J.; Samuelson, L.A.; Kumar, J. *Nano Lett.* 2003, 3(4): 523.
41. Chen, J.; Officer, D.L.; Pringle, J.; MacFarlane, D.R.; Too, C.O.; Wallace, G.G. *Electrochem. Solid-State Lett.* 2005, 8(10): A528.
42. Saito, Y.; Kubo, W.; Kitamura, T.; Wada, Y.; Yanagida, S. *J. Photochem. Photobiol. A: Chem.* 2004, 164: 153.
43. Christian-Pandya, H.; Vaidyanathan, S.; Galvin, M. *Handbook of Conducting Polymers: Conjugated Polymers Processing and Applications*, Eds. Skotheim, T. and Reynolds, J.R. (3rd edition), CRC Press, Boca Raton, 2007: 5-1.
44. Hyodo, K. *Electrochim. Acta* 1994, 39: 265.
45. De Paoli, M.A.; Casalbore-Miceli, G.; Giroto, E.M.; Gazotti, W.A. *Electrochim. Acta* 1999, 44: 2983.
46. Abrissani, C.; Bongini, A.; Mastragostino, M.; Zanelli, A.; Barbarella, G.; Zambianchi, M. *Adv. Mat.* 1995, 7: 57.

47. Sapp, S.A.; Sotzing, G.R.; Reynolds, J.R. *Chem. Mat.* 1998, 10: 2101.
48. Coskun, Y.; Cirpan, A.; Toppare, L. *Polymer* 2004, 45: 4989.
49. Krishnamoorthy, K.; Ambade, A.V.; Mishra, S.P.; Kanungo, M.; Contractor, A.Q.; Kumar, A. *Polymer* 2002, 43, 6465.
50. Sonmez, G.; Sonmez, H.B.; Shen, C.K.F.; Wudl, F. *Adv. Mater.* 2004, 16(21): 1905.
51. Santos, M.J.L.; Rubira, A.F.; Pontes, R.M.; Basso, E.A.; Girotto, E.M. *J. Solid State Electrochem.* 2006, 10: 117.
52. Cutler, C.A.; Bouguettaya, M.; Kang, T.-S.; Reynolds, J.R. *Macromolecules* 2005, 38: 3068.
53. Lu, W.; Fadeev, A.G.; Qi, B.; Smela, E.; Mattes, B.R.; Ding, J.; Spinks, G.M.; Mazurkiewicz, J.; Zhou, D.; Wallace, G.G.; MacFarlane, D.R.; Forsyth, S.A.; Forsyth, M. *Science* 2002, 297: 983.
54. Lu, W.; Fadeev, A.G.; Qi, B.; Mattes, B.R. *Synth. Met.* 2003, 135–136: 139.
55. Baughman, R.H. *Synth. Met.* 1996, 78(3): 339.
56. Madden, J.D.; Schmid, B.; Hechinger, M.; Lafontaine, S.R.; Madden, P.G.; Hover, F.S.; Kimball, R.; Hunter, I.W. *IEEE J. Oceanic Eng.* 2004, 29: 738.
57. Andrews, M.K.; Jansen, M.L.; Spinks, G.M.; Zhou, D.; Wallace, G.G. *Sens. Act. A* 2004, 114: 65.
58. Wu, Y.; Zhou, D.; Spinks, G.M.; Innis, P.C.; McGill, W.M.; Wallace, G.G. *Smart Mater. Struct.* 2005, 14: 1511.
59. Ding, J.; Liu, L.; Spinks, G.M.; Zhou, D.; Wallace, G.G.; Gillespie, J. *Synth. Met.* 2003, 138: 391.
60. Gandhi, M.R.; Murray, P.; Spinks, G.M.; Wallace, G.G. *Synth. Met.* 1995, 73(3): 247.
61. Hara, S.; Zama, T.; Takashima, W.; Kaneto, K. *Smart Mater. Struct.* 2005, 14: 1501.
62. Hara, S.; Zama, T.; Takashima, W.; Kaneto, K. *J. Mater. Chem.* 2004, 14: 1516.
63. Smela, E.; Gadeguard, N. *Adv. Mater.* 1999, 11: 953.
64. Hara, S.; Zama, T.; Takashima, W.; Kaneto, K. *Synth. Met.* 2005, 149: 199.
65. Wu, Y.; Alici, G.; Spinks, G.M.; Wallace, G.G. *Synth. Met.* 2006, 156: 1017.
66. Lewis, T.; Spinks, G.M.; Wallace, G.G.; De Rossi, D.; Pachetti, M. *Polym. Preprints* 1997, 38(2): 520.
67. Zhou, D.; Spinks, G.M.; Wallace, G.G.; Tiyapiboonchaiya, C.; MacFarlane, D.R.; Sun, J. *Electrochim. Acta* 2003, 48: 2355.
68. Wang, E.; Liu, U.; Samec, Z.; Dvorak, C. *Electroanalysis* 1990, 2: 623.
69. Price, W.E.; Wallace, G.G.; Zhao, H. *J. Electroanal. Chem.* 1992, 334: 11.
70. Zhao, H.; Price, W.E.; Wallace, G.G. *Polymer* 1993, 34: 117.
71. Mirmohseni, A.; Price, W.E.; Wallace, G.G.; Zhao, H. *J. Int. Mat. Syst. Struc.* 1993, 4: 43.
72. Mirmohseni, A.; Price, W.E.; Wallace, G.G. *Polymer Gels and Networks* 1993, 1: 61.
73. Zinger, B.; Miller, L.K. *J. Am. Chem. Soc.* 1984, 106: 6861.
74. Feldheim, D.L.; Elliot, C.M.J. *Membr. Sci.* 1992, 70: 9.
75. Kamada, K.; Kamo, J.; Motonaga, A.; Iwasaki, T.; Hosokawa, H. *Polymer J.* 1994, 26: 141.
76. Anderson, M.R.; Mattes, B.J.; Reiss, H.; Kaner, R.B. *Science* 1991, 353: 1412.
77. Liang, W.; Martin, C.R. *Chem. Mater.* 1991, 3: 390.
78. Ge, H.; Teasdale, P.R.; Wallace, G.G. *J. Chrom.* 1990, 544: 305.
79. Zhou, Q.-X.; Miller, L.L.; Valentine, J.R. *J. Electroanal. Chem.* 1989, 261: 147.
80. Lin, Y.; Wallace, G.G. *Journal of Controlled Release* 1994, 30: 137.
81. Huang, H.; Liu, C.; Liu, B.; Cheng, G.; Dong, S. *Electrochim. Acta* 1998, 43(9): 999.
82. Wadhwa, R.; Lagenaur, C.F.; Cui, X.T. *J. Controlled Release* 2006, 110: 531.
83. Spinks, G.M.; Tallman, D.E.; Dominis, A.J.; Wallace, G.G. *J. Solid State Electrochem.* 2002, 6(2): 85.



84. Tallman, D.E.; Spinks, G.; Dominis, A.; Wallace, G.G. *J. Solid State Electrochem.* 2002, 6: 73.
85. Spinks, G.M.; Tallman, D.E.; Dominis, A.J.; Wallace, G.G. *J. Solid State Electrochem.* 2002, 6: 85.
86. Tallman, D.E.; Pae, Y.; Bierwagen, G.P. *Corrosion* 1999, 55(8): 779.
87. Santos, J.R.; Mattoso, L.H.C.; Motheo, A.J. *Electrochim. Acta* 1997, 43(3–4): 309.
88. Racicot, R.; Brown, R.; Yang, S.C. *Synth. Met.* 1997, 85(1–3): 1263.
89. Brusiz, V.; Angelopoulos, M.; Graham, T. *J. Electrochem. Soc.* 1997, 144(2): 436.
90. Lu, W.K.; Basak, S.; Elsenbaumer, R.L. Corrosion inhibition of metals by conductive polymers, *Handbook of Conducting Polymers*, edited by T.A. Skotheim, R.L. Elsenbaumer, and J.R. Reynolds (Marcel Dekker, New York, 1998), pp. 881–920.
91. Fahlman, M.; Jasty, S.; Epstein, A.J. *Synth. Met.* 1997, 85(1–3): 1323.
92. Tallman, D.E. and Bierwagen, G.P. *Handbook of Conducting Polymers: Conjugated Polymers Processing and Applications*, Eds. Skotheim, T. and Reynolds, J.R. (3rd edition), CRC Press, Boca Raton, 2007: 15-1.
93. Guiseppi-Elie, A.; Wallace, G.G.; Matsue, T. *Handbook of Conducting Polymers*, 2nd edition, Marcel Dekker, New York, 1998, chapter 33.
94. Adeloju, S.B.; Wallace, G.G. *Analyst* 1996, 121(8): 1147.
95. Barisci, J.N.; Conn, C.; Wallace, G.G. *Trends Polym. Sci.* 1996, 4(9): 307.
96. Imisides, M.D.; John, R.; Wallace, G.G. *Chem. Tech.* 1996, 26(5): 19.
97. Lewis, T.W.; Wallace, G.G.; Smyth, M.R. *Analyst* 1999, 124(3): 213.
98. Smyth, M.R.; Zhao, H.; Wallace, G.G. *Trends Anal. Chem.* 1999, 18(4): 245.
99. Ahuja, T.; Mir, I.A.; Kumar, D.; Rajesh, *Biomaterials* 2007, 28: 791.
100. Sugiyasu, K., and Swager, T.M. *Bull. Chem. Soc. Jap.*, 2007, 80: 2074.
101. Sadik, O.A.; Wallace, G.G. *Electoanalysis.* 1993, 5: 555.
102. Lin, Y.P.; Wallace, G.G. *J. Electroanal. Chem.* 1988, 27: 145.
103. Imisides, M.D.; Wallace, G.G. *J. Electroanal. Chem.* 1988, 246: 181.
104. Ulmana, W.; Waller, J. *Anal. Chem.* 1986, 58: 2979.
105. Lin, Y.; Wallace, G.G. *Anal. Chim. Acta* 1992, 263: 71.
106. Hammerle, M.; Schuhmann, W.; Schmidt, H.L. *Sens. Act. B* 1992, 86: 106.
107. Sadik, O.; Wallace, G.G. *Anal. Chim. Acta.* 1993, 279: 209.
108. Sadik, O.; Wallace, G.G. *Analyst* 1994, 6: 1997.
109. Guiseppi-Elli, A.; Brahim, S. and Wilson, A.M. *Handbook of Conducting Polymers: Conjugated Polymers Processing and Applications*, Eds. Skotheim, T. and Reynolds, J.R. (3rd edition), CRC Press, Boca Raton, 2007: 12-1.
110. Gardner, J.W.; Pearce, T.C.; Friel, S.; Bartlett, P.N.; Blair, N. *Sens. Act. B* 1994, 18–19: 240.
111. Partridge, A.C.; Harris, P.; Andrew, M.K. *Analyst* 1996, 121: 1349.
112. Gibson, T.D.; Prosser, O.; Hulbert, J.N.; Marshall, R.W.; Corroran, P.; Lowery, P.; Ruck-Keene, E.A.; Heron, S. *Sens. Act. B* 1997, 44: 413.
113. Barisci, J.N.; Andrews, M.K.; Partridge, A.C.; Harris, P.; Wallace, G.G. *Sens. Act. B* 2002, 84: 252.
114. Stella, R.; Serra, G.; De Rossi, D.; Barisci, J.N.; Wallace, G.G. *Sens. Act.* 2000, 63: 1.
115. Hodgson, A.J.; Spencer, M.J.; Wallace, G.G. *React. Polym.* 1992, 18: 77.
116. Hodgson, A.J.; Gilmore, K.; MacKenzie, I.; Wallace, G.G.; Ogata, N.; Aoki, T. *Proc. ACS Div. Polym. Mater. Sci. Eng.* ACS, 1993, 216.
117. Hodgson, A.J.; Gilmore, K.J.; Small, C.; Wallace, G.G.; MacKenzie, I.; Ogata, N.; Aoki, T. *Supramol. Sci.* 1994, 1: 77.
118. Schmidt, C.E.; Shastri, V.R.; Vacanti, J.P.; Langer, R. *Proc. Natl. Acad. Sci. USA* 1997, 94: 8948.
119. Garner, B.; Hodgson, A.J.; Wallace, G.G.; Underwood, P.A. *J. Mat. Sci.* 1999, 10: 19.
120. Kotwal, A.; Schmidt, C.E. *Biomat.* 2001, 22: 1055.

121. Cui, X.; Lee, V.A.; Raphael, Y.; Wiler, J.A.; Hetke, J.F.; Anderson, D.J.; Martin, D.C. *Biomed. Mater. Res.* 2001, 56: 261.
122. Di Giglio, E.; Sabbatini, L.; Colucci, S.; Zambonin, G. *J. Biomat. Sci. Polymer Edn.* 2000, 11: 1073.
123. Innis, P.C.; Moulton, S.E.; Wallace, G.G. *Handbook of Conducting Polymers: Conjugated Polymers Processing and Applications*, Eds. Skotheim, T. and Reynolds, J.R. (3rd edition), CRC Press, Boca Raton, 2007: 11-1.
124. Thompson, B.C.; Moulton, S.E.; Ding, J.; Richardson, R.; Cameron, A.; O'Leary, S.; Clark, G.M.; Wallace, G.G. *J. Controlled Release* 2006, 116: 285.
125. Richardson, R.T.; Thompson, B.; Moulton, S.; Newbold, C.; Lum, M.G.; Cameron, A.; Kapsa, R.; Clark, G.; O'Leary, S.; Wallace, G.G. *Biomaterials* 2007, 28: 513.
126. Zhou, D.; Wallace, G.G.; Spinks, G.M.; Liu, L.; Cowan, R.; Saunders, E.; Newbold, C. *Synth. Met.* 2003, 135: 39.
127. Smela, E. *Advanced Materials* 2003, 15: 481.
128. Immerstrand, C., Holmgren-Peterson, K., Magnusson, K.-E., Jager, E., Krogh, Skoglund, M., Selbing, A. and Ingnas, O., *MRS Bulletin*, 2002, June: 461.
129. Jager, E.W.H.; Smela, E.; Ingnas, O. *Science* 2000, 290: 1540.
130. Hsu, T.-R. *MEMS and Microsystems: Design and Manufacture*, 1st ed. Boston: McGraw Hill, 2002.
131. Spinks, G.M. and Smela, E. *Handbook of Conducting Polymers: Conjugated Polymers Processing and Applications*, Eds. Skotheim, T. and Reynolds, J.R. (3rd edition), CRC Press, Boca Raton, 2007: 14-1.
132. Jager, E.W.H.; Ingnas, O.; Lundstrom, I. *Science* 2000, 288: 2335.
133. McGovern, S.T.; Spinks, G.M.; Wallace, G.G. *Sens. Act. B: Chem.* 2005, B107: 657.
134. Lee, S.-K.; Lee, S.-J.; An, H.-J.; Cha, S.-E.; Chang, J.K.; Kim, B.; Pak, J.J. Presented at Smart Structures and Materials, Electroactive Polymer Actuators and Devices, San Diego, CA, 2002.
135. Berdichevsky, Y.; Lo, Y.-H. Presented at Mat. Res. Soc. Symp. Fall 2003 Meeting, Boston, 2003.
136. Pettersson, P.F.; Jager, E.W.H.; Ingnäs, O. Presented at IEEE-EMBS Special Topic Conference on Microtechnologies in Medicine & Biology, Lyon, France, 2000.
137. Zhao, B.; Moore, J.S.; Beebe, D.J. *Anal. Chem.* 2002, 74: 4259.
138. Someya, T.; Dodabalapur, A.; Gelperin, A.; Katz, H.E.; Bao, Z. *Langmuir* 2002, 18: 5299.
139. Isaksson, J.; Tengstedt, C.; Fahlman, M.; Robinson, N.; Berggren, M. *Adv. Mater.* 2004, 16: 316.
140. Causley, J.; Stitzel, S.; Brady, S.; Diamond, D.; Wallace, G. *Synth. Met.* 2005, 151: 60.
141. Martin, C.R.; Penner, R.M.; van Dyke, L.S. *In Functional Polymers*. Bergbreker, D.E. (Ed.). Plenum Press, New York, 1989.
142. Heinze, J.; Dietrich, M. *Mat. Sci. Forum* 1989, 42: 63.
143. Doblhofer, K. and Rajeshwar, K. Electrochemistry of conducting polymers, in *Handbook of Conducting Polymers*, edited by Terje A. Skotheim, Ronald L. Elsenbaumer, and John R. Reynolds (Marcel Dekker, New York, 1997), pp. 531–588.
144. Buttry, D.A. *J. Electroanal. Chem.* 1990, 17: 1.
145. Deakin, M.R.; Buttry, D.A. *Anal. Chem.* 1989, 61: 1147.
146. Fletcher, S.; John, R.; Talaie, A.; Wallace, G.G. *J. Electroanal. Chem.* 1991, 319: 365.
147. Talaie, A.; Wallace, G.G. *Mat. Sci. Forum* 1995, 185: 189.
148. Pei, Q.; Ingnas, O. *J. Phys. Chem.* 1992, 96: 10507.
149. Pei, Q.; Ingnas, O. *J. Phys. Chem.* 1993, 97: 6034.
150. John, R.; Mirmohseni, R.; Teasdale, P.R.; Wallace, G.G. *TrAC* 1993, 12: 94.
151. Johnson, E.L.; Stevenson, R. *Basic Liquid Chromatography*. Varian, California, 1978.
152. Chehimi, M.M.; Pigois-Landurea, E.; Delamar, M. *J. Chim. Phys.* 1992, 81: 1173.

153. Chehimi, M.M.; Abel, M.L.; Pigois-Landurea, E.; Delamar, M. *Synth. Met.* 1993, 60: 183.
154. Andrade, J.D. (Ed.). *Polymer Surface Dynamics*. Plenum Press, New York, 1987.
155. Kendig, M.; Addison, R.; Jean Jaquet, S. *J. Electrochem. Soc.* 1990, 137: 2690.
156. Teasdale, P.R.; Wallace, G.G. *React. Polymer* 1995, 24: 157.
157. Bining, G.; Rohrer, H.; Gerber, C.; Weibel, E. *Phys. Rev. Lett.* 1982, 49: 57.
158. Barisci, J.N.; Stella, R.; Spinks, G.M.; Wallace, G.G. *Electrochim. Acta* 2000, 46: 519.
159. Barisci, J.N.; Stella, R.; Spinks, G.M.; Wallace, G.G. *Synth. Met.* 2001, 124: 407.
160. Otero, T.F.; Beneochea, M. *Langmuir* 1999, 5: 1323.
161. Chainet, E.; Billon, M. *J. Electroanal. Chem.* 1998, 451(1–2): 273.
162. Albuquerque, J.E.; Mattoso, L.H.C.; Balogh, D.T.; Faria, R.M.; Masters, J.G.; MacDiarmid, A.G. *Synth. Met.* 2000, 113: 19.
163. Xia, Y.; Wiesinger, J.M.; MacDiarmid, A.G.; Epstein, A.J. *Chem. Mater.* 1995, 7: 443.
164. Avlyanov, J.K.; Min, Y.; MacDiarmid, A.G.; Epstein, A.J. *Synth. Met.* 1995, 72: 65.
165. Kuzmany, H.; Sariciftci, N.S. *Synth. Met.* 1987, 18: 353.
166. Koziel, K.; Lapkowski, M.; Lefrant, S. *Synth. Met.* 1995, 69: 137.
167. Rapta, P.; Dunsch, A.P.L. *Synth. Met.* 2001, 119: 409.
168. Okamoto, H.; Kotaka, T. *Polymer* 1998, 39: 4349.
169. Zimmermann, A.; Künzelmann, U.; Dunsch, L. *Synth. Met.* 1998, 93: 17.
170. Ansari, R.; Wallace, G.G. *Polymer* 1994, 35(11): 2372.
171. Pud, A.A. *Synth. Met.* 1994, 66(1): 1.
172. Lewis, T.W.; Spinks, G.M.; Wallace, G.G.; Mazzoldi, A.; DeRossi, D. *Synth. Met.* 2001, 122(2): 379.
173. Crowley, K.; Cassidy, J. *J. Electroanal. Chem.* 2003, 547: 75.
174. Quillard, S.; Louarn, G.; Lefrant, S.; MacDiarmid, A.G. *Physical Review B* 1994, 50: 12496.
175. Pereira da Silva, J.E.; de Faria, D.L.A.; Cordoba de Torresi, S.I.; Temperini, M.L.A. *Macromolecules* 2000, 33: 3077.
176. Lapkowski, M.; Berrada, K.; Quillard, S.; Louarn, G.; Lefrant, S.; Pron, A. *Macromolecules* 1995, 28: 1233.
177. Neudeck, A.; Dunsch, A.P.L. *Synth. Met.* 1999, 107: 143.
178. Kahol, P.K.; Dyakonov, A.J.; McCormick, B.J. *Synth. Met.* 1997, 89: 17.
179. Rapta, P.; Dunsch, L. *Synth. Met.* 2001, 119: 409; and references cited therein.
180. Streeter, I.; Wain, A.J.; Thompson, M.; Compton, R.G. *J. Phys. Chem. B* 2005, 109: 12636; and references cited therein.
181. He, J.; Gelling, V.J.; Tallman, D.E.; Bierwagen, G.P. *Abstr. Pap.—Am. Chem. Soc.* 2000, 220th, OLY: 201.

---

## 2 Assembly of Polypyrroles

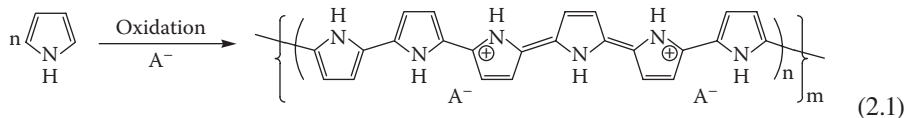
Stability and homogeneity of materials were formerly viewed as desirable properties by scientists. Any modifications made to such materials required ingenious and complex chemical processes. Although these properties will always have a place in structural components, a new generation of materials have been discovered by scientists that are defined by their heterogeneity and dynamic properties. As can be concluded from studying natural materials and reactions, which have evolved to a level of complexity and diversity using simple building blocks, the capability to change in response to their environment is a powerful one. We now strive to recreate such sophisticated behavior using conducting polymers as simple building blocks.

Polypyrroles (PPy's) are formed by the oxidation of pyrrole or substituted pyrrole monomers. In the vast majority of cases, these oxidations have been carried out by either (1) electropolymerization at a conductive substrate (electrode) through the application of an external potential or (2) chemical polymerization in solution by the use of a chemical oxidant. Photochemically initiated and enzyme-catalyzed polymerization routes have also been described but are less developed. These various approaches produce polypyrrole (PPy) materials with different forms—chemical oxidations generally produce powders, whereas electrochemical synthesis leads to films deposited on the working electrode, and enzymatic polymerization gives aqueous dispersions. The conducting polymer products also possess different chemical/electrical properties. These alternative routes to PPy's are therefore discussed separately in this chapter.

This chapter deals with the creation of conducting PPy's, including the parameters that are important in affecting the polymerization process. Chapter 3 discusses how these synthesis parameters influence the polymer properties.

### **ELECTROPOLYMERIZATION—“A COMPLEX PROCESS OVERSIMPLIFIED”**

PPy can be formed by the oxidation of pyrrole at a suitable anode. Upon application of a positive potential, an insoluble, conducting polymeric material is deposited at the anode. The polymerization reaction can be represented simply as:



[ $m$  relates to the polymer chain length, which determines molecular weight].

In this representation (Equation 2.1),  $A^-$  is a counterion necessary to balance the charge on the polymer backbone. The counterion content is high (can be greater than 50% w/w) and is usually incorporated between the PPy planes<sup>1</sup> that are predominantly  $\alpha$ - $\alpha$  bonded<sup>2</sup> (as shown). In an "ideal" PPy (Figure 2.1), it is assumed that the geometry is such that the counterion is intercalated between the planar polymer chains.<sup>2</sup> In real materials, this idealized structure must be distorted somewhat because highly insoluble and highly crosslinked materials are formed.<sup>3</sup> The molecular structure of PPy is further described later in this chapter.

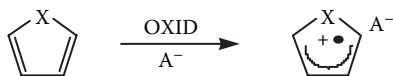
The simplistic polymerization process (Equation 2.1) and the idealized structure (Figure 2.1) both belie the complexity of this polymerization process.<sup>4</sup> A greater understanding of this process has led to the development of innovative processing approaches in recent years. As pointed out in the introduction, intelligent material structures require a dynamic character. This dynamic, interactive nature is present right from the point when polymer synthesis is initiated; hence, the assembly of these materials is not as straightforward as illustrated in Equation 2.1. The first step (monomer oxidation) is slow<sup>5</sup>; the radical-radical coupling, deprotonation, and subsequent oxidation are fast. Polymerization is believed to proceed via a radical-radical coupling mechanism,<sup>6</sup> wherein the natural repulsion of the radicals is assumed to be negated by the solvent, the counterion, and even the monomer. Chain growth then continues until the charge on the chain is such that a counterion is incorporated. Eventually, as the polymer chain exceeds a critical length, the solubility limit is exceeded, and the polymer precipitates on the electrode surface.

A major point of contention involves where radical-radical coupling occurs and whether continued growth is in solution or from the electrode surface. At least some polymerization occurs in solution,<sup>7</sup> but how much depends on the experimental conditions employed. This polymer then interacts with the bare electrode or previously deposited polymer as the reaction proceeds to produce the final structure.

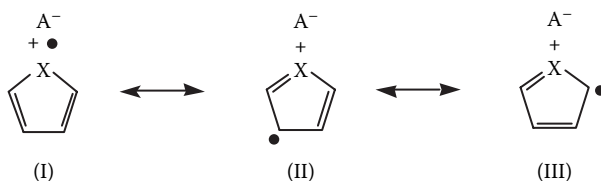
Once the initial layer of PPy is deposited, it becomes a reactant that determines the course of the remainder of the polymerization process. Polymerization occurs more readily (at a lower potential) on the already-deposited PPy than on the anode surface. This process of product becoming reactant continues until the reaction is stopped. A more detailed investigation of the polymerization process reveals the intricacies involved in producing these sophisticated dynamic structures. Thus, the overall process may be broken into several discrete steps, as shown in Figure 2.1 (details are available in Reference 4).

The electrochemical conditions, electrode material, solvent, counterion, and monomer all influence the nature of the processes occurring. For example, if the applied potential is too low (under certain conditions), the rate of polymerization will be such that no precipitate forms. If the solvent is nucleophilic (or contains

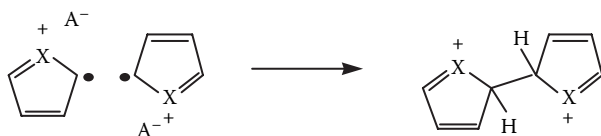
**Step 1. Monomer Oxidation**



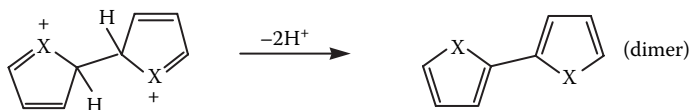
*Resonance forms:*



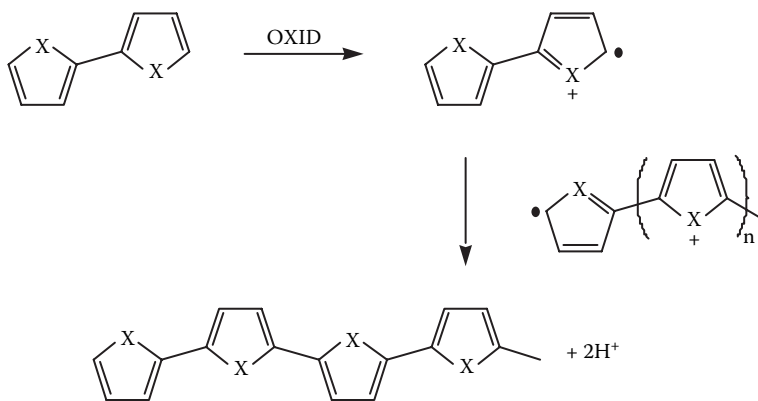
**Step 2. Radical-Radical Coupling**



**Step 3. Deprotonation/Re-Aromatization**



**Step 4. Chain Propagation**



**FIGURE 2.1** A more detailed look at PPy formation.

dissolved oxygen), it will react with the free-radical intermediates. If the electrode material is extremely polar, at the potential required for polymerization, deposition may be discouraged. In addition, the solvent, monomer, counterion, and substrate interactions are all important because they dictate the solubility and/or deposition of the resultant polymer.

Another issue arising from closer examination of the mechanism is the question of what actually controls the rate of polymerization, and hence, the structure of the polymer. Again, all the parameters mentioned earlier play a role in determining the overall rate of reaction.<sup>8</sup> The complexity arises because the role that each plays varies depending on the stage of polymerization. For example, in the initial stages of polymerization, the electrode substrate plays a critical role that diminishes once the reaction is initiated. On the other hand, the monomer may be present in excess when the reaction is initiated, but due to depletion, it may become the rate-determining factor as the reaction proceeds.

With respect to the rate-determining step, the electrochemical reactions occurring at the cathode cannot be ignored. Particularly in a two-electrode cell, this electrochemical step may become the rate-determining factor. This is the case, for example, when reduction of water is the cathodic reaction. Reactions occurring at the auxiliary electrode (the cathode) in Figure 2.2 are usually assumed to involve reduction of the supporting electrolyte cation, dissolved oxygen, or solvent itself, unless an auxiliary reagent such as an electroactive metal ion or ferricyanide is intentionally added. The auxiliary electrode reaction will then consume this additive.

The hydrodynamics of the electrochemical system and temperature are also important because these control the rate of transport of reactants and products to and from the electrochemical reaction zone. This in turn determines the polymerization efficiency. Hydrodynamics are also important in determining the form of the PPy produced. For example, using a flow-through cell and in appropriate chemical envi-

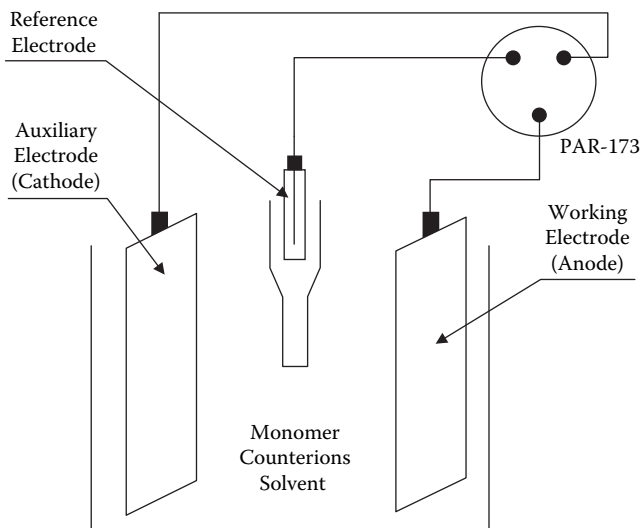


FIGURE 2.2 The three-electrode electropolymerization cell.

ronments, stable colloidal dispersions rather than insoluble films can be produced (see section titled “The Polymerization Environment/Cell Design”).

Aspects of polymerization efficiency have been studied previously<sup>9</sup> using electrochemical quartz crystal microbalance techniques, which allow the amount of polymer deposited to be weighed *in situ*. This is achieved by depositing polymer on a gold-coated quartz crystal whose oscillating frequency is continually monitored (see Chapter 1). The change in frequency can then be related to the change in mass and plots of charge ( $Q$ ) versus mass obtained. These workers found that the efficiency was low in the early stages of polymerization and then increased to a constant level. They also found that the final electrolytic efficiency decreased as the monomer concentration decreased, and varied depending on the electrolyte/solvent combination employed. In a sense, the electrode acts as a product collection device, interacting with appropriate components of the polymerization process. These results emphasize the competitive nature of the electrodeposition process and the fact that the polymer forms first in solution and then deposits onto the working electrode. Given the complexity of the polymerization process, each of the experimental properties that control it will now be considered, in turn.

## THE POLYMERIZATION ENVIRONMENT/CELL DESIGN

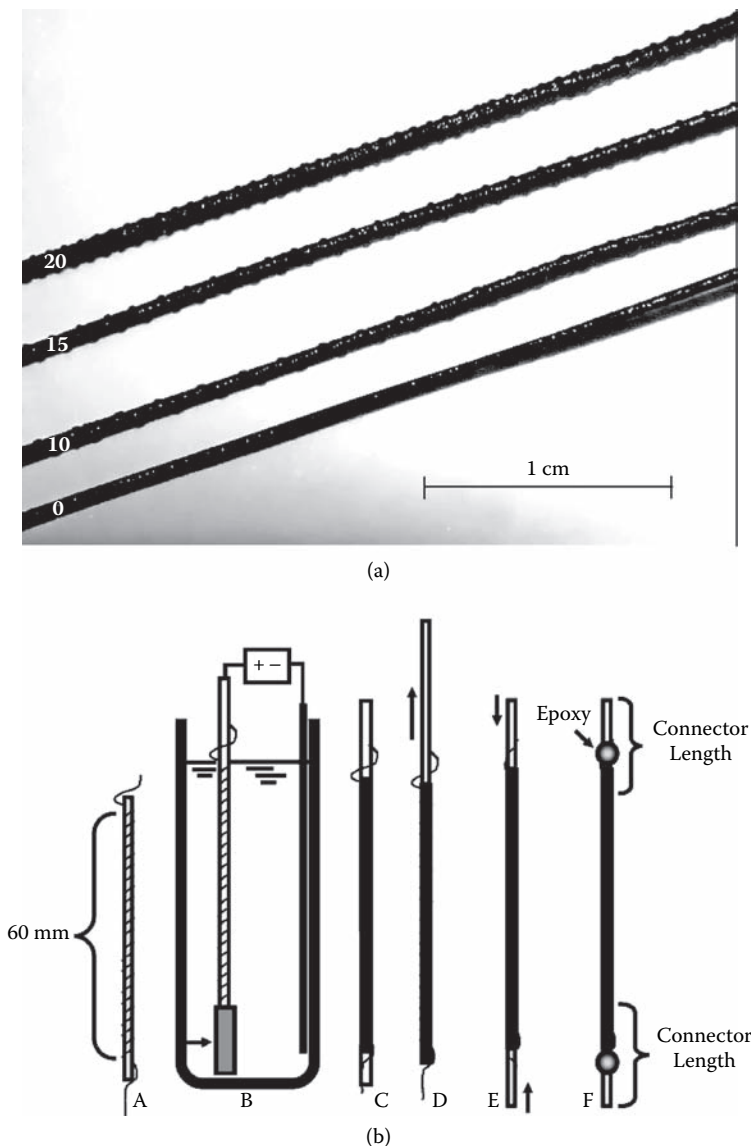
Although the setup required to induce electropolymerization is simple (Figure 2.2), the setup required to deliver a product of the necessary quality for real applications requires some thought and is still the subject of numerous studies. For example, in our own work,<sup>10</sup> we have found that the use of concentric counter electrodes is essential to coat wire electrodes in a uniform fashion. In more recent work,<sup>11</sup> we have verified the need for a helical wire interconnect to ensure efficient charge injection into hollow PPy fibers of micrometer dimensions but centimeters in length (Figure 2.3).

Most laboratory setups employ a three-electrode potentiostated system to ensure effective potential control and to maximize the reproducibility of the polymerization process. The positioning of the auxiliary electrode is critical in that it determines the electrical field generated, which can influence the quality and evenness of the polymer deposited. The electrode system shown in Figure 2.2 includes a reference electrode. A two-electrode cell can also be used, usually with galvanostatic (constant current) electropolymerization methods, but care must be taken to avoid overoxidation of the PPy through poor control of the potential.

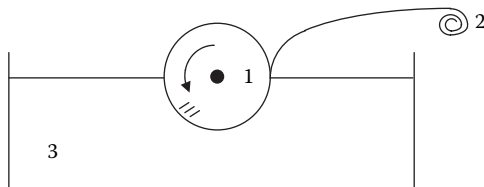
Two major considerations accentuated by the nature of conducting polymer synthesis are  $iR$  drop effects and the hydrodynamics of the cell. As polymer is deposited on the anode, the resistance of the electrode (substrate and polymer) usually increases. The cell hydrodynamics, importantly, regulate the movement of reactants (monomer/lower-molecular weight oligomers) and products (higher-molecular-weight oligomers and polymers) to/from the electrode. During growth, variations on the order of millivolts or slight changes in the hydrodynamics of the system may have a dramatic influence on the polymer produced.

With respect to cell design, the working electrode geometry, the anode–cathode separation, and the nature of the working electrode all influence the nature of the polymer formed. The use of a thermostated cell is essential for manufacturing





**FIGURE 2.3** Photographs (A) of hollow polymer tubes with helical interconnect used for actuation testing. The pitch of the helix can be altered with examples shown in (A) of 20, 15, and 10 turns/cm. A hollow tube with no helix (0 turns/cm) is also shown. Schematic diagram (B) showing method of construction for these actuators. (A) 25  $\mu\text{m}$  platinum wire is wrapped around the 125  $\mu\text{m}$  wire as a spiral; (B) Polymer synthesis—the assembly is placed in polymer electrolyte solution (0.5 M Py, 0.25 M TBA  $\text{PF}_6$  in propylene carbonate) and electroplated for 24 h at  $-28^\circ\text{C}$ ; (B) Polymer coating forms around wire and spiral; (C) 125  $\mu\text{m}$  center wire is withdrawn from the polymer tube/helix; (D) Two short connectors of 125  $\mu\text{m}$  wire are inserted into each end; (E) 25  $\mu\text{m}$  wire is pulled tight around these ends for a good electrical connection and epoxy-glued (F) to hold it in place.



**FIGURE 2.4** Rotary drum anode (1) used for continuous production of CEP polymer tape on collector roller (2), which is continuously stripped from anode as it is deposited from the electropolymerization bath (3).

polymers in a reproducible fashion. Given the chemical steps involved in the polymerization process, the hydrodynamics and temperature control of the cell design are important. Not only does the temperature influence the rates of transport in the cell but it is also important in determining the extent to which unwanted side reactions occur. For example, it is known that the radicals generated during polymerization can react with oxygen to form an inferior product. At higher temperatures, such reactions would proceed more rapidly. Several workers<sup>12</sup> have shown that polymers with higher conductivity are produced from polymerizations carried out at low temperature. In our own work, temperatures as low as  $-28^{\circ}\text{C}$ , using propylene carbonate (PC) as solvent, have been necessary to achieve optimal polymer conductivity.

The transport of reactants and products to and from the reaction zone is extremely dependent on the cell hydrodynamics and on whether the solution is stationary or moving. Products generated at the auxiliary electrode may also be critical, and for this reason, the auxiliary electrode should be separated or placed downstream.

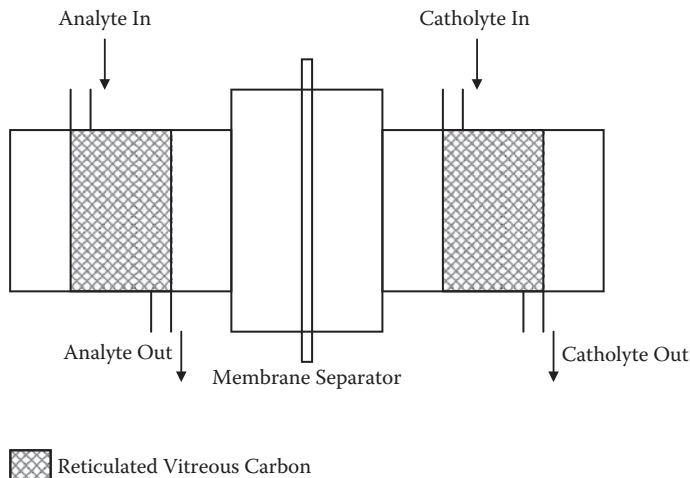
Continuous processing using electrodeposition requires that

- A mechanically stable and conductive polymer be deposited
- The polymer be continuously removed from the electrochemical cell

Continuous processing cells have been described previously by Naarmann.<sup>13</sup> The most popular approach involves the use of a rotated drum electrode. Polymer is electrodeposited onto the electrode as it passes through the cell and then continuously stripped from the electrode as it rotates out of the cell (Figure 2.4).

In our own laboratories,<sup>14</sup> we have used the fact the polymerization occurs in solution to develop a flow-through electrochemical cell (Figure 2.5) to produce colloids<sup>15,16,17,18</sup> or water-soluble<sup>19,20,21</sup> CEPs continuously. The use of a highly porous anode (reticulated vitreous carbon—RVC) ensures that a high surface area is available for electropolymerization and that a flowing solution can be used to prevent polymer deposition. The use of steric stabilizers (such as polyethylene oxide or polyvinylalcohol) in the flow-through electrolyte (see use of stabilizers—under “Chemical Polymerization”) also helps prevent deposition and promotes colloid formation. Both PPy and polyaniline (PAN) colloids have been prepared using this approach.

The beauty of this electrochemical approach to production of colloids is that a range of dopants ( $\text{A}^-$ ) can be incorporated into the polymer. For example, functional dopants such as corrosion inhibitors,<sup>15</sup> proteins,<sup>16</sup> and polyelectrolytes<sup>17</sup> have been incorporated. Even dopants that produce chiral activity within the conducting poly-



**FIGURE 2.5** A flow-through electrochemical cell.

mer colloid have been successfully incorporated.<sup>18</sup> This approach can also be used to produce novel nanocomposite structures. For example, a conducting polymer layer has been coated onto nanosized polyurethane.<sup>22,23</sup>

Other workers<sup>24</sup> have used similar principles to enable continuous production of conducting polymer fibers in a flow-through electrochemical cell. As with the hydrodynamic system described in the preceding text, polymer is produced at the anode and continuously removed from the cell in the form of a fiber. Alternatively, other fibers such as Kevlar<sup>®</sup> or nylon can be coated using such hydrodynamically controlled polymerization systems.

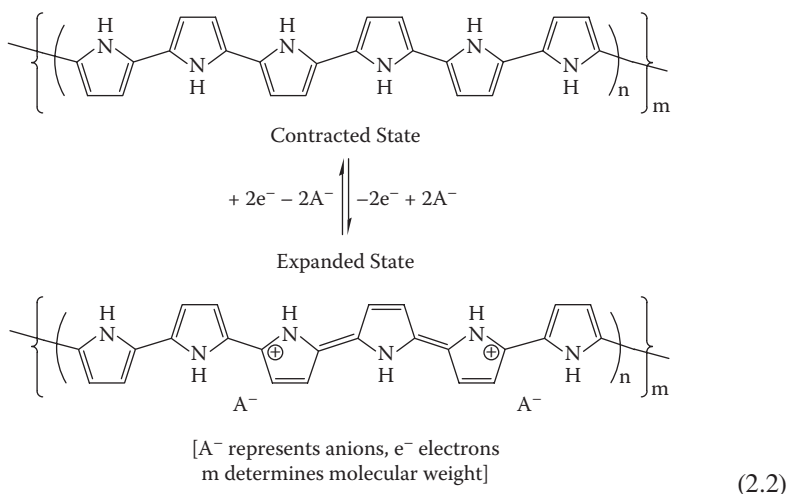
The hydrodynamic aspects of cell design have been studied using a rotating electrode setup.<sup>25</sup> As the electrode rotation speed is increased, the potential required to sustain constant-current deposition increases. The hydrodynamics increase the rate of oligomer transport away from the electrode and therefore prevent polymer deposition.

## ELECTROCHEMICAL CONDITIONS

The simplest means of inducing the polymerization process is to apply a sufficiently positive constant potential. The potential chosen will influence the rate of oxidation and, therefore, polymerization. If the rate of polymerization is too slow, oxidation of the pyrrole monomer may occur without deposition, because the critical chain length may not be reached, and hence, the solubility will not be exceeded before the products leave the reaction zone near the electrode surface. However, the upper value of the potential is limited by a process that results in overoxidation of the polymer. This results in a less conductive and more porous polymer product<sup>26,27</sup> with inferior mechanical properties. In general, because of the heterogeneity of electrode substrates (see later text), constant potential growth does not result in even coatings on electrode surfaces. In addition, constant potential growth is sensitive to  $iR$  drop effects. As the polymer is deposited, electrode resistance ( $R$ ) increases and the effective potential drops, thereby changing the growth characteristics of the polymer.

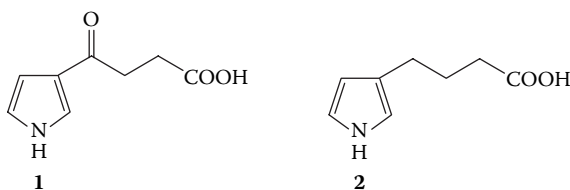
An alternative is to apply a constant current to drive the reaction. This usually results in more even film growth although local variations in current density will produce a heterogeneous polymer. The rate of polymerization is dictated by the current density applied. Again, if the rate is too low, oxidation without deposition may occur. However, if the rate is too high, the potential may stray into the region where overoxidation of the polymer occurs.

Finally, transient potential/current waveforms may be used for polymerization. Cyclic voltammetric growth has mostly been used to carry out mechanistic studies. The use of pulsed current or potential is not a common practice. Recently, however, pulsed-current methods<sup>28,29</sup> have been used by Mitchell and coworkers to produce more ordered anisotropic films. The use of transient waveforms adds another dimension to electropolymer growth, because the oxidation/reduction of the polymer according to Equation 2.2 will occur during growth, and the effect of this on the polymerization process must be considered.

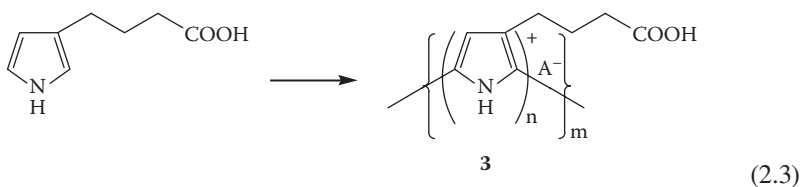


In fact it is this oxidation/reduction process that results in the more ordered structure obtained by Mitchell and coworkers. They postulate that deposition will be regulated by the oxidation/reduction process.

Transient waveforms can also be used to modify the monomer prior to polymerization *in situ*. For example, the polymerization of monomer **1** does not proceed if a constant positive potential is applied.



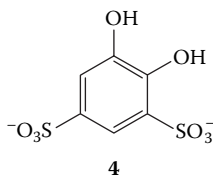
However, when a transient waveform is used, reduction of monomer **1** to form **2** can occur at negative potentials. The polymerization of **2** proceeds according to Equation 2.3 as the working electrode is exposed to more positive potentials.<sup>30</sup>



### ELECTRODE MATERIALS

The electrode substrate should be considered an integral part of the polymer production process,<sup>31,32,33</sup> particularly in the initial stages of growth. The nature of the electrode material determines how easily the pyrrole monomer can be oxidized. It also determines the degree of adsorption of the monomer, the oligomers, and finally, the polymer that occurs during polymerization. Whether or not deposition occurs depends on the surface energy of the electrode and controls the hydrophobic/hydrophilic nature of the deposited polymer. It has been postulated that some oxide-containing electrodes undergo covalent-bonding reactions with the polymer to form an extremely adherent film.<sup>34</sup> It is possible to use electrodes as templates to produce nanostructured electrodeposits (see later section on nanostructured PPy).

It is known that deposition on substrates where nonconductive metal oxide layers are formed at positive potentials is difficult. This includes electrodes made of stainless steel, tantalum, and aluminum. However, the rate of oxide formation is important because we have shown that stainless steel is an ideal substrate for deposition of some PPy's. The rate of oxide formation depends on the solution and the electrochemical conditions employed. If the polymer can deposit before the onset of metal oxide formation, then consistent films of excellent quality can be deposited. This is aptly demonstrated with the successful electrocoating of aluminum when the electrocatalyst Tiron **4** is used.



The Tiron mediates the monomer/oligomer oxidation process resulting in a significant decrease in the polymerization potential. Tiron does also interact with aluminum and may assist in binding the polymer product to the surface.

Other workers have shown that the use of specific dopants to assist in rapid deposition and/or metal passivation of active metals can help in this regard. For example, oxalic acid<sup>35</sup> or molybdate<sup>36</sup> containing electrolytes have been used to facilitate

electrodeposition of PPy on Al. Others have used ammonium oxalate electrolyte to facilitate the coating of nickel-plated copper.<sup>37</sup>

The adhesion of the polymer to the electrode surface is another consideration. For example, the polymer can be generated at an electrode such as tantalum, where it will not deposit. In our laboratories<sup>38</sup> we have used the fact that deposition of PPy onto tantalum is difficult in the design of an electrochemical slurry cell to coat silica particles. The polymer generated at the tantalum anode does not deposit there; instead, it deposits on the more receptive (silica particle) surfaces in the electrochemical cell. This represents a unique polymerization process whereby the polymer is generated electrochemically in an environment that allows nonconductive substrates to be coated, resulting in unique composite structures.

An interesting result obtained recently shows that the substrate employed may dictate the surface (polymer/solution) properties of even relatively thick polymers.<sup>39</sup> For example, with polymers grown from dodecyl sulfate (DS)-containing electrolytes, the nature of the substrate used dictated the hydrophobicity/hydrophilicity of the conducting polymer–solution interface. Polymers grown on a carbon-foil substrate shown to be hydrophobic produced a more hydrophilic polymer surface. Finally, those grown on platinum, a more hydrophilic substrate, produce a more hydrophobic polymer.

These results indicate that the surfactant counterion is capable of imparting either hydrophobic or hydrophilic properties to the polymer, depending on the substrate material. This may be due to a different orientation of the surfactant counterion within the polymer for each substrate. Because the carbon foil has a much more hydrophobic surface, the surfactant counterions could be expected to align themselves more, with the nonpolar end toward the substrate and the charged end toward the solution on the carbon-foil material. This would explain the difference in surface interactions between the polymers on these two substrates.

The size of the working electrode is also important. This will influence the electropolymerization process in that the conductivity decrease during deposition can be minimized; also, depletion effects are more pronounced with large electrodes. With smaller (< 20  $\mu\text{m}$  diameter) electrodes, electropolymerization can be carried out in low-conductivity media; also, the rate of transport to and from the electroactive center is markedly enhanced. In some cases, this latter feature can be a problem in that the enhanced rate of transport away from the microelectrode causes increased difficulty in obtaining a polymer deposit.

The *auxiliary electrode* used is usually electrochemically inert, yet capable of maintaining rapid cathodic reactions to maintain the desired polymerization rate at the working electrode surface. During deposition at anodic potentials, the auxiliary electrode is exposed to (sometimes extreme) negative potentials. The increase in pH (due to the reduction of dissolved oxygen in the solution and to the reduction of water itself) may interfere with the polymerization process; hence, the positioning of the auxiliary electrode is of paramount importance. To prevent an increase in pH, easily reduced species such as copper or silver salts may be added. This provides a more facile electrode reaction at the cathode and prevents electrode reactions that result in a change in pH.

When cyclic voltammetric growth or pulsed-potential deposition is used, the behavior of the auxiliary electrode at anodic potentials is also important because

exposure to extreme positive potentials may occur. If easily oxidized (e.g., stainless steel), the release of metal ions into solution can interfere with the polymerization process at the anode. Alternatively, generation of products from water oxidation or organic solvent oxidation can cause problems. This again emphasizes the need to control the reactions occurring at the auxiliary electrode.

## THE SOLVENT

Given that some of the solvent becomes an integral part of the final product and participates in the auxiliary electrode reaction, it is more than just a reaction medium. It is a reactant and should be considered as such. The solvent will also have an effect in determining the conformational nature of the polymer. This effect is analogous to that observed with other macromolecules, such as proteins, that can fold in aqueous solution to protect their hydrophobic groups but unfold in more nonpolar solvents to expose the hydrophobic groups. The choice of solvent is critical, and its role should be considered in light of the detailed polymerization mechanism.

Obviously, the solvent should be as pure as possible. Even the presence of dissolved oxygen may pose problems as it reacts with radical intermediates and is reduced at the auxiliary electrode to form hydroxide during the polymerization process. There is a major attraction in the use of pyrrole over other heterocyclics because this monomer is water soluble. Aqueous solvents are preferred to organic solvents from the point of view of cost, ease of handling, safety, and the range of counterions that can be used.

The solvent should, of course, be capable of dissolving the monomer and counterion at appropriate concentrations, and it should not decompose at potentials required for polymerization. If the products of such decomposition reactions are innocuous, no problems should arise. However, other reagents (e.g., metal ions) can be added to control the auxiliary electrode reaction if necessary, as described earlier.

The interaction of the solvent with the electrode, substrate, monomer, and counterion should also be considered. Even before a potential is applied, it is these interactions that will determine the conditions within the electroreaction zone because the degree of adsorption of the monomer and counterion will be solvent dependent. As the electropolymerization reaction proceeds, the nature of the solvent will also determine the solubility of the resultant polymer. Somewhat independently, the nature of the solvent will control the extent of interaction of these products with the electrode.

The nucleophilicity of the solvent is also important<sup>40</sup> because a more nucleophilic solvent is likely to react with the free-radical intermediates. Dong and Ding<sup>41</sup> suggest that PPy grown electrochemically in aqueous solvent reacts with water molecules to produce carboxyl groups that inhibit further growth. However, the importance of water molecules in hydrating the polymer has also been discussed.<sup>42</sup> These workers have shown that with an optimal amount of water (2–4% in the polymer, or one water molecule for every five to ten pyrrole rings), the water appears to participate in a favorable way in the redox reaction—decreasing the activation barrier. Interestingly, drying the polymer at 40°C for 2–3 h reduces the water content to this level, and it is extremely difficult to dry any further. With some polymeric systems, we have recently found<sup>43</sup> that thin layers of polymer contain large percentages of water (see

later under “The Counterion/Cation Effect”). Interestingly, when dehydrated and then exposed to moisture, the polymers exhibit hygroscopic properties, rapidly reabsorbing water from the atmosphere. In addition, the counterions incorporated during polymerization may have solvent molecules associated with them. In the case where water is the solvent, hydrated counterions and/or cations will be incorporated.

In the case of acetonitrile solvent, where the solvation of anions is unlikely to occur, pyrrole can solvate anions itself.<sup>44</sup> This may explain why PPy films formed from acetonitrile with perchlorate counterions are less porous; with pyrrole solvating the counterion during synthesis, a denser structure would be expected. This also results in polymers that are more conductive and have lower capacitance and greater electrochemical reversibility than those grown from water. Similar differences in conductivity were observed between acetonitrile and water when DS was used as the counterion,<sup>45</sup> although the differences in conductivity were not so marked. The presence of DS probably provides some protection from the nucleophilic solvent. In other work,<sup>46</sup> we have shown that pyrrole can be reversibly oxidized in surfactant-containing media (i.e., the surfactant stabilizes the free radical produced). This reversibility could not be detected in the absence of surfactants.

The use of specific solvents that stabilize  $\pi$  segments along the polymer chain give rise to increased conductivity and stability of PPy. Propylene carbonate has proved to be a useful solvent in this regard.<sup>47</sup> This will influence subsequent polymerization processes, as the deposition of a more conductive polymer leads to more efficient electrochemistry as the polymerization proceeds.

More recently, the use of ionic liquid (IL) electrolytes (Figure 2.6) to prepare conducting polymers has been investigated. These unusual solvents are molten (liquid) salts at low temperature (< 100°C). They function as the solvent and also provide the electrolyte ions. It has been shown that PPys grown from these solvents have distinctly different morphologies from those electrosynthesized from conventional electrolytes.<sup>48</sup> Electrochemical growth of PPy at an IL–air interface results in a microporous web of conducting polymers (Figure 2.7).<sup>49</sup>

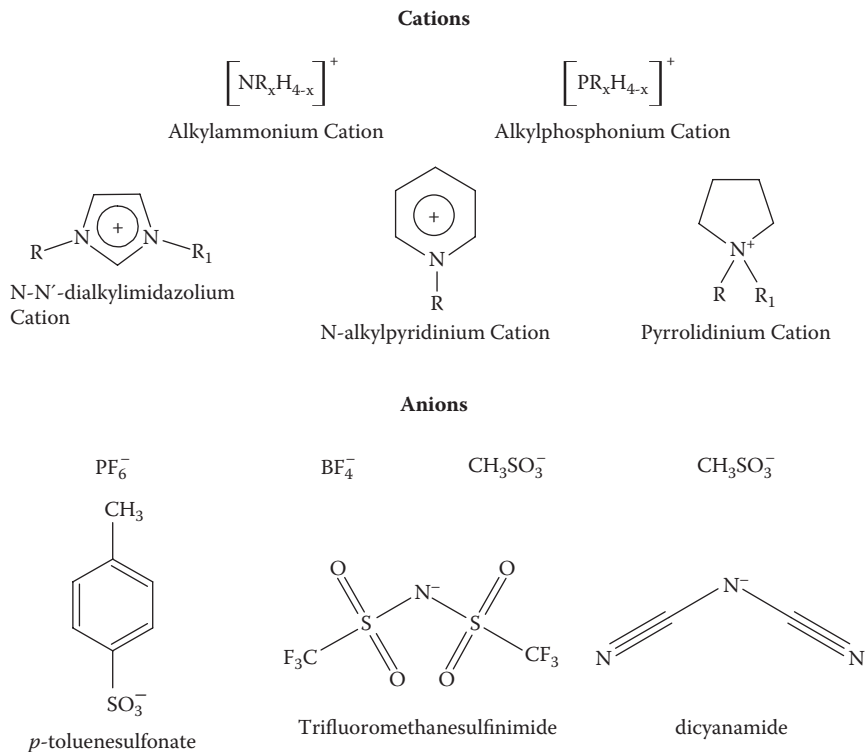
## THE COUNTERION/CATION EFFECT: CHOICE OF ELECTROLYTE

Numerous workers<sup>50,51,52,53</sup> have studied the effect of the counterion on the electropolymerization process. The high concentration of counterion employed means that it can have a dramatic effect on the polymerization process. The electrolyte will influence the conductivity of the solution, the polymer properties and, hence, the rate of polymerization. The nature of the electrolyte salt employed can also have a marked effect on polymer–solvent interactions.

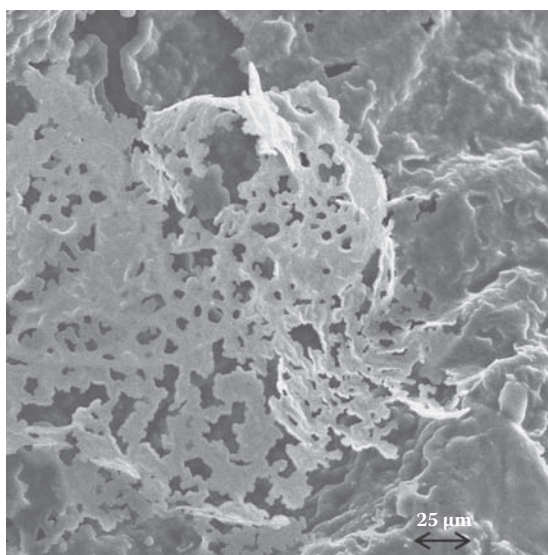
This latter phenomenon has not yet been studied in detail as far as conducting polymers are concerned. However, in other areas the ability of particular salts to dehydrate macromolecular (in this case proteins) structures has been known for some time.<sup>54</sup> This dehydration can have a marked effect on the polymeric structure produced with conducting polymers and the inherent stability of the structure obtained.<sup>55</sup>

It has been shown that the concentration of counterion employed not only has an effect on the amount of anion incorporated into the polymer but also on its structure





**FIGURE 2.6** Typical ionic liquid ions.



**FIGURE 2.7** Fine-structured poly(pyrrole) film formed on the ionic liquid surface using 10 ms voltage pulses. (Source: Dr. Jenny Pringle, Monash University, Australia.)

and morphology.<sup>56</sup> These differences in morphology will influence surface area and the subsequent rate of polymerization.

Other workers have carried out electropolymerization in the presence of chemical oxidants.<sup>57</sup> This results in the production of much more porous, yet mechanically stable conducting polymer materials.

For efficient polymerization, the counterion should be readily incorporated. Therefore, some studies have suggested that small size and high charge density are preferable. We have shown, however, that polyelectrolytes are readily incorporated.<sup>43</sup> This affects the subsequent polymerization process because polymers with very high water content are obtained. Formation of the open hydrophilic polymer network encourages continued growth of such structures because the polymer prefers to grow and deposit in the more hydrophobic regions.

The counterion should also be stable both chemically and electrochemically; otherwise, breakdown products may interfere in the polymerization process. If it is electroactive at potentials lower than the monomer oxidation potential, it can be incorporated using potentiostatic methods but not with constant-current techniques because the counterion will be preferentially oxidized.

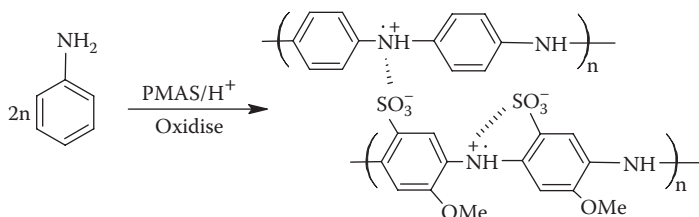
The counterion may be catalytic,<sup>51</sup> in which case it will have a dramatic effect on the polymerization process. For example, Tiron **4** (shown earlier) has a catalytic effect on the electropolymerization of pyrrole, thereby enabling the process to be carried out at a more rapid rate at lower applied potentials. The ability of the counterion to ion pair with charged oligomers produced as part of the polymerization process will also have an effect.

The “magical” counterions in terms of conductivity and mechanical properties appear to be sulfonated aromatics,<sup>58,59,60,61,62</sup> in particular, *para*-toluene sulfonate (pTS). It has been shown that the benzene sulfonates induce a degree of crystallinity<sup>28,29</sup> that results in higher conductivity. This higher conductivity enables the polymerization process to proceed efficiently. It has also been suggested that the sulfonated aromatics exhibit surfactant-like behavior as the radicals are stabilized and presumably protected from unwanted side reactions with the solvent, oxygen, or other nucleophiles.

The direct incorporation of biological dopants into inherently conducting polymers is providing a number of new opportunities in areas such as biosensors, bioreactors, and novel surfaces for cell culturing (see Chapter 1). For example, oligonucleotides have been incorporated directly as dopants,<sup>63</sup> as has salmon sperm DNA<sup>64</sup> and even intact red blood cells.<sup>65</sup>

An interesting option in terms of dopants is to incorporate an inherently conducting polymer such as a sulfonated polyaniline (PMAS; Figure 2.8) as the molecular dopant. An interesting electrically conducting hydrogel (>90% [w/w] H<sub>2</sub>O) with multiple electrochemical switches is the result.<sup>66</sup>

The counterion employed also has a marked effect on the electropolymerization process in organic solvents. For example, the polymerization of poly(methyl carboxypyrrole) (PMCP) proceeds differently in *para*-toluenesulfonic acid (pTS), tetrabutylammonium perchlorate (TBAP), tetrabutylammonium tetrafluoroborate (TBABF<sub>4</sub>), and tetrabutylammonium hexafluorophosphate (TBAPF<sub>6</sub>).<sup>63</sup> As reported in that work, the rate of polymerization (at constant potential) and the time required for the onset of polymer deposition varied with the counterion employed.



**FIGURE 2.8** Polymerization of aniline in the presence of PMAS.

There is no doubt that the counterion incorporated during synthesis influences the ability of the polymer to interact with different solvents and other molecules. These “surface properties” also influence the interfacial structure and properties that are critically important when conducting polymers are integrated with other materials and structures.

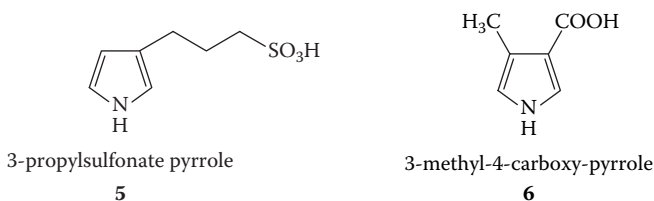
### THE MONOMER

A number of *N*-substituted pyrroles have been prepared previously.<sup>64</sup> Such substitution lowers the electronic conductivity of the resultant materials and usually results in deterioration of the polymer’s mechanical properties.

Pyrroles substituted in the 3 or 4 ( $\beta$ ) position are usually preferred. It has been shown that  $\alpha$ -substituted monomers do not undergo polymerization, because these sites are required for polymer formation. Provided the substituents are not electron withdrawing and/or too bulky, these monomers are easily oxidized and yield polymers with good conductivity.<sup>65,67</sup>

The derivatized monomers will influence the electropolymerization process in various ways. Differing functional groups will influence the solubility of the monomer, oligomers, and resultant polymer. For example, PPy’s can be made soluble in organic solvents by alkylation at the 3-position.<sup>68,69</sup> This influences the polymerization process because polymer may always be produced at the bare electrode (because there is no deposit). The production of soluble polymers provides a well-controlled means of polymerization. An indication of the achievable solubilities is given in Table 2.1. Although the side chain promotes solubility, the degree attainable is still dependent on the dopant incorporated and the solvent used for electropolymerization.

Some functional groups will have a dramatic effect on the polymerization process because they will provide self-doping. For example, monomers **5** and **6** exhibit this phenomenon.



**TABLE 2.1**  
**Solubility Data at 25°C for PODP**

| Polymer   | Solubility (g/L)                |                  |        |
|---|---------------------------------|------------------|--------|
|   | CH <sub>2</sub> Cl <sub>2</sub> | CCl <sub>4</sub> | Xylene |
| PODP-ClO <sub>4</sub> (electrodeposited from CH <sub>2</sub> Cl <sub>2</sub> )                        | 36                              | 52.5             | 57     |
| PODP-ClO <sub>4</sub> (electrodeposited from THF)   | 3.5                             | 13.5             | 30.5   |
| PODP-ClO <sub>4</sub> (electrodeposited from THF/CH <sub>3</sub> CN media)                            | 5                               | 1                | 0      |
| PODP-ClO <sub>4</sub> (electrodeposited from CCl <sub>4</sub> /CH <sub>2</sub> Cl <sub>2</sub> media) | 10                              | 5                | 1      |
| PODP-pTS (electrodeposited from CH <sub>2</sub> Cl <sub>2</sub> /CH <sub>3</sub> CN media)            | 40                              | 34               | 51     |

The ionizable –SO<sub>3</sub>H and –COOH groups provide the charge required to dope the polymer during oxidation and polymerization. For example, in the case of **6**, this results in a polymer with a very low additional counterion content. Monomer **5** can be polymerized without additional counterion.

Water-soluble polymers can also be produced by functionalizing the monomer with an alkyl sulfonate group. Havinga and coworkers<sup>70</sup> have shown that a polymer paste is formed upon oxidation of monomers such as **5**, shown earlier.

## CHEMICAL POLYMERIZATION

The number of experimental variables available with chemical polymerization is greatly reduced because no electrochemical cell or electrodes are employed. The range of dopant counterions (A<sup>-</sup>) that may be incorporated into the PPy backbone during polymerization has also, until recently, been generally limited to ions associated with the oxidant. However, chemical polymerization remains of interest for processing purposes because it may be easier to scale up this batch process and it results in the formation of powders or colloidal dispersions. Furthermore, it is possible to use chemical deposition to coat other nonconducting materials.

Pyrrole polymerizations have a significant advantage in terms of flexibility over polyaniline syntheses, described later in Chapter 4, in that they may be carried out in neutral aqueous solution (i.e., no acid is required). A range of organic solvents may also be employed, the limitation being the requirement to dissolve both the pyrrole monomer and the oxidant.

## MECHANISM OF CHEMICAL POLYMERIZATION

It is usually assumed that the mechanism of chemical polymerization is similar to that described earlier in electropolymerization. However, work in our own laboratories<sup>71</sup> highlights the fact that it is difficult to duplicate the products of electropolymerization using a chemical oxidant. Studies using 3-methyl-4-carboxy-pyrrole have demonstrated that polymers obtained with both techniques are similar in chemical composition but differ markedly with respect to polymer morphology.

## INFLUENCE OF POLYMERIZATION CONDITIONS

### THE OXIDANT

The most widely used chemical oxidants have been ammonium persulfate,  $(\text{NH}_4)_2\text{S}_2\text{O}_8$ , and  $\text{FeCl}_3$ , although hydrogen peroxide and a range of transition metal salts (e.g.,  $\text{Fe}^{3+}$ ,  $\text{Ce}^{4+}$ ,  $\text{Cu}^{2+}$ ,  $\text{Cr}^{6+}$ , and  $\text{Mn}^{7+}$ ) have also been employed. The use of  $\text{H}_2\text{O}_2$  (with  $\text{Fe}^{3+}$  catalyst) is attractive environmentally, as the only by-product is water. For the metal-based oxidants considered by Chao and March,<sup>72</sup> infrared (IR) spectroscopy confirmed that similar PPy backbones were formed in each case.

For one-electron oxidants such as  $\text{FeCl}_3$ , an [oxidant]/[pyrrole] molar ratio of ca. 2.3 is usually employed. Two electrons are required for the oxidation of each pyrrole unit, with the remaining 0.3 electrons being used for ca. 30% oxidative doping of the neutral PPy product into its conducting form, which carries a positive charge on about every third pyrrole unit. However, with respect to polymer conductivity, Miyata and coworkers have shown that control of the redox potential in solution by adjusting the concentration of the redox couple can be used to advantage.<sup>73</sup> The use of binary systems (mixtures of two different oxidants) has also proved useful in this regard.<sup>74</sup> If the oxidizing strength is too high, the rate of polymerization is too fast, resulting in an aggregated, low-conductivity material.

The use of halogens as oxidizing agents has also been reported,<sup>75</sup> resulting in a PPy/X product containing halide ( $\text{X}^-$ ) ions as the dopant counterions. These same workers used chemical polymerization to produce PPy-polymethylpyrrole copolymers.

Kang and coworkers<sup>76</sup> have also used organic electron acceptors such as 2,3-dichloro-5,6-dicyano-*p*-benzoquinone (DDQ) and chloranil. A solvent effect was observed when polymerization was carried out using DDQ. Polymerization in acetonitrile gave the lowest conductivity, and in water it was slightly better. A similar solvent dependence was observed for chloranil oxidations.

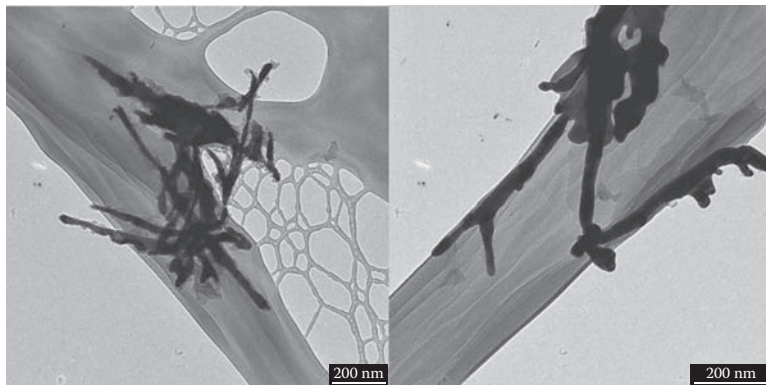
### THE SOLVENT

Solvent effects have also been reported for the polymerization of pyrrole using  $\text{FeCl}_3$  as oxidant.<sup>77</sup> The conductivities of the PPy products prepared in water and alcohols ranging from MeOH to octanol were considerably higher than for the polymers prepared under the same conditions in acetonitrile, tetrahydrofuran, chloroform, and benzene.

A biphasic solvent system consisting of ionic liquids and  $\text{H}_2\text{O}$  has also been used as the solvent media for chemical polymerization of the conducting polymers poly(pyrrole), poly(terthiophene), and poly(3,4-ethylenedioxythiophene). Using gold chloride as the oxidant, unusual highly fibrillar conducting polymer morphologies were observed at the polymer-ionic liquid interface (Figure 2.9).<sup>78</sup>

### POLYMERIZATION TEMPERATURE

The vast majority of chemical polymerizations of pyrrole have been carried out between 0°C and room temperature. In one of the few systematic studies of the influence of temperature, Miyata and coworkers<sup>77</sup> examined polymerization with  $\text{FeCl}_3$



**FIGURE 2.9** Poly(terthiophene) from interfacial polymerization using  $\text{AuCl}_3$  in water layer and terthiophene in ionic liquid 1-ethyl-3-methylimidazolium bis(trifluoromethanesulfonimide),  $\text{emINTf}_2$ .

in MeOH solvent over the range  $-20$  to  $-60^\circ\text{C}$ . Maximum conductivity was observed for the PPy product synthesized at  $0^\circ\text{C}$ .

### THE DOPANT COUNTERION ( $\text{A}^-$ )

The dopant anions ( $\text{A}^-$ ) incorporated into conducting PPy's are positioned interstitially between the polymer chains and, as discussed earlier for electropolymerization, their nature consequentially influences both the polymerization process and the properties of the resultant polymers. In initial chemical polymerization studies, the incorporated anions were limited to those arising from the oxidant employed; for example,  $\text{FeCl}_3$  and  $(\text{NH}_4)_2\text{S}_2\text{O}_8$  oxidants provided  $\text{Cl}^-$  and  $\text{HSO}_4^-/\text{SO}_4^{2-}$  counterions, respectively. These could in many cases be subsequently replaced by a range of other anions through either ion-exchange or redox cycling.

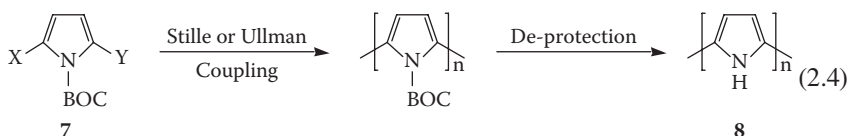
More recently, it has been found that anions such as polyelectrolytes and surfactant-like anions, for example, dodecylbenzenesulfonate (DBSA), can be inserted directly into PPy products during polymerization in competition with anions arising from the oxidant. This very useful development will be discussed later in a section dealing with PPy processability.

### ACHIEVING REGIOSELECTIVE COUPLING WITH PYRROLE MONOMERS

For the formation of PPy's with extended  $\pi$ -conjugation and high electrical conductivity, it is necessary to have only 2,5'-couplings, through the preferential linking of radical cations of type (III) as depicted in Figure 2.1. Unfortunately, 2,3'- and 2,4'-couplings also occur, leading to structural defects (branching) in the resultant polymers. This results in diminished supramolecular order and lower electrical conductivity, as well as decreased crystallinity and the impairment of other properties.

Synthetic routes to structurally perfect oligomers of PPy, involving only 2,5'-couplings of the individual pyrrole repeat units (idealized structure shown in Equa-

tion 2.1), have been successfully devised. For example, 2,5-disubstituted pyrrole monomers **7** ( $X = \text{Br}$ ,  $Y = \text{SnMe}_3$ ) bearing a *tert*-butoxycarbonyl (BOC) protecting group on the N center have been polymerized to oligomers with 16–20 pyrrole units, through a Stille coupling using organometallic reagents (Equation 2.4).<sup>79</sup> Reductive Ullman coupling of 2,5-dibromo-*N*-BOC-pyrrole has similarly yielded oligomers with up to 20 pyrrole units.<sup>80</sup> A less sophisticated way to at least reduce the opportunity for unwanted 2,3'- and 2,4'-couplings is to employ the dimer, 2,2'-bipyrrole as the substrate in a standard chemical polymerization.<sup>81</sup>



## IN SITU CHEMICAL POLYMERIZATION

The previous chemical polymerization routes usually precipitate the conducting PPy's as black powders. However, it has been found that PPy's may also be deposited as films on the surfaces of insulating substrates by immersing the substrates in the polymerization solution. Careful control of the polymerization conditions can maximize film deposition rather than bulk precipitation,<sup>82</sup> as illustrated elegantly by Saurin and Armes<sup>83</sup> for the deposition of PPy onto printed circuit boards. They employed the Fe(III) complex of 5-sulfosalicylic acid as a mild chemical oxidant rather than an Fe(III) salt and a high oxidant-to-monomer ratio. *In situ* chemical deposition has now become established as a simple and cost-effective method for the deposition of thin films of PPy on a wide range of substrate materials, examples of which are described in the following text.

*Deposition on glass/plastics.* Kuhn, MacDiarmid, and coworkers<sup>84</sup> have shown that *in situ* polymerization of pyrrole (0.009 *M*) with FeCl<sub>3</sub> (0.02 *M*) in the presence of HCl or an organosulfonic acid dopant (0.003 *M*) leads to the facile deposition of thin, uniform PPy films on glass substrates and overhead transparencies. The conductivity of the films was highest for hydrophobic substrates. In related studies using (NH<sub>4</sub>)<sub>2</sub>S<sub>2</sub>O<sub>8</sub> as oxidant, they found that the *in situ* deposition of PPy films occurs more readily on hydrophobic surfaces, such as Si/SiO<sub>2</sub> and glass pretreated with octadecylsiloxane, than on related hydrophilic surfaces.<sup>85</sup> They exploited these different deposition rates to produce patterned microstructures of conducting PPy's by a microcontact "stamp"-printing technique. PPy features as small as 2 μm could thereby be produced.

PPy may be similarly coated on low-density polyethylene (LDPE), whereas grafting of the LDPE surface with acrylic acid enhances film growth and adhesion.<sup>86</sup> The *in situ* oxidation of pyrrole by Fe(III) can also be used to deposit PPy films on polystyrene substrates.<sup>87</sup> In a variation of this method, polyimide films exhaustively soaked in pyrrole (with up to 14% monomer uptake) have been coated with PPy via oxidation with FeCl<sub>3</sub> in acetonitrile solvent.<sup>88</sup> The resultant material shows electrical conductivity of ca.  $4 \times 10^{-2} \text{ S cm}^{-1}$ .

*Deposition on Fibers/Fabrics.* Following pioneering studies by Kuhn and coworkers,<sup>89</sup> a wide variety of textile substrates have been successfully coated with

conducting PPy's through *in situ* chemical polymerization. These include nylon fabrics, where H-bonding between carboxyl groups on the nylon backbone and pyrrole monomers is believed to lead to a more ordered PPy product.<sup>90</sup> Vapor-phase *in situ* deposition has also been employed, for example, by passing pyrrole vapor over cotton thread coated with the oxidant  $\text{FeCl}_3$ .<sup>91</sup> Typically, the surface resistance of such conducting polymer-coated fabrics decreases the greater the polymer deposition.

It has been shown that conducting PPy's can be formed by exposing a layer of the oxidant salt (e.g.,  $\text{FeCl}_3$ ) to pyrrole monomer in the vapor phase.<sup>92</sup> Adherent conducting polymer films can be produced in this way. Interestingly, the vapor-phase polymerization method gives rise to a highly swollen polymer structure containing excess oxidant. This is readily removed using a washing step.<sup>93</sup> By including functional molecules such as organometallic catalysts or even enzymes in the wash solution, this provides a convenient way to load the conducting polymers with functional molecules.<sup>94</sup>

## ROUTES TO MORE PROCESSABLE PPy'S

Both chemically and electrochemically synthesized PPy's are typically insoluble in water and organic solvents, and are infusible because of strong intermolecular and intramolecular interactions of their polymer chains. There has been intense research over the past decade to overcome this serious hindrance to their processibility and subsequent utilization. Several approaches have now been developed to improve the solubility of PPy's, namely (1) counterion-induced solubilization, (2) colloid formation, and (3) side-chain-induced solubilization. Each of these will be discussed in turn.

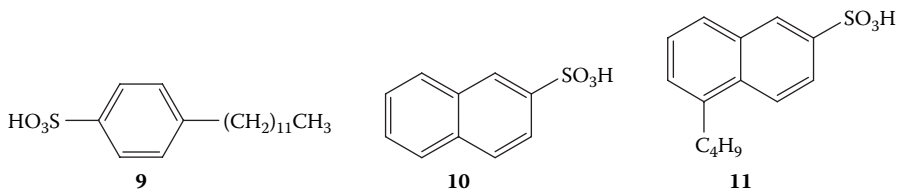
### COUNTERION-INDUCED SOLUBILIZATION

An important breakthrough in PPy chemistry was the discovery by Lee and coworkers<sup>95</sup> in 1995 of a chemical polymerization route to an unsubstituted PPy that was soluble in organic solvents. They exploited the surfactant-like qualities of added dodecylbenzenesulfonate (DBSA; **9**) as a dopant anion to solubilize PPy formed during oxidation of pyrrole by aqueous  $(\text{NH}_4)_2\text{S}_2\text{O}_8$ . The PPy/DBSA product, isolated as a black powder in 42% yield after 40 h reaction at  $0^\circ\text{C}$ , was very soluble in *m*-cresol, and could be dissolved in weakly polar solvents such as chloroform and dichloromethane by the addition of an equimolar amount of dodecylbenzenesulfonic acid. A film cast from chloroform solution exhibited an electrical conductivity of  $5 \text{ S cm}^{-1}$ , and its UV-visible spectrum was similar to that of electrochemically deposited PPy.

The solubilizing ability of the DBSA dopant is believed to arise from the long-chain dodecyl group reducing the interactions between the PPy chains as well as assisting solvation by the organic solvents. Subsequent studies have shown that a range of other large, surfactant-like sulfonic acids, added during polymerization of pyrrole by aqueous  $(\text{NH}_4)_2\text{S}_2\text{O}_8$ , can similarly cause dopant-ion-induced solubilization of PPy.<sup>96,97,98</sup> These include  $\beta$ -naphthalenesulfonic acid (NSA, **10**), 5-butyl-naphthalenesulfonic acid (BNSA, and **11**) and anthraquinonesulfonic acid (AQSA). Freestanding films of the doped PPy products may be cast from solutions in *m*-cre-

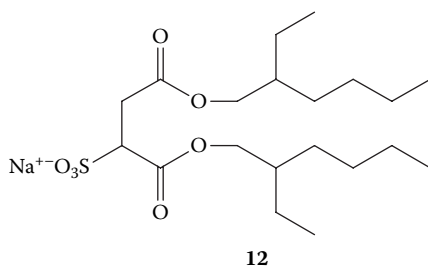


sol,  $\text{CHCl}_3$ , DMSO or *N*-methylpyrrolidinone (NMP) solvents, exhibiting electrical conductivities in the range  $10^{-2}$ – $1 \text{ S cm}^{-1}$ . Marked changes in the UV-visible spectrum of PPy/DBSA when dissolved in the preceding range of solvents indicate a strong solvent dependence for the polymer chain conformation (see Chapter 3).



When camphorsulfonic acid (HCSA) is used as the sulfonic acid dopant in related syntheses, a highly conducting ( $\delta = 15 \text{ S cm}^{-1}$ ) PPy/HCSA product is isolated, but it is completely insoluble in any solvent.<sup>96</sup> This latter polymer may be prepared in soluble form by analogous chemical polymerization of pyrrole in organic solvents such as  $\text{CHCl}_3$ , THF, or  $\text{CH}_3\text{NO}_2$ . However, it is nonconductive, emphasizing the influence of the polymerization solvent on the properties of the PPy product. A similar solvent effect was observed when PPy/HCSA was prepared using  $\text{H}_2\text{O}_2$  as the oxidant (with  $\text{Fe}^{3+}$  catalyst).<sup>99</sup> Kudoh has used aqueous  $\text{Fe}_2(\text{SO}_4)_3$  as the oxidant to produce a similar range of surfactant-solubilized PPy's.<sup>100</sup>

In a recent development, the first alcohol-soluble PPy's have been synthesized by the oxidation of pyrrole with aqueous  $(\text{NH}_4)_2\text{S}_2\text{O}_8$  using di(2-ethylhexyl) sulfosuccinate sodium salt (NaDEHS; **12**) as the dopant anion.<sup>101</sup> This dopant contains both nonpolar alkyl chains and polar oxygen centers, the latter of which are believed to form H-bonds with alcohol solvents, thereby facilitating dissolution.



## COLLOIDAL PPy DISPERSIONS

Other workers have used additives to enable the preparation of effectively “water-soluble” conductive polymer colloids. As early as 1986, Bjorklund and Liedberg<sup>102</sup> observed that when pyrrole was oxidized by  $\text{FeCl}_3$  in the presence of aqueous methylcellulose (MWt 100,000), a PPy/methylcellulose sol was formed that could be characterized by scanning electron microscopy. Thin films could be obtained from the sol, exhibiting a conductivity of ca.  $0.2 \text{ S cm}^{-1}$ . Subsequently, a range of neutral, water-soluble steric stabilizers such as poly(vinylalcohol), poly(ethyleneoxide) (PEO), or poly(vinylpyridine) have been successfully

employed to produce stable, relatively monodispersed colloidal sols.<sup>103,104,105,106</sup> Cationic and anionic polyelectrolytes have also been used.<sup>107,108</sup>  $\text{FeCl}_3$  has been the most common oxidant employed for PPy colloid preparation. In contrast to bulk PPy syntheses,  $(\text{NH}_4)_2\text{S}_2\text{O}_8$  has found little application. It has been suggested that its more rapid oxidation of pyrrole monomers may lead to uncontrolled fast nucleation, causing macroscopic precipitation.

Colloidal PPy's prepared in aqueous solution are generally spherical. Particle size is very dependent on the synthetic conditions (stabilizer, oxidant, etc.), with sizes between 30 and 445 nm being described by Armes and Vincent.<sup>104</sup> The electrical conductivities of the PPy colloids are frequently a few orders of magnitude lower than those observed for macroscopically precipitated PPy's. This presumably arises from the insulating nature of the attached polymeric stabilizers. Data reported by Armes and Aldissi<sup>109</sup> indicate that the thickness of the stabilizer is in the range of 33–36 nm. They also showed that it is possible to strip the stabilizer (PEO) after chemical polymerization and to replace it with another one. They indicated that the molecular weight and nature of the stabilizer, as well as the concentration and nature of the oxidant, influence particle size.

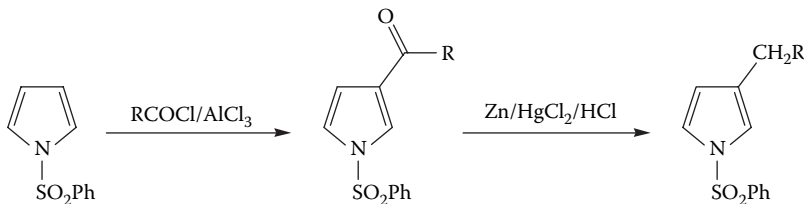
These same workers described an inverse emulsion-type polymerization process.<sup>109</sup> They used a conventional process in which microemulsions of water in hydrocarbon readily form in the presence of Aerosol-OT(AOT). The droplets are essentially swollen cells, where radius is controlled by the water/AOT ratio. As droplets collide, hydrophilic reagents contained in them are exchanged. When pyrrole and  $(\text{NH}_4)_2\text{S}_2\text{O}_8$  dispersions were mixed, eventually a sediment appeared. However, if poly(vinyl pyrrolidone) (PVP) was added at different intervals, stable dispersions of small particles could be prepared.

Armes and Aldissi<sup>109</sup> reported the synthesis of PPy colloids in nonaqueous solvents by the polymerization of pyrrole with  $\text{FeCl}_3$  in alkylester solvents using poly(vinylacetate) as a stabilizer. The same stabilizer has been similarly used to give PPy colloidal dispersions in 2-methoxyethanol and acetonitrile/methanol.<sup>110</sup> Methylacetate, methylformate, and propylformate solvents have also been used for colloidal PPy formation.<sup>111,112</sup> A greater rate of polymerization was observed than that found in water, which may account for the broader particle size distribution in organic solvents compared with  $\text{H}_2\text{O}$ . Once again, these studies highlighted the influence of the nature of the solvent on the conductivity of the PPy colloids. Solvents with more polar character gave rise to colloids with higher conductivities.

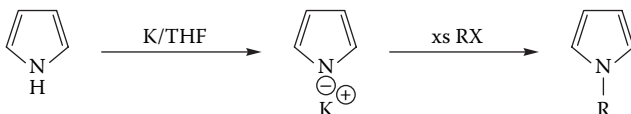
Others<sup>113</sup> have highlighted the role of the solvent in enabling the steric stabilizer to function in the colloid-forming role. At room temperature, they showed that poly(vinylmethylether), which does not function as a steric stabilizer in water, does so in ethanol. However, the colloids produced in an ethanol-containing solution were much lower in conductivity.

### SIDE-CHAIN-INDUCED SOLUBILIZATION

The presence of flexible alkyl or alkoxy groups in the 3-ring position or the N center of polypyrrole renders the polymer soluble in organic solvents. The appropriate 3-alkyl substituted pyrrole monomers may be synthesized by Friedel–Crafts



**FIGURE 2.10** Synthesis of alkylated pyrroles.

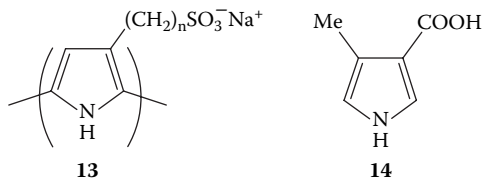


**FIGURE 2.11** Route to *N*-functionalized pyrrole monomers.

alkylation of *N*-protected pyrrole, followed by Clemmensen reduction, as illustrated in Figure 2.10.<sup>114</sup> Electrochemical or chemical oxidation (e.g.,  $\text{FeCl}_3$ ) of the substituted monomer then yields the poly(3-alkylpyrrole) products.<sup>115,116</sup> The enhanced processibility of these 3-alkyl- and 3-alkoxy-substituted PPy's comes, however, at the price of reduced electric conductivity, because of steric crowding by the substituents twisting the polymer backbone from planarity. It should also be noted that, unlike analogous substituted polythiophenes where routes to regioregular polymers have been developed (see Chapter 6), these 3-substituted PPy's are presumably mixtures of regioisomers (head-to-tail, head-to-head, tail-to-tail, etc.).

*N*-functionalized pyrrole monomers are available by the general route shown in Figure 2.11, involving reaction of pyrrole with potassium metal (in THF) to yield a pyrrole-1-yl potassium compound, which may be attacked by a variety alkyl and aryl halides. Chemical or electrochemical polymerization then yields the *N*-substituted PPy's. Although soluble in organic solvents, their electrical conductivities are unfortunately even lower than those of the 3-substituted PPy's. An interesting example, involving a reactive substituent, is the *N*-vinylpyrrole monomer, whose vinyl group may be polymerized by radical polymerization and the pyrrole units oxidatively polymerized with  $\text{FeCl}_3$ .<sup>117</sup>

The introduction of alkylsulfonic acid substituents onto the pyrrole rings, as in the series of 3-substituted polymers **13** ( $n = 3, 4, \text{ or } 6$ ), results in water-soluble PPy's.<sup>118</sup> These polymers were obtained through either electrochemical or chemical ( $\text{FeCl}_3$ ) oxidative polymerization of the appropriate substituted monomers. They are self-doped by the anionic sulfonate substituents and exhibit electrical conductivities in the range  $10^{-3}$ – $0.5 \text{ S cm}^{-1}$ . In our laboratories, we have alternatively synthesized **13** ( $n = 4$ ) via an electrohydrodynamic processing technique using a flow-through cell with reticulated vitreous carbon anode and cathode, obtaining a polymer with a molecular weight of ca. 10,500 and a conductivity of  $0.01 \text{ S cm}^{-1}$ .<sup>119</sup> A water-soluble carboxylic acid substituted PPy **14** has also been reported, obtained by electrochemical oxidation of 3-methylpyrrole-4-carboxylic acid in  $\text{CH}_3\text{CN}$ .<sup>120</sup>

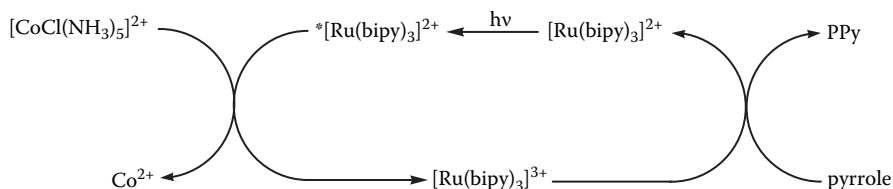


## PHOTOCHEMICALLY INITIATED POLYMERIZATION

Several photochemical routes to PPy have been described that have advantages in some applications over the conventional chemical and electrochemical syntheses. Shimidzu and coworkers<sup>121</sup> reported that visible light irradiation of an aqueous pyrrole solution in the presence of  $[\text{Ru}(\text{bipy})_3]^{2+}$  (bipy = 2,2'-bipyridine) as the photosensitizer and  $[\text{CoCl}(\text{NH}_3)_5]^{2+}$  as a sacrificial oxidant led to the deposition PPy/Cl. This powdery product exhibited a relatively low conductivity ( $3 \times 10^{-4} \text{ S cm}^{-1}$ ) compared to PPy/Cl prepared via standard chemical or electrochemical methods. The photochemically initiated polymerization is believed to proceed via the mechanism shown in Figure 2.12, where oxidation of the pyrrole is performed by the strong oxidant  $[\text{Ru}(\text{bipy})_3]^{3+}$  generated by oxidative quenching of the photo-excited  $^*[\text{Ru}(\text{bipy})_3]^{2+}$  species by the sacrificial Co(III) complex. By employing the anionic polymeric membrane Nafion to absorb both the photosensitizer and the sacrificial oxidant, and irradiating with a laser at 490 nm through a photomask, Shimidzu and coworkers<sup>121</sup> further demonstrated the ability to deposit fine ( $10 \mu\text{m}$ ) patterns of conducting PPy directly on the Nafion membrane. Other researchers<sup>122</sup> have similarly employed the complex  $[\text{Cu}(\text{dpp})_2]^+$  (dpp = 2,9-diphenyl-1,10-phenanthroline) as photosensitizer and *p*-nitrobenzyl bromide as the sacrificial oxidant to photodeposit conducting PPy on a variety of surfaces such as paper and glassy carbon.

## ENZYME- AND ACID-CATALYZED POLYMERIZATIONS

Aizawa and Wang have reported<sup>123</sup> that the copper-containing enzyme, bilirubin oxidase (BOX), catalyzes the oxidative polymerization of pyrrole to give thin films of PPy on substrates such as glass, plastic, or platinum plates. The BOX was first adsorbed onto the matrix support from an aqueous acetate buffer solution (pH 5.5), followed by incubation with the pyrrole monomer (0.2 M) in acetate buffer (pH 6) for several hours at room temperature. The deposited PPy film was reported to have similar properties to PPy made by conventional chemical or electrochemical methods.



**FIGURE 2.12** Photoelectrochemical generation of polypyrrole.

Treatment of pyrrole with aqueous 6.0 M HCl is reported to rapidly (< 1 min) yield the trimer, 2,5-dipyrrole-2-yl-pyrrolidine, in which the central heterocyclic ring is saturated.<sup>124</sup> The use of longer reaction times (4 h) or higher temperatures (100°C) has been shown to lead to the formation of polymeric species that possess alternating pyrroline and pyrrolidine groups together with varying degrees of ring-opened pyrrole units.<sup>125</sup> These brown polymers are nonconductive, but the presence of amine and carbonyl functional groups along their chains may prove useful for further derivatization.

## THE QUEST FOR EXTRA FUNCTIONALITY

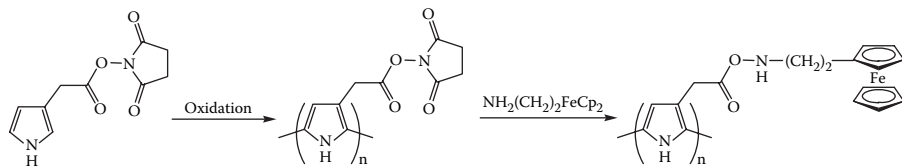
It has proved possible to add a wide range of additional functionalities to the parent polypyrrole (PPy) structure, opening up an exciting array of potential applications for these materials. Two distinct approaches to achieving this additional functionality have been successfully employed, namely:

1. Covalent attachment of specific groups to the PPy backbone (either before or after polymerization)
2. Incorporation of specific dopant anions (as discussed previously in this chapter)

The attachment of simple substituents such as alkyl or methoxy groups to the backbone of PPy's is well known to markedly enhance their solubility in organic solvents and, consequently, their processability (see the preceding text). Covalent binding of more sophisticated substituents to PPy can provide a wide range of other attributes. A number of these are discussed in the following text, with particular emphasis on the synthesis of derivatized PPy's with sensing capabilities.

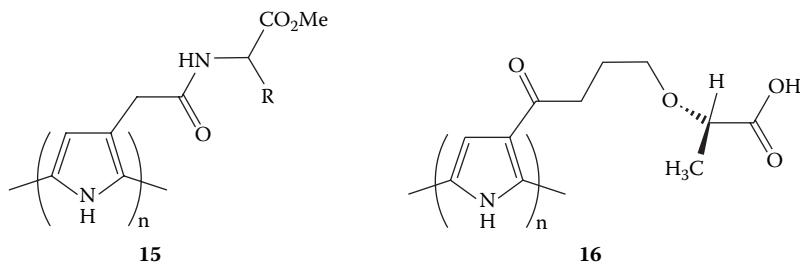
The usual approach has been to synthesize a monomer or dimer containing the appropriate recognition group, and this is subsequently oxidized to produce the conducting polymer.<sup>126</sup> A drawback with this approach to functionalized polymers is that the synthesis of the initial substituted monomer may be complex and time consuming. In addition, subsequent oxidation to the desired polymer may prove difficult because of steric hindrance by the functional group or electronic effects that shift the oxidation potential of the monomer. A significant recent development, therefore, is a route involving the facile modification of preformed PPy's containing good leaving groups such as *N*-hydroxysuccinamide.<sup>127</sup> Using this approach, crown ethers and electroactive groups such as ferrocene, as well as oligonucleotides have been covalently attached to the pyrrole rings (e.g., Figure 2.13).<sup>127,128</sup> This generic approach should be extendable to analogous polythiophenes and polyanilines (PAn's).

Another significant development has been the synthesis of chiral PPy's. These were first prepared by Baughman and coworkers<sup>129</sup> by the electropolymerization of pyrrole monomers bearing chiral substituents covalently attached to the pyrrole N centers. However, the chiroptical properties of these polymers were not investigated. Subsequently, Delabouglise and Garnier<sup>130</sup> prepared a series of chiral PPy's **15** (R = CH<sub>2</sub>OH, CHMe<sub>2</sub>, Ph) by electropolymerizing pyrrole monomers

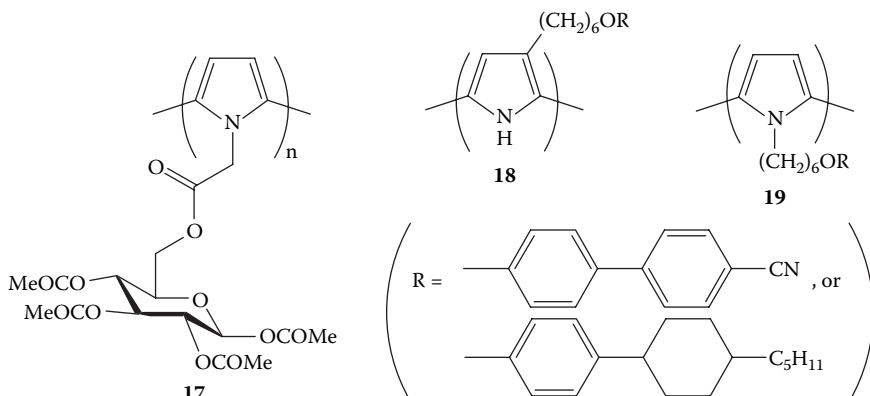


**FIGURE 2.13** Covalent attachment of ferrocene to polypyrrole.

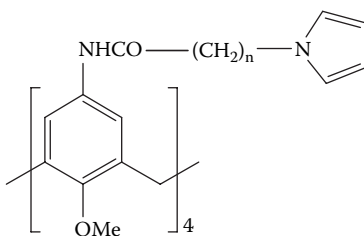
with amino acid substituents at the 3-position of the pyrrole ring. As with other 3-substituted PPy's, these novel polymers exhibited lower conductivities (ca.  $1 \text{ S cm}^{-1}$ ) compared to unsubstituted PPy's. Circular dichroism studies showed them to be optically active, and it was suggested that the presence of the chiral amino acid substituents on the pyrrole rings caused the polymer chains to preferentially adopt a one-handed helical arrangement. Recently, optically active PPy's containing (–)-ethyl-L-lactate as the chiral inducing agent (e.g., polymer **16**) have been similarly electrochemically synthesized.<sup>131</sup> Although their circular dichroism spectra were not recorded, they were shown to possess enantioselective recognition properties (see Chapter 3).



An optically active PPy **17** has also been synthesized by the electropolymerization of pyrrole monomer bearing a homochiral sugar covalently attached to the pyrrole nitrogen.<sup>132</sup> This chiral polymer discriminated between (+)- and (–)- camphorsulfonate ions as potential anionic dopants in cyclic voltammetry studies.



Other interesting recent examples of poly(3- or *N*-substituted pyrrole)s are the polymers **18** and **19**, which contain either cyclohexylphenyl or biphenyl groups to give liquid crystalline properties.<sup>133</sup> These can be prepared by either potentiostatic electropolymerization or by chemical oxidation using  $\text{FeCl}_3$  and 1-naphthalenesulfonic acid. The products are of relatively low molecular weight ( $M_n = 2,500\text{--}10,300$ , depending on synthesis conditions) and low conductivity ( $10^{-4}\text{--}10^{-7} \text{ S cm}^{-1}$ ) after  $\text{I}_2$  doping. A mesophase was observed only for the lower-molecular-weight ( $M_n < 5,000$ ) materials. Pyrrole monomers have also been synthesized with calix[4]arenes grafted to the N atom of the pyrrole ring.<sup>134,135</sup> Electropolymerization to give films of the corresponding *N*-substituted PPy's **20** was more facile for the monomer with the longer alkyl spacing arm length ( $n = 4$ ).



20

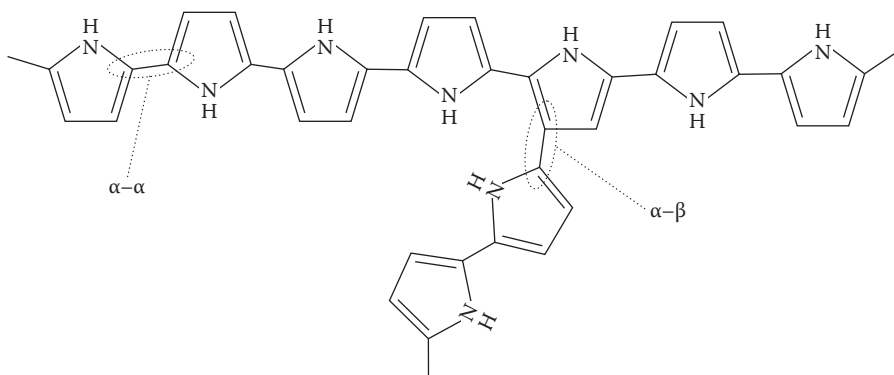
## MOLECULAR STRUCTURE AND MICROSTRUCTURE OF PPy

The polymerization conditions used to prepare PPy not only determine the polymer composition but also influence the structure of the polymer from the molecular level to the microscopic level. In this section, studies characterizing the detailed structure of PPy films, coatings, particles, and colloidal dispersions are reviewed. These studies provide the foundation for understanding the properties of PPy's, as described in Chapter 3.

### MOLECULAR WEIGHT, BRANCHING, AND CROSSLINKING

A key structural parameter for all thermoplastic polymer materials is the molecular weight. The molecular weight has a profound effect on physical properties such as mechanical strength and toughness and the viscosity of polymer solutions and polymer melts. Because synthetic polymers contain a distribution of molecular weights, it is most informative to measure the full distribution using techniques such as gel permeation chromatography (GPC) and to obtain the average molecular weight from such distribution.

Unfortunately, the intractable nature of PPy has made molecular weight determinations virtually impossible. Methods such as GPC and other techniques including light scattering, viscosity measurements, and vapor pressure osmosis, all require the polymer to be dissolved completely. Because PPy prepared by conventional methods does not dissolve, these analyses have not been possible.



**FIGURE 2.14** Polypyrrole chain structure showing  $\alpha-\alpha$  and  $\alpha-\beta$  couplings leading to chain branching and crosslinking.

The intractable nature of PPy is a strong indication that the unsubstituted polymer is substantially crosslinked. In the case of crosslinked polymers, the molecular weight parameter becomes meaningless, and it is the density of crosslinking that is strongly correlated to physical properties such as strength, toughness, and solvent swellability. Direct evidence of chemical crosslinking in PPy is rare, but  $^{15}\text{N}$  NMR studies have shown evidence of both  $\alpha-\alpha$  and  $\alpha-\beta$  linkages.<sup>136</sup> In more recent times, theoretical methods have been used to estimate the probability of branched structures forming during polymerization of pyrrole. These simulations give a degree of branching on the order of 20% for room temperature polymerization and show a slight dependency of branching on polymerization temperature (increasing with increasing temperature).<sup>137</sup> These estimates agree well with recent XPS studies of PPy/PF<sub>6</sub> and PPy/DBSA that show the degree of branching/crosslinking as 33 and 22%, respectively.<sup>138</sup> The branched and crosslinked structures are shown in Figure 2.14.

Only in specific instances has it been possible to prepare soluble PPy, as summarized in a recent review.<sup>139</sup> Two approaches have been used: alkyl-substituted pyrroles (as described earlier) and the use of certain dopants. In the former case, it is likely that the alkyl substituents block the branching and crosslinking reactions that occur in conventional preparations of PPy. Tritium-labeled 2,2'-dimethylpyrrole was studied by Nazzari and Street,<sup>140</sup> and their studies showed a molecular size of between 100 and 1000 pyrrole units. It has been reported that PPy's soluble in alcohols and other organic solvents can be prepared using solubilizing dopants. Solubilities of up to 11% (w/w) were obtained using sodium bis(2-ethylhexyl) sulfosuccinate as a doping agent.<sup>141</sup> Analysis of polymers formed with this dopant gave an average molecular weight of 62,000 (303 pyrrole rings) and conductivities of 12 S cm<sup>-1</sup>. The dopant-induced solubility is thought to be due to the dopant destabilizing the polymer-polymer interactions relative to the polymer-solvent interactions.<sup>142</sup> The large size of the dopant reduces the number of side chains and crosslinks, and so the inter-chain interactions are weakened.<sup>138</sup> Synthesis conditions have been found to affect the solubility and conductivity of PPy films cast from PPy solutions. Higher conductivities are obtained when polymerization is carried out using a higher oxidant-to-monomer ratio, and lower polymerization temperatures and shorter polymerization



times.<sup>139</sup> Lower temperatures favor the formation of a more linear polymer that is more soluble and gives higher conductivity. Longer polymerization times lead to higher yields and higher doping levels, but when large dopants such as DBSA are used, the interchain interaction is reduced, leading to lower conductivity.

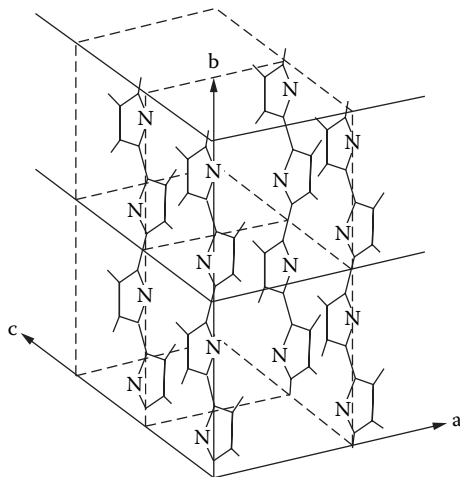
Turcu and coworkers<sup>142</sup> compared the optical properties of PPy/DBSA and the soluble fraction extracted from the as-prepared polymer. The IR spectra indicated that the soluble fraction contained shorter conjugation lengths. The conjugation lengths were also sensitive to the type of solvent used, with chloroform giving longer conformation lengths and higher conductivity than *m*-cresol.

### CRYSTALLINITY AND MOLECULAR ORDER

Several studies have investigated the manner in which polymer chains are arranged in the solid state for PPy. The chief investigative tool in these studies is x-ray diffraction, where scattering of incident x-rays occurs at specific angles related to the spacing between molecular layers in ordered crystal structures. The earliest studies by Mitchell<sup>143</sup> and Mitchell and Geri<sup>144</sup> revealed a molecular anisotropy in electrochemically prepared PPy/pTS (*para*-toluene sulfonate) films. The anisotropy was interpreted as being due to all *trans*-coupled PPy chains lying in planes parallel to the electrode surface, but randomly oriented in the direction perpendicular to the electrode. Further studies on other dopants revealed that anisotropy was mainly observed when planar dopants were used. In such cases, the planar dopant is regarded as a template for ordering the polymer chains. In contrast, nonplanar dopants, such as  $\text{ClO}_4^-$ ,  $\text{BF}_4^-$ , and  $\text{SO}_4^{2-}$ , produce films that appear isotropic in x-ray diffraction studies.<sup>145,146</sup> The degree of anisotropy was found to increase with lower polymerization temperature,<sup>144</sup> high anodic polymerization potentials,<sup>144</sup> high dopant:monomer molar ratios in the polymerization electrolyte,<sup>147</sup> and mechanical stretching.<sup>148,149</sup> One study of thin PPy coatings suggested a degree of crystallinity of 68%.<sup>150</sup> In all cases, the conditions that favor an increase in molecular anisotropy also favor an increase in electrical conductivity, suggesting that the anisotropy is due to molecular orientation favoring an increase in conjugation length.

More detailed studies of the molecular structure of PPy/PF<sub>6</sub> (hexafluorophosphate) have recently been published. Nogami and coworkers<sup>151</sup> have reported scattering peaks due to amorphous order that is independent of the film orientation. This finding is consistent with those described earlier because the PF<sub>6</sub><sup>-</sup> counterion is symmetrical and does not induce orientational order. Recent studies by Yoon and coworkers<sup>152</sup> suggested a partially crystalline structure, with the polymer chain aligned along the *b*-direction and stacked along the *c*-direction in a monoclinic arrangement (Figure 2.15). Polymerization conditions that favor higher conductivity (low temperatures and low current densities) also produce a higher degree of crystallinity (up to 37%) and a larger crystallite domain length (up to 2.6 nm or ~ 8 pyrrole rings).

A recent detailed x-ray diffraction (XRD) study of PPy/PF<sub>6</sub> during electrochemical cycling revealed new insights into the microstructure.<sup>153</sup> In the fully oxidized state, the XRD patterns could be interpreted as dopant ions homogeneously dis-



**FIGURE 2.15** Schematic illustration of crystalline structure of PPy/PF<sub>6</sub>.

tributed in both amorphous and crystalline regions. During the initial reduction of the polymer, the proportion of amorphous regions diminished as might be expected because of the egress of dopant ions. In addition, the XRD peaks associated with crystalline regions increased in intensity, suggesting that the remaining dopant ions formed more ordered structures with the polymer chains. Continued reduction of the polymer then produced a decrease in intensity of the crystalline peaks resulting from the further loss of dopant ions and a decrease in interchain interaction arising from  $\pi$ - $\pi$  stacking.

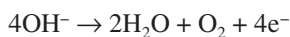
Although most of the available literature supports the planar *trans* arrangement for electrochemically prepared PPy, one study suggests an alternative conformation. Davidson and coworkers<sup>154</sup> found clear evidence of a helical structure produced from an all *cis* coupling of pyrrole rings. These workers used dodecyl sulfate as dopant, but also argue that all published literature on XRD of PPy is also consistent with the helical structure. Furthermore, the helical structure is identical to that proposed for poly(3-alkylthiophenes) as described further in Chapter 6.

Although molecular anisotropy has been noted in several PPy films, the overall degree of crystallinity is very low in these materials. The work by Davidson and coworkers<sup>154</sup> on thin PPy films (prepared at very short polymerization times) provides evidence of crystal formation, but the crystal growth is not maintained as the film thickens. Thus, the polymer first formed on the electrode surface may have a high degree of order but does not extend into the bulk structure of thick films.

## SURFACE MORPHOLOGY AND FILM DENSITY

The most readily observed structure of PPy samples is the peculiar surface morphology common to all electropolymerized PPy films and coatings. The morphology consists of nodules ranging in size to hundreds of microns and that themselves consist of aggregations of smaller particles. The structure has been referred to as a “cauliflower”- or “fractal”-like surface.

Many studies have considered the origin of the cauliflower morphology in PPy, and many factors have been identified as influencing the type of structure formed. For example, the type of dopant used during electropolymerization profoundly affects the surface morphology. Even when using two similar anions (chloride and bromide), significant differences were observed in the polymer structure at the nanoscale and microscale.<sup>155</sup> Recently, Lemon and Haigh<sup>156</sup> have reported that the nodular morphology arises from gas evolution at the working electrode during electropolymerization. Thus, the simultaneous formation of O<sub>2</sub> gas at the electrode surface and polymer formation results in polymer forming over the gas bubble and producing a roughened surface. The reaction occurring is suggested as



Yoon and coworkers<sup>152</sup> have also observed large (5–10 μm diameter) pores on the electrode side of PPy films prepared on unpolished platinum electrodes. Well-ordered microstructures have been formed on electrode surfaces by using gas bubbles as templates. Thus, microscale shapes in the form of cups, bowls, and bottles have been formed from PPy doped with camphorsulfonic acid.<sup>157</sup>

More recent studies have used atomic force microscopy (AFM) to determine surface morphology and surface roughness of electrochemically prepared PPy films. Li and coworkers<sup>158</sup> showed that the nodular surface arises very early in the electropolymerization process, where “microislands” first form on the (gold) electrode surface. With longer polymerization times, the film thickness increases and the film surface consists of close-packed nodular grains of submicron diameters. Barisci and coworkers<sup>159</sup> found a strong correlation between the surface potential of PPy films and the nodular surface morphology. These workers concluded that the nodules are dopant-rich, high-conductivity regions where nuclei initially formed and around which polymer subsequently grew preferentially. This growth concept had been previously described by Yang and coworkers<sup>160</sup> and Jeon and coworkers.<sup>161</sup> Interestingly, MacDiarmid and coworkers<sup>162</sup> have shown that a similar globular surface morphology is also found in chemically polymerized PPy films when deposited on various substrates.

The influence of dopant type on surface morphology has been studied using AFM by Silk and coworkers.<sup>163,164</sup> For thin films (< 1 μm thick), the PPy films prepared with four different dopants (Cl<sup>-</sup>, ClO<sub>4</sub><sup>-</sup>, SO<sub>4</sub><sup>2-</sup>, and dodecyl sulfate) were indistinguishable, with all consisting of globules of 100–300 nm in diameter and 10–30 nm in height. With thicker films (> 5 μm thick), however, clear differences were observed: the sulfate- and dodecyl-sulfate-doped films maintained approximately the same surface structure in thick films as in the thinner films. However, the Cl<sup>-</sup>- and ClO<sub>4</sub><sup>-</sup>-doped films generated large cauliflower structures consisting of large protrusions of ~2 μm in diameter and 0.5–1 μm in height. These protrusions showed a substructure of the smaller globules seen in thinner films. For all dopant types, the diameter of the smaller globules increased linearly with the square root of film thickness, suggesting a similar growth mechanism for all dopant types. Similar structures and similar dependence of globule diameter and film thickness has also been reported for PAN films, suggesting that globule formation and growth is common to both electrochemically formed polymers.

The electrode material has also been found to influence the surface morphology of electrochemically prepared PPy films. In our own work, we used transmission electron microscopy (TEM) to investigate the cross-sectional structure of PPy films prepared on different substrates.<sup>165</sup> In all cases, the large surface globules were observed to be the caps of cone-shaped structures that extended to the electrode surface of the PPy film (see Chapter 3). Interestingly, Yoon and coworkers showed that the cauliflower-type surface morphology could be virtually eliminated by carefully polishing the electrode surface.<sup>152</sup>

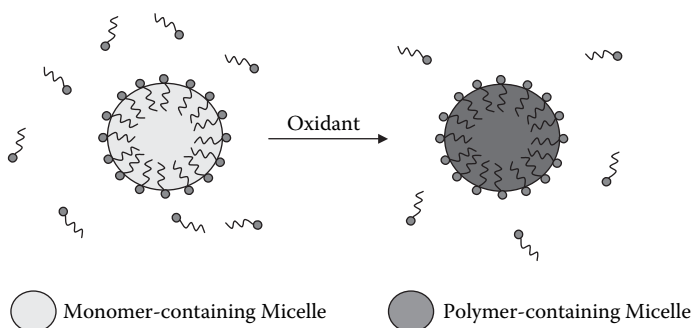
The film densities reported for PPy have been shown to be highly dependent on dopant and preparation conditions. For example, the low-temperature polymerization ( $-40^{\circ}\text{C}$ ) of pyrrole with  $\text{PF}_6^-$  counterion produces films with a density of  $1.4 \text{ g/cm}^3$ .<sup>152</sup> In contrast, the same films prepared at room temperature have much lower densities of  $0.6\text{--}0.8 \text{ g/cm}^3$ .

## NANOSTRUCTURED PPy'S

One approach to the formation of CEP nanoparticles is through the use of micellar polymerization and microemulsion techniques. The advantage of such an approach is that the particle size can be predefined by establishing the appropriate size and geometry of the templating micelle (Figure 2.16).

Using this approach Jang and coworkers<sup>166</sup> have reported the synthesis of PPy nanoparticles at the 2 nm scale. Typical surfactants used in the preparation of these sub-5-nm particles were quaternary ammonium-based cations such as octyltrimethylammonium bromide or decyltrimethylammonium bromide. Reactions at room temperature produced nanoparticles with diameters on the order of 10 nm, whereas at  $70^{\circ}\text{C}$  ca. 50 nm diameter particles were observed.

Selvan and coworkers<sup>167,168</sup> utilized a block copolymer micelle of polystyrene-block-poly(2-vinylpyridine) in toluene exposed to tetrachloroauric acid that was selectively adsorbed by the micelle structure. On exposure of this solution to pyrrole monomer, doped PPy was obtained concurrently with the formation of metallic gold nanoparticles. The product formed consisted of a monodispersed (7–9 nm) gold core surrounded by a PPy shell. Dendritic nanoaggregate structures were also reported



**FIGURE 2.16** Schematic illustrating micellar/microemulsion nanoparticle synthesis. (With permission from G. G. Wallace and P. C. Innis, *J. Nanosci. Nanotech.* 2, 441 (2002). © 2002, American Scientific Publishers.)

to form via a vapor-phase polymerization of the pyrrole monomer onto cast films of the block copolymer.

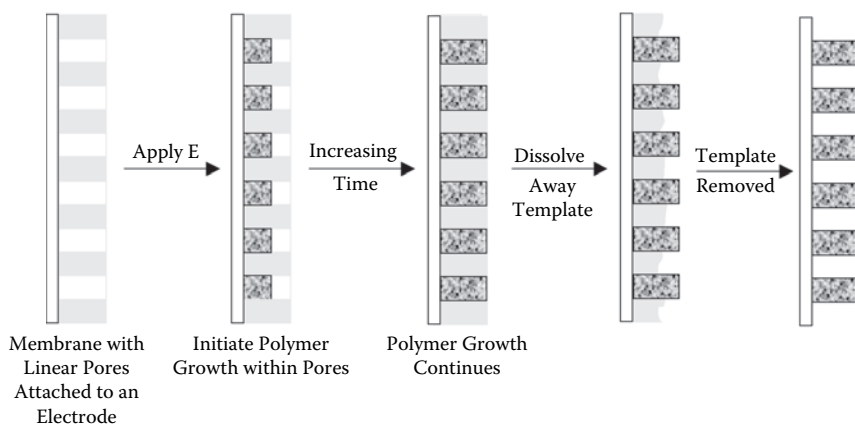
PPy nanotubes have also been synthesized by inducing polymerization in an inverse microemulsion.<sup>169</sup> Nanotubes were synthesized by using bis(2-ethylhexyl)sulfosuccinate (20.3 mmol) in hexane (40 mL), which form tubelike or rodlike micelles. The oxidant ( $\text{FeCl}_{3(\text{aq})}$ ) is effectively trapped in the core of the micelle. Addition of pyrrole then results in interfacial polymerization at the micelle surface, resulting in hollow nanotubes 95 nm in diameter and up to 5  $\mu\text{m}$  in length. The electrical conductivity of these nanotubes was up to 30  $\text{S cm}^{-1}$ .

A comprehensive study indicating how nanostructure can be influenced by the use of appropriate anionic or cationic surfactants, and even the oxidant used, has been produced recently by Zhang and coworkers.<sup>170</sup>

Chitosan has been used as a molecular template to promote formation of nano-sized PPy particles on silica.<sup>171</sup> Interestingly, another biomolecule (Heparin) has been shown to have a similar templating effect. In the case of Heparin, it acts as both the molecular dopant and a (nano) structure-directing template.<sup>172</sup> Interestingly, the fibrils continue to grow in this form even after they leave the constraints of the membrane,<sup>173</sup> indicating that once a pattern of growth is imprinted, it continues.

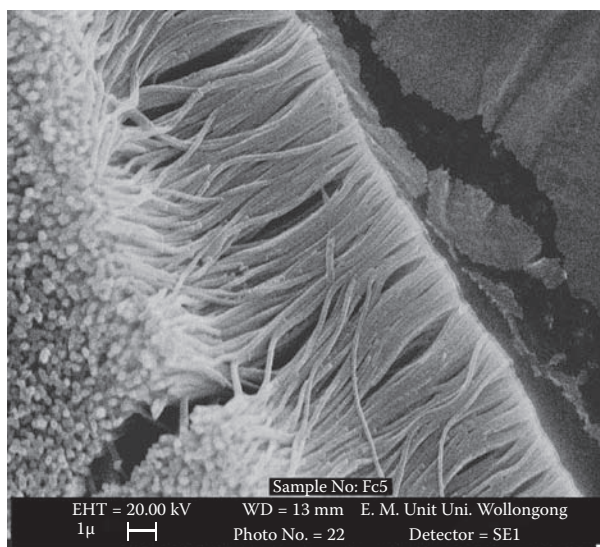
Conducting polymers have been grown within zeolites.<sup>174,175</sup> With channels as small as 0.3 nm, this allows assembly of single molecular wires. Conductivities of  $10^{-9}$   $\text{S cm}^{-1}$  for such wires contained within zeolites have been reported, and this increases to  $10^{-2}$   $\text{S cm}^{-1}$  when the polymer is extracted from the host structure.

Martin and coworkers<sup>176,177,178</sup> have used controlled pore-size membranes as templates to electrochemically grow fibrillar mats of CEPs. Similar structures have also been produced using nanoporous particle track-etched polycarbonate membranes with both PPy<sup>179,180,181,182</sup> and PAN<sup>183</sup> via chemical and electrochemical techniques. The approach involves the oxidation of the monomer within the pores of a template. This is achieved electrochemically as illustrated in Figure 2.17. The electrode sub-

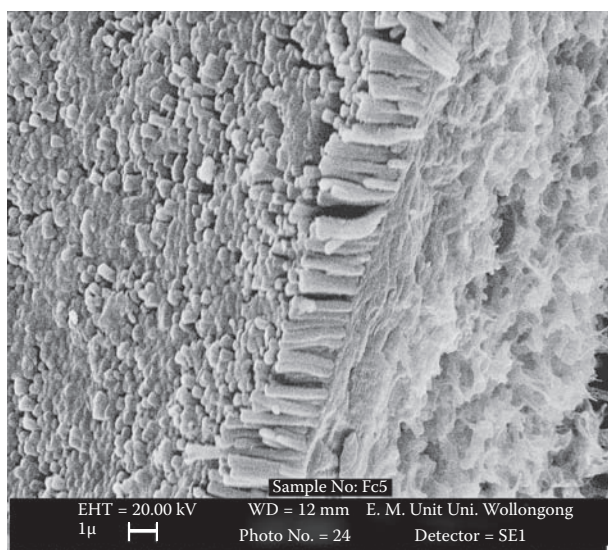


**FIGURE 2.17** Assembly of fibrillar CEPs using controlled pore-size templates. (With permission from G. G. Wallace and P. C. Innis, *J. Nanosci. Nanotech.* 2, 441 (2002). © 2002, American Scientific Publishers.)

strate used can be a conventional flat surface system such as solid gold, platinum, or glassy carbon, resulting in structures such as shown in Figure 2.18a. Alternatively, more novel electrode substrates such as platinized PVDF membranes with nominal pore size of  $0.45\ \mu\text{m}$  can be used (Figure 2.18b).

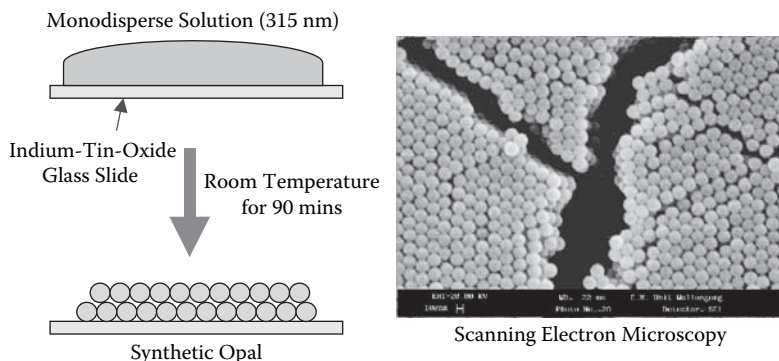


(a)

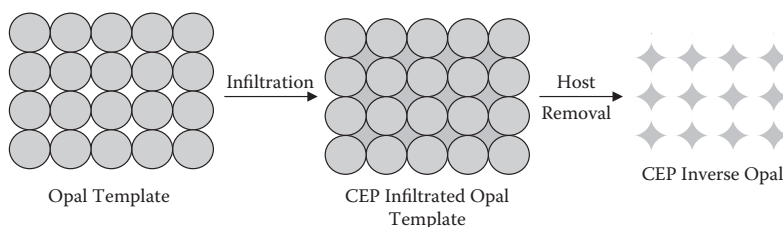


(b)

**FIGURE 2.18** Scanning electron micrographs of fibrillar structure of PPy/pTS on (a) a flat electrode surface and (b) a PVDF membrane. (With permission from V. Misoska, Ph.D. thesis, University of Wollongong, 2002.)



**FIGURE 2.19** Self-assembly of opal structures onto electrode substrates via monodispersed colloidal dispersions. (With permission from V. Misoska, Ph.D. thesis, University of Wollongong, 2002.)



**FIGURE 2.20** Schematic illustrating preparation of an inverse CEP opal using a synthetic opal template. (With permission from G. G. Wallace and P. C. Innis, *J. Nanosci. Nanotech.* 2, 441 (2002). © 2002, American Scientific Publishers.)

Other templates used to assist assembly of nanostructured conducting polymers are synthetic opals<sup>184,185,186,187,188,189</sup> based on polystyrene or silica spheres. Opal templates provide a route to establishing high range order in the nanodomain, resulting in high surface-to-volume ratios. Template opal structures (Figure 2.19) are preformed from monodisperse spherical colloidal particles that are permitted to self-assemble into close-packed arrays via a sedimentation process assisted by either gravity or pressure/microfiltration. After template formation, conducting polymer is formed by infiltration of monomer into the void spaces within the structure, followed by subsequent oxidative polymerization. The final stage is the removal of the templating core to leave an inverse structure from the templating material with essentially the same optical properties as the original host<sup>186</sup> (Figure 2.20). Others<sup>184,185</sup> used a similar templating approach but prepared self-assembled polystyrene (PS) latex opals onto gold substrates followed by the direct electropolymerization of PPy, PAN, and polybithiophene (PBT) into the interstitial void spaces of the host matrix. Using this approach, interchanneling between adjacent template layers was evident, giving evidence for the formation of a 3-D macroporous nanostructure.

Others have shown that molecular templates, such as a polyacrylate film predeposited on a carbon electrode, can be used effectively to create PPy nanowires via electrochemical oxidation of pyrrole.<sup>190,191</sup> Electropolymerization in the presence of

pyrenesulfonic acid also results in formation of nanowires with diameters in the range 150–200 nm.<sup>192</sup>

Shen and Wan<sup>193</sup> have shown that chemical oxidation of pyrrole (by APS) in the presence of  $\beta$ -naphthalenesulfonic acid ( $\beta$ -NSA) results in the formation of tubules down to ca. 200 nm in diameter. The tubular structures had reasonable conductivity ( $10 \text{ S cm}^{-1}$ ) and were soluble in *m*-cresol. In later work,<sup>194</sup> it was reported that the morphology was significantly influenced by the concentration of the  $\beta$ -NSA. Granular morphologies were present when  $[\beta\text{-NSA}]$  was less than 0.2 M, whereas on increasing the  $\beta$ -NSA concentration, fiber formation became the dominant morphology.

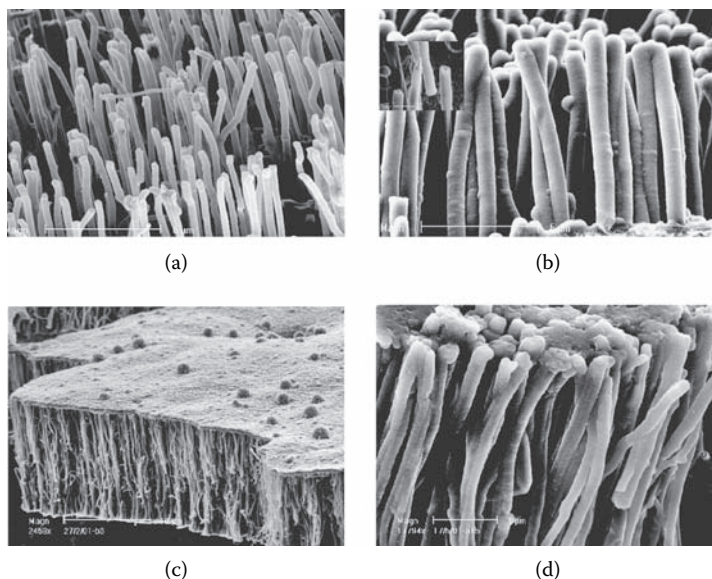
Other morphology types have also been noted using the  $\beta$ -NSA anion, namely, hollow microspheres ranging from 450 to 1370 nm (with inner wall thicknesses of 20–250 nm,) and conductivities of up to  $190 \text{ mS cm}^{-1}$ .<sup>195</sup>

Others<sup>196</sup> have used lipid tubules as templates during chemical oxidation of pyrrole to form nanofibers with diameters between 10 and 50 nm and lengths reaching up to several hundred microns.

Thin 50–100 nm freestanding PPy nanofilms have been synthesized, utilizing oxidative interfacial polymerization at a water–chloroform interface.<sup>197</sup> Thicker 3–4  $\mu\text{m}$  PPy films have been produced via this method.<sup>198</sup> Control over the final film thickness was achieved by removal of the immiscible solvents from above and below the nucleating film after a few minutes of polymerization. Stirring of the interfacial solutions resulted in the inhibition of polymer nucleation at the interface. Thin 5 nm PPy films on mica and graphite surfaces have also been formed via a micellar polymerization route.<sup>199</sup> The thin films were formed owing to the surfactant (CTAB and SDS) in solution adsorbing to the substrate surface as a thin-film micelle containing the pyrrole monomer, which was subsequently polymerized by ferric chloride solution.

Recent work aimed at other objectives may also provide an interesting route to the production of CEP-containing nanocomposites: this is in the use of carbon nanotubes (CNTs) as host “platforms.” CNTs in their own right possess interesting electronic properties and, when combined with other conjugated polymers, synergistic effects have been observed.<sup>200,201</sup> Our studies have focused on the use of aligned carbon nanotubes as templates for CEP deposition. Our recent work in this area<sup>202</sup> has revealed significant improvements when PPy glucose oxidase (GOD) is coated onto aligned CNTs for use as biosensors (Figure 2.21). We have also shown that CEPs can be highly effective dispersants for CNTs, presumably attaching themselves to the CNT structure. The properties of these novel dispersants of nanomaterials are yet to be investigated.





**FIGURE 2.21** Aligned carbon nanotubes with a bioactive conducting polymer: (a) Pure CNT array before treatment, (b) aligned CEP–CNT coaxial nanowires; inset shows clear image of single tube coated with PPy, (c) PPy only deposited on the top of CNT surface because of high density of tubes, and (d) polymer formed on both outside of walls and the top of the surface of the CNT array. (With permission from *Electroanalysis*, 15, 1089 (2003). © 2003, Wiley-VCH.)

## REFERENCES

1. Street, G.B.; Lindsey, S.E.; Nazaal, A.I.; Wynne, K. *J. Mol. Cryst. Liq. Cryst.* 1985, 118: 137.
2. Street, G.B.; Clarke, T.C.; Geiss, R.H.; Lee, V.Y.; Nazaal, A.I.; Pfluger, P.; Scott, J.C. *J. Physique*. 1983, C3: 599.
3. Nazaal, A.I.; Street, G.B. *J. Electroanal. Chem.* 1983, 27: 342.
4. John, R.; Wallace, G.G. *J. Electroanal. Chem.* 1991, 306: 157.
5. Scharitker, B.R.; Garcia-Pastariza, E.; Marina, W. *J. Electroanal. Chem.* 1991, 300: 85.
6. Andrieux, C.P.; Audebert, P.; Haipot, P.; Saveant, J.M. *J. Phys. Chem.* 1991, 95: 10158.
7. Beck, F.; Oberst, M. *Mackromol. Chem. Macromol. Symp.* 1987, 8: 97.
8. John, R.; Wallace, G.G. *Polym. Int.* 1992, 27: 255.
9. Baker, C.K.; Reynolds, J.R. *J. Electroanal. Chem.* 1988, 251: 307.
10. Imisides, M.D.; Wallace, G.G. *J. Electroanal. Chem.* 1988, 246: 181.
11. Ding, J.; Liu, L.; Spinks, G.M.; Zhou, D.; Gillespie, J.; Wallace, G.G. *Synth. Met.* 2003, 138: 391.
12. Ogasawara, M.; Funahashi, K.; Iwata, K. *Mol. Cryst. Liq. Cryst.* 1985, 118: 1159.
13. Naarmann, H. *Synth. Met.* 1991, 41: 1.
14. Eisazadeh, H.; Spinks, G.; Wallace, G.G.; *Polymer* 1994, 35: 3801.
15. Innis, P.C.; Spinks, G.; Wallace, G.G. *Antec* 1998, 1229.
16. Barisci, J.N.; Harper, G.; Hodgson, A.J.; Liu, L.; Wallace, G.G. *Reactive Funct. Polym.* 1999, 39: 269.

17. Davey, J.M.; Innis, P.C.; Partridge, A.C.; Ralph, S.F.; Too, C.O.; Wallace, G.G. *Coll. Surf.* 2000, 175: 291.
18. Aboutanos, V.A.; Kane-Maguire, L.A.P.; Wallace, G.G. *Synth. Met.* 2000, 114: 313.
19. Guo, R.; Barisci, J.N.; Innis, P.C.; Too, C.O.; Zhou, D.; Wallace, G.G. *Synth. Met.* 2000, 114: 267.
20. Zhou, D.; Innis, P.C.; Shimizu, S.; Maeda, S.; Wallace, G.G. *Synth. Met.* 2000, 114: 287.
21. Innis, P.C.; Chen, Y.C.; Ashraf, S.; Wallace, G.G. *Polymer* 2000, 41: 4065.
22. Reece, D.A.; Innis, P.C.; Ralph, S.F.; Wallace, G.G. *Coll. Surf.* 2002, 207: 1.
23. Aboutanos, V.A.; Kane-Maguire, L.A.P.; Wallace, G.G. *Synth. Met.* 2000, 114: 313.
24. Li, S.; Macosko, W.; Whire, H.S. *Science* 1993, 259: 957.
25. Lin, Y.; Wallace, G.G. *Electrochim. Acta* 1994, 39: 1409.
26. Beck, F.; Braun, P.; Oberst, M. *Ber. Bunsens. Phys. Chem.* 1987, 91: 967.
27. Fruend, B.; Bodalbhai, L.; Brajter-toth, A. *Talanta* 1991, 38: 95.
28. Kiani, M.S.; Mitchell, G.R. *Synth. Met.* 1992, 48: 203.
29. Kiani, M.S.; Bhatt, N.V.; Davies, F.J.; Mitchell, G.R. *Polymer* 1992, 33: 4113.
30. Too, C.O.; Ashraf, S.A.; Ge, H.; Gilmore, K.J.; Pyne, S.G.; Wallace, G.G. *Polymer* 1993, 34: 2684.
31. Rodriguez, I.; Marcos, M.L.; Velasco, J.G. *Electrochim. Acta* 1987, 32: 1181.
32. Cheung, K.M.; Bloor, D.; Steven, G.C. *Polymer* 1988, 29: 1709.
33. Gregory, R.V.; Kimbrell, W.C.; Kuhn, H.H. *Synth. Met.* 1989, 28: C823.
34. Tallman, D.E.; Vang, C.; Bierwagon, G.P.; Wallace, G.G. *J. Electrochem. Soc.*, 2002, 149: C173.
35. Akundy, G.S.; Iroh, J.O. *Polymer* 2001, 42: 9665.
36. Lehr, I.L.; Saidman, S.B. *Electrochim. Acta* 2006, 51: 3249.
37. Tüken, T.; Yazici, B.; Erbil, M. *Progr. Org. Coat.* 2005, 54: 372.
38. Ge, H.; Wallace, G.G. *J. Liq. Chrom.* 1990, 13: 3261.
39. Teasdale, P.R.; Wallace, G.G. *React. Polym.* 1995, 24: 157.
40. Ko, J.M.; Rhee, H.W.; Park, S.M.; Kim, C.Y. *J. Electrochem. Soc.* 1990, 3: 905.
41. Dong, S.; Ding, J. *Synth. Met.* 1987, 20: 119.
42. Mermillod, N.; Tanguy, J.; Periot, F. *J. Electrochem. Soc.* 1986, 133: 1073.
43. Hodgson, A.J.; Gilmore, K.; Small, C.; Wallace, G.G.; MacKenzie, I.; Aoki, T.; Ogata, N. *Supramol. Science* 1994, 1: 77.
44. Visy, C.S.; Lukkari, J.; Pajunen, T.; Kankare, J. *Synth. Met.* 1989, 22: 289.
45. Ko, J.; Rhee, H.W.; Kim, C.Y. *Makromol. Chem. Macromol. Symp.* 1990, 33: 353.
46. Gilmore, K.; John, R.; John, M.; Wallace, G.G.; Spencer, M.J.; Teasdale, P.; Xhao, H. *Proc. ACS Symp. Electrochem. Microheterogeneous Fluids* 1992, 225.
47. Skotheim, T.A. *Handbook of Conducting Polymers.* Marcel Dekker, New York, 1986.
48. Pringle, J.M.; Efthimiadis, J.; Howlett, P.C.; Efthimiadis, J.; MacFarlane, D.R.; Chaplin, A.B.; Hall, S.B.; Officer, D.L.; Wallace, G.G.; Forsyth, M. *Polymer* 2004, 45: 1447.
49. Pringle, J.M.; Forsyth, M.; Wallace, G.G.; MacFarlane, D.R. *Macromolecules* 2006, 39: 7193.
50. Sun, B.; Jones, J.J.; Burford, P.R.; Skyllas-Kazaces, M. *J. Mat. Sci.* 1989, 24: 4024.
51. Zinger, B.J. *Electroanal. Chem.* 1988, 244: 115.
52. Vork, F.T.A.; Schuermans, B.C.A.M.; Barendrecht, E. *Electrochim. Acta* 1990, 35: 567.
53. Cheung, K.M.; Bollor, D.; Stevens, G.C. *J. Mat. Sci.* 1990, 25: 3814.
54. Hearn, M.T.W. *Anal. Sci.* 1991, 7: 1519.
55. Lewis, T.W. Ph.D. Thesis, University of Wollongong, 2000.
56. Shen, Y.; Qiu, J.; Qian, R. *Makromol. Chem.* 1987, 188: 2041.
57. Omastova, M.; Kosima, S.; Skakalova, B.; Jancula, D. *Synth. Met.* 1993, 53: 227.
58. Price, W.E.; Wallace, G.G.; Zhao, H. *J. Memb. Sci.* 1994, 87: 47.

59. Qin, R.; Qiu, J. *Polym. J.* 1987, 19: 157.
60. Qian, M.; Diaz, A.F.; Logan, A.J.; Kroonbi, M.; Bargon, J. *Mol. Cryst. Liq. Cryst.* 1982, 83: 265.
61. Kuwabata, S.; Okamoto, K.; Yoneyama, H. *J. Chem. Soc. Farad. Trans.* 1988, 84: 2317.
62. Naarmann, H. 1986, U.S. Patent No. 4,569,734.
63. Ge, H.; Ashraf, S.A.; Gilmore, K.; Too, C.O.; Wallace, G.G. *J. Electroanal. Chem.* 1992, 340: 41.
64. Deronsier, A.; Moutet, J.C. *Acc. Chem. Res.* 1982, 249: 22.
65. Castelvetro, V. et al. *New Polym. Mat.* 1990, 2: 93.
66. Zhao, H.; Wallace, G.G. *Polym. Gels Networks* 1998, 6: 233.
67. Imisides, M.D.; John, R.; Riley, P.J.; Wallace, G.G. *Electroanalysis* 1991, 3: 789.
68. Masuda, H.; Tanaka, S.; Kaeriyama, K.J. *Polym. Sci. Part A. Polym. Chem.* 1990, 28: 1831.
69. Ashraf, S.A.; Chen, F.; Too, C.O.; Wallace G.G. *Polymer* 1996, 37: 2811.
70. Havinga, E.F.; Ten Hoeve, W.; Meijer, W.; Wynberg, H. *Chem. Mater.* 1989, 1: 650.
71. Ge, H.; Wallace, G.G. *Polymer* 1993, 34: 2007.
72. Chao, T.H.; March, J.J. *Polym. Sci. Part A. Polym. Chem.* 1988, 26: 743.
73. Whang, Y.E.; Han, J.H.; Nalwa, H.S.; Watanabe, T.; Miyata, S. *Synth. Met.* 1991, 41: 3043.
74. Whang, Y.E.; Han, J.H.; Motobe, T.; Watanabe, T.; Miyata, S. *Synth. Met.* 1991, 45: 151.
75. Neoh, K.G.; Kang, E.T.; Tan, T.C. *J. Appl. Polym. Sci.* 1989, 38: 2009.
76. Kang, E.T.; Neoh, K.G.; Tan, T.C.; Ong, Y.K. *J. Polym. Sci. Part A. Polym. Chem.* 1987, 25: 2143.
77. Whang, Y.E.; Han, J.H.; Nalwa, H.S.; Watanabe, T.; Miyata, S. *Synth. Met.* 1991, 41–43: 3043; and references cited therein.
78. Pringle, J.M.; Ngamna, O.; Lynam, C.; Wallace, G.G.; Forsyth, M.; MacFarlane, D.R. *Macromolecules* 2007, 40: 2702.
79. Martina, S.; Enkelmann, V.; Wegner, G.; Schlüter, A.D. *Synth. Met.* 1992, 51: 299.
80. Groenendaal, L.; Peerlings, H.W.I.; van Dongen, J.L.J.; Havinga, E.E.; Vekemans, J.A.J.M.; Meijer, E.W. *Macromolecules* 1995, 28: 116.
81. Lindenberger, H.; Schäfer-Siebert, D.; Roth, S.; Hanack, M. *Synth. Met.* 1987, 18: 37.
82. Malinauskas, A. *Polymer* 2001, 42: 3957; and references cited therein.
83. Saurin, M.; Armes, S.P. *J. Appl. Polym. Chem.* 1995, 56: 41.
84. Avlyanov, J.K.; Kuhn, H.H.; Josefowicz, J.Y.; MacDiarmid, A.G. *Synth. Met.* 1997, 84: 153.
85. Huang, Z.; Wang, P.-C.; MacDiarmid, A.G.; Xia, Y.; Whitesides, G. *Langmuir* 1997, 13: 6480.
86. Neoh, K.G.; Teo, H.W.; Kang, E.T.; Tan, K.L. *Langmuir* 1998, 14: 2820; and references cited therein.
87. De Marcos, S.; Wolfbeis, O.S. *Sens. Mater.* 1997, 9: 253.
88. Meador, M.A.B.; Hardy Green, D.; Auping, J.V.; Gaier, J.R.; Ferrara, L.A.; Papadopoulos, D.S.; Smith, J.W.; Keller, D.J. *J. Appl. Polym. Sci.* 1997, 63: 821.
89. Gregory, R.V.; Kimbrell, W.C.; Kuhn, H.H. *Synth. Met.* 1989, 28: C823.
90. Martin, C.R. *Science* 1994, 266: 1961; and references cited therein.
91. Tan, S.N.; Ge, H.L. *Polymer* 1996, 37: 965.
92. Winther-Jensen, B.; Chen, J.; West, K.; Wallace, G.G. *Macromolecules* 2004, 37: 5930.
93. Winther-Jensen, B.; Chen, J.; West, K.; Wallace, G.G. *Polymer* 2005, 46: 4664.
94. Chen, J.; Winther-Jensen, B.; Lynam, C.; Ngamna, O.; Moulton, S.; Zhang, W.; Wallace, G.G. *Electrochem. Solid-State Lett.* 2006, 9: H68.

95. Lee, J.Y.; Kim, D.Y.; Kim, C.Y. *Synth. Met.* 1995, 74: 103.
96. Lee, J.Y.; Song, K.T.; Kim, S.Y.; Kim, Y.C.; Kim, D.Y.; Kim, C.Y. *Synth. Met.* 1997, 84: 137.
97. Oh, E.J.; Jang, K.S.; Suh, J.S.; Kim, H.; Kim, K.H.; Yo, C.H.; Joo, J. *Synth. Met.* 1997, 84: 147.
98. Shen, Y.; Wan, M. *Synth. Met.* 1998, 96: 127.
99. van der Sanden, M.C.M. *Synth. Met.* 1997, 87: 141.
100. Kudoh, Y. *Synth. Met.* 1996, 79: 17.
101. Jang, K.S.; Han, S.S.; Suh, J.S.; Oh, E.J. *Synth. Met.* 2001, 119: 107.
102. Bjorklund, R.B.; Liedberg, B. *J. Chem. Soc., Chem. Commun.* 1986, 1293.
103. Armes, S.P. In *Handbook of Conducting Polymers. 2nd Edition* Skotheim, T.A.; Elsenbaumer, R.L.; Reynolds, J.R. (Eds.). Marcel Dekker, New York, 1998, p. 423.
104. Armes, S.P.; Vincent, B. *J. Chem. Soc., Chem. Commun.* 1987, 288.
105. Cawdery, N.; Obey, T.M.; Vincent, B. *J. Chem. Soc. Chem. Commun.* 1988, 1189.
106. Markham, G.; Obey, T.M.; Vincent, B. *Coll. Surf.* 1990, 51: 239.
107. Armes, J.P.; Aldissi, M.; Agnew, S.F. *Synth. Met.* 1989, 28: C837.
108. Beadle, P.M.; Armes, S.P.; Greaves, S.; Watts, J.F. *Langmuir* 1996, 12: 1784.
109. Armes, S.P.; Aldissi, M. *Synth. Met.* 1990, 37: 137.
110. Beaman, M.; Armes, S.P. *Colloid Polym. Sci.* 1993, 271: 70.
111. Cooper, E.C.; Vincent, B.J. *Coll. Interf. Sci.* 1989, 132: 592.
112. Aldissi, M.; Armes, S. P. *Progr. Org. Coat.* 1991, 19: 21.
113. Digar, M.L.; Battacharyou, S.N.; Mandal, B.M. *Polymer* 1994, 35: 377.
114. Anderson, H.J.; Loader, C.E.; Xu, R.X.; Le, N.; Gogan, N.J.; McDonald, R.; Edwards, L.G. *Can. J. Chem.* 1985, 63: 896.
115. Salmon, M.; Kanazawa, K.K.; Diaz, A.F.; Krounbi, M. *J. Polym. Sci., Polym. Lett.* 1982, 20: 187.
116. Chan, H.S.O.; Munro, H.S.; Davies, C.; Kang, E.T. *Synth. Met.* 1988, 22: 365.
117. Castelvetro, V.; Colligiani, A.; Ciardelli, F.; Ruggieri, G.; Giordano, M. *New Polym. Mater.* 1990, 2: 93.
118. Havinga, E.E.; ten Hoeve, W.; Meijer, E.W.; Wynberg, H. *Chem. Mater.* 1989, 1: 650.
119. Innis, P.C.; Chen, Y.C.; Ashraf, S.; Wallace, G.G. *Polymer* 2000, 41: 4065.
120. Pickup, P.G. *J. Electroanal. Chem.* 1987, 225: 273.
121. Segawa, H.; Shimidzu, T.; Honda, K. *J. Chem. Soc., Chem. Commun.* 1989, 132.
122. Kern, J.-M.; Sauvage, J.-P. *J. Chem. Soc., Chem. Commun.* 1989, 657.
123. Aizawa, M.; Wang, L. In *Polymeric Materials Encyclopedia, Vol. 3*. J.C. Salamone (Ed.). CRC Press, Boca Raton, FL, 1996, p. 2107; and references cited therein.
124. Potts, H.A.; Smith, G.F. *J. Chem. Soc.* 1957, 4018.
125. Hawkins, S.J.; Ratcliffe, N.M. *J. Mater. Chem.* 2000, 10: 2057.
126. Higgins, S.J. *Chem. Soc. Rev.* 1997, 26: 247; and references cited therein.
127. Godillot, P.; Korri-Youssoufi, H.; Srivastava, P.; El Kassmi, A.; Garnier, F. *Synth. Met.* 1996, 83: 117.
128. Garnier, F.; Korri-Youssoufi, H.; Srivastava, P.; Mandrand, B.; Delair, T. *Synth. Met.* 1999, 100: 89.
129. Elsenbaumer, R.L.; Eckhardt, H.; Iqbal, Z.; Toth, J.; Baughman, R.H. *Mol. Cryst. Liq. Cryst.* 1985, 118: 111.
130. Delabouglise, D.; Garnier, F. *Synth. Met.* 1990, 39: 117.
131. Pleus, S.; Schwientek, M. *Synth. Met.* 1998, 95: 233.
132. Moutet, J.-C.; Saint-Aman, E.; Tran-Van, F.; Angibeaud, P.; Utille, J.-P. *Adv. Mater.* 1992, 4: 511.
133. Hasegawa, H.; Kijima, M.; Shirakawa, H. *Synth. Met.* 1997, 84: 177.
134. Chen, Z.; Gale, P.A.; Beer, P.D. *J. Electroanal. Chem.* 1995, 393: 113.

135. Buffenoir, A.; Bidan, G.; Chalameau, L.; Soury-Lavergne, I. *J. Electroanal. Chem.* 1998, 451: 261.
136. Ribo, J.M.; Dicko, A.; Valles, M.A.; Claret, J.; Daliemer, P.; Ferrer-Anglada, N.; Bonnett, R.; Bloor, D. *Polymer* 1993, 34: 1047.
137. Yurtsever, E.; Esenturk, O.; Pamuk, H.O.; Yurtsever, M. *Synth. Met.* 1998, 98: 229.
138. Joo, J.; Lee, J.K.; Baeck, J.S.; Kim, K.H.; Oh, E.J.; Epstein, J. *Synth. Met.* 2001, 117: 45.
139. Cho, S.H.; Song, K.T.; Lee, J.Y. in *Handbook of Conducting Polymers: Theory, Synthesis, Properties and Characterization*, Eds. Skotheim, T. and Reynolds, J.R. (3rd Edition), CRC Press, Boca Raton, FL, 2007: 8–1.
140. Nazzal, A.I.; Street, G.B. *J. Chem. Soc. Chem. Commun.* 1984, 2: 83.
141. Oh, E.J.; Jang, K.S. *Synth. Met.* 2001, 119: 109.
142. Turcu, R.; Graupner, W.; Filip, C.; Bot, A.; Brie, M.; Grecu, R. *Adv. Mater. Opt. Electron.* 2000, 9: 157.
143. Mitchell, G.R. *Polym. Commun.* 1986, 27: 346.
144. Mitchell, G.R.; Geri, A. *J. Phys. D: Appl. Phys.* 1987, 2: 1346.
145. Mitchell, G.R.; Davis, F.J.; Kiani, M.S. *Br. Polym. J.* 1990, 23: 157.
146. Pruneanu, S.; Graupner, W.; Oniciu, L.; Brie, M.; Turcu, R. *Mater. Chem. Phys.* 1996, 46: 55.
147. Pruneanu, S.; Resel, R.; Leising, G.; Brie, M.; Graupner, W.; Oniciu, L. *Mater. Chem. Phys.* 1997, 48: 240.
148. Yamaura, M.; Hagiwara, T.; Iwata, K. *Synth. Met.* 1988, 26: 209.
149. Jang, K.S.; Moon, B.; Oh, E.J.; Hong, H.J. *Polymer-Korea* 2003, 27: 323.
150. Ashrafi, A.; Golozar, M.A.; Mallakpour, S. *Synth. Met.* 2006, 156: 1280.
151. Nogami, Y.; Pouget, J.P.; Ishiguro, T. *Synth. Met.* 1994, 62: 257.
152. Yoon, C.O.; Sung, H.K.; Kim, J.H.; Barsoukov, E.; Kim, J.H.; Lee, H. *Synth. Met.* 1999, 99: 201.
153. Warren, M.R.; Madden, J.D. *Synth. Met.* 2006, 156: 724.
154. Davidson, R.G.; Hammond, L.C.; Turner, T.G.; Wilson, A.R. *Synth. Met.* 1996, 81: 1.
155. Eftekhari, A.; Kazemzad, M.; Keyanpour-Rad, M. *Polym. J.* 2006, 38: 781.
156. Lemon, P.; Haigh, J. *Mater. Res. Bull.* 1999, 34: 665.
157. Qu, L.T.; Shi, G.Q.; Yuan, J.Y.; Han, G.Y.; Chen, F. *J. Electroanal. Chem.* 2004, 561: 149.
158. Li, J.; Wang, E.; Green, M.; West, P.E. *Synth. Met.* 1995, 74: 127.
159. Barisci, J.N.; Stella, R.; Spinks, G.M.; Wallace, G.G. *Electrochim. Acta* 2000, 46: 519.
160. Yang, R.; Evans, D.F.; Christensen, L.; Hendrickson, W.A. *J. Phys. Chem.* 1990, 94: 6117.
161. Jeon, D.; Kim, J.; Gallagher, M.C.; Willis, R.F.; Kim, Y.T. *J. Vac. Sci. Technol.* 1991, B9: 1154.
162. Avlyanov, J.K.; Kuhn, H.H.; Josefowicz, J.Y.; MacDiarmid, A.G. *Synth. Met.* 1997, 84: 153.
163. Silk, T.; Hong, Q.; Tamm, J.; Compton, R.G. *Synth. Met.* 1998, 93: 59.
164. Silk, T.; Hong, Q.; Tamm, J.; Compton, R.G. *Synth. Met.* 1998, 93: 65.
165. Gandhi, M.; Spinks, G.M.; Burford, R.P.; Wallace, G.G. *Polymer* 1995, 36: 4761.
166. Jang, J.; Oh, J.H.; Stucky, G.D. *Angew. Chem. Int. Ed.* 2002, 41: 4016.
167. Selvan, S.T. *Chem. Commun.* 1998, 351.
168. Selvan, S.T.; Spatz, J.P.; Klok, H.-A.; Moller, M. *Adv. Mater.* 1998, 10: 132.
169. Jang, J.; Yoon, H. *Chem. Commun.* 2003, 720.
170. Zhang, X.; Zhang, J.; Song, W.; Liu, Z. *J. Phys. Chem. B* 2006, 110: 1158.
171. Yang, X.; Dai, T.; Lu, Y. *Polymer* 2006, 47: 441.
172. Shi, S.; Ge, D.; Wang, J.; Jiang, Z.; Ren, L.; Zhang, Q. *Macromol. Rapid Commun.* 2006, 27: 926.

173. Mansouri, J.; Burford, R.P. *J. Memb. Sci.* 1994, 87: 23.
174. Wu, C.G.; Bein, T. *Science* 1994, 264: 1757.
175. Zuppiroli, L.; Beuneu, F.; Mory, J.; Enzel, P.; Bein, T. *Synth. Met.* 1993, 55: 5081.
176. Cepak, V.M.; Martin, C.R. *Chem. Mat.* 1999, 11: 1363.
177. Martin, C.R. *Acc. Chem. Res.* 1995, 28: 61.
178. Martin, C.R. *Science* (1994) 266: 1961.
179. Duchet, J.; Legras, R.; Demoustier-Champagne, S. *Synth. Met.* 1998, 98: 113.
180. Demoustier-Champagne, S.; Duchet, J.; Legras, R. *Synth. Met.* 1999, 101: 20.
181. Demoustier-Champagne, S.; Stavaux, P.-Y. *Chem. Mater.* 1999, 11: 829.
182. Mativetsky, J.M.; Datars, W.R. *Physica B* 2002, 324: 191.
183. Delvaux, M.; Duchet, J.; Stavaux, P.-Y.; Legras, R.; Demoustier-Champagne, S. *Synth. Met.* 2000, 113: 275.
184. Misoska, V.; Price, W.; Ralph, S.F.; Wallace, G.G. *Synth. Met.* 2001, 121: 1501.
185. Bartlett, P.N.; Birkin, P.R.; Ghanem, M.A.; Toh, C.S. *J. Mater. Chem.* 2001, 11: 849.
186. Wang, D.; Caruso, F. *Adv. Mater.* 2001, 13: 350.
187. Yoshino, Y.; Kawagashi, Y.; Tatsuhara, S.; Kajii, H.; Lee, S.; Fujii, A.; Ozaki, M.; Zakhidov, A.; Vardeny, Z.V.; Ishikawa, M. *Microelectron. Eng.* 1999, 47: 49.
188. Cassagneau, T.; Caruso, F. *Adv. Mater.* 2002, 14: 34.
189. Krauss, T.F.; De La Rue, R. *Prog. Quantum Elect.* 1999, 23: 51.
190. Jerome, C.; Labaye, D.; Bodart, I.; Jerome, R. *Synth. Met.* 1999, 101: 3.
191. Jerome, C.; Jerome, R. *Agnew. Chem. Int. Ed.* 1998, 37: 2488.
192. Lu, G.; Li, C.; Shi, G. *Polymer* 2006, 47: 1778.
193. Shen, Y.; Wan, M. *J. Polym. Sci.* 1999, 37: 1443.
194. Liu, J.; Wan, M. *J. Mater. Chem.* 2001, 11: 404.
195. Wei, Z.; Wan, M. *Adv. Mater.* 2002, 14: 1314.
196. Qi, Z.; Lennox, R.B. *Electrochem. Proc.* 1997, 5: 173.
197. Sree, U.; Yamamoto, Y.; Deore, B.; Hiigi, H.; Nagaoka, T. *Synth. Met.* 2002, 131: 161.
198. Lu, Y.; Shi, G.; Li, C.; Liang, Y. *J. Appl. Polym. Sci.* 1998, 70: 2169.
199. Yuan, W.-L.; O'Rear, E.A.; Grady, B.P.; Glatzhofer, D.T. *Langmuir* 2002, 18: 3343.
200. Cochet, M.; Maser, W.K.; Benito, A.M.; Callejas, M.A.; Martinez, M.T.; Benoit, J.M.; Schreiber, J.; Chauret, O. *Chem. Comm.* 2001, 1450.
201. Fan, J.; Wan, M.; Zhu, D.; Chang, B.; Pan, Z.; Xie, S. *J. App. Polym. Sci.* 1999, 74: 2605.
202. Gao, M.; Dai, L.; Wallace, G.G. *Electroanalysis* 2003, 15: 1089.



---

# 3 Properties of Polypyrroles

The assembly of polypyrroles (PPy's) is an intricate process and determines the molecular structure and microstructure of the polymer obtained. This in turn influences the chemical, electrical, and mechanical properties of the material. It is impossible to optimize a single property of materials such as polypyrrole (PPy) in isolation. The chemical, electrical, and mechanical properties are inextricably linked.

To function as intelligent materials, conducting polymers must be capable of stimuli recognition, information processing, and response actuation. As a result, they must possess appropriate chemical properties that change in response to stimuli and appropriate electrical properties that allow information to be transported within the structure and switches to be actuated. The mechanical properties must also be considered, because the creation of materials with ideal chemical and electrical properties, but with inappropriate mechanical properties, will be of questionable value.

To fully optimize the material properties, the relationships between the structure and the properties must be thoroughly understood. The current state of knowledge concerning the electrical, chemical, and mechanical properties of PPy structures are reviewed in this chapter.

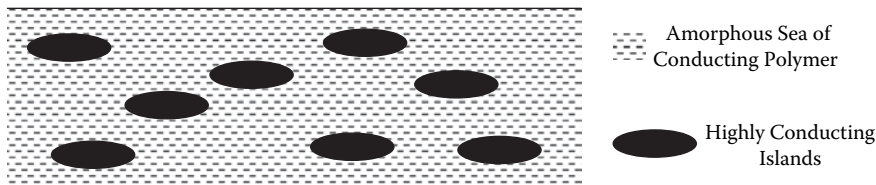
## **ELECTRICAL PROPERTIES: CONDUCTIVITY**

The electrical properties of intelligent materials are important as they determine the following:

- The ability to transport information from one part of the structure to another
- The ability to store information
- The ability to trigger responses
- The ability to convert and/or store energy

Electrical conductivity in PPy involves the movement of positively charged carriers and/or electrons along polymer chains and the hopping of these carriers between chains. It is generally believed that the intrachain hopping resistance is much greater than the interchain transport resistance.





**FIGURE 3.1** Highly conducting islands of polymer in a sea of amorphous, less conducting polymer.

Electron and x-ray diffraction data suggest that the polymer chains in electrochemically synthesized PPy lie parallel to the substrate electrode surface, as described in Chapter 2. This is reflected in the anisotropic nature of the conductivity of PPy.<sup>1</sup> The resistance along the surface of the film is known to be less than that across the film. However, this anisotropy is lost with thicker films.

At a more microscopic level, the variation of the bulk conductivity observed as a function of temperature is best explained using a model consisting of highly conducting islands of polymer in a sea of amorphous, less conducting material<sup>2,3</sup> as depicted in Figure 3.1.

Conductivity within conducting electroactive polymers (CEPs) is a complex issue. A polymer that can exhibit conductivity across a range of some 15 orders of magnitude most likely utilizes different mechanisms under different conditions. In addition to the electronic conductivity exhibited by CEPs, they possess ionic conductivity because of the solvent or electrolyte incorporated during synthesis. The experimental parameters encountered during synthesis (as listed and discussed in Chapter 2) have an effect on the polymer conductivity. In particular, the electrochemical conditions, the solvent, the counterion, and monomers used during synthesis influence the electronic properties of the resulting polymer.

The electrochemical conditions during synthesis can be manipulated to vary the concentration of electrons removed per unit time. This, of course, will have a dramatic effect on the resulting polymer. The polymer must be grown at potentials anodic enough to initiate polymerization, yet care must be taken not to overoxidize, because this results in less conductive materials. Previous workers<sup>4</sup> studied the effect of increased current density during growth on the conductivity of PPy/DS (DS = dodecyl sulfate) polymers. Over the range 2.0–8.8 mA/cm<sup>2</sup>, they indicated that initially an increase in conductivity was observed that leveled out and then dropped off again at higher current densities. As Diaz and Lacroix pointed out,<sup>5</sup> however, the optimal current density depends on the counterion/solvent system under investigation. They have shown that the quality of the films obtained deteriorated with the presence of nucleophiles during polymerization. Water itself can act as a nucleophile, attacking the pyrrole ring to form carboxyl groups that break up the polymer chain, thereby causing a decrease in conductivity and mechanical properties. The magnitude of this effect is electrolyte dependent because surfactants, for example, are known to stabilize the pyrrole radical<sup>6</sup> even in nucleophilic solvents. Despite this enhanced stability, other workers have shown that PPy/DS has higher conductivity when grown from CH<sub>3</sub>CN rather than water.<sup>7</sup>

It has been shown<sup>8</sup> that a cauliflower structure was observed for polymers grown from water because of hydrophobic effects. Such unevenness decreases conductivity. Aavapiryanont and coworkers<sup>9</sup> have also shown that the presence of small amounts of water affects the rate of growth and polymer conductivity. More recently, Trivedi and coworkers have shown that conducting polymers grown from ionic liquids have improved conductivity.<sup>10</sup>

The most studied of all variables is the counterion. Several workers<sup>11,12,13</sup> have shown that the incorporated counterion has a dramatic effect on the conductivity of the polymer. For a given counterion, the concentration employed also affects the conductivity of the resultant polymer.<sup>14</sup> Maddison and Jenden<sup>15</sup> even showed that counterion exchange after synthesis has an effect on the polymer conductivity. Conductivity decreases as the electron affinity of the counterion is increased. It has been reported<sup>16</sup> that the degree of oxidation of the polymer does not vary appreciably as the counterion is varied. The trend in conductivity is related to the nucleophilicity of the counterion employed; this may be due to some sort of anion-induced localization of the radical cation in the polymer. The effect of even slight changes in the molecular structure of the counterion on the conductivity of a range of PPy's has been studied<sup>17</sup> (Table 3.1). In some cases, the use of mixed counterion systems also has a marked effect on conductivity<sup>18</sup> (Table 3.2).

Other workers<sup>19</sup> indicated that anions can be exchanged after polymer growth with minimal effect on conductivity, suggesting that the polymer superstructure is determined during synthesis and the incorporation of other ions has minimal effect on this. The addition of functional groups to the pyrrole monomer influences the electronic properties of the resultant polymer. Steric effects introduced by bulky functional groups, for example, decrease the conductivity, particularly when present as N-substituents.<sup>20</sup> The presence of substituents on the 3-position of the pyrrole ring has less effect, but still results in a decrease in conductivity (see Table 3.3).

Other workers<sup>21</sup> have shown that conductivity can be improved by stretching the polymer after growth. The increase in conductivity occurred in the direction of stretching, and was caused by alignment of polymer units.

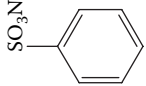
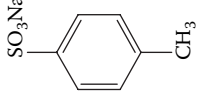
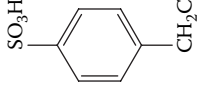
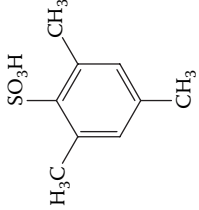
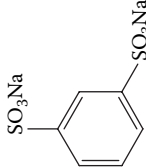
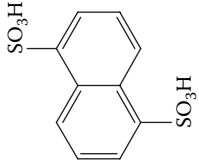
The conditions applied during chemical polymerization also influence the conductivity of the resultant polymer. For example, Kang and coworkers<sup>22</sup> used simultaneous chemical polymerization (using I<sub>2</sub> or Br<sub>2</sub>) at 0–4°C to produce more highly conducting polymers. Whang and coworkers<sup>23</sup> have shown that judicious choice of the Fe<sup>II</sup>/Fe<sup>III</sup> ratio, in order to manipulate the  $E^\circ$  value of the oxidizing solution, results in greatly improved conductivities.

## SWITCHING PROPERTIES

The fact that these unique polymer materials conduct electricity is fascinating enough, but the ability to switch their properties *in situ* using simple electrical stimuli is intriguing. Of course, this ability is dependent on possessing conductivity initially.

Charge can be reversibly added to or removed from a conducting polymer by cycling the material through oxidized and reduced states. As the switch from oxidized to reduced state occurs, there is a concomitant decrease in the conductivity.

**TABLE 3.1**  
**Effect of the Counterion on the Tensile Strength and Conductivity of Polypyrrole (PPy) Films**

| Counterions            | PPy/BSA<br> | PPy/pTS<br> | PPy/EBS<br> | PPy/MS<br> | PPy/BS<br> | PPy/NPS<br> |
|------------------------|--|--|---|---|---|--|
| Tensile strength (MPa) | 17–23  | 70–80  | 60–70   | 36–47   | 40–55   | 40–50  |
| Conductivity (S/cm)    | 19–20  | 90–110   | 90–110  | 50–70   | 47–70   | 50–70  |

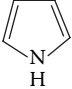
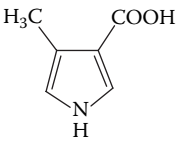
**TABLE 3.2**  
**Effect of Adding Dodecyl Sulfate (DS) to Polypyrrole/(PPy) Para-Toluene Sulfonate (pTS) Films**

| Composition of Polymerization Solution | 0.2 M PPy     | 0.2 M PPy   | 0.2 M PPy  | 0.2 M PPy  | 0.2 M PPy  | 0.2 M PPy  | 0.2 M PPy  |
|--|---------------|-------------|------------|------------|------------|------------|------------|
|  | 0.05 M pTS    | 0.05 M pTS  | 0.05 M pTS | 0.05 M pTS | 0.05 M pTS | 0.05 M pTS | 0.05 M pTS |
|  | No SDS        | 0.0025 M DS | 0.005 M DS | 0.01 M DS  | 0.02 M DS  | 0.05 M DS  | No pTS     |
| Composition of membranes               | PPy/pTS (pTS) | PPy/pTS/DS  | PPy/pTS/DS | PPy/pTS/DS | PPy/pTS/DS | PPy/pTS/DS | PPy/DS     |
| Conductivity (S/cm)                    | 105 ± 10      | 94 ± 8      | 82 ± 5     | 73 ± 7     | 70 ± 7     | 65 ± 7     | 40 ± 9     |
| Tensile strength (MPa)                 | 70 ± 6        | 63 ± 6      | 55 ± 6     | 24 ± 5     | 12 ± 3     | 5 ± 2      | 3 ± 2      |
| Thickness (µm)                         | 4.0 ± 0.3     | 4.5 ± 0.3   | 5 ± 0.3    | 5.5 ± 0.3  | 6.0 ± 0.3  | 6.3 ± 0.3  | 9.0 ± 0.4  |

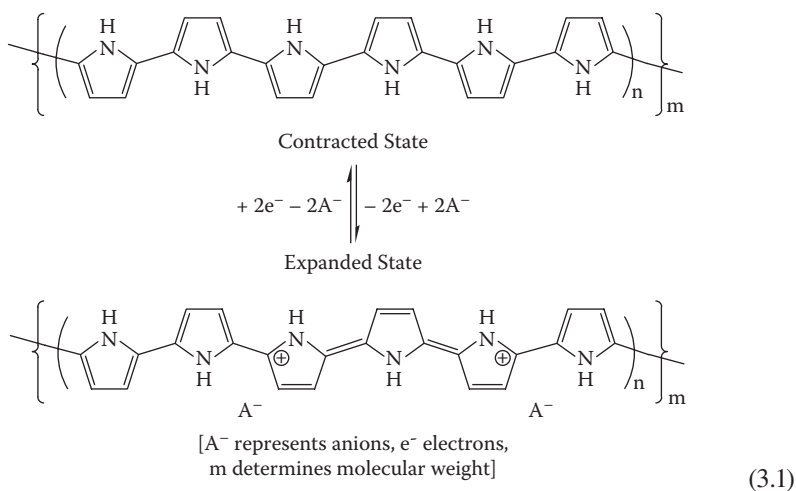
*Note:* All films were prepared using the same electrochemical conditions. Polymerization current density = 2 mA/cm<sup>2</sup>; polymerization time = 10 min; amount of charge passed = 1.2 C/cm<sup>2</sup>.

*Source:* From Zhao, H.; Price, W.E.; Wallace, G.G. *J. Memb. Sci.* 1994, 87: 47.

**TABLE 3.3**  
**Effect of Substituents on Conductivity**  
**of PPy's**

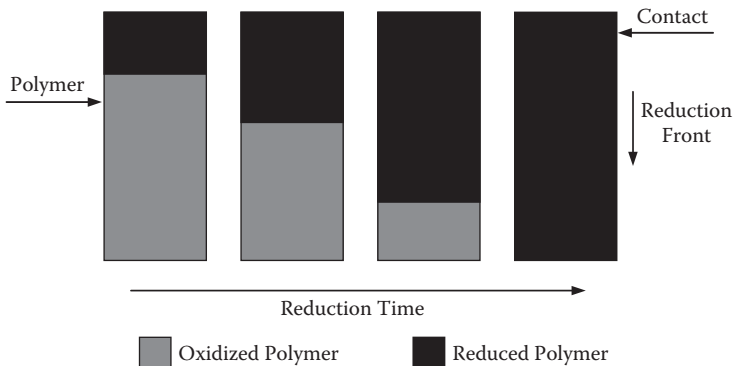
|   | Typical Conductivity Range |
|---|----------------------------|
|  | 90–110                     |
|  | 2                          |

The process for PPy's is often described rather simplistically as indicated in Equation 3.1:

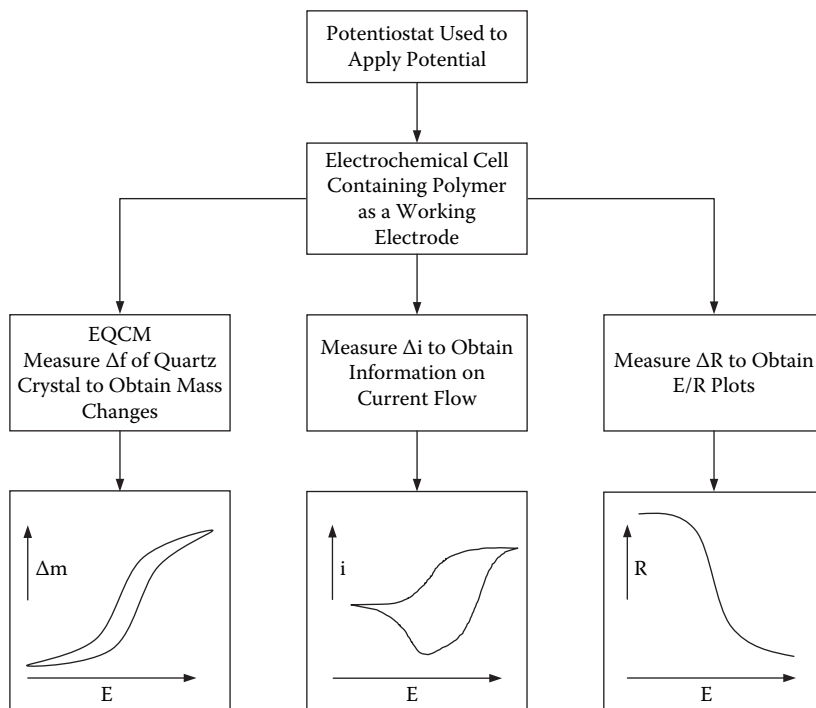


The switch involves mass and charge transport in the film, and charge transfer at the point of electrical contact (usually an inert electrode substrate). It has been shown previously<sup>24</sup> that reduction proceeds from the point of electrical contact, as does reoxidation (Figure 3.2).

At a molecular level, it is envisaged that the reduction front percolates through the polymer material, limited (in simple cases) by the diffusion of anions out of the polymer material. The composition of the film is not uniform but varies with time during the conversion process. Upon reoxidation, anions must be reinserted into the polymer, usually a slower process. The reoxidation is less energy efficient because the reduced polymer is less conductive.



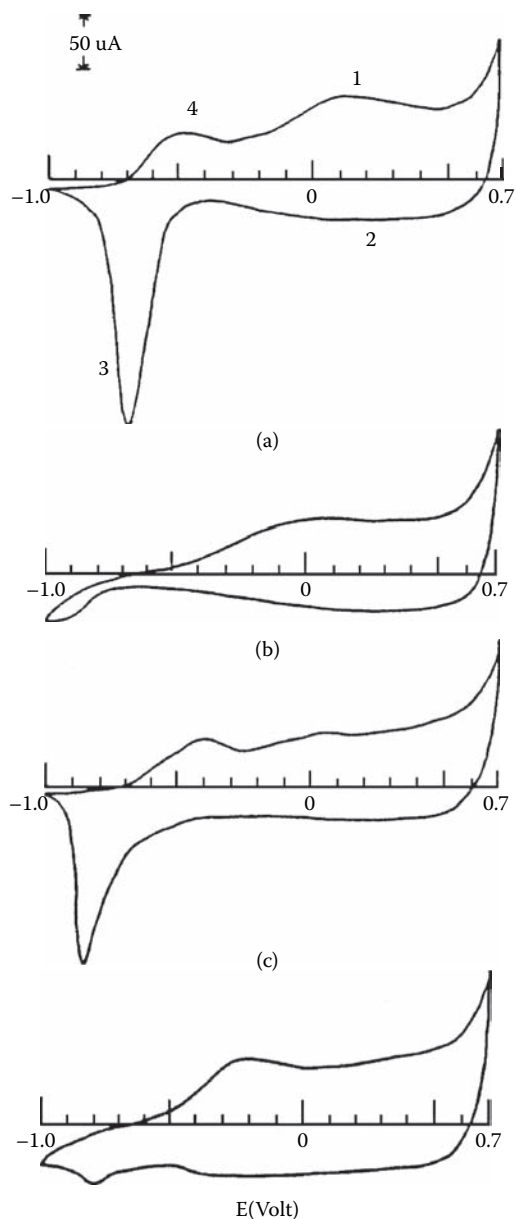
**FIGURE 3.2** Schematic illustrating reduction of a conducting polymer.



**FIGURE 3.3** The multidimensional analyses technique used to obtain  $\Delta i$ ,  $\Delta m$ , and  $\Delta R$  as the polymer is oxidized and reduced. ( $\Delta i$  = changes in current flow,  $\Delta m$  = changes in mass, and  $\Delta R$  = transitions in resistance).

As discussed in Chapter 1, these processes can be studied more closely *in situ* using a number of techniques (Figure 3.3). One technique allows current flow, mass changes, and transitions in resistance to be monitored *in situ* as the polymer is oxidized or reduced.

A typical cyclic voltammogram and a corresponding cyclic resistogram for a well-defined polymer system are shown in Chapter 1, Figure 1.23. The mass



**FIGURE 3.4** Cyclic voltammograms obtained for PPy/pTS coated electrodes: (a) 0.2 M KCl, (b) 0.2 M  $\text{CaCl}_2$ ; and for PPy/MS coated electrodes: (c) 0.2 M KCl, (d) 0.2 M  $\text{CaCl}_2$ . Scan rate: 20 mV/s. (From Zhao, H.; Price, W.E.; Wallace, G.G. *J. Memb. Sci.* 1994, 87: 47. p. 51. With permission from Elsevier Science-NL, Sara Burgerhartstraat, 1055 kV Amsterdam, The Netherlands.)

changes observed can be attributed to anion movement (see Equation 3.1) as the polymer is oxidized and reduced. As the polymer is reduced, a well-defined resistance transition is also observed, which is reversed upon reoxidation. The resistance changes observed do not accompany the current flow due to oxidation/reduction but lag behind it owing to the ion-exchange process occurring more slowly.

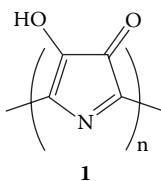
The following factors are important as far as the design of intelligent material systems is concerned:

- The electrical potential of transitions
- The rate of transitions
- Molecular events occurring during transitions

Several parameters will influence the electrochemical switching process. The most important are

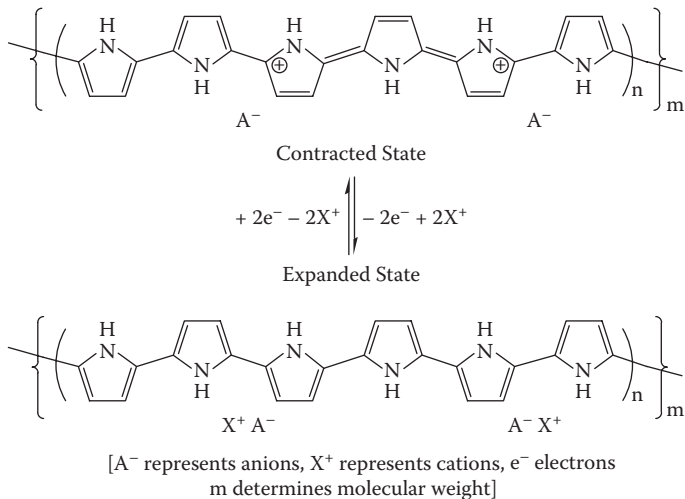
- The anion or cation incorporated during synthesis
- The solvent/electrolyte system used

The effect of the anion on the cyclic voltammograms obtained during cyclic voltammetry is shown in Figure 3.4. These cycles can be repeated, provided the potential range is restricted. If the potential applied is too positive, overoxidation of the polymer occurs.<sup>25,26</sup> This overoxidation process ultimately results in the formation of the following product **1**:



This polymeric material has inferior electrical and mechanical properties. If the potential applied is too negative, hydrogen evolution and subsequent deterioration of the polymer occur. Using the same electrochemical quartz crystal microbalance (EQCM) techniques, previous workers<sup>27,28,29</sup> have shown that cations ( $X^+$ ) are incorporated during the reduction of PPy's with large counterions that cannot be removed according to Equation 3.2:





(3.2)

As the polymer is reduced, anions are no longer electrostatically attracted and can leave the polymer; however, if this process is too slow, then charge compensation may be achieved by cation incorporation, the cation coming from the electrolyte in which the polymer is reduced. In some cases, where the anion incorporated during the synthesis is bulky (e.g., a polyelectrolyte such as polyvinyl sulfonate) and/or has a bulky hydrophobic component (e.g., a surfactant molecule such as dodecyl sulfate), the cation incorporation process will predominate and the polymer mass will increase upon reduction (see Chapter 1). The change in resistance, at least in solution as measured here, is much less when cation rather than anion movement predominates in the polymer oxidation/reduction process.

Although the role of the solvent during synthesis is probably more important in determining the conductivity and porosity of the polymer (as these contribute to the kinetics of switching), it may also be important in determining the electrodynamic properties. It has been shown that water will solvate polymers such as PPy,<sup>30</sup> and this influences conductivity, and consequently, switching. Also, other workers<sup>31,32</sup> have shown that there is substantial movement of solvent in or out of the polymer during the oxidation/reduction process, which may also contribute to changes in mass.

Even subtle changes in the counterion play a direct role in influencing switching characteristics. For example, it has been shown that the counterion incorporated during synthesis affects the ion-exchange selectivity series (Table 3.4), which then influences switching characteristics. Because charge can only move in tandem with a chemical transformation, the mobility/affinity (for the polymer) of the counterion is extremely important. Visy and coworkers<sup>33</sup> indicated that the nature of the counterion is only important when dehydrated. They observed major differences with different counterions in acetonitrile, but with other data quoted for water no major difference was found. Others<sup>34</sup> have shown that the counterion incorporated during synthesis affects both the potential and the rate of switching processes.

The effect of even subtle changes in the structure of sulfonated counterions influences the switching process. These changes are evident in the cyclic resistograms<sup>35</sup>

**TABLE 3.4**  
**Ion-Exchange Sequence**

| Polymer Composition | Ion-Exchange Sequence  |
|---------------------|--|
| PPy/Cl              | $\text{Br}^- > \text{SCN}^- > \text{SO}_4^{2-} > \text{I}^- > \text{CrO}_4^{2-}$               |
| PPy/ $\text{ClO}_4$ | $\text{SCN}^- > \text{Br}^- > \text{I}^- > \text{SO}_4^{2-} > \text{CrO}_4^{2-}$               |
| Conventional resin  | $\text{SO}_4^{2-} > \text{I}^- > \text{CrO}_4^{2-} > \text{Br}^- = \text{SCN}^- > \text{Cl}^-$ |

recorded during the switching of a number of PPy's with different sulfonated counterions. These small differences at a molecular level are often amplified during switching. Not only do the initial steps depend on anion-exchange processes, but subsequent steps during switching are also influenced by the chemical (e.g., hydrophobic or hydrophilic) and physical (e.g., resistance) characteristics induced in the polymer by the inserted ions.

Salmon and coworkers<sup>16</sup> showed that the nature of the monomer was important in determining the switching potential. Specifically, he found that poly-*N*-methylpyrrole was more difficult to oxidize or reduce than PPy, and that intermediate potentials were required to switch copolymers of these two pyrroles. An elegant study by Delabougli and Garnier showed how attaching various amino acids to the polymer backbone could be used to modify the switching characteristics.<sup>36</sup>

Salmon and coworkers<sup>16</sup> reported that although *N*-substituted pyrroles could be switched, it required greater potentials to do so. This was not always due to conductivity changes (e.g., *N*-phenyl [ $\sigma = 10^{-3} \text{ S cm}^{-1}$ ,  $E^\circ = 650 \text{ mV}$ ] and *i*-butyl [ $\sigma = 2 \times 10^{-5} \text{ S cm}^{-1}$ ,  $E^\circ = 600 \text{ mV}$ ]). Presumably, this was due to differing monomer/counterion affinities.

Other workers have shown that the use of copolymers of pyrrole with substituted pyrroles (*N*-methylpyrrole, in this case) can be used to alter the switching potential.<sup>37</sup> In our laboratories, studies involving a functionalized PPy<sup>38</sup> have shown that the switching characteristics are markedly affected by the counteranion incorporated during the synthesis. Obviously, this counteranion effect can be amplified by the presence of certain substituents.

Zhang and Dong<sup>39</sup> have shown the importance of the supporting electrolyte on the switching properties using *in situ* resistance- and current-measuring techniques. Both the potential required to trigger the switching and the rate of switching are determined by the supporting electrolyte. The solubility of the ions in the solvent used and their affinity for the polymer matrix determine the switching behavior. In some electrolytes where the anion of the electrolyte is difficult to incorporate (e.g., DS), this has a marked effect on the switching characteristics, resulting in cation incorporation.

The electrolyte can also have another effect, not commonly recognized by many researchers, the *chaotropic effect*.<sup>40</sup> This effect, more commonly discussed in biochemical circles, is related to variations in the water-structuring ability of different salts. This ability is used, for example, to dehydrate and salt out macromolecular proteins. The same effect can be expected with conducting polymers. As well as ion-size effects, this may be used to explain the large shifts in switching potentials observed in different electrolytes<sup>41</sup> when the cation was varied and the difference in overoxidation potentials observed in different electrolytes.<sup>42</sup>

The presence of nucleophiles during potential scanning decreases polymer stability because the polymer becomes reactive at anodic potentials.<sup>43</sup> This finding was used to demonstrate the formation of covalent bonds between OH<sup>-</sup> or CN<sup>-</sup> and pyrrole at positive potentials.

The use of ionic liquid electrolytes has been shown to influence electrochemical switching potentials.<sup>44</sup> However, even more significant with the use of ionic liquid electrolytes is the ability to greatly expand the electrochemical potential window within which conducting polymers retain their physical and mechanical properties.<sup>45,46</sup>

The size of the electrode also affects switching properties. The ability to switch at high scan rates has been demonstrated previously by other workers, using micro-electrodes.<sup>47</sup> Conversely, larger electrodes will be slower to switch, and the degree (percentage of material affected) of switching will be much less efficient.

## CHEMICAL AND BIOCHEMICAL PROPERTIES

The chemical properties of the CEP structure determine the ability to recognize particular stimuli and respond to them appropriately. In addition, these properties determine how the conducting polymer interacts with other materials in the construction of composite intelligent material structures. Most polymers are capable of, and indeed do, interact with other molecules. Such molecules may be part of larger molecular structures (important in the area of compatible materials), or they may be solvent molecules (such interaction can influence many processes including dissolution) or specific molecules in a solvent or gaseous medium.

As shown in Table 3.5, all such interactions can be broken down into definable modes of molecular interactions. Organized in appropriate spatial and temporal domains, these interactions combine to give rise to chemical recognition phenomena such as complexation and enzyme or antibody/antigen interactions. In a more general sense, how these interactions are influenced by environmental stimuli determines the behavior of the polymer system.

The most common interaction of polymers is with solvents. However, only a limited number of studies have been carried out to investigate the effect of solvents on PPy's. We have considered the use of dynamic contact angle analyses and have shown that the ability of PPy's to interact with water is influenced by the counterion employed during synthesis and the presence of functional groups on the polymer backbone.<sup>48</sup> These preliminary studies have also shown that in the process of exposing PPy's to water, the polymer structure responds by becoming easier to wet. This is evident from the subsequent dynamic contact angle scan, showing that the polymer is reluctant to shed water that has previously been incorporated. Using more conventional contact angle measurements, we have determined that the wettability of conducting PPy's is markedly affected by the counterion incorporated during synthesis (Table 3.6).

Even simple PPy's (with simple counterions such as chloride or nitrate incorporated) are inherently versatile molecular structures, capable of undergoing all the interactions listed in Table 3.5. Most particularly, they are strong anion exchangers<sup>49,50,51</sup> that are also capable of undergoing hydrophobic interactions. Other ion-exchange groups (e.g., carboxy groups)<sup>52</sup> or self-doping sulfonate groups<sup>53</sup> can be

**TABLE 3.5**  
**Summary and Examples of the Types of Molecular Interactions**

| Molecular Interaction | Example | Relative Strength      | Distance Dependence | Directionality |
|-----------------------|---------|------------------------|---------------------|----------------|
| Ionic                 |         | Very strong            | $1/r$               | No             |
| Ion-dipole            |         | Strong                 | $1/r^2$             | Yes            |
| Polar                 |         | Moderate               | $1/r^3$             | Yes            |
| Ion-induction         |         | Weak                   | $1/r^4$             | No             |
| Dipole-induction      |         | Very weak              | $1/r^6$             | No             |
| London dispersion     |         | Very weak <sup>a</sup> | $1/r^6$             | No             |

<sup>a</sup> London dispersion forces increase with the size and polarizability of the molecule.

Permanent dipole moment.

Induced dipole moment.

Instantaneous dipole moment.

**TABLE 3.6**  
**Contact Angles Determined**  
**for Different PPy's**

| Substrate | Contact Angle (°) |
|-----------|-------------------|
| ITO       | 75.6              |
| PPy/Cl    | 65.0              |
| PPy/DS    | 59.7              |
| PPy/PAA   | 37.8              |

PPy = polypyrrole; ITO = indium tin oxide coated glass; DS = dodecyl sulfate; PAA = poly(acrylic acid).

added to the monomer prior to polymerization to modify these properties. For example, we have used the presence of the carboxy group to produce chromatographic stationary phases capable of separating small molecules or proteins by cation-exchange chromatography.<sup>52</sup> In these cases, the cation-exchange interactions took place on the carboxy groups.

A dramatic impact on chemical properties is achieved by the appropriate choice of counterion. The counterion employed during synthesis can have a marked effect on the anion-exchange selectivity series of conducting polymers.<sup>54</sup> Table 3.4 shows the anion-exchange selectivity series obtained for both polypyrrole chloride and polypyrrole perchlorate. As illustrated, polypyrrole salts do not behave similar to conventional ion-exchange resins.

The interplanar distance of neutral PPy has been reported to be 2.41 Å. If the anions are intercalated between the planes of PPy chains, as has been suggested previously (see Chapter 2), then the interplanar spacing should expand according to the size of the anions incorporated during synthesis. It appears that a small interplanar space is formed when small anions such as Cl<sup>-</sup> are used as counterions during polymerization. This small interplanar spacing makes it difficult to replace the anion within the polymer plane with a much larger anion from solution. This then affects subsequent ion-exchange processes.

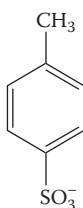
Results obtained from our work correlate with those predicted by the postulated hypothesis. The ionic radii of some ions used for ion-exchange investigations are as follows:

|           |                 |                 |                |                               |                               |                                |
|-----------|-----------------|-----------------|----------------|-------------------------------|-------------------------------|--------------------------------|
| Ions      | Cl <sup>-</sup> | Br <sup>-</sup> | I <sup>-</sup> | SO <sub>4</sub> <sup>2-</sup> | ClO <sub>4</sub> <sup>-</sup> | CrO <sub>4</sub> <sup>2-</sup> |
| Radii (Å) | 1.81            | 1.95            | 2.16           | 2.30                          | 2.36                          | 2.40                           |

The ion-exchange sequence (Table 3.4) on PPy/ClO<sub>4</sub> follows this sequence. Therefore, CrO<sub>4</sub><sup>2-</sup> was found to be more difficult to exchange with ClO<sub>4</sub><sup>-</sup> compared to other ions. The selectivity toward SO<sub>4</sub><sup>2-</sup> over CrO<sub>4</sub><sup>2-</sup> is amazing given the difference in size of 0.1 Å. This is probably due to the larger size of CrO<sub>4</sub><sup>2-</sup>, but suggests that the polymer chains are held rigidly in place once the polymer is formed. A similar

trend was noted on PPy/Cl. However, as  $\text{Cl}^-$  is smaller than  $\text{ClO}_4^-$ , lesser  $\text{Cl}^-$  could be exchanged.

In extreme cases, the incorporation of larger hydrophobic counterions (e.g., dodecyl sulfate) results in the formation of a polymer not capable of anion exchange but quite hydrophobic in nature.<sup>55,56</sup> Counterions that are intermediate in nature [e.g., *para*-toluenesulfonate **2**] induce intermediate behavior because they are charged, relatively small anions and have some hydrophobic character.

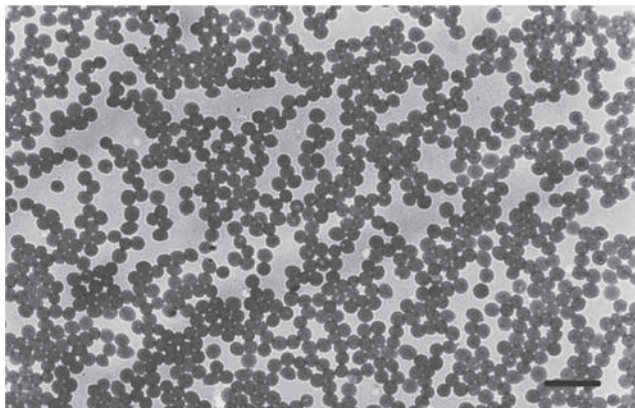


*Para*-toluene sulfonate (pTS)  
**2**

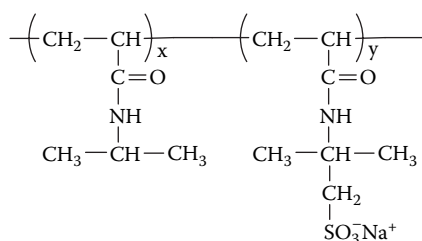
Polyelectrolytes may also be incorporated as counterions during synthesis<sup>57,58,59,60</sup> and as they would be difficult to remove, the anion-exchange capacity is again reduced as the cation-exchange capacity concomitantly increases.

It is also possible to incorporate a range of chemically functional counterions into PPy.<sup>61,62,63</sup> The fact that pyrrole can be polymerized from aqueous solutions enables a wide range of counterions to be included in the structure. In cases where a counterion with a specific activity is incorporated, the polymer may act as no more than a carrier or a means of electronic communication. Numerous examples of inclusion of antibodies<sup>64,65,66,67</sup> and enzymes<sup>68,69,70,71,72</sup> have been reported. In some cases, additives (molecular carriers) have been used to facilitate the incorporation of these large, low-charge-density molecules.<sup>73</sup> For example, the interaction of anionic surfactants with proteins to produce higher-charged molecules can be used to enhance incorporation. Another novel approach to facilitating protein incorporation involved the attachment of the biomolecule to colloidal gold prior to electropolymerization. Using appropriate assembly techniques, the bioactivity of such components can be retained even after immobilization in the conducting polymer.

It is also possible to integrate the chemical properties of other functional molecules into the conducting polymer by direct inclusion as the molecular dopant. For example, electrocatalysts,<sup>74,75,76</sup> complexing agents,<sup>77,78,79</sup> and polynucleotides<sup>80,81</sup> or even DNA<sup>82</sup> have all been incorporated to induce the specific properties of these molecules. We have successfully incorporated mammalian red blood cells during electrosynthesis, using polyelectrolytes in the synthesis mixture (Figure 3.5).<sup>83</sup> It is also possible to covalently attach bioactive sites to conducting polymers directly.<sup>84,85,86</sup> The use of such approaches to attach digionucleotides<sup>83,84</sup> is particularly exciting in that it provides a platform for a new range of DNA testing technologies. A range of temperature-sensitive polyelectrolytes<sup>87,88,89</sup> **3** have also been incorporated into conducting polymers to make the properties of the resultant materials temperature dependent.

Scale bar 30  $\mu\text{m}$ .

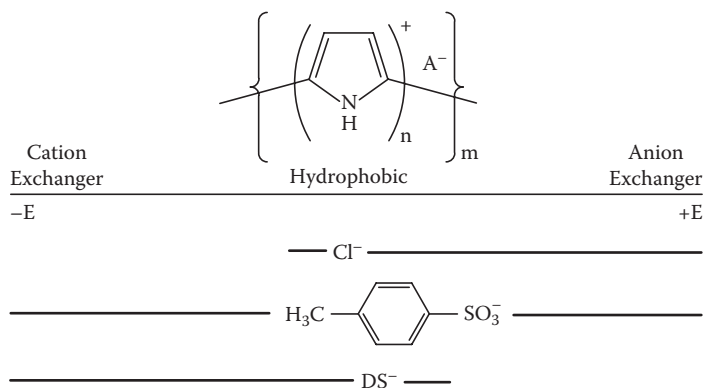
**FIGURE 3.5** A matrix formed by electropolymerizing pyrrole using human red blood cells and poly(vinyl sulfate) as dopant anion (using a current density of  $0.5 \text{ mA}\cdot\text{cm}^{-2}$  for 10 sec).



3

We have also shown how ion-exchange properties and hydrophobic character can be adjusted.<sup>90,91</sup> The potential stimuli or chemical property behavior is dependent on the counterion incorporated during synthesis, as discussed previously. As illustrated in Figure 3.6, the chemical interaction properties (cation exchange, hydrophobic, and anion exchange) and the way they vary as a function of potential are markedly dependent on the counterion ( $\text{Cl}^-$ ,  $\text{pTS}^-$ , or  $\text{DS}^-$ ) incorporated during synthesis.

In addition, the activity of incorporated functional molecules such as proteins can be altered by application of appropriate electrical stimuli.<sup>64,65,92,93</sup> In a previous work,<sup>94</sup> incorporation of proteins into phases suitable for affinity chromatography was demonstrated. It was also shown that the application of electrical potential influences the Ag–Ab interaction during the column load-up stage of the experiment. Although the mechanism is not absolutely clear, perhaps the application of potential changes the protein conformation owing to changes in the hydrophobicity of the polymer surface. Attempts to reverse the Ab–Ag interaction using applied potentials on the affinity column were unsuccessful. However, by using the same principles in the form of a sensing technology incorporated into a flow-injection analysis system and a repetitive-pulsed-potential waveform routine, reversibility of the interaction could be attained,<sup>65</sup> and the same phenomena have been used more recently in the development of new biosensing technologies.<sup>66,67,92,93,95</sup>

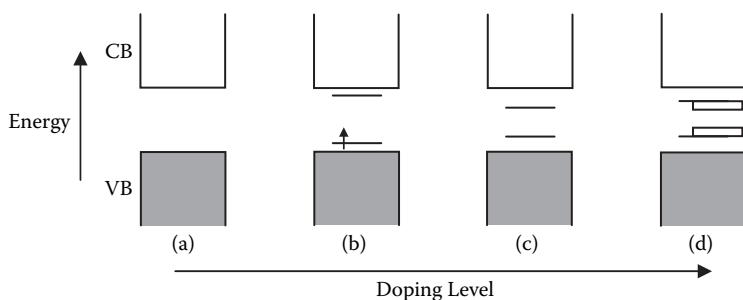


**FIGURE 3.6** A schematic illustration of the effect of applied potential on the ion-exchange properties of PPy's containing different counteranions (DS = dodecyl sulfate).

## OPTICAL PROPERTIES OF PPY'S

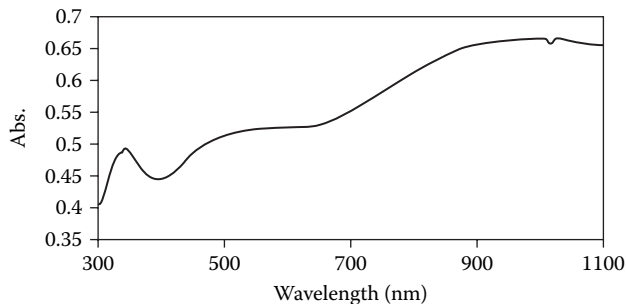
### ELECTRONIC BAND STRUCTURE

Figure 3.7 shows the electronic levels or bands proposed by Bredas and coworkers<sup>96</sup> for PPy, on the basis of semiempirical theoretical calculations, as it is progressively doped from its neutral undoped state to a maximum of ca. 35% doping. In its neutral state, PPy is predicted to have a very large  $\pi$ - $\pi^*$  (valence  $\rightarrow$  conduction) band gap of 3.2 eV. When one electron is removed to form a polaron (radical cation), two polaronic levels appear in the band gap as shown in Figure 3.7b. The lower of these polaronic levels is half-filled for such partly doped PPy's (with one positive charge for every 4–6 monomer units), as confirmed by an electron spin resonance (ESR) signal for the unpaired electron. Further electron removal results in the formation of a spinless bipolaron and the energy levels shown in Figure 3.7c (together with the loss of the ESR signal). These electronic states coalesce into bipolaron bands (Figure 3.7d) with further doping to ca. 35% (one positive charge for every three pyrrole monomer units). The  $\pi$ - $\pi^*$  band gap is also predicted<sup>90</sup> to increase to 3.6 eV.



**FIGURE 3.7** Calculated electronic levels or bands for PPy's with increasing doping (CB = conduction band, VB = valence band): (a) neutral polymer, (b) polaron orbitals form, (c) bipolaron orbitals form, and (d) bipolaron bands form.





**FIGURE 3.8** UV-visible spectrum of PPy/DNA grown galvanostatically ( $2 \text{ mA cm}^{-2}$ ) for 2 min onto ITO-coated glass from an aqueous solution containing 0.2 M pyrrole and 0.2% w/v salmon sperm DNA.

### UV-VISIBLE-NIR SPECTRA: DEPENDENCE ON DOPING LEVEL AND CHAIN CONFORMATION

The UV-visible spectra of PPy's and their changes with varying doping levels have, in a number of cases, been correlated with the previous predictions, as first discussed by Bredas and coworkers.<sup>96</sup> For example, the change in color of neutral PPy from pale yellow to gray-black as it is electrochemically oxidized to PPy/ $\text{ClO}_4$  is accompanied by progressive changes in the UV-visible-NIR (NIR = near infrared) spectrum consistent with the initial appearance of polarons and their subsequent replacement by bipolarons.<sup>97</sup> In general, highly doped PPy's exhibit two characteristic bipolaron bands at ca. 1.0 and 2.6 eV (1240 and 475 nm) as well as a  $\pi$ - $\pi^*$  band.<sup>98,99</sup>

A typical UV-visible spectrum obtained for PPy/DNA is shown in Figure 3.8. This reveals a  $\pi$ - $\pi^*$  band and bipolaron bands at ca. 525 and 1000 nm.

The position and shape of the bipolaron/polaron bands have been shown to be very dependent on environmental factors such as the deposition surface or solvent. These changes in UV-visible-NIR spectra are believed to arise from (and to be indicative of) conformational changes in the PPy chains. For example, whereas conducting PPy films deposited on hydrophilic glass surfaces exhibit an absorption band at ca. 1180 nm, this band is replaced by an intense free-carrier tail extending to 2600 nm for analogous films deposited on hydrophobic, silanized glass.<sup>100</sup> By analogy with related studies of polyanilines (see Chapter 5), the presence of the free-carrier tail for PPy deposited on hydrophobic surfaces is attributed to the adoption of an *extended coil* conformation by the polymer chains. This contrasts with the *compact coil* conformation favored on hydrophobic surfaces.

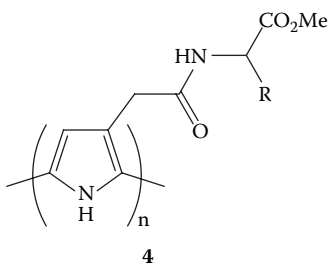
Similar marked changes in their UV-visible-NIR spectra occur for the recently discovered<sup>101</sup> "soluble" PPy's when the organic solvent is varied.<sup>97,102,103,104</sup> For example, the bipolaron band observed at 475 nm for PPy/DBSA (DBSA = dodecylbenzenesulfonate) in chloroform solvent undergoes a large blue shift to ca. 425 nm with *m*-cresol or dimethyl sulfoxide (DMSO) as solvent.<sup>97,100</sup> This suggests a shorter conjugation length for the PPy in *m*-cresol and DMSO. This is consistent with the lower electrical conductivity observed for PPy/DBSA films cast from solutions in *m*-cresol than from chloroform solutions.<sup>99</sup> The intensity of the NIR bipolaron band of PPy/

DBSA is also very sensitive to the nature of the organic solvent. Oh and coworkers<sup>103</sup> reported that this NIR band is more intense in relatively nonpolar solvents such as chloroform than in the aromatic solvents *m*-cresol or benzylalcohol, and is markedly reduced in the polar solvents DMSO and *N*-methyl pyrrolidinone (NMP) as well as blue-shifted to ca. 850–900 nm. These spectral changes were attributed to micelle formation by the DBSA and solvent interactions with the PPy chains. This leads to rearrangement of the polymer backbone from an extended coil conformation in chloroform to a relatively compact coil one in NMP and DMSO.

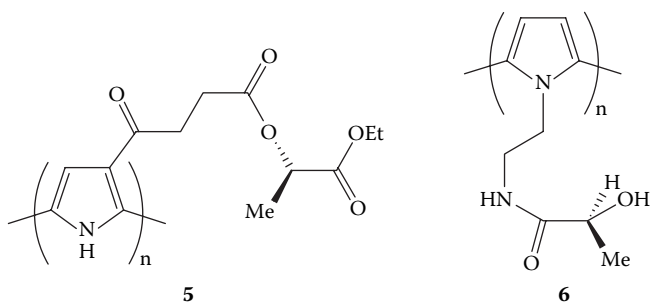
Similar changes have been recently observed in the intensity and wavelength of the NIR bipolaron band of the polymer PPy/DEHS [DEHS = di(2-ethylhexyl)sulfosuccinate] in alcohol solvents of varying polarity.<sup>102</sup> The nonpolar 2-ethylhexyl groups are believed to solvate the PPy chains more effectively in weakly polar alcohols such as *t*-butyl alcohol, resulting in an extended coil conformation and an intense NIR free-carrier tail. In contrast, in polar ethanol or 2,2,2-trifluoroethanol solvents this solvation is less effective, leading to the adoption of a compact coil conformation and markedly less-intense NIR absorption.

## CHIROPTICAL PROPERTIES OF OPTICALLY ACTIVE PPy'S

The first reported circular dichroism (CD) study of chiral PPy's was by Delabouglise and Garnier<sup>105</sup> on the polymers **4** (R = CH<sub>2</sub>OH, CHMe<sub>2</sub>, and Ph), in which a series of amino acids are covalently bound at the 3-position of each pyrrole ring. They exhibit a CD band at ca. 470 nm associated with the absorption band at 460 nm. This optical activity is believed to be induced by the presence of the chiral amino acid substituents, leading to the adoption of a one-handed helical structure by the PPy chains.



More recently, Pleus and Schwientek<sup>106</sup> prepared a series of related chiral PPy's bearing (–)-ethyl L-lactate as the chiral functional group located at either the pyrrole ring 3-position or the ring N centre (e.g., polymers **5** and **6**). Although no CD studies were carried out on the PPy films, cyclic voltammograms recorded in the presence of (+)– or (–)-CSA<sup>–</sup> (CSA<sup>–</sup> = camphor sulfonate) revealed them to be enantioselective. Preferential doping of the chiral PPy by the (–)-CSA<sup>–</sup> anion took place, as indicated by the substantially higher charge passed when cycling the potential in the presence of this enantiomer rather than (+)-CSA<sup>–</sup>. Similar enantioselectivity between the (+)– and (–)-CSA<sup>–</sup> ions is exhibited by optically active films of the polymer **6**, which has a glucose derivative covalently bound at the pyrrole N centers.<sup>107</sup>



## ELECTROCHEMICAL ASYMMETRIC SYNTHESIS, CHIRAL SEPARATIONS, AND SENSING

Very significantly, recent studies by Pleus and coworkers<sup>108</sup> have revealed that the conducting films **5** and **6** may be employed as chiral electrodes for the enantioselective electroreduction of acetophenone and 4-methylbenzophenone in DMF to their corresponding alcohols, using DMF/LiBr as electrolyte and phenol as the proton donor. The nature of the electrolyte used for electrodeposition of the polymers influenced the optical purity of the chiral alcohol products obtained with enantioselectivities as high as 58% being achieved.

Separation of enantiomeric amino acids using chiral-conducting PPy membranes has also been reported by Ogata.<sup>109</sup> The enantioselective membranes were prepared by electrodeposition of PPy in the presence of the chiral dopants poly(L-glutamic acid) or dextran sulfate onto a platinum-coated poly(vinylidene difluoride) membrane. The chiral separation of racemic tryptophan was demonstrated. In an alternative approach, Nagaoka and coworkers<sup>110</sup> have prepared molecularly imprinted PPy (by overoxidation of PPy doped with L-lactate and L-glutamate) for use in chiral separations. These chiral dopant anions were removed during electrochemical overoxidation and a complementary cavity for the anion created. The resultant imprinted PPy's exhibited high enantioselectivity for the L-acids over the D-enantiomers. A column packed with carbon fibers modified with the imprinted PPy's was used for the enantioselective uptake of the particular acid anion.

Recently, Costello and coworkers<sup>111</sup> developed chiral vapor-phase sensors based on chiral poly(3-substituted pyrroles). The chiral PPy's were fabricated into chiral sensors using a three-step process: (1) coating of the chiral monomer onto poly(vinylidene)difluoride (PVDF) membrane, (2) polymerization of the monomer within the membrane structure using an excess of aqueous ferric chloride oxidant, and (3) mounting the membrane between silver contacts to obtain the sensor. Chiral discrimination and sensor properties of the sensors were investigated using enantiomers of butanol, limonene, and carvone. The chiral polymer sensors were found to show differential changes in electrical resistance and mass when exposed to different enantiomers in the vapor phase. The results suggested that the chiral side group on the pyrrole repeat units plays the main role in the selective adsorption characteristics of the polymers.

## MECHANICAL PROPERTIES OF PPy

To be functional, any material must possess adequate mechanical properties to withstand the stresses and strains that occur during service. For example, stand-alone membranes must be sufficiently stiff to maintain their shape and sufficiently strong to resist rupture when subjected to pressure gradients. Similarly, coatings are subjected to high stress resulting from the different thermal expansion between coating and substrate. Thus, the coating material must show high ductility, so that it is able to expand and contract without cracking or delaminating. Membranes and coatings are just two of the many potential applications for CEPs, but they demonstrate the key importance of mechanical properties.

It is commonly recognized by researchers in this field that the mechanical properties of PPy's vary widely from strength and tenacity to extreme brittleness. Consequently, it is necessary to understand how the mechanical properties are affected by the chemical structure, the processing conditions, and the conditions of use (service environment). The ultimate aim is to develop and understand causal relationships between the structure of the PPy and the mechanical properties. Such relationships would enable the deliberate manipulation of the structure (e.g., by controlling the processing conditions) to produce desired mechanical properties.

The published work on the mechanical properties of PPy is reviewed below. Most of this work has been conducted on dry films, which is discussed first. Some recent work on the adhesion of PPy to electrode materials is also presented along with the results of investigations into environmental effects on mechanical properties.

### DRY-STATE MECHANICAL PROPERTIES

Several investigators have specifically studied the mechanical properties of PPy, whereas numerous others have reported such properties as incidental to other findings. The most commonly reported values are the Young's modulus ( $E$ , a measure of material stiffness), the tensile strength ( $\sigma_B$ ), and the percentage of elongation to break ( $\epsilon_B$ , a measure of ductility or brittleness). All tests described in Table 3.7 have been conducted in tension, using thin films as samples (apart from Bloor and coworkers<sup>12</sup> who used 1-mm-thick plates).

The most pertinent feature in Table 3.7 is the vast range of mechanical properties that have been reported for PPy. It is apparent that the composition of the polymer (e.g., counterion type) and the polymerization conditions have a significant effect on the polymer properties. However, the relationships are not straightforward. For example, Wynne and Street<sup>13</sup> have shown that acetonitrile solvent yields PPy films with very good mechanical properties, whereas Sun and coworkers<sup>11</sup> and others have reported the opposite. It is clear that systematic analyses are required to elucidate the determinants of the mechanical properties of PPy's.

Most of the previous studies have been empirical in nature. However, they have been important in demonstrating those factors that influence the mechanical properties. For example, mechanical properties of PPy films have been observed to improve as the polymerization temperature decreases. Sun and coworkers<sup>11</sup> have observed that the tensile strength of PPy/pTS increases as the synthesis temperature

**TABLE 3.7**  
**Summary of Mechanical Properties of PPy's**

| Polymerization Conditions <sup>a</sup>  | $E$ (GPa) | $s_b$ (MPa) | $\epsilon_g$ (%) | Variables Studied  | Reference               |
|---|-----------|-------------|------------------|--|-------------------------|
| Vitreous carbon and platinum<br>ACN + 0.5% water<br>Various counterions<br>$E_{app} = 3-6$ V<br>CD = 0.51-7.44 mA/cm <sup>2</sup> | —         | 18-55       | 7-27             | $E_{app}$ and CD during polymerization<br>Action of water during polymerization<br>Different counterions | Buckley et al. [117]    |
| Carbon electrode<br>Water or ACN + 0.7% water<br>pTIS-<br>$E_{app} = 3$ V<br>CD = 0.016 mA/cm <sup>2</sup><br>T = 0°C             | 1.2-3.5   | 35-76       | 16-50            | Plasticizing effect of residual solvent<br>Effect of polymerization solvent                              | Wynne and Street [113]  |
| Platinized electrodes<br>PC (with and without water)<br>pTIS-<br>CD = 0.3-3.2 mA/cm <sup>2</sup>                                  | 3.3-4.1   | 34-65       | 2.6-6.0          | 1 mm plates prepared<br>CD during polymerization varied<br>Plasticizing effect of water                  | Bloor et al. [112]      |
| Various solvents<br>pTIS-<br>$E_{app} = 0.8-1.3$ V  | —         | 8-59        | 7-17             | Effect of large additions of water to<br>ACN solvent<br>Effect of solvent additives                      | Diaz and Hal [120]      |
| Stainless steel<br>Water<br>Various counterions<br>CD = 1.3 mA/cm <sup>2</sup>  | —         | 17-68       | 1-10             | Various counterions  | Wettermark et al. [124] |

|   |         |          |                      |  |                          |
|---|---------|----------|----------------------|--|--------------------------|
| Titanium<br>ACN + 1% water or ACN +<br>PC + 1% water<br>pTS <sup>-</sup> E <sub>app</sub> = 0.7–1.1 V<br>CD = 0.7–3.5 mA/cm <sup>2</sup><br>T = 20 or –40°C       | 0.9–4.3 | 2–59     | 2–24                 | Reaction temperature<br>Aging<br>Added plasticizers  | Sun et al. [11]          |
| Titanium<br>PC + 1% water<br>pTS <sup>-</sup><br>E <sub>app</sub> = 1.0 V<br>CD = 0.3–1.0 mA/cm <sup>2</sup><br>T = 0 or 25°C                                     | 1.0–2.7 | 36–43    | 3–26                 | Aging  | Cvetko et al. [123]      |
| Carbon and platinum<br>PC + 1% water<br>PF <sub>6</sub> <sup>-</sup><br>Various E <sub>app</sub> and CD<br>Various T  | —       | —        | 670–180 <sup>b</sup> | Effect of polymerization conditions<br>on elongation of films  | Hagiwara et al.<br>[115] |
| Platinum<br>Iso-propylalcohol + diethylene<br>glycol or poly(ethylene glycol)<br>Boron trifluoride diethyl etherate<br>Constant E <sub>app</sub><br>T = 0 or 15°C | —       | 5.5–83.7 | 0.57–6.81            | Effect of cosolvents during<br>polymerization and effect of<br>polymerization temperature<br>Films formed on the front side and<br>back side of the working electrode<br>were compared | Wang et al. [116]        |

<sup>a</sup> Where reported, the polymerization conditions are summarized as: working electrode; solvent; counterion; applied potential (E<sub>app</sub>) if potentiostatic growth; current density (CD) if galvanostatic growth; polymerization temperature (T).

<sup>b</sup> Tested at 150°C.

pTS<sup>-</sup> = *p*-toluene sulfonate; ACN = acetonitrile; PC = propylene carbonate.

decreases. Similarly, Hagiwara and coworkers<sup>114,115</sup> have observed that the elongation to break of PPy/CIO<sub>4</sub> and PPy/PF<sub>6</sub> films, respectively, increase upon decreasing polymerization temperature. Sun and coworkers<sup>11</sup> attributed the differences in mechanical properties to changes in the molecular structure of the polymer (e.g., conjugation length or molecular weight) caused by the decreasing reaction temperature. Wang and coworkers<sup>116</sup> have shown that smoother films formed at lower polymerization temperatures lead to higher tensile strength and elongation to break, suggesting that the nodular surface structure and porosity act as stress concentrators.

The applied potential and current density used during electropolymerization have also been found to be significant variables. A steady decrease in the tensile strength of PPy/pTS films has been observed as the applied potential during polymerization was increased.<sup>117</sup> Another study reported lower tensile strengths for more highly doped PPy.<sup>118</sup> Other workers<sup>119</sup> have also reported a decrease in the Young's modulus of PPy/pTS with increasing applied potential during electropolymerization. No specific explanation has been offered for the behavior; however, it has been suggested<sup>117</sup> that the change in the mechanical properties may be associated with a decrease in the density of the films as the potential of polymerization was increased, with a "more open, mechanically less durable material" being produced. Hagiwara and coworkers<sup>114,115</sup> observed an increase in the elongation to break of PPy films as the potential was increased during polymerization. This was also accompanied by variations in film density. A similar correlation between density and mechanical strength has been noted by Wang and coworkers.<sup>116</sup> Higher densities and strengths were obtained by addition of specific cosolvents to the polymerization bath. Also, a comparison of films obtained on the front side (facing the cathode) and back side of the anode revealed a higher density and strength in the latter. Simple electron microscope (SEM) micrographs confirmed a more porous, rougher structure in the low-density films.

The solvent used during electropolymerization also affects mechanical properties. For example, Wynne and Street<sup>113</sup> observed that the incorporation of a small amount of water with acetonitrile as the polymerization solvent improves the mechanical properties of the PPy/pTS films. This was attributed either to differences in the composition or in molecular weight. However, the latter was not determined, and minimal differences were reported in the former. In contrast, others<sup>120</sup> have shown that large additions of water to acetonitrile result in a substantial decrease in strength. It has also been noted that PPy/pTS films formed from propylene carbonate were superior to those formed from acetonitrile solvent in terms of mechanical properties, but again, reasons were not suggested.<sup>121</sup>

Several researchers have observed that PPy films may be plasticized by solvents such as water, leading to a decrease in brittleness.<sup>11,107,113,117</sup> Wynne and Street<sup>113</sup> showed that PPy/pTS reversibly absorbs moisture, causing plasticization of the films. Sun and coworkers<sup>11</sup> have noted that the loss of moisture from PPy/pTS films with time leads to embrittlement, and the incorporation of phthalate plasticizers into the films improved ductility. Similarly, several workers<sup>122,123</sup> have used surfactants as counterions, resulting in a good plasticizing effect.

By far the most important processing variable for mechanical properties is the type of counterion used (Table 3.7). The effects of various counterions incorporated

into PPy films on the mechanical properties have been studied by several workers.<sup>117,121,123</sup> For example, Cvetko and coworkers<sup>123</sup> observed that the pTS<sup>-</sup> counterion produced flexible films, whereas all other counterions investigated produced brittle films. These other counterions included BF<sub>4</sub><sup>-</sup>, AsF<sub>6</sub><sup>-</sup>, ClO<sub>4</sub><sup>-</sup>, HSO<sub>4</sub><sup>-</sup>, BrC<sub>6</sub>H<sub>4</sub>SO<sub>3</sub><sup>-</sup>, and CF<sub>3</sub>COO<sup>-</sup>. Our own studies (Tables 3.1 and 3.2) have also demonstrated the dramatic effect the choice of counterion has on tensile strength.

Buckley and coworkers<sup>117</sup> have further investigated the effects of counterion structure on the mechanical properties of PPy films by using variations on the pTS<sup>-</sup> structure, for example, C<sub>6</sub>H<sub>5</sub>SO<sub>3</sub><sup>-</sup>, CH<sub>3</sub>CH<sub>2</sub>C<sub>6</sub>H<sub>4</sub>SO<sub>3</sub><sup>-</sup>, and CH<sub>3</sub>(CH<sub>2</sub>)<sub>11</sub>C<sub>6</sub>H<sub>4</sub>SO<sub>3</sub><sup>-</sup>. The pTS<sup>-</sup> counterion again showed the best results. Buckley and coworkers have demonstrated that the current density used during polymerization may have a more significant effect, because the *p*-dodecylbenzenesulfonate counterion gives very similar mechanical properties to the pTS<sup>-</sup> when a similar current density was used. These workers suggested that the wide variations in properties reported may be attributed to differences in polymerization conditions.

The key to understanding the properties of PPy films is to develop an understanding of the relationship between the structure of the polymer and its mechanical properties. Unfortunately, few studies have been devoted to gaining such an understanding. This is due, in part, to the intractable nature of PPy films that makes structural characterization difficult.

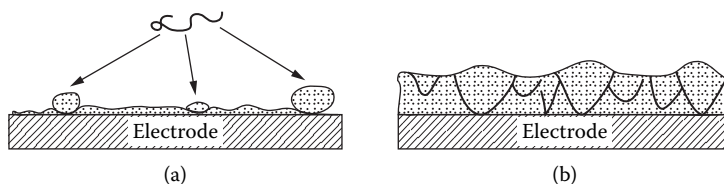
The molecular weight of PPy is one variable that has sometimes been quoted as a possible explanation for differences in the mechanical properties of PPy's prepared in different ways. Wynne and Street<sup>113</sup> suggested that the change in mechanical properties of PPy/pTS with changing solvent might be due to production of polymers having different molecular weights. Others<sup>11</sup> have also proposed that differences in molecular weight may account for the different mechanical properties observed in PPy/pTS films prepared at different temperatures. Unfortunately, the molecular weights of polymers were not determined in these studies; consequently, it is not possible to confirm these assertions.

Buckley and coworkers<sup>117</sup> have noted a correlation between the composition of the PPy, in terms of the ratio of counterion to monomer and the tensile strength of the films. These workers observed that the concentration of counterion intercalated with the polymer depends upon the potential applied during polymerization. However, they noted that the change in mechanical properties could also be due to changes in the density of films,<sup>117</sup> as also noted in a more recent study.<sup>116</sup> Thus, the effect of counterion content and polymerization potential on the mechanical properties of the films remains unknown.

Crosslinking is likely to significantly affect the mechanical properties of the polymer; the greater the degree of crosslinking, the more brittle the material. Unfortunately, there have been no reports on the effect of polymerization conditions or counterion type on the degree of crosslinking produced in polypyrrole. Consequently, it is not known to what extent crosslinking varies as a result of differing conditions and to what extent it affects the mechanical properties.

Numerous x-ray diffraction studies have been conducted on PPy films in order to characterize the degree of molecular order (as described earlier). It has been noted<sup>124</sup> that the degree of alignment increased as the applied potential and temperature of





**FIGURE 3.9** Illustration of proposed deposition mechanism leading to cone/nodule formation and fracture points for CEPs: (a) preferential deposition occurs at discrete sites on the electrode surface resulting in “microisland” formation, and (b) microislands form upward and outward with continued deposition.

polymerization decreased. As reported above, the mechanical properties of PPy films were observed to improve under such conditions. Thus, there may be some correlation between molecular order and the mechanical properties of the films.

A greater degree of order has been observed upon mechanically stretching the films.<sup>114,115</sup> This stretching is believed to orient the molecular chains in the direction of the applied stress. However, the effects of stretching on mechanical properties have not been reported.

Several studies have shown that electrochemically prepared films have an inhomogeneous nodular (or “cauliflower”) structure.<sup>125</sup> A number of studies have reported the morphology of PPy films as a function of various processing variables; however, little is known of the mechanism of formation of the nodular structure or the effect of this structure on mechanical properties.

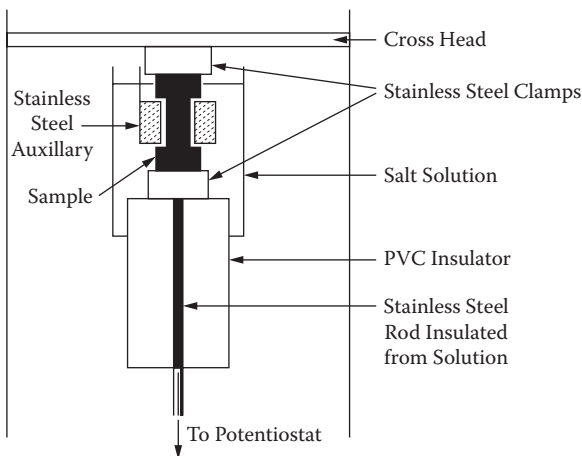
Qian and Qui<sup>126</sup> have observed that the morphology of PPy films depends upon the type of counterion used. For example,  $\text{ClO}_4^-$ ,  $\text{BF}_4^-$ , and  $\text{PF}_6^-$  yielded films with high concentrations of voids, whereas PPy/pTS films consisted of densely packed nodules. Other workers have noted a dependence of the density of PPy films on the polymerization conditions.<sup>115,116,117</sup> Thus, the change in film morphology may explain the effect of counterion type and polymerization conditions on mechanical properties, as surveyed previously.

One study in our laboratories investigated the direct link between PPy film morphology and mechanical properties.<sup>126</sup> Observation of the fracture surfaces of the films showed a roughened surface with cone-shaped features (Figure 3.9), similar to those observed in transmission electron microscope (TEM) micrographs of the film cross sections (described earlier). It was concluded from this study that the cone boundaries are points of weakness within the film that allow easier crack propagation. Thus, films with less prominent boundaries should show improved fracture resistance.

On the basis of these reports, it seems that the relationship between the morphology of PPy films and mechanical properties needs to be further assessed. Once this relationship is known, the effects of smaller scale variations in structure can be determined.

## ENVIRONMENTAL EFFECTS ON MECHANICAL PROPERTIES

Some information is available about the environmental effects on the mechanical properties of PPy. For most intelligent polymer systems, mechanical properties need to be stable with time in the service environment. One study has tracked the changes



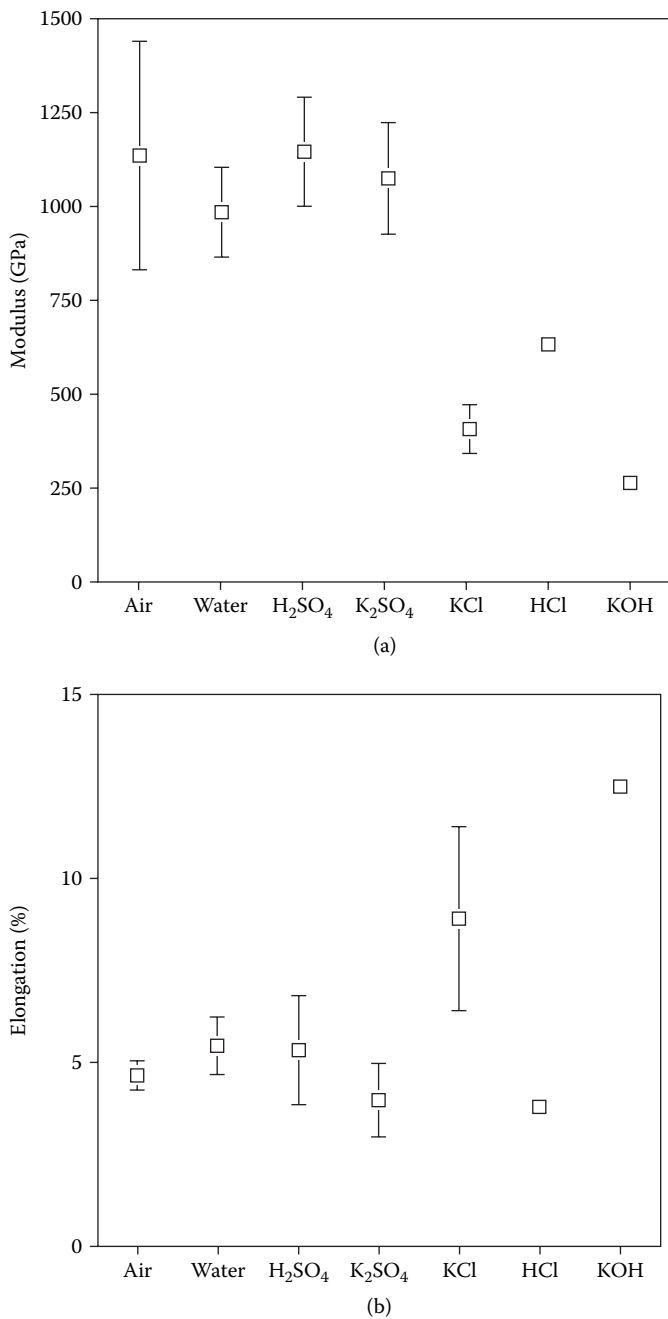
**FIGURE 3.10** *In situ* cell for mechanical testing. (From *Polymer*, Vol. 36, No. 25, “Film substrate and mechanical properties of electrochemically prepared PPy,” M. Gandhi and coworkers, p. 4762. With permission from Elsevier Science Ltd., Oxford, England.)

in the mechanical properties of PPy during aging over 12 months.<sup>118</sup> However, some systems may require mechanical actuation properties of the polymer; indeed, such actuation may need to occur in response to environmental changes. For these reasons, it is instructive to study the effects of environment on mechanical properties.

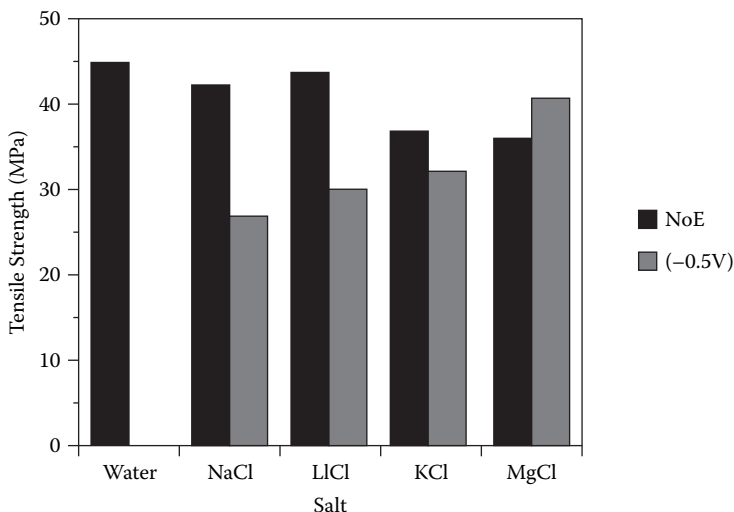
Two aspects of the mechanical properties of PPy in different environments have been studied in our laboratories<sup>127</sup>: the effects of different salt solutions and the effect of an applied potential. The latter was achieved using the experimental setup shown in Figure 3.10. In both cases, the Young’s modulus, elongation at break, and tensile strength were measured. Additionally, in the latter, the mechanical actuating behavior of the PPy was also examined. The actuating behavior of conductive polymers has also been studied by other workers and was reviewed in Chapter 1.

Figures 3.11a and 3.11b show the effect of different aqueous environments on the mechanical properties of PPy/pTS. It is clear that the films become more ductile in potassium chloride and potassium hydroxide solutions. Little change in properties is noted for films in air, water, sulfuric acid, or potassium sulfate. The reasons for these changes are not clear at present, although it is known that alkaline solutions have a degradative effect on PPy.<sup>128</sup> These processes are likely to cause a reduction in the molecular weight and/or crosslink density of the polymer, and hence increase its ductility. The sensitivity of the polymer to environmental conditions demonstrates the importance of determining its behavior in the actual service environment.

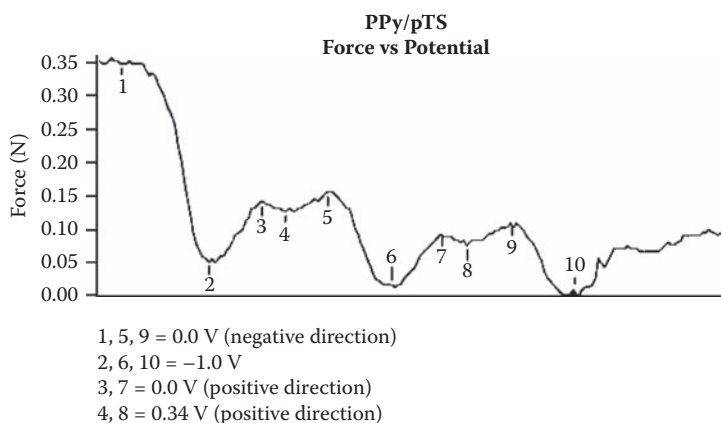
When electrical potentials are applied, equally dramatic changes in mechanical properties have been observed.<sup>129</sup> That is, negative potential induced a much higher plasticity in the PPy/pTS samples. When tested without an applied potential, the samples showed classical brittle behavior with an elongation at break of 10%. However, when the polymer was reduced, the elongation at break increased to approximately 20%. The electrolyte solution influenced the changes in mechanical properties, with divalent cations requiring a more negative potential to induce ductility. This correlates with the ease of ion transport into the polymer. Application of



**FIGURE 3.11** (a) Young's moduli of PPy/pTS films tested immediately after immersion in various aqueous environments (the modulus in air is included for comparison). (b) Elongation at break of PPy/pTS films tested immediately after immersion in various environments (the elongation in air is included for comparison).



**FIGURE 3.12** Effect of applied potential on tensile strength.



**FIGURE 3.13** Changes in force recorded for a stretched PPy film subjected to a cyclically varying potential.

positive potentials was found to have a minimal effect on the mechanical properties compared to the dry-state behavior. The effect of an applied potential (in different electrolytes) on the tensile strength is shown in Figure 3.12.

The changes in force within a PPy/pTS film held at a constant strain and subjected to cyclically varying potential have been studied (Figure 3.13). Such changes are caused by contraction or swelling of the polymer, which can be correlated with ion flow out of or into it.

The actuation force or movement generated during redox cycling is directly related to the concomitant changes in mechanical properties. Using a simple linear elastic model of the small-strain mechanical properties of PPy, it has been shown that the actuation strain ( $\epsilon\sigma$ ) at a constant applied stress ( $\sigma$ ) is accurately predicted from Equation 3.3

$$\varepsilon_{\sigma} = \varepsilon_0 + \sigma \left( \frac{1}{Y'} - \frac{1}{Y} \right) \quad (3.3)$$

where  $\varepsilon_0$  is the actuation strain at zero applied stress, and  $Y$  and  $Y'$  are the Young's moduli before and after the actuation voltage has been applied. In a typical PPy actuation experiment, a positive voltage that causes oxidation of the polymer induces swelling due to the ingress of dopant ions. The oxidation also causes an increase in the Young's modulus. As a consequence of the modulus shift, the net actuation strain ( $\varepsilon_{\sigma}$ ) decreases with increasing applied stress ( $\sigma$ ). Similarly, the stress generated by the actuator (at fixed length) is also affected by the modulus shift:

$$\Delta\sigma_{\sigma} = Y'\varepsilon_0 + \sigma \left( \frac{Y' - Y}{Y} \right) \quad (3.4)$$

so that a smaller stress is generated when Young's modulus increases and the polymer swells during oxidation. Several studies of modulus changes during redox cycling have confirmed that it is generally true that the modulus increases during oxidation,<sup>130,131,132</sup> although the change is much reduced in ionic liquid electrolytes.

## CONCLUSIONS

Obviously, the way in which CEPs such as PPy's are assembled has a dramatic effect on their chemical, electrical, and mechanical properties. This information can be used to advantage by those of us involved in material design from the molecular level. Factors influencing the electrical and chemical properties of CEPs continue to be studied, adding more information to the already massive databank indicating that these are not simple systems.

Fully understanding the mechanical, electrical, and chemical properties of a material is vital for its successful application. The literature reports confirm that the properties of PPy's vary widely, and are related to composition and processing conditions in a complex way. Thus, the study of the basic properties must be conducted at a fundamental level, by developing structure–property relationships. This, however, requires a greater understanding of the structure of PPy's, both at the molecular and supramolecular levels.

A further aspect that has not been described in detail is the effect of service environments on the properties of the PPy's. Although the effects of aging on electrical properties have received most attention, the changes in mechanical and chemical properties are less well known. If PPy's are to be confidently used in service, their performance must be assessed at various temperatures, under varying strain rates and cyclic loads, in contact with various liquid or gaseous media, and under the influence of applied electrical fields. Recent studies have begun to explore the influence of changes in mechanical properties during redox cycling on the performance of PPy as an electromechanical actuator. Such studies highlight the problems—and also opportunities—that arise in these dynamic materials.

## REFERENCES

1. Mitchell, G.R.; Geri, A. *J. Phys. D. Appl. Phys.* 1987, 20: 1346.
2. Kaiser, A.B. *Adv. Mat.* 2001, 13: 927.
3. Kohlman, R.S.; Zibold, A.; Tanner, D.B.; Inas, G.G.; Ishiguro Min, Y.G.; MacDiarmid, A.G.; Epstein, A.J. *Phys. Rev. Lett.* 1997, 78: 3915.
4. Peres, R.C.D.; Pernout, J.M.; De Paili, M.A. *J. Polym. Sci. Part A. Polym. Chem.* 1991, 29: 225.
5. Diaz, A.F.; Lacroix, J.C. *New J. Chem.* 1988, 12: 171.
6. Gimore, K.J.; John, M.J.; Teasdale, P.R.; Zhao, H.; Wallace, G.G. *ACS Symp. Ser. Electrochemistry in Microheterogeneous Fluids.* 1992: 225.
7. Ko, J.M.; Rhee, H.W.; Park, S.M.; Kim, C.Y. *J. Electrochem. Soc.* 1990, 137: 905.
8. Ribo, J.M.; Dico, A.; Valles, M.A.; Ferrer, N.; Bonnett, R.; Bloor, D. *Synth. Met.* 1989, 33: 403.
9. Aavapiryanont, S.; Chandler, A.K.; Gunawardena, G.A.; Pletcher, D.J. *Electroanal. Chem.* 1984, 177: 279.
10. Geetha, S.; Trivedi, D.C. *Synth. Met.* 2005, 155: 306.
11. Sun, B.; Jones, J.J.; Burford, R.P.; Skyllas-Kazacos, M. *J. Mat. Sci.* 1989, 24: 4024.
12. Kuwabata, S.; Natamura, J.; Yoneyama, H. *J. Chem. Soc. Chem. Comm.* 1988: 779.
13. Wegner, G.; Wernet, W.; Glatzhorer, D.T.; Ulanski, J.; Krohnke, C.; Mohammadi, M. *Synth Met.* 1987, 18: 1
14. Shen, Y.; Qiu, J.; Qian, R. *Makromol. Chem.* 1987, 188: 2041.
15. Maddison, D.S.; Jenden, C.M. *Polym. Int.* 1992, 27: 231.
16. Salmon, M.; Diaz, A.F.; Logan, A.J.; Krounbi, M.; Bargar, J. *Mol. Cryst. Liq. Cryst.* 1983, 83: 1297.
17. Zhao, H.; Price, W.E.; Wallace, G.G. *J. Memb. Sci.* 1994, 87: 47.
18. Zhao, H.; Price, W.E.; Teasdale, P.R.; Wallace, G.G. *React. Polym.* 1994, 23: 213.
19. Yamaura, M.; Sato, K.; Hagiwara, T.; Iwata, K. *Synth. Met.* 1992, 48: 337.
20. Diaz, A. *Chem. Script.* 1981, 17: 145.
21. Ogasawara, M.L.; Funahashi, K.; Iwata, K. *Mol. Cryst. Liq. Cryst.* 1985, 118: 159.
22. Kang, E.T.; Neoh, K.G.; Ti, H.C. *Sol. State. Comm.* 1986, 60: 457.
23. Whang, Y.E.; Han, J.J.; Nalwa, H.S.; Watanabe, T.; Miyata, S. *Synth. Met.* 1991, 41: 3043.
24. Tezuka, Y.; Ohyama, S.; Ishii, T.; Aoki, K. *Bull. Chem. Soc. Jpn.* 1991, 64: 2045.
25. Beck, F.; Barsch, U.; Micahel, R. *J. Electroanal. Chem.* 1993, 351: 169.
26. Schlenoff, J.B.; Xu, H. *J. Electrochem. Soc.* 1992, 139: 2397.
27. Tanguy, J.; Slama, M.; Hoclet, M.; Baudouin, J.L. *Synth. Met.* 1989, 28: C145.
28. Naoi, K.; Lien, M.; Smyrl, W.H. *J. Electrochem. Soc.* 1991, 138: 440.
29. Reynolds, J.R.; Sundaresan, N.S.; Pomerantz, M.; Basak, S.; Baker, C.K. *J. Electroanal. Chem.* 1988, 250: 355.
30. Duffit, G.L.; Pickup, P.G. *J. Phys. Chem.* 1991, 95: 9634.
31. Peres, R.C.D.; De Paoli, M.A.; Torresi, R.M. *Synth. Met.* 1992, 48: 259.
32. Naoi, K.; Lien, M.; Smyrl, W.H. *J. Electroanal. Chem.* 1989, 272: 273.
33. Visy, C.; Lukkari, J.; Pajunen, T.; Kanakare, J. *Synth. Met.* 1989, 22: 289.
34. Vork, F.T.A.; Schuermans, B.C.A.; Barendrecht, E. *Electrochim. Acta.* 1990, 35: 567.
35. Talaie, A.; Wallace, G.G. *Synth. Met.* 1994, 63: 83.
36. Delabouglise, D.; Garnier, F. *J. Chim. Phys.* 1992, 89: 1131.
37. Nishizawa, M.; Sawaguchi, T.; Matuse, T.; Uchida, I. *Synth. Met.* 1991, 45: 241.
38. Ge. H.; Ashraf, S.A.; Gilmore, K.J.; Too, C.O.; Wallace, G.G. *J. Electroanal. Chem.* 1992, 340: 41.
39. Zhang, W.; Dong, S. *Electrochim. Acta.* 1993, 38: 441.
40. Hearn, M.T.W. *Anal. Sci.* 1991, 7: 119.

41. Iseki, M.I.; Saito, K.; Ikematsu, M.; Sugiyama, Y.; Kuhara, K.; Mizukami, A. *J. Electroanal. Chem.* 1993, 358: 221.
42. Lewis, T.W. PhD Thesis, University of Wollongong, 1998.
43. Beck, F.; Michaelis, R. *Werkstoffe and Korrosion*, 1991, 42: 341.
44. Boxall, D.L.; Osteryoung, R.A. *J. Electrochem. Soc.* 2004, 151: E41.
45. Lu, W.; Fadeev, A.G.; Qi, B.; Smela, E.; Mattes, B.R.; Ding, J.; Spinks, G.M.; Mazurkiewicz, J.; Zhou, D.; MacFarlane, D.R.; Forsyth, S.A.; Forsyth, M.; Wallace, G.G. *Science* 2002, 297: 983.
46. Ding, J.; Zhou, D.; Spinks, G.; Forsyth, S.; Forsyth, M.; MacFarlane, D.; Wallace, G. *Chemistry of Materials* 2003, 15: 2392.
47. Andrieux, C.P.; Audebert, P.; Hapiot, P.; Nechtschein, M.; Odin, C. *J. Electroanal. Chem.* 1991, 305: 153.
48. Teasdale, P.R.; Wallace, G. G. *J. Electroanal. Chem.* 1995, 241: 157.
49. John, R.; Wallace, G.G. *J. Electroanal. Chem.* 1993, 354: 154.
50. Ge, H.; Wallace, G.G. *React. Polym.* 1992, 18: 113.
51. Qian, R. *Makromol. Chem. Macromol. Symp.* 1990, 33: 327.
52. Ge, H.; Gilmore, K.G.; Ashraf, S.; Too C.O.; Wallace, G.G. *J. Liq. Chrom.* 1993: 16.
53. Reynolds, J.R.; Sundaresan, N.S.; Pomerantz, M.; Basaks; Baker, C.K. *J. Electroanal. Chem.* 1988, 256: 355.
54. Sadik, O.; Wallace, G.G. *Electroanal.* 1993, 5: 555.
55. Rhee, H.W.; Jean, E.J.; Kim, J.S.; Kim, C.Y. *Synth. Met.* 1989, 28: C605.
56. Ko, J.M.; Rhee, H.W.; Kim, C.Y. *Makromol. Chem. Macromol. Symp.* 1990, 33: 353.
57. Shimidzu, T.; Ohtani, A.; Honda, K. *J. Electroanal. Chem.* 1988, 251: 323.
58. Zhong, C.; Doblhofer, K. *Electrochim. Acta.* 1990, 35: 1971.
59. Naoi, K.; Lien, M.; Smyrl, W.H. *J. Electrochem. Soc.* 1991, 138: 440.
60. Mirmohseni, A.; Price, W.E.; Wallace, G.G. *Poly. Gels. Networks.* 1993, 1: 61.
61. Shimidzu, T. In *Lower Dimensional Systems and Molecular Electronics*. Metzger, R.M. (Ed.). Plenum Press, New York, 1991: 653.
62. Lewis, T.W.; Smyth, M.R.; Wallace, G.G. *Analyst.* 1999, 99: 121.
63. Wallace, G.G.; Kane-Maguire, L.A.P.; *Adv. Materials.* 2002, 14: 953.
64. Wallace, G.G.; Maxwell, K.; Lewis, T.W.; Hodgson, A.T.; Spencer, M.J. *J. Liq. Chrom.* 1990, 13(15): 3091.
65. Barnett, D.; Sadik, O.A.; John, M.J.; Wallace, G.G. *Analyst.* 1994, 119: 1997.
66. Sadik, O.A.; Van Emon, J.M. *Biosens. Bioelectronics.* 1996, 11: 1.
67. Bender, S.; Sadik, O.A. *Env. Sci. Tech.* 1998, 32: 788.
68. Foulds, N.C.; Lowe, C.R. *Anal. Chem.* 1988, 60: 2473.
69. Couves, L.D.; Porter, S.J. *Synth. Met.* 1989, 28: C761.
70. Adeljou, S.B.; Shaw, S.J. Wallace, G.G. *Anal. Chim. Acta.* 1997, 341: 155.
71. Compagnone, D.; Feclerici, G.; Banister, J.V. *Electroanal.* 1995, 7: 1151.
72. Lu, W.; Zhou, D.; Wallace, G.G. *Anal. Comm.* 1998, 35: 245.
73. Carden, P.; Hodgson, A.J.; John, R.; Spencer, M.J.; Wallace, G.G. In *Am. Chem. Soc. Symp. Ser. Electrochemistry in Colloids and Dispersions.* 1992: 235.
74. El Hourch, A.; Belcadi, S.; Moisy, P.; Crouigneau, P.; Legel, J.M.; Lamy, C.J. *Electroanal. Chem.* 1992, 339.
75. Malinaukis, A. *Synth. Met.* 1999, 107: 75.
76. Lapowski, M.; Bidan, G.; Founier, M. *Pol. J. Chem.* 1991, 65: 1547.
77. Riley, P.J. Wallace, G.G. *J. Electroanal. Chem.* 1991, 3: 191.
78. Lin, Y.; Wallace, G.G. *Anal. Chim. Acta.* 1992, 263: 71.
79. Saunders, B.R.; Fleming, R.J.; Murray, K.S. *Chem. Mater.* 1995, 7: 1082.
80. Wang, J.; Jiang, M. *Langmuir* 2000, 16: 2269.
81. Wu, Y.; Moulton, S.E.; Too, C.O.; Zhou, D.; Wallace, G.G. *The Analyst* 2004, 129: 585.

82. Misoska, V.; Price, W.; Ralph, S.; Ogata, N.; Wallace, G.G. *Synth. Met.* 2001, 123: 279.
83. Campbell, T.E.; Hodgson, A.J.; Wallace, G.G. *Electroanal.* 1999, 11: 215.
84. Schumann, W.; Lammert, R.; Uhe, B.; Schmidt, H. *Sensors and Actuators, B.* 1990, 1: 537.
85. Livache, T.; Roget, A.; Dejean, E.; Bartlet, C.; Bidan, G.; Teouk, R. *Nucl. Acids Research.* 1994, 22: 2915.
86. Garnier, F.; Karri-Youssoufi, H.; Srivastava, P.; Mandrand, B.; Delair, T. *Synth. Met.* 1999, 100: 89.
87. Kim, B.C.; Spinks, G.M.; Too, C.O.; Wallace, G.G.; Bae, Y.H.; Ogata, N. *Reactive & Functional Polymers* 2000, 44: 245.
88. Saunders, B.R.; Saunders, J.M.; Mrkic, J.; Dunlop, E.H. *Phys. Chem. Chem. Phys.* 199, 1: 1563.
89. Shim, W.S.; Lee, Y.H.; Yeo, I-H., Lee, J.Y.; Lee, D.S. *Synth. Met.* 1999, 104, 119.
90. Ge, H.; Wallace, G.G. *J. Liq. Chrom.* 1990, 13: 3261.
91. Ge, H.; Wallace, G.G. *J. Chrom.* 1991, 588: 25.
92. Sadik, O.A.; Wallace, G.G. *Anal. Chim. Acta.* 1993, 279: 209.
93. Barnett, D.; Laing, D.G.; Skopec, S.; Sadik, O.A.; Wallace, G.G. *Anal. Lett.* 1994, 27: 2417.
94. Hodgson, A.J.; Lewis, T.W.; Maxwell, K.M.; Spencer, M.J.; Wallace, G.G. *Journal of Liquid Chromatography* 1990, 13: 3091.
95. Gooding, J.; Wasioowych, C.; Barnett, D.; Hibbert, D.B.; Barisci, J.N.; Wallace, G.G. *Biosensors and Bioelectronics* 2004, 20: 260.
96. Bredas, J.L.; Street, G.B. *Acc. Chem. Res.* 1985, 18: 309.
97. Furukawa, Y.; Tazawa, S.; Fuji, Y.; Harada, I. *Synth. Met.* 1988, 24: 329.
98. Hu, Y.; Yang, R.; Evans, D.F.; Weaver, J.H. *Phys. Rev. B.* 1991, 44: 13660.
99. Turco, R.; Graupner, W.; Filip, C.; Bot, A.; Brie, M.; Grecu, R. *Adv. Mater. Opt. Electron.* 1999, 9: 157; and references cited therein.
100. Huang, Z.; Wang, P.-C.; Feng, J.; MacDiarmid, A.G.; Xia, Y.; Whitesides, G.M. *Synth. Met.* 1997, 85: 1375.
101. Lee, J.Y.; Kim, D.Y.; Kim, C.Y. *Synth. Met.* 1995, 74: 103.
102. Turco, R.; Giurgiu, L.V.; Ordean, R.; Grecu, R.; Brie, M. *Synth. Met.* 2001, 119: 287.
103. Oh, E.J.; Jang, K.S.; Suh, J.S.; Kim, H.; Kim, K.H.; Yo, C.H.; Joo, J. *Synth. Met.* 1997, 84: 147.
104. Jang, K.S.; Han, S.S.; Suh, J.S.; Oh, E.J. *Synth. Met.* 2001, 119: 107.
105. Delabouglise, D.; Garnier, F. *Synth. Met.* 1990, 39: 117.
106. Pleus, S.; Schwientek, M. *Synth. Met.* 1998, 95: 233.
107. Moutet, J.-C.; Saint-Aman, E.; Tran-Van, F.; Angibeaud, P.; Utille, J.-P. *Adv. Mater.* 1992, 4: 511.
108. Schwientek, M.; Pleus, S.; Hamann, J. *Electroanal. Chem.* 1999, 461: 94.
109. Ogata, N. *Macromol. Symp.* 1997, 118: 693.
110. Deore, B.; Yakabe, H.; Shiigi, H.; Nagaoka, T. *Analyst.* 2002, 127: 935; and references cited therein.
111. de Lacy Costello, B.P.J.; Ratcliffe, M.N.; Sivanand, P.S. *Synth. Met.* 2003, 139: 43.
112. Bloor, D.; Hercliff, R.D.; Galiotis, C.G.; Young, R.J. *Electronic Properties of Polymers and Related Compounds.* Kuzmany, H.; Mehring, M.; Roth, S. (Eds.). Springer-Verlag, Berlin, 1985, p179.
113. Wynne, K.J.; Street, G.B. *Macromolecules.* 1985, 18: 2361.
114. Ogasarara, M.; Funahashi, K.; Demura, T.; Hagiwara, T.; Iowata, K. *Synth. Met.* 1986, 14: 61.
115. Hagiwara, T.; Hirasaka, M.; Sato, K.; Yamaura, M. *Synth. Met.* 1990, 36: 241.
116. Wang, X.-S.; Xu, J.-K.; Shi, G.-Q.; Lu, X. *J. Mater. Sci.* 2002, 37: 5171.

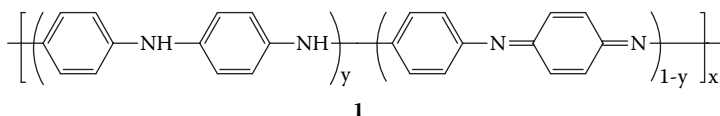


117. Buckley, L.J.; Roylance, D.K.; Wnek, G.E. *J. Polym. Sci. Pt. B: Poly. Phys.* 1987, 25: 2179.
118. Kaynak, A.; Rintoul, L.; Graeme, A. *Mater. Res. Bull.* 2000, 35: 813.
119. Yoshino, K.; Tabata, M.; Satoh, M.; Kaneto, K.; Ohsawa, T. *Technol. Rep. Osaka Uni.* 1985, 35: 231.
120. Diaz, A. F.; Hal, G. *IBM J. Res. Dev.* 1993, 27(4): 342.
121. Moss, B.K.; Burford, R.P.; Skyllas-Kazacos, M. *Materials Forum.* 1989, 13: 35.
122. Peres, R. C. D.; Perout, S. M.; Depaoli, M. *Synth. Met.* 1989, 28: C59.
123. Cvetko, B.F.; Brungs, M.P.; Burford, R.P.; Skyllas-Kazacos, M. *J. App. Electrochem.* 1987, 17: 1198.
124. Wettermark, U.G.; Worrell, G.A.; Chem, C.S. *Polym. Mater. Sci. Eng.* 1991, 64: 267.
125. Mitchell, G. *J. Phys. D. Appl. Phys.* 1987, 20: 1346.
126. Qian, R.; Qui, J. *Polym. J.* 1987, 19: 157.
127. Burford, R.; Gandhi, M.; Spinks, G.M.; Wallace, G.G. *Polymer.* 1995, 36: 4761.
128. Moss, B.; Ph.D. Thesis, University of New South Wales, 1993.
129. Gandhi, M.; Murray, R.; Spinks, G.M.; Wallace, G.G. *Synth. Met.* 1995, 73: 247.
130. Spinks, G.M.; Liu, L.; Zhou, D.; Wallace, G.G. *Advanced Functional Materials* 2002, 12: 437.
131. Koehler, S.; Bund, A.; Efimov, I. *J. Electroanal. Chem.* 2006, 589: 82.
132. Otero, T.F.; Cascales, J.J.L.; Arenas, G.V. *Mater. Sci. Eng. C* 2007, 27: 18.

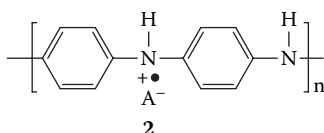
# 4 Synthesis of Polyanilines

Polyaniline (PAn) has been known for over a century since the synthesis of the so-called aniline blacks that enjoyed early use as cotton dyes in the 1860s. Systematic studies<sup>1,2</sup> of its properties before World War I led to the proposal by Green and Woodhead<sup>2</sup> of an aniline octamer structure and the existence of several oxidation states. Only sporadic studies of PAn's were undertaken over the following 70 years until investigations by MacDiarmid and coworkers in the mid-1980s,<sup>3,4</sup> and in particular, the discovery of electrical conductivity for its *emeraldine salt* (ES) form, led to an explosion of interest in this fascinating polymer.

PAn is now accepted to have the general polymeric structure shown as **1**. It differs from most other conducting electroactive polymers, such as polypyrroles (PPy's; Chapters 2 and 3) and polythiophenes (Chapter 6), in that it possesses three readily accessible oxidation states. These range from the fully reduced ( $y = 1$ ) *leucoemeraldine* state to the half-oxidized ( $y = 0.5$ ) emeraldine form to the fully oxidized ( $y = 0$ ) *pernigraniline* state. The ES form **2** is the state with the highest conductivity.



$y = 1$  (leucoemeraldine), 0.5 (emeraldine) and 0 (pernigraniline) as base forms



emeraldine salt (ES), PAn.HA

PAn also differs from PPy's and polythiophenes in that the N heteroatom participates directly in the polymerization process (PAn is a *ladder* polymer that polymerizes *head to tail*) and participates in the conjugation of the conducting form of the polymer to a greater extent than the N and S heteroatoms in PPy and polythiophene.

In addition, PAN is unique among the conducting electroactive polymers in that it can be rapidly converted between base and salt forms by treatment with acid or base. These reversible redox and pH-switching properties (see Chapter 5 for details), together with the electrical conductivity of its ES form **2**, its ease and cheapness of synthesis, and its good environmental stability have led to PAN becoming the most extensively studied conducting organic polymer over the past decade, and a wide range of potential applications are currently being developed.

PAN's are most commonly prepared through the chemical or electrochemical oxidative polymerization of the respective aniline monomers in acidic solution. However, a range of polymerization techniques has now been developed, including

1. Electrochemical polymerization
2. Chemical polymerization
3. Photochemically initiated polymerization
4. Enzyme-catalyzed polymerization
5. Polymerization employing electron acceptors

## ELECTROCHEMICAL POLYMERIZATION

The electrochemical cell arrangement described for production of PPy (see Chapter 2) is applicable to the electropolymerization of PAN. The polymerization cell design is of equal importance for the preparation of PAN as for PPy. All the requirements of the cell design apply, and the same versatility of the form of assembly can be attained, although in practice PAN has not been investigated as extensively as the latter in this regard. The only additional requirement of a polymerization cell for PAN is that the electrode and construction materials should be stable in acid media.

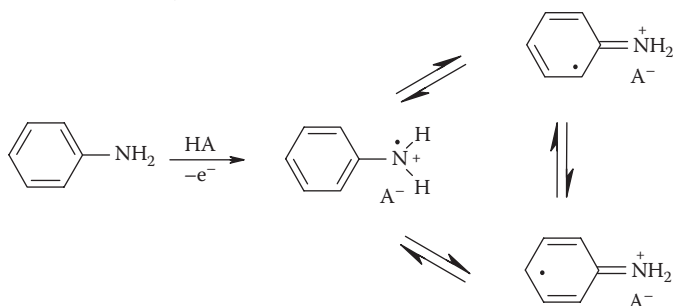
Electrochemical polymerization is routinely carried out in an acidic aqueous solution of aniline. This low pH is required to solubilize the monomer and to generate the PAN/HA (HA = acid) emeraldine salt as the only conducting form of PAN. Constant potential (potentiostatic) or potentiodynamic techniques are generally employed because the overoxidation potential for PAN is very close to that required for monomer oxidation.

Defects due to overoxidation of the polymer have been proposed; however, the exact nature of overoxidation is not known. One theory is that crosslinking occurs,<sup>5</sup> whereas another proposes the opening of the chain after the formation of a paraquinone.<sup>6</sup> It is reported that a short-term increase of the applied potential to 0.9–1.1 V (versus Ag/AgCl) during potentiostatic deposition gives more adherent films.<sup>7</sup>

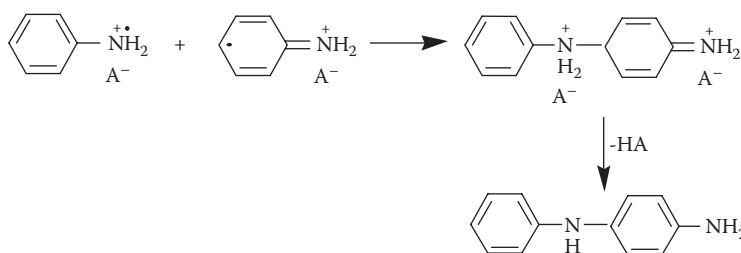
## MECHANISM OF ELECTROCHEMICAL POLYMERIZATION

The generally accepted mechanism for the electropolymerization of aniline is an  $E(CE)_n$  process, as presented in Figure 4.1.<sup>8–10</sup> Formation of the radical cation of aniline by oxidation on the electrode surface (step 1) is considered the rate-determining step. This is followed by coupling of radicals, mainly *N*- and *para*-forms, and elimi-

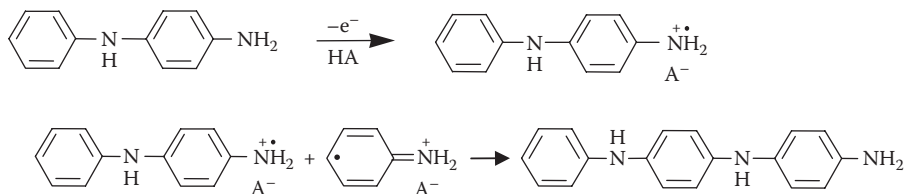
## Step 1. Oxidation of Monomer



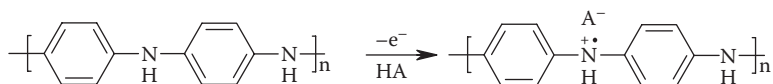
## Step 2. Radical Coupling and Rearomatization



## Step 3. Chain Propagation



## Step 4. Oxidation and Doping of the Polymer



**FIGURE 4.1** Electropolymerization of aniline.

nation of two protons. The dimer (oligomer) formed then undergoes oxidation on the electrode surface along with aniline. The radical cation of the oligomer couples with an aniline radical cation, resulting in propagation of the chain. The acid (HA) present in the solution dopes the formed polymer to give PAN/HA (step 4).

The growth of PAN has been found to be self-catalyzing<sup>11,12</sup>; the more polymer deposited, the higher the rate of polymer formation. A mechanism for this has been proposed, involving adsorption of the anilinium ion onto the most oxidized form of PAN, followed by electron transfer to form the radical cation and subsequent reoxidation of the polymer to its most oxidized state.<sup>12</sup>

## ELECTRODE MATERIALS

A variety of working electrodes may be used, including platinum or gold plates, glassy carbon, reticulated vitreous carbon, as well as indium-tin-oxide (ITO)-coated glass. As with PPy's, the electrode substrate plays a critical role in determining the extent of polymer deposition and the nature of the deposit formed. In extreme conditions, the surface chemistry of the electrode can be so incompatible that no PAN will deposit; in fact, surface treatments of ITO exploit this phenomenon in microcontact printing to allow patterns of conducting polymers to be produced on the substrate.<sup>13</sup> Others have shown that the inherent conductivity of the underlying substrates can have a dramatic effect on the conductivity of the resulting polymer deposited.<sup>14</sup>

For some applications, especially in the area of corrosion protection, the electropolymerization of PAN onto active substrate is of interest. Lacroix and coworkers<sup>15</sup> have achieved this by first coating mild steel with a very thin PPy layer and then electrocoating PAN over it. Others have electrodeposited PAN-PPy composites on aluminum<sup>16</sup> or steel<sup>17</sup> surfaces using oxalic acid electrolytes. A number of ring-substituted anilines have also been directly electrodeposited on active iron substrates using an oxalic acid electrolyte.<sup>18</sup>

## CONCENTRATION AND NATURE OF THE DOPANT ACID (HA)

The electropolymerization of aniline is almost always carried out in strong aqueous acids (HA) at a low pH of  $\leq 2$ . Only a few polymerizations have been performed at higher pH values ( $\geq 3$ ). An *in situ* UV-visible spectroscopic study of the galvanostatic (constant-current) polymerization of aniline in aqueous HCl at pH between 0.2 and 3.7 showed that typical PAN/HCl emeraldine salts were formed using  $\text{pH} \leq 1.7$ . However, the film deposited at pH 3.7 was quite different in nature, its spectrum being consistent with an oligomeric material with chains of short conjugation length, interrupted sometimes with heterojunctions or *ortho*-coupling.<sup>19</sup>

The dopant  $\text{A}^-$  incorporated into the polymer is usually the conjugate base from this acid. As with other conducting electroactive polymers (CEPs), the nature of the anion is critical in determining the morphology,<sup>20</sup> conductivity,<sup>21</sup> and subsequent switching characteristics of the polymer (see later in this chapter and Chapter 5). It also plays a critical role during growth, because some oligomers or polymers (e.g., those containing  $\text{HSO}_4^-/\text{SO}_4^{2-}$ ) are inherently more soluble and this delays the onset of precipitation onto the electrode surface.<sup>22</sup> The PAN grown from oxyacids has a sponge-like structure. Those grown from HCl form a spaghetti-like structure because, as with PPy, the anion used influences the rate of polymerization.<sup>23</sup>

It has been shown that addition of polyelectrolytes to the polymerization solution can result in the incorporation of these larger molecules as dopants even when the acid is in excess.<sup>24</sup> Others have shown that the addition of inert salts (e.g., LiCl,  $\text{CaCl}_2$ ) to the acid electrolyte can result in significant increases in molecular weight: up to  $160,000 \text{ gmol}^{-1}$ .<sup>25</sup>

A significant development in PAN chemistry was our report<sup>26,27</sup> of the first optically active PAN's, prepared through the electrochemical polymerization of aniline in the presence of the chiral dopant acids (+)- or (-)-10-camphorsulfonic acid (HCSA). Films of the emeraldine salts PAN/(+)-HCSA and PAN/(-)-HCSA can be

readily deposited on ITO-coated glass electrodes using either potentiostatic (0.8–1.1 V versus Ag/AgCl), potentiodynamic (sweeping the potential from –0.2 to 1.0 V), or galvanostatic (applied current density of 0.5 mAcm<sup>-2</sup>) methods. These films exhibit strong circular dichroism (CD) bands in the visible region (see Chapter 5), indicating the induction of chirality into the PAN chains by the (+)- and (–)-HCSA dopants. Analogous electrochemical oxidation of the monomer 2-methoxyaniline in the presence of (+)- and (–)-HCSA has provided a similar route to optically active poly(2-methoxyaniline), POMA/HCSA, films.<sup>28</sup>

The converse approach to inducing chirality into conducting polymer chains, namely, the incorporation of an optically active cation, has also been successfully employed in our laboratories to produce the first optically active water-soluble sulfonated PAN. Poly(2-methoxyaniline-5-sulfonic acid) has been prepared in optically active form through the electropolymerization of 2-methoxyaniline-5-sulfonic acid in the presence of (*R*)-(+)- or (*S*)-(–)-1-phenylethylamine.<sup>29</sup> The optical activity and electroactivity of the chiral sulfonated PAN's are retained when immobilized on poly(4-vinylpyridine) (see Chapter 5).

## SOLVENT

The electropolymerization of aniline has almost always been carried out in aqueous solution. However, a limited number of studies have described polymerization from organic solvents. In 1989, Watanabe and coworkers<sup>30</sup> electropolymerized aniline (0.10 M) in 0.10 M LiClO<sub>4</sub>/acetonitrile solution at a Pt-coated glass working electrode by applying a constant potential of 2.0 V (versus standard calomel electrode) for 1 h. The UV-visible spectrum and redox switching properties of the polymeric material obtained were consistent with those of the formation of PAN. Others have used acetonitrile<sup>31</sup> with dodecylbenzenesulfonate as the dopant anion to facilitate solubility of aniline.

More recently, several papers have appeared in which 2-halogeno-substituted (*X* = Cl, Br, I) anilines were potentiodynamically polymerized in acetonitrile solvent containing 0.03 M HClO<sub>4</sub>/0.10 M [Bu<sub>4</sub>N] ClO<sub>4</sub><sup>-</sup> by sweeping the potential between –0.30 and +1.9 V (versus Ag/AgCl).<sup>32–34</sup> The polymers obtained again showed UV-visible spectral and cyclic voltammetric behavior characteristics of PAN's. However, their electrical conductivities (ca. 10<sup>-3</sup> S/cm) were 3–4 orders of magnitude lower than that typically found for unsubstituted PAN/HA salts, perhaps due to the steric influence of the halogeno substituents. The potentiostatic electropolymerization of a range of *N*-alkylanilines (alkyl ranging from methyl to dodecyl) has also been reported in either acetonitrile or dimethylsulfoxide solvent.<sup>35</sup> However, the extremely low conductivities (ca. 10<sup>-10</sup> S/cm) of all the products except for the *N*-hexyl, -heptyl, and -octyl polymers suggest that they are not typical emeraldine salts.

Acetonitrile was also used as the solvent for the first successful synthesis of a PAN/PPy copolymer via galvanostatic (constant-current) electropolymerization of mixtures of aniline (0.5 M) and pyrrole (0.1–1.0 M) in acetonitrile solvent in the presence of CF<sub>3</sub>COOH as acid and tetraethylammonium tetrafluoroborate as supporting electrolyte. Differential scanning calorimetry and Fourier transform infrared (FTIR) measurements confirmed that the electrically conducting product was a mixture of PAN, PPy, and a random PAN/PPy copolymer.<sup>36</sup>

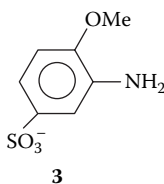
Ionic liquid electrolytes have recently been used for the electrosynthesis of PAn.<sup>37</sup> The rate of polymerization of aniline was found to be high, and adhesion of the conducting polymer product to the metal electrode was enhanced.

### TEMPERATURE

A remarkable recent example of the influence of electropolymerization temperature on the properties of PAn products is observed in the potentiostatic polymerization of aniline in the presence of chiral (+)-HCSA to give optically active PAn/(+)-HCSA films. The CD spectra of the polymers electrodeposited at  $\leq 25^\circ\text{C}$  were inverted compared to the spectra of analogous emeraldine salts deposited at  $\geq 40^\circ\text{C}$ , indicating an inversion of the preferred helical hand for PAn chains.<sup>38</sup> The observations may be rationalized in terms of a temperature-induced interconversion between two initially (kinetically) formed diastereomeric PAn products.

### MONOMER TYPE

A tremendous range of monomer derivatives of aniline has been investigated,<sup>39–45</sup> with many of them forming polymers having properties significantly different from those of PAn. In most instances the conductivity, electroactivity, and other electrochemical attributes of the resultant polymers have been studied. The electronic properties have also been investigated.<sup>46</sup> However, the chemical properties of these substituted PAn's have not been investigated to any great extent. Other workers<sup>47,48</sup> have attached sulfonate groups to PAn after polymerization to make the polymer water soluble. Alternatively, the functionalized aniline monomer **3** containing a methoxy and a sulfonate group has been polymerized electrochemically to produce water-soluble conducting PAn's.<sup>49</sup> Using a flow-through electrochemical method, accurate control over molecular weight, and hence conductivity, can be obtained. It is also possible to produce copolymers with aniline using this approach.



### COLLOIDAL PAN'S

Using a flow-through electrochemical cell, we have developed an electrohydrodynamic route to PAn colloids (rather than the more traditional chemical oxidation route), including dispersions with novel functionality. For example, we recently reported the first optically active PAn colloids, obtained through the electropolymerization of aniline in the presence of poly(styrenesulfonate) as an electrosteric stabilizer and (+)-HCSA as the chiral inducing agent.<sup>50</sup> Chiral PAn colloids have also been synthesized using the core-shell technique, in which PAn/(+)-HCSA/SiO<sub>2</sub><sup>51</sup> and PAn/(+)-HCSA/PU (PU = polyurethane)<sup>52</sup> nanocomposites were generated through

the electropolymerization of aniline onto the surface of small silica (20 nm) and PU (40 nm) particles in aqueous dispersion. In the case of the PAN/HA/PU dispersions, the film-forming properties of the PU component assisted the subsequent formation of uniform, strongly adhering conducting polymer films. The chiroptical properties of these novel chiral PAN colloids are described in Chapter 5.

## CHEMICAL POLYMERIZATION

Chemical synthesis has the advantage of being a simple process capable of producing bulk quantities of CEPs on a batch basis. To date, it has been the major commercial method of producing PAN's, several companies producing bulk powders, dispersions, and coated products.

For chemical polymerization, the oxidizing force is supplied by a chemical oxidant in the solution. The most widely employed chemical oxidant has been aqueous ammonium persulfate,  $(\text{NH}_4)_2\text{S}_2\text{O}_8$ , leading to the incorporation of  $\text{HSO}_4^-/\text{SO}_4^{2-}$  as the dopant anions ( $\text{A}^-$ ) in the PAN/HA product. Acidic conditions ( $\text{pH} \leq 3$ ) are usually required to assist the solubilization of the aniline in water and to avoid excessive formation of undesired branched products.<sup>53</sup> An  $(\text{NH}_4)_2\text{S}_2\text{O}_8$ /aniline molar ratio of  $< 1.2$  is usually employed. As the  $\text{S}_2\text{O}_8^{2-}$  anion is a two-electron oxidizer (acceptor), this suggests that a little over two electrons are removed from each aniline monomer during polymerization.

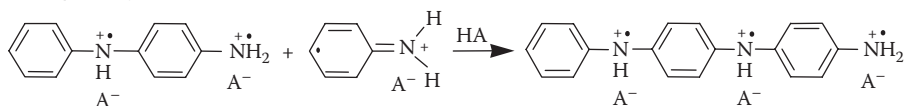
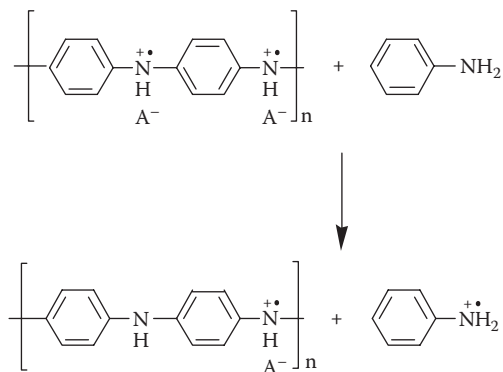
### MECHANISM OF CHEMICAL POLYMERIZATION

The chemical polymerization of aniline by  $(\text{NH}_4)_2\text{S}_2\text{O}_8$  is believed to proceed in its initial stages by a mechanism similar to that described earlier for electrochemical polymerization.<sup>54-56</sup> The first step involves the formation of the aniline radical cation. In the second step, coupling of *N*- and *para*-radical cations occurs, with subsequent rearomatization of the dication of *p*-aminodiphenylamine (PADPA). It is then oxidized to the diradical dication. Although *head-to-tail* (i.e., *N-para*) coupling is predominant, some coupling in the *ortho*-position also occurs, leading to defects in conjugation in the resultant polymer.

A significant variation from the electropolymerization route occurs in the subsequent chain propagation and product formation steps (Figure 4.2). The initial polymer product has been confirmed from spectroscopic studies<sup>57,58</sup> to be the fully oxidized pernigraniline salt form of PAN, which is not surprising in view of the high oxidizing power (2.16 V, versus Ag/AgCl) of ammonium persulfate. When the oxidant is completely consumed, the remaining aniline in solution reduces the pernigraniline to form the final product, the green ES (step 4). Color changes during the reaction reflect the described steps: during the second step the solution is pink because of PADPA; during the third step the solution becomes deep-blue because of formation of protonated pernigraniline; and in the final step green ES precipitates.

The properties of PAN's, such as electrical conductivity, morphology, molecular weight, and stereoregularity, are sensitive to the polymerizing conditions employed. On the basis of extensive studies, the influence of various polymerization conditions on the properties of ESs (PAN/HA) are summarized in the following sections.



*Propagation of Chain**Reduction of Pernigraniline Salt to Emeraldine Salt (ES)***FIGURE 4.2** Chemical polymerization of aniline.**POLYMERIZATION TEMPERATURE**

Chemical polymerizations of aniline with  $(\text{NH}_4)_2\text{S}_2\text{O}_8$  were initially performed at room temperature. However, later studies showed that the PAN obtained was of relatively low molecular weight and contained significant defect sites such as undesirable branching due to *ortho*-coupling.<sup>59,60</sup> Subsequently, the most widely employed temperature for chemical polymerization of aniline monomers has been ca. 1–5°C, as described by MacDiarmid and coworkers,<sup>61</sup> providing a PAN whose emeraldine base (EB) forms have molecular weights ( $M_w$ ) of 30,000–60,000 g mol<sup>-1</sup>.

For industrial applications, it is desirable to have PAN's with high molecular weights ( $M_w$  ca. 100,000) and low polydispersity ( $\text{PD} < 2.0$ ). The use of low temperatures down to –30° or –40°C (achieved through the addition of salts such as LiCl and CaF<sub>2</sub>) has led to the formation of PAN's with much higher molecular weights (up to 400,000).<sup>62–65</sup> The <sup>13</sup>C NMR studies of leucoemeraldine base (LB) forms of the PAN products (obtained by subsequent reduction) revealed that the most structurally regular PAN was obtained at –30°C. However, these reactions generally require over 48 h to complete, and the polydispersity is relatively high ( $\text{PD} > 2.5$ ). Researchers at DuPont Technologies have recently reported that the best results are achieved by polymerization at 0°C in the presence of higher concentrations of LiCl or NaCl (5–10 M), under which conditions polymerization is complete within 3 h with a higher yield (80%) and superior polydispersity ( $\text{PD} < 2.0$ ).<sup>66</sup>

**NATURE AND CONCENTRATION OF THE DOPANT ACID (HA)**

The nature and concentration of the protonic acid (HA) employed in aniline polymerization with  $\text{S}_2\text{O}_8^{2-}$  have a significant effect on the physicochemical properties

and molecular weights of the PAN/HA products. For example, the polymerization reaction time using  $\text{HClO}_4$  as the dopant acid was observed to be ca. twice as long as that using  $\text{HCl}$ ,  $\text{HNO}_3$ , or  $\text{H}_2\text{SO}_4$ , which may be associated with a more compact morphology for the PAN/ $\text{HClO}_4$  products.<sup>67</sup>

Chemical oxidation of aniline to give conducting PAN/HA emeraldine salts is typically carried out at low pH (0–2) using strong aqueous acids. In one of the few studies of polymerization at higher pH, Fu and Elsenbaumer<sup>68</sup> established from calorimetric and UV-visible spectral studies that materials of low molecular weight and low electrical conductivity were formed in media of pH 4–6. Their properties were inconsistent with the formation of ESs. There has been considerable recent interest in the chemical polymerization of aniline at relatively high pH because of the unusual nanostructures formed. From the early stages of the polymerization of aniline with ammonium persulfate in aqueous  $\text{HCl}$  at pH values of 3–4, MacDiarmid and coworkers<sup>69</sup> have isolated yellow-brown products that they propose (from spectroscopic and elemental analyses) to be a new class of polymeric or oligomeric azane species containing N-N bonds in their backbones. Related studies by Stejskal and coworkers<sup>70</sup> of the polymerization of aniline by the same oxidant in 0.4 M aqueous acetic acid suggest that the oligomeric and nonconducting (conductivity ca.  $10^{-10}$  S/cm) species formed initially at pH > 4 have phenazine-like structures formed as a result of ortho-coupling of aniline monomers.

Other recent papers indicate that PAN-like materials can in fact be grown from chemical oxidation of aniline in basic solutions of aqueous  $\text{NaOH}$ .<sup>71,72</sup> These species again possess unique nanostructures such as nanotubes and hollow microspheres that may have exciting potential applications in nanoscience.

## NATURE OF THE OXIDANT

A wide range of other chemical oxidants has also been successfully employed for the polymerization of aniline monomers. Although the standard electrode potential for  $\text{FeCl}_3$  is low (0.77 V) compared to  $(\text{NH}_4)_2\text{S}_2\text{O}_8$ , it has proved to be a particularly useful oxidant, resulting in PAN's with  $M_w > 20,000$ . Maximum yield and molecular weight of the PAN/ $\text{HCl}$  product are reported<sup>73</sup> to occur without added acid. The optimum reaction temperature (35°C) is higher than that found earlier for  $(\text{NH}_4)_2\text{S}_2\text{O}_8$  ( $\leq 0^\circ\text{C}$ ), which may be due to the slower electron transfer rate of  $\text{FeCl}_3$ . The polymer product has electrochemical properties similar to that of PAN produced with  $(\text{NH}_4)_2\text{S}_2\text{O}_8$ . Solid-state  $^{13}\text{C}$  NMR studies of the corresponding EBs (obtained by alkaline dedoping) also show the  $\text{FeCl}_3$ - and  $(\text{NH}_4)_2\text{S}_2\text{O}_8$ -derived polymers to be very similar. The use of  $\text{FeCl}_3$  also enables polymerization to be carried out in polar organic solvents such as methanol rather than in water.

Other chemical oxidants that have been examined include ceric ammonium sulfate,<sup>74</sup> potassium dichromate,<sup>75</sup> and hydrogen peroxide,<sup>76</sup> although it is reported that optimal conductivities are obtained when  $(\text{NH}_4)_2\text{S}_2\text{O}_8$  is used as oxidant. It has been suggested that the polymerization process is less dependent on the oxidation potential of the particular oxidant (see Table 4.1) than on the degradation processes associated with each.

**TABLE 4.1**  
**Commonly Used Oxidants and Their**  
**Oxidation Potentials**

| Oxidant                               | $E^0$ (V, versus Standard Hydrogen Electrode) |
|---------------------------------------|---|
| $(\text{NH}_4)_2\text{S}_2\text{O}_8$ | 1.94  |
| $\text{H}_2\text{O}_2$                | 1.78  |
| $\text{Ce}(\text{SO}_4)_2$            | 1.72  |
| $\text{K}_2\text{Cr}_2\text{O}_7$     | 1.23  |
| $\text{FeCl}_3$                       | 0.77  |

### NATURE OF THE SOLVENT

Chemical polymerization of aniline and substituted anilines has generally been carried out in aqueous solution. Addition of 0.2–0.6 v/v acetone, tetrahydrofuran (THF), or ethanol to the reaction mixture was found to slow down the polymerization of aniline using  $(\text{NH}_4)_2\text{S}_2\text{O}_8/\text{HCl}$ , with reaction times varying on the order  $t_{\text{acetone}} \sim t_{\text{THF}} > t_{\text{ethanol}}$ .<sup>77</sup> The yields of ES products (ca. 65%) and the electrical conductivities of the products (ca. 10 S  $\text{cm}^{-1}$ ) were similar in each case to those obtained without added organic solvent, but their molecular weights were lower. Similarly, Kuramoto and coworkers<sup>78,79</sup> have polymerized the dodecylbenzenesulfonic acid (DBSA) salt of aniline (dissolved in chloroform) with  $(\text{NH}_4)_2\text{S}_2\text{O}_8$  (in a small amount of water). A homogeneous green/black suspension was obtained from which the PAN/DBSA ES product could be readily isolated by the addition of excess methanol or acetone. PAN has also been prepared in acetonitrile and chloroform solvents using  $\text{Fe}(\text{ClO}_4)_3$  and tetrabutylammonium periodate as the oxidant, respectively.<sup>80,81</sup>

### INTERFACIAL POLYMERIZATION

The chemical polymerization of aniline at the interface between two immiscible solvents provides an attractive alternative route to PAN's. Such interfacial polymerization was first demonstrated in 1994 by Michaelson and McEvoy,<sup>82</sup> who produced a freestanding PAN film at the interface between a solution of aniline/sodium dodecylsulfate in carbon tetrachloride and an aqueous oxidant solution containing ammonium persulfate/HCl. The analogous interfacial polymerization of a range of *N*-alkylanilines and *o*-alkylanilines using hexane and water phases for chemical oxidation with ammonium persulfate has also been briefly described.<sup>83</sup>

### SELF-STABILIZED DISPERSION POLYMERIZATION

Another exciting new approach to the synthesis of defect-free PAN is self-stabilized dispersion polymerization (SSDP), recently reported by Lee and coworkers.<sup>84</sup> In this process, aniline solution in aqueous HCl was added to a chloroform–water mixture and stirred to give a cloudy colloid to which was added ammonium persulfate oxidant in HCl, producing the green ES product. The difference between SSDP and

interfacial polymerization described in the previous section (where reaction occurs at the interface between two liquid phases, each containing one of the reactants) is that polymerization occurs in the aqueous phase.

The authors hypothesized that the organic phase in SSDP would separate the insoluble aniline oligomers and grown PAN chains from the reactive ends of the chains in the aqueous phase, thereby hindering unwanted side-branching (*ortho*-coupling) and crosslinking. This goal appears to have been achieved; the PAN products obtained (after conversion to camphorsulfonate salts) were found to have unprecedentedly high electrical conductivities ( $\delta$ ) of up to 1300 S/cm and to exhibit  $\delta$  versus temperature profiles consistent with metallic character.<sup>85</sup> The availability of such a simple route to high-performance, metal-like PAN opens up new opportunities for CEP applications in *plastic electronics*.

### ACHIEVING REGIOSELECTIVE COUPLING WITH ANILINE MONOMERS

For the oxidative formation of PAN with extended  $\pi$ -conjugation and high conductivity, the regioselective head-to-tail *para*-coupling of the initially formed radical cations is required, as depicted in Figures 4.1 and 4.2. However, the coupling of the N-centered radical cation with the *ortho*-sited radical also occurs to a limited extent, resulting in branched PAN chains. The extent of such *ortho*-coupling has been estimated by <sup>13</sup>C NMR spectroscopy to be ca. 5% for chemically synthesized emeraldine base. This undesired coupling can be reduced by the use of aniline monomers bearing blocking substituents in the *ortho*-position. However, these are generally less readily oxidized than the parent aniline, and the ES products are less conducting because of the twisting of PAN chains from planarity caused by steric interactions by the ring substituents.

### TEMPLATE-GUIDED SYNTHESIS

Employing a polyelectrolyte to bind to and preferentially align the aniline monomers before polymerization (e.g., by  $S_2O_8^{2-}$ ) has shown promise in facilitating the desired head-to-tail coupling of the aniline substrates. During polymerization, the anionic polyelectrolytes such as poly(styrenesulfonate) and poly(acrylate)<sup>86–88</sup> also provide the required counterions for charge compensation in the doped PAN products. This can lead to water-soluble or water-dispersed ES products.

### COMPARISON OF CHEMICALLY AND ELECTROCHEMICALLY PREPARED PAN FILMS

Until recently, it has been generally considered<sup>89,90</sup> that PAN's prepared by the alternative chemical and electrochemical routes have similar chemical structures, although differences in morphology were noted and there was disagreement in the literature as to which route produces material of higher molecular weight.<sup>91,92</sup> Significantly, from a comparison of the CD spectra of chemically and electrochemically prepared PAN/(+)-HCSA films (see Chapter 5), we have recently found the first unequivocal evidence that these PAN's possess different structures or conformations for their chains.<sup>93</sup>

## VAPOR-PHASE DEPOSITION

An alternative to solvent-phase synthesis of CEPs is vapor-phase polymerization (VPP). This route was first used for PAN's in 1998 for the deposition of conducting PAN films on cotton fibers, by impregnating the thread with  $(\text{NH}_4)_2\text{S}_2\text{O}_8$  oxidant and then exposing the surface to aniline vapor.<sup>94</sup> Polyacrylamide films coated with conducting PAN (conductivity ca.  $10^{-5} \text{ S cm}^{-1}$ ) have been similarly prepared.<sup>95</sup>

More recently, using the chiral Fe(III) salt Fe(III)(R)-(+)-camphorsulfonate [Fe(III)(R)-HCSA] as chemical oxidant, the direct vapor-phase deposition of optically active PAN/(+)-HCSA films has been achieved on nonconductive substrates such as glass and poly(ethylene terephthalate). Postpolymerization cyclic voltammetric and Raman spectral studies showed that these chiral ES films possessed stable electrochemical activity in acidic environments.<sup>96</sup>

## PHOTOCHEMICALLY INITIATED POLYMERIZATION

Kobayashi and coworkers<sup>97,98</sup> have recently reported the photochemically initiated polymerization of aniline by irradiation with visible light of either bilayer or single-layer films containing  $[\text{Ru}(\text{bipy})_3]^{2+}$  as initiator and methylviologen ( $\text{MV}^{2+}$ ) as sacrificial oxidant. Irradiation of  $[\text{Ru}(\text{bipy})_3]^{2+}$  near its absorption band at 452 nm leads to the generation of the triplet excited state  $^*[\text{Ru}(\text{bipy})_3]^{2+}$  species. Electron transfer between  $^*[\text{Ru}(\text{bipy})_3]^{2+}$  and  $\text{MV}^{2+}$  generates the strong oxidant  $[\text{Ru}(\text{bipy})_3]^{3+}$ , responsible for the oxidation/polymerization of aniline to PAN.

These studies focused on the deposition of PAN on bilayer or single-layer electrodes for image formation and use in molecular electronics, rather than bulk PAN synthesis. Using appropriate masks, these photochemical routes were shown to have exciting potential for the generation of patterns of CEPs on substrates (with definitions as low as  $2 \mu\text{m}$ ). It was, however, observed that small amounts of aniline dimer (e.g.,  $10^{-3} \text{ M}$ ) were necessary in the aniline monomer ( $0.3 \text{ M}$ ) substrate solution to achieve photopolymerization. This was attributed to the lower oxidation potential of the dimer compared to aniline, with the dimeric radical cation formed in the initial oxidation step then reacting with aniline monomer to give an even more readily oxidized trimer, eventually leading to PAN.

We have independently explored the use of both  $[\text{Ru}(\text{bipy})_3]^{2+}$  and  $[\text{Ru}(\text{phen})_3]^{2+}$  as polymerization photo-initiators for the bulk synthesis of PAN's. By employing the Co(III) complexes  $[\text{CoCl}(\text{NH}_3)_5]^{2+}$  and  $[\text{Co}(\text{H}_2\text{O})(\text{NH}_3)_5]^{3+}$  as the sacrificial oxidants rather than methylviologen, we found<sup>99</sup> that aniline can be readily photopolymerized to PAN/ $\text{HNO}_3$  and PAN/HCSA salts *without* needing the addition of aniline dimer. Facile polymerization of substituted anilines could be similarly achieved yielding, for example, poly(*n*-butylaniline)/ $\text{HNO}_3$  and poly(2,5-dimethoxyaniline)/ $\text{HNO}_3$  salts.

## ENZYME-CATALYZED POLYMERIZATION

Recently, there has been considerable interest in the use of enzymes such as horseradish peroxidase (HRP) as catalysts for the synthesis of PAN's and PPy's with

oxidants such as peroxide.<sup>100,101</sup> Although this method has the advantage of being environmentally benign (the  $\text{H}_2\text{O}_2$  oxidant is converted into water), early studies produced polymers with low molecular weight and extensive chain branching. Samuelson and coworkers<sup>102,103</sup> have largely overcome these problems for the HRP-catalyzed synthesis of PAn through an elegant approach using polyelectrolytes such as poly(styrenesulfonate) (PSS) as templates in the reaction mixture to induce more structural order during PAn growth. The PSS plays three roles in this approach:

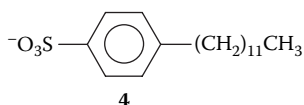
1. Serves as a template that aligns the aniline monomers before polymerization so as to promote the desired head-to-tail coupling
2. Provides the counterions for doping the synthesized PAn to the conducting emeraldine salt form
3. Imparts water solubility to the PAn/PSS product

Another advantage of this enzyme-catalyzed route to colloidal PAn salts is the considerably higher pH that can be employed compared to the previous chemical and electrochemical polymerization methods. Horseradish peroxidase immobilized on chitosan powder as a solid support has also been found to catalyze the  $\text{H}_2\text{O}_2$  oxidation of aniline to a similar PAn/PSS product, opening up the prospect of enzyme reuse and the design of enzyme reactors for PAn synthesis.<sup>104</sup>

The mild ( $\text{pH} = 4.3$ ) conditions for these HRP-catalyzed syntheses have led to the similar employment of more delicate biological polyelectrolytes such as DNA as aligning templates.<sup>105,106</sup> In the latter case, electrostatic interactions between the DNA phosphate groups and protonated aniline monomers before polymerization are believed to provide the preferential alignment leading to *para*-directed coupling of the aniline units. As discussed in Chapter 5, the binding of DNA to PAn in the PAn/DNA product leads to a remarkable, reversible change in the conformation of DNA chains.<sup>107</sup>

## POLYMERIZATION USING ELECTRON ACCEPTORS

Kuramoto and coworkers<sup>108</sup> have developed a novel route to conducting PAn's through the reaction of dodecylbenzenesulfonic acid salts (**4**) of aniline or 2-methoxyaniline with the strong organic electron acceptor dichlorodicyanobenzoquinone (DDQ) in chloroform solvent. The PAn/DBSA product was isolated by the addition of excess methanol and acetone to the polymerization mixture, simultaneously removing oligomers and other organic by-products. In contrast, the weaker organic electron acceptors chloranil and tetracyanoquinodimethane (TCNQ) showed no oxidative polymerization activity. These researchers have more recently extended this approach to the synthesis of optically active PAn's with the polymerization of aniline and its substituted analogs 2-methoxyaniline, 2-ethoxyaniline, and *o*-toluidine with DDQ in mixed chloroform/THF solvent.<sup>107,109</sup>



## MISCELLANEOUS POLYMERIZATION METHODS

Plasma polymerization of aniline in the absence of a solvent or a chemical oxidant, giving neutral undoped PAN, was first described in 1984.<sup>110</sup> This method has been further developed<sup>111,112</sup> recently with, for example, Cruz and coworkers, describing the deposition of PAN film using radio frequency (RF) glow discharges between stainless steel electrodes and at 0.02–0.08 atm pressures. The aniline monomer reacts with electrons in the plasma, and the polymer deposits on the reactor wall after growth.<sup>100</sup>

Recently, acidic (0.6 M H<sub>2</sub>SO<sub>4</sub>) aniline solutions have been reported to undergo slow (10 d), spontaneous polymerization on platinum or palladium foil surfaces, providing a novel, *electroless polymerization* route to PAN.<sup>113</sup> X-ray photoelectron spectroscopy and FTIR spectral studies suggest that the deposited PAN materials are in the rarely reported *nigraniline* oxidation state, intermediate between the well-known emeraldine and pernigraniline states.

## ROUTES TO MORE PROCESSABLE PAN'S

Emeraldine salts prepared by the previous chemical (and electrochemical) oxidative routes are typically amorphous, infusible solids that are insoluble in both organic solvents and water. These intractable characteristics have hindered the development of applications for PAN, and considerable research has been carried out over the past decade to develop routes to more readily processable PAN's.

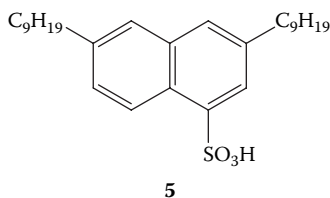
Approaches that have proved successful in enhancing processibility include (1) emulsion polymerization and (2) synthesis of colloidal PAN's. The former leads to PAN that is soluble in organic solvents, whereas the latter provides effectively water-soluble materials. An alternative has been side-chain functionalization, involving the polymerization of ring or *N*-substituted aniline monomers bearing either alkyl or alkoxy groups (to enhance solubility in organic solvents) or sulfonate or carboxylate groups (to induce water solubility). These approaches are discussed in the following sections.

### EMULSION POLYMERIZATION

In initial emulsion polymerization studies,<sup>114,115</sup> oxidation of the aniline monomer was carried out in xylene–water or chloroform–water emulsions containing DBSA. PAN/DBSA polymers with high molecular weights were obtained, with a higher degree of crystallinity, and the polymers exhibited a fibril structure. These differences in properties were attributed to the fact that the higher solubility of the PAN product in the emulsion sustained the polymerization reaction.<sup>103</sup> Further applications of this synthetic route include the preparation of a PAN/chlorophyll material, which exhibits good solubility in organic solvents such as chloroform, benzene, and THF.<sup>116</sup>

However, the PAN products were not easily recovered and generally were isolated by breaking the emulsion (e.g., by adding acetone), to precipitate the ES. A major development with this method was therefore the discovery of a direct synthesis of an ES that is highly soluble in organic solvents by workers at Monsanto.<sup>117</sup> The method uses a reverse emulsion procedure involving initial formation of emul-

sion particles consisting of a water-soluble organic solvent (e.g., 2-butoxyethanol), a water-insoluble surfactant-like dopant (dinonylnaphthalenesulfonic acid, DNNSA; **5**), aniline, and water, with  $(\text{NH}_4)_2\text{S}_2\text{O}_8$  as oxidant. As the reaction proceeds, the mixture changes from an emulsion to a two-phase system, with the PAn product remaining in the organic phase. This solution is typically diluted with toluene and has been sold commercially under the trade name PANDA<sup>TM</sup>.



The PAn/DNNSA is highly soluble (it is not a dispersion) in nonpolar organic solvents such as xylene and toluene, common solvents used in many paints. It has a molecular weight ( $M_w$ ) > 22,000 and an electrical conductivity of  $10^{-5} \text{ S cm}^{-1}$ . Interestingly, treatment of a PAn/DNNSA film with methanol or acetone leads to a marked (five orders of magnitude) increase in conductivity, which is believed to arise from extraction of excess DNNSA dopant causing an increase in polymer crystallinity.

## COLLOIDAL PAN DISPERSIONS

The most commercially successful method of producing processable forms of CEPs has been the aqueous colloidal dispersion route pioneered by Vincent and Armes<sup>118–120</sup> (see two recent reviews by Armes<sup>121</sup> and Wessling<sup>122</sup>). Unlike the methods discussed earlier, which all require extensive derivatization of the aniline monomer, dispersions are readily formed from unsubstituted aniline and are readily manufactured in bulk quantities.

The major route to colloidal (effectively water soluble) PAn has been through the chemical oxidation ( $\text{S}_2\text{O}_8^{2-}$ ) of the monomer in the presence of polymeric steric stabilizers and electrosteric stabilizers (polyelectrolytes), such as poly(vinyl alcohol), poly(*N*-vinyl pyrrolidone), poly(ethylene oxide), poly(styrene sulfonate), dodecylbenzene sulfonate, and dextran sulfonate. It has been found that the stabilizer can act simultaneously as a dopant, imparting new functionality to the polymer or additional compatibility for the final application.

Colloid formation during chemical synthesis occurs because of the formation of small, growing PAn particles in aqueous solution adsorbing the stabilizer onto their outer layers, typically through hydrogen bonding. The adsorbed outer layer then stabilizes the particle and prevents coalescence. Typical particle sizes range from 60 to 300 nm<sup>123</sup> and are strongly dependent on the type of stabilizer, oxidant type and concentration, monomer concentration, temperature, etc., and they can exist as either discrete particles or group together as conglomerate structures. Recently, colloidal PAn/HCl/DBSA dispersions containing 10–20 nm particles and PAn/HCl/PVA [PVA = poly(vinyl alcohol)] dispersions with particles as small as 5 nm have been reported,<sup>124,125</sup> the latter in mixed DMSO–water solvent.



We have shown that such colloids are electroactive and can be electrodeposited.<sup>126</sup> However, the electrodeposited films are not coherent and redissolve once the negative potential is removed. Optically active colloidal PAN nanocomposites of the type PAN/HCSA/polyacrylic acid have also recently been synthesized using the chemical oxidation route, by the oxidation of aniline with  $(\text{NH}_4)_2\text{S}_2\text{O}_8$  in the presence of (+)- or (-)-HCSA as the dopant acid and polyacrylic acid as the steric stabilizer.<sup>127</sup>

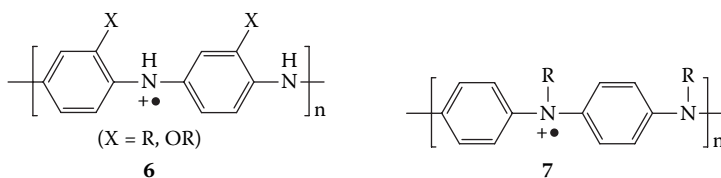
Alternatively, the *core-shell* approach has been employed to generate aqueous dispersions (or nanocomposites) in which PAN's are deposited on the surfaces of nanoparticles such as silica<sup>128,129</sup> or  $\text{TiO}_2$ <sup>130</sup> during polymerization. The resultant core-shell structures often group together as conglomerate structures described as having a raspberry-like morphology.<sup>131</sup>

A detailed  $^1\text{H}$  NMR kinetic investigation<sup>132</sup> of the polymerization of aniline in  $\text{DCI}/\text{D}_2\text{O}$  solution has revealed no significant differences between the rates of dispersion polymerization using a poly(ethylene oxide)-based stabilizer and standard precipitation polymerization in the absence of any stabilizer. However, faster polymerization of aniline was observed in the presence of 20 nm silica particles, leading to PAN-silica nanocomposites. In contrast, slower polymerization occurred in the presence of surfactant micelles to form surfactant-stabilized PAN particles, presumably owing to the high solution viscosity.

## SUBSTITUTED PAN'S

### ALKYL- AND ALKOXY-SUBSTITUTED PAN'S

A wide range of alkyl- and alkoxy-substituted PAN's of the general types **6** and **7** have been synthesized by the chemical or electrochemical oxidation of appropriately substituted aniline monomers.<sup>133</sup> Such substitution imparts markedly improved solubility in organic solvents to the emeraldine salt products compared to the parent (unsubstituted) PAN/HA salts. The poly(2-methoxyaniline) (POMA) species, in particular, has been the subject of extensive studies.<sup>134-137</sup> This species has the additional attractive feature of being soluble in water after being wet with acetone.



The substituted PAN products often have much lower molecular weights than the parent unsubstituted PAN, although  $M_w$  values as high as  $400,000 \text{ g mol}^{-1}$  have been reported for POMA by controlled chemical polymerization at  $-40^\circ\text{C}$ .<sup>58</sup> This improvement in processability for substituted PAN's is also generally gained at the expense of a large decrease in electrical conductivity, due to twisting of the polymer chains from planarity by the bulky substituents.

Oxidative polymerization of substituted aniline monomers is frequently more difficult than that of aniline. A significant recent advance has therefore been the

synthesis of the novel poly(aniline boronic acid), which can be readily converted into a range of other substituted PAN's, including previously inaccessible polymers (*vide infra*).<sup>138</sup>

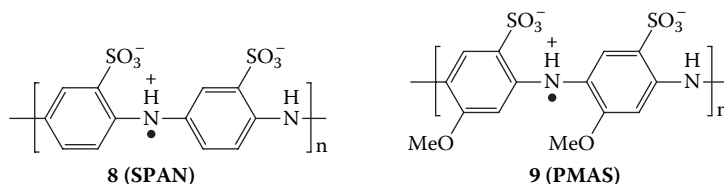
### COVALENTLY BOUND CHIRAL SUBSTITUENTS

A significant recent development has been the synthesis of PAN's in which chiral substituents have been covalently attached to the aniline rings. Chiral ethers were bound to the aniline monomer before its chemical oxidation by persulfate,<sup>139</sup> producing chiral PAN's possessing strong optical activity as evidenced by their CD spectra. Previous routes to chiral PAN's had employed chiral dopant anions to induce chirality into PAN chains.

### SULFONIC ACID SUBSTITUTED PAN'S

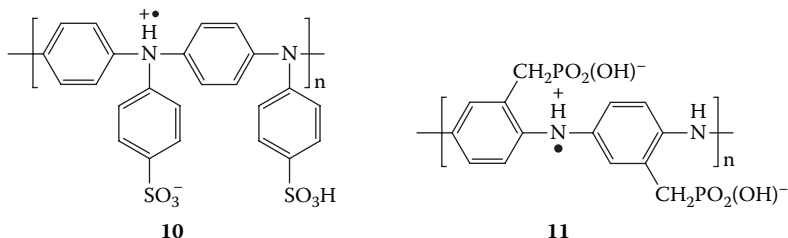
There has also been considerable interest in the polymerization of sulfonated aniline monomers in the hope of producing water-soluble sulfonated PAN's. Attempts to polymerize *o*- or *m*-aminobenzenesulfonic acid using both chemical and electrochemical means have generally been unsuccessful, which has been attributed to steric and electronic deactivation by the electron-withdrawing sulfonic acid substituent.<sup>140,141</sup> However, Young and coworkers<sup>142</sup> have reported that *o*- and *m*-aminobenzenesulfonic acid can be synthesized by a novel, high-pressure (19 kbar) procedure using  $(\text{NH}_4)_2\text{S}_2\text{O}_8$  as oxidant in the presence of 5.0 M LiCl and 5%  $\text{FeSO}_4$ , yielding the fully sulfonated, self-doped PAN (SPAN; **8**). However, its UV-visible spectrum is inconsistent with an emeraldine salt.

The related fully sulfonated, self-doped polymer poly(2-methoxyaniline-5-sulfonic acid) (PMAS; **9**) may be prepared under normal atmospheric pressure by the oxidation of 2-methoxyaniline-5-sulfonic acid (MAS) monomer with aqueous  $(\text{NH}_4)_2\text{S}_2\text{O}_8$  in the presence of ammonia or pyridine (to permit dissolution of the MAS monomer).<sup>141</sup> The polymerization pH was therefore  $\geq 3.5$ . Subsequent studies showed that the product consisted of two fractions: a major fraction with  $M_w$  of ca. 10,000 Da whose electrical conductivity and spectroscopic and redox switching properties were consistent with a PAN emeraldine salt, as well as a nonconducting, electroinactive oligomer ( $M_w$  ca. 2,000 Da).<sup>143,144</sup> Pure samples of each of these materials can be obtained using cross-flow dialysis.<sup>145</sup>



The self-doped polymer, poly{*N*-(4-sulfophenyl)aniline} **10**, bearing a sulfonated substituent on each of its N centers, has also been prepared by oxidizing the relevant monomer with  $(\text{NH}_4)_2\text{S}_2\text{O}_8$  in aqueous HCl.<sup>146,147</sup> Phosphonic acid substituents can also be utilized to generate self-doping PAN's, as illustrated by the oxidation using

$\text{S}_2\text{O}_8^{2-}$  of the monomer *o*-aminobenzylphosphonic acid to give the novel polymer **11**.<sup>148</sup> Its low conductivity (ca.  $10^{-3} \text{ S cm}^{-1}$ ) may arise from H-bonding between the  $\text{PO}_2(\text{OH})^-$  substituents and  $\text{NH}^+$  radical cation sites on the polymer chain, causing significant charge-pinning.



### POSTPOLYMERIZATION MODIFICATION: ENHANCING FUNCTIONALITY

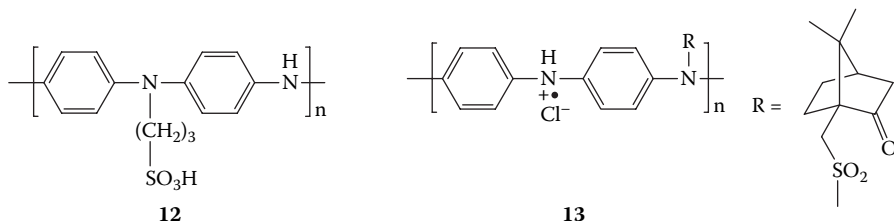
An alternative approach to increasing the solubility, and hence the processability of PAN, has been a variety of postpolymerization methods. Such modifications have also been pursued in order to introduce added functionality to PAN, allowing their use in a range of applications such as chemical and biochemical sensors. The postpolymerization modifications typically involve either (1) chemical reactions on preformed emeraldine base (EB), leucoemeraldine base (LB), or pernigraniline base (PB) leading to covalent binding of groups to the aniline rings or N centers, or (2) doping of preformed EB with agents such as Brönsted acids (HA), Lewis acids, and metal complexes, or organic electron acceptors. These various approaches are summarized in the following sections.

#### COVALENTLY SUBSTITUTED PAN'S

In addition to their direct synthesis from sulfonated aniline monomers described earlier, a number of water-soluble, self-doped sulfonated PAN's may also be prepared by postpolymerization methods. The most widely investigated has been the synthesis of the ring-substituted SPAN **8**. Treatment of EB with fuming sulfuric acid gave a SPAN product with ca. 50% of the aniline rings sulfonated.<sup>140</sup> Subsequently, it was found that up to 70% of the aniline rings could be sulfonated by similar treatment of LB, giving a polymer with enhanced electrical conductivity (ca.  $1 \text{ S cm}^{-1}$ ).<sup>149</sup> The substitution of amino and alkylthio groups onto the aniline rings of PAN has similarly been achieved through the treatment of EB (or PB) with alkyl amines and alkylthiols.<sup>150</sup>

Deprotonation of the amine centers in EB by treatment with NaH in DMSO, followed by reaction with 1,3-propanesulfone, provides a route to the water-soluble, self-doped polymer **12**, in which a  $-(\text{CH}_2)_3\text{SO}_3\text{H}$  group is covalently attached to ca. 50% of the N centers along the polymer chain.<sup>151</sup> The use of the fully reduced LB as substrate should lead to a higher degree of N-substitution. This has been confirmed in a related study where subsequent treatment of the deprotonated LB with alkyl halides has provided a general route to poly(*N*-alkylaniline)s, with alkyl chains varying in length from butyl to octadecyl.<sup>152</sup>

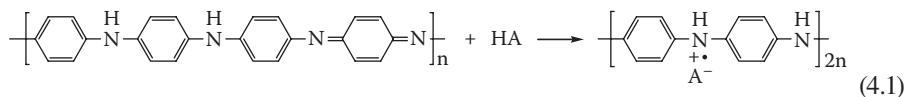
In our laboratories, we have used a related approach to covalently attach chiral camphorsulfonate groups to N centers of PAN, by the reaction of EB with (1S)-(+)-10-camphorsulfonyl chloride in NMP/pyridine.<sup>153</sup> The optically active product **13**, isolated as the HCl salt, is believed to preferentially adopt a one-handed helical conformation for its polymer chains. This provides the first example of chiral induction in a PAN species through a covalently attached group. A significant advantage for the product **13** compared to the chiral PAN/HCSA salts described earlier is that it consequently retains its optical activity upon alkaline dedoping in solution to its EB form.



A factor hindering the expansion of PAN chemistry to date has been the lack of a generic route to variously substituted derivatives. An exciting development in this respect is the recent synthesis of the novel poly(aniline boronic acid).<sup>138</sup> Aromatic boronic acids are versatile chemical precursors, undergoing a wide range of transformations and this provides a facile route to a wide range of substituted PAN's that are difficult to synthesize directly from their respective monomers. This approach has been successfully demonstrated for the synthesis of poly(hydroxyaniline) and for poly(halogenoaniline).<sup>138</sup>

### DOPING OF EB WITH BRÖNSTED ACIDS (HA)

PAN is unique among inherently conducting polymers in that it can be converted into a conducting form by a nonredox, acid-doping process, exemplified by the doping of EB with Brönsted acids (HA) to yield electronically conducting PAN/HA emeraldine salts (Equation 4.1). A wide variety of acids may be employed, ranging from inorganic acids such as HCl, HNO<sub>3</sub>, H<sub>2</sub>SO<sub>4</sub>, H<sub>3</sub>PO<sub>4</sub>, and HBF<sub>4</sub> to organic sulfonic and carboxylic acids.



In an important discovery in the early 1990s, Cao and coworkers<sup>154</sup> found that organic solvent solubility can be imparted to conducting PAN salts by the incorporation of surfactant-like dopant acids (HA). For example, by doping EB with large bifunctional protonic acids such as HCSA or DBSA, it is possible to solubilize fractions of these polymers in their fully doped state into solvents such as *m*-cresol, chloroform, toluene, and xylene. This solubilization is caused by the hydrocarbon “tail” in the dopants, while the sulfonate (SO<sub>3</sub><sup>-</sup>) “head” forms an ionic bond with radical cation NH<sup>+</sup> sites on the PAN chains. There is some debate as to whether this approach pro-

duces true solutions or forms dispersions in organic media. In practical terms the result is the same—solution-processable, unsubstituted conducting polymers in the doped state.

Films of the PAN/HCSA and PAN/DBSA polymers may be cast from these solutions; the properties of the films are highly dependent on the solvent employed.<sup>155,156</sup> This is attributed to the solvent's ability to produce either a rodlike (more highly conducting) or coil-like (less conducting) polymer structure (see Chapter 5). The solubility of these polymers in organic solvents has also facilitated the preparation of conducting blends of PAN with various insulating polymers.<sup>157,158</sup> The blends can exhibit a very low percolation threshold, believed to arise from the formation of an interpenetrating network morphology.<sup>159</sup>

It has recently been shown that acid doping of EB can also be carried out in the solid state.<sup>160</sup> For example, the mechanical blending of stoichiometric amounts of solid EB and HCSA or picric acid leads to electrically conducting PAN/HA salts.

Water-soluble ESs can also be prepared by this acid-doping technique. For example, doping of EB with phosphonic acid containing poly(ethyleneglycol)monoethyl ether (PEGME) as a hydrophilic tail gives a mildly conducting PAN that is soluble (or dispersible) in water.<sup>161</sup>

With the water-soluble poly(*o*-methoxyaniline) (POMA), Mattoso and coworkers<sup>162</sup> have reported the self-assembly of multilayer conducting polymer films by depositing alternating layers of the POMA cation and polyanionic dopants such as poly(styrenesulfonate) and poly(vinylsulfonate) onto a glass substrate. This concept has been further developed with POMA by employing the anion of poly(3-thiopheneacetic acid) as the polyanionic dopant, giving novel self-assembled films in which both the cationic and anionic components are electroactive polymers.<sup>163</sup>

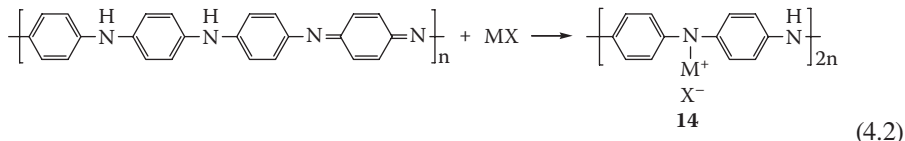
We have employed a related approach in generating films containing alternating layers of the anionic, water-soluble sulfonated polyaniline PMAS **9** and the polycation, poly(vinylpyridine).<sup>164</sup> The analogous self-assembly of multilayer films of the sulfonated SPAN **8** and the light-sensitive polycation, diazoresin, has also been described recently.<sup>165</sup>

## INCORPORATION OF CHIRAL DOPANT ANIONS OR CATIONS

This synthetically facile acid-doping approach (Equation 4.1) has also been successfully employed by us and others to produce optically active PAN's. The addition of the chiral dopant (+)- or (-)- HCSA to EB in organic solvents such as *N*-methylpyrrolidinone rapidly generates optically active PAN/HCSA salts in solution, where the PAN chains are believed to adopt a one-handed helical arrangement (see Chapter 5).<sup>166,167</sup> Optically active PAN/HCSA films can be cast onto glass from these solutions. We have observed similar, but less rapid, chiral induction by doping the EB forms of the ring-substituted polymers poly(2-methoxyaniline) (POMA) and poly(*ortho*-toluidine) with (+)- and (-)-HCSA.<sup>168,169</sup> Optically active PAN's can also be similarly produced by employing other chiral dopant acids such as (+)- or (-)- tartaric acid and *O,O'*-dibenzoyl derivatives.<sup>170</sup>

### DOPING OF EB WITH LEWIS ACIDS

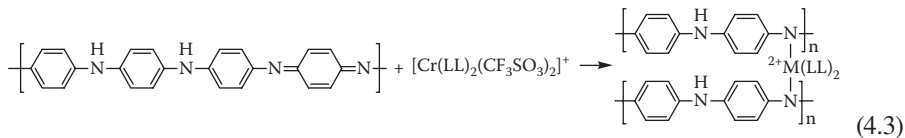
Solutions of EB may be also readily doped with a range of metal salts and Lewis acids in a process (Equation 4.2) reminiscent of the Brønsted acid doping of EB described earlier. Similar to protonic doping, binding of the metal ions to imine N sites on the EB chains is believed to occur, leading to conducting PAN products of the general type **14**.



Considerable attention has been paid to the doping of EB with LiCl and other lithium salts because of its significance to lithium-ion rechargeable batteries.<sup>171–173</sup> The coordination of transition metal ions such as Zn(II) and Pd(II) to PAN N centers has also been described by several research groups.<sup>160,174–176</sup> For the reaction of Pd(II) species with EB, a redox reaction involving partial oxidation of the PAN to its pernigraniline state and concomitant reduction of Pd<sup>2+</sup> to Pd<sup>0</sup> is reported to accompany the complexation reaction.<sup>177</sup> The Pd-containing PAN species have significant catalytic activity for a range of reactions. Similar doping and redox processes have been suggested during the related reaction of CuCl<sub>2</sub> with EB in NMP solvent.<sup>178</sup>

Complexation (doping) of EB with classic Lewis bases such as AlCl<sub>3</sub>, GaCl<sub>3</sub>, SnCl<sub>4</sub>, and FeCl<sub>3</sub> solubilizes PAN in acetonitrile and nitromethane, solvents that will not dissolve EB or its protonated PAN/HA ESs.<sup>179</sup> This improved solubility is attributed to metal doping at all the PAN basic sites, eliminating H-bonding between adjacent polymer chains, which is one of the major contributors to poor PAN solubility (see Chapter 5).

The generation of octahedral transition metal (TM) complexes of PAN through related reactions of EB with complexes containing readily removable ligands should have considerable advantages over the aforementioned doping with simple metal salts. These include a variety of fixed geometric (*cis* or *trans*) and chiral configurations, distinctive redox/spectroscopic properties associated with their metal–ligand interactions, and their potential use as probes for the nature and site of metal binding to PAN. To this end, we have doped EB in CHCl<sub>3</sub> solvent with the Cr(III) complexes *cis*-[Cr(L-L)<sub>2</sub>(CF<sub>3</sub>SO<sub>3</sub>)<sub>2</sub>]<sup>+</sup> (L-L = 1,2 diaminoethane; 1,10-phenanthroline or 2,2'-bipyridine) and *cis*- and *trans*- [Cr(cyclam)(CF<sub>3</sub>SO<sub>3</sub>)<sub>2</sub>]<sup>+</sup> containing readily replaced triflate ligands, as summarized in Equation 4.3.<sup>180</sup> In the *cis*-[Cr(phen)<sub>2</sub>(CF<sub>3</sub>SO<sub>3</sub>)<sub>2</sub>]<sup>+</sup> case, strong support for coordination of Cr(III) to imine N sites on the polymer chains came from photoluminescence studies on the related reaction with the aniline tetramer.



In a recent fascinating development of this approach, Hirao and coworkers<sup>181</sup> have produced chiral induction in poly(*ortho*-toluidine) via the complexation of EB with chiral Pd(II) complexes bearing one labile coordination site. The chirality of the ligand moieties of the Pd complex is believed to induce a propeller twist of the PAN backbone.

### DOPING OF EB WITH ORGANIC ELECTRON ACCEPTORS

“Pseudodoping” of EB by a range of organic acceptors has also been reported by Kang and coworkers,<sup>182,183</sup> producing charge transfer complexes with conductivities as high as  $0.1 \text{ S cm}^{-1}$ . On the basis of the maximum conductivity achieved, the complexing/doping ability of the organic acceptors with EB decreases in the order: TCNE  $\sim$  *o*-chloranil  $>$  DDQ  $>$  *o*-bromanil  $>$  *p*-fluoranil  $>$  *p*-chloranil. With *o*-chloranil, x-ray photoelectron spectroscopic (XPS) studies show the formation of Cl<sup>-</sup> ions and positively charged N centers on the PAN chains and a concomitant decrease in imine N sites. This indicates that the charge transfer interaction between the electron acceptor and EB must proceed beyond the simple formation of a charge transfer complex, consistent with pseudodoping of EB. Similar charge transfer interactions are observed between *o*-chloranil or *o*-bromanil and substituted EBs to give substituted PAN's such as poly(2-chloroaniline), poly(3-chloroaniline), and poly(2-ethyl-aniline).<sup>184</sup> However, XPS data reveal less extensive charge transfer, presumably owing to steric hindrance associated with the aniline ring substituents.

### ION IMPLANTATION

Ion implantation has recently been employed as an alternative doping method to convert neutral, nonconducting PAN into a conducting form. For example, bombarding PAN with high energy (24 keV) I<sup>+</sup> ions is reported<sup>185</sup> to cause a 12 orders of magnitude increase in the conductivity of the polymer.

### STRUCTURE OF PAN

PAN's formed by both the chemical and electrochemical processes have been extensively studied to establish structure–property relationships. In this section, the structural studies of PAN are reviewed; the influence of structure on properties is considered in Chapter 5. The description of PAN structure is complicated by its complexity. As described earlier, PAN can exist in six different forms (the salt or base forms of leucoemeraldine, emeraldine, and pernigraniline). In addition, the protonated forms of PAN also have counteranions intimately associated with the positively charged PAN chains. Finally, it has also been observed that PAN's may contain considerable amounts of solvent molecules.

### MOLECULAR STRUCTURE AND CONFORMATION

PAN formed by either the electrochemical or chemical process give essentially linear chains with predominantly *para* head-to-tail couplings. As reviewed previously, variations to the linear structure have been introduced by substitutions on the ben-

zene ring. Only the unsubstituted PAN's are described in the following sections, as fewer structural studies have been reported on substituted PAN's.

## MOLECULAR WEIGHT

A few studies have investigated the molecular weight of PAN as prepared by standard methods. In an early work, MacDiarmid and Epstein<sup>186</sup> reported that normal gel permeation chromatography (GPC) techniques could be used to determine molecular weight distributions of PAN. The EB form of PAN was dissolved in NMP with 0.5 wt% LiCl to prevent gelation. Using narrow polystyrene standards, the PAN molecular weight was estimated to be 64,452 ( $M_w$ ) and 25,283 ( $M_n$ ), giving a polydispersity of 2.55. The molecular weights could be increased (to  $M_w = 440,000$ ;  $M_n = 127,000$ ; PDI = 3.5) by cooling the reaction solution to  $-9^\circ\text{C}$  (in the presence of LiCl) to precipitate anilinium hydrochloride and to minimize the concentration of free aniline in the solution. These authors also compared the molecular weights obtained from GPC (using polystyrene standards) and that obtained from light scattering of leucoemeraldine solutions. The leucoemeraldine was obtained by reducing the EB using hydrazine, and the molecular weight by light scattering was found to be approximately one half of that estimated using GPC.

More recently, Mattes and coworkers<sup>187</sup> have investigated the effect of polymerization temperature on the molecular weight of chemically synthesized PAN. Using polystyrene standards, the molecular weights ( $M_w$ ) increased from 31,000 to 235,000 as the polymerization temperature decreased from 0 to  $-40^\circ\text{C}$ . LiCl was used during polymerization, while the EB was dissolved in NMP using 2-methylaziridine as an antigelation agent.

Mattes and coworkers also determined the Mark–Houwink constants for PAN EB in NMP. The Mark–Houwink equation relates the intrinsic viscosity (solution viscosity at infinite dilution) to the polymer molecular weight:

$$[\eta] = KM_w^\alpha$$

where  $[\eta]$  is the intrinsic viscosity and  $K$  and  $\alpha$  are the Mark–Houwink constants. By relating the intrinsic viscosity of four different EB samples to their weight average molecular weight (determined from GPC using polystyrene standards), the Mark–Houwink constants were determined to be  $K = 1.2 \times 10^{-4} \text{ dl g}^{-1}$  and  $\alpha = 0.77$ . These values are in the range expected for flexible chain conformations. In a comparative study of different polymerization methods, Jayakannan and coworkers<sup>188</sup> found that the intrinsic viscosity (and, therefore, molecular weight) decreased in the listed order for PAN ES (doped with pTS) prepared by

1. Redoping an EB sample prepared by chemical polymerization of aniline in HCl solution giving ES–Cl and subsequent deprotonation using ammonium hydroxide
2. Direct polymerization of aniline in a water–toluene stirred mixture containing pTS acid dopant



### 3. Interfacial polymerization of aniline in a water–toluene stirred mixture containing pTS acid dopant

The importance of using LiCl to prevent polymer aggregation has been demonstrated by Angelopoulos and coworkers<sup>189</sup> in GPC studies. These workers noted that without LiCl the GPC chromatogram showed a bimodal distribution. The high molecular weight peak, however, disappeared when LiCl was added to the solution, suggesting that this peak was due to polymer aggregation. NMP can H-bond to the PAN, but this solvent does not sufficiently solvate the polymer to disrupt all PAN interactions. Thus, additives such as LiCl must be added to prevent PAN H-bonding interactions.

## CHAIN CONFORMATION

A number of studies have considered the nature of the PAN conformation in solution as an effect of solvent/dopant/oxidation state. As described in Chapter 5, the PAN can form either tight coils or expanded chains depending on the nature of the solvent used. This behavior is typical of polymers in either “poor” or “good” solvents, but has a significant impact on the electrical properties of conjugated polymers, as described in Chapter 5 for PAN.

## BULK STRUCTURE

### NANOSCALE HETEROGENEITY

There is considerable evidence and widespread acceptance that PAN forms a heterogeneous structure in its emeraldine salt (ES) form. The evidence comes mainly from electronic transport studies in which the temperature dependence of conductivity fits a charge-hopping model.<sup>190</sup> It is proposed that small domains of highly ordered polymer are surrounded by less ordered material and that electron transport is dominated by the slow conduction through the latter. In the ordered regions, it is suggested that the polymer chains lie flat, allowing a longer conjugation length as the  $\pi$  orbitals can overlap. In the amorphous regions, the chains are more twisted, causing less overlap of  $\pi$  orbitals and shorter conjugation lengths.

Recently, there have been a number of studies that provide direct evidence of the heterogeneous structure of PAN ES. In our own work (see Chapter 1, Figure 1.30),<sup>191</sup> we have used a variant of the scanning tunneling microscope to probe the electronic structure of ES. In this technique (called *current-imaging tunneling spectroscopy* [CITS]), the I–V characteristics of the polymer are mapped with nanometer resolution. For PAN ES, it was found that small (20–80 nm) domains having metallic-like I–V curves were surrounded by an insulating matrix. The structure fitted very well with the description provided by conductivity modeling.

## CRYSTALLINITY, MOLECULAR ORDER, AND CONFORMATION IN SOLID STATE

The exact nature of the structure of the ordered phase in PAN is an ongoing research area. The elucidation of such structure is complicated by the various means of pro-

ducing ES films or coatings: direct electropolymerization or through acid doping (protonation) of EB. The latter technique has the advantage that the EB is highly soluble, and good-quality films and coatings can be cast from the solution. Subsequent treatment of the EB films gives the ES. It has been known for some time that certain dopants render the PAn ES soluble. Thus, it is also possible to form films and coatings by direct casting from ES solutions. However, as described previously, the nature of the solvent used for the ES can profoundly affect the conformation of the PAn in solution, and these conformational differences are also carried over to the cast films. The following sections review the structural studies of solution-cast and electropolymerized PAn in both the EB and ES forms.

Pouget and coworkers made an exhaustive study of PAn crystallinity in 1991,<sup>192</sup> and this work remains the main reference point for more recent studies. Pouget and coworkers report two forms of crystallinity in the ES form of PAn and that these two structures are produced by different processing methods. The so-called ES-I structure is produced by direct polymerization of aniline in acid to produce the doped PAn ES, either electrochemically or by using chemical oxidants. Deprotonation of the ES-I produces an amorphous EB (denoted EB-I), and reprotonation of EB-I once again generates the ES-I structure. A new crystallographic structure is produced, however, when EB-I is dissolved in solvents such as NMP and cast as a film; the EB is crystalline with a degree of crystallinity ~50%. This structure is denoted EB-II. When EB-II is doped with HCl, it produces the ES-II structure, again with a degree of crystallinity of 50%, but fundamentally different from the ES-I structure. Curiously, when ES-II is deprotonated, it produces an amorphous EB, and reprotonation of this amorphous EB gives the ES-II structure (not ES-I). More specific descriptions of these crystal structures and a summary of more recent studies are given in the following sections.

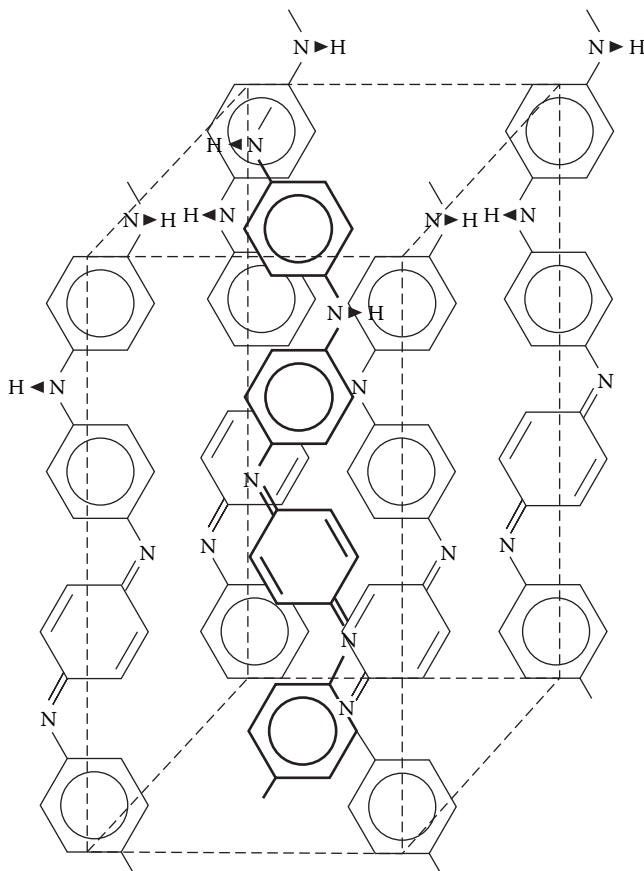
## SOLUTION-CAST EMERALDINE BASE

The EB form of PAn can be either crystalline or amorphous depending on its preparation conditions. The crystalline form (EB-II) has a degree of crystallinity of up to 50% and a crystallite size of 5–15 nm.<sup>192</sup> The crystal structure has been indexed as an orthorhombic lattice with the polymer chains oriented in the *c*-direction. The lattice parameters enable the ring-N-ring angle ( $\delta$ ) about the amine nitrogen to be estimated as between 131 and 141°. Furthermore, modeling of the structure enables an estimate of the ring tilt angle ( $\theta$ ), where the phenyl rings are tilted out of the plane defined by the N atoms by +30° and -30° for alternating rings. The chain structure is represented in Figure 4.3, and the proposed<sup>192</sup> orthorhombic structure is shown in Figure 4.4.

Some studies have examined the effect of solvent on the structure of EB films cast from solutions. For example, Ou and Samuels<sup>193</sup> found that EB films cast from NMP solution were partially crystalline, as evidenced by shoulders appearing above the amorphous band in x-ray diffraction (XRD) studies. However, when the EB was cast from a solution in *N,N'*-dimethyl propylene urea (DMPU), no evidence of crystallinity was observed. Whereas the NMP solutions were unstable (undergoing gelation owing to the formation of H-bonded networks between the PAn chains), the



**FIGURE 4.3** Definition of the chain angles  $\delta$  (bond angle ring-amine N-ring) and  $\theta$  (ring torsional twist).



**FIGURE 4.4** Proposed EB-II orthorhombic crystal structure for emeraldine base.

DMPU solutions were stable probably because the DMPU can itself H-bond to the PAn. The implication of these observations is that the structure formed in solution is likely to become nucleation sites for crystallization upon solidification by solvent evaporation. Disrupting the solution structure reduces the number of nucleation sites and effectively prevents crystallization. Contrasting results have been reported by Angelopoulos and coworkers,<sup>189</sup> who showed that crystallinity was only observed in films cast from low concentrations of EB in NMP (< 10 wt%). The interpretation

from these results was that the solution network in higher concentrations actually impedes crystal formation upon solvent evaporation.

There is general agreement that increased crystallinity of EB can be induced by mechanically stretching the films or fibers. Ou and Samuels<sup>193</sup> estimate the crystallinity for undrawn EB to be 11–15%, which increases to 20–30% with a draw ratio of 3.5. Mechanical drawing also results in a high degree of anisotropy, with the crystallites oriented in the draw direction. XRD studies by Fischer and coworkers<sup>194</sup> confirm the increase in crystallinity with drawing of EB fibers. The increase in crystallinity was attributed to the nucleation of new crystallites rather than to the growth of existing crystals. These workers also noted an orientation effect of the amorphous phase, so that highly drawn ( $L/L_0 = 4.5$ ) EB has an amorphous phase analogous to the nematic liquid crystal structure.

## EMERALDINE SALT FROM PROTONATION OF EB

Protonation of the EB can produce two types of ES crystal structures. The structures are denoted ES-I (from protonation of amorphous EB-I) and ES-II (from protonation of EB-II).

The ES-II structure, similar to the EB-II structure from which it is formed, is likely to have an orthorhombic lattice. Model calculations show the ring tilt angle to be close to  $0^\circ$ , accounting for the higher conductivity of the ES compared to EB. The formation of the ES-II structure by doping EB-II can be visualized by a shift of the middle chain in Figure 4.4 by  $\vec{b}/2$  and  $+\vec{c}/2$  and insertion of dopant ions between the (a,c) layers.<sup>192</sup>

The ES-I structure is less well defined, but likely involves a tilting of the chains with respect to the (a,b) basal plane. There are similarities between the EB-II structure and the ES-I structure in terms of d-spacings, and a model ES-I structure can be derived from the EB-II structure by inserting a dopant ion in the channel delimited by four adjacent chains.<sup>192</sup> A compact structure is obtained by assuming that the dopant sits in the hollow of the polymer chain zig-zag. Good agreement of calculated and experimental XRD spectra is obtained by assuming such a structure, although some subtle differences remain unexplained.<sup>192</sup> The model structure assumes a ring tilt angle of  $0$ – $15^\circ$  and a chain twist angle (of the chain with respect to the  $c$ -axis) of  $20$ – $30^\circ$ .

More detailed studies of the ES-I structure have shown variations depending on the type of dopant. When ES is prepared by protonating EB using different acids, the crystal structure has been shown to be dependent on the type of acid used.<sup>187</sup> Small dopant ions, such as pTS and 5-sulfosalicylic acid, induce less crystalline ordering than larger dopants such as CSA and DBSA. The latter give diffraction peaks that suggest a larger degree of separation between polymer chains, as described in detail in the following sections.

## SOLUTION-CAST EMERALDINE SALT

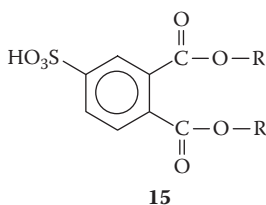
ES films can be prepared directly from solutions when particular counterions are used to impart solubility. The most extensively studied system is the camphorsul-

fonic-acid-doped ES as cast from a *m*-cresol solution. Luzny and coworkers have considered the crystal structure of camphorsulfonic-acid-doped polyaniline (PAn/CSA) as cast from *m*-cresol.<sup>195</sup> Although presenting a clear crystal structure with a degree of crystallinity of 25%, the unit cell structure has no resemblance to the structures formed by the EB.

In fact, Minto and Vaughan<sup>196</sup> argue that the PAn/CSA crystal structure is a variation of the ES-I crystal structure described earlier. The interactions between the phenyl rings in the CSA<sup>-</sup> anion and the polymer produce a more planar structure of the polymer chains compared with the ES-I structure (ring tilt angle up to 15°). The planar arrangement also reduces the interchain separation from  $a = 0.426$  nm for ES-I (HCl-doped) to  $a = 0.35$  nm for PAn/CSA. Furthermore, Minto and Vaughan describe a liquid-crystal-like order in the amorphous phase of PAn/CSA owing to the ordering and solvation by residual *m*-cresol solvent. Finally, the unstretched films examined by them showed a preferred orientation of the polymer chains parallel to the substrate.

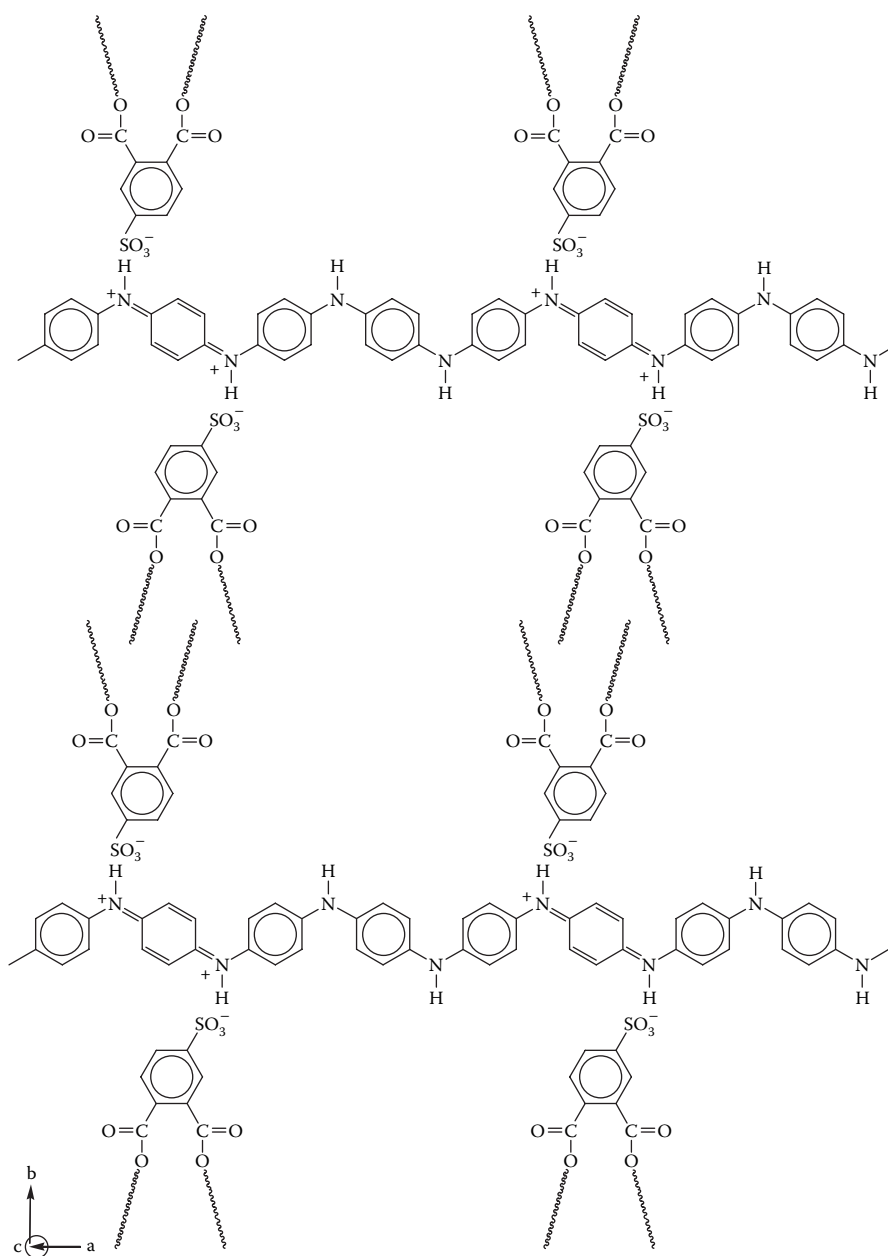
More recent studies have shown the consistency of the crystal structure of PAn/CSA to be variable and highly dependent on the conditions of film preparation. Saravanan and coworkers<sup>197</sup> have reported a crystallinity as high as 56% in CSA-doped PAn. Djurado and coworkers<sup>198</sup> have speculated that the influence of chain branching during polymerization may play a role in the nature of the crystal structure formed.

Pron and coworkers<sup>199</sup> have investigated the crystal structure of other soluble ESs. In these studies, the solubility of the ES was induced using dialkyl ester sulfonate dopants (**15**), where R = *n*-pentyl, *n*-octyl, *n*-dodecyl, or other alkyl chains:



The general model of the crystal structure proposed by Pron and coworkers<sup>199</sup> is shown schematically in Figure 4.5. In this structure, the alkyl chains separate the ordered PAn chains and the separation of the latter depends on the alkyl chain length. In fact, detailed analysis suggests that the alkyl chains are interdigitated, as shown in the figure. Similar structures have been proposed for DBSA-doped PAn.<sup>200</sup>

A similar layered, or lamellar, structure has been described by Laska and coworkers<sup>201</sup> for PAn ES doped with alkyl phosphates. These dopants both solubilize and plasticize the polymer. The effect of doping level on the microstructure has been reported, with the degree of crystallinity generally decreasing with an increasing level of doping. The fully doped ES had a degree of crystallinity almost half that of the lightly doped structure (dopant:aniline at unit molar ratio of 0.2). It was proposed that the increased concentration of bulky dopant ions around the PAn chains at the fully doped state (dopant:aniline at unit molar ratio of 0.5) disrupted the ordered structure.



**FIGURE 4.5** Layered stacking of emeraldine salt chains with *n*-alkyl diester dopants separating the chains in the *b*-direction.

## ELECTROPOLYMERIZED EMERALDINE SALT

The crystal structure of electropolymerized PAN ES has been shown to conform to the ES-I structure, at least for simple counterions such as  $\text{Cl}^-$ . Zhu and coworkers<sup>202</sup> used STM/AFM to obtain high-resolution images of both electrochemically grown and solution-cast PAN films with different dopants. They found a high degree of molecular ordering with extended PAN chains stacked in parallel rows and separated by a distance that correlated with dopant size. The interchain separation was found to be 0.4 nm for  $\text{Cl}^-$ -doped ES, close to the expected chain separation for the ES-I crystal structure. The interchain distance increased to 0.7 nm for  $\text{ClO}_4^-$  dopants and 1.4 nm for pTS-doped ES. These separations were found to closely agree with molecular mechanics calculations. More recently, it has been shown that the presence of neutral KI salts increased the crystallinity of electrochemically prepared PAN.<sup>203</sup>

## INFLUENCE OF WATER AND “SECONDARY DOPANTS” ON PAN CRYSTALLINITY

An increase in crystallinity of PAN ES has been reported by the incorporation of secondary plasticizing agents. Pron and coworkers<sup>199</sup> have shown that the incorporation of an “external” plasticizer enhances the crystallinity of dialkyl-ester-doped PAN. The use of dioctylphthalate or tritolyl phosphate was shown to increase the intensity of WAXD scattering peaks and to also increase the electrical transport properties. With about 30 wt% of external plasticizer added (with respect to the PAN base), it is estimated that one plasticizer molecule is associated with 13.5–14 PAN repeat units. The analysis of the XRD peaks shows that the plasticizer does not enter the crystalline domains and must, thus, remain in the amorphous regions. The plasticizer, therefore, is believed to enhance the crystallization of the PAN by allowing greater chain flexibility during the latter stages of film casting.

## MORPHOLOGY AND DENSITY

The film morphology of electrochemically prepared PAN has been shown by many workers to be fibrillar in nature and often quite porous. In contrast, solution-cast films are flat and featureless with little porosity. The density of cast PAN films has been found to depend on the dopant and degree of crystallinity,<sup>204</sup> as expected. Conditions that favor lower crystallinity (such as higher polymerization temperature) and the incorporation of bulky dopants will produce lower-density films. The density of electropolymerized coatings will also be affected by the porosity and coating morphology. The factors influencing the morphology of electropolymerized PAN are reviewed in the following text.

Armes and coworkers have investigated the structure of both PAN colloid particles [stabilized with poly(vinyl alcohol)] and electrochemically prepared PAN films. In both cases the fundamental morphology was nanoparticles of up to 20 nm in diameter. Colloid particles were *rice grain* shaped. Thick films showed submicron-sized features that appear to be aggregates of the smaller particles.

Several other studies have indicated that the PAN film morphology changes during the polymerization process. Abrantes and coworkers,<sup>205</sup> for example, used ellip-

sometry techniques to investigate the thickness and properties of PAN/SO<sub>4</sub> films prepared potentiodynamically. These workers found clear evidence of a less dense structure forming at longer polymerization times. Desilvestro and Scheifele<sup>206</sup> have reviewed some of the early structural studies on PAN. They report that SEM and ellipsometry studies have shown that thin (< 150 nm) PAN films prepared electrochemically are compact with densities of ~1.45 g/cm<sup>3</sup>. Thicker films become very porous with a granular or fibrous surface structure. Films that are many tens of microns thick can have porosities in excess of 80%.

On the basis of studies of polymerization of aniline in a number of supporting electrolytes, Desilvestro and Scheifele<sup>206</sup> have proposed the following growth mechanism for electrodeposited PAN. There is an induction period initially in which a dense layer of globular morphology is deposited. Polymerization then proceeds from localized globules, leading to fibrils of roughly uniform diameter. Further deposition occurs at the active ends of fibrils and at branch points (which are evenly distributed). Partial thickening of the fibrils also takes place during further polymerization. Porosities are consistently reduced when faster polymerization occurs (e.g., potentiodynamic polymerization, higher aniline concentrations).

A number of studies have investigated the effect of counterion on PAN film morphology. In our own studies, we have commonly observed a powdery deposit for electrochemically prepared PAN (see Chapter 5). Comparing small counterions, Duic and coworkers<sup>207</sup> found a correlation between film morphology and conductivity. Fibrous morphologies were produced by using four acids, with the diameter of the fibrils decreasing with different anions as follows: HSO<sub>4</sub><sup>-</sup> > NO<sub>3</sub><sup>-</sup> > Cl<sup>-</sup> > ClO<sub>4</sub><sup>-</sup>. The rate of polymerization (under identical potentiodynamic conditions) followed the same order; it is possibly related to specific anion adsorption on the electrode promoting a higher concentration of the anion at the polymerization site. The Cl<sup>-</sup> ion promotes less branching of fibrils than the oxyacids, and the lower degree of branching may account for the lower conductivity (10<sup>-3</sup> S/cm) of the PAN/Cl compared with the PAN prepared from oxyacid electrolytes (1–8 S/cm).

Hwang and Yang<sup>208</sup> have compared the morphology and porosity of PAN prepared with polyelectrolytes. Similarly to other workers, they found that HCl produces a porous, fibrous network with fiber diameters ~100 nm. The addition of poly(acrylic acid) produced extended, long needles of PAN loosely connected together. Other polyelectrolytes, such as poly(vinylsulfonate) and poly(styrenesulfonate), produce more globular surface structures.<sup>208</sup> Yang has advanced the hypothesis that the morphology is determined by H-bonding interactions between the anilinium ions and the polyelectrolyte chains to produce the so-called *double strand* PAN.

The morphology of *in situ* deposited PAN's using chemical oxidants is very similar to that of thin electrodeposited films. For thin films (60 nm thick), AFM studies reveal granular features of 50–100 nm in diameter that are densely packed giving smooth films.<sup>209</sup> Thicker films are much rougher with granular features up to 200 nm in diameter.

The growth mechanism of *in situ* deposited films proposed by Stejskal and coworkers<sup>210</sup> has similarities to that described earlier for electrodeposited PAN. It is important to note that the *in situ* method produces both a surface coating as well as the normal powdery precipitate from the bulk of the solution. It is proposed by



Stejskal that aniline radical cations adsorb on the substrate surface during an *induction period* before bulk polymerization is observed. The adsorbed species promote the formation of a dense film initially on the substrate surface. Once this film has formed, further growth occurs on the PAN surface in a manner similar to the growth of localized globules during electropolymerization. The surface roughness of *in situ* PAN films may be further increased by the incorporation of PAN precipitates from the bulk solution.

## NANOSTRUCTURED POLYANILINES

As for PPy's, there has been an explosion of interest in the synthesis of PAN's with nanodimensions, as such materials have been shown to have enhanced electronic and electrochemical properties. Formation of PAN nanoparticles has been achieved via polymerization in micelles, using either sodium dodecyl sulfate (SDS)<sup>211</sup> or DBSA<sup>212–214</sup> as the surfactant stabilizer. Particle sizes in the range of 10–30 nm with conductivities as high as 24 S cm<sup>-1</sup> have been reported.

Control of the micelle size utilized in the formation of PAN nanoparticles has been achieved by tailoring the stabilizer to modify the resulting micelle dimensions. Kim and coworkers<sup>215,216</sup> used amphiphilic polymer molecules and hydrophobically end-capped poly(ethylene oxide) [PEO], and varied the hydrophilic regions in it to control the final micelle size. The resultant nanostructures ranged from 20 to approximately 300 nm in size, depending on the molecular weight of the hydrophilic PEO midsection.

Using inverse microemulsions, it has been shown that small monodisperse PAN particles can be produced.<sup>217–219</sup> Particle sizes in the range of 10–35 nm diameter were obtained. After washing to remove the surfactant, chemically prepared materials exhibited conductivities of up to 10 S cm<sup>-1</sup>, whereas for electrochemically prepared materials conductivities as high as 200 S cm<sup>-1</sup> were reported. Gan and coworkers used<sup>218</sup> an inverse microemulsion approach that involved the formation of barium sulfate nanoparticles, which were then coated by PAN. These composite nanoparticles had a reported conductivity from 0.017 to 5 S cm<sup>-1</sup>, with particles ranging in size from 10 to 20 nm. Xia and Wang<sup>220</sup> have used ultrasonication during inverse microemulsion polymerization of PAN to produce spherical nanoparticles with diameters of 10–50 nm and conductivities on the order of 10 S cm<sup>-1</sup>. The ultrasonication was found to increase the rate of polymerization of aniline, which is typically slow when the microemulsion route is used. Rate increases are obtained by acceleration of heterogeneous liquid–liquid chemical reactions in solution. A secondary advantage is the prevention of aggregation due to particle agitation induced by ultrasonication.

Physical templates have also been used to facilitate the growth of PAN nanostructures. Nanofibril arrays were prepared by chemically depositing PAN into 20–200 nm pores in anodic aluminum oxide film (30–60 μm thick) that was subsequently etched away with 0.3 M H<sub>3</sub>PO<sub>4</sub> or through ultrasonication.<sup>221</sup>

Hollow CEP cigar-shaped nanotubes with sealed ends, synthesized via the track-etched polycarbonate template route, have also been reported by Mativetsky and Datars.<sup>222</sup> These materials exhibited a small drop in conductivity as the diameter decreased from 400 to 50 nm, contrary to previous reports.<sup>223–224</sup> The small decrease

in conductivity on the order of  $50 \text{ mS cm}^{-1}$  is believed to result from an increase in the electron scattering within the nanocylinder walls or from the presence of large impedances in the nanostructure.

Choi and Park<sup>226</sup> have modified surfaces with cyclodextrins to assist in the electroformation of PAN nanowires. Others have utilized the concept of molecular templates to form PAN supramolecular rods with electrical conductivity improved by two orders of magnitude.<sup>227</sup>

A template-guided synthesis of water-soluble chiral-conducting PAN in the presence of (S)-(-)- and (R)-(+)-2-pyrrolidone-5-carboxylic acid [(S)-PCA and (R)-PCA] has been reported to produce nanotubes.<sup>228</sup> The structures prepared have outer diameters of 80–220 nm with an inner tube diameter of 50–130 nm. It was proposed that the tubular structures form as a result of the hydrophobic aniline being templated by the hydrophilic carboxylic acid groups of the PCA in aqueous media during chiral tube formation. The resultant tubes were shown to be optically active, suggesting that the PAN chains possess a preferred helical screw.

McCarthy and coworkers<sup>126,229</sup> reported a template-guided synthesis of water-soluble chiral PAN nanocomposites. The nanoparticles were prepared by the physical adsorption of aniline monomer onto a templating poly(acrylic acid) in the presence of (+)- or (-)-CSA, followed by chemical oxidation. Using this approach, optically active nanocomposites of approximately 100 nm diameter were formed. Earlier work by Sun and Yang<sup>230</sup> using polyelectrolytes produced similar nonchiral dispersions in which the PAN chain is interwound with a water-soluble polymer by electrostatic forces.<sup>231</sup> Similar work by Samuelson and coworkers utilized DNA as a chiral template for PAN.<sup>232</sup>

The concept of using molecular templates has been taken a step further by Zhang and Wan<sup>233</sup> by the incorporation of 10 nm  $\text{Fe}_3\text{O}_4$  nanomagnet particles into the  $\beta$ -NSA nanorods and nanotubes that are 80–100 nm in diameter. These PAN/ $\beta$ -NSA/ $\text{Fe}_3\text{O}_4$  nanostructures were observed to exhibit superparamagnetic behavior (i.e., hysteresis loop effects). More importantly, both the electrical conductivity and magnetic properties of these nanoparticles could be manipulated by control over the loading level of the nanomagnetic particles. Increased loading of the  $\text{Fe}_3\text{O}_4$  nanoparticle decreased the conductivity from *ca.*  $70 \text{ mS cm}^{-1}$  for no loading to *ca.*  $10 \text{ mS cm}^{-1}$  at 20 wt%, while inducing the superparamagnetic behavior in the nanocomposite.

Self-assembled PAN nanofibers and nanotubes that also exhibit photoisomerization functionality have been described by Huang and Wan<sup>234</sup>; azobenzenesulfonic acid (ABSA) was used as the molecular templating surfactant, dopant, and photoactive agent. The nanostructures formed were similar to those synthesized by Wan and coworkers<sup>228,235–237,233</sup> (discussed previously), with diameters of 110–130 nm and fiber lengths of 3–8  $\mu\text{m}$ . The photoinduced isomerization, from *trans* to *cis*, of the ABSA dopant was observed using UV-visible spectroscopy at 430 nm ( $n-\pi^*$  transition) after irradiation of the nanocomposites at 365 nm (for 0, 2, 6, 10, and 12 min) by UV-visible spectroscopy from 300 to 800 nm. The photoisomerization of the composite material was observed to be slower than that for ABSA owing to steric hinderance as a result of the *trans*-ABSA interacting along the polymer backbone.

Recent elegant studies by Kaner and coworkers<sup>238,239</sup> have shown that interfacial polymerization provides a facile and versatile method to produce PAN's as nanofi-

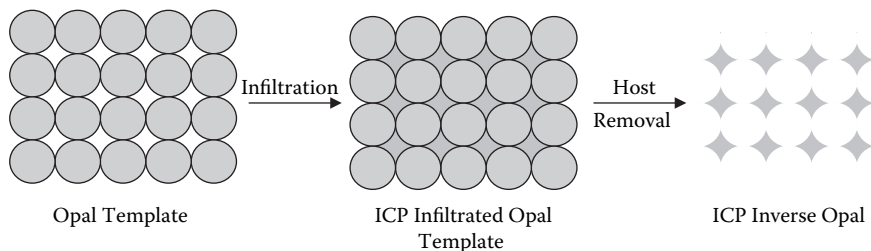
bers with diameters between 30 and 120 nm, depending on the nature of the dopant anion employed. In addition, by constraining the aniline polymerization to the solvent interface, this synthetic approach is believed to hinder undesired reactions such as *ortho*-coupling and lead to PAN's with fewer defects.

There are a number of alternate routes that are capable of producing nanoparticles in the absence of a precursor substrate or a molecular template. For example, He and coworkers<sup>240</sup> have described a technique in which PAN is deposited between two nanoelectrodes to form a nanojunction. As the junction is decreased in size to just a few nanometers, abrupt switching characteristics are observed as opposed to the more gradual transition observed during electrochemical switching of PAN structures with larger dimensions. A further report from the same laboratory<sup>241</sup> added a new dimension by initiating growth of PAN between an STM tip and a gold substrate. The STM tip was modified to allow only a few nanometers to take part in the growth of the nanowire. During growth, the tip and substrate were monitored at 20–100 nm resolution. After growth, the nanowire could be stretched by moving the STM tip to produce wires up to 200 nm in length and with diameters as low as 6 nm. These structures had conductivities of about 5 S cm<sup>-1</sup>.

Electrodeposition of PAN containing (C60) fullerene as dopant<sup>242,243</sup> has been shown to result in 2-D or 3-D fibrillar structures.<sup>243,244</sup> Diameters from 10 to 100 nm with fibril lengths of up to 3000 nm were observed. The fibrillar network had conductivities in the range 10–100 S cm<sup>-1</sup>. 2-D networks have been prepared using pulsed-potential techniques, whereas 3-D networks were observed to form over longer synthesis times. With this approach, there is apparent control over the density of contact points for the individual nanonetworks.

Electrospinning<sup>245,246</sup> is another recent nontemplated method. This simple approach is based on the electrostatic fiber spinning of composite fibers of PAN with poly(ethylene oxide), polystyrene, or polyacrylonitrile. These fibers are formed when a high electric field (5–14 kV) is placed between the tip of a metallic anodic spinning needle loaded with the dissolved polymer solution (0.5–4 wt% PAN and 2–4 wt% host polymer) and an opposing cathode plate separated by 20 cm. The presence of the high electric field causes the electrostatic forces on the polymer-loaded solution at the needle tip to overcome the surface tension, thereby expelling a polymer fiber from the surface toward the opposing cathodic plate. The transit time from the anode tip to the cathode plate is accompanied by a desolvation and drying process, in part assisted by the electrostatic charges placed upon the solvent molecules causing electrostatic repulsion. The resulting nanofiber composite is reported to have lengths in the meter range and is collected as an interwoven mesh with large surface-to-volume ratios (~10<sup>3</sup> m<sup>2</sup>/g). These fibers are ohmic in nature. Fiber dimensions of < 100 nm have been routinely produced by this technique. More recently,<sup>245</sup> fibers of PAN have been directly spun from a 20 wt% solution of PAN (Versicon<sup>TM</sup>) in 98% sulfuric acid at 5 kV. The electrospinning method has also been extended to produce continuous PAN/poly(ethylene oxide) monofilament nanofibers down to 60 nm diameter at a maximum spin rate of 1130 m/min and a conductivity of 33 S cm<sup>-1</sup>.<sup>247</sup>

Aligned polymer nanowire structures have been developed using an electrochemical deposition technique to form aligned PAN arrays on smooth and textured electrode substrates without the need for a porous templating structure.<sup>248,249</sup> Ori-



**FIGURE 4.6** Schematic showing the approach used to produce highly ordered inverse opal structures with conducting polymers.

ented polymer nanowires were formed using a preprogrammed constant-current deposition method in which the current density was stepped down throughout the nanowire growth.

In order to create novel nanostructures, PAN's have been recently deposited on aligned carbon nanotubes<sup>250</sup> or into the interstitial spaces of inverse opals<sup>251,252</sup> to create novel, ordered 3-D networks (Figure 4.6). Molecular templates (such as cyclodextrin) have also been added to electrode surfaces to facilitate the electrodeposition of nanostructures.<sup>253</sup>

## DEPOSITION IN NANOSCALE MATRICES

An elaboration of this technique, incorporating the concept of template-guided synthesis, is the use of nanoporous matrices such as zeolites and polycarbonates as a template within whole pores to perform the chemical polymerization of aniline monomers. For example, Wu and Bein<sup>254</sup> have prepared nanofilaments of conducting PAN in the 3-nm-wide channels (pores) of the aluminosilicate host, MCM-41, through initial adsorption of aniline vapor into the dehydrated host followed by oxidation with  $(\text{NH})_2\text{S}_2\text{O}_8$ .

## REFERENCES

1. Willstater, R.; Cramer, J. *Ber.* 1910, 43: 2976; 1911, 44: 2162.
2. Green, A.G.; Woodhead, A.E. *J. Chem. Soc.* 1910, 97: 2388; 1912, 101: 1117.
3. MacDiarmid, A.G.; Chiang, J.C.; Halpern, M.; Huang, W.S.; Mu, S.L.; Somasiri, N.L.; Wu, W.; Yaniger, S.I. *Mol. Cryst. Liq. Cryst.* 1985, 121: 173.
4. Huang, W.S.; Humphrey, B.D.; MacDiarmid, A.G. *J. Chem. Soc. Faraday Trans 1.* 1986, 8: 2385.
5. Kobayashi, T.; Yoneyama, H.; Tamura, H. *J. Electroanal. Chem.* 1984, 177: 293.
6. Hyodo, K.; Oomae, M. *Electrochim. Acta.* 1990, 35: 827.
7. Barbero, C.; Kotz, R.; Kalaji, M.; Nyholm, L.; Peter, L.M. *Synth. Met.* 1993, 55: 1545.
8. Genies, E.M.; Tsintavis, C.; Syed, A.A. *Mol. Cryst., Liq. Cryst.* 1985, 121: 181.
9. Wei, Y.; Sun, Y.; Patel, S.; Tang, X. *Polymer Preprints.* 1989, 30: 228.
10. Zotti, G.; Cattarin, S.; Comisso, N. *J. Electroanal. Chem.* 1984, 177: 387.
11. Genies, E.M.; Tsintavis, C. *J. Electroanal. Chem.* 1985, 195: 109.
12. Zotti, G.; Cattarin, S.; Comisso, N. *J. Electroanal. Chem.* 1988, 239: 387.
13. Huang, Z.; Wang, P.C.; MacDiarmid, A.G.; Xia, Y.; Whilesides, G. *Langmuir.* 1997, 13: 6480.

14. Pastil, S.F.; Bedkar, A.G.; Agashe, C. *Mat. Letters*. 1992, 14: 307.
15. Camalet, J.L.; Lacroix, J.C.; Aeiyaich, S.; Chane-Ching, K.I.; Lacaze, P.C. *Synth. Met.* 1999, 102: 1386.
16. Akundy, G.S.; Rajagopalan, R.; Iroh, J.O. *J. App. Polymer Sci.* 2002, 83: 1970.
17. Rajagopalan, R.; Iroh, J.O. *Electrochim. Acta.* 2001, 46: 2443.
18. Sazou, D. *Synth. Met.* 2001, 118: 133.
19. Okamoto, H.; Kotaka, T. *Polymer.* 1998, 39: 4349.
20. Porter, T.L.; Minove, D.; Sykes, A.G. *J. Vac. Sci. Technol.* 1995, May/June: 1286.
21. Duic, L.J.; Mandic, Z.; Kvacicek, F.J. *Polym. Sci.* 1994, 32: 105.
22. Cordova, R.; Del Valle A.; Arratia, A.; Gomez, H.; Schrebler, R. *J. Electroanal. Chem.* 1994, 377: 75.
23. Duic, I.J.; Mandic, Z.; Kovacicek, F. *J. Polym. Sci. Part A. Polym. Chem.* 1994, 32: 105.
24. Hyodo, K.; Nozaki, M. *Electrochim. Acta.* 1988, 33: 165.
25. Mattozo, L.H.C.; Faria, R.M.; Bulhoes, L.O.S.; MacDiarmid, A.G. *Polymer.* 1994, 35: 5104.
26. Majidi, M.R.; Kane-Magurie, L.A.P.; Wallace, G.G. *Polymer.* 1994, 45: 3113.
27. Majidi, M.R.; Kane-Maguire, L.A.P.; Wallace, G.G. *Aust. J. Chem.* 1998, 51: 23.
28. Norris, I.D.; Kane-Maguire, L.A.P.; Wallace, G.G. *Macromolecules.* 2000, 33: 3237.
29. Strounina, E.V.; Kane-Maguire, L.A.P., Wallace, G.G. *Synth. Met.* 1999, 106: 129.
30. Watanabe, A.; Mori, K.; Mikuni, M.; Nakamura, Y.; Matsuda, M. *Macromolecules.* 1989, 22: 3323.
31. Lapkowski, M.; Fryczkowski, R. *Polish. J. Chem.* 1994, 68: 1597.
32. Sahin, Y.; Percin, S.; Alsancak, G.Ö. *Journal of Applied Polymer Science.* 2003, 89: 1652.
33. Sahin, Y.; Percin, S.; Sahin, M.; Özkan, G. *Journal of Applied Polymer Science.* 2003, 90: 2460.
34. Sahin, Y.; Percin, S.; Sahin, M.; Özkan, G. *Journal of Applied Polymer Science.* 2004, 91: 2302.
35. Yano, J.; Ota, Y.; Kitani, A. *Materials Letters.* 2004, 58: 1934.
36. Fusalba, F.; Belanger, D. *J. Phys. Chem.* 1999, 103: 9044.
37. Li, M.C.; Ma, C.A.; Liu, B.Y.; Jin, Z.M. 2005, 7: 209.
38. Pornputtkul, Y.; Kane-Maguire, L.A.P.; Wallace, G.G. *Macromolecules.* 2006, 39: 5604.
39. Wei, Y.; Sun, Y.; Patel, S.; Tang, X. *Polymer Preprints.* 1989, 30: 228.
40. Dao, L.H.; LeClerc, M.; Guay, J.; Chevalier, J.W. *Synth. Met.* 1989, 29: E377.
41. Manohar, S.K.; MacDiarmid, A.G.; Cromack, K.R.; Ginder, J.M.; Epstein, A.J. *Synth. Met.* 1989, 29: 49.
42. Ohsaka, T.; Ohnuki, Y.; Oyama, N. *J. Electroanal. Chem.* 1984, 161: 399.
43. Dao, L.H.; Guay, J.; LeClerc, M. *Synth. Met.* 1989, 29: E383.
44. Commison, N.; Daolio, S.; Engoli, G.; Zecchin, S.; Zotti, G. *J. Electroanal. Chem.* 1988, 255: 97.
45. LeClerc, M.; Guay, J.; Dao, L.H. *Macromolecules.* 1989, 22: 649.
46. Bonnell, D.A.; Angelopoulos, S. *Synth. Met.* 1989, 33: 301.
47. Hany, P.; Genies, E.M.; Santier, C. *Synth. Met.* 1989, 31: 369.
48. Yue, J.; Epstein, A.J. *J. Am. Chem. Soc.* 1990, 112: 2800.
49. Zhou, D.; Innis, P.C.; Wallace, G.G.; Shimizu, S.I.; Maeda, S. *Synth. Met.* 2000, 114: 287.
50. Innis, P.C.; Norris, I.D.; Barisci, J.N.; Kane-Maguire, L.A.P.; Wallace, G.G. *Macromolecules.* 1998, 31: 6521.
51. Aboutanos, V.; Barisci, J.N.; Kane-Maguire, L.A.P.; Wallace, G.G. *Synth. Met.* 1999, 106: 89.

52. Aboutanos, V.; Kane-Maguire, L.A.P.; Wallace, G.G. *Synth. Met.* 2000, 114: 313.
53. Cao, Y.; Andreatta, A.; Heeger, A.J.; Smith, P. *Polymer.* 1989, 30: 2305.
54. Genies, E.M.; Boyle, A.; Lapkowski, M.; Tsintavis, C. *Synth. Met.* 1990, 36: 139.
55. Tzou, K.; Gregory, R.V. *Synth. Met.* 1992, 47: 267.
56. Stilwell, D.E.; Park, S.-M. *J. Electrochem. Soc.* 1998, 135: 2254.
57. Manohar, S.K.; MacDiarmid, A.G.; Epstein, A.J. *Bull. Am. Phys. Soc.* 1989, 34: 582.
58. MacDiarmid, A.G.; Epstein, A.J. *In Science and Applications of Conducting Polymers.* W.R. Salaneck, W.R.; Clark, D.T.; Samuelson, E.J. (eds). Adam Hilger, Bristol, UK. 1990, 53.
59. Adams, P.N.; Apperley, D.C.; Monkman, A.P. *Polymer.* 1993, 34: 328.
60. Kenwright, A.M.; Feast, W.J.; Adams, P.N.; Milton, A.J.; Monkman, A.P.; Say, B.J. *Polymer.* 1992, 33: 4292.
61. MacDiarmid, A.G.; Chiang, J.C.; Richter, A.F.; Somarisi, N.L.D. *In Conducting Polymers, Special Applications.* L. Alcacer (ed). Reidel, Dordrecht, 1987, 105.
62. Mattoso, L.H.C.; MacDiarmid, A.G.; Epstein, A.J. *Synth. Met.* 1994, 68: 1.
63. Adams, P.N.; Monkman, A.P. *Synth. Met.* 1997, 87: 165; and references cited therein.
64. Beadle, P.M.; Nicolau, Y.F.; Banka, E.; Rannou, P.; Djurado, D. *Synth. Met.* 1998, 95: 29.
65. Stejskal, J.; Riede, A.; Hlavata, D.; Prokes, J.; Helmstedt, M.; Holler, P. *Synth. Met.* 1998, 96: 55.
66. Min, G. *Synth. Met.* 2001, 119: 273.
67. Morales, G.M.; Miras, M.C.; Barbero, C. *Synth. Met.* 1999, 101: 686.
68. Fu, Y.; Elsenbaumer, R.L. *Chem. Mater.* 1994, 6: 671.
69. Venancio, E.C.; Wang, P.-C.; MacDiarmid, A.G. *Synth. Met.* 2006, 156: 357.
70. Stejskal, J.; Sapurina, I.; Trchová, M.; Konyushenko, E.N.; Holler, P. *Polymer.* 2006, 47: 8253.
71. Long, Y.; Chen, Z.; Ma, Y.; Zhang, Z.; Jin, A.; Gu, C.; Zhang, L.; Wei, Z.; Wan, M. *Appl. Phys. Lett.* 2004, 84: 2205; and references cited therein.
72. Wang, X.; Liu, N.; Yan, X.; Zhang, W.; Wei, Y. *Chem. Lett.* 2005, 34: 42.
73. Yasuda, A.; Shimidzu, T. *Synth. Met.* 1993, 61: 239.
74. Syed, A.A.; Dinesan, M.K. *Talanta.* 1991, 38: 815; and references cited therein.
75. Pron, A.; Genoud, F.; Menardo, C.; Nechstein, M. *Synth. Met.* 1988, 24: 193.
76. Sun, Z.; Geng, Y.; Jing, J.L.; Wang, F. *Synth. Met.* 1997, 84: 99; and references cited therein.
77. Geng, Y.; Li, J.; Sun, Z.; Jing, X.; Wang, F. *Synth. Met.* 1998, 96: 1.
78. Kuramoto, N.; Tomita, A. *Synth. Met.* 1997, 88: 147.
79. Kuramoto, N.; Takahashi, Y. *React. Funct. Polym.* 1998, 37: 33.
80. Inoue, M.; Navarro, E.R.; Innoue, M.B. *Synth. Met.* 1989, 30: 199.
81. Epstein, A.J.; Ginder, J.M.; Zuo, F.; Bigelow, R.W.; Tanner, D.B.; Richter, A.F.; Huang, W.-S.; MacDiarmid, A.G. *Synth. Met.* 1987, 18: 303.
82. Michaelson, J.C.; McEvoy, A.J. *J. Chem. Soc., Chem. Commun.* 1994, 79.
83. Falcou, A.; Longeau, A.; Marsacq, D.; Hourquebie, P.; Duchêne, A. *Synth. Met.* 1999, 101: 647.
84. Lee, S.-H.; Lee, D.-H.; Lee, K.; Lee, C.-W. *Adv. Funct. Mater.* 2005, 15: 1495.
85. Lee, K.; Cho, S.; Park, S.H.; Heeger, A.J.; Lee, C.-W.; Lee, S.-H. *Nature.* 2006, 441: 65.
86. Sun, L.; Liu, H.; Clark, R.; Yang, S.C. *Synth. Met.* 1997, 84: 67; and references cited therein.
87. Angelopoulos, M.; Patel, M.; Shaw, J.M.; Labianca, N.C.; Rishton, S.A. *J. Vac. Sci. Technol. B.* 1993, 11: 2794.
88. Chen, S.-A.; Lee, H.-T. *Macromolecules.* 1995, 28: 2858.
89. Genies, E.M.; Boyle, A.; Lapkowski, M.; Tsintavis, C. *Synth. Met.* 1990, 36: 139.

90. Chinn, D.; DuBow, J.; Liess, M.; Josowicz, M.; Janata, J. *Chem. Mater.* 1995, 7: 1504.
91. Mattoso, L.H.C.; Faria, R.M.; Bulhoes, L.O.S.; MacDiarmid, A.G. *Polymer.* 1994, 35: 5104.
92. Hatchett, D.W.; Josowicz, M.; Janata, J. *J. Electrochem. Soc.* 1999, 146: 4535.
93. Norris, I.D.; Kane-Maguire, L.A.P.; Wallace, G.G. *Macromolecules.* 1998, 31: 6529.
94. Tan, S.N.; Ge, H.L. *New Polym. Mater.* 1998, 5: 169.
95. Das, B.K.; Kar, S.; Chakraborty, S.; Chabroborty, D.; Gangopadhyay, S.J. *Appl. Polym. Sci.* 1998, 69: 841.
96. Chen, J.; Winther-Jensen, B.; Pornputtkul, Y.; West, K.; Kane-Maguire, L.; Wallace, G.G. *Electrochem. Solid-State Letts.* 2006, 9: C9.
97. Teshima, K.; Uemura, S.; Kobayashi, N.; Hirohashi, R. *Macromolecules.* 1998, 31: 6783; and references cited therein.
98. Kim, Y.; Fukai, S.; Kobayashi, N. *Synth. Met.* 2001, 119: 337.
99. Kane-Maguire, L.A.P.; Pirkle, B.; Watson, R.; Dozier, T.; Kane-Maguire, N.A.P. *Symposium on Functional Polymers and Electrochemistry; Proc. 11th Royal Australian Chemical Institute Convention.* Canberra, Australia, Feb. 2000: 14.
100. Aizawa, M.; Wang, L. In *Polymeric Materials Encyclopedia.* J.C. Salamre (ed). CRC Press, Boca Raton, Florida, 1996, 3: 2107.
101. Akkara, J.A.; Kaplan, D.L.; John, V.J.; Tripathy, S.K. In *Polymeric Materials Encyclopedia.* J.C. Salamre (ed). CRC Press, Boca Raton, Florida, 1996, 3: 2116.
102. Samuelson, L.A.; Anagnostopoulos, A.; Alva, K.S.; Kumar, J.; Tripathy, S.K. *Macromolecules.* 1998, 31: 4376.
103. Liu, W.; Kumar, J.; Tripathy, S.K.; Senecal, K.J.; Samuelson, L.A. *J. Am. Chem. Soc.* 1999, 121: 71.
104. Jin, Z.; Su, Y.; Duan, Y. *Synth. Met.* 2001, 122: 237.
105. Liu, W.; Cholli, A.L.; Nagarajan, R.; Kumar, J.; Tripathy, S.; Bruno, F.F.; Samuelson, L. *J. Am. Chem. Soc.* 1999, 121: 11345.
106. Nagarajan, R.; Liu, W.; Kumar, J.; Tripathy, S.K.; Bruno, F.F.; Samuelson, L.A. *Macromolecules.* 2001, 34: 3921.
107. Nagarajan, R.; Tripathy, S.K.; Kumar, J.; Bruno, F.F.; Samuelson, L.A. *PMSE.* 2000, 83: 546.
108. Su, S.-J.; Kuramoto, N. *Macromolecules.* 2001, 34: 7249.
109. Su, S.-J.; Kuramoto, N. *Chem. Mater.* 2001, 13: 4787.
110. Hernandez, R.; Diaz, A.F.; Waltman, R.; Bargon, J. *J. Phys. Chem.* 1984, 88: 3333.
111. Gong, X.; Dai, L.; Mau, A.W.H.; Griesser, H.J. *J. Polym. Sci. A.* 1998, 36: 633.
112. Cruz, G.J.; Morales, J.; Castillon Ortega, M.M.; Olayo, R. *Synth. Met.* 1997, 88: 213.
113. Chen, Y.; Kang, E.T.; Neoh, K.G. *Appl. Surface Science.* 2002, 185: 267.
114. Cao, Y.; Smith, P.; Heeger, A.J. U.S. Patent 5,232,631, 1993.
115. Osterholm, J.-E.; Cao, Y.; Klavetter, F.; Smith, P. *Polymer.* 1994, 35: 2902.
116. Jin, C.-Q.; Park, S.-M. *Synth. Met.* 2001, 124: 443.
117. Kinlen, P.J.; Liu, J.; Ding, Y.; Graham, C.R.; Remsen, E.E. *Macromolecules.* 1998, 31: 1735.
118. Vincent, B.; Waterson, J. *J. Chem. Soc., Chem. Commun.* 1990, 683.
119. Armes, S.P.; Aldissi, M.I.; Agnew, S.; Gottesfield, S. *Mol. Cryst. Liq. Cryst.* 1990, 1745.
120. Armes, S.P.; Aldissi, M. *Polymer.* 1991, 32: 2043.
121. Armes, S.P. In *Handbook of Conducting Polymers.* T.A. Skotheim, R.L. Elsenbaumer, J.R. Reynolds (eds). Marcel Dekker, New York. 1998.
122. Wessling, B. In *Handbook of Conducting Polymers.* T.A. Skotheim, R.L. Elsenbaumer, J.R. Reynolds (eds). Marcel Dekker, New York. 1998.
123. Armes, S.P.; Aldissi, M.; Idzorek, G.C.; Keaton, P.W.; Rowton, L.J.; Stradling, G.L.; Collopy, M.T.; McColl, D.B. *J. Colloid Interface Sci.* 1991, 141: 119.

124. Kim, B.J.; Oh, S.G.; Han, M.G.; Im, S.S. *Synth. Met.* 2001, 122: 297.
125. Ghosh, P.; Siddhanta, S.K.; Haque, S.R.; Chakrabarti, A. *Synth. Met.* 2001, 123: 83.
126. Eisazadeh, H.; Spinks, G.M.; Wallace, G.G. *Polym. Int.* 1995, 37: 87.
127. McCarthy, P.A.; Huang, J.; Yang, S.-C.; Wang, H.-L. *Langmuir.* 2002, 18: 259.
128. Stejskal, J.; Kratochvil, P.; Armes, S.P.; Lascelles, S.F.; Riede, A.; Helmstedt, M.; Prokes, J.; Krivka, I. *Macromolecules.* 1996, 29: 6814.
129. Kuramoto, N.; Takahashi, Y.; Nagai, K.; Koyama, K. *React. Funct. Polym.* 1996, 30: 367.
130. Somani, P.R.; Marimuthu, R.; Mulik, U.P.; Sainkar, S.R.; Amalnerkar, D.P. *Synth. Met.* 1999, 106: 45.
131. Gill, M.; Mykytiuk, J.; Armes, S.P.; Edwards, J.L.; Yeats, T.; Moreland, P.J.; Mollett, C. *J. Chem. Soc., Chem. Commun.* 1992, 108.
132. Gill, M.T.; Chapman, S.E.; DeArmitt, C.L.; Baines, F.L.; Dadswell, C.M.; Stamper, J.G.; Lawless, G.A.; Billingham, N.C.; Armes, S.P. *Synth. Met.* 1998, 93: 227.
133. Leclerc, M.; Guay, J.; Dao, L.H. *Macromolecules.* 1989, 22: 649.
134. Macinnes, D.; Funt, B.L. *Synth. Met.* 1988, 25: 235.
135. D'Aprano, G.; Leclerc, M.; Zotti, G.; Schiavon, G. *Chem. Mat.* 1995, 7: 33; and references cited therein.
136. Dao, L.H.; Bergeron, J.Y.; Chevalier, J.W.; Nguyen, M.T.; Paynter, R. *Synth. Met.* 1991, 41-43: 655.
137. Kang, E.T.; Neoh, K.G.; Tan, K.L.; Wong, H.K. *Synth. Met.* 1992, 48: 231.
138. Shoji, E.; Freund, M.S. *Langmuir.* 2001, 17: 7183.
139. Goto, H. *Macromol. Chem. Phys.* 2006, 207: 1087.
140. Yue, J.; Wang, Z.H.; Cromack, K.R.; Epstein, A.J.; MacDiarmid, A.G. *J. Am. Chem. Soc.* 1991, 113: 2665; and references cited therein.
141. Shimizu, S.; Saitoh, T.; Yuasa, M.; Yano, K.; Maruyama, T.; Watanabe, K. *Synth. Met.* 1997, 85: 1337.
142. Chan, H.S.O.; Neuendorf, A.J.; Ng, S.-C.; Wong, P.M.L. Young, D.J. *Chem. Commun.* 1998, 1327.
143. Guo, R.; Barisci, J.N.; Innis, P.C.; Too, C.O.; Wallace, G.G.; Zhou, D. *Synth. Met.* 2000, 114: 267.
144. Strounina, E.V.; Shepherd, R.; Kane-Maguire, L.A.P.; Wallace, G.G. *Synth. Met.* 2003, 135-136: 289.
145. Masdarolomoo, F.; Innis, P.C.; Ashraf, S.; Wallace, G.G. *Synth. Met.* 2005, 153: 181.
146. DeArmitt, C.; Armes, C.P.; Winter, J.; Uribe, F.A.; Gottesfeld, J.; Mombourquette, C. *Polymer.* 1993, 34: 158.
147. Nguyen, M.T.; Kasai, P.; Miller, J.L.; Diaz, A.F. *Macromolecules.* 1994, 27: 3625.
148. Chan, H.S.O.; Ho, P.K.H.; Ng, S.C.; Tan, B.T.G.; Tan, K.L. *J. Am. Chem. Soc.* 1995, 117: 8517.
149. Wei, X.-L.; Wang, Y.Z.; Long, S.M.; Bobeczko, C.; Epstein, A.J. *J. Am. Chem. Soc.* 1996, 118: 2545.
150. Han, C.-C.; Hseih, W.-D.; Yeh, J.-Y.; Hong, S.-P. *Chem. Mater.* 1999, 11: 480.
151. Chen, S.-A.; Hwang, G.-W. *J. Am. Chem. Soc.* 1995, 117: 10055.
152. Zheng, W.-Y.; Levon, K.; Laakso, J.; Osterholm, J.-E. *Macromolecules.* 1994, 27: 7754.
153. Reece, D.A.; Kane-Maguire, L.A.P.; Wallace, G.G. *Synth. Met.* 2001, 119: 101.
154. Cao, Y.; Smith, P.; Heeger, A.J. *Synth. Met.* 1992, 48: 91.
155. MacDiarmid, A.G.; Epstein, A.J. *Synth. Met.* 1995, 69: 85.
156. Avlyanar, J.K.; Min, Y.; MacDiarmid, A.G.; Epstein, A.J. *Synth. Met.* 1995, 72: 65.
157. Cao, Y.; Smith, P.; Heeger, A.J. *Synth. Met.* 1992, 48: 91.
158. Anand, J.; Palaniappan, S.; Sathyanarayana, D.N. *Prog. Polym. Sci.* 1998, 23: 993; and references cited therein.



159. Yang, C.Y.; Cao, Y.; Smith, P.; Heeger, A.J. *Synth. Met.* 1992, 53: 293.
160. Stejskal, J.; Sapurina, I.; Trchova, M.; Prokes, J.; Krivka, I.; Tobolkova, E. *Macromolecules.* 1998, 31: 2218.
161. Geng, Y.H.; Sun, Z.C.; Li, J.; Jing, X.B.; Wang, X.H.; Wang, F.S. *Polymer.* 1999, 40: 5723.
162. Mattoso, L.H.C.; Zucolotto, V.; Patterno, L.G.; van Griethuijsen, R.; Ferreira, M.; Campana, S.P.; Oliveira, O.N. *Synth. Met.* 1995, 71: 2037.
163. Mello, S.V.; Pereira, E.C.; Oliveira, O.N. *Synth. Met.* 1999, 102: 1204.
164. Tallman, D.E.; Wallace, G.G. *Synth. Met.* 1997, 90: 13.
165. Cao, T.; Wei, L.; Yang, S.; Zhang, M.; Huang, C.; Cao, W. *Langmuir.* 2002, 18: 750.
166. Havinga, E.E.; Bouman, M.M.; Meijer, E.W.; Pomp, A.; Simenon, M. *Synth. Met.* 1994, 66: 93.
167. Majidi, M.R.; Kane-Maguire, L.A.P.; Wallace, G.G. *Polymer.* 1995, 36: 3597.
168. Majidi, M.R.; Kane-Maguire, L.A.P.; Wallace, G.G. *Polymer.* 1996, 37: 359.
169. Norris, I.D.; Kane-Maguire, L.A.P.; Wallace, G.G.; Mattoso, L.H.C. *Aust. J. Chem.* 2000, 53: 89.
170. Syed, S.A.; Kane-Maguire, L.A.P.; Majidi, M.R.; Pyne, S.G.; Wallace, G.G. *Polymer.* 1997, 38: 2627.
171. Chen, S.-A.; Lin, L.-C. *Macromolecules.* 1995, 28: 1239.
172. Saprigin, A.; Kohlman, R.S.; Long, S.M.; Brenneman, K.R.; Epstein, A.J.; Angelopoulos, M.; Liao, Y.-H.; Zheng, W.; MacDiarmid, A.G. *Synth. Met.* 1997, 84: 767.
173. Saprigin, A.V.; Brenneman, K.R.; Lee, W.P.; Long, S.M.; Kohlman, R.S.; Epstein, A.J. *Synth. Met.* 1999, 100: 55.
174. Ruokolainen, J.; Eerikainen, H.; Torkkeli, M.; Serimaa, R.; Jussila, M.; Ikkala, O. *Macromolecules.* 2000, 33: 9272.
175. Higuchi, M.; Ikeda, I.; Hirao, T. *J. Org. Chem.* 1997, 62: 1072.
176. Hirao, T.; Yamaguchi, S.; Fukuhura, S. *Tetrahedron Lett.* 1999, 40: 3009; and references cited therein.
177. Hasik, M.; Drelinkiewicz, A.; Wenda, E. *Synth. Met.* 2001, 119: 335.
178. Higuchi, M.; Imoda, D.; Hirao, T. *Macromolecules.* 1996, 29: 8277.
179. Genoud, F.; Kulszewicz-Bajer, I.; Bedel, A.; Oddou, J.L.; Jeandey, C.; Pron, A. *Chem. Mat.* 2000, 12: 744; and references cited therein.
180. Kane-Maguire, L.A.P.; Kane-Maguire, N.A.P. ACS National Meeting, San Francisco, March 2000.
181. Moriuchi, T.; Shen, X.; Hirao, T. *Tetrahedron.* 2006, 62: 12237.
182. Khor, S.H.; Neoh, K.G.; Kang, E.T. *J. Appl. Polym. Sci.* 1990, 40: 2015.
183. Kang, E.T.; Neoh, K.G.; Tan, T.C.; Khor, S.H.; Tan, K.L. *Macromolecules.* 1990, 23: 2918.
184. Kang, E.T.; Neoh, K.G.; Tan, K.L. *Eur. Polym. J.* 1994, 30: 529.
185. Tong, Z.S.; Wu, M.Z.; Pu, T.S.; Xhou, F.; Liu, H.Z. *Synth. Met.* 1995, 68: 125.
186. MacDiarmid, A.G.; Epstein, A.J. *Mater. Res. Soc. Symp. Proc.* 1992, 247: 565.
187. Yang, D.; Adams, P.N.; Mattes, B.R. *Synth. Met.* 2001, 119: 301.
188. Jayakannan, M.; Annu, S.; Ramalekshi, S. *J. Polym. Sci. Pt B - Polym. Phys.* 2005, 43: 1321.
189. Angelopoulos, M.; Dipietro, R.; Zheng, W.G.; MacDiarmid, A.G.; Epstein, A.J. *Synth. Met.* 1997, 84: 35.
190. Zuo, F.; Angelopoulos, M.; MacDiarmid, A.G.; Epstein, A.J. *Phys. Rev. B: Condens. Matter.* 1989, 39: 3570.
191. Yau, S.T.; Barisci, J.N.; Spinks, G.M. *Appl. Phys. Lett.* 1999, 74: 667.
192. Pouget, J.P.; Jozefowicz, M.E.; Epstein, A.J.; Tang, X.; MacDiarmid, A.G. *Macromolecules.* 1991, 24: 779.
193. Ou, R.; Samuels, R. *J. Polym. Sci., Part B: Polym. Phys.* 1999, 37: 3473.

194. Fischer, J.E.; Tang, X.; Scherr, E.M.; Cajipe, V.B.; MacDiarmid, A.G. *Synth. Met.* 1991, 41: 661.
195. Luzny, W.; Banka, E. *Macromolecules.* 2000, 33: 425.
196. Minto, C.D.G.; Vaughan, A.S. *Polymer.* 1997, 38: 2683.
197. Saravanan, S.; Mathai, C.J.; Anantharaman, M.R.; Venkatachalam, S.; Prabhakaran, P.V. *J. Pys. Chem. Solids.* 2006, 67: 1496.
198. Djurado, D.; Nicolau, Y.F.; Rannou, P.; Luzny, W.; Samuelsen, E.J.; Terech, P.; Bee, M.; Sauvajol, J.L. *Synth. Met.* 1999, 101: 764.
199. Dufour, B.; Rannou, P.; Fedorko, P.; Djurado, D.; Travers, J.-P.; Pron, A. *Chemistry of Materials.* 2001, 13: 4032.
200. Levon, K.; Ho, K.H.; Zheng, W.Y.; Laakso, J.; Karna, T.; Taka, T.; Osterholm, J.E. *Polymer.* 1995, 36: 2733.
201. Laska, J.; Djurado, D.; Lunzy, W. *Eur. Polym. J.* 2002, 38: 947.
202. Zhu, C.; Wang, C.; Yang, L.; Bai, C.; Wang, F. *Appl. Phys. A: Mater. Sci. Process.* 1999, 68: 435.
203. Sharma, M.; Kaushik, D.; Singh, R.R.; Pandey, R.K. *J. Mater. Sci-Mater. In Electronics.* 2006, 17: 537.
204. Stejskal, J.; Hlavata, D.; Holler, P.; Trchova, M.; Prokes, J.; Sapurina, I. *Polym. Int.* 2004, 53: 294.
205. Abrantes, L.M., Correia, J.P., Savic, M., Jin, G. *Electrochimica Acta.* 2001, 46: 3181.
206. Desilvestro, J.; Scheifele, W. *J. Mater. Chem.* 1993, 3: 263.
207. Duic, L.; Mandic, Z.; Dovacicek, F. *J. Polym. Sci.; Pt. A: Polym. Chem.* 1994, 32: 105.
208. Hwang, J.H.; Yang, S.C. *Synth. Met.* 1989, 29: E271.
209. Avlyanov, J.K.; Josefowicz, J.Y.; MacDiarmid, A.G. *Synth. Met.* 1995, 73: 205.
210. Sapurina, I.; Riede, A.; Stejskal, J. *Synth. Met.* 2001, 123: 503.
211. Kim, B.J.; Oh, S.G.; Han, M.G.; Im, S.S. *Synth. Met.* 2001, 122: 297.
212. Han, M.G.; Cho, S.K.; Oh, S.G.; Im, S.S. *Synth. Met.* 2002, 126: 53.
213. Samuelson, L.; Liu, W.; Nagarajan, R.; Kuman, J.; Bruno, F.F.; Cholli, A.; Tripathy, S. *Synth. Met.* 2001, 119: 271.
214. Moulton, S.E.; Innis, P.C.; Kane-Maguire, L.A.P.; Ngamna, O.; Wallace, G.G. *Current Applied Physics.* 2004, 4: 402.
215. Kim, D.; Choi, J.; Kim, J.-Y.; Han, Y.-K.; Sohn, D. *Macromolecules.* 2002, 35: 5314.
216. Kim, D.; Kim, J.-Y.; Kim, E.-R.; Sohn, D. *Mol. Cryst. Liq. Cryst.* 2002, 377: 345.
217. Gan, L.M.; Chew, C.H.; Chan, H.S.O.; Ma, L. *Polym. Bull.* 1993, 31: 347.
218. H.S.O. Chan, L.M. Gan, C.H. Chew, L. Ma and S.H. Seow, *J. Mat. Chem.* 3, 1109 (1993).
219. Gan, L.M.; Zhang, L.H.; Chan, H.S.O.; Chew, C.H. *Mat. Chem. Phys.* 1995, 40: 94.
220. Xia, H.; Wang, Q. *J. Nanoparticle Research.* 2001, 3: 401.
221. Wang, Z.; Chen, M.; Li, H.-L.; *Mater. Sci. Eng. A.* 2002, 328: 33.
222. Mativetsky, J.M.; Datars, W.R. *Physica B.* 2002, 324: 191.
223. Duchet, J.; Legras, R.; Demoustier-Champagne, S. *Synth. Met.* 1998, 98: 113.
224. Demoustier-Champagne, S.; Duchet, J.; Legras, R. *Synth. Met.* 1999, 101: 20.
225. Demoustier-Champagne, S.; Stavaux, P.-Y. *Chem. Mater.* 1999, 11: 829.
226. Choi, S.J.; Park, S.M. *Adv. Mat.* 2000, 12: 1547.
227. Kosenen, H.; Ruokolainen, J.; Knaapila, M.; Torkkeli, M.; Jokela, K.; Serimaa, R.; Brinke, G.T.; Bras, W.; Mankman, A.P.; Ikkala, O. *Macromol.* 2000, 33: 8671.
228. Wan, M.; Yang, Y. *J. Mater. Chem.* 2002, 12: 897.
229. Li, W.; McCarthy, P.A.; Liu, D.; Huang, J.; Yang, Z.C.; Wang, H.-L.; *Macromolecules.* 2002, 35: 9975.
230. Sun, L.; Yang, S.C. *Mater. Res. Soc. Symp. Proc.* 1994, 328: 167.
231. Sun, L.; Liu, H.; Clark, R.; Yang, S.C. *Synth. Met.* 1997, 84: 67.

232. Samuelson, L.; Liu, W.; Nagarajan, R.; Kuman, J.; Bruno, F.F.; Cholli, A.; Tripathy, S. *Synth. Met.* 2001, 119: 271.
233. Zhang, Z.; Wan, M. *Synth. Met.* 2003, 132: 205.
234. Huang, K.; Wan, M. *Chem. Mater.* 2002, 14: 3486.
235. Shen, Y.; Wan, M. *J. Polym. Sci.* 1999, 37: 1443.
236. Wei, Z.; Wan, M. *Adv. Mater.* 2002, 14: 1314.
237. Zhang, Z.; Wei, Z.; Wan, M. *Macromolecules.* 2002, 35: 5937.
238. Huang, J.; Virji, S.; Weiller, B.H.; Kaner, R.B. *J. Amer. Chem. Soc.* 2003, 125: 314.
239. Huang, J.; Kaner, R.B. *J. Amer. Chem. Soc.* 2004, 126: 851.
240. He, H.; Zhu, J.; Tao, J.; Nagahara, L.A.; Amlani, I.; Tsui, R. *J. Am. Chem. Soc.* 2001, 123: 7730.
241. He, H.X.; Li, C.Z.; Tao, N.J. *App. Phys. Lett.* 2001, 78: 811.
242. Langer, J.J.; Czajkowski, I. *Adv. Mat. Opt. Electr.* 1997, 7: 149.
243. Langer, J.J.; Framski, G.; Joachimiak, R. *Synth. Met.* 2001, 121: 1281.
244. Magnus Persson, S.H.; Dyreklev, P.; Inganas, O. In *Atomic and Molecular Wires* pp. 119–128. Joachim, S.; Roth, S. (Eds), Kluwer Publishers, 1997, Netherlands
245. MacDiarmid, A.G.; Jones, W.E.; Norris, I.D.; Gao, J.; Johnson, A.T.; Pinto, N.J.; Hone, J.; Han, B.; Ko, F.K.; Okuzaki, H.; Llaguno, M. *Synth. Met.* 2001, 119: 27.
246. Norris, I.D.; Shaker, M.M.; Ko, F.K.; MacDiarmid, A.G. *Synth. Met.* 2000, 114: 109.
247. Lee, S-H.; Yoon, J-W.; Suh, M.H. *Macromol. Res.* 2002, 10: 282.
248. Liu, J.; Lin, Y.; Liang, L.; Voigt, J.A.; Huber, D.L.; Tian, Z.R.; Coker, E.; McKenzie, B.; McDermott, M.J. *Chem. Eur. J.* 2003, 9: 604.
249. Liang, L.; Liu, J.; Windisch, C.F.; Exarhos, G.X.; Lin, Y. *Angew. Che. Int. Ed.* 2002, 41: 3665.
250. Gao, M.; Huang, S.; Dai, L.; Wallace, G.G.; Gao, R.; Wang, Z. *Agnewandte. Chemie.* 2000, 39: 3664.
251. Wang, D.; Caruso, F. *Adv. Mat.* 2001, 13: 350.
252. Bartlett, P.N.; Birkin, P.R.; Ghanem, H.A.; Toh, C-S. *J. Mater. Chem.* 2001, 11: 849.
253. Choi, S-J.; Park, S-M. *Adv. Mat.* 2000, 12: 1547.
254. Wu, C.G.; Bein, T. *Science.* 1994, 264: 1757.
255. Aimes, S.P.; Aldissi, M.; Hawley, M.; Beery, J.G.; Gottesfeld, S. *Langmuir.* 1991, 7: 1447.

---

# 5 Properties of Polyanilines

As with polypyrrole (PPy), the electrical, chemical, and mechanical properties of polyaniline (PAn) are inextricably linked. In addition, PAn has spectacular optical and chromic properties that distinguish it from other conducting electroactive polymers (CEPs). The current state of knowledge concerning properties of PAn is reviewed in this chapter.

## ELECTRICAL PROPERTIES

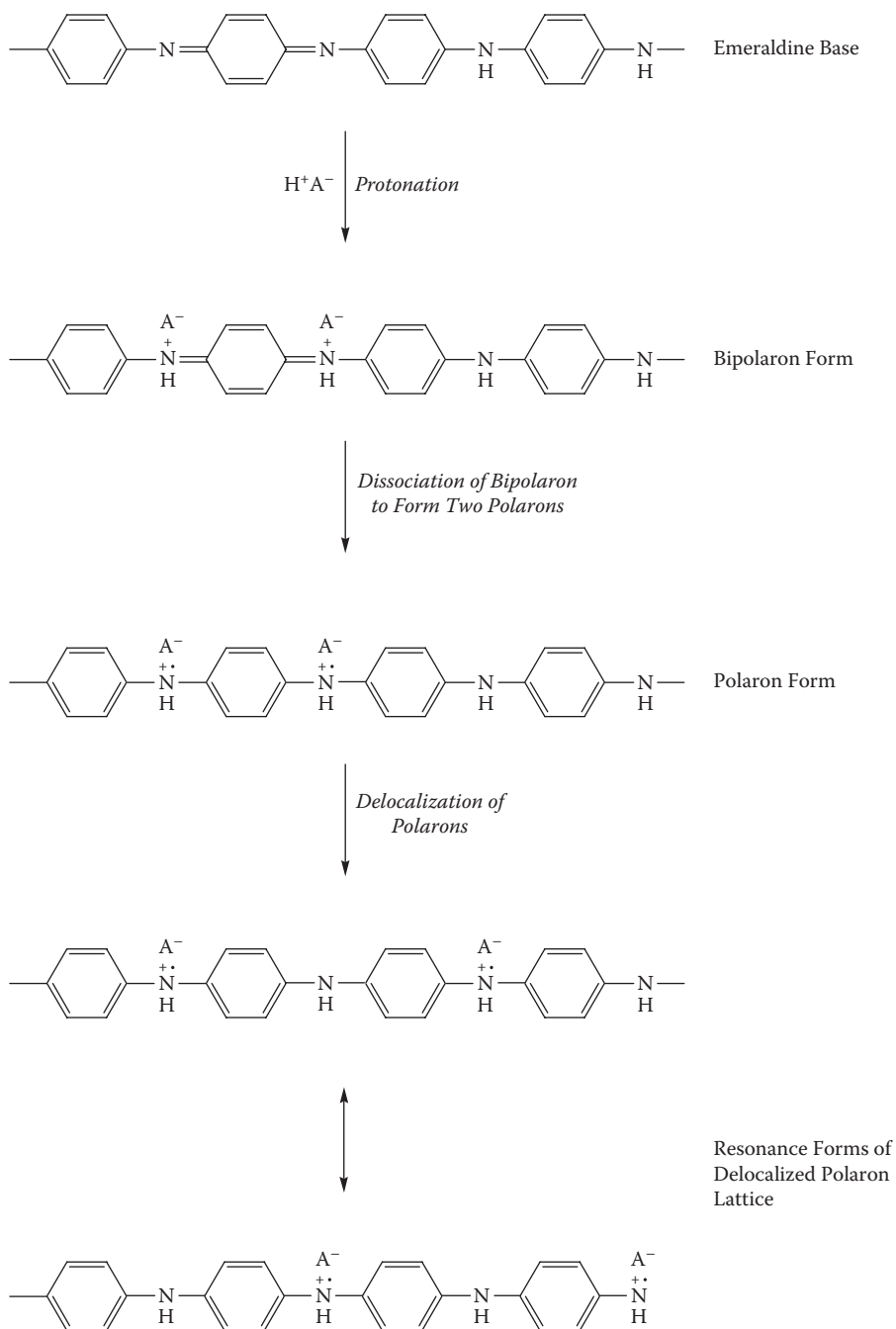
### CONDUCTIVITY

PAn has an electronic conduction mechanism that seems to be unique among conducting polymers, as it is doped by protonation as well as by undergoing the p-type doping described for PPy. This results in the formation of a nitrogen radical cation rather than the carbonium ion of other p-doped polymers.<sup>1</sup> Many of the unusual properties of PAn's arise because of the A-B nature of the polymer configuration, whereas most other conducting polymers are of the A-A type. Furthermore, the B component is the basic N heteroatom, which is involved with the conjugation in polyaniline PAn more than the heteroatoms in PPy and similar polymers. Therefore, the conductivity of PAn depends on both the oxidation state of the polymer and its degree of protonation.

PAn can exist in a range of oxidation states. The one that can be doped to the highly conducting state is called *emeraldine*. In the base form it consists of amine (-NH-) and imine (=N-) sites in equal proportions. The imine sites can be protonated<sup>2</sup> to the bipolaron (dication) emeraldine salt form. However, this undergoes a further rearrangement to form the delocalized polaron lattice, which is a polysemiquinone radical cation salt. The structures at each stage of this process are shown in Figure 5.1.

Although theoretical calculations have predicted that the bipolaron state is energetically more favored than the polaron,<sup>2</sup> it is widely agreed that polarons are the charge carriers responsible for the high-conductivity PAn.<sup>3,4,5,6,7</sup> It has been proposed that the presence of coulombic interactions, dielectric screening, and local disorder in the PAn lattice act to stabilize the delocalized polaron state.<sup>8</sup> It has also been shown that bipolaron states do exist in PAn, but they are few in number and are not associated with the conducting regions of the polymer.<sup>8</sup>

The conductivity of the PAn/HA emeraldine salts (ES) is dependent upon the temperature<sup>9</sup> as well as humidity and, hence, polymer water content.<sup>10,11</sup> In general, attachment of functional groups decreases the conductivity, whereas the formation of copolymers between aniline and functionalized aniline results in polymers with intermediate conductivity. In addition, the preparation conditions,<sup>12,13</sup> particularly as



**FIGURE 5.1** The doping of emeraldine base with protons to form the conducting emeraldine salt form of polyaniline (a polaron lattice).

they relate to the formation of structural defects<sup>14</sup> and the polymer morphology,<sup>15,16</sup> influence conductivity. It has also been reported that the conductivity of PAN is dependent on the solvent it is cast from or exposed to. This phenomenon has been referred to as *secondary doping*.<sup>17,18</sup> The solvent causes a change in the polymer conformation that results in increased conductivity.

However, the most significant dependence of the conductivity of PAN is on the proton-doping level.<sup>19</sup> The maximum conductivity occurs when PAN is 50% doped by protons, to give the polaron lattice structure shown in Figure 5.1. Under these conditions, the conduction mechanism is similar to that for the other polymers described, with the polaron states overlapping to form midgap bands. The electrons are thermally promoted at ambient temperatures to the lower energy-unfilled bands that permits conduction.<sup>20</sup>

Even so, the occurrence of a charge exchange phenomenon is necessary to produce the conductivity levels observed, even in 50% doped PAN, because of the presence of structural defects other than those caused by inadequate protonation of the nitrogen sites. It is proposed that this involves interchain or intrachain proton exchange as well as electron transport. This explains the observed dependence of conductivity on the ambient humidity, as the presence of water within the polymer lattice would facilitate this proton-exchange phenomenon.<sup>16</sup>

At doping levels higher than 50%, some amine sites are protonated, and at levels lower than this, some imine sites remain unprotonated. In both instances, delocalization of the charge carriers over the polymer backbone is disrupted, thereby reducing the polymer conductivity. When significant proportions of these nonconducting phases occur, PAN behaves in a manner equivalent to a conducting system in which metallic islands are dispersed throughout a nonconducting media. In such a system, transport of the charge carriers occurs through “charge energy-limited tunneling” involving long-range hopping. This is similar to that which occurs in granular conduction models, except that it occurs on a molecular scale in PAN. This complex relationship between the conductivity of PAN and the chemical nature of its environment has resulted in great efforts to characterize these phenomena and, particularly recently, to find applications where these unusual properties are of benefit. Further discussion of this aspect appears in the section on the switching properties of PAN.

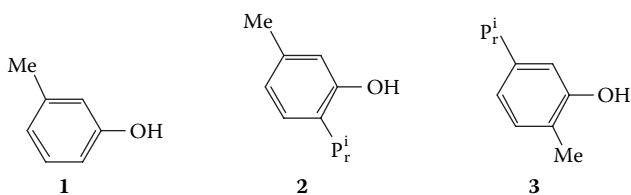
There has been much recent interest in enhancing the order and consequent conducting properties of conducting PAN salts via *postpolymerization* treatment with an appropriate “secondary dopant.” In particular, much attention has focused on the influence of *m*-cresol **1** solvent or vapor on the properties of the ES PAN/(±)-HCSA salt obtained by doping emeraldine base (EB) with racemic (±)-10-camphorsulfonic acid (HCSA).<sup>21,22,23</sup> Emeraldine salt films cast from such doping reactions in DMSO, DMF, *N*-methylpyrrolidinone (NMP), and chloroform solvents are considered to possess a *compact coil* conformation of their PAN chains.<sup>23,24</sup> These tightly coiled chains exhibit a characteristic localized polaron band at ca. 800 nm in their UV-visible spectra and show relatively low electrical conductivities (typically 0.1–1 S/cm). In contrast, PAN's cast from similarly doped solutions in *m*-cresol solvent have been assigned an *expanded coil* conformation on the basis of their markedly higher electrical conductivities (150–200 S/cm) and strikingly different absorption spectra.<sup>23,24</sup> Most diagnostic is the replacement of the high-wavelength (ca. 800 nm)

polaron band by an intense, broad free-carrier tail absorption in the near-infrared (1000–2500 nm) region.

*Meta*-cresol vapor has also been shown to have a major effect on the properties of PAN/(±)-HCSA salts. Exposure to *m*-cresol vapor of films originally cast in the compact coil conformation causes a change to an expanded coil arrangement for the polymer chain and a large (ca. two orders of magnitude) increase in electrical conductivity.<sup>23,25</sup> Once again, associated with these changes is the disappearance of the localized polaron band in the visible absorption spectrum at ca. 800 nm characteristic of the compact coil conformation and its replacement by a strong, broad free-carrier tail in the near-infrared region.

In both the liquid and gas phases, the *m*-cresol is considered to act as a secondary dopant for the PAN chains, leading to the previous conformational changes. Theoretical studies<sup>26,27</sup> suggest that the effects associated with *m*-cresol arise from a synergistic combination of interactions between the *m*-cresol, HCSA, and PAN chains. These involve H-bonding between the phenolic OH group of the *m*-cresol and the carbonyl group of the HCSA, and  $\pi$ -stacking of phenyl rings in the secondary dopant and the PAN chain.

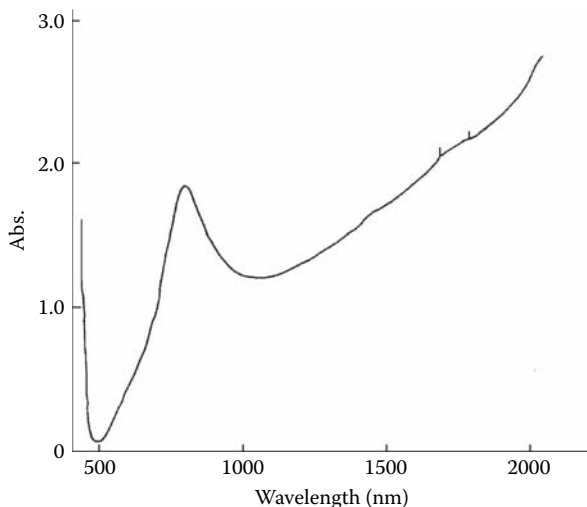
Other phenolic compounds have also been shown to cause similar changes in conformation and physical properties of PAN/HCSA salts.<sup>24,28</sup> Most of these, for example, *m*-cresol, are highly corrosive and toxic, limiting their desirability for processing and enhancing the electrical conductivity of PAN's. However, we have recently found that the structurally related molecules thymol **2** and carvacrol **3**, which are much less toxic than *m*-cresol, can also function as effective secondary dopants for PAN/(+)-HCSA films and increase the electrical conductivity by up to two orders of magnitude.<sup>28</sup>



The UV–visible spectrum for PAN/(±)-HCSA obtained by doping EB with (±)-HCSA in carvacrol is shown in Figure 5.2.

## METALLIC POLYANILINE

Although conducting electroactive polymers (CEPs) have been known for three decades, the goal of producing a polymer with transport properties typical of a metal has to date eluded researchers. CEPs such as PAN emeraldine salts have not exhibited the monotonic decrease in resistivity with temperature expected of a metal, and their electrical conductivities are not as high as one would theoretically expect. In consequence, their microstructures are generally regarded to consist of islands of highly conducting, crystalline regions surrounded by regions of amorphous nonconducting material.



**FIGURE 5.2** UV-visible spectrum for PAN/(±)-HCSA obtained by doping EB with (±)-HCSA in carvacrol.

The recent report<sup>29</sup> of PAN/HCSA salts possessing unprecedentedly high electrical conductivities of up to 1300 S/cm and that exhibit resistivity versus temperature profiles typical of a metal is, therefore, highly significant. These remarkable PAN's were prepared via a novel self-stabilized dispersion polymerization route (see Chapter 4) that minimizes defects in the PAN product arising from undesirable *ortho*-coupling and crosslinking during the polymerization. Further support for the superior nature of these new PAN materials is their high crystallinity evidenced from x-ray diffraction (XRD) studies. This route to improved, high-performance PAN may open up exciting new prospects in “plastic electronics.”

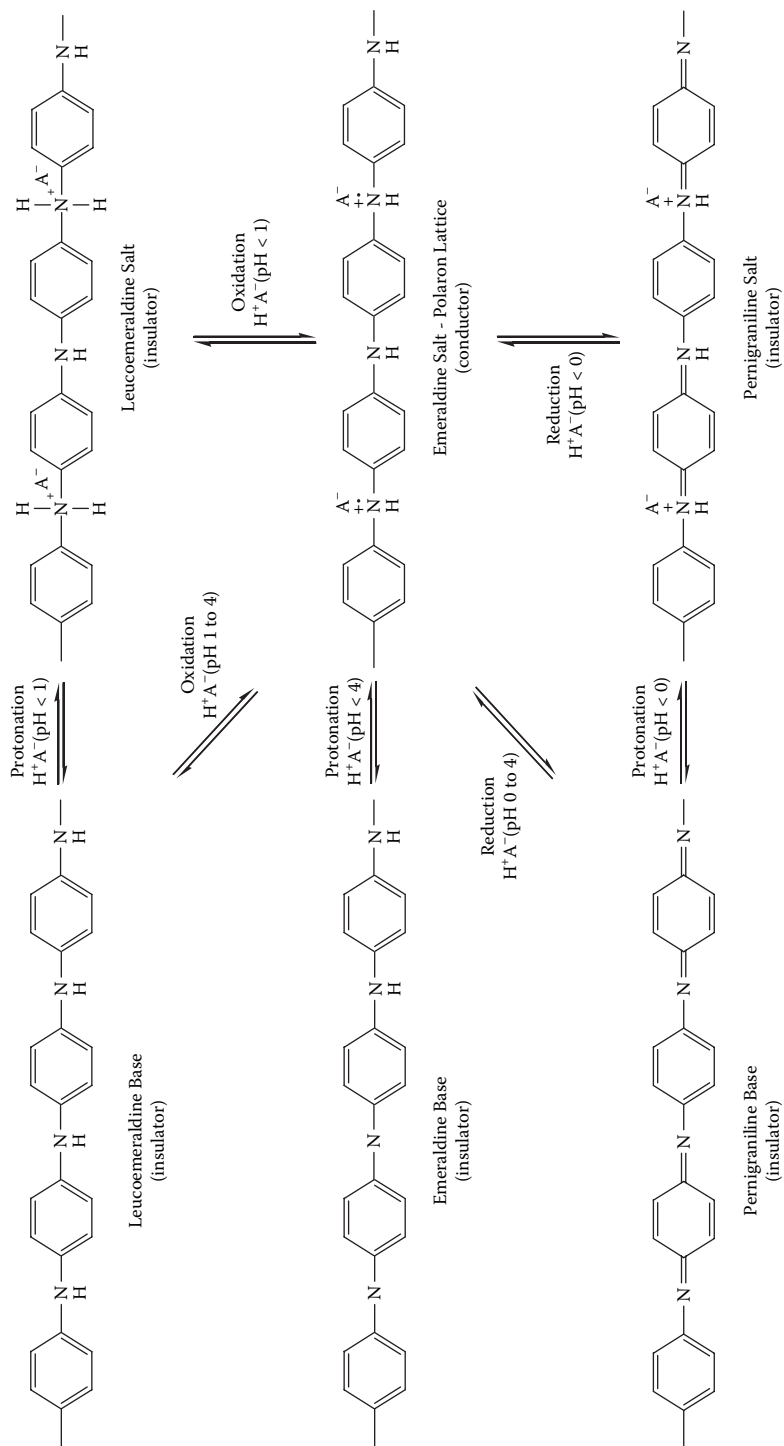
## SWITCHING PROPERTIES

PAN is an interesting material that undergoes two distinct redox processes when in the protonated state (Figure 5.3).<sup>30</sup> These processes are readily observed using cyclic voltammetry (Figure 5.4). The most conductive form of PAN is the emeraldine salt form that occurs between approximately +0.20 and +0.60 V versus Ag/AgCl. At less positive potentials, the fully undoped form (leucoemeraldine) is less conductive, as is the fully oxidized form (pernigraniline) at higher potentials.

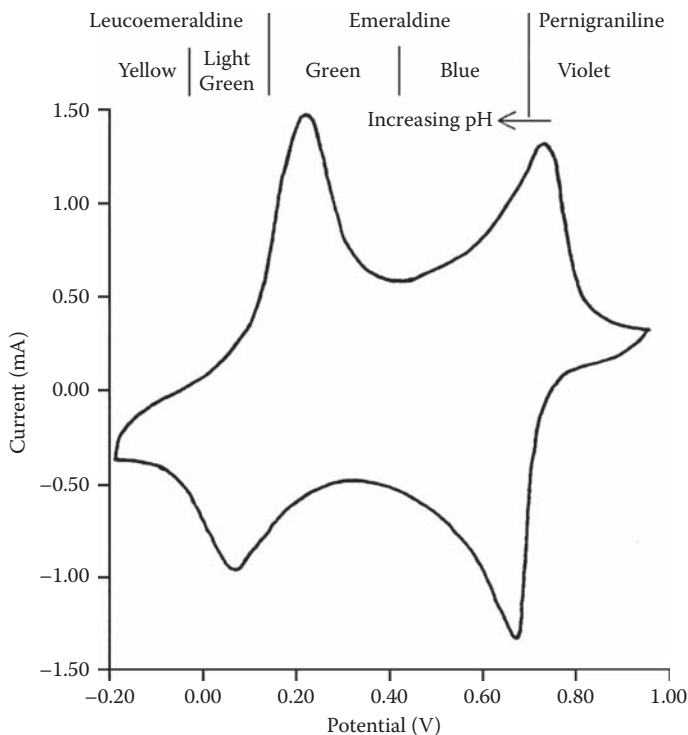
The doping reaction is the same as that which occurs during the polymerization process, and the dedoping reaction is the reverse process. Many of the side reactions that can occur during polymerization can also be a problem during doping, particularly those involving overoxidation.

PAN can be “switched” by the addition of acids and bases that protonate and deprotonate the base sites within the polymer. This leads to the dependence of the polymer states, and thus the reactions, on the pH of the solutions. At solutions of pH greater than 4, PAN loses its electroactivity entirely because the emeraldine salt, the only conducting form of the polymer, cannot form.





**FIGURE 5.3** The protonation/deprotonation and redox reactions between the various forms of polyaniline.



**FIGURE 5.4** Cyclic voltammogram of PAN/HCl on a glassy carbon electrode; 1 M HCl(aq); 50 mV/s; the potentials at which structure and color changes occur and the change in the potential of the second redox reaction with pH are shown as well. The second oxidation peak moves to a less positive potential with increasing pH.

If the PAN polymer is exposed to potentials greater than the second oxidation process, a third voltammetric response appears upon cycling the potential. This is due to oxidation/reduction of a degradation product.<sup>31</sup> In fact, insoluble degradation products are formed, probably owing to chain scission by hydrolysis of amine groups to form benzoquinone and acrylamine terminations.

PAN has been shown to exhibit similar redox behavior in both aqueous and non-aqueous media.<sup>32</sup> However, in organic solvents, the second (more positive) oxidation response is irreversible owing to the lack of protons in such media.

Thus, PAN undergoes transitions between various states. Therefore, its chemical properties are varied and can be controlled by application of a potential and/or an acid or base. Not only do the conductivity and chemical properties of PAN change but the color of the polymer also changes between each of these states.<sup>33,34</sup> These chromatic changes in PAN have led to an interest in its use for display devices, redox and pH indicators, and other applications.

The electrochemical switching of PAN can be readily monitored by cyclic voltammetry. However, because of the dependence of the switching on the protonation level of the solution, the peak potentials vary with the pH. A signature voltammogram for PAN at a pH of 0 is shown in Figure 5.4, including the potentials at which structural

and color changes occur. The trend observed for the peak potential with increasing pH is also indicated. The rate of switching depends on the electrolyte used<sup>35</sup> (with smaller ions, the switching is faster) and the solvent employed.<sup>36</sup>

It has been established that when polyelectrolytes are incorporated as dopants in PAN, the switch from conducting to nonconducting material is shifted to very-high-pH solutions, enabling electrochemistry to be carried out on PAN in neutral solutions.<sup>37</sup> Poly(methoxyanilines) have been used as the basis of electromechanical actuating; changes in dimensions in the thickness direction of more than 20% were reported as the polymers are doped and dedoped.<sup>38,39</sup> Similar effects are observed if some level of self-doping is introduced into the PAN backbone.<sup>40</sup>

## CHEMICAL PROPERTIES

Many of the properties of PPy mentioned in earlier chapters apply to PAN as well. The electron-rich, nonpolar backbone of the polymer is dispersed with functional groups of the N heteroatom that may participate in hydrogen bonding, as well as introduce a polar functional group to the various forms. In the conducting state, PAN also has a positive charge delocalized over the backbone of the polymer and over a much larger range than in traditional ion-exchange materials. The ion-exchange properties of PAN may be derived from a similar source to PPy, although in the PAN, the positive charge is in the form of a radical cation rather than a dication. The effect of this difference on the chemical properties cannot be predicted with certainty. The dependence of this state of the polymer on the pH of its environment will also make a major contribution to the observed chemical properties.

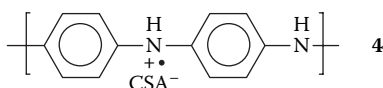
Several studies<sup>41,42</sup> have indicated that the strongest chemical interaction of PAN is anion-exchange properties and that these properties differ in several ways from those of conventional ion-exchange resins. The reason may be attributed to the charge delocalization. Charge configurational phenomena have also been observed in studies with amino acid interactions on PAN.<sup>43</sup> For example, it has been shown that for two amino acids with similar charge densities but different molecular configurations, the ability to interact with PAN was markedly different. Studies involving inverse chromatography<sup>44</sup> have shown that PAN's are more hydrophilic than PPy, as may be expected from the increased charge density. It has also been observed that PAN stationary phases are capable of discriminating between polyaromatic hydrocarbons on the basis of planarity and/or length-to-breadth ratio.<sup>44</sup>

A smaller range of counterions has been incorporated into PAN than into PPy; therefore, the range of chemical interactions imparted by the counterions has not been as significant. A number of different functional groups have been added to the aniline monomer although these have predominantly been investigated for their influence on the conductivity or polymerization of PAN, as mentioned previously. However, these may also be used to introduce various chemical interactions to PAN, in a manner similar to that described for PPy.

Incorporation of bioactive molecules into PAN is not so readily achieved because electropolymerization must normally be carried out at low pH. However, thin polymeric coatings containing enzymes have been produced by polymerization from buffer solutions (pH = 7).<sup>45</sup> Tatsuma and coworkers<sup>46</sup> have immobilized

horseradish peroxidase into films composed of a sulfonated PAN and poly(L-lysine) or poly(ethyleneimine). In other work, Ogura and coworkers added tungsten trioxide to polyaniline–polyvinylsulfate electrodes, and they used these to facilitate the electroreduction of CO<sub>2</sub> to lactic acid, formic acid, ethanol, and methanol.<sup>47</sup> In another report from the same laboratory,<sup>48</sup> a range of different Fe complex structures were added to PAN prussian blue films to enable the electrocatalytic reduction of CO<sub>2</sub>.

Films of optically active PAN salts, such as PAN/(+)-HCSA **4** or the optically active EB derived from them, have recently been shown<sup>49</sup> to exhibit discrimination toward chiral compounds such as the enantiomers of CSA- and amino acids. The studies suggest that these novel chiral materials may indeed have potential for the separation of enantiomeric chemicals, such as chiral drugs.



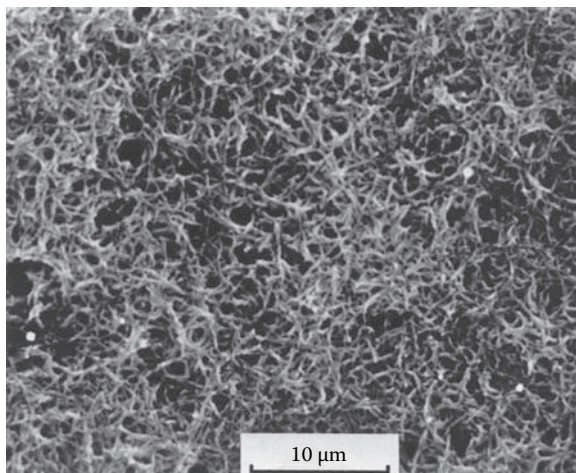
## MECHANICAL PROPERTIES OF POLYANILINE

The mechanical properties of PAN differ considerably between the electrochemically prepared polymer and that produced from solvent casting. As described earlier, electropolymerized emeraldine salts are highly porous and, consequently, have low mechanical strength. Freestanding films may be prepared electrochemically, but their poor mechanical properties limit their usefulness. In contrast, the polymers made from solution are much less porous and are widely used as freestanding films and fibers. The effect of polymer structures and morphology on PAN mechanical properties are described in the following text.

## ELECTROCHEMICALLY PREPARED FILMS

A limited number of studies have considered the effects of electropolymerization conditions on the mechanical properties of PAN. Kitani and coworkers,<sup>50</sup> for example, have shown that it is possible to prepare freestanding films from PAN in the reduced (leucoemeraldine) state. When oxidized to the emeraldine state, the films became brittle. Similar behavior was described in Chapter 3 for PPy and the change in mechanical properties in that case was related to the increased interchain bonding between charged chains resulting in a decrease in toughness. Presumably, a similar explanation applies to PAN.

The polymerization potential has also been found to influence the mechanical properties of polyaniline PAN/HA emeraldine salt films.<sup>50</sup> The most extensible films were formed at a polymerization potential of 0.65 V (versus Ag/Ag<sup>+</sup>), which displayed an extension to break of around 40%. Preparation of the PAN/HA films at 0.8 V and 1.0 V resulted in more brittle films. It was suggested that degradation of the PAN at polymerization potentials in excess of 0.8 V might explain the poor properties of the 1.0 V film. The difference in behavior of the films prepared at 0.65 V and 0.8 V was attributed to differences in their crosslink density. Unfortunately,



**FIGURE 5.5** Scanning electron micrograph of polyaniline/HCl.

structural characterizations of the PAN films prepared under these conditions were not conducted, making it impossible to explore the structure–property relationships in more detail.

Our studies have shown that the electropolymerization method produces a powdery deposit (Figure 5.5) and that the adhesion of the deposit to the working electrode depends on the reaction conditions. For example, a finer powder PAN/HNO<sub>3</sub> salt produced by using the NO<sub>3</sub><sup>-</sup> counterion gave stronger adhesion than the coarser PAN/HCl produced when the Cl<sup>-</sup> counterion was used. Also, cyclic application of the electropolymerization potential gave the most strongly adherent deposits, whereas galvanostatic growth gave a polymer that was less adherent. Finally, the potentiostatic method produced the lowest adhesion. To date, the effect of these parameters on other mechanical properties of the coatings and films has not been reported.

PAN can be successfully plasticized to improve the ductility and toughness. Residual solvent (e.g., NMP) in solution-cast films and fibers undoubtedly affects the mechanical properties by increasing elongation at break and reducing the elastic modulus. Fedorko and coworkers<sup>51,52</sup> have recently demonstrated dramatic improvements in the ductility of PAN films using plasticizing dopants. Thus, the di(2-ethylhexyl)ester of 4-sulfophthalic acid (DEHEPSA) was used to prepare PAN that was soluble (in the ES form) in dichloroacetic acid. Cast films had similar conductivities to PAN/HCSA of ~ 100 S/cm. Tensile testing gave an elongation at break of 28% for the PAN/DEHEPSA films compared with only 2% for the ES-CSA. The tensile strength for both films was similar: 14 and 16 MPa, respectively. This tensile strength is comparable with that obtained for unoriented EB films. PAN gels have also been prepared containing large amounts of solvents such as NMP or *m*-cresol. In one study,<sup>53</sup> high-conductivity gels (up to 100 S/cm) have been prepared with Youngs moduli up to 1 MPa (typical of rubber).

Most fibers (see Chapter 7) and films of PAN have been prepared from a solution of EB and converted to the emeraldine salt by acid doping. The choice of dopant acid

has a profound effect on mechanical properties. In fact, MacDiarmid and coworkers<sup>54</sup> have shown that the mechanical properties depend in a complex way on dopant, casting solvent, and polymer molecular weight. EB films have also been thermally crosslinked, with the degree of crosslinking (controlled by the thermal treatment temperature) greatly affecting the tensile strength.<sup>55</sup> Although the strength increased with crosslinking, the ability to protonate the EB using acids was diminished. Full details of the effects of polymer structure (as influenced by dopant and solvent) on the mechanical properties are yet to be elucidated.

Thermal analysis has been used to study thermal transitions in PAN, specifically the glass transition. This polymer has been shown to display a distinct glass temperature ( $T_g$ ) with the transition being sensitive to the degree of plasticization. DMA studies<sup>56</sup> on PAN-EB films cast from NMP have shown multiple transitions at 142, 198, and 272°C. The lower temperature transitions disappeared when residual NMP was removed, suggesting that the highest temperature transition represents the  $T_g$  of PAN-EB. Gregory<sup>57</sup> has evaluated the thermal properties of the LB form of PAN using differential scanning calorimetry (DSC) and DMA. A broad endotherm was observed at ~385°C, substantially higher in temperature than the  $T_g$  at ~200°C. The endotherm was attributed to melting of a crystalline phase as supported by x-ray diffraction (XRD) and microscopy data. DMA data also confirmed significant softening of the polymer at ~375°C. The fibers and films used by Gregory were prepared from DMPU, a solvent that inhibits gelation of the EB in solution.

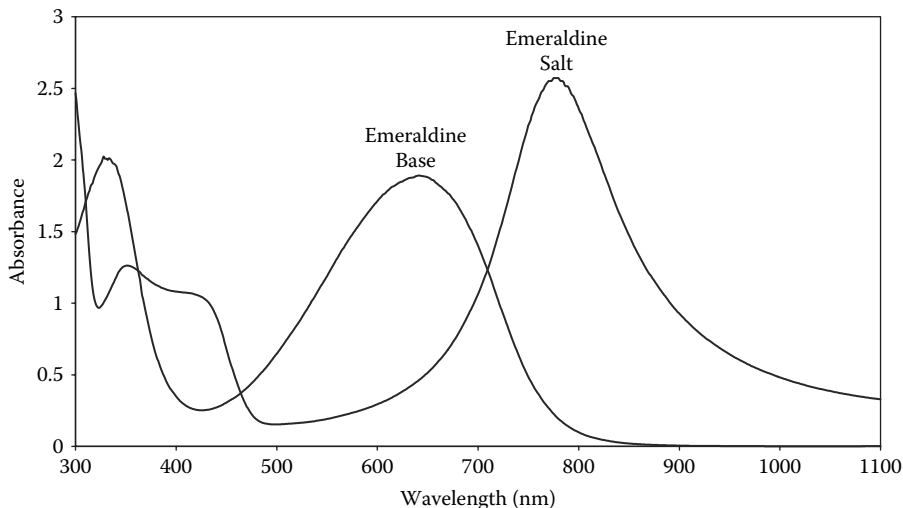
## OPTICAL PROPERTIES OF POLYANILINES

Semiempirical molecular orbital calculations,<sup>58</sup> and more recently, *ab initio* calculations<sup>59</sup> on the conducting emeraldine salt form of PAN predict, in contrast to PPy and polythiophene, the presence of a single broad polaron band deep in the band gap. This band is half-filled, giving rise to an ESR signal.<sup>60</sup>

These band-structure calculations are in agreement with the observed UV–visible–NIR spectra. In their compact coil conformation, emeraldine salt typically exhibit three peaks: a  $\pi$ – $\pi^*$  (band gap) band at ca. 330 nm and two visible-region bands at ca. 430 and 800 nm that may be assigned as  $\pi \rightarrow$  polaron band and polaron  $\rightarrow \pi^*$  band transitions, respectively<sup>61</sup> (see Figure 5.6).

## BASE FORMS OF POLYANILINE

Electronic band structures have also been calculated for each of the base forms of PAN, namely: the fully reduced leucoemeraldine base (LEB), the half-oxidized EB, and the fully oxidized pernigraniline base (PB).<sup>62</sup> The observed UV–visible spectra of LEB, EB, and PB are in good agreement with these calculated band structures. The lowest energy absorption band for LEB occurs at ca. 320 nm and may be assigned to the  $\pi$ – $\pi^*$  electronic transition, that is, between the valence and conduction bands. For EB, as well as a similar low-wavelength  $\pi$ – $\pi^*$  band, there is a strong band at ca. 600 nm that has been attributed to a local charge transfer between a quinoid ring and the adjacent imine-phenyl-amine units giving rise to an intramolecular charge



**FIGURE 5.6** UV-visible spectra of polyaniline showing EB and ES forms.

transfer exciton.<sup>63</sup> PB also exhibits two absorption peaks: a  $\pi$ - $\pi^*$  band at ca. 320 nm and a band at ca. 530 nm assigned to a Peierls gap transition.

Protonation of PB causes a violet-to-blue color change due to the formation of pernigraniline salt (PS). This color change is associated with the loss of the PB band at 530 nm and the appearance of a strong PS peak at ca. 700 nm.

In general, conjugated polymers such as PAN show a strong coupling between their electronic structure and geometric features such as the polymer chain conformation. There have been a number of theoretical studies examining the influence of PAN chain conformation and, in particular, the role of phenyl and phenyl/quinoid torsional angles along the chain, on the electronic structure of PAN (and consequently their electronic absorption spectra). These include semiempirical calculations by Brédas and coworkers<sup>62,64,65</sup> and by de Oliveira and coworkers<sup>66</sup> on oligomeric models of the PAN base forms LB, EB, and PB, as well as some *ab initio* calculations.<sup>67</sup>

The position and intensity of the absorption bands for PAN species are, therefore, sensitive to the conformation adopted by the polymer chains, as well as the conjugation length. With emeraldine salt, the  $\lambda_{\max}$  for the longest-wavelength absorption band is red-shifted for polymers with longer conjugation length. Most interest in this particular polaron band has centered, however, on its use as a diagnostic test for the conformation of the PAN chains. As seen in Figure 5.6, this band typically appears as a strong peak in the region 750–850 nm when the PAN chains adopt a *compact coil* conformation. However, when an *extended coil* conformation is adopted, this localized polaron band is replaced by a broad, strong free-carrier tail in the NIR, with  $\lambda_{\max}$  red-shifted to 1500–2500 nm. The delocalization of the polaron along the PAN chain in this extended coil conformation results in a much-enhanced electrical conductivity.

As a consequence, there has been extensive recent interest in exploring means of modifying PAN chain conformations, using UV-visible-NIR spectra (and asso-

ciated circular-dichroism [CD] spectra for chiral PAN) to monitor such changes. The influence of secondary dopants such as *m*-cresol and carvacrol on the conformation of PAN's was discussed earlier in this chapter,<sup>21-28</sup> whereas other significant advances in this area are summarized later in the section entitled "Solvatochromism and Thermochromism."

## CIRCULAR DICHOISM SPECTRA

The first reported optically active PAN's were the PAN/(+)-HCSA and PAN/(-)-HCSA salts (HCSA = 10-camphorsulfonic acid), prepared in our laboratories by the electropolymerization of aniline in the presence of either (+)- or (-)-HCSA.<sup>68,69</sup> The optically active dopant anions are believed to induce a preferred one-handed helical arrangement in the PAN chains in these emeraldine salts **4**, giving rise to intense CD bands in the visible region. Recent studies by Li and Wang<sup>70</sup> have shown that PAN/(+)-HCSA films of exceptionally high optical activity can be electrochemically deposited by polymerizing the aniline monomer in the presence of small amounts of aniline oligomers.

An alternative facile approach to optically active PAN is the doping of EB with optically active dopant anions such as (+)- or (-)- CSA<sup>-</sup> in a variety of organic solvents.<sup>71,72,73</sup> The PAN/(+)-HCSA and PAN/(-)-HCSA salts exhibit mirror-imaged circular dichroism (CD) spectra, indicating enantioselectivity in the doping of the EB chains with (+)- and (-)-HCSA. Figure 5.7 shows the CD spectrum of PAN/(+)-HCSA in NMP solvent. It exhibits bisignate CD bands at ca. 720 and 795 nm associated with the high-wavelength polaron absorption band observed (Figure 5.6) at ca. 775 nm. Overlapping bisignate CD bands are also observed at lower wavelengths (including a characteristic band at ca. 450 nm), associated with the low-wavelength polaron band and  $\pi$ - $\pi^*$  absorption band observed in this region.

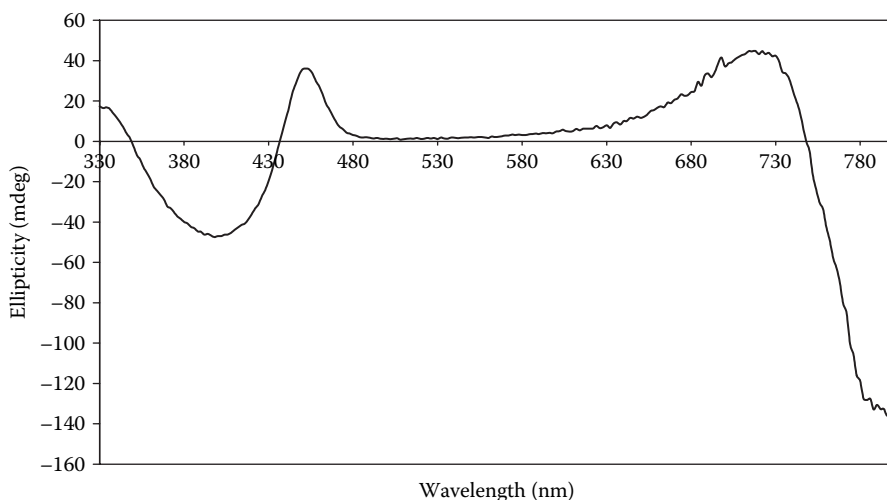


FIGURE 5.7 CD spectrum of PAN/(+)-HCSA in NMP solvent.



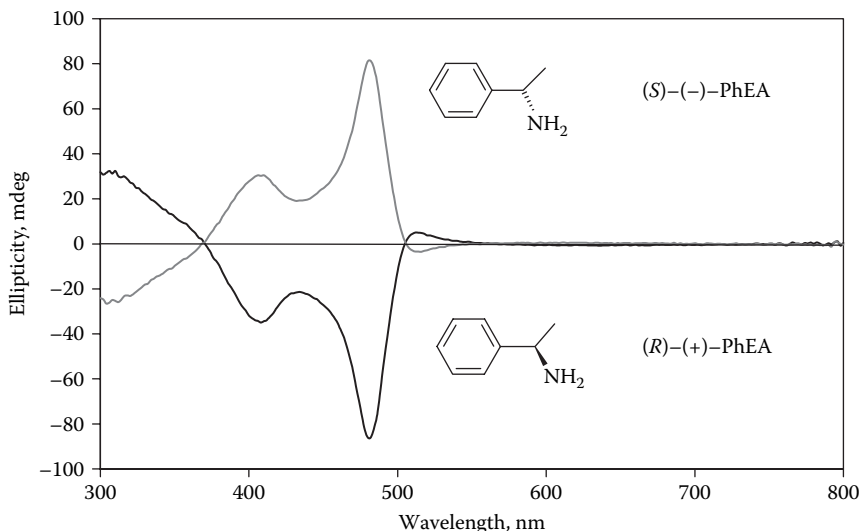
We have rationalized the optical activity of these PAN/HCSA (and related PAN/tartrate) salts in terms of the preferential adsorption of a one-handed helical conformation by the PAN chains, depending on which enantiomer of the CSA<sup>-</sup> anion is employed in the doping.<sup>68,69,73,74</sup> Alternatively, as suggested by Meijer and coworkers<sup>75</sup> (and has been established for chiral poly(alkylthiophenes); see Chapter 6), the observed optical activity may arise from the formation of chiral supramolecular aggregates. However, in contrast to chiral poly(alkylthiophenes), PAN/(+)-HCSA exhibits a strong CD spectra in “good” solvents such as NMP and DMPU (where interchain aggregation is believed to be minimized) as well as in “poor” solvents, supporting one-handed helical chains as a major contribution to the observed CD spectra of PAN.HCSA salts in organic solvents.

Optically active poly(2-methoxyaniline)/HCSA (POMA/(+)-HCSA and POMA/(–)-HCSA) salts can also be made either electrochemically or by the previous doping method, again exhibiting bisignate CD bands associated with the visible-region absorption bands.<sup>76,77</sup> More recently, optically active POMA/HCSA and poly(2-ethoxyaniline)/HCSA salts have also been generated by the oxidation of the corresponding substituted aniline monomers with the electron acceptor 2, 3-dichloro-5,6-dicyanobenzoquinone (DDQ) in organic solvents such as chloroform/THF mixture.<sup>78,79</sup>

Optically active films of PAN/(+)-HCSA and POMA/(+)-HCSA may be dedoped in 1 M NH<sub>4</sub>OH to give the corresponding optically active EBs,<sup>69,76</sup> and the oxidation (with S<sub>2</sub>O<sub>8</sub><sup>2-</sup>) and reduction (with N<sub>2</sub>H<sub>4</sub>) of such films have also been shown to yield optically active PB and LEB films, whose chiroptical properties have been exhibited by CD spectra.<sup>80</sup>

In an alternative approach, optically active forms of the anionic fully sulfonated PAN, poly(2-methoxyaniline-5-sulfonic acid) [PMAS] can be generated via the incorporation of the ammonium ions of chiral amines or aminoalcohols as the counter cations. This was achieved either during electropolymerization of the MAS monomer<sup>81</sup> or via addition of the chiral ammonium cations to preformed PMAS.<sup>82</sup> The PMAS polymer chains (or assemblies of chains) are believed to preferentially adopt a one-handed helical conformation, the chiral induction being initiated by acid–base interaction of the chiral amines with “free” sulfonic acid groups on the PMAS chains. CD spectra of these polymers show that enantiomeric amines such as (*R*)-(+)- and (*S*)-(–)-1-phenylethylamine induce the opposite helical hands for the PMAS chains (see Figure 5.8). However, there was no clear correlation between the CD signals for the PMAS.(amine) films and the configuration of structurally diverse amines.

CD is a very sensitive spectroscopic tool for probing chain conformations in optically active polymers. For example, with peptides, CD spectroscopy has been widely employed to estimate the proportion of the chain present as the alternative  $\alpha$ -helix,  $\beta$ -sheet, and random coil conformations.<sup>83</sup> Following the discovery of electrochemical<sup>68,69</sup> and chemical<sup>71,72</sup> routes to chiral PAN. HCSA and related ring-substituted PAN's, we have employed CD spectroscopy extensively to (1) distinguish between extended coil and compact coil PAN conformations, (2) probe redox and pH switching in PAN, (3) characterize conformational changes in solvatochromism and thermochromism for PAN, and (4) distinguish unequivocally between the conformations/structures of electrochemically and chemically prepared PAN. Similar valuable information on



**FIGURE 5.8** CD spectra of spun-cast 1:1 PMAS/(+)-PhEA and PMAS/(-)-PhEA films.

PAn structures and chiral recognition properties has been increasingly reported by other research groups over the last few years, as summarized in the following text.

## CHIRAL DISCRIMINATION AND ASYMMETRIC INDUCTION WITH CHIRAL POLYANILINES

Kaner and coworkers<sup>84,85</sup> have recently reported enantiomeric discrimination of amino acids by chiral PAn films. The EB form of PAn doped with (*S*)-(+)- or (*R*)-(-)-10-camphorsulfonic acid was used to separate racemates of DL-amino acids. The interactions of the chiral PAn films with amino acids suggested that the chiral recognition ability of dedoped PAn is size and shape dependent. These properties may be useful in the employment of chiral PAn as a chiral stationary phase for chromatography.

A striking example of asymmetric induction by chiral PAn's has been the recent demonstration that thin optically active PAn film layers can act as platforms to induce optical activity in PAn's containing only achiral dopants that are subsequently electrochemically deposited on these surfaces.<sup>86</sup> The origin of this remarkable macromolecular asymmetric induction is currently uncertain. Interestingly, Samuelson and coworkers<sup>87</sup> have recently observed related asymmetric induction in the horseradish peroxidase catalyzed synthesis of PAn/(+)-HCSA/PAA, PAn/(-)-HCSA/PAA and PAn/(rac)-HCSA/PAA nanocomposites (PAA = polyacrylic acid), where the PAn chains adopted the same helical hand, irrespective of the hand of HCSA employed.

## SOLVATOCHROMISM AND THERMOCHROMISM

Marked changes in the UV-visible and CD spectra of PAn/HCSA salts have been widely reported by changing the nature of the organic solvent, the solvatochromism being associated with changes in the PAn backbone conformation/structure. How-

ever, there have been few studies of thermochromism. We have recently shown from CD studies of PAN/(+)-HCSA that the conformation of electrochemically deposited films is changed upon heating to 140°C from a largely extended coil conformation to a compact coil conformation.<sup>88</sup> This study also unequivocally established that electrochemically and chemically prepared PAN/(+)-HCSA salts have different conformations/structures.

Kaner and coworkers<sup>89</sup> have reported that in the doping of EB with (+)-HCSA, the presence of water in the NMP solvent causes the PAN/(+)-HCSA formed to have an inverted CD spectrum compared to that exhibited by the chiral salt formed in the absence of water. More recent studies in our laboratories<sup>90</sup> of similar chiral doping of EB in a range of organic solvents (NMP, DMSO, DMF, and DMPU) containing 1–10% v/v water reveal marked changes in CD spectra due to the presence of water, in some cases, leading to inversion of configuration. These inversions may arise from prior H-bonding of the EB substrate by water, which competes with H-bonding between the dopant (+)-HCSA carbonyl group and the PAN amine groups believed to be responsible for chiral induction in the polymer chains. Surprisingly, the presence of 25–50% water in the organic solvent leads to optically inactive PAN. Kuramoto and coworkers<sup>78,91</sup> have also recently observed fascinating solvent-mediated changes in the CD spectra for PAN/(+)-HCSA salts produced via their electron acceptor route. They have also pointed out<sup>78,79</sup> that PAN/(+)-HCSA and POMA/(+)-HCSA salts prepared from water and organic solvents possess different conformations.

## REFERENCES

1. Bredas, J.L.; Chance, R.R.; Silbey, R. *Phys. Rev. B* 1982, 26: 5843.
2. Angelopoulos, M.; Asturias, G.E.; Ermer, S.P.; Scherr, E.M.; MacDiarmid, A.G.; Akhtar, M.; Kiss, Z.; Epstein, A. *J. Mol. Cryst. Liq. Cryst.* 1988, 160: 151.
3. Epstein, A.J.; Ginder, J.M.; Zuo, F.; Biegelow, R.E.; Wou, H.S.; Tanner, D.B.; Fichter, A.F.; Huang, W.S.; MacDiarmid, A.G. *Synthetic Metals* 1987, 18: 303.
4. Nakajima, T.; Kawagoe, T. *Synthetic Metals* 1989, 28: C629.
5. Watanabe, A.; Mori, K.; Mikuni, M.; Nakamura, Y.; Matsuda, M. *Macromolecules* 1989, 22: 3323.
6. Focker, W.W.; Wnck, G.E.; Wei, Y. *J. Phys. Chem.* 1987, 91: 5813.
7. Zhang, D.; Hwang, J.H.; Yang, S.C. *Mat. Res. Soc. Symp. Proc.* 1990, 173: 305.
8. Bonnell, D.A.; Angelopoulos, M. *Synthetic Metals* 1989, 33: 301.
9. Javadi, H.H.; Cromack, K.R.; MacDiarmid, A.G.; Epstein, A.J. *Phys. Rev. B* 1989, 39: 3579.
10. Angelopoulos, M.; Ray, A.; MacDiarmid, A.G.; Epstein, A.J. *Synthetic Metals* 1987, 21: 21.
11. Wei, Y.; Hariharan, R.; Patel, S. A. *Macromol.* 1990, 23: 758.
12. Fosong, W.; Jinsong, T.; Lixiang, W.; Hongfang, Z.; Zhishen, M. *Mol. Cryst. Liq. Cryst.* 1988, 160: 175.
13. Pron, A.; Genoud, F.; Menardo, C.; Nechschein, M. *Synthetic Metals* 1988, 24: 193.
14. Thyssen, A.; Borgerding, A.; Schiltze, J.W. *Makromol. Chem. Macromol. Symp.* 1987, 8: 1423.
15. Schacklette, L.W.; Baughman, R.H. *Mol. Cryst. Liq. Cryst.* 1990, 189: 193.
16. Lu, Y.; Li, J.; Wu, W. *Synthetic Metals* 1989, 30: 87.
17. MacDiarmid, A.J.; Epstein, A.J. *Synthetic Metals* 1995, 69: 85.
18. Avlyanar, J.K.; Min, Y.; MacDiarmid, A.J.; Epstein, A.J. *Synthetic Metals* 1995, 72: 65.

19. Chiang, J.; MacDiarmid, A.G. *Synthetic Metals* 1986, 13: 193.
20. Tanaka, J.; Mashita, N.; Mizoguchi, J.; Kume, K. *Synthetic Metals* 1989, 29: E175.
21. Cao, Y.; Smith, P.; Heeger, A.G. *Synthetic Metals* 1992, 48: 91.
22. Cao, Y.; Smith, P. *Polymer*. 1993, 34: 3139.
23. MacDiarmid, A.G.; Epstein, A.J. *Synthetic Metals* 1994, 65: 103, and references cited therein.
24. Xia, Y.; Wiesinger, J.M.; MacDiarmid, A.G. *Chem. Mater.* 1995, 7: 443.
25. Xia, Y.; MacDiarmid, A.G.; Epstein, A.J. *Macromolecules* 1994, 27: 7212.
26. Ikkala, O.T.; Pietilä, L.-O.; Ahjopalo, L.; Österholm, H.; Passiniemi, P.J. *J. Chem. Phys.* 1995, 103: 9855.
27. Ikkala, O.T.; Pietilä, L.-O.; Passiniemi, P.; Vikki, T.; Österholm, H.; Ahjopalo, L.; Österholm, J.-E. *Synthetic Metals* 1997, 84: 55.
28. Norris, I.D.; Kane-Maguire, L.A.P.; Dai, L.; Zhang, F.; Mau, A.W.H.; Wallace, G.G. *Aust. J. Chem.* 2002, 55: 253.
29. Lee, K.; Cho, S.; Park, S.H.; Heeger, A.J.; Lee, C.-W.; Lee, S.-H. *Nature* 2006, 441: 65.
30. Huang, W.S.; Humphrey, B.D.; MacDiarmid, A.G. *J. Chem. Soc. Faraday Trans.* 1985, 82: 2385.
31. Foot, P.J.S.; Simon, R. *Phys. D. Appl. Phys.* 1989, 22: 1598.
32. Watanabe, A.; Mori, K.; Mikon, M.; Nakamura, Y.; Matsuda, M. *Macromol.* 1989, 22: 3323.
33. Batich, C.D.; Laitinen, H.A.; Tamura, H. *J. Electroanal. Chem.* 1990, 137: 883.
34. Habib, M.A. *Langmuir* 1988, 4: 1302.
35. Grzeszczuk, M.; Olszak, G.S. *J. Electroanal. Chem.* 1993, 359: 161.
36. LaCroix, J.C.; Diaz, A.F. *J. Electrochem. Soc.* 1988, 135: 1457.
37. Bartlett, P.N.; Wallace, E.N.K. *J. Electroanal. Chem.* 2000, 486: 23.
38. Kaneko, M.; Kaneto, K. *Polymer J.* 2001, 33: 104.
39. Kaneko, M.; Kaneto, K. *Synthetic Metals* 1999, 102: 1350.
40. Karayakin, A.A.; Strakhova, A.K.; Yatsimirsky, A.K. *J. Electroanal. Chem.* 1994, 371: 259.
41. Syed, A.A.; Dinesan, M.K. *Synthetic Metals* 1990, 36: 209.
42. Syed, A.A.; Dinesan, M.K. *Analyst* 1992, 117: 611.
43. Teasdale, P.R.; Wallace, G.G. *Polymer Int.* 1994, 35: 197.
44. Chriswanto, H.; Wallace, G.G. *Chromatographia* 1996, 42, 191.
45. Shinohara, H.; Chiba, T.; Aizawa, M. *Sens. Actuators.* 1988, 13: 79.
46. Tatsuma, T.; Ogawa, T.; Sato, R.; Oyama, N. *J. Electroanal. Chem.* 2001, 501: 180.
47. Endo, N.; Miho, K. Y.; Ogura, K. *J. Mol. Catalysis A.* 1997, 127: 49.
48. Nakayama, M.; Ino, M.; Ogura, K. *J. Electroanal. Chem.* 1997, 440: 251.
49. Guo, H.; Eogan, V.; Knobler, C.M.; Kanar, R.B. *Polym. Prep.* 1999, 40: 506.
50. Kitani, A.; Kaya, M.; Tsujioka, S.I.; Sasaki, K. *J. Polym. Sci.: Polym. Chem.* 1988, 26: 1531.
51. Fedorko, P.; Fraysse, J.; Dufresne, A.; Planes, J.; Travers, J.P.; Olinga, T.; Kramer, C.; Rannou, P.; Pron, A. *Synthetic Metals* 2001, 119: 445.
52. Dufour, B.; Rannou, P.; Fedorko, P.; Djurado, D.; Travers, J.P.; Pron, A. *Chem. Mater.* 2001, 13: 4032.
53. Gonzalez, I.; Munoz, M.E.; Santamaria, A.; Pomposo, J.A.; Grande, H.; Rodriguez-Parra, J. *Macromol. Rapid Commun.* 2002, 23: 659.
54. Jeong, S.K.; Suh, J.S.; Oh, E.J.; Park, Y.W.; Kim, C.Y.; MacDiarmid, A.G. *Synthetic Metals* 1995, 69: 171.
55. Tan, H.H.; Neoh, K.G.; Liu, F.T.; Kocherginsky, N.; Kang, E.T., *J. Appl. Polym. Sci.* 2001, 80: 1.
56. Han, M.G.; Lee, Y.J.; Byun, S.W.; Im, S.S. *Synthetic Metals* 2001, 124: 337.

57. Gregory, R.V. *Annu. Tech. Conf.—Soc. Plast. Eng.* 1999, 57th: 1515.
58. Stafström, S.; Brédas, J.L.; Epstein, A.J.; Woo, H.S.; Tanner, D.B.; Huang, W.S.; MacDiarmid, A.G. *Phys. Rev. Lett.* 1987, 59: 1464.
59. Baird, N.C.; Wang, H. *Chem. Phys. Lett.* 1993, 202: 50.
60. Zhuang, L.; Zhou, Q.; Lu, J. *J. Electroanal. Chem.* 2000, 493: 135; and references cited therein.
61. Xia, Y.; Wiesinger, J.M.; MacDiarmid, A.G.; Epstein, A.J. *Chem. Mater.* 1995, 7: 443.
62. Libert, J.; Cornil, J.; dos Santos, D.A.; Brédas, J.L. *Phys. Rev. B.* 1997, 56: 8638; and references cited therein.
63. McCall, R.P.; Ginder, J.M.; Leng, J.M.; Ye, H.J.; Manohar, S.K.; Masters, J.G.; Asturias, G.E.; MacDiarmid, A.G.; Epstein, A.J. *Phys. Rev. B.* 1990, 41: 5202.
64. Brédas, J.L.; Quattrocchi, C.; Libert, J.; MacDiarmid, A.G.; Ginder, J.M.; Epstein, A.J. *Phys. Rev. B.* 1991, 44: 6002.
65. Barta, P.; Kugler, T.; Salaneck, W.R.; Monkman, A.P.; Libert, J.; Lazzaroni, R.; Brédas, J.L. *Synthetic Metals* 1998, 93: 83.
66. de Oliveira, Z. T.; dos Santos, M.C. *Chem. Phys.* 2000, 260: 95.
67. Jansen, S.A.; Duong, T.; Major, A.; Wei, Y.; Sein, L.T. *Synthetic Metals* 1999, 105: 107; and references cited therein.
68. Majidi, M.R.; Kane-Maguire, L.A.P.; Wallace, G.G. *Polymer* 1994, 35: 3113.
69. Majidi, M.R.; Kane-Maguire, L.A.P.; Wallace, G.G. *Aust. J. Chem.* 1998, 51: 23.
70. Li, W.; Wang, H.-S. *Adv. Funct. Mater.* 2005, 15: 1793.
71. Havinga, E.E.; Bouman, M.M.; Meijer, E.W.; Pomp, A.; Simenon, M.M.J. *Synthetic Metals* 1994, 66: 93.
72. Majidi, M.R.; Kane-Maguire, L.A.P.; Wallace, G.G. *Polymer* 1995, 36: 3597.
73. Majidi, M.R.; Kane-Maguire, L.A.P.; Wallace, G.G. *Polymer* 1996, 37: 359.
74. Ashraf, S.A.; Kane-Maguire, L.A.P.; Majidi, M.R.; Pyne, S.G.; Wallace, G.G. *Polymer* 1997, 38: 2627.
75. Langeveld-Voss, B.M.W.; Janssen, R.A.J.; Meijer, E.W. *J. Mol. Struct.* 2000, 521: 285, and references cited therein.
76. Norris, I.D.; Kane-Maguire, L.A.P.; Wallace, G.G. *Macromolecules* 2000, 33: 3237.
77. Norris, I.D.; Kane-Maguire, L.A.P.; Wallace, G.G.; Mattose, L.H.C. *Aust. J. Chem.* 2000, 53: 89.
78. Su, J.-J.; Kuramoto, N. *Macromolecules* 2001, 34: 7249.
79. Su, S.-J.; Kuramoto, N. *Chem. Mater.* 2001, 13: 4787.
80. Kane-Maguire, L.A.P.; Norris, I.D.; Wallace, G.G. *Synthetic Metals* 1999, 101: 817.
81. Strounina, E.V.; Kane-Maguire, L.A.P.; Wallace, G.G. *Synthetic Metals* 1999, 106: 129.
82. Strounina, E.V.; Kane-Maguire, L.A.P.; Wallace, G.G. *Polymer* 2006, 47: 8088.
83. Creighton, T.E. In *Proteins, Structures and Molecular Properties, 2nd Edition*. W.H. Freeman and Co, New York. Chapter 5, 1993.
84. Guo, H.; Knobler, C.M.; Kaner, R.B. *Synthetic Metals* 1999, 101: 44.
85. Kaner, R.B. *Synthetic Metals* 2002, 125: 65.
86. Pornputtkul, Y.; Kane-Maguire, L.A.P.; Innis, P.C.; Wallace, G.G. *Chem. Commun.* 2005: 4539.
87. Thiyagarajan, M.; Samuelson, L.A.; Kumar, J.; Cholli, A.L. *J. Am. Chem. Soc.* 2003, 125: 11502.
88. Norris, I.D.; Kane-Maguire, L.A.P.; Wallace, G.G. *Macromolecules* 1998, 31: 6529.
89. Egan, V.; Barrstein, R.; Hohmann, L.; Tran, T.; Kaner, R.B. *J. Chem. Soc. Chem. Commun.* 2001, 801.
90. Boonchu, C.; Kane-Maguire, L.A.P.; Wallace, G.G. *Synth. Met.* 2003, 135–136: 241.
91. Hino, T.; Kumakura, T.; Kuramoto, N. *Polymer* 2006, 47: 5295.

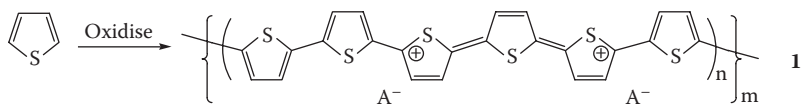
# 6 Synthesis and Properties of Polythiophenes

Polythiophenes (PTh's) (**1** shown subsequently) have much in common with polypyrroles. They are formed from a cyclopentadiene molecule, but which has an S heteroatom. Thiophene is oxidized to form a conducting electroactive polymer (CEP), with the greatest conductivity obtained from  $\alpha$ - $\alpha$  linkages. There are some important differences between polythiophenes and polypyrroles, and these are discussed here.

## SYNTHESIS OF POLYTHIOPHENE

### ELECTROPOLYMERIZATION

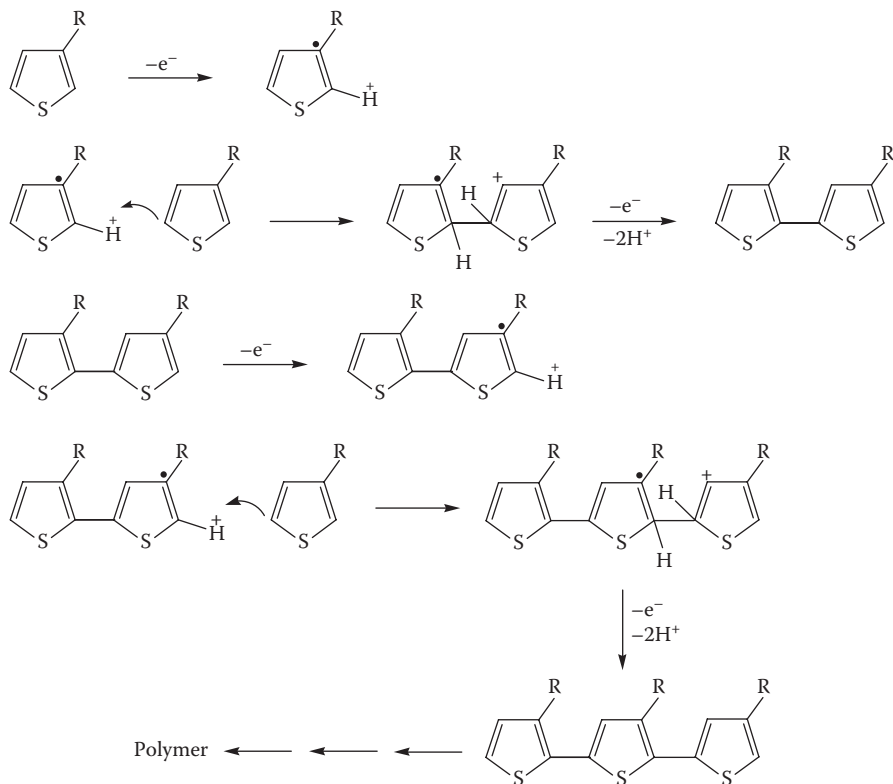
Polythiophene **1** can be synthesized either electrochemically or chemically using a simple oxidation process according to



$A^-$  molecular dopant, *m* determines molecular weight (6.1)

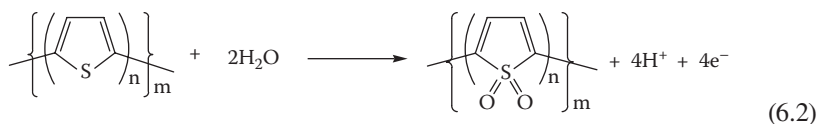
As with polypyrrole,  $A^-$  is a counterion incorporated into the polymer during growth to balance the charge on the polymer backbone, and *m* is a parameter proportional to the molecular weight. As with polypyrroles, the mechanism of polymerization involves formation of radical cations that react with one another or the starting monomer to develop the polymeric structure (Figure 6.1). The reaction of the radical cation with the thiophene monomer has been elegantly demonstrated in studies in which small amounts of bi- or ter-thiophene were added to reduce the polymerization potential.<sup>1</sup> Even after the additive was consumed, polymerization continued at lower potentials.

This is particularly important because the development of systems utilizing thiophene have been thwarted by the "polythiophene paradox."<sup>2</sup> It has been clearly shown that at potentials required to oxidize the thiophene monomer, the polymer itself becomes overoxidized. This overoxidation process proceeds according to Equation 6.2,<sup>3</sup> and results in deterioration in the chemical and physical properties of the polymer.

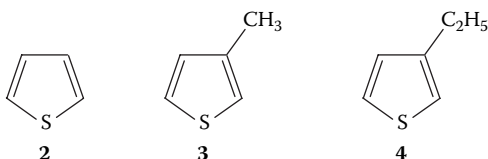


**FIGURE 6.1** Polymerization of thiophene (where R = H or a substituent).

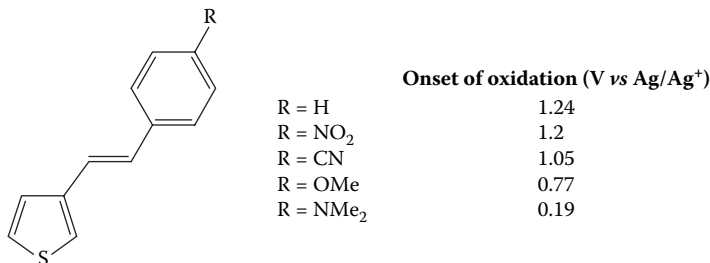
Therefore, if using constant-current or constant-potential polymerization, the product obtained will be a mixture of polythiophene and overoxidized polythiophene.



Various substituted thiophenes have been produced, the most common being 3-alkyl thiophenes. Sato and coworkers<sup>4</sup> carried out a comprehensive study using thiophene (Th **2**), 3-methylthiophene (MTh **3**), and 3-ethylthiophene (ETH **4**).



They found that all the monomers could be oxidized to form conducting polymers, and that the oxidation potentials increased such that MTh < ETH < Th. The



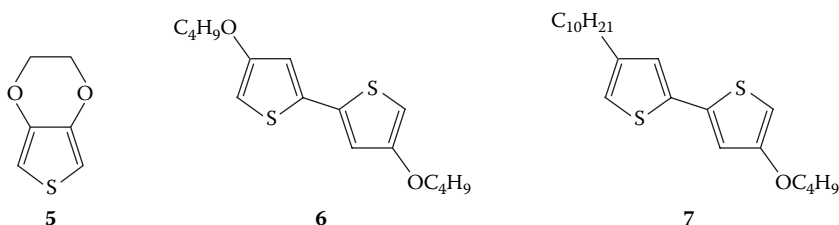
**FIGURE 6.2** Effect of substituents on oxidation potential of substituted thiophenes.

fact that ETH was harder to oxidize than MTH was attributed to steric effects. Lowering of the oxidation potential by addition of alkyl groups at a  $\beta$  carbon position avoids the polythiophene paradox during polymerization.

Other workers<sup>5,6</sup> have minimized overoxidation during polymerization by using bithiophenes or terthiophenes as starting materials for the polymerization process. The polymerization potential has been shown to decrease such that terthiophene < bithiophene < thiophene. As reviewed by Roncali, polythiophenes produced from these starting materials generally have lower conductivity.<sup>7</sup> However, addition of small amounts of bithiophene<sup>8</sup> influences the polymerization process and results in polymers with increased conjugation length and, therefore, fewer structural defects. This translates to improved electronic properties.

We<sup>9,10</sup> have recently shown that the attachment of a range of electron-donating or electron-withdrawing groups through a conjugated linker (Figure 6.2) has a dramatic effect on polymerization potential and subsequent photovoltaic performance.<sup>9,10</sup>

A range of alkoxy groups<sup>11</sup> **5**, **6**, **7** has also been added to the bithiophene starting material to reduce the oxidation potential even further. Attachment of the alkyl group **7** also facilitates the solubility of the polymer in nonpolar organic solvents.



A range of copolymers involving functional thiophenes have also been formed electrochemically. For example, Sato and coworkers<sup>12</sup> formed a copolymer containing 3-dodecylthiophene and 3-methylthiophene. The material had a solubility of 75 (w/w)% in chloroform and a conductivity of 220 S cm<sup>-1</sup>.

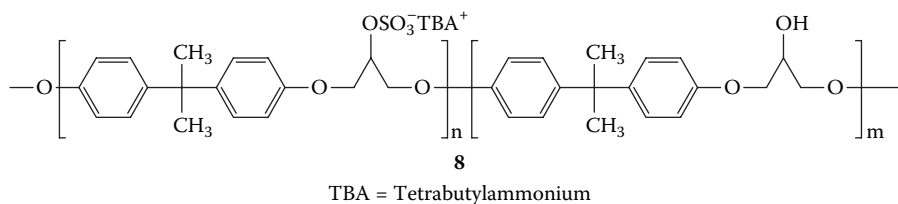
Polythiophenes are normally produced from nonaqueous media because the monomer is more soluble in these. Also, a wider electrochemical potential window is available, and this is required as polythiophene is more difficult to oxidize than pyrrole. The influence of water on the polymerization process for thiophene and on the redox switching properties has been studied.<sup>13,14</sup> The presence of water as low as



1% causes mislinkages and a subsequent deterioration in polymer properties.<sup>13</sup> Other authors<sup>15</sup> have claimed that optimal polymers are produced from propylene carbonate.<sup>4</sup> These same workers also point out that the minimum thiophene concentration required to enable polymerization is solvent dependent. The required minimal monomer concentration decreases for solvents with a large dielectric constant. They claim that solvents with a high dielectric constant (having an electron-withdrawing substituent) influence the reactivity of the intermediate cation radical and, therefore, play an important role in the polymerization process.

The counterion employed can also affect the rate of polymerization at a fixed potential. The effect of the counterion's chemical nature on the oxidation of 3-methylthiophene was found to be potential dependent.<sup>15</sup> At relatively low anodic potentials (+1.25 to +1.34 V), the initial rate of reaction was found to be quickest when the  $\text{ClO}_4^-$  anion was used as dopant. The next quickest rate was with the  $\text{BF}_4^-$  ion, closely followed by  $\text{PF}_6^-$ . This trend was similar to the oxidation potentials measured by cyclic voltammetry. At higher anodic potentials (+1.40 to +1.5 V), the  $\text{ClO}_4^-$  ion showed the slowest reaction rate. At even higher potentials (> +1.50 V), the reaction involving  $\text{ClO}_4^-$  was severely inhibited, with currents dropping to low values. The perchlorate ion is known to undergo oxidation at these potentials to form  $\text{ClO}_4$ . This species may well have reacted with the intermediate monomer radicals to inhibit the polymerization process.

Recently novel polyelectrolytes **8** have been incorporated into polythiophene structures and found to generate a mechanically strong electroactive deposit.<sup>16</sup>



The ability to incorporate different counterions into any conducting polymer backbone is largely dictated by the requirement for mutual monomer—counterion solubility. Whereas for polyanilines this is limited by the need for acid conditions to dissolve the monomer, for polythiophenes it is often limited by the need for an organic solvent to achieve monomer dissolution.

Ionic liquids introduce a new possibility in this regard, as their ability to provide dissolution is often unpredictable and sometimes useful. These ionic liquid properties have been used recently to achieve incorporation of dye molecules into polyterthiophene.<sup>17</sup>

Polythiophenes have been polymerized on a range of substrates<sup>15</sup> including Pt, Au, Cr, and Ni. However, as with polypyrrole, they do not grow on more easily oxidized substrates such as Cu, Ag, Pb, or Zn.

Other workers have shown that polymerization of functional thiophenes from aqueous media is possible if surfactants are used to help solubilize the monomer.<sup>18,19,20,21</sup> In the case of SDS being used as a solubilizing agent for bithiophene,<sup>18</sup> it was also found to lower the oxidation potential and inhibit the dissolution of the

iron, enabling electropolymerization on this active substrate. SDS was also found to lower the oxidation potential of EDOT structure **5**<sup>19</sup> and other copolymers containing alkoxythiophene and bithiophene groups.<sup>20</sup>

The effect of temperature on the polymerization process for thiophene<sup>22</sup> has been investigated. Results show that when polymerization is carried out at 15–20°C, polymers with optimal properties are obtained. Ultrasonication has been used to improve the efficiency (improved yield, lowering of polymerization potentials) of the electropolymerization process for polythiophene.<sup>23</sup>

### CHEMICAL POLYMERIZATION

As with polypyrrole, polythiophene can be produced using a chemical oxidant. However, owing to the limited solubility of thiophene, this reaction must be carried out in nonaqueous media. Copper (II) perchlorate has been used as an oxidizing agent in acetonitrile to yield a simultaneous polymerization/doping process.<sup>24</sup> This results in polymer materials with conductivities of approximately 8 S cm<sup>-1</sup>. Alternatively,<sup>25</sup> the Grignard reaction can be used (Figure 6.3) to produce polythiophene, which is the first time conventional synthesis techniques have been used. Others<sup>26</sup> have used a chemical polymerization process that ensures the production of well-defined head-to-tail (HT)-coupled poly(3-alkylthiophenes).

The first controlled chemical syntheses of polythiophene were reported in 1980 by two different groups; they used metal-catalyzed coupling of 2,5-dibromothiophene (Equation 6.3).<sup>27,28</sup> In both cases, the dibromothiophene substrate was first reacted with Mg in THF, replacing either the 2- or 5-bromo substituent with MgBr. Self-coupling was then achieved, with either Ni(bipy)Cl<sub>2</sub><sup>27</sup> or M(acac)<sub>2</sub> (M = Co, Ni,

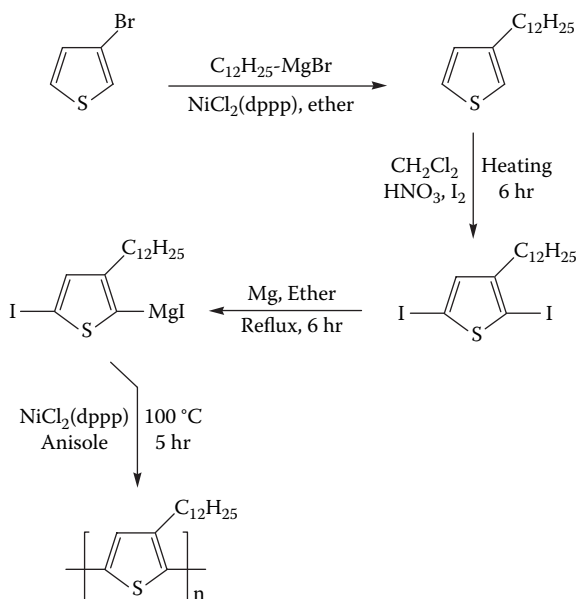
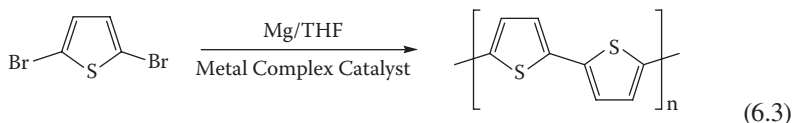


FIGURE 6.3 Chemical synthesis of alkylated polythiophenes.

Pd) or  $\text{Fe}(\text{acac})_3$ <sup>28</sup> as catalyst, the condensation reactions eventually leading to polythiophenes of low molecular weight.



Such polycondensation dehalogenation reactions remain a commonly employed route to polythiophene, and a range of solvents, halogenothiophene substrates, and other metal-based catalysts have been examined, as recently reviewed.<sup>29</sup> For example, the reaction of 2,5-dibromothiophene with  $\text{Ni}(\text{cyclooctadiene})_2$  and triphenylphosphine in DMF leads to an almost quantitative yield of polythiophene.<sup>30</sup> Solid-state <sup>13</sup>C NMR studies confirm exclusive 2,5-coupling of the thiophene repeat units in the polymeric product. The 2,5-dichlorothiophene monomer is less active as a substrate in such reactions; however, the corresponding 2,5-diiodothiophene is reported to be a good substrate.<sup>31</sup>

The direct oxidative polymerization of a thiophene monomer has also been successfully employed to prepare polythiophene, for example, using  $\text{FeCl}_3$  in chloroform solvent.<sup>32</sup>  $\text{MoCl}_5$  may be similarly employed as both the oxidant and dopant.<sup>33</sup> Subsequent reduction with ammonia of the doped polythiophene products from these  $\text{FeCl}_3$  and  $\text{MoCl}_5$  oxidations provides the neutral polymer.

Despite their low molecular weights, these unsubstituted polythiophenes are insoluble in THF and other common organic solvents, and are also infusible. Their poor processability has therefore led to extensive studies of alkyl- and alkoxy-substituted polythiophenes in the hope of enhancing solubility in organic solvents and allowing melt processing. Synthetic approaches to these substituted polythiophenes are described in the following text.

### VAPOR-PHASE POLYMERIZATION

Vapor-phase polymerization (VPP) has also been employed in a few cases to prepare polythiophene-based films. This approach was first successfully used by de Leeuw and coworkers<sup>34</sup> in 1994 to prepare smooth films of poly(3,4-ethylenedioxythiophene) (PEDOT) using ferric *p*-toluenesulfonate as the oxidant. Imidazole was added as inhibitor to suppress the polymerization of the EDOT monomer until the solvent was evaporated. Fe(III) sulfonates do not have sufficient oxidizing power in VPP to produce coherent and conducting polythiophenes from the thiophene monomer itself. However, Winther-Jensen and coworkers<sup>35</sup> have recently prepared polybithiophene (PBTh) and polyterthiophene (PTTh) via the vapor-phase polymerization of the more readily oxidized bithiophene and terthiophene using Fe(III) tosylate as oxidant. Both polymers were formed in their blue, oxidized state, but spontaneously reduced to their neutral, yellow-orange state upon washing in ethanol. The cyclic voltammograms of the PBTh and PTTh films on Pt-coated PET foils in 0.10 M  $[\text{Bu}_4\text{N}]\text{ClO}_4/\text{acetonitrile}$  were similar to those previously described<sup>36</sup> for analogous electrochemically produced films, confirming their electroactivity.

Vapor-phase polymerization has been used to create a PEDOT structure into which even delicate biomolecules such as enzymes can be incorporated during the subsequent washing step.<sup>37</sup>

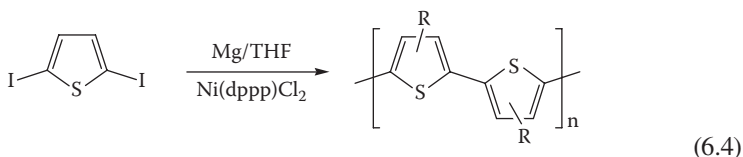
## UV POLYMERIZATION OF OLIGOTHIOPHENES

There have been several reports indicating that oligothiophenes can also be polymerized by UV irradiation.<sup>38,39,40</sup> In a recent study in 2004, Huisman and coworkers<sup>40</sup> showed that when thin films of bithiophene and terthiophene were irradiated with a 150 W xenon lamp, dimerization occurred, giving quarterthiophene (4T) and sexi-thiophene (6T), respectively. Similar photochemical dimerizations were achieved with solutions of bithiophene and terthiophene in chloroform or toluene, or when films of nanocrystalline titanium dioxide (nc-TiO<sub>2</sub>) soaked with bithiophene and terthiophene were irradiated. The latter approach provides a convenient method to partly fill nc-TiO<sub>2</sub> pores with 4T and 6T oligothiophenes, which is of potential use in the fabrication of photovoltaic devices. Interestingly, the authors reported a photovoltaic response when nc-TiO<sub>2</sub>/4T or nc-TiO<sub>2</sub>/6T interpenetrating structures were irradiated with visible light.

## SUBSTITUTED POLYTHIOPHENES

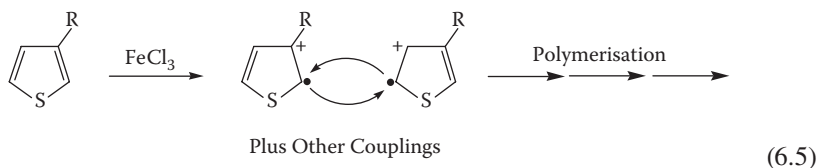
### POLY(3-ALKYLTHIOPHENES) AND POLY(3-ALKOXYTHIOPHENES)

Elsenbaumer and coworkers<sup>41,42</sup> reported the first synthesis of soluble poly(3-alkylthiophenes) in 1985, using the metal-catalyzed cross-coupling polymerization shown in Equation 6.4, with 2,5-diiodo-3-alkylthiophenes as substrates. Poly(3-alkylthiophene) products with butyl or longer alkyl substituents were found to be soluble in a wide range of common organic solvents, such as chloroform, dichloromethane, THF, toluene, and nitrobenzene, permitting the casting of thin films of the polymers. Melt processing into films was also possible, whereas <sup>1</sup>H NMR studies confirmed that only 2,5'-couplings had occurred. Undesirable 2,3'- and 2,4'-couplings (leading to branching structural defects) were absent, presumably owing to steric hindrance by the 3-alkyl group.

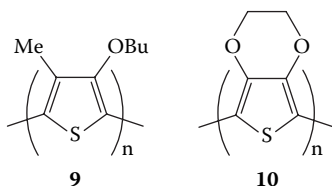


The direct oxidative polymerization of 3-alkylthiophenes with FeCl<sub>3</sub> in an organic solvent such as chloroform has also been widely used to prepare poly(3-alkylthiophenes) with molecular weights between 30,000 and 300,000.<sup>29,33,43,44,45</sup> This route, like the Grignard-type coupling methods mentioned earlier, proceeds by 2,5'-couplings of the alkylthiophene repeat units, with little or no undesirable 2,4'-couplings. This is consistent with a mechanism proposed for FeCl<sub>3</sub>-based polymerizations, involving initial oxidation of the 3-alkylthiophenes to radical cations with the radi-

cal centers predominantly located on the thiophene ring 2- and 5-positions, followed by chain propagation (Equation 6.5).<sup>46</sup>



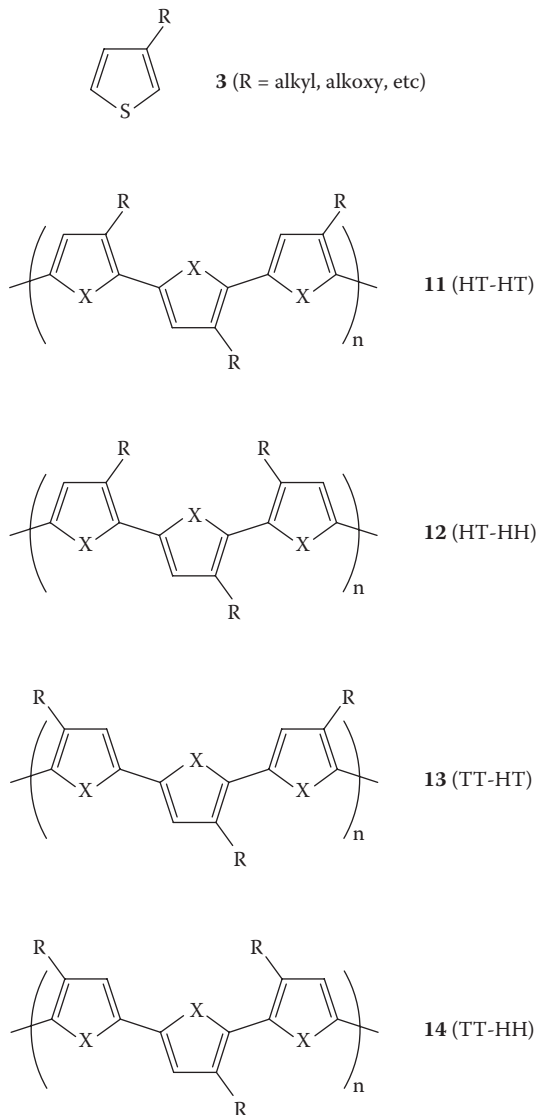
The  $\text{FeCl}_3$  oxidative polymerization route has also been employed for the synthesis of poly(3-alkoxythiophenes).<sup>29,47,48</sup> Increasing the alkoxy substituent chain length leads to improved solubility in organic solvents. The smaller steric demands of the alkoxy groups compared to the corresponding alkyl substituents results in less twisting of the polythiophene backbone. An extreme illustration of this is in the polymerization of 3,4-disubstituted thiophene monomers. Whereas the presence of two alkyl substituents causes marked twisting of the polymer chain from planarity and a consequent large decrease in electrical conductivity,<sup>47</sup> a film of poly(3-butoxy-4-methylthiophene) **9** exhibits a UV-visible spectrum ( $\lambda_{\text{max}} = 545 \text{ nm}$ ) typical of a highly conjugated (planar) polymer and has high conductivity after doping with  $\text{FeCl}_3$  ( $\delta = 2 \text{ S cm}^{-1}$ ).<sup>48</sup> Another interesting and useful disubstituted polymer is PEDOT **10**. This can be readily prepared by the  $\text{FeCl}_3$  oxidation of the corresponding monomer, and has an exceptionally high conductivity ( $\delta = 13\text{--}30 \text{ S cm}^{-1}$ , depending on the organic solvent employed in the synthesis).<sup>49</sup>



Alkoxy-substituted bithiophenes have also been successfully polymerized, using  $\text{Cu}(\text{ClO}_4)_2$  as oxidant.<sup>50</sup> As with related  $\text{FeCl}_3$  oxidations of alkyl-substituted bithiophenes,<sup>51</sup> these dimeric substrates are easier to oxidize than the corresponding substituted thiophene monomers, due to their lower oxidation potentials.

Despite the predominant 2,5'-coupling with both the 3-alkyl and 3-alkoxy thiophene monomer substrates, the presence of the ring substituents introduces a further structural complication. Coupling of the substituted thiophene units can now lead to four possible triad regioisomers for the resultant polymers, depending on whether the coupling occurs in a 2,5'-head-to-tail (HT), 2,2'-head-to-head (HH), or 5,5'-tail-to-tail (TT) manner. These structures **11–14** for the polythiophene products are depicted in Figure 6.4 (X = S).

When a mixture of these regioisomers is formed, the resulting substituted polythiophenes are described as *regiorandom* or irregular. This has major implications for the properties of the polymers. Strong steric interactions between alkyl (R) groups in cases of HH couplings, as in regioisomers **12** and **14**, cause marked twisting of

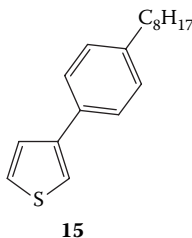


**FIGURE 6.4** Structures of substituted polythiophenes.

the polymer chain from planarity, thereby decreasing the conjugation length and electrical conductivity of the polythiophene. In contrast, the less sterically crowded *regioregular* HT–HT structure **11** results in little twisting, and this species can adopt an almost planar arrangement for its polymer backbone. These predictions are supported by gas-phase molecular mechanics and *ab initio* calculations.<sup>52,53</sup>

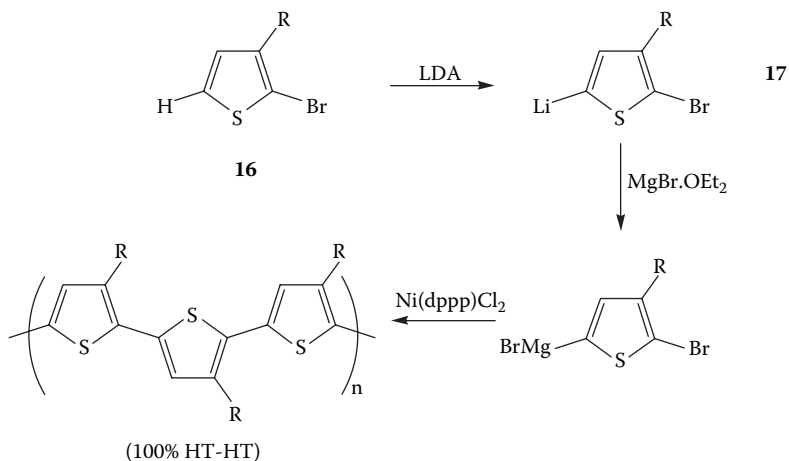
<sup>1</sup>H NMR studies have shown that metal-catalyzed cross-coupling polymerizations of 3-alkylthiophenes such as reactions 6.4, generally lead to regiorandom polythiophenes. A similar situation holds for polymerizations performed by the oxidation

of 3-alkylthiophenes with  $\text{FeCl}_3$ .<sup>33,43,44,45</sup> The poly(3-alkylthiophene) products from this latter route usually have only ca. 70–80% HT coupling; i.e., they are *regiorandom*. However, it has been reported that in the polymerization of 3-(4-octylphenyl)-thiophene **15**, the slow addition of the  $\text{FeCl}_3$  oxidant can result in up to 94% HT couplings.<sup>54</sup> Improved polymerization conditions have similarly led to an 84% HT polymer from  $\text{FeCl}_3$  oxidation of 3-octylthiophene.<sup>55</sup>



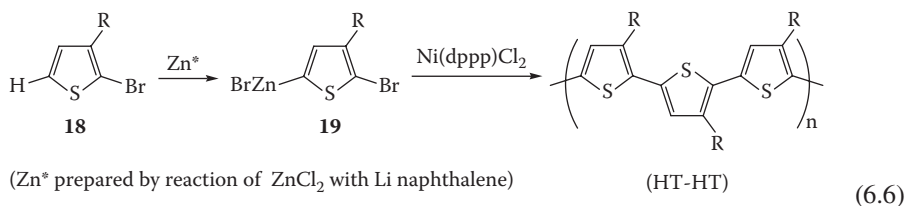
## REGIOREGULAR SUBSTITUTED POLYTHIOPHENES

An important development has been the discovery of effective routes to highly regioregular (HT) poly(3-alkylthiophenes). The first such regiospecific polymerization was reported by McCullough and Lowe<sup>56</sup> in 1992. This one-pot synthesis involves the regioselective lithiation of 2-bromo-3-alkylthiophene **16** and subsequent *in situ* generation of the Grignard reagent **17**, followed by polymerization via the addition of  $\text{NiCl}_2(\text{dppf})$  catalyst, to give poly(3-alkylthiophenes) with 98–100% HT–HT couplings (Figure 6.5). These regioregular polymers ( $M_n = 20,000\text{--}40,000$ ) possess markedly improved properties over the related regiorandom polymers, including enhanced electrical conductivity, nonlinear optical properties, and crystallinity. For example, regioregular poly(3-dodecylthiophene) exhibits a conductivity of  $1000\text{ S cm}^{-1}$ , compared to  $20\text{ S cm}^{-1}$  for its regiorandom analog.<sup>57</sup>



**FIGURE 6.5** Regioregular synthesis of substituted polythiophene.

In a second useful approach to regioregular (HT) poly(3-alkylthiophenes), developed by Rieke and coworkers,<sup>58</sup> highly reactive zinc ( $Zn^*$ ) is reacted with 2,5-dibromo-3-alkylthiophene substrates **18** to yield metallated species **19** with high regiospecificity. Treatment of this intermediate with the cross-coupling catalyst  $NiCl_2(dppp)$  results in a regioregular (HT) poly(3-alkylthiophene) (Equation 6.6). The polythiophene products from the alternative McCullough and Rieke synthetic routes have similar properties.

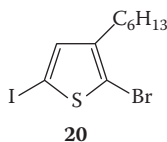


An alternative, less sophisticated approach to regioregular substituted polythiophenes is the use of asymmetric 3,4-disubstituted thiophene monomers as substrates, resulting in the selective activation of either the 2- or 5- positions on the thiophene ring. Using this method, poly(3-alkoxy-4-methylthiophenes) with > 95% HT couplings have been prepared via  $FeCl_3$  oxidation.<sup>48,59</sup>

Using these chemical synthetic approaches, a wide range of substituted polythiophenes have now been prepared, bearing functional groups that impart specific properties to the polymers such as water solubility, sensor capabilities, and chirality. Some specific examples are described here.

### REGIOREGULAR POLY(3-ALKYLTHIOPHENES) WITH LOW POLYDISPERSITIES AND CONTROLLED MOLECULAR WEIGHTS

Although poly(3-alkylthiophenes) with high HT regioselectivity are available from the preceding routes, their polydispersities ( $M_w/M_n$ ) before subsequent fractionation are typically high, and their molecular weights not readily controlled. A significant recent development has therefore been the report by Yokozawa and coworkers<sup>60</sup> of the polymerization of 2-bromo-3-hexyl-5-iodothiophene **20** by the  $Ni(dppp)Cl_2$  catalyst to give poly(3-hexylthiophene) in high yield, having greater than 98% HT coupling, and possessing a low polydispersity of 1.30–1.39. The molecular weight of the polymer product was also closely controlled by the **20**:catalyst ratio employed. This new synthetic route should be extendable to the production of other HT poly(3-alkylthiophenes) of requisite molecular weight and low polydispersity, assisting the development of superior electrical and optical devices.



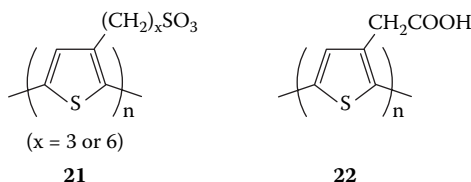


## POLYTHIOPHENES WITH SPECIAL FUNCTIONAL GROUPS

### WATER-SOLUBLE POLYTHIOPHENES

Self-doped water-soluble sulfonated polythiophenes of type **21** ( $x = 3$  or  $6$ ) have been prepared by the  $\text{FeCl}_3$  oxidation of the corresponding monomers.<sup>61,62,63</sup>  $^1\text{H}$  and  $^{13}\text{C}$  NMR studies of these self-doped polymers in  $\text{D}_2\text{O}/\text{DMSO-d}_6$  or  $\text{D}_2\text{O}/\text{acetonitrile-d}_3$  showed a HT:HH ratio of 4:1 in both cases.<sup>63</sup> Related poly[(3-thienyl)alkane sulfonic acid] polymers **21** ( $x = 2, 6, 10$ ) have been similarly chemically synthesized, wherein the doping level was found to be dependent on the length of the alkyl side chain.<sup>64</sup> More recently, self-doped conducting sulfonated polythiophene films have been prepared via electropolymerization of thiophene in acetonitrile solvent containing fluorosulfonic acid.<sup>65</sup> The degree of thiophene ring sulfonation and water solubility of the resultant polymers increased with increasing concentration of fluorosulfonic acid employed, whereas the electrical conductivity decreased, presumably because of the twisting of the polymer chains caused by the presence of the sulfonic acid ring substituents.

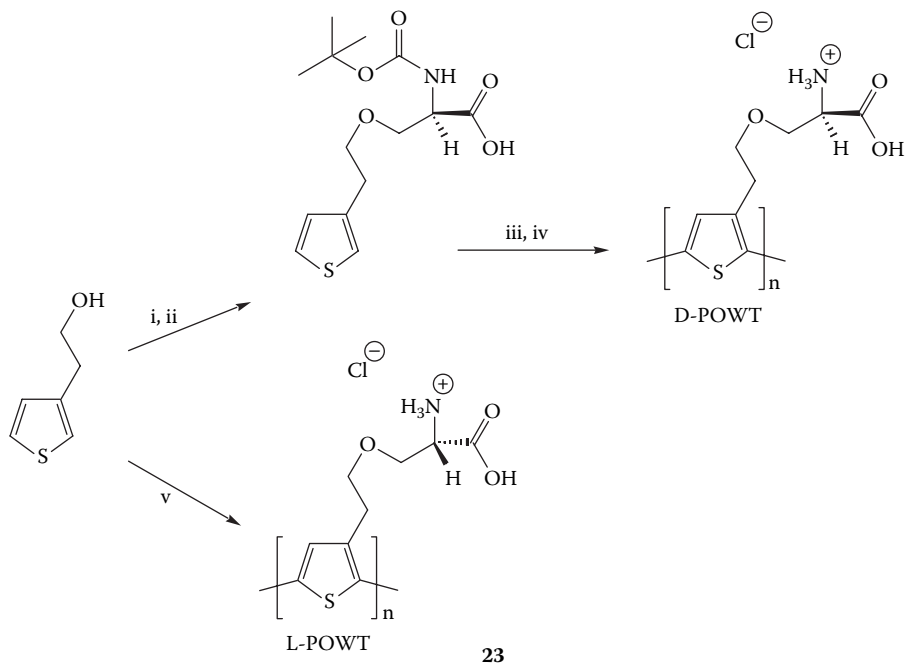
Related water-soluble polythiophenes with carboxylic acid substituents covalently bound at the thiophene ring 3-position have also been reported. For example, poly(3-thiophene acetic acid) **22** has been synthesized by Osada and coworkers<sup>66</sup> in 75% yield by  $\text{FeCl}_3$  oxidation of 3-thiophene methyl acetate, followed by alkaline hydrolysis and protonation. Its hydrogel has also been described.<sup>67</sup> The polymer has a molecular weight of 16,000 and a polydispersity of 2.8.  $^1\text{H}$  NMR studies show it to be regiorandom, with less than 40% HT–HT couplings.<sup>66</sup> At around pH 5–6 in aqueous solution, the polymer main chain of **22** undergoes an abrupt conformational change from the aggregated to the extended state, caused by electrostatic repulsions between the dissociated carboxylic acid substituents. McCullough and coworkers<sup>68</sup> have also prepared novel regioregular water-soluble polythiophenes with a propionic acid group at the ring 3-position that self-assemble through carboxylic acid dimer pairs between adjacent chains. These undergo dramatic pH- and cation-induced color changes attributed to “unzipping” of the purple self-assembled state to a yellow, disassembled, and twisted structure.



Another interesting water-soluble polythiophene is **23** (L-POWT), bearing a chiral amino acid side chain, which was prepared by Inganäs and coworkers<sup>69</sup> by oxidative polymerization with  $\text{FeCl}_3$  (Figure 6.6). The chiroptical and solvatochromic properties of this optically active polymer are described later.

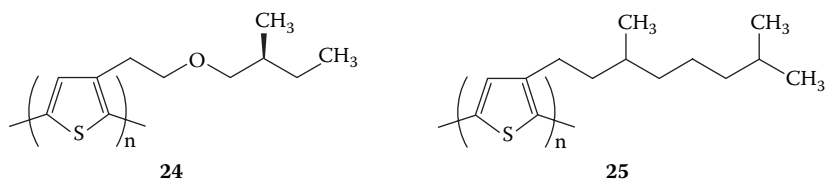
### ORGANIC-SOLVENT-SOLUBLE CHIRAL POLYTHIOPHENES

A large number of optically active polythiophenes have been prepared through the chemical polymerization of monomers bearing chiral substituents covalently bound



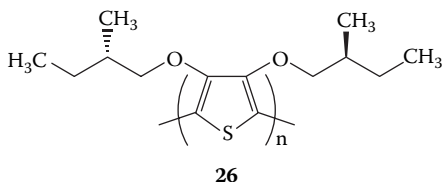
**FIGURE 6.6** (i) TsCl, pyridine,  $\text{CHCl}_3$ , 86%; (ii) N-t-Boc-D-Ser,  $\text{K}_2\text{CO}_3$ , DMF,  $35^\circ\text{C}$ , 57%; (iii)  $\text{CH}_2\text{Cl}_2/\text{TFA}$  (1:1), quant.; (iv)  $\text{FeCl}_3$ , TBA-trifluoromethanesulfonate,  $\text{CHCl}_3$ ,  $15^\circ\text{C}$ , 61%; and (v) using N-t-Boc-L-ser. (From Andersson, M.; Ekeblad, P.O.; Hjertberg, T.; Wennerström, O.; Inganäs, O. *Polym. Commun.* 1991, 32: 546. With permission.)

at the 3-position of the thiophene ring. For example, Meijer and coworkers<sup>70</sup> prepared the regioregular (HT) chiral polythiophene **24** by polymerizing the (*S*)-(+)-2-phenylbutyl ether of 3-propylthiophene by the McCullough method. The strong optical activity observed for the polymer is induced by the chiral substituent and is believed to be associated with aggregation of the polymer chains. Polymer **24** is soluble in a range of organic solvents, its chiroptical properties showing marked solvent and temperature dependence.

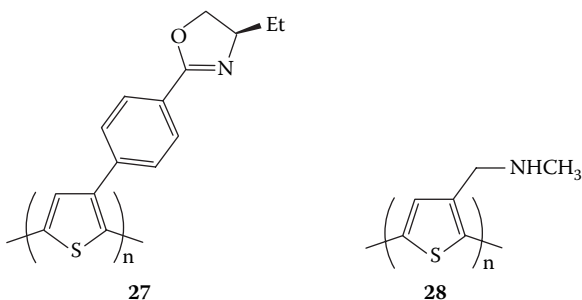


Similar thermochromic and solvatochromic effects have been observed by Bidan and coworkers<sup>71</sup> for the optically active polymer **25** prepared in a regiospecific fashion (100% HT-HT coupling) by the McCullough method. In contrast, the analogous regiorandom polymer prepared by oxidation with  $\text{FeCl}_3$  in chloroform has only weak optical activity. However, the disubstituted chiral polythiophene **26**, synthesized by

Meijer and coworkers<sup>72</sup> through the  $\text{FeCl}_3$  route, is strongly optically active and also exhibits solvatochromism and thermochromism. This optical activity is again believed to be associated with a chiral  $\pi$ -stacked aggregated phase of the polymer, which is highly ordered owing to the stereoregular structure of the substituent side chains.

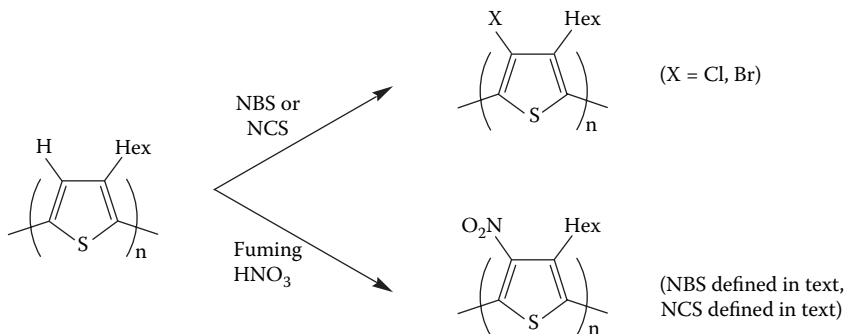


Other optically active polythiophenes recently prepared using the regiospecific McCullough approach are **27** and **28**. The former polymer bears a chiral oxazoline group in its side chain, and complexation of this group by metal ions induces solvent-dependent chirality in the polythiophene.<sup>73,74</sup> Polythiophene formed using monomer **28** is water soluble and becomes optically active upon binding to DNA.<sup>75</sup> To our knowledge, this represents the first example of induction of chirality into an achiral polythiophene through binding to a chiral moiety.



## POSTPOLYMERIZATION MODIFICATION: ENHANCING FUNCTIONALITY

The synthesis of many substituted polythiophenes from their respective monomers is difficult because of the intolerance of the functional group to the synthetic conditions or owing to electronic/steric retardation of the polymerization by the substituent. As described in Chapters 2 and 4 for polypyrroles and polyanilines, postpolymerization modification of preformed polythiophenes provides an alternative approach for preparation of functionalized polythiophenes. For example, nucleophilic substitution of overoxidized polythiophenes with methoxy and halogeno groups in the 4-ring position has been described.<sup>76,77</sup> More recently, facile electrophilic substitutions of poly(3-hexylthiophene) to give 4-halogeno (Cl, Br) and 4-nitro derivatives have been shown to produce high yields (> 90%) (Figure 6.7).<sup>78</sup> Halogenations were carried out using *N*-bromosuccinamide (NBS) and *N*-chlorosuccinamide



**FIGURE 6.7** Electrophilic substitutions of polythiophenes.

(NCS) in chloroform at room temperature, and nitration employed fuming nitric acid at 0°C. The halogenated polythiophenes may be useful precursors for further derivatization/functionalization.

## STRUCTURE OF POLYTHIOPHENES

In this section, the structural studies of polythiophenes are reviewed; the influence of structure on properties is considered in subsequent sections. The description of polythiophene structures include the alkyl-substituted thiophenes, such as poly(3-alkylthiophenes) (P3ATH's).

## MOLECULAR STRUCTURE AND CONFORMATION

The molecular structure of chemically polymerized 3-pentylthiophene has been reported in one study.<sup>79</sup> Such polymers [poly(3-alkylthiophenes) with alkyl groups longer than 4 carbons] are soluble in common solvents, and therefore, conveniently studied using techniques including NMR, GPC, and others. Proton NMR analysis of the chemically prepared poly(3-pentylthiophenes) (P3PTh) showed that 81% of the polymer content was HT configuration, the remainder being HH or TT sequences. Infrared spectra taken of the P3PTh powder showed the absence of 2-4-coupled thiophenes. The conclusion was that all sequences were 2,5'-coupled.

A comparison of doped and undoped PTh by <sup>13</sup>C NMR has been reported by Hotta and coworkers.<sup>80</sup> Their results show remarkably simple spectra for both forms of the polymer consistent with all 2,5' ( $\alpha$ - $\alpha'$ ) coupling and in contrast to the more complex spectra obtained for polypyrrole.<sup>81</sup> The doped PTh showed an upfield shift compared with the undoped PTh, consistent with an increase in electron density of the former.

## MOLECULAR WEIGHT

The study by Czerwinski and coworkers,<sup>79</sup> described earlier, included an analysis of the molecular weight of soluble poly(3-pentylthiophene) by GPC. An estimate of the polymer molecular weight was made using polystyrene standards, and the average

molecular size was determined to be 118 repeat units. The polydispersity was 4.8, which is typical for such chemically oxidized polymers. A study of the effect of synthesis conditions on the molecular weight of a chemically polymerized terthiophene (3,3'-didodecyl-2,2':5,2'-terthiophene) has shown that higher molecular weights (with no insoluble material) could be obtained by carefully purifying the oxidant, and with slow addition of oxidant to the monomer solution.<sup>82</sup> The measurement of the molecular weight of soluble PTh's is discussed by Verilhac and coworkers.<sup>83</sup>

## ELECTROPOLYMERIZED POLYTHIOPHENES

### CRYSTALLINITY, MOLECULAR ORDER, CONFORMATION IN SOLID STATE

As with polypyrroles, electrochemically prepared polythiophenes show small degrees of crystallinity (~5%). The nature of the crystal structure has been investigated using x-ray diffraction. Ito and coworkers showed that electrochemically deposited PTh had a preferred molecular orientation parallel to the electrode surface.<sup>84</sup> Again, this structural feature is the same as that observed in polypyrrole (Chapter 2). Later work by these same researchers<sup>85</sup> investigated the reduced form of the electropolymerized PTh. The reduced PTh showed a crystallinity that was tentatively assigned an orthorhombic unit cell on the basis of earlier work by Mo and coworkers.<sup>86</sup> Reflections of the (110) and (200) planes were identified, and corresponded to the unit cell dimensions  $a = 0.780$  nm,  $b = 0.555$  nm, and  $c = 0.803$ . Mechanical drawing of the reduced PTh (draw ratio 1.8) showed preferential orientation of the  $c$ -axis parallel to the film surface. Satoh and coworkers<sup>87</sup> have also noted a preferred orientation parallel to the film surface upon mechanical drawing of the reduced PTh. However, the orientation effect was not as strong as that noted by Ito,<sup>85</sup> and the assigned crystal structure was somewhat different (orthorhombic  $a = 0.108$  nm,  $b = 0.474$  nm,  $c = 0.756$  nm). The differences in the two studies may reflect the influence of different electrochemical preparation conditions.

Surprisingly high crystallinity has been recently reported<sup>88</sup> for electrochemically polymerized thiophene using a nickel electrode with an ionic liquid ( $\text{BF}_3^-$  diethyl ether:  $(\text{C}_2\text{H}_5)_3\text{O}^+\text{BF}_4^-$ ) electrolyte. The estimated degree of crystallinity of the PTh films made in this way was over 70%, and the structure was assigned to a monoclinic unit cell with parameters  $a = 0.624$  nm,  $b = 0.593$  nm,  $c = 596$  nm, and  $\beta = 103.6^\circ$ . The obtained films showed high tensile strengths (80 MPa) but relatively low conductivity ( $3.5 \times 10^{-2}$  S  $\text{cm}^{-1}$ ). Another study has shown that the use of small amounts of a hydrogen scavenger reduces the instance of hydrogenation during electrochemical polymerization of thiophene.<sup>89</sup> The effect is a greater degree of packing of the PTh chains, this time with the thiophene rings oriented perpendicular to the electrode surface. Very high tensile strengths (135 MPa) and conductivities (1300 S  $\text{cm}^{-1}$ ) were reported for these PTh films.

Electrochemically prepared alkylated polythiophenes have been investigated by Garnier and coworkers.<sup>90,91</sup> When comparing polythiophene and monosubstituted polyalkylthiophenes, these workers found an increase in crystallinity of the substituted thiophenes in comparison to the unsubstituted polythiophene. The degree of crystallinity was low (5%), but the crystal structure was assigned to a hexagonal cell

( $a = 0.97$  nm,  $c = 1.22$  nm). The structure could be described by a helical conformation with 11 thiophene units making one loop of the coil.

### MORPHOLOGY AND DENSITY

The film morphology of electrochemically prepared polythiophene has been shown in numerous studies to be almost identical to that commonly observed for polypyrrole (described in Chapter 2). A nodular surface is observed for both unsubstituted and 3-alkyl substituted thiophenes.<sup>92</sup> As with PPy, the electrochemical preparation of PTh at higher current densities produced rougher surface morphologies. The similarity in morphologies suggest a similar growth mechanism for electrochemically polymerized PPy and PTh.

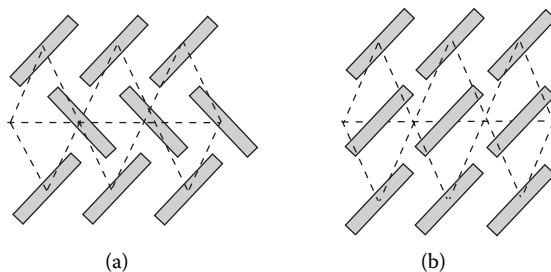
A number of studies have investigated the effect of film thickness on PTh morphology. As with PPy, the films show a rougher surface texture with increasing polymerization time.<sup>93,94</sup> Tourillon and Garnier also compared unsubstituted PTh and 3-methyl-substituted P3MTh and found different morphologies. In both cases, thin films gave flat and featureless surfaces. Thicker films (0.5–1.0  $\mu\text{m}$ ), however, showed wrinkled roughness for PTh and nodular roughness for P3MTh when both were oxidized and doped with  $\text{PF}_6^-$ . A much flatter surface was produced when P3MTh was doped with  $\text{CF}_3\text{SO}_3^-$ . Different morphologies were observed in the reduced state, which also depended on the dopant present in the oxidized form of the polymer.

Masuda and coworkers<sup>95</sup> have considered the morphology of PTh's produced by an entirely different electrochemical procedure. In their work, the starting monomer was 2,5-bis(trimethylsilyl)thiophene (BTMSTh), which produces unsubstituted PTh upon electropolymerization. Masuda and coworkers<sup>95</sup> found that  $\text{PF}_6^-$ -doped PTh produced from thiophene monomer gave a nodular surface morphology, whereas  $\text{BF}_4^-$  gave a much flatter surface. However, for PTh produced from BTMSTh, the surface morphology was completely different: a fine nodular texture was produced with  $\text{PF}_6^-$  as dopant, but a rough nodular structure was produced with  $\text{BF}_4^-$  as dopant.

It is apparent that the determinants of the PTh morphology are complex, as with other conducting polymers. However, the effects on mechanical and electrical properties, as well as switching properties, are likely to be significant and worthy of further investigation.

### SOLUTION-CAST POLYTHIOPHENES

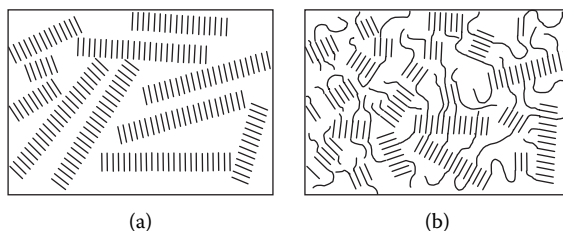
A great deal of work has been done to characterize the structure of films cast from chemically prepared polythiophenes.<sup>96</sup> Most of this work has been conducted on undoped PTh's because of their importance in electronic devices, such as thin-film transistors and photovoltaics. Depending on composition and processing conditions, the crystallinity can be as high as 30% in polythiophenes.<sup>97</sup> A layered structure is usually formed in PTh crystals between extended chains held together by  $\pi$ -stacking, with additional structural order introduced by alkyl side-chain interactions in functionalized PTh's.<sup>98</sup> Chemically synthesized PTh powders exhibit a



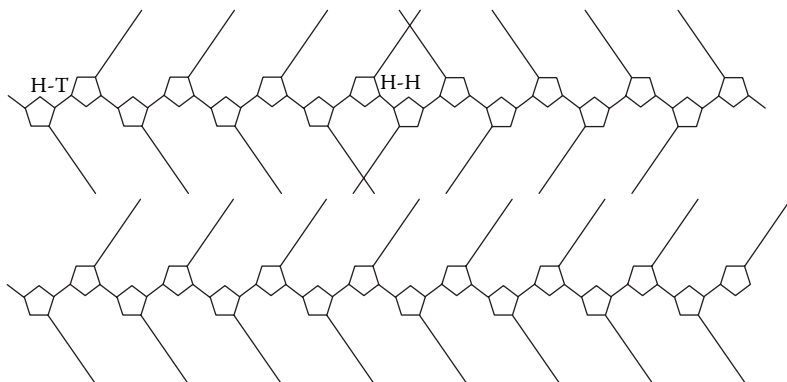
**FIGURE 6.8** Illustration of stacking arrangements proposed for polythiophene (PTh) and poly(3-alkylthiophenes) in their undoped state. (From Winokur, M.J., in *Handbook of Conducting Polymers. Conjugated Polymers. Theory, Synthesis, Properties and Characterisation*, 3rd edition, Skotheim, T.A. and Reynolds, J.R. (Eds.), CRC Press, Boca Raton, 2007, 17–1). Oriented chains extend into and out of the page. (a) herringbone stacking arrangement, (b) lamellar stacking arrangement.

partially crystalline structure in which the chains align and pack in a herringbone arrangement (Figure 6.8a) in the crystalline regions.<sup>98</sup> Polyalkylthiophenes adopt a simple layered-type structure because of interactions between the alkyl chains on neighboring polymer molecules (Figure 6.8b).<sup>98</sup> Commercially important PEDOT shows less-well-defined structural order.<sup>98</sup>

A number of studies have considered how PTh composition and molecular weight influence crystallinity. Regioregular HT poly(3-alkyl thiophenes) produce more crystalline materials than their nonregioregular counterparts.<sup>99,100</sup> The HT coupling allows regular packing of the alkyl side chains (Figure 6.9). HH and TT couplings disrupt the regularity of the structure (Figure 6.9) and lead to lower crystallinity.<sup>101</sup> Although it has been reported that higher molecular weights lead to higher degrees of crystallinity,<sup>97</sup> it has also been shown that lower molecular weights produce more-well-defined crystals.<sup>83,102</sup> Atomic force microscopy (AFM) studies have shown regular rodlike crystallites in low-molecular-weight regioregular PTh's. Higher-molecular-weight samples show less-well-resolved crystals.<sup>83</sup> The orientation of the extended chains is perpendicular to the long axis of the rod-shaped crystals, and the crystal width is correlated with molecular weight. In high-molecular-weight PTh's it



**FIGURE 6.9** Illustration of chain structure of poly(3-alkylthiophene) showing effect of head–head (HH) coupling in a mainly head–tail (HT) coupled chain. (From Jeffries-El, M. and McCullough, R.D., in *Handbook of Conducting Polymers. Conjugated Polymers. Theory, Synthesis, Properties and Characterisation*, 3rd edition, Skotheim, T.A. and Reynolds, J.R. (Eds.), CRC Press, Boca Raton, 2007, 9–1. With permission.)



**FIGURE 6.10** Illustration of chain stacking of poly(3-alkylthiophene) in rodlike structures at (a) low and (b) high molecular weight. (From Verilhac, J.M.; LeBlevenec, G.; Djurado, D.; Rieutord, F.; Chouiki, M.; Travers, J.P.; Pron, A. *Synth. Met.* 2006, 156: 815. With permission.)

is likely that a single chain passes between one crystal and another. The individual crystals are then less well defined. A schematic illustration of the crystal structure in low- and high-molecular-weight regioregular PTh's is given in Figure 6.10.

X-ray diffraction (XRD) studies have shown that the interchain spacing is dependent on the alkyl chain length.<sup>103</sup> Comparison of various side-chain lengths for P3AT's<sup>79</sup> shows an increase in interchain spacing. The interchain spacing increases about 0.16 nm for each methylene group in the side chain. Recent studies have shown some discrepancies in this general behavior, with some long side chains actually giving smaller interchain separations.<sup>104</sup> It is possible that in these cases, side chains on neighboring polymer molecules interdigitate. However, in one study, it was shown that such interdigitating chains are unlikely and, instead, a different crystal structure forms that involves a greater tilt angle of the side branches.<sup>104</sup>

Processing conditions have also been shown to affect the crystallinity of PTh's. In particular, surface treatments applied to substrates have been shown to have a significant effect on the ordering of adjacent PTh crystals. For example, the addition of silane hydrophobic treatments to silicon induces an alignment in the PTh chains such that the thiophene ring is oriented perpendicular to the substrate surface.<sup>105</sup> Other surface treatments lead to ordering with the thiophene ring oriented parallel to the substrate surface.<sup>106</sup> A distinct layered structure has been observed in doped poly(3-hexylthiophene), where doping is higher in disordered layers between less doped and more highly crystalline layers.<sup>106</sup> Doped poly(3,4-ethylenedioxythiophene) (PEDOT) also is reported to have a layered structure, with  $\pi$ -stacked chains separated by layers of dopant ions.<sup>107</sup> In addition, the solution-casting processes can also influence the nature of the crystals formed. Thus, slow evaporation of solvent or annealing after casting typically produce higher degrees of crystallinity.<sup>105,108</sup>

PEDOT has been synthesized via the micellar route with sodium dodecyl sulfate and dodecylbenzene sulfonic acid.<sup>109,110</sup> It has been obtained with particle diameters of 35 to 100 nm and conductivities on the order of 50 S cm<sup>-1</sup>. Nanocomposites containing polythiophene and poly(*N*-vinylcarbazole) have been formed with average



particle size in the range 20–80 nm.<sup>111</sup> However, the dc conductivities measured were low, on the order of  $10^{-6}$  S cm<sup>-1</sup>. Reverse cylindrical micelles obtained by adding the oxidant FeCl<sub>3</sub> to a solution containing sodium bis(2-ethylhexyl)sulfosuccinate were used to facilitate oxidation of EDOT and the subsequent formation of PEDOT. Nanorods with diameters of  $40 \pm 20$  nm, lengths of  $200 \pm 30$  nm, and conductivities of 72 S cm<sup>-1</sup> were recorded.<sup>112</sup> MacDiarmid and coworkers<sup>113</sup> have used V<sub>2</sub>O<sub>5</sub> nanofibers as sacrificial seeds to promote formation of PEDOT nanofibers (3–10 μm long and 100–180 nm in diameter) with pressed pellet conductivity of 16 S cm<sup>-1</sup>. Others have used vapor-phase polymerization to produce nanodimensional coatings of PEDOT with low resistance and high transparency.<sup>114</sup> As for polypyrroles and polyanilines, physical templates have been used to produce nanodimensional structures of polythiophenes.<sup>115</sup>

## PROPERTIES OF POLYTHIOPHENES

Because polythiophene itself is prone to overoxidation during polymerization, most practical work has been carried out using alkylated thiophenes, which have higher overoxidation potentials. Synthesis of functionalized thiophenes (such as alkylated monomers) is much easier to achieve than that of its pyrrole counterpart. The decreased activity of the sulfur group compared to that of the –NH group means that the laborious steps involved in protecting the heteroatom during synthesis are not required for thiophene.

### CONDUCTIVITY

To achieve high conductivities, the polythiophene paradox must be overcome. The polymerization process and conductivity of the resultant material are influenced by the concentration of monomer used during polymerization<sup>116</sup> because, if this is too low, the overoxidation reaction predominates, at least when galvanostatic polymerization is used. Synthesis at reduced temperatures will help avoid overoxidation and can be used to increase the conductivity of the resultant material.<sup>117</sup>

As stated earlier, the presence of alkyl functional groups on the monomer<sup>118</sup> can be used to advantage in preventing overoxidation of the polythiophenes during synthesis. Conductivities as high as 7500 S cm<sup>-1</sup> have been obtained for poly(methylthiophene).<sup>119</sup>

As with polypyrroles, the counterion used during electropolymerization influences the conductivity of polythiophenes.<sup>120,121</sup> Electrochemically produced copolymers<sup>122</sup> of 3-dodecylthiophene (DTh) and 3-methylthiophene (MTh) have been shown to exhibit conductivities intermediate to the two homopolymers. The actual value depends on the ratio of MTh to DTh in the polymer.

Other workers have reported that thinner, more compact polymers are more conductive than polymers grown to be thicker.<sup>123</sup> It has been shown that the conductivity of poly(2-octylthiophenes) decreases when exposed to atmospheres of higher humidity. This is presumably due to dedoping<sup>124</sup> of the polymer, although swelling at higher humidity would also decrease conductivity. This same group of researchers<sup>125</sup> has shown that the conductive properties of polythiophenes could be stabi-

lized by heat treatment. This thermal annealing process increased the crystallinity of the polymer.

The conductive properties of alkylated thiophenes are known to be unstable, particularly at elevated temperatures. The mechanism of thermal undoping has been associated with thermal mobility. Consequently, various workers<sup>126</sup> have considered synthesis of random copolymers (e.g., thiophene and 3-octylthiophene), with well-distributed octyl side groups leaving space around the main chains to accommodate dopants.

In general, the conductivity of materials produced using the chemical oxidation process is lower. Higher conductivities can be obtained by chemical production of copolymers; for example, using poly(methylthiophene) and polyurethane,<sup>127</sup> conductivities as high as  $26 \text{ S cm}^{-1}$  have been reported.

The conductivity of polythiophenes in the undoped state is particularly important in electronics applications.<sup>105</sup> Both molecular weight and morphology have been found to significantly affect the charge carrier mobility in PTh's. Because the morphology is strongly influenced by the molecular weight, it has proved difficult to determine how each of these factors individually affects crystallinity. In low-molecular-weight PTh's, the conductivity is limited mainly due to poor conduction between crystal grains.<sup>105</sup> The surface of these grains is covered by insulating alkyl side chains, so the grain boundaries become conduction barriers. The conductivity of such films can be greatly increased by controlling the morphology. For example, substrate surface treatments that produce aligned crystals will produce higher in-plane charge mobilities because individual crystals can join in the  $\pi$ -stacking direction.<sup>105</sup> Higher-molecular-weight PTh's are less affected by processing conditions, because grain boundaries are blurred as individual chains pass from one grain to another. Higher charge carrier mobilities are found in higher-molecular-weight PTh's.<sup>128</sup>

## MECHANICAL PROPERTIES OF POLYTHIOPHENES

As with polyanilines, polythiophenes can either be prepared directly by electropolymerization, or by casting from solutions (for alkyl-substituted thiophenes). Most interest has focused on the latter because of their improved mechanical properties compared with those of electrochemically prepared films. The factors influencing the mechanical properties of PTh's are reviewed in this section.

Mechanical properties of electrochemically prepared PTh's have generally been poor;<sup>129</sup> however, recent reports have described the preparation of PTh films having extremely high tensile strength and modulus.<sup>130</sup> In one study, electropolymerization of thiophene monomers was conducted in a solvated Lewis acid to lower the oxidation potential. The resultant films had tensile strengths of 140 MPa,<sup>131</sup> with conductivities of  $\sim 100 \text{ S cm}^{-1}$ . Similarly, high tensile strengths (135 MPa) with very high modulus (46 GPa) and reasonable elongation to break (4%) were obtained when thiophene was electropolymerized in the presence of a hydrogen scavenger. These samples also produced very high conductivities (up to  $1300 \text{ S cm}^{-1}$ ).<sup>130</sup> The results were attributed to more regioregular structure produced with fewer crosslinks.

Wang and Feng have reported on the effect of film thickness on the mechanical properties of PTh films prepared using the same Lewis acid/hydrogen scavenger

electropolymerization.<sup>132</sup> The modulus obtained from these studies was in the range 3–7 GPa, which is more typical of unoriented polymers, and was found to be higher in thin films. Similarly, films having a thickness less than 10  $\mu\text{m}$  were slightly stronger ( $\sim 100$  MPa) than thicker films (80–100 MPa). Thicker films were found to be slightly porous, hence, leading to lower modulus and tensile strengths. Strains at failure were between 2 and 6%.

The relationship between the mechanical properties and the morphology of electrochemically prepared PTh has been examined by Ito and coworkers.<sup>133</sup> Their results showed that the Young's modulus ( $E$ ) and breaking strength ( $\sigma_b$ ) decreased by approximately 50% when the current density during polymerization increased from 0.7 to 5.0  $\text{mA}/\text{cm}^2$ . The oxidized PTh films were powdery, which presumably reduced the strength and gave a lower elongation at break. A higher current density for growth produced excessively high cell potentials that were thought to cause degradation of the polymer. The higher current density also increased the roughness of the surface nodules, and the same relationship between nodular boundaries and tensile strength observed for polypyrroles (see Chapter 3) is also likely to hold for the PTh films. Thus, higher current densities produce a rougher morphology and weaker boundaries between the nodules, which results in mechanical failure at lower stress and strain.

The effect of doping on mechanical properties has been reported by a number of workers. Yoshino and coworkers<sup>134</sup> observed that undoped PTh had a higher stiffness ( $E = 1300$  MPa) and tensile strength ( $\sigma = 55$  MPa) than PTh doped with  $\text{BF}_4^-$  ( $E = 360$  MPa;  $\sigma = 15$  MPa). Similarly, Ito and coworkers observed that the mechanical properties ( $E$ ,  $\sigma_b$  and, strain at break,  $\epsilon_b$ ) of electrochemically reduced PTh films were all increased compared with the as-prepared, oxidized films.<sup>133</sup> Again, the reduced films showed lower strength, modulus, and elongation at break when prepared at a higher current density. In the best case (current density 0.7  $\text{mA}/\text{cm}^2$ ), the reduced PTh had  $E \sim 3.3$  GPa, yield stress  $\sim 70$  MPa,  $\sigma_b \sim 265$  MPa, and  $\epsilon_b \sim 95\%$ . The general observation of increased stiffness and strength for the reduced polythiophene is the opposite of that observed for polypyrroles (see Chapter 3). In the case of polypyrroles, the oxidized state was observed to be stiffer, stronger, but less ductile than the reduced state owing to the ionic crosslinking induced by the ionic nature of the polymer. In the case of PTh, it is possible for the increased solvent content that accompanies oxidation to cause a plasticization effect that is greater than the ionic crosslinking, so that the oxidized films are more ductile and flexible.

Moulten and Smith<sup>135,136</sup> have reported the effects of doping and alkyl-substituent length on the mechanical properties of P3ATH's cast from 3% solutions in chloroform. In contrast to the studies reported previously for electrochemically prepared PTh, it was shown that the alkylthiophenes became stiffer (by an order of magnitude) and stronger (doubled) when doped with  $\text{FeCl}_3$ . They also noted that anhydrous  $\text{FeCl}_3$  doping produces brittle polymers; further, this problem could be avoided by using 1 M  $\text{FeCl}_3 \cdot 6\text{H}_2\text{O}$ , presumably because of the plasticization by water molecules. The increase in stiffness and strength of PTh upon doping was attributed to more effective interchain bonding through  $\pi$ - $\pi$  overlaps of neighboring thiophene rings.

Mechanical drawing of PTh films and fibers has also been observed to increase the stiffness and strength.<sup>85,136</sup> Ito and coworkers showed that drawing the reduced PTh increased  $E$  to 8.5 GPa and  $\sigma_b$  to 265 MPa (draw ratio of 1.8).<sup>85</sup> Commonly observed in many polymers (including other CEPs), the increased stiffness and strength is attributed to the alignment of the macromolecules in the draw direction. Moulten and Smith<sup>136</sup> observed similar behavior with 3-substituted polythiophenes; however, the increase in stiffness and strength were not as significant as reported by Ito and coworkers.<sup>133</sup> In fact, for a given draw ratio, the increase in stiffness and strength decreased as the length of the alkyl chain increased. Similar results have been obtained by Van de Leur and coworkers<sup>137</sup> using dynamic mechanical analysis of hexyl-, octyl-, and dodecyl-substituted PTh's.

The mechanical properties of PTh's have been modeled by Moulten and Smith<sup>136</sup> in terms of the macromolecular structure and intermolecular bonding. On the basis of their model, these authors have found good agreement between the measured and predicted Young's modulus. Thus, the effect of the alkyl side chain can be explained by a dilution effect, whereby longer side chains result in greater separation of macromolecules. This means that there are fewer load-bearing covalent bonds per unit cross-sectional area, so the stiffness is lower. In addition, these workers found that coupling defects (i.e., head-head and tail-tail couplings in P3ATH's) reduce the effective  $\pi$ - $\pi$  overlaps between macromolecules and also reduce stiffness. A slight variation in the number of such defects was observed in the three P3ATH's studied—defects were slightly higher in the octyl- and dodecyl-substituted PTh's compared with the hexyl-substituted PTh.

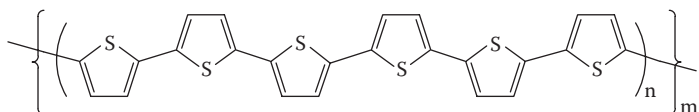
## CHEMICAL PROPERTIES

Studies of the chemical properties of polythiophenes have been limited. As with polypyrroles, a hydrophobic backbone is formed, and the polymer has ion-exchange properties. Modification of chemical properties by incorporation of appropriate counterions is not so readily addressable because polymerization must be carried out from nonaqueous solution and occurs at more anodic potentials compared to pyrrole.

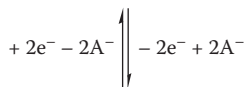
However, some workers have incorporated a selection of counterions.<sup>121,122,123</sup> Others<sup>138</sup> have incorporated heteropolyanions with a view to their use as electrocatalytic electrodes. The fact that thiophenes are easier to derivatize than pyrroles is also attractive in that chemical functionality can be introduced by derivatization. A range of functional groups have been introduced<sup>139,140,141,142,143,144</sup> to modify the chemical properties of polythiophenes. The ability to attach active groups such as amino acids provides an attractive route for modifying the molecular recognition properties of the resultant polymers. The decreased activity of the sulfur group compared to the NH group also means that derivatization after polymerization is more easily accomplished.<sup>145</sup>

## SWITCHING PROPERTIES

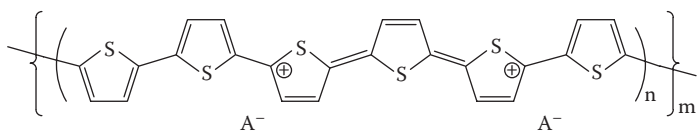
As with polypyrroles, the properties of the polythiophenes can be modulated by application of electrical stimuli according to Equation 6.7:



Contracted State in Reduced Form



Expanded State in Oxidized Form



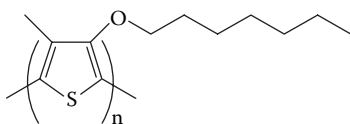
[A<sup>-</sup> represents anions, e<sup>-</sup> electrons  
m determines molecular weight]

**Polythiophene - a dynamic (electroactive) polymer structure**

(6.7)

This picture is undoubtedly oversimplified. Different sites are switched at different potentials, and when A<sup>-</sup> is relatively immobile, cation movement accompanies the oxidation/reduction process.

The switching properties are determined by the electrochemical conditions employed during growth, the counterion incorporated, and the substituents attached to the thiophene ring.<sup>146</sup> For example, poly(3-heptoxy-4-methylthiophene) **29** switches at 0.76 V, whereas under the same conditions, poly(3-octylthiophene) switches at 1.01 V. The electrolyte used for switching also has a marked effect on the potential, rate, and reversibility of the switching process.<sup>147</sup>



poly (3-heptoxy-4-methylthiophene)  
P3H4MTh

**29**

Polythiophenes are in general more hydrophobic materials than polypyrroles. Electrochemical switching is not so efficient in aqueous media. Therefore, some workers have used the ability to attach functional groups such as polyethers<sup>148</sup> to increase hydrophilicity and improve electrochemical behavior in aqueous solutions.

### N-DOPING OF POLYTHIOPHENES

Polythiophenes, similarly to other polyheterocycles, exhibit hole-dominated transport (p-doping). However, electron-dominated transport (or n-doping) has begun to attract increasing interest. Decreasing the polymer band gap should produce polymers with

more positive reduction potentials and that are therefore more accessible to n-doping, and this has been successfully achieved by the use of donor and acceptor units in the polymer structure (see reviews by Roncali,<sup>149</sup> and Meijer and coworkers<sup>150</sup>). For example, Reynolds and coworkers<sup>151</sup> have synthesized a family of polymers based on an alternating 3,4-ethylenedioxythiophene dimer (BiEDOT) donor and pyridine-type acceptor. By varying the strength of the substituted pyridine acceptors, they have more recently generated thiophene-based polymers with readily accessible reduced forms and three or more distinct oxidation states of various colors, which can be switched electrochemically. Manipulation of the polymer band gap in this manner promises to provide novel devices for applications such as electrochromics.

## OPTICAL PROPERTIES OF POLYTHIOPHENES

### Electronic Band Structure and UV-Visible Spectra

Theoretical studies indicate that neutral polythiophene (similar to polypyrrole) has a nondegenerate ground state, with mesomeric aromatic and quinoidal structures of nonequivalent energy.<sup>152</sup> Oxidative doping leads to the formation of two bands in the band gap corresponding to a polaron (radical cation). However, both calculations<sup>152,153</sup> and measurements of UV-visible spectra during increasing doping<sup>154</sup> suggest that the polarons are unstable compared with spinless bipolarons (dications). The two subgap absorption bands that appear at ca. 0.5 and 1.5 eV with increasing doping of polythiophene have therefore generally been assigned to electronic transitions involving bipolarons. However, other studies of lightly doped poly(3-methylthiophene) suggest that polarons may instead be involved.<sup>155</sup>

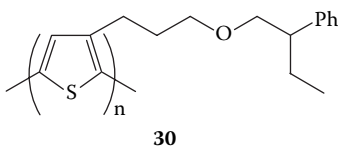
The majority of UV-visible spectral studies have been carried out on neutral polythiophenes, whose spectra are dominated by the band gap  $\pi$ - $\pi^*$  transition. The position of this peak has been widely used as a measure of the conjugation length of the polymer backbone, undergoing a red shift with increasing conjugation length. Extensive comparisons have been made between regioregular and regioirregular poly(3-alkylthiophenes), where the much-lower-energy  $\pi$ - $\pi^*$  transitions of regioregular polymers indicates a longer conjugation length compared to corresponding regioirregular polythiophenes.<sup>156</sup> Another feature of the regioregular poly(alkylthiophenes) is the appearance of vibronic structures on the  $\pi$ - $\pi^*$  absorption bands.

### Thermochromism and Solvatochromism in Poly(3-alkylthiophenes)

A striking feature of neutral poly(3-alkylthiophenes) is their thermochromism, observed both in the solid and solution states.<sup>157,158</sup> Upon heating, a marked blue shift occurs for the highest-wavelength  $\pi$ - $\pi^*$  absorption band. Similar marked changes in color are observed upon transferring from a "poor" solvent to a "good" solvent.<sup>157-159</sup> In both cases, these color changes have been attributed to a twisting of the polythiophene backbone from an essentially planar to a less ordered nonplanar conformation. This is supported by theoretical calculations.<sup>160</sup> Further evidence for the conformational changes occurring in these systems comes from circular dichroism (CD) spectral studies of optically active poly(3-alkylthiophenes), described in the following text.

### CHIROPTICAL PROPERTIES OF OPTICALLY ACTIVE POLYTHIOPHENES

A wide range of optically active polythiophenes have been reported, prepared in general through electrochemical or chemical oxidation of monomers in which a chiral substituent is covalently attached to the 3-position of the thiophene ring. The first example was the electrochemically prepared polymer **30**, which exhibited a very large optical rotation ( $[\alpha]_D = +3000^\circ$ ) compared to the corresponding monomer ( $[\alpha]_D = +21^\circ$ ).<sup>161</sup> This high optical activity was interpreted in terms of the adoption of a one-handed helical conformation by the polythiophene main chain induced by the presence of the chiral propyl-2-phenylbutyl ether substituent. Unfortunately, no CD spectrum was recorded. However, cyclic voltammograms of (*S*)-**30**, recorded in acetonitrile solvent in the presence, alternately, of (+)- and (–)-camphorsulfonic acid (HCSA), revealed significant chiral discrimination by the polymer in its doping with the enantiomeric CSA<sup>–</sup> anions (50% higher with (+)-CSA<sup>–</sup> compared to (–)CSA<sup>–</sup>). The opposite enantioselectivity was observed with (*R*)-**30**.

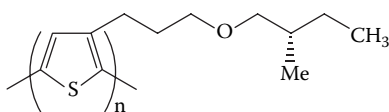


Inganas and coworkers<sup>162</sup> have reported the CD spectrum of the related chiral polythiophene **23**, which contains a chiral amino acid group attached to the thiophene units by an ether linkage. In water solvent, a pair of exciton-coupled CD bands are observed in the visible region associated with the  $\pi$ – $\pi^*$  transition band in the UV-visible spectrum at ca. 430 nm. These chiroptical features are attributed to a helical conformation adopted by the polymer backbone under the influence of the chiral side chain. However, in methanol solvent, no CD bands are observed, and the  $\pi$ – $\pi^*$  absorption band is blue-shifted. This suggests a change in the polymer chain conformation in methanol solvent to a more planar arrangement.

In a series of elegant papers, Meijer and coworkers<sup>70,163,164,165</sup> have observed remarkable solvent- and temperature-dependent CD spectra for a range of regio-regular (HT) chiral polythiophenes. For example, although the regio-regular polythiophene **24** is optically inactive in the good solvent chloroform, the successive addition of the poor solvent methanol results in the progressive appearance of three (overlapping) exciton-coupled CD bands corresponding to the three vibronic bands of the  $\pi$ – $\pi^*$  transition seen at 512, 540, and 592 nm in the visible spectrum.<sup>70</sup> An extremely high chiral anisotropy factor ( $g = \Delta\epsilon/\epsilon$ ) of ca. 2.2% was determined for a solution of **24** in 40% CHCl<sub>3</sub>/60% CH<sub>3</sub>OH. The authors attributed the observed optical activity to the helical packing of the polymer chains into a chiral supramolecular aggregate induced by the optical active side chains, rather than the adoption of a helical conformation by individual polythiophene chains. Films of polymer **24** spun-cast from solution also show optical activity associated with the  $\pi$ – $\pi^*$  absorption band, but this is lost upon heating above the polymer melting point of 160°C. Surprisingly, whereas the original polymer optical activity is recovered upon slow cooling, rapid

cooling generates a film with the inverse CD spectrum, indicating the formation of a chiral superstructure of opposite handedness.

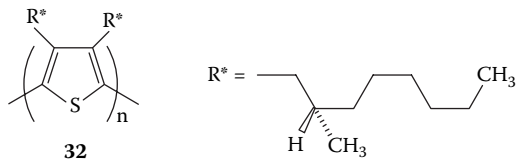
This sensitivity of the handedness of chiral-substituted polythiophenes to the conditions under which microaggregation occurs has been further confirmed in detailed thermochromic and solvatochromic studies by Meijer and coworkers<sup>163,164,165</sup> on **24** and the related chiral polythiophenes **31** and **26**. Polymers **24** and **31** are optically inactive in dichloromethane solvent at room temperature, but develop strong CD spectra upon cooling to  $-73^{\circ}\text{C}$ .<sup>163</sup> In contrast, in 1-decanol solvent, **24** and **31** are optically active at room temperature, presumably because of their ability to form a chiral-aggregated phase at room temperature in this poor solvent. Significantly, the CD spectra in 1-decanol are inverted compared to those recorded in dichloromethane, indicating the adoption of opposite handedness by the chiral superstructures. The sensitivity of the hand of the chiral organization of the polymer chains to the ordering conditions suggests only a small difference in energy between the two diastereomeric forms.<sup>163</sup> The disubstituted chiral polythiophene **26** similarly only exhibits optical activity at room temperature in the presence of poor solvents such as methanol.<sup>72,164</sup> In this aggregated form, the photoluminescence spectrum of **26** is also circularly polarized.<sup>165</sup> Heating the solution to  $120^{\circ}\text{C}$  causes a conformational change to an optically inactive disordered form.<sup>72,164</sup>

**31**

Similar remarkable inversions of CD spectra have been reported by Bidan and coworkers<sup>71</sup> for the stereoregular form of the chiral polythiophene **25**. This polymer is optically inactive in the good solvent chloroform. No change occurs in the UV-visible and CD spectra upon addition of up to 30% of the poor solvent methanol. However, from 35 to 37.5% methanol, strong CD bands appear in the visible region between 430 and 630 nm, presumably associated with the formation of a chiral aggregate. Interestingly, the addition of further methanol (42–50%) results in the progressive appearance of an inverted CD spectrum, consistent with the adoption of a chiral superstructure of the opposite hand. Other researchers<sup>74</sup> have recently reported similar inversions of chirality for optically active polymer **27**, bearing a chiral oxazoline residue in its side chain.

However, another paper<sup>166</sup> reports what appears to be the first example of an optically active substituted polythiophene in a good solvent, that is, where the polymer is believed to be in an unaggregated form. This disubstituted polymer **32** exhibits bisignate CD bands at ca. 300 and 337 nm, associated with the  $\pi-\pi^*$  absorption band at 318 nm. The large blue shift of this  $\pi-\pi^*$  absorption band compared to other poly(3-alkylthiophene)s indicates a short conjugation length for this polymer, arising from twisting of the polythiophene backbone from planarity. It was suggested that the observed bisignate CD bands of unequal rotational strength arise from diastereomeric helical sections of the chains, with the majority adopting a (+)- Cotton screw-sense and the minority a (–)-screw-sense.





Recently, optically active polythiophenes, incorporating as ring substituents chiral selectors such as (*R*)-(-)- and (*S*)-(+)-*N*-(3,5-dinitrobenzoyl)- $\alpha$ -phenylglycine used in Pirkle-type stationary phases, have been synthesized.<sup>167</sup> These may have potential in enantioselective analysis of chiral chemicals using high performance liquid chromatography (HPLC).

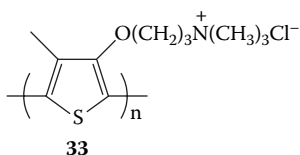
The chiral polythiophene, poly(3-[(*S*)-5-amino-5-carboxyl-3-oxapentyl]-2,5-thiophenylene) hydrochloride, L-POWT, ring-functionalized with the amino acid L-serine, has been synthesized by Inganäs and coworkers,<sup>69,168</sup> and was found to exhibit pH-dependent UV-visible, fluorescence emission, and CD spectra. At a pH equal to the isoelectric point of the amino acid, the polythiophene chains separate and adopt a nonplanar right-handed helical conformation. Increasing the pH leads to a more planar conformation of the backbone and aggregation of the polymer chains.

More recently, the analogous chiral polythiophene, D-POWT, containing the enantiomeric amino acid D-serine in its side chain, has been synthesized.<sup>169</sup> It exhibits pH-dependent optical phenomena similar to L-POWT, indicating that the nonplanar-to-planar conformation of the polythiophene backbone is not affected by the enantiomeric stereochemistry of the zwitterionic amino acid side chain. However, the L- and D-POWT polymers have mirror-imaged CD spectra, showing that the chirality of the zwitterionic side chain is reflected in the conformation of the polymer backbone. In subsequent studies,<sup>170</sup> these enantiomeric-substituted polythiophenes have been used as conformation-sensitive optical probes for the detection of pH-induced conformational changes within a synthetic peptide. Interaction of the polymers with the peptide initially induced a more planar conformation for the backbone, separation of the polymer chains, and an increase in fluorescence emission. Specific chiral recognition could be quantified as differences in fluorescence emission based on both single- and two-photon excitation from the two enantiomeric polymers, which interact differently with the peptide.

The regioregular (HT) poly[3-{4-(*R*)-4-ethyl-2-oxazolin-2-yl}phenyl]thiophene] **27** bears a chiral oxazoline residue. This polymer was found<sup>73</sup> to exhibit strong CD bands associated with its  $\pi$ - $\pi^*$  bands when complexed with metal ions such as copper (II) and iron (III) in the good solvent chloroform, despite the fact that no aggregation was observed. The induced chirality in this case is believed to arise from the main chain chirality. However, in the absence of metal ions, although optically inactive in chloroform, it generates an induced CD when poor solvents such as methanol and acetone are added.<sup>74,171</sup> Membrane filtration, XRD, and AFM measurements indicate that the polymer chirality induced in these mixed solvents arises from the formation of chiral aggregates. Interestingly, chirality of these supramolecular aggregates is reported<sup>172</sup> to be reversibly switched “on” and “off” via electron transfer. The CD vanishes upon oxidative doping of the polymer main chain, presumably because of

the formation of a more rigid planar conformation, but is regenerated upon subsequent chemical reduction with amines such as triethylenetetramine. Such a redox-induced supramolecular chirality switch may provide novel molecular devices for applications such as data storage.

A fascinating recent development has been the preparation of a supramolecular chiral, insulated “molecular wire” by self-assembly between an achiral water-soluble polythiophene **33** and a natural polysaccharide, schizophyllan (SPG).<sup>173</sup> SPG is a  $\beta$ -1,3-glucan that exists as a right-handed triple helix (t-SPG) in water and as a single random coil (s-SPG) in dimethylsulfoxide (DMSO). The achiral polythiophene **33** exhibited no CD spectrum in water or water–DMSO mixtures. However, upon addition of s-SPG–DMSO, an intense CD spectrum was induced in the  $\pi$ – $\pi^*$  region, which was stable at temperatures as high as 90°C. The induction of polythiophene main chain chirality is believed to arise from intrachain effects rather than interchain  $\pi$ -stacking, with a predominantly one-handed helical structure being induced via interpolymer complexation of the polythiophene with s-SPG. Such molecular wires based on conjugated polymers have potential applications in areas such as molecular electronics and sensor signal amplification.



Chiral disubstituted PEDOTs have recently been prepared for the first time via transesterification of 3,4-dimethoxythiophene monomers with chiral glycols followed by potentiodynamic oxidation.<sup>174</sup> An alternative approach to optically active PEDOTs has also been recently described, which involves the electrochemical polymerization of the EDOT monomer in aqueous hydroxypropyl cellulose (HPC) as a polymer lyotropic liquid crystal to give a chiral PEDOT/HPC hybrid.<sup>175</sup> The PEDOT prepared in this chiral nematic liquid crystal exhibited optically active electrochromism in that it could be electrochemically switched between a dark blue reduced state and a sky blue oxidized form that exhibited a different CD spectrum.

## CONCLUSIONS

Polythiophenes, although maintaining dynamic properties (switching characteristics) similar to polypyrroles, are distinct in a number of ways. The chemistry is such that a wide range of molecular building blocks in the form of functionalized monomers are more readily produced. For example, this enables addition of redox groups, light-harvesting groups, and other metal-complexing groups covalently to the polymer backbone. The switching characteristics are also different in that polythiophenes are in general more difficult to oxidize and to overoxidize. However, the fact that polythiophenes must normally be prepared from nonaqueous media limits the range of dopants that can be incorporated. The use of surfactants to solubilize thiophene monomers in water is an interesting approach to overcoming this limitation.

## REFERENCES

1. Wei, Y.; Chan, C.C.; Tran, J.; Jang, G.W.; Hsueh, K.F. *Chem. Mat.* 1991, 3: 888.
2. Krische, B.; Zagorska, M. *Synth. Met.* 1989, 28: 263.
3. Beck, F.; Barsch, U.; Michaelis, R. *J. Electroanal. Chem.* 1993, 351: 169.
4. Sato, M.A.; Tanaka, S.; Am, K.J. *Synth. Met.* 1986, 14: 279.
5. Krische, B.; Zagorska, M.; Hellberg, J. *Synth. Met.* 1993, 58: 295.
6. Krische, B.; Zagorska, M. *Synth. Met.* 1989, 33: 257.
7. Roncali, J. *Chem. Rev.* 1992, 92: 711.
8. Wei, Y.; Tian, J. *Polymer* 1992, 33: 4872.
9. Cutler, C.A.; Burrell, A.K.; Officer, D.L.; Too, C.O.; Wallace, G.G. *Synth. Met.* 2002, 128: 35.
10. Cutler, C.A.; Burrell, A.K.; Collis, G.E.; Dastoor, P.C.; Officer, D.L.; Too, C.O.; Wallace, G.G. *Synth. Met.* 2001, 123: 225.
11. Faid, K.; Cloutier, R.; LeClerc, M. *Synth. Met.* 1993, 55: 1272.
12. Sato, M.; Shimizu, T.; Yamauchi, A. *Makromol. Chem.* 1990, 191: 313.
13. Beck, F.; Barsch, U. *Makromol. Chem.* 1993, 194: 2725.
14. Turcu, R.; Pana, O.; Bratu, I.; Bogdon, M. *J. Mol. Elect.* 1990, 6: 1.
15. Tanaka, K.; Schichiri, T.; Wang, S.; Yamabe, T. *Synth. Met.* 1988, 24: 203.
16. Ding, J.; Price, W.E.; Ralph, S.F.; Wallace, G.G. *Synth. Met.* 2000, 110: 123.
17. Murray, P.S.; Ralph, S.F.; Too, C.O.; Wallace, G.G. *Electrochimica Acta* 2006, 51: 2471.
18. Dazzaoui, E.A.; Aeiyaeh, S.; Lacaze, P.C. *Synth. Met.* 1996, 83: 159.
19. Sakmeche, N.; Aeiyaeh, S.; Aaron, J.J.; Jouini, M.; Lacroix, J.C.; Lacaze, P.C. *Langmuir* 1999, 15: 2566.
20. Gningue-Sall, D.; Fall, M.; Dieng, M.M.; Aaron, J.J.; Lacaze, P.C. *Phys. Chem. Chem. Phys.* 1999, 1: 1731.
21. Fall, M.; Dieng, M.M.; Aaron, J.J.; Aeiyaeh, S.; Lacaze, P.C. *Synth. Met.* 2001, 118: 149.
22. Oterom, T.F.; Azelain, E.L. *Polym. Comm.* 1988, 29: 21.
23. Osawa, S.; Ho, M.; Tanaka, X.; Kuwano, J. *J. Polym. Sci. Part B.* 1992, 30: 19.
24. Inoue, M.B.; Velazquez, E.F.; Inoue, M. *Synth. Met.* 1988, 24: 224.
25. Nalwa, H.S. *Die Angew. Makromol. Chem.* 1991, 188: 105.
26. McCulloch, R.D.; Lowe, R.D.; Jayaraman, M.; Ewbank, P.C.; Anderson, D.L.; Tristram-Nagle, S. *Synth. Met.* 1993, 55: 1198.
27. Yamamoto, T.; Sanechika, K.; Yamamoto, A. *J. Polym. Sci., Polym. Lett. Ed.* 1980, 18: 9.
28. Lin, J.W.P.; Dudek, L.P. *J. Polym. Sci., Polym. Chem. Ed.* 1980, 18: 2869.
29. McCullough, R.D. *Adv. Mater.* 1998, 10: 93; and references cited therein.
30. Yamamoto, T.; Morita, A.; Miyazaki, Y.; Maruyama, T.; Wakayama, H.; Zhou, Z.H.; Nakamura, Y.; Kanbara, T.; Sasaki, S.; Kubota, K. *Macromolecules* 1992, 25: 1214.
31. Kobayashi, M.; Chen, J.; Chung, T.C.; Moraes, F.; Heeger, A.J.; Wudl, F. *Synth. Met.* 1984, 9: 77.
32. Yoshino, K.; Hayashi, S.; Sugimoto, R. *Jpn. J. Appl. Phys.* 1984, 23: L899.
33. Sugimoto, R.; Takeda, S.; Gu, H.B.; Yoshino, K. *Chemistry Express* 1986, 1: 635.
34. de Leeuw, D.M.; Kraakman, P.A.; Bongaerts, P.F.G.; Mutsaers, C.M.; Klaassen, D.B.M. *Synth. Met.* 1994, 66: 263.
35. Winther-Jensen, B.; Chen, J.; West, K.; Wallace, G. *Macromolecules* 2004, 37: 5930.
36. Zotti, G.; Schiavon, G. *Synth. Met.* 1990, 39: 183.
37. Chen, J.; Winther-Jensen, B.; Lynam, C.; Ngamna, O.; Moulton, S.; Zhang, W.; Wallace, G.G. *Electrochemical and Solid-State Letters* 2006, 9(7): H68.
38. Fujitsuka, M.; Sato, T.; Segawa, H.; Shimidzu, T. *Chem. Lett.* 1995, 99.

39. Nishio, S.; Okada, S.; Minamimoto, Y.; Okumura, M.; Matsuzaki, A.; Sato, H. *J. Photochem. Photobiol. A: Chem.* 1998, 116: 245.
40. Huisman, C.L.; Huijser, A.; Donker, H.; Schoonman, J.; Goossens, A. *Macromolecules* 2004, 37: 5557.
41. Jen, K.Y.; Oboodi, R.; Elsenbaumer, R.L. *Polym. Mater. Sci. Eng.* 1985, 53: 79.
42. Miller, G.G.; Elsenbaumer, R.L. *J. Chem. Soc., Chem. Commun.* 1986, 1346.
43. Leclerc, M.; Diaz, F.M.; Wegner, G. *Makromol. Chem.* 1989, 190: 3105.
44. Pomerantz, M.; Tseng, J.J.; Zhu, H.; Sproull, S.J.; Reynolds, J.R.; Uitz, R.; Arnott, H.J.; Haider, H.I. *Synth. Met.* 1991, 41-43: 825.
45. McCullough, R.D.; Williams, S.P.; Tristram-Nagle, S.; Jayarman, M.; Ewbank, P.C.; Miller, L. *Synth. Met.* 1995, 69: 279.
46. Niemi, V.M.; Knuutila, P.; Osterholm, J.-E.; Korvola, J. *Polymer* 1992, 33: 1559.
47. Leclerc, M.; Daoust, G. *J. Chem. Soc., Chem. Commun.* 1990, 273.
48. Daoust, G.; Leclerc, M. *Macromolecules* 1991, 24: 455.
49. Heywang, G.; Jonas, F. *Adv. Mater.* 1992, 4: 116.
50. Gallazzi, M.C.; Castellani, L.; Marin, R.A.; Zerbi, G. *J. Polym. Sci., Polym. Chem. Ed.* 1993, 31: 3339.
51. Souto Maior, R.M.; Hinkelmann, K.; Eckert, H.; Wudl, F. *Macromolecules* 1990, 23: 1268.
52. McCullough, R.D.; Lowe, R.D.; Jayaraman, M.; Anderson, D.L. *J. Org. Chem.* 1993, 58: 904.
53. Barbarella, G.; Bongini, A.; Zambianchi, M. *Macromolecules* 1994, 27: 3039.
54. Andersson, M.R.; Selse, D.; Berggren, M.; Jarvinen, H.; Hjertberg, T.; Inganäs, O.; Wennerstrom, O.; Osterholm, J.-E. *Macromolecules* 1994, 27: 6503.
55. Jarvinen, H.; Lahtinen, L.; Nasman, J.; Hormi, O.; Tammi, A.-L. *Synth. Met.* 1995, 69: 299.
56. McCullough, R.D.; Lowe, R.D. *J. Chem. Soc., Chem. Commun.* 1992, 70.
57. McCullough, R.D.; Tristram-Nagle, S.; Williams, S.P.; Lowe, R.D.; Jayaraman, M. *J. Am. Chem. Soc.* 1993, 115: 4910.
58. Chen, T.-A.; Rieke, R.D. *Synth. Met.* 1993, 60: 175.
59. Fréchet, M.; Belletête, M.; Bergeron, J.-Y.; Durocher, G.; Leclerc, M. *Macromol. Chem. Phys.* 1997, 198: 1709.
60. Yokoyama, A.; Miyakoshi, R.; Yokozawa, T. *Macromolecules* 2004, 37: 1169.
61. Ikenoue, Y.; Saida, Y.; Kira, M.; Tomozawa, H.; Yashima, H.; Kobayashi, M. *J. Chem. Soc., Chem. Commun.* 1990, 1694.
62. Arroyo-Villan, M.I.; Diaz-Quijada, G.A.; Abdou, M.S.A.; Holdcroft, S. *Macromolecules* 1995, 28: 975.
63. Diaz-Quijada, G.A.; Pinto, B.M.; Holdcroft, S. *Macromolecules* 1996, 29: 5416.
64. Chen, S.-A.; Hua, M.-Y. *Macromolecules* 1993, 26: 7108.
65. Udum, Y.A.; Pekmez, K.; Yildiz, A. *Synth. Met.* 2004, 142: 7.
66. Kim, B.-S.; Chen, L.; Gong, J.; Osada, Y. *Macromolecules* 1999, 32: 3964.
67. Chen, L.; Kim, B.-S.; Nishino, M.; Gong, J.P.; Osada, Y. *Macromolecules* 2000, 33: 1232.
68. McCullough, R.D.; Ewbank, P.C.; Loewe, R.S. *J. Am. Chem. Soc.* 1997, 119: 633; and references cited therein.
69. Andersson, M.; Ekeblad, P.O.; Hjertberg, T.; Wennerstrom, O.; Inganäs, O. *Polym. Commun.* 1991, 32: 546.
70. Bouman, M.M.; Meijer, E.W. *Adv. Mater.* 1995, 7: 385.
71. Bidan, G.; Guillerez, S.; Sorokin, V. *Adv. Mater.* 1996, 8: 157.
72. Langeveld-Voss, B.M.W.; Janssen, R.A.J.; Meijer, E.W. *J. Molec. Struct.* 2000, 521: 285; and references cited therein.
73. Yashima, E.; Goto, H.; Okamoto, Y. *Macromolecules* 1999, 32: 7942.

74. Goto, H.; Yashima, E.; Okamoto, Y. *Chirality* 2000, 12: 396.
75. Ewbank, P.C.; Nuding, G.; Suenaga, H.; McCullough, R.D.; Shinkai, S. *Tetrahedron Lett.* 2001, 42: 155.
76. Harada, H.; Fuchigami, T.; Nonaka, T. *J. Electroanal. Chem.* 1991, 303: 139.
77. Qi, Z.; Rees, N.G.; Pickup, P. *Chem. Mat.* 1996, 8: 701.
78. Li, Y.; Vamvounis, G.; Holdcroft, S. *Macromolecules* 2001, 34: 141.
79. Czerwinski, W.; Kreja, L.; Chrzaszcz, M.; Kaubski, A. *J. Mater. Sci.* 1994, 29: 1191.
80. Hotta, S.; Hosaka, T.; Shimotsuma, W. *J. Chem. Phys.* 1984, 80: 954.
81. Street, G.; Clarke, T.; Krounbi, M.; Kanazawa, K.; Lee, V.; Pfluger, P.; Scott, J.; Weiser, G. *Mol. Cryst. Liq. Cryst.* 1982, 83: 253.
82. Gallazzi, M.C.; Bertarelli, C.; Montoneri, E. *Synth. Met.* 2002, 128: 91.
83. Verilhac, J.M.; LeBlevenec, G.; Djurado, D.; Rieutord, F.; Chouiki, M.; Travers, J.P.; Pron, A. *Synth. Met.* 2006, 156: 815.
84. Ito, M.; Shioda, H.; Tanaka, K. *J. Polym. Sci.: Part C: Polym. Lett.* 1986, 24: 147.
85. Ito, M.; Tsuruno, A.; Osawa, S.; Tanaka, K. *Polymer* 1988, 29: 1161.
86. Mo, Z.; Lee, K.B.; Moon, Y.B.; Kobayashi, M.; Heeger, A.J.; Wudl, F. *Macromol.* 1985, 18: 1972.
87. Satoh, M. Yamasaki, H., Aoki, S. and Yoshino, K., *Mol. Cryst. Liq. Cryst.* 1988, 159: 289.
88. Li, C.; Shi, G.; Liang, Y.; Sha, Z. *Polymer* 1997, 38: 6421.
89. Jin, S.; Cong, S.X.; Xue, G.; Xiong, H.M.; Mansdorf, B.; Cheng, S.Z.D. *Adv. Mater.* 2002, 14: 1492.
90. Garnier, F.; Tourillon, G.; Barraud, J.Y.; Dexpert, H. *J. Mater. Sci.* 1985, 20: 2687.
91. Tourillon, G.; Garnier, F. *Mol. Cryst. Liq. Cryst.* 1985, 118: 221.
92. Waltman, R.J.; Bargon, J.; Diaz, A.F. *J. Phys. Chem.* 1983, 87: 1459.
93. Tourillon, G.; Garnier, F. *J. Polym. Sci.* 1984, 22: 33.
94. Yassar, A.; Roncali, J.; Garnier, F. *Macromol.* 1989, 22: 804.
95. Masuda, H.; Taniki, Y.; Kaeriyama, K. *J. Polym. Sci.; Polym. Chem.* 1992, 30: 1667.
96. Jeffries-El, M. and McCullough, R.D., in *Handbook of Conducting Polymers. Conjugated Polymers. Theory, Synthesis, Properties and Characterisation*, 3rd edition, Skotheim, T.A. and Reynolds, J.R. (Eds.), CRC Press, Boca Raton, 2007, 9-1.
97. Kaniowski, T.; Luzny, W.; Niziol, S.; Sanetra, J.; Trznadel, M. *Synth. Met.* 1998, 92: 7.
98. Winokur, M.J., in *Handbook of Conducting Polymers. Conjugated Polymers. Theory, Synthesis, Properties and Characterisation*, 3rd edition, Skotheim, T.A. and Reynolds, J.R. (Eds.), CRC Press, Boca Raton, 2007, 17-1.
99. Chen, T.A.; Rieke, R.D. *J. Am. Chem. Soc.* 1992, 114: 10087.
100. McCullough, R.D.; Lowe, R.D. *J. Chem. Soc. - Chem. Commun.* 1992, 1: 70.
101. Luzny, W.; Pron, A. *Synth. Met.* 1997, 84: 573.
102. Kline, R.J.; McGehee, M.D.; Kadnikova, E.N.; Liu, J.S.; Frechet, J.M.J. *Adv. Mater.* 2003, 15: 1519.
103. Fell, H.J.; Samuelsen, E.J.; Mardalen, J.; Andersson, M.R. *Synth. Met.* 1995, 69: 283.
104. Meille, S.V.; Romita, V.; Caronna, T.; Lovinger, A.J.; Catellani, M.; Belobrzecakaja, L. *Macromolecules* 1997, 30: 7898.
105. Kline, R.J.; McGehee, M.D. *Polymer Reviews* 2006, 46: 27.
106. Kim, D.H.; Jang, Y.; Park, Y.D.; Cho, K. *Macromolecules* 2006, 39: 5843.
107. Kirchmeyer, S.; Reuter, K and Simpson, J.C., in *Handbook of Conducting Polymers. Conjugated Polymers. Theory, Synthesis, Properties and Characterisation*, 3rd edition, Skotheim, T.A. and Reynolds, J.R. (Eds.), CRC Press, Boca Raton, 2007, 10-1.
108. Takashima, W.; Nagamatsu, S.; Pandey, S.S.; Endo, T.; Yoshida, Y.; Tanigaki, N.; Rikukawa, M.; Yase, S.; Kaneto, K. *Synth. Met.* 2001, 119: 563.
109. Oh, S.-G.; Im, S.-S. *Current Appl. Phys.* 2002, 2: 273.
110. Choi, J.W.; Han, M.G.; Kim, S.Y.; Oh, S.G.; Im, S.S. *Synth. Met.* 2004, 141: 293.

111. Ballav, N.; Biswas, M. *Polym. Int.* 2004, 53: 198.
112. Jang, J.; Chang, M.; Yoon, H. *Adv. Mater.* 2005, 17: 1616.
113. Zhang, X.; MacDiarmid, A.G.; Manohar, S.K. *Chem. Commun.* 2005, 5328.
114. Kim, J.; Kim, E.; Won, Y.; Lee, H.; Suh, K. *Synth. Met.* 2003, 139: 485.
115. Rajesh, B.; Ravindranathan Thampi, K.; Bonard, J.-M.; Xanthopoulos, N.; Mathieu, H.J.; Viswanathan, B. *J. Phys. Chem. B* 2004, 108: 10640.
116. Wei, Y.; Tian, J. *Polymer* 1992, 33: 4872.
117. Otero, T.F.; Azelain, E.L. *Polym. Comm.* 1988, 29: 21.
118. Tanaka, K.; Schichiri, T.; Wang, S.; Yamambe, T. *Synth. Met.* 1988, 24: 203.
119. Sato, M.; Tanaka, S.; Ama, K.J. *Synth. Met.* 1986, 14: 279.
120. Tourillon, G.; Garnier, F. *J. Phys. Chem.* 1983, 87: 2289.
121. Tourillon, G.; Garnier, F. *J. Electroanal. Chem.* 1984, 161: 407.
122. Sato, M.; Shimizu, T.; Yamauchi, A. *Makromol. Chem.* 1990, 191: 313.
123. Yassar, A.; Roncali, J.; Garnier, F. *Macromol.* 1989, 22: 804.
124. Taka, T. *Synth. Met.* 1993, 55: 4985.
125. Taka, T.; Punkka, E.; Isotalo, H. *Synth. Met.* 1993, 55: 4979.
126. Pei, Q.; Ingnas, O.; Gustafsson, G.; Granstrom, M.; Anderson, M.; Hjertberg, T.; Wennerstrom, O.; Osterholm, J.E.; Laakso, J.; Harvinen, H. *Synth. Met.* 1993, 55: 1221.
127. Xu, X.; Ishikawa, A.; Kobayashi, A.; Satoh, M.; Hasegawa, E. *Synth. Met.* 1993, 55: 4973.
128. Street, R.A.; Northrup, J.E.; Salleo, A. *Phys. Rev. B.* 2005, 15: 1519.
129. Roncali, J. *Chem. Rev.* 1992, 92: 711.
130. Jin, S.; Cong, S.; Xue, G.; Xiong, H.; Mansdorf, B.; Cheng, S.Z.D. *Adv. Mater.* 2002, 14: 1492.
131. Shi, G.; Jin, S.; Xue, G.; Li, C. *Science* 1995, 267: 994.
132. Wang, X.-S.; Feng, X.Q. *J. Mater. Sci. Lett.* 2002, 21: 715.
133. Ito, M.; Tsuruno, A.; Osawa, S.; Tanaka, K. *Polymer* 1988, 29: 116.
134. Yoshino, K.; Tabata, M.; Satoh, M.; Kaneto, K.; Hasegawa, T. *Tech. Rep.* 1985, 35: 231.
135. Moulten, J.; Smith, P. *Synth. Met.* 1991, 40: 13.
136. Moulten, J.; Smith, P. *Polymer* 1992, 33: 2340.
137. Van de Leur, R.H.M.; De Ruiter, B.; Breen, J. *Synth. Met.* 1993, 55: 4956.
138. Lapowski, M.; Biadan, G.; Fournier, M. *Pol. J. Chem.* 1991, 65: 1547.
139. Koktar, D.; Joshi, V.; Ghosh, P.K. *J. Chem. Soc. Chem. Comm.* 1988, 917.
140. Rughooputh, S.D.D.V.; Nowak, M.; Hotta, S.; Heeger, A.J.; Wudl, F. *Synth. Met.* 1987, 21: 41.
141. Andersson, M.; Ekeblad, P.O.; Hjertberg, T.; Wennerstrom, O.; Ingnas, O. *Polym. Comm.* 1991, 32: 546.
142. Ikenoue, Y.; Tomozawa, H.; Saida, Y.; Kira, M.; Yashima, H. *Synth. Met.* 1991, 40: 333.
143. Patil, A.O.; Ikenoue, Y.; Basecu, N.; Colaneri, N.; Chen, J.; Wudl, F.; Heeger, A.J. *Synth. Met.* 1987, 20: 151.
144. Bryce, M.R.; Chissel, A.; Kathiramanathan, P.; Parker, D.; Smith, N.R.M. *J. Chem. Soc. Chem. Comm.* 1987, 466.
145. Torres, W.; Fox, M.A. *Chem. Mat.* 1990, 2: 158.
146. Roncali, J.; Garreau, R.; Lemaire, M. *J. Electroanal. Chem.* 1987, 218: 107.
147. Chen, S.A.; Tsai, C.C. *Macromol.* 1993, 26: 2234.
148. Marque, P.; Roncali, J.; Garnier, F. *J. Electroanal. Chem.* 1987, 218: 107.
149. Roncali, J. *Chem. Rev.* 1997, 97: 173.
150. van Mullekom, H.A.M.; Vekemans, J.A.J.M.; Havinga, E.E.; Meijer, E.W. *Mater. Sci. Eng.* 2001, 32: 1.

151. Irvin, D.J.; DuBois, C.J.; Reynolds, J.R. *Chem. Commun.* 1999, 2121.
152. Bredas, J.L.; Themans, B.; Andre, J.M.; Chance, R.R.; Silby, R.; *Synth. Met.* 1984, 9: 265.
153. Lauchlan, L.; Etamad, S.; Chung, T.C.; Heeger, A.J.; MacDiarmid, A.G. *Phys. Rev. B.* 1981, 24: 3701.
154. Chung, T.C.; Kaufman, J.H.; Heeger, A.J.; Wudl, F. *Phys. Rev. B.* 1984, 30: 702.
155. Herbake, G.; Meier, E.; Kobel, W.; Egli, M.; Kiess, H.; Tosatti, E. *Solid State Commun.* 1985, 55: 419.
156. McCullough, R.D. *Adv. Mat.* 1998, 10: 93; and references cited therein.
157. Roncali, J. *Chem. Rev.* 1992, 92: 711; and references cited therein.
158. Leclerc, M.; Faid, K. In *Handbook of Conducting Polymers*. 2nd. Edn. T.A. Skotheim, R.L. Elsenbaumer, J.R. Reynolds(eds). Marcel Dekker, New York, 1998, p. 695; and references cited therein.
159. Rughooputh, S.D.D.V.; Hotta, S.; Heeger, A.J.; Wudl, F. *J. Polym. Sci. Polym. Phys. Ed.* 1987, 25: 1071.
160. Thomas, B.; Salaneck, W.R.; Bredas, J.L. *Synth. Met.* 1989, 28: C359.
161. Lemaire, M.; Delabouglise, D.; Garreau, R.; Guy, A.; Roncali, J. *J. Chem. Soc., Chem. Commun.* 1988: 658.
162. Andersson, M.R.; Selse, D.; Berggren, M.; Jarvinen, H.; Hjertberg, T.; Inganäs, O.; Wennerstrom, O.; Osterholm, J.-E. *Macromolecules* 1994, 27: 6503.
163. Langeveld-Voss, B.M.W.; Christiaans, M.P.T.; Janssen, R.A.A.; Meijer, E.W. *Macromolecules* 1998, 31: 6702.
164. Langeveld-Voss, B.M.W.; Peeters, E.; Janssen, R.A.; Meijer, E.W. *Synth. Met.* 1997, 84: 611.
165. Langeveld-Voss, B.M.W.; Janssen, R.A.A.; Christiaans, M.P.T.; Meskers, S.C.J.; Dekkers, H.P.J.M.; Meijer, E.W. *J. Am. Chem. Soc.* 1996, 118: 4908.
166. Fujiki, M.; Nakashima, H.; Koe, J.R.; Takigawa, H. *Polym. Preprints* 1999, 40: 523.
167. Ramos, J.C.; Souto-Maior, R.M.; Navarro, M. *Polymer* 2006, 47: 8095.
168. Nilsson, K.P.R.; Andersson, M.R.; Inganäs, O. *J. Phys.: Condens. Matter.* 2002, 14: 10011, and references cited therein.
169. Nilsson, K.P.R.; Olsson, J.D.M.; Konradsson, P.; Inganäs, O. *Macromolecules* 2004, 37: 6316.
170. Nilsson, K.P.R.; Olsson, J.D.M.; Stabo-Eeg, F.; Lindgren, M.; Konradsson, P.; Inganäs, O. *Macromolecules* 2005, 38: 6813.
171. Goto, H.; Okamoto, Y.; Yashima, E. *Macromolecules* 2002, 35: 4590.
172. Goto, H.; Yashima, E. *J. Am. Chem. Soc.* 2002, 124: 7943.
173. Li, C.; Numata, M.; Bae, A.-H.; Sakurai, K.; Shinkai, S. *J. Am. Chem. Soc.* 2005, 127: 4548.
174. Caras-Quintero, D.; Bäuerle, P. *Chem. Commun.* 2004, 926.
175. Goto, H.; Akagi, K. *Chem. Mater.* 2006, 18: 255.

---

# 7 Processing and Device Fabrication

All the practical uses of conductive electroactive polymers (CEPs), including intelligent material systems, require the ability to integrate them into other structures or to implement innovative device fabrication protocols using them. As pointed out in previous chapters, the optimization of chemical properties results in some compromise in electrical and mechanical properties, and vice versa. There is a further requirement for the use of integrated material systems in the development of intelligent structures, and from that arises the need to spatially resolve function. The discrete physical location of sensing and actuating loci throughout a “mechanically stable” structure is required for many applications. Practically useful, intelligent structures based on these materials can, therefore, only be realized if the properties of CEPs can be retained and a structural integrity obtained by weaving the active components throughout other synthetic or naturally occurring systems. This can be achieved either by combining the conducting polymers within other structures or devices after polymerization or by assembling the conducting polymer within a host matrix.

## INTEGRATION/FABRICATION AFTER POLYMERIZATION

For most conventional polymer structures, blending is used to achieve the desired properties of the composite structure. Conventional polymers are amenable to this approach, because they are either soluble in common organic solvents or fusible (melt before decomposing). This has generally not been the case with CEPs, although significant advances have been made through modifications to the polymer structure. Outlined in the following text are recent advances in the integration of CEPs into other polymer structures by either solution or melt processes.

## SOLUTION-PROCESSABLE CEPs

Polyaniline (PAn) is most amenable to solution processing. The emeraldine base (EB) form of PAn is soluble in selected solvents such as methyl pyrrolidinone<sup>1</sup> or strong acids.<sup>2,3</sup> More recently, it has been discovered that solubility of the doped form can be induced by the use of appropriate “surfactant-like” molecules as dopants.<sup>4</sup> Camphorsulfonic acid (HCSA) and dodecylbenzenesulfonic acid have proved particularly useful in this regard. Once solubilized, these PAn’s can be cast into sheets or blended with other conventional polymer structures. For example, the pres-



ence of the surfactant counterion facilitates the blending process<sup>5</sup> with polymers such as:

- Polyethylene
- Nylons
- Polycarbonate
- Polystyrene
- Poly(vinylacetate)
- Poly(vinylchloride) (PVC).

When PAN/CSA is dissolved in *m*-cresol with poly(methyl methacrylate)-(PMMA), this can be spun-cast to form optically transparent films.<sup>5</sup>

Pron and coworkers<sup>6</sup> have blended PAN with cellulose acetate and cast from *m*-cresol to produce highly transparent and conductive ( $\approx 1 \text{ S cm}^{-1}$ ) PAN. Addition of plasticizers (in particular, phenylphosphonic acid) not only resulted in more flexible films but lowered the percolation threshold for PAN to an amazing 0.05% (w/w).

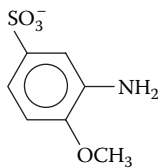
De Paoli and coworkers<sup>7</sup> have used the more soluble poly(*o*-methoxyaniline) doped with *p*-toluene sulfonic acid to prepare a composite blend with poly(epichlorohydrin-*co*-ethylene oxide), but conductivities were relatively low ( $10^{-3} \text{ S cm}^{-1}$ ) even with a high 50% (w/w) conducting polymer loading.

Others<sup>8</sup> have blended PAN doped with dodecylbenzenesulfonic acid with poly(vinyl alcohol) (PVA) in water or with polyacrylate in organic solvents to obtain transparent conductive composites.

Solution processing of polypyrroles (PPy's) and polythiophenes has been limited by these materials' lack of solubility. To overcome this, some work<sup>9,10,11</sup> has been concerned with attaching alkyl groups to PPy's or polythiophenes to increase solubility. This has had the desired effect of increasing solubility in common solvents such as  $\text{CH}_2\text{Cl}_2$  or  $\text{CHCl}_3$ , in some cases to levels in excess of 300 g/L polymer.

The solubility of polythiophenes has also been increased by attaching alkoxy groups to bithiophene monomers.<sup>12</sup> Other workers<sup>13,14,15</sup> have been concerned with producing pyrroles and thiophenes with alkyl-sulfonated chains attached to increase the water solubility of the polymer.

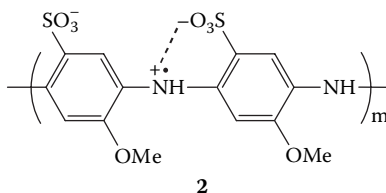
Sulfonate groups have also been attached to PAN either after<sup>16</sup> or before<sup>17</sup> polymerization to induce water solubility. The latter approach requires addition of a methoxy (electron-donating group) to the aniline ring to counterbalance the effects of the electron-withdrawing sulfonate group during polymerization—see structure **1**.



**1**

Solubility, and hence processability, is improved at the expense of the electrical (decreased conductivity) properties of the polymer. The flow-through electro-

synthesis approach described in Chapter 2 has been used to prepare PMAS **2**.<sup>18,19</sup> Subsequently, we developed a purification scheme that enables removal of low-molecular-weight by-products that arise from the monomer oxidation process. Removal of these by-products has a dramatic effect on the electronic properties of the water-soluble polymer obtained, increasing conductivity by approximately two orders of magnitude to  $1 \text{ S cm}^{-1}$ .<sup>20</sup>



Given the lack of solubility of conducting polymers that have the desired electrochemical and/or chemical properties, colloidal processing provides an attractive alternative. Colloids are readily dispersed throughout other solutions for subsequent processing into other structures. Conductive electroactive colloids of PPy's or PAN's are readily prepared by carrying out the oxidative polymerization in the presence of a steric stabilizer.<sup>21</sup> Stabilizers such as PVA, poly(vinyl pyrrolidone) (PVP), and poly(ethylene oxide) (PEO) have been used, and conducting polymer particles with sizes in the range 10–100 nm can be prepared. While the conductivity of the colloids is less than that of electrodeposited films, it is respectable (up to  $10 \text{ S cm}^{-1}$ ).

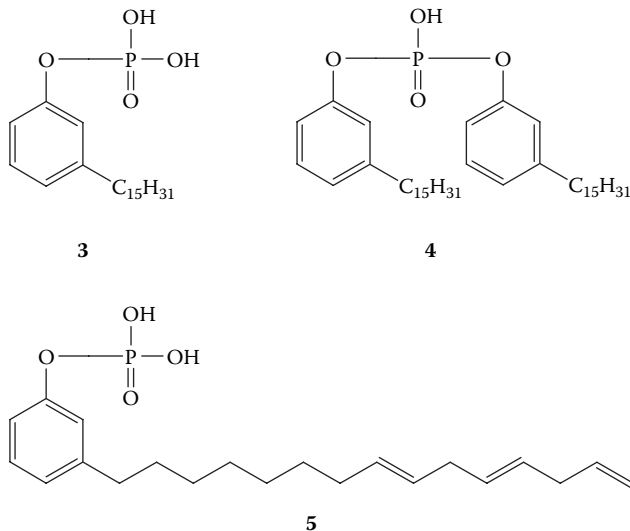
Once formed, these colloids may be used for further processing. For example, they can be mixed with paints.<sup>22</sup> The products formed are as conductive as those obtained when carbon black is added to paints. However, they are also electroactive and presumably (at least the colloidal component) retain the unique chemical properties of the conducting polymer.

In some cases, larger conducting polymer particles have been mixed with other polymers. For example, Bose and coworkers<sup>23</sup> incorporated chemically synthesized polypyrrole (PPy) into PVC or nafion. After casting, the materials were shown to be electroactive and demonstrated electrocatalytic properties.

## MELT-PROCESSABLE CEPS

As with solution processing, there have been significant recent advances in melt processing of CEPs.<sup>24,25,26</sup> Again, most interest has been with PAN. The most successful approach has been to use specific dopants to induce melt processability. Thus, various dopants, such as **3–5** (Figure 7.1), have been used that combine an acid group (e.g., sulfonic or phosphoric acid) with hydrophobic segments. The latter cause a plasticization of the host PAN and reduce the strong interchain bonding caused by its aromaticity, H-bonding, and charge delocalization. Once suitably plasticized, the doped PAN is able to be fused to form free-standing films by hot pressing.

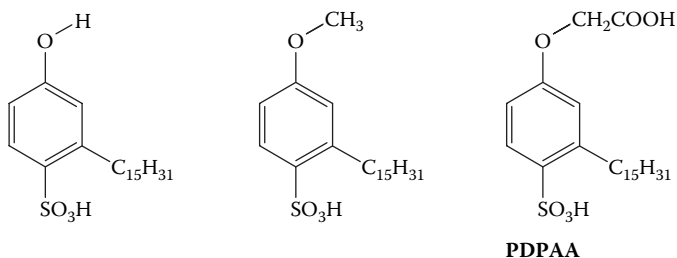
In one series of studies, Paul and Pillai<sup>25</sup> used various phosphate ester dopants to induce melt processability in PAN. Conductivities as high as  $1.8 \text{ S cm}^{-1}$  were



**FIGURE 7.1** Dopants used to induce thermal processing.

reported for melt-pressed pellets of PAn/PDPPA.<sup>26</sup> The doped polymers were found to be thermally stable up to 200°C so that melt pressing at 160°C did not induce any thermal degradation. Blends of the phosphate-ester-doped PAn were readily prepared with PVC by dry mixing at room temperature followed by hot pressing. The blends were found to give flexible films with a percolation threshold of 5% PAn content (by weight) and a conductivity of  $2.5 \times 10^{-2} \text{ S cm}^{-1}$  for a blend having 30 wt% PAn/PDPPA in PVC.

In other work, Paul and coworkers<sup>26</sup> have reported melt-processed PAn using sulfonic acid dopants (Figure 7.2). These dopants also gave flexible free-standing films of doped PAn after hot pressing, exhibiting higher conductivities than the phosphate-ester-doped PAn (up to  $65 \text{ S cm}^{-1}$  for doped systems prepared by an emulsion polymerization technique). The conductivity was dependent upon the pressing temperature, reaching a maximum at around 140°C. The decline in conductivity at higher pressing temperatures was probably due to thermal crosslinking of the PAn, reducing electron delocalization.



**FIGURE 7.2** Structures of sulfonic acid dopants used.

These demonstrations of melt processability for PAn provide an avenue for the convenient preparation of films and fibers of CEPs. The absence of solvent makes the melt-processing route more attractive and environment-friendly than alternative solvent processing. In addition, the melt-processable CEPs are then easily incorporated into polymer blends using the well-developed processing techniques (extrusion and so on) widely used for thermoplastic polymers.

## ASSEMBLY OF CONDUCTING POLYMERS IN HOST MATRICES

Conducting polymers can be integrated into other structures at the point of assembly using either the chemical or the electrochemical oxidative route.

## CHEMICAL POLYMERIZATION

The simplest approach is to have a suitable host structure imbibe the oxidant or monomer. This material is then exposed to the monomer or oxidant, respectively, and the polymer material is grown throughout. For example, Bjorklund and Lundstrom<sup>27</sup> described a procedure in which cellulose paper was first exposed to a metal salt ( $\text{FeCl}_3$ ) that would act as the polymerization agent. The metal salt-soaked paper was then exposed to the pyrrole monomer in liquid or vapor form. Materials with conductivities of approximately  $2 \text{ S cm}^{-1}$  could be produced using this approach.

We have found similar results in our laboratories making impregnated papers with PPy and PAn for inverse thin-layer chromatography.<sup>28</sup> The method we used to prepare PAn-modified paper was to load filter paper strips with aniline, which was allowed to diffuse throughout the paper for about 10 min. The strips were then immersed in  $\text{FeCl}_3$  that had been acidified with HCl. The PAn adheres well to the filter paper when it is dried, and no problems with chemical instability were observed. The morphology of the polymer surface was that of the filter paper substrate.

It was noted by MacDiarmid and Epstein as early as 1989 that PAn salts may also be deposited as films on a variety of substrates by immersing the substrate in the polymerization mixture.<sup>29</sup> In fact, during standard chemical polymerization, one often observes the deposition of a thin, extremely adherent green emeraldine salt (ES) film on the walls of glass reaction vessels, as well as the bulk precipitation of PAn/HA powder. By judicious manipulation of the polymerization conditions such as reagent concentrations/ratios and modification of the substrate surface, one can maximize the surface deposition as opposed to polymer precipitation.<sup>30</sup> This phenomenon has been developed into a widely useful *in situ* polymerization technique for the preparation of PAn films on a variety of insulating surfaces such as glass and plastics, as well as on fibers and fabrics.

## DEPOSITION ON GLASS/PLASTICS

*In situ* polymerization of aniline is generally carried out in aqueous  $(\text{NH}_4)_2\text{S}_2\text{O}_8/\text{HCl}$ . The glass support is typically removed from the reaction mixture during the polymerization at the stage when a blue/violet film of pernigraniline salt has formed on its surface. This film is then reduced to the green ES product by reaction with a separate

aniline/HCl solution.<sup>31</sup> Alternatively, the glass support may be left immersed in the reaction mixture until the polymerization is complete.<sup>32</sup>

The *in situ* deposition of conducting PAN films was found by MacDiarmid and coworkers<sup>33</sup> to occur more readily on hydrophobic surfaces, such as Si/SiO<sub>2</sub> and glass pretreated with octadecylsiloxane (OTS), than on related hydrophilic surfaces. They exploited these different deposition rates to produce patterned microstructures of PAN, by the microcontact “stamp” printing of patterned hydrophilic films of OTS on hydrophilic glass substrates before the aniline polymerization. Conducting PAN features as small as 2 μm in lateral dimension could be produced with this method. In collaboration with Alan MacDiarmid, we have prepared optically active PAN/(+)-HCSA and PAN/(-)-HCSA films on glass using this *in situ* route, by replacing the HCl in the polymerization solution by (+)- or (-)- camphorsulfonic acid.<sup>34</sup>

Not surprisingly, in view of the preceding preference for hydrophobic surfaces, PAN can also be deposited by the *in situ* method on supports such as low-density polyethylene (LDPE).<sup>35</sup> Modification of the LDPE surface by grafting with acrylic acid promotes the growth and adhesion of the PAN films. Conducting PAN coating may be similarly deposited on PVC and PMMA surfaces through chemical oxidative polymerization.<sup>36</sup>

An important development, pioneered by Kuhn and coworkers,<sup>37,38</sup> has been the deposition of conducting PAN's onto fibers and fabrics. Not only hydrophobic fibers such as polyesters and polypropylene but also hydrophilic textiles such as rayon and cotton can be coated with PAN with this *in situ* polymerization method. PAN/nylon-6 composite films have also been prepared by adsorbing aniline onto thin nylon-6 films and then treating with aqueous (NH<sub>4</sub>)<sub>2</sub>S<sub>2</sub>O<sub>8</sub>.<sup>39</sup> The composite films exhibited a low percolation threshold requiring just 4% PAN for electrical conductivity.

Quartz fibers and Kevlar have also been coated. A uniform adherent, conducting, and electroactive coating is produced using this simple approach. The mechanical properties of the base textile are not significantly affected. The authors suggest that the adherent coating arises from the fact that it is not the monomer or oxidant that is adsorbed onto the textile, but rather the radical and/or oligomers.

Nylon, glass fabric, and glass wool<sup>40</sup> have been coated with PAN using similar procedures. In this case, the material to be coated is soaked in a solution containing aniline and a doping agent such as benzene sulfonic acid, *p*-toluene sulfonic acid, 5-sulfosalicylic acid, or sulfuric acid is added with the oxidant (ammonium peroxydisulfate). The fibers appear to be uniformly coated with the CEP, and the coatings obtained are electroactive.

PAN has been integrated into other structures (polyethylene, polyterephthalate, polyester, and polystyrene) by soaking in monomer solutions and then exposing to acidic oxidant (FeCl<sub>3</sub>) solutions.<sup>41</sup> Results suggest that the polymers were swollen by the aniline monomer and that polymerization occurred within these swollen media to produce dispersed PAN granules. Conductivities on the order of 10<sup>-1</sup> S cm<sup>-1</sup> were obtained.

PPy has been coated on PMMA or polyethylene spheres<sup>42</sup> using a chemical polymerization process. The spheres were dispersed in methanol and then added to water containing FeCl<sub>3</sub> oxidant. Pyrrole dissolved in water was subsequently added.

The coated spheres could be mixed with noncoated spheres of PMMA and hot-pressed to obtain films with conductivities of  $3.5 \text{ S cm}^{-1}$ .

Other workers have coated nylon by imbibing pyrrole into the film followed by exposure to oxidant.<sup>43</sup> Polymerization only occurred in the surface layer ( $5 \mu\text{m}$ ), resulting in the formation of a heterogeneous structure. Nylon 6,6 (N66) with incorporated PPy had a much higher initial modulus of 2.6 GPa, compared to 1.7 GPa for N66 alone. However, the elongation to break was also markedly reduced, from 350% for N66 to 60% for N66/PPy.

Kelkar and Bhat<sup>44</sup> described a modified method for making nylon-PPy composites. In the modified method, the nylon is first doped with copper chloride. Because  $\text{CuCl}_2$  acted as an initiation site for polymerization, the authors argue that this resulted in more continuous conducting polymer chains throughout the nylon and a higher bulk conductivity.

Chemical polymerization onto sulfonated (dopant-containing) synthetic polymers has also been described.<sup>45</sup> Sulfonated polyethylene-polystyrene was exposed to monomer and then the oxidant. A mixture of  $\text{Fe}^{\text{II}}$  and  $\text{Fe}^{\text{III}}$  led to more accurate control of the  $E^\circ$  value of solution. These same workers also described a novel chemical/electrochemical method, in which pyrrole was initially polymerized using a low concentration of  $\text{Fe}^{\text{III}}$ . The reduced  $\text{Fe}^{\text{III}}$  could then be reoxidized electrochemically to regenerate the oxidant. Using this chemical/electrochemical process, composite polymers with conductivities as high as  $35 \text{ S cm}^{-1}$  were obtained.

PPy's have been integrated into other structures by polymerizing in the presence of a dissolved polymer. For example,<sup>46</sup> polymerization of pyrrole has been achieved in a solution of polycarbonate dissolved in  $\text{CHCl}_3$  with  $\text{FeCl}_3$  as oxidant. The composite was then precipitated using a nonsolvent such as methanol, ethanol, or acetone. The resultant structure was polycarbonate with conducting PPy dispersed throughout the matrix.

A similar procedure was used to produce PPy-poly(ethylene-co-vinyl acetate) [PEVA] composites.<sup>47</sup> The host polymer can be dissolved in a toluene solution with pyrrole. A concentrated dispersion is then formed by adding it to an aqueous solution containing a surfactant. An aqueous solution of the oxidant ( $\text{FeCl}_3$ ) is then introduced to form the polymer. The conductivity of the resultant materials is approximately  $5 \text{ S cm}^{-1}$ . The PEVA-based composites can be processed into films and other shaped articles by hot pressing at approximately  $100\text{--}150^\circ\text{C}$  and  $15\text{--}20 \text{ MPa}$  pressure for 1 h. The mechanical properties are determined by the PEVA content. For example, for composites of PPy-PEVA containing 20% (w/w) PPy, soft flexible films that can be extended up to 600% were produced. For pure PPy films, elongations of less than 5% are achievable.

From the same laboratory, another report<sup>48</sup> describes the use of this approach to prepare PPy/poly(alkyl methacrylate). In this case, a chloroform solution of poly(alkyl methacrylate) and pyrrole is dispersed in an aqueous surfactant solution whereupon the oxidant is added. The PPy deposits on the host polymer, and again a nonsolvent is used to precipitate the composite. The composites can then be hot-pressed to obtain films or other objects. Compared to cold pressing, hot pressing improves the mechanical properties but decreases the conductivities. In the hot-pressed materials, a distinct PPy phase could not be observed.

A similar approach<sup>49</sup> was used to prepare PAN/poly(alkylmethacrylate) composites. Sodium persulfate was used as the oxidant in acidic (HCl) media, and the composite was precipitated by the addition of methanol. Again, hot pressing was found to improve the mechanical properties, and conductivities of  $2 \text{ S cm}^{-1}$  were obtained. Although higher conductivities could be obtained with cold pressing, the mechanical properties were inferior.

PAN composites have been formed by polymerizing aniline in the presence of a latex.<sup>50</sup> The latexes were chlorinated copolymers (Haloflex EP 252), which were film-forming latexes. Interestingly, the thermal stability of the resultant composite was better than either of the individual components. Polyaniline–polyacrylamide<sup>51</sup> composites have been prepared by carrying out a chemical oxidation of aniline in the presence of polyacrylamide. Films that could be cast were stable up to  $250^\circ\text{C}$ . However, conductivities were low (approximately  $5 \times 10^{-2} \text{ S cm}^{-1}$ ).

An alternative approach<sup>52</sup> involves polymerization of conventional polymer in the presence of a soluble conducting polymer (alkylated thiophene) to form a semi-interpenetrating network. The polythiophene was dissolved in solutions of styrene and divinyl benzene; conductivities in the range  $0.01\text{--}0.10 \text{ S cm}^{-1}$  were obtained.

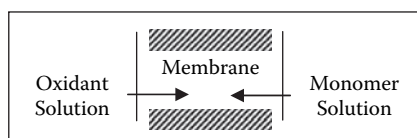
Conducting polymers have been formed inside other porous structures such as crosslinked polystyrene.<sup>53,54</sup> In the latter report, attachment of alkyl chains to the pyrrole improved the wetting characteristics, and hence, the mechanical properties of the composite.

An interesting approach to conducting polymer composite formation was reported by Mohammadi and coworkers,<sup>55</sup> who used Cu(II) complexed to poly(vinylpyridine) as the oxidant. They reported that composites with adequate mechanical and electrical properties can be obtained using this approach.

## INTERFACIAL POLYMERIZATION

Where the support material to be employed is porous to the monomer and/or oxidant, a novel approach termed *interfacial* or *diaphragmatic chemical* polymerization may be used (Figure 7.3).

Essentially, a membrane transport cell is used with oxidant on one side and monomer solution on the other. Where polymerization occurs depends on the relative mobility of the oxidant and the monomer.<sup>56</sup> In fact, this can be used to localize conducting polymer formation within the membranes. For example, with a nafion membrane and the use of  $\text{S}_2\text{O}_8^{2-}$  as oxidant, polymerization is restricted to the oxidant side of the membrane owing to anion exclusion (nafion is negatively charged). When  $\text{Fe}^{3+}$  is used as oxidant, polymerization occurs throughout the membrane. The use of different solvents can also affect the transport processes for oxidant and monomer. This



**FIGURE 7.3** Interfacial polymerization to produce conducting polymer membrane.

was used to fix the point of polymerization by other coworkers who prepared PPy–PVC structures.<sup>57</sup> Similar procedures have been used to coat PPy onto cellulose acetate and PVC.<sup>58</sup> Others have used a vapor-phase interfacial polymerization approach to produce thin conducting polymer coatings on conventional membranes.<sup>59</sup>

## ELECTROCHEMICAL INTEGRATION

Provided electrodes can somehow be embedded into another polymeric material that has sufficient porosity to allow monomer and counterion species to ingress, electropolymerization can also be used to make composite materials.

Electropolymerization can be used to coat other substrates, not just planar electrodes, resulting in the production of conducting polymer “composites.” For example, electrochemical methods have been used to coat spherical graphite particles in a pulsed bed reactor.<sup>60</sup> In fact, the substrate to be coated need not be conductive. Electropolymerization can be used to coat other structures by producing polymer in solution that is subsequently deposited onto other surfaces. This is possible because conducting polymers are formed in solution even when electrochemical methods are used. Judicious cell design, therefore, enables conducting polymers to be produced at an electrode where they are not adhesive, and to coat other surfaces that adsorb the CEPs more readily. For example, nonconductive silica particles can be coated using this method.<sup>61</sup> This same principle has been used to coat fibers in a flow-through electrochemical cell (Figure 7.4).<sup>62</sup> For poly(3-methylthiophene) and PPy fiber, growth rates of approximately  $30 \text{ cm h}^{-1}$  are achievable. Coated Kevlar or polyester string shows good adhesion of CEPs. Stand-alone conducting polymer fibers (with conductivities of  $6.2 \text{ S cm}^{-1}$ ) have also been produced using this approach.

Electrochemical polymerization has also been used to coat natural fibers such as cotton, silk, and wool<sup>63</sup> or synthetic carbon fibers<sup>64</sup> with PPy.

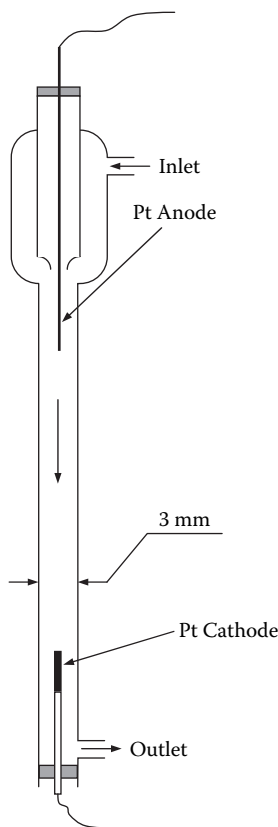
As early as 1984,<sup>65,66</sup> it was reported that conductive polymer composites could be prepared electrochemically by polymerizing pyrrole on a working electrode coated with the support polymer (e.g., PVC). According to Wang and coworkers,<sup>67</sup> the uniformity and conductivity of the polymer were improved if electrolyte was incorporated into the PVC before inducing electropolymerization.

Other workers have prepared poly(*N*-methylpyrrole)/poly(biphenol-A-carbonate) (PC) using this approach.<sup>68</sup> The electrodes were dip-coated with the PC and then electropolymerization was induced. Thermogravimetric analysis verified that a graft copolymer was produced. A similar procedure has been used to prepare PAN composites with the same host polymer.<sup>69</sup> The *in situ* electrochemical polymerization process has also been used to prepare polyacrylonitrile/PPy composite films.<sup>70</sup>

With these systems, conducting polymers start to grow from the electrode side. If polymerization times are short, only the electrode side is conductive, enabling a degree of spatial control that allows structures to be formed. As pointed out earlier, this may be important in producing intelligent material structures where localized polymerization is required to provide spatial distribution of function.

PPy/polyurethane (PU) composites with conductivities as high as  $1 \text{ S cm}^{-1}$  have also been prepared.<sup>71</sup> The PU was initially cast on indium–tin oxide coated glass electrodes, whereupon electropolymerization was carried out. The condition employed





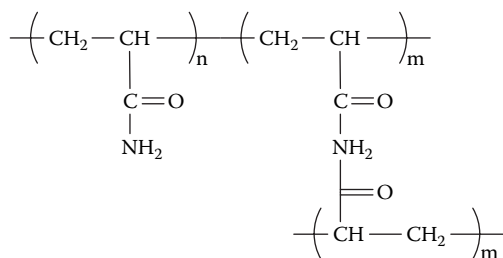
**FIGURE 7.4** Schematic of the electrochemical flow cell used to grow conducting poly(3-MeTh) on fibers. A centrifugal pump is used to pump the electrolyte solution through the gel. (From Li, S.; White, H.S. *J. Electrochem. Soc.* 1993, 140: 2473. With permission.)

during polymerization has a marked effect on the mechanical and electrical properties obtained.

PPy/poly(vinyl-methylketone) (PVMK) composites have been prepared using both chemical and electrochemical polymerization.<sup>72</sup> Both PPy and PVMK are capable of forming intramolecular hydrogen bonds, as evidenced in the resultant composites. The morphologies of the blends produced using the two approaches are different, the chemically prepared material being more thermally stable.

A similar approach has been used to prepare PAN/PVA composites.<sup>73</sup> In this case, the PVA is dip-coated using a DMSO solution, and the electropolymerization is initiated before the DMSO is completely removed. PAN has been electropolymerized<sup>74</sup> onto a platinum electrode wrapped in an aromatic copolyamide. PAN–nafion composites can be prepared using the coating-electropolymerization method.<sup>75</sup>

PAN–nitrilic rubber composites<sup>76</sup> have been prepared using rubber-coated anodes for electropolymerization. The resultant material has the mechanical properties of a crosslinked elastomer with the electrical and electro-optical properties



**FIGURE 7.5** Crosslinked polyacrylamides.

of PAN. The polymer composite properties vary markedly with the electrolyte used during electropolymerization.

PAN/PC composites have been prepared<sup>77</sup> using the materials wherein the electrode is initially dip-coated with the host (PC) polymer. As for the corresponding PPy composite discussed earlier, Fourier Transform Infrared (FTIR) and Differential Scanning Calorimetry (DSC) data suggest that the resulting product is not a simple composite but involves H-bonding between the two compounds.

Hydrogels are fascinating polymeric structures (an open porous network containing sometimes > 90% water by weight) that are ideally suited for electrochemistry. Crosslinked polyacrylamides (Figure 7.5) and agarose gels are two commonly used examples.

The polyacrylamides are readily modified chemically to change both their physical and chemical properties. The mechanical properties of these gels are such that electrodes can be cast in the gel at the time of polymerization/gelation. Monomer and electrolyte can then be introduced to the gel, and polymerization induced electrochemically. The electrochemical gel cell setup is shown in Figure 7.6. Upon application of an appropriate negative potential, conducting polymer growth is initiated and eventually “fills” the gel (Figure 7.6).

Retaining the open porous structure of gels, these polymers contain approximately 90% water<sup>78,79</sup> (Figure 7.7). They retain the redox switching characteristics of PPy films and the inherent ability of the hydrogel host to be dehydrated and rehydrated. Presumably, this is because the growth of the conducting polymer is regulated by the crosslinked hydrogel network. The resultant gel composites are electroactive and electrically conducting. The large open porous structure results in a high degree of electrochemical efficiency, which in turn improves the controlled-release capabilities of the conducting polymer. This has been demonstrated by comparing the release profiles of a sulfonated dye from a simple PPy structure and from a conducting polymer–gel composite. In the latter case, the rate of electrically stimulated release increased by more than an order of magnitude.<sup>79</sup>

The mechanical infrastructure provided by the gels enables polymers of large dimensions and various shapes to be produced. The conducting polymer will grow throughout the gel. By appropriate placement of electrodes, it is possible to grow composite structures with conducting polymers strategically placed with predetermined spatial resolution throughout the gel.

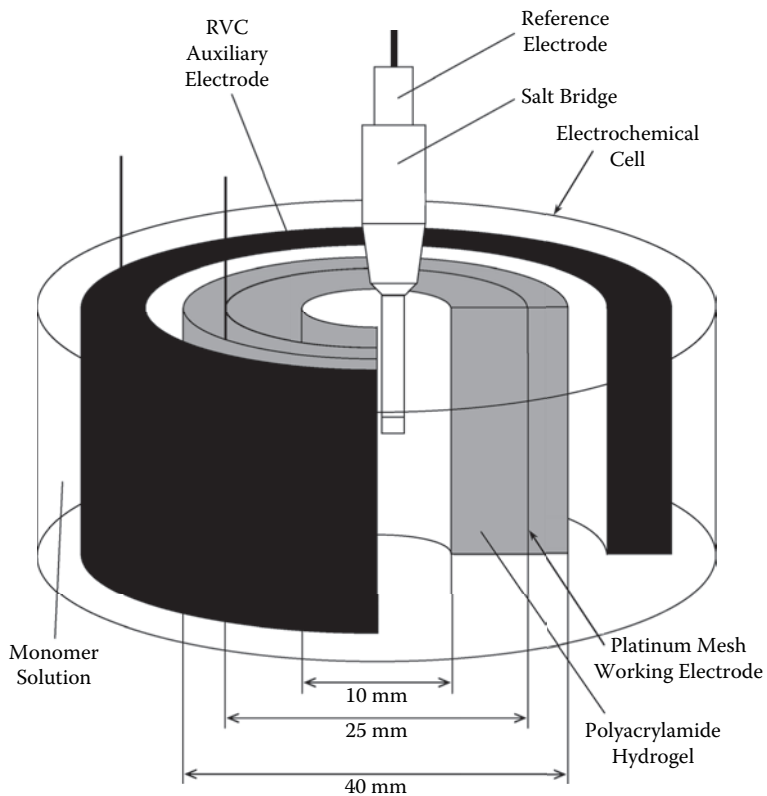


FIGURE 7.6 The gel cell.



FIGURE 7.7 A slab of polypyrrole gel composite.

This ability to pattern in three or two dimensions is critical to the development of intelligent material structures containing conducting electroactive polymers. Advances in patterning are described in the following section.

## DEVICE FABRICATION

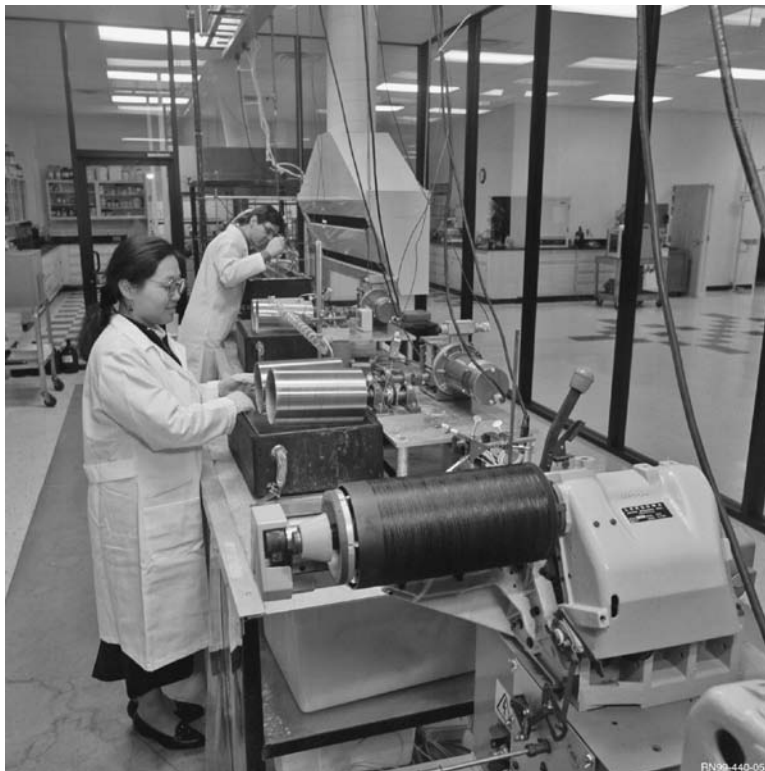
Processable conducting polymers, either by melt or solution means, are suitable for fabrication into the myriad of devices envisaged for these dynamic polymer systems. The nature of the fabrication process is necessarily determined by the performance required of the final product. However, the ultimate size and cost of the fabricated part are equally as important as the performance characteristics. In this section, we review some recent developments in the area of printing and fiber-spinning technologies that will impact the fabrication of conducting polymer devices in the future.

## FIBER-SPINNING TECHNOLOGIES

Fibers are useful building blocks for devices because of the well-developed spinning and weaving technologies that are available and because of the increasing use of high-performance fibers in advanced materials. Mass production of fibers and their weaving into textiles dates back to the early stages of the Industrial Revolution. The alignment of polymer chains (natural or synthetic) along the fiber axis enhances performance: both conductivity and mechanical properties of conducting polymers have been shown to be improved by producing fibers (including a draw process). The assembly of fibers through weaving and other processes is the basis of the mass production of textiles, carpets, and even paper products. Utilizing these well-developed technologies for the construction of conducting polymer-based devices is an extremely attractive prospect.

It is in the emerging field of electronic textiles that fiber spinning and conducting polymer technologies merge. An electronic textile contains electronic components seamlessly integrated into a conventional fabric structure. Although some examples seem futuristic (computers or mobile phones built into a sports jacket), others appear more achievable. For example, the addition to conventional fabrics of fibers that can also provide energy storage (batteries, capacitors) or energy conversion (photovoltaic, thermal energy harvesting, etc.) will be extremely useful for persons living or traveling in remote areas. The energy fabrics can be manufactured into tents and blankets, and the energy device can be used to power all manner of electrical devices from communications to cooking. Another application is in the area of biomedical monitoring. Here, a number of sensor fibers are built into garments and the sensor responses recorded, and in some scenarios automatically transmitted to health service providers. The range of potential applications is immense and includes baby monitors and triage services for injured soldiers.

Already solution-processable conducting polymers have been used to develop fiber products that may be used in the applications described earlier. In one commercial operation (Santa Fe Science and Technology, Inc.), continuous lengths of PAN fibers are made by a wet-spinning operation. The continuous nature of the operations enables control of fiber diameter and electronic properties. Conductivities of



**FIGURE 7.8** The polyaniline fiber-spinning facility at Santa Fe Science and Technology, United States (photo courtesy Ben Mattes).

up to  $1000 \text{ S cm}^{-1}$  have been reported and the mechanical properties are described as being similar to Nylon-6. Figure 7.8 shows the SFST fiber-spinning operation and the resultant product.

A number of workers have shown that it is necessary to synthesize PAN to high molecular weights to successfully prepare fibers and films with adequate mechanical properties. Laughlin and Monkman<sup>80</sup> have shown that a molecular weight of 130,000 g/mol is sufficient, whereas Mattes and coworkers<sup>81</sup> have investigated the effect of molecular weight in the range 100,000–300,000 g/mol. The higher the molecular weight, the more the films could be drawn and the higher was the tensile strength. Mattes and coworkers<sup>82</sup> have prepared PAN emeraldine base (EB) fibers by wet spinning. As-spun fibers had a modulus of 0.54 GPa, tensile strength of 15 MPa, and elongation at break of 9%, which were altered by drawing (4x) to 1.85 GPa, 63 MPa, and 6%, respectively.

As expected, the stretching of PAN films and fibers has a dramatic effect on the mechanical properties. In another study, EB films could be stretched by over 5 times their original length (at  $140^\circ\text{C}$ ), and this process was shown to produce a 10-fold increase in tensile strength (to 226 MPa<sup>83</sup>). Similarly, thermal stretch-orientation of EB fibers produces a tensile strength of 318 MPa, which reduces to 150 MPa when

HCl-doped to the emeraldine salt. Similar increases in elastic modulus would be expected to result from the mechanical drawing, because the process causes considerable alignment of the polymer chains in the draw direction. In one study, drawn EB films gave a room temperature modulus of 12 GPa,<sup>84</sup> which is considerably higher than is typical of unoriented polymers. Such mechanical orientation also increases the crystallinity<sup>84</sup> and conductivity of the PAN films and fibers.

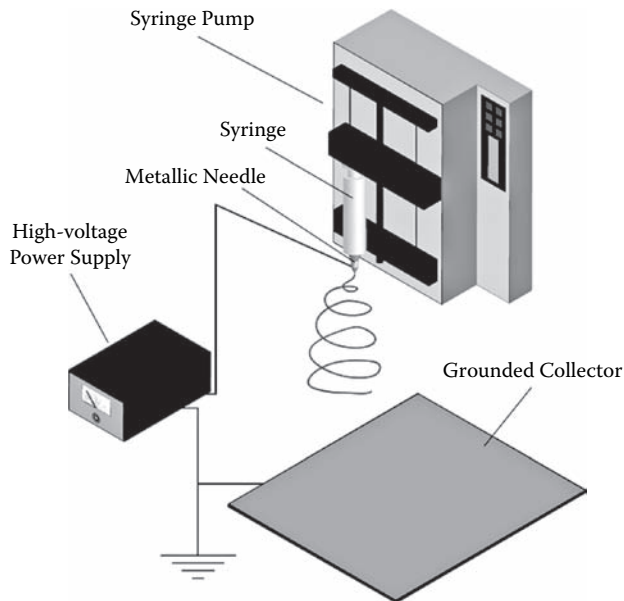
Direct preparation of PAN ES films and fibers from solution is also possible. Monkman and coworkers<sup>85</sup> have reported ES fibers showing a modulus of 2 GPa and tensile strength of 97 MPa with a conductivity of 600 S cm<sup>-1</sup>. These fiber properties were obtained after high-temperature drawing and annealing of the as-spun fibers. Similarly, in our own laboratories, we have produced PAN ES fibers in a one-step spinning process with and without carbon nanotubes as reinforcement.<sup>86</sup> The drawn fibers had a modulus of 3.4 GPa, tensile strength of 170 MPa, and elongation at break of 9%. With the addition of 0.76% (w/w) carbon nanotubes, these properties changed to 7.3 GPa, 255 MPa, and 4%. In addition, the conductivity increased from 500 to 700 S/cm with the addition of the nanotubes. In comparison, PAN ES fibers prepared by first wet-spinning leucoemeraldine and then post-treating to produce the ES showed inferior mechanical and electrical properties: modulus 3.5 GPa, tensile strength 45 MPa, elongation at break 4.6%, and conductivity 96 S/cm.<sup>87</sup>

An important hardware addition in the development of fiber-spinning protocols is the availability of customized wet-spinning apparatus from Nakamura Services Co. in Japan (Figure 7.9).

Recently,<sup>88,89,90</sup> there has also been much interest in the formation of nanofibers using electrospinning. The method (illustrated in Figure 7.10) is a straightforward way to make long polymer fibers with diameters ranging from 100 nm to 2 μm.



**FIGURE 7.9** The customized wet-spinning apparatus at the Intelligent Polymer Research Institute, University of Wollongong.



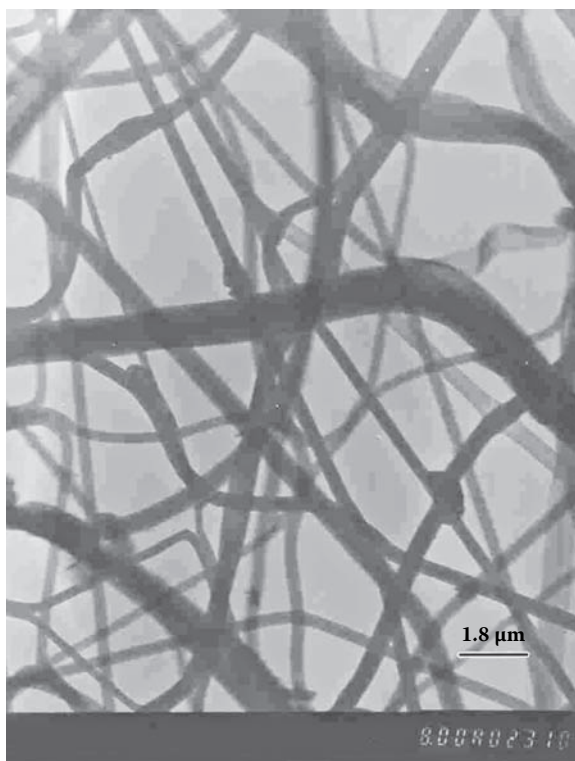
**FIGURE 7.10** Schematic diagram of electrospinning. (From Dan Li, Jesse T. McCann, and Younan Xia, *Electrospinning: A simple and versatile technique for producing ceramic nanofibers and nanotubes*, *J. Am. Ceram. Soc.*, 2006, 89, 1861–69. With permission.)

The method involves dissolving the polymer in a suitable solvent and then applying a large voltage difference between a metal capillary containing the solution (e.g., a syringe) and a target. The target may be a metal foil upon which the nanofibers deposit. The high voltage induces the free charges in the polymer solution to move, and the result is a jet of solution that flows from the capillary to the target to form an oriented network (Figure 7.10). Recently, a method was also reported for fiber alignment using a modified electrospinning method.<sup>89</sup> Conducting polymer fibers have recently been formed by the electrospinning process as reported by MacDiarmid and coworkers,<sup>90</sup> whereas Figure 7.11 shows fibers containing polythiophenes produced in this manner with one of our collaborators.

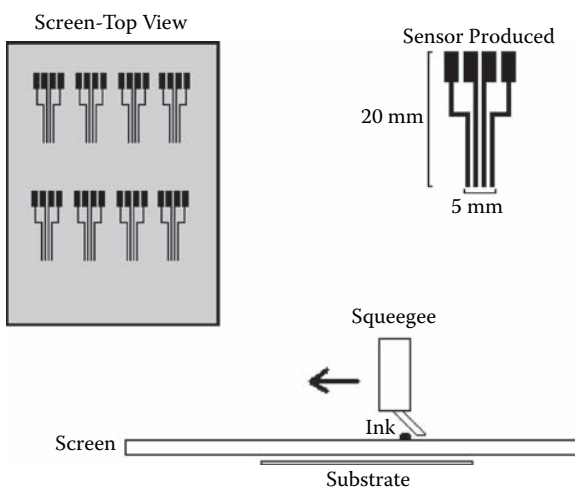
## PRINTING TECHNOLOGIES

Printing is also an old art that is now seen in a new light for fabrication of advanced products including electronic components. Solution-processable CEPs are inherently suitable for fabrication using printing methods, and their availability is already leading to low-cost sensors and cheap, disposable electronics.

In our own laboratories,<sup>91</sup> we have used conventional screen-printing techniques for the manufacture of sensors (Figure 7.12). In one example, conducting tracks of ~1 mm in width and 17 mm long were printed onto plastic substrates, and conducting polymer was subsequently deposited over the tracks to make a four-probe gas sensor. Similar techniques have been used to generate all-polymer field-effect transistors. The great advantage of screen printing is its suitability for coating fabrics. Thus,



**FIGURE 7.11** Electrospun fibers of poly(vinylalcohol) containing sulfonated polyaniline.



**FIGURE 7.12** The screen-printing process involved in preparation of carbon track electrodes on polymer substrates.



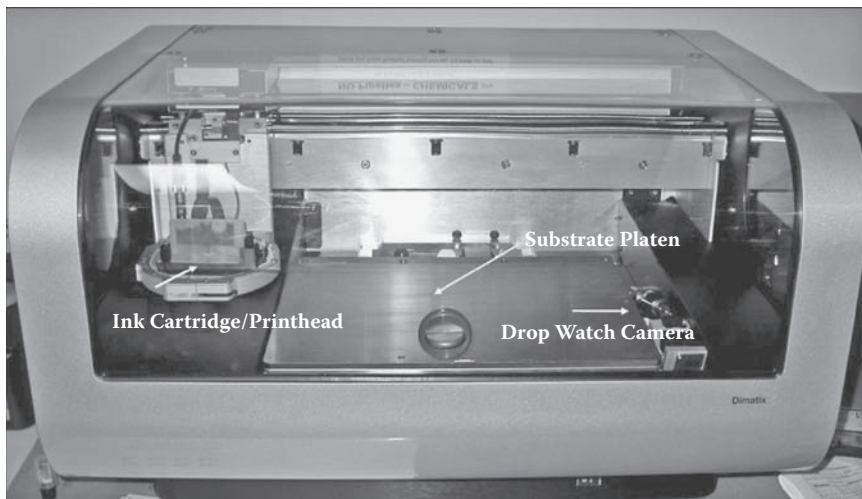
screen printing provides a new option for preparing electronic textiles in addition to the CEP fiber structures described earlier. The biggest disadvantage of screen printing is that only 100  $\mu\text{m}$  resolution is typically available, making it unsuitable for microfabrication.

Recent developments show, however, that microscale electronics can be made even with readily available ink-jet printers. De Rossi and coworkers<sup>92</sup> have used ink-jet printing to make 3-D structures from soluble conducting polymers. Several groups have reported the production of polymer light-emitting diodes using ink-jet printing to deposit lines or pixels. The thickness of the deposited layers is  $\sim 200$  nm, and the minimum width is limited to  $\sim 200$  nm. The resolution is ultimately limited by the ink-jet printing process, which involves the deposition of droplets onto the substrate. The droplet size and spreading before evaporation determine the resolution. Richard Friend and coworkers<sup>93</sup> from the Cavendish Laboratory, University of Cambridge, have significantly improved the resolution of the ink-jet printing process by first patterning the surface with hydrophilic and hydrophobic regions. Using such methods, these researchers were able to prepare features to 5  $\mu\text{m}$  in width and prepared all-polymer transistor circuits that showed performance similar to those made by photolithography methods.

Yoshioka and Jabbour have used a desktop ink-jet printer to prepare PEDOT/PSS electrodes as components for organic light-emitting diodes.<sup>94</sup> We have prepared PAN nanodispersions that are amenable to printing from a desktop unit.<sup>95</sup> This has been used as a convenient route to producing novel chemical-sensing surfaces. Reactive printing in which the oxidant is delivered using ink-jet printing to produce patterns followed by exposure to monomer in the vapor phase is an alternative approach to obtaining printed patterns.<sup>96</sup>

A significant advance for these involved in the use of ink-jet printing for device fabrication is the introduction of much more flexible ink-jet printing hardware. For example, the Dimatix printer (Figure 7.13) enables printing of solutions/dispersions using a range of solvents with temperature control of both the printing head and the substrate stage. We have used this system to print PAN-based “inks” with high resolution and low resistivity.<sup>97</sup>

Similar techniques have been used to generate finer resolution by microcontact printing methods. These methods are suitable for preparing features as small as 100 nm.<sup>98</sup> The process involves forming a rubber stamp, the surface of which is painted with a masking ink. The ink is transferred to the substrate and forms the pattern of the stamp on the substrate. The stamped areas can then be coated with soluble conducting polymers. In one example, polythiophenes were deposited on hydrophilic areas formed in a prior microprinting step. In another process, a polythiophene derivative was directly stamped onto a conductive ITO-glass surface although the feature size was quite large (100  $\mu\text{m}$ ). A final variation of the microcontact printing technique has been widely explored by Alan MacDiarmid and colleagues.<sup>99</sup> In this method, the surface to be coated is stamped with a hydrophobic self-assembled monolayer (e.g., organothiol on a gold surface), and a conducting polymer is deposited by electropolymerization. MacDiarmid’s contribution was to use the same technique but with chemical-initiated polymerization. Conducting polymer lines and other shapes could then be deposited on virtually any substrate, including flexible plastics. In yet



**FIGURE 7.13** Dimatix DMP2800 ink-jet printer.

another variation, Honholtz and MacDiarmid<sup>100</sup> also showed that the mask could be made by a regular office laser printer. A printed substrate could be uniformly coated by *in situ* polymerization and the laser-printed regions subsequently removed by ultrasonication.

These examples serve to illustrate the enormous interest in mass production techniques for preparing low-cost devices based on conducting electroactive polymers. No doubt, the future development of such techniques will lead to commercial products allowing the integration of electronics into a number of conventional host structures. The most dramatic of which may include flexible plastic electronic components and electronic textiles and fabrics. These developments have been hastened by the recent advent of processable conducting polymers. Tremendous opportunities now arise in marrying these processable conducting polymers with the age-old arts of knitting, weaving, and printing.

## REFERENCES

1. Angelopoulos, M.; Atruisa, G.E.; Ermer, S.P.; Ray, A.; Scherr, E.M.; MacDiarmid, A.G.; Akhtar, M.; Kiss, Z.; Epstein, A. *J. Mol. Cryst. Liq. Cryst.* 1988, 20: 151.
2. Cao, Y.; Smith, P.; Heeger, A.J. In *Conjugated Polymeric Materials: Opportunities in Electronics, Opto-electronics and Molecular Electronics*. Bredas, J.L.; Chance, R.R. (Eds.). Kluwer Academic Publishers, Dordrecht, The Netherlands, 1990.
3. Andretta, A.; Cao, Y.; Chiang, J.C.; Heeger, A.J.; Smith, P. *Synth. Met.* 1988, 26: 383.
4. Cao, Y.; Smith, P.; Heeger, A.J. *Synth. Met.* 1992, 48: 91.
5. Heeger, A.J. *Synth. Met.* 1993, 55: 3471.
6. Pron, A.; Nicolau, F.; Genond, F.; Nechstein, M. *J. Appl. Polym. Sci.* 1997, 63: 971.
7. Gazolti, W.A.; Faez, R.; De Paoli, M.A. *Eur. Polym. J.* 1999, 35: 35.
8. Su, S.J.; Kuramoto, N. *Synth. Met.* 2000, 108: 121.
9. Ruhe, J.; Ezquerra, T.; Wegner, G. *Makromol. Chem. Rapid. Commun.* 1989, 10: 103.
10. Walwa, H.S. *Die Angewandte Makromolekulare Chemie* 1991, 188: 105.

11. Ashraf, S.A.; Chen, F.; Too, C.O.; Wallace, G.G. *Polymer* 1996, 37: 2811.
12. Faid, K.; Cloutier, R.; LeClerc, M. *Synth. Met.* 1993, 55: 1272.
13. Patil, A.O.; Ikenoue, Y.; Basescu, N.; Colaneri, N.; Chen, J.; Wudl, F.; Heeger, A.J. *Synth. Met.* 1987, 20: 151.
14. Ikenoue, Y.; Uotani, N.; Patil, A.O.; Wudl, F.; Heeger, A.J. *Synth. Met.* 1989, 30: 305.
15. Ikenoue, Y.; Tomozawa, H.; Saida, Y.; Kira, M.; Yashima, H. *Synth. Met.* 1991, 40: 333.
16. Yue, J.; Wang, Z.H.; Cromack, K.R.; Epstein, A.J.; MacDiarmid, A.G. *J. Am. Chem. Soc.* 1991, 113: 2665.
17. Shimizu, S.; Saitoh, T.; Uzawa, M.; Yuasa, M.; Yano, K.; Muruyama, T.; Watanabe, K. *Synth. Met.* 1997, 85: 1337.
18. Guo, R.; Barisci, J.N.; Innis, P.C.; Too, C.O.; Zhou, D.; Wallace, G.G. *Synth. Met.* 2000, 114: 267.
19. Zhou, D.; Innis, P.C.; Shimizu, S.; Maeda, S.; Wallace, G.G. *Synth. Met.* 2000, 114: 287.
20. Masdarolomoor, F.; Innis, P.C.; Ashraf, S.; Wallace, G.G. *Synth. Met.* 2005, 153: 181.
21. Aldissi, M.; Armes, S.P. *Progr. Org. Coat.* 1991, 19: 21.
22. Eisazadeh, H.; Spinks, G.; Wallace, G.G. *Mat. Forum.* 1993, 17: 241.
23. Bose, C.S.C.; Basak, S.; Rajeshwark, K. *J. Electrochem. Soc.* 1992, 139: L75.
24. Paul, R.K.; Pillai, C.K.S. *J. Appl. Polym. Sci.* 2001, 80: 1354.
25. Paul, R.K.; Pillai, C.K.S. *Polym. Int.* 2001, 50: 381.
26. Paul, R.K.; Vijayanathan, V.; Pillai, C.K.S. *Synth. Met.* 1999, 104: 189.
27. Bjorklund, R.B.; Lundstrom, I. *J. Electron. Mater.* 1984, 13: 211.
28. Teasdale, P.R.; Wallace, G.G. *Polym. Int.* 1994, 3: 197.
29. MacDiarmid, A.G.; Epstein, A.J. *Faraday Discuss. Chem. Soc.* 1989, 88: 317.
30. Malinauskas, A. *Polymer* 2001, 42: 3957; and references cited therein.
31. Zheng, W.; Min, Y.; MacDiarmid, A.G.; Angelopoulos, M.; Liao, Y.-H.; Epstein, A.J. *Synth. Met.* 1997, 84: 63.
32. Stejskal, J.; Sapurina, I.; Prokes, J.; Zemek, J. *Synth. Met.* 1999, 105: 195.
33. Huang, Z.; Wang, P.-C.; MacDiarmid, A.G.; Xia, Y.; Whitesides, G. *Langmuir* 1997, 13: 6480.
34. Kane-Maguire, L.A.P.; MacDiarmid, A.G.; Norris, I.D.; Wallace, G.G.; Zheng, W. *Synth. Met.* 1999, 106: 171.
35. Neoh, K.G.; Teo, H.W.; Kang, E.T.; Tan, K.L. *Langmuir* 1998, 14: 2820; and references cited therein.
36. Wan, M.X.; Li, M.; Li, J.C.; Liu, Z.X. *Thin Solid Films* 1995, 259: 188.
37. Gregory, R.V.; Kimbrell, W.C.; Kuhn, H.H. *Synth. Met.* 1989, 28: C823.
38. Armes, S.P.; Gottesfeld, S.; Beery, J.G.; Garzon, F.; Mombourquette, C.; Hawley, M.; Kuhn, H.H. *J. Mater. Chem.* 1991, 1: 525.
39. Byun, S.W.; Im, S.S. *Polymer* 1998, 39: 485.
40. Trivedi, D.C.; Dhawan, S.K. *J. Mater. Chem.* 1992, 2: 1091.
41. Wan, M.; Yang, J. *J. App. Polym. Sci.* 1993, 49: 1639.
42. Yoshino, K.; Morita, S.; Yin, X.H.; Onoda, M.; Yamamoto, H.; Watanuki, T.; Isa, I. *Synth. Met.* 1993, 55: 3562.
43. Chen, Y.; Qian, R.; Li, G.; Li, Y. *Polym. Comm.* 1991, 32: 189.
44. Kelkar, D.S.; Bhat, N.V. *Polymer* 1993, 34: 986.
45. Zinger, B.; Kijel, D. *Synth. Met.* 1991, 41: 1013.
46. Pouzet, S.; LeBolay, N.; Ricard, A.; Jousse, F. *Synth. Met.* 1993, 55: 1079.
47. Yang, S.; Ruckenstein, E. *Synth. Met.* 1993, 60: 249.
48. Ruckenstein, E.; Yang, S. *Polymer* 1993, 34: 4655.
49. Yang, S.; Ruckenstein, E. *Synth. Met.* 1993, 59: 1.

50. Beadle, P.; Armes, S.P.; Gottesfeld, S.; Mombourquette, C.; Houltan, R.; Andrews, W.D.; Agnew, S.F. *Macromolecules* 1992, 25: 2526.
51. Bhat, N.V.; Joshi, N.V. *J. Appl. Polym. Sci.* 1993, 50: 1423.
52. Wang, Y.; Rubner, M.F. *Macromolecules* 1992, 25: 3284.
53. Ruckenstein, E.; Park, J.S. *J. Appl. Polym. Sci.* 1991, 42: 925.
54. Ruckenstein, E.; Chen, J.H. *J. Appl. Polym. Sci.* 1991, 43: 1209.
55. Mohammadi, A.; Paul, D.W.; Ingnas, O.; Nilsson, J.O.; Lundstrom, I. *J. Polym. Sci. Part A. Polym. Chem.* 1994, 32: 495.
56. Iyoda, T.; Ohtani, A.; Honda, K.; Simidzu, T. *Macromolecules* 1990, 23: 1971.
57. Nakata, M.; Kise, H. *Polym. J.* 1993, 2: 91.
58. Dubistky, Y.A.; Zhubanov, B.A. *Synth. Met.* 1993, 53: 303.
59. Martin, C.R.; Liang, W.; Menan, V.; Parthasarathy, R.; Parthasarathy, A. *Synth. Met.* 1993, 55: 3766.
60. Pouzet, S.; Le Bolay, N.; Ricard, A. *Synth. Met.* 1993, 55: 1495.
61. Ge, H.; Wallace, G.G. *Anal. Chem.* 1989, 61: 2391.
62. Li, S.; White, H.S. *J. Electrochem. Soc.* 1993, 140: 2473.
63. Bhadani, S.N.; Kumari, M.; Sen Gupta, S.; Sahu, G. *J. Appl. Polym. Sci.* 1997, 64: 1073.
64. Iroh, J.O.; Chen, Y. *Polymer Composites* 1999, 20: 482.
65. Niwa, O.; Tamamura, T. *J. Chem. Soc. Chem. Commun.* 1984, 817.
66. De Paoli, M.; Waltman, R.J.; Diaz, A.F.; Bargan, J. *J. Chem. Soc. Chem. Commun.* 1984, 1015.
67. Wang, T.T.; Tasaka, S.; Hutton, R.S.; Lu, P.Y. *J. Chem. Soc. Chem. Commun.* 1985, 1343.
68. Geibler, U.; Hallensleben, M.L.; Toppare, L. *Adv. Mater.* 1991, 3: 104.
69. Dogan, S.; Akbulut, U.; Toppare, L. *Synth. Met.* 1992, 53: 29.
70. Park, Y.H.; Myeong, H.H. *J. Appl. Polym. Sci.* 1973, 45: 992.
71. Chiu, H.T.; Lin, J.S.; Huang, L.T. *J. Appl. Electrochem.* 1992, 22: 528.
72. Wang, H.L.; Fernandez, J.E. *Macromolecules* 1992, 25: 179.
73. Wang, H.L.; Fernandez, J.E. *Macromolecules* 1993, 26: 3336.
74. Xue, Z.; Bi, X.Y. *J. Appl. Polym. Sci.* 1993, 47: 2073.
75. Sung, J.Y.; Huang, H.J. *Anal. Chim. Acta* 1991, 246: 275.
76. Tassi, E.L.; De Paoli, M.A.; Panero, S.; Scrosati, B. *Polymer* 1994, 35: 565.
77. Dogan, S.; Akbulut-U.; Toppare, L. *Synth. Met.* 1992, 53: 29.
78. Kim, B.C.; Spinks, G.M.; Wallace, G.G.; John, R. *Polymer* 2000, 41: 1783.
79. Small, C.J.; Too, C.O.; Wallace, G.G. *Polym. Gels Networks* 1997, 5: 251.
80. Laughlin, P.J.; Monkman, A.P. *Synth. Met.* 1997, 84: 765.
81. Adams, P.N.; Bowman, D.; Brown, L.; Yang, D.; Mattes, B.R. *Proc. SPIE—The Int. Soc. Opt. Eng.* 2001, 4329: 475.
82. Wang, H.L.; Romero, R.J.; Mattes, B.R.; Zhu, Y.T.; Winokur, M.J. *J. Polym. Sci. Pt B. Polym. Phys.* 2000, 38: 194.
83. MacDiarmid, A.G.; Epstein, A.J. *Mater. Res. Soc. Symp. Proc.* 1992, 247: 565.
84. Okuzaki, H.; Kira, T.; Kunugi, T. *J. Appl. Polym. Sci.* 2000, 75: 566.
85. Pomfret, S.J.; Adams, P.N.; Comfort, N.P.; Monkman, A.P. *Polymer* 2000, 41: 2265.
86. Mottaghitalab, V.; Spinks, G.M.; Wallace, G.G. *Polymer* 2006, 47: 4996.
87. Mottaghitalab, V.; Xi, B.B.; Spinks, G.M.; Wallace, G.G. *Synth. Met.* 2006, 156: 796.
88. Reneker, D.H.; Chun, I. *Nanotechnology* 1996, 7: 216.
89. Theron, A.; Zussman, E.; Yarin, A.L.; *Nanotechnology* 2001, 12: 384.
90. MacDiarmid, A.G.; Jones, W.E.; Norris, I.D.; Gao, J.; Johnson, A.T.; Pinto, N.J.; Hone, J.; Han, B.; Ko, F.K.; Okuzaki, H.; Llaguno, M. *Synth. Met.* 2001, 119: 27.
91. Shepherd, R.L.; Barisci, J.N.; Collier, W.A.; Hart, A.L.; Partridge, A.C.; Wallace, G.G. *Electroanalysis* 2002, 14: 575.

92. Pede, D.; Serra, G.; De Rossi, D. *Mater. Sci. Eng.* 1998, C5: 289.
93. Sirringhaus, H.; Kawase, T.; Friend, R.H.; Shimida, T.; Inbasekaran, M.; Wu, W.; Woo, E.P. *Science* 2000, 290: 2123.
94. Yoshioka, Y.; Jabbour, G.E. *Synth. Met.* 2006, 156: 779.
95. Ngamna, O.; Morrin, A.; Killard, A.J.; Moulton, S.E.; Smyth, M.R.; Wallace, G.G. *Langmuir* 2007, 23: 8569.
96. Winther-Jensen, B.; Clark, N.; Subramanian, P.; Helmer, R.; Ashraf, S.; Wallace, G.; Spiccia, L.; MacFarlane, D. *J. Appl. Polym. Sci.* 2007, 104: 3938.
97. Small, W.R.; Masdarolomoor, F.; Wallace, G.G.; in het Panhuis, M. *J. Mat. Chem.* 2007, 17: 4359.
98. Holdcroft, S. *Adv. Mater.* 2001, 12: 1753.
99. Huang, Z.; Wang, P-C.; MacDiarmid, A.G.; Xia, Y.; Whitesides, G. *Langmuir* 1997, 13: 6480.
100. Honholtz, D.; MacDiarmid, A.G. *Synth. Met.* 2001, 121: 1327.

---

# Index

## A

AABSA (azobenzenesulfonic acid), 169  
Academic research, 5, 9–10  
Acetonitrile solvent, 71, 141  
Acid-catalyzed polymerization, 83–84  
AFM, *see* Atomic force microscopy (AFM)  
Agarose gels, 241  
Aligned polymer nanowire structures, 170–171  
Alkyl- and alkoxy-substitutions  
    polyanilines synthesis, 152  
    polythiophenes, 203–206  
Allied Signal (company), 17  
Aluminum, corrosion protection, 22  
Aniline monomers, 147  
Anionic species, 21  
Anions  
    chemical sensors, 23  
    dopant counterion, 77  
    polyaniline synthesis, 156–158  
Applications  
    areas, 9  
    biomedical, 9, 24, 26–27, 30–31  
    electromagnetic interference, 11  
    electronics, 217  
    electrostatic discharge, 11  
    metal replacement, 11  
    shorter-term opportunities, 10  
    utilization of conductivity, 11–12  
Approaches, polyaniline synthesis, 150–152  
AQSA (anthraquinonesulfonic acid), 79  
Artificial muscles, 27, 30–31  
Assembly, in host matrices, 235  
Asymmetric induction, 193  
Atomic force microscopy (AFM)  
    chiroptical properties, polythiophenes, 224  
    polyaniline morphology and density, 167  
    scanning probe microscopy, 43, 44  
    solution-cast polythiophenes, 214  
    surface morphology and film density, 90  
Auxiliary electrodes, 69

## B

Base forms, polyanilines, 189–191  
Batteries, 9, 13  
BIEDOT (3,4-ethylenedioxythiophene), 221  
Bilirubin oxidase (BOX), 83  
Bioactive molecule incorporation, 186

Biochemical properties, 114–118  
Biomedical applications  
    application area, 9  
    artificial muscles, 27, 30–31  
    cellular communications, 26–27  
    fundamentals, 24  
    sensors, 27  
Bionic Ear, 27, 30  
Biosensors, 23  
Bithiophenes, 199–200  
BNSA (butyl-naphthalenesulfonic acid), 79  
BOX (bilirubin oxidase), 83  
Braille, 17–18  
Branching, 86–88  
Brønsted acids  
    Lewis acids, 157  
    polyanilines, postpolymerization  
        modification, 155–156  
Bulk structure, polyaniline synthesis, 160

## C

Cambridge Display Technologies (company), 16  
Cambridge University, 15–16  
Carbon nanotubes (CNT)  
    fiber-spinning technologies, 245  
    nanostructured approach, 95  
    nanostructured polyanilines, 171  
Cationic species, 21  
Cauliflower structure/surface  
    conductivity, 105  
    dry-state mechanical properties, 128  
    surface morphology and film density, 89–90  
Cavendish Laboratory, 248  
CD, *see* Circular dichroism (CD) spectra and spectroscopy  
Cellular communications, 26–27  
Chain conformation, 160  
Chaotropic effect, 113  
Characterization tools, 32  
Charge delocalization, 186  
CHCl<sub>3</sub> solvent, 80  
Chemical analysis, 37, 39–40  
Chemical polymerization  
    polyaniline synthesis, 143–147  
    polypyrroles assembly, 75  
    polythiophene synthesis, 201–202  
    processing and device fabrication, 235

- Chemical properties
    - polyanilines, 186–187
    - polypyrroles, 114–118
    - polythiophenes, 219
  - Chemical sensors, 22–24
  - Chiral characteristics
    - discrimination, 193
    - dopant anions/cations, 156–158
    - induction, poly(*ortho*-toluidine), 158
    - separations, 122
  - Chiroptical properties
    - polypyrroles, 121
    - polythiophenes, 222–225
  - Chitosan, 92
  - Chloranil
    - electron acceptors polymerization, 149
    - oxidants, 76
  - Circular dichroism (CD) spectra and spectroscopy
    - chiroptical properties, polythiophenes, 222–225
    - fundamentals, 46, 47–48
    - polyanilines, 191–192
    - solvatochromism, 221
    - thermochromism, 221
  - CITS, *see* Current-imaging tunneling spectroscopy (CITS)
  - Clemmenson reduction, 82
  - CNT, *see* Carbon nanotubes (CNT)
  - Cochlear explant, 27
  - Cochlear implant, 27
  - Cold pressing, 237
  - Colloidal dispersions
    - polyaniline synthesis approach, 150, 151–152
    - polypyrroles assembly, 80–81
  - Colloids
    - polyaniline electrochemical polymerization, 142–143
    - solution-processable CEPs, 233
  - Colors and color changes
    - chemical polymerization mechanism, 143
    - electrochromic devices, 16–17
    - switching properties, 185–186
    - water-soluble polythiophenes, 208
  - Communications tools, 32
  - Compact coil conformation
    - conductivity, 181
    - level and chain conformation, 120
    - polyaniline base forms, 190
  - Complexation, *see* Doping
  - Conductive electroactive polymers, 5
  - Conductivity
    - alkylated thiophenes, 217
    - obtaining higher, 87
    - polyaniline electrical properties, 179, 181–182
    - polypyrroles, 103–105
    - polythiophenes, 216–217
  - Conformation
    - electropolymerized polythiophenes, 212–213
    - polyaniline synthesis, 158–161
    - polythiophenes, 211–212
  - Controlled-release devices, 21–22
  - Copper, corrosion protection, 22
  - Core-shell approach, 152
  - Corrosion protection, 22, 140
  - Counterion/cation effect, 71, 73–74
  - Counterion-induced solubilization, 79–80
  - Counterions
    - chemical properties, 116–117, 186
    - conductivity, 105
    - dry-state mechanical properties, 126–127
    - electropolymerization, 200
    - morphology and density, 167
    - polythiophene properties, 219–220
  - Covalently bound chiral substitution, 153
  - Covalent substitution, 154–155
  - CRC Cochlear Implant, 27
  - Cross-coupling, 205
  - Crosslinking
    - dry-state mechanical properties, 127
    - electrochemically prepared films, 187
    - melt-processable CEPs, 234
    - polyacrylamides, 241
    - polypyrroles assembly, 86–88
    - polythiophene properties, 217
    - self-stabilized dispersion polymerization, 147
  - Crystallinity
    - electropolymerized polythiophenes, 212–213
    - polyaniline synthesis, 160–161, 166
    - polypyrroles assembly, 88–89
  - Current-imaging tunneling spectroscopy (CITS)
    - nanoscale heterogeneity, 160
    - scanning probe microscopy, 44
  - CV, *see* Cyclic voltammetry (CV)
  - Cyclic resistogram, 109
  - Cyclic voltammetry (CV)
    - electrochemical conditions, 67
    - electrochemical methods, 33–34
    - electrode materials, 69–70
    - localized electrochemical mapping, 51
    - switching properties, 109, 183
    - vapor-phase deposition, 148
  - Cyclodextrins, 169, 171
- ## D
- DBSA (dodecylbenzenesulfonate)
    - Brönsted acids, 155
    - counterion-induced stabilization, 79–80
    - dopant counterion, 77
    - level and chain conformation, 120–121
    - nanostructured polyanilines, 168
  - DCA, *see* Dynamic contact angle (DCA) analysis

- DDQ (2,3-dichloro-5,6-dicyano-*p*-benzoquinone), 76
- DEHPSA (di(2-ethylhexyl)ester of 4-sulfophthalic acid), 188
- Delocalization, charge, 186
- Dendritic nanoaggregate structures, 91–92
- Density
- polyanilines, 166–168
  - surface morphology and films, 89–91
- Deposition
- electrode materials, 68
  - polyaniline synthesis, 171
  - in situ* chemical polymerization, 78–79
- Deposition, on glass/plastics, 235–238
- Devices, fabrication, 243, *see also* Processing and device fabrication
- Diaphragmatic chemical polymerization, 238–239
- Differential scanning calorimetry (DSC)
- electrochemical integration, 241
  - electrochemically prepared films, 189
  - solvents, 141
- Dimatix printer, 248
- Display technologies, 15–16
- DMA, 189
- DMF, 194
- DMPU (*N,N'*-dimethyl propylene urea)
- solution-cast emeraldine base, 161–162
  - solvatochromism and thermochromism, 194
- DMSO (dimethylsulfoxide)
- counterion-induced stabilization, 80
  - electrochemical integration, 240
  - solvatochromism and thermochromism, 194
- Dodecylbenzenesulfonic acid, 231
- Dopants
- anions/cations, 156–158
  - counterion ( $A^-$ ), 77
  - polyaniline chemical polymerization, 144–145
  - polyaniline electrochemical polymerization, 140–141
- Doping
- polythiophene properties, 220–221
  - secondary, 166, 181
- Double-strand polyanilines, 167
- Dow Chemical (company), 16
- Dry-state properties, 123, 126–128
- DSC, *see* Differential scanning calorimetry (DSC)
- Ductility, 188
- DuPont (company), 16
- Dynamic contact angle (DCA) analysis, 40–42
- E**
- EAMEX, 17
- EB, *see* Emeraldine base (EB)
- EC-AFM, *see* Electrochemical atomic force microscopy (EC-AFM)
- EC-STM, *see* Electrochemical scanning tunneling microscopy (EC-STM)
- EDOT
- chiroptical properties, polythiophenes, 225
  - electropolymerization, 201
  - vapor-phase polymerization, 202
- EFM, *see* Electrical force microscopy (EFM)
- EIS, 51
- Electrical force microscopy (EFM), 44–45
- Electrically stimulated light emission, 15–16
- Electrical properties
- polyanilines, 179–183
  - polypyrroles, 103–105
- Electrochemical atomic force microscopy (EC-AFM), 46
- Electrochemical properties and conditions
- asymmetric synthesis, 122
  - integration, 239–243
  - polymerization, 138–143
  - polypyrroles assembly, 66–75
  - prepared films, 187–189
  - pumping, 20
  - switching/energy storage/conversion, 12–14
  - tools, 32–35
- Electrochemical quartz crystal microbalance (EQCM)
- fundamentals, 35
  - localized electrochemical mapping, 51
  - switching properties, 111
- Electrochemical scanning tunneling microscopy (EC-STM), 46
- Electrochromics, 16–17
- Electrode materials
- polyaniline electrochemical polymerization, 140
  - polypyrroles assembly, 68–70
- Electrodeposition, 31
- Electroless polymerization, 150
- Electrolyte choice, 71, 73–74
- Electromagnetic interference (EMI), 11
- Electromechanical actuators, 17–18
- Electromechanical analysis (EMA), 36–37
- Electron acceptor polymerization, 149
- Electron-beam patterning resolution, 12
- Electronic band structure
- optical properties, 119
  - polythiophene optical properties, 221
- Electronic nose systems, 23–24
- Electronic textiles, *see* Fiber-spinning technologies
- Electron spin resonance (ESR) spectroscopy
- fundamentals, 49, 51
  - polyaniline optical properties, 189



Electropolymerization, *see also* Polymerization  
 polypyrroles assembly, 59–60, 62–63  
 polythiophenes, 197–201, 212–213

Electrospinning  
 fiber-spinning technologies, 245–246  
 nanostructured polyanilines, 170

Electrostatic discharge (ESD), 11

Elongation at break, 129, *see also* Young's modulus

EMA, *see* Electromechanical analysis (EMA)

Emeraldine base (EB)  
 chiral discrimination, 193  
 chiral dopant anions/cations, 156  
 circular dichroism spectra, 191–192  
 conductivity, 179  
 electrochemically prepared films, 188–189  
 enhancing functionality, 154–155  
 fiber-spinning technologies, 244  
 Lewis acids, 157  
 molecular structure, 160–161  
 molecular weight, 159  
 polyaniline base forms, 189–190  
 polyaniline synthesis, 161–163  
 salt from protonation, 163  
 solution-cast, 161–163  
 solution-processable CEPs, 231  
 solvatochromism and thermochromism, 194

Emeraldine salt (ES) and salt state  
 chemical polymerization, 235  
 conductivity, 137, 179  
 controlled-release devices, 22  
 deposition, on glass/plastics, 235  
 electrochemically prepared films, 187–189  
 electropolymerized, 166  
 fiber-spinning technologies, 245  
 molecular structure, 160–161  
 nanoscale heterogeneity, 160  
 polyanilines, 150, 163–166  
 solution-cast, 163–164  
 sulfonic acid substitution, 153

EMI, *see* Electromagnetic interference (EMI)

Emulsion polymerization, 150–151

Environmental effects on, 128–132

Enzyme-catalyzed polymerization  
 polyaniline synthesis, 148–149  
 polypyrroles assembly, 83–84

EQCM, *see* Electrochemical quartz crystal microbalance (EQCM)

ESD, *see* Electrostatic discharge (ESD)

ESR, *see* Electron spin resonance (ESR) spectroscopy

Etching, 31

Expanded/extended coil conformation  
 conductivity, 181  
 level and chain conformation, 120  
 polyaniline base forms, 190

Extra functionality, 84–86

## F

Fabrication after polymerization, 231

Fabrics  
 deposition, on glass/plastics, 236  
*in situ* chemical polymerization, 78–79

Fibers  
 polymerization environment/cell design, 66  
*in situ* chemical polymerization, 78–79

Fiber-spinning technologies, 243–246

Films  
 chemical properties, 187  
 comparison, 147  
 density, 89–91  
 freestanding, 187  
 polythiophene properties, 218  
 thickness, 213

Flow-through electrochemical cell, 65

Fourier transform infrared (FTIR)  
 nigraniline oxidation state, 150  
 solvents, 141

Freestanding films, 187

Friedel-Crafts alkylation, 81–82

Fullerene, 170

Functional groups  
 conductivity, 105  
 monomer, 74

Functionality, enhanced, 84–86

## G

Galvanic coupling, 22

Gel permeation chromatography (GPC), 86

Gels, 241

Ge series probe, 39

Glass deposition, 78

Glass fabrics, 236

Glass wool, 236

Glucose oxidase (GOD), 95

GOD, *see* Glucose oxidase (GOD)

GPC, *see* Gel permeation chromatography (GPC)

Grignard reaction and coupling methods  
 chemical polymerization, 201  
 substituted polythiophenes, 203, 206

## H

Halogens, oxidants, 76

HCSA (camphorsulfonic acid)  
 Brønsted acids, 155  
 chiral discrimination, 193  
 chiral dopant anions/cations, 156  
 circular dichroism spectra, 191–192  
 counterion-induced stabilization, 80  
 solution-processable CEPs, 231  
 solvatochromism and thermochromism, 193–194

- Head-to-tail couplings and position  
  Brönsted acids, 155  
  chemical polymerization mechanism, 143  
  fundamentals, 137  
  molecular structure and conformation, 158  
  regioselective coupling, 147
- Heeger, Alan, 5, 8
- Heparin, 92
- Heteropolyanions, 219
- High-performance liquid chromatography (HPLC), 224
- High-pressure liquid chromatography (HPLC), 40
- <sup>1</sup>H NMR studies  
  colloidal dispersions, 152  
  substituted polythiophenes, 205
- Hoechst (company), 16
- Hollow microspheres, 95
- Honeywell International (company), 17
- Horseradish peroxidase (HRP)  
  chemical properties, 186–187  
  photochemically initiated polymerization, 148–149
- Hot pressing, 237
- HPC (hydroxypropyl cellulose), 225
- HPLC, *see* High-pressure liquid chromatography (HPLC)
- I**
- IBM (company), 12
- IL, *see* Ionic liquids (IL)
- Implantable devices, 24, 30
- Indium tin oxide (ITO)-coated glass  
  circular dichroism spectroscopy, 48  
  polyaniline electrode material, 140  
  UV-visible spectroscopy, 47
- Induction period, 168
- Ink-jet printers, 248
- In situ* chemical polymerization, 78–79
- In situ* spectroscopy, 46
- Integration/fabrication after polymerization, 231
- Intelligent materials  
  defined, 2  
  fundamentals, 2–4, 51, 53  
  historical developments, 4–5  
  selection of, 32  
  structures, 3  
  systems, 3
- Intelligent Polymer Research Institute (IPRI)  
  Braille, 17–18  
  CEP unique features, 5  
  electromechanical analysis, 36
- Interchain spacing, 215
- Interfacial polymerization  
  nanostructured polyanilines, 169–170  
  polyaniline chemical polymerization, 146  
  processing and device fabrication, 238–239
- Interstitial spaces, 171
- Inverse chromatography, 37
- Inverse electrochemical thin-layer chromatography (ITLC), 40
- Inverse microemulsion approach, 168
- Inverse opals, 171
- Inverse thin-layer chromatography, 235
- Ionic liquids (IL)  
  electrolytes, 71  
  electropolymerization, 200
- Ion implantation, 158
- ITLC, *see* Inverse electrochemical thin-layer chromatography (ITLC)
- J**
- John Hopkins University, 13
- K**
- Kevlar  
  deposition, on glass/plastics, 236  
  polymerization environment/cell design, 66
- Kinetic investigation, 152
- Knee sleeve, biomechanic sensors, 27
- L**
- Ladder polymer, 137
- LB, *see* Leucoemeraldine base (LB) and base state
- LDPE (low-density polyethylene), 236
- LEIS, *see* Localized electrochemical impedance spectroscopy (LEIS)
- Leucoemeraldine base (LB) and base state  
  conductivity, 137  
  controlled-release devices, 22  
  enhancing functionality, 154  
  fiber-spinning technologies, 245  
  polyaniline base forms, 189–190
- Lewis acids  
  chiral dopant anions/cations, 157–158  
  polythiophene properties, 217
- Light-induced charge separation, *see* Polymer photovoltaics
- Linköping University, 31
- Lipid tubules, 95
- Lithium salts  
  Lewis acids, 157  
  molecular weight, 159–160
- Lithography, 31
- Localized electrochemical impedance spectroscopy (LEIS), 51

Localized electrochemical mapping, 51  
 Lycra, 27

## M

MacDiarmid, Alan, 5, 8  
 Macromolecular building blocks, 5  
 Mark-Houwink constants, 159  
 Mars Explorer, 17  
 Masks, 148  
 Material level, 4–5, *see also* Intelligent materials  
 McCullough synthetic route and method, 207–210  
*m*-cresol  
   conductivity, 182  
   counterion-induced stabilization, 79  
   level and chain conformation, 120–121  
 Mechanical properties  
   dry-state properties, 123, 126–128  
   environmental effects on, 128–132  
   polyanilines, 187  
   polypyrroles, 123–132  
   polythiophenes, 217–219  
 Mechanisms  
   polyaniline chemical polymerization, 143  
   polyaniline electrochemical polymerization, 138–139  
 Melt-processable CEPs, 233–235  
 Membranes  
   application area, 9  
   chiroptical properties, polythiophenes, 224  
   utilization limitations, 21  
 MEMS, *see* Micro-electromechanical systems (MEMS)  
 Metal ions, 23  
 Metallic polyaniline, 182–183  
 Metals  
   controlled-release devices, 22  
   replacement, applications, 11  
 Microcontact printing methods, 248  
 Micro-electromechanical systems (MEMS), 31–32  
 Microfluid applications, 31–32  
 Microislands, 90  
 MicroMuscle, 17  
 MicroMuscle AB, 30  
 Microrobot arm, 31  
 Microstructure, polypyrroles assembly, 86–91  
 Mitsubishi Rayon (company), 12  
 Molecular level, 4–5, *see also* Intelligent materials  
 Molecular order  
   electropolymerized polythiophenes, 212–213  
   polyaniline synthesis, 160–161  
   polypyrroles assembly, 88–89  
 Molecular probes, 37, 39

Molecular structure  
   polyaniline synthesis, 158–159  
   polypyrroles assembly, 86–91  
   polythiophenes, 211–212  
 Molecular weight  
   polyaniline synthesis, 159–160  
   polypyrroles assembly, 86–88  
   polythiophenes, 211–212  
 Monomers  
   polyaniline electrochemical polymerization, 142  
   polypyrrole electrochemical conditions, 74–75  
 Morphology  
   electropolymerized polythiophenes, 213  
   polyaniline synthesis, 166–168  
 Movement, artificial muscles, 27, 30–31  
 Movement, redox cycling, 131–132

## N

Nanoscale heterogeneity, 160  
 Nanoscale matrices, 171  
 Nanostructures  
   polyaniline synthesis, 168–171  
   polypyrroles assembly, 91–95  
 NASA (National Aeronautics and Space Administration), 17  
 Near-infrared (NIR) region, 47  
 Nerve cells, 27  
 Neurotrophin, 27  
 Nitrilic rubber composites, 240  
 NMP (*N*-methylpyrrolidinone)  
   counterion-induced stabilization, 80  
   solution-cast emeraldine base, 161–162  
   solvatochromism and thermochromism, 194  
 North Shore Hospital Service, 30  
 NSA ( $\beta$ -naphthalenesulfonic acid), 79  
 Nucleophilicity, 70  
 Nylon, 236

## O

Octahedral transition metal (TM) complexes, 157  
 Opals  
   nanostructured approach, 94  
   nanostructured polyanilines, 171  
 Optical properties and activity  
   chemical properties, 187  
   chiral dopant anions/cations, 156  
   chiroptical properties, 121  
   circular dichroism spectra, 191–192  
   colloidal dispersions, 152  
   electronic band structure, 119  
   polyanilines, 189  
   polypyrroles, 119–121

- polythiophenes, 221
- UV-visible-NIR spectra, 120–121
- Organic electron acceptors
  - chiral dopant anions/cations, 158
  - oxidants, 76
- Organic-solvent-soluble chiral polythiophenes, 208–210
- ortho*-coupling
  - dopant acid, 140
  - metallic polyaniline, 183
  - regioselective coupling, 147
  - self-stabilized dispersion polymerization, 147
- ortho*-position, 143
- OTS (octadecylsiloxane), 236
- Overoxidation
  - polythiophenes, 197–199
  - Raman spectroscopy, 48
- Oxidants, 145–146
- Oxide formation rate, 68
- P**
- PanAquas, 12
- para*-head-to-tail, *see* Head-to-tail couplings and position
- PB, *see* Pernigraniline base (PB) and state
- PC composites, 241
- PCEMP (poly(3-carbethoxy-4-methylpyrrole)), 42
- PCMP (poly(3-carboxy-4-methylpyrrole)), 42
- PEDOT (poly(3,4-ethylenedioxythiophene))
  - chiroptical properties, polythiophenes, 225
  - ink-jet printer, 248
  - solution-cast polythiophenes, 214–216
  - substituted polythiophenes, 204
  - vapor-phase polymerization, 202–203
- PEO (poly(ethyleneoxide))
  - colloidal dispersions, 80
  - nanostructured polyanilines, 168
- Pernigraniline base (PB) and state
  - conductivity, 137
  - enhancing functionality, 154
  - polyaniline base forms, 189–190
- PEVA (poly(ethylene-*co*-vinyl acetate)), 237
- Philips (company), 11, 16
- Photochemically initiated polymerization
  - polyaniline synthesis, 148
  - polypyrroles assembly, 83
- Photoisomerization, 169
- Photovoltaic devices and systems, 14–15
- Piezoelectric polymers, 18
- Pirkle-type stationary phases, 224
- Plasma polymerization, 150
- Plastic chip, 11–12
- Plasticization, 126
- Plastics, 78
- PLEDs, *see* Polymer light-emitting diodes (PLEDs)
- PMAS (poly(2-methoxyaniline-5-sulfonic acid))
  - Brönsted acids, 156
  - circular dichroism spectra, 192
  - electrolyte choice, 73
  - electron spin resonance, 49
- PMCP (poly(methyl carboxypyrrole)), 73
- PMMA (poly(methyl methacrylate)), 236
- Polyacrylate predeposition, 94
- Polyanilines
  - asymmetric induction, 193
  - base forms, 189–191
  - chemical, 186–187
  - chiral discrimination, 193
  - circular dichroism spectra, 191–192
  - conductivity, 179, 181–182
  - electrical, 179–183
  - electrochemically prepared films, 187–189
  - fundamentals, 179
  - mechanical, 187
  - metallic polyaniline, 182–183
  - optical, 189
  - solvatochromism, 193–194
  - structure, 1
  - switching, 183–186
  - thermochromism, 193–194
- Polyanilines, synthesis
  - alkyl- and alkoxy-substitution, 152
  - aniline monomers, 147
  - approaches, 150–152
  - Brönsted acids, 155–156
  - bulk structure, 160
  - chain conformation, 160
  - chemical polymerization, 143–147
  - chiral dopant anions/cations, 156–158
  - colloidal dispersions, 151–152
  - colloids, 142–143
  - conformation, 158–161
  - covalently bound chiral substitution, 153
  - covalent substitution, 154–155
  - crystallinity, 160–161, 166
  - density, 166–168
  - deposition, 171
  - dopant acid, 140–141, 144–145
  - dopants, secondary, 166
  - electrochemical polymerization, 138–143
  - electrode materials, 140
  - electroless polymerization, 150
  - electron acceptors polymerization, 149
  - electropolymerized, 166
  - emeraldine base, 161–163
  - emeraldine salt, 163–166
  - emulsion polymerization, 150–151
  - enzyme-catalyzed polymerization, 148–149
  - film comparison, 147
  - fundamentals, 137–138

- interfacial polymerization, 146
- ion implantation, 158
- Lewis acids, 157–158
- mechanism, 138–139, 143
- molecular order, 160–161
- molecular structure, 158–159
- molecular weight, 159–160
- monomer type, 142
- morphology, 166–168
- nanoscale heterogeneity, 160
- nanoscale matrices, 171
- nanostructured polyanilines, 168–171
- organic electron acceptors, 158
- oxidant, 145–146
- photochemically initiated polymerization, 148
- plasma polymerization, 150
- postpolymerization modification, 154–156
- regioselective coupling, 147
- salt from protonation, 163
- self-stabilized dispersion polymerization, 146–147
- solid state conformation, 160–161
- solution-cast, 161–164
- solvent, 141–142, 146
- structure, 158
- substitution, 152–154
- sulfonic acid substitution, 153–154
- temperature, 142, 144
- template-guided synthesis, 147
- vapor-phase deposition, 148
- water, influence, 166
- Polycondensation dehalogenation reactions, 202
- Polyelectrolytes
  - dopant counterion, 77
  - incorporation as counterions, 117
- PolyIC (company), 12
- Polymerization, *see also* Electropolymerization
  - acid-catalyzed, 83–84
  - chemical polymerization, 75, 143–147, 201–202, 235
  - conditions influence, 76–77
  - diaphragmatic chemical polymerization, 238–239
  - electrochemical properties and conditions, 138–143
  - electrode materials, 140
  - electroless, 150
  - electron acceptors, 149
  - emulsion, 150–151
  - environment/cell design, 63, 65–66
  - enzyme-catalyzed, 83–84, 148–149
  - fabrication after, 231
  - interfacial, 146, 169–170, 238–239
  - photochemically initiated, 83, 148
  - plasma, 150
  - rate, 62, 140
  - UV, oligothiophenes, 203
  - vapor-phase polymerization, 148, 202–203
- Polymerization environment/cell design, 66
- Polymer light-emitting diodes (PLEDs)
  - application area, 9
  - display technologies, 15–16
- Polymer nanowire structures, 170–171
- Polymer photovoltaics, 14–15
- Polypyrroles, assembly
  - acid-catalyzed polymerization, 83–84
  - branching, 86–88
  - chemical polymerization, 75
  - colloidal dispersions, 80–81
  - counterion/cation effect, 71, 73–74
  - counterion-induced solubilization, 79–80
  - crosslinking, 86–88
  - crystallinity, 88–89
  - dopant counterion ( $A^-$ ), 77
  - electrochemical conditions, 66–75
  - electrode materials, 68–70
  - electropolymerization, 59–60, 62–63
  - enzyme-catalyzed polymerization, 83–84
  - extra functionality, 84–86
  - film density, 89–91
  - functionality, enhanced, 84–86
  - fundamentals, 59, 66–68, 76
  - microstructure, 86–91
  - molecular order, 88–89
  - molecular structure, 86–91
  - molecular weight, 86–88
  - monomer, 74–75
  - nanostructured approach, 91–95
  - photochemically initiated polymerization, 83
  - polymerization conditions influence, 76–77
  - polymerization environment/cell design, 63, 65–66
  - regioselective coupling, 77–78
  - side-chain-induced solubilization, 81–82
  - in situ* chemical polymerization, 78–79
  - solvent, 70–71, 76
  - surface morphology, 89–91
  - temperature, 76–77
- Polypyrroles, properties
  - biochemical, 114–118
  - chemical, 114–118
  - chiral separations, 122
  - chiroptical properties, 121
  - conductivity, 103–105
  - dry-state properties, 123, 126–128
  - electrical, 103–105
  - electrochemical asymmetric synthesis, 122
  - electronic band structure, 119
  - environmental effects on, 128–132
  - fundamentals, 103, 132
  - mechanical, 123–132
  - optical, 119–121
  - sensing, 122

- structure, 1
  - switching, 105–114
  - UV-visible-NIR spectra, 120–121
  - Polythiophenes
    - alkyl- and alkoxy substitutions, 203–206
    - chemical polymerization, 201–202
    - conformation, 211–213
    - crystallinity, 212–213
    - electropolymerization, 197–201, 212–213
    - fundamentals, 225
    - molecular order, 212–213
    - molecular structure, 211–212
    - molecular weight, 211–212
    - morphology, 213
    - paradox, 197
    - regioregular substitution, 206–207
    - solid state conformation, 212–213
    - solution-cast, 213–216
    - special functional groups, 208–211
    - structure, 1, 211
    - substitution, 203–207
    - synthesis, 197–202
    - UV polymerization, oligothiophenes, 203
    - vapor-phase polymerization, 202–203
  - Polythiophenes, properties, 216–225
    - chemical, 219
    - chiroptical, 222–225
    - conductivity, 216–217
    - doping, 220–221
    - electronic band structure, 221
    - mechanical, 217–219
    - optical, 221
    - solvatochromism, 221
    - switching, 219–220
    - thermochromism, 221
    - UV-visible spectra, 221
  - Polyurethane (PU) composites, 239
  - Poly(vinylalcohol) (PVA)
    - colloidal dispersions, 80
    - solution-processable CEPs, 232
  - Poly(vinylchloride) (PVC), 236
  - Poly(vinyl-methylketone) (PVMK) composites, 240
  - Poly(vinylpyridine)
    - Brönsted acids, 156
    - colloidal dispersions, 80
  - POMA (poly(*o*-methoxyaniline))
    - Brönsted acids, 156
    - chiral dopant anions/cations, 156
    - circular dichroism spectra, 192
  - Postpolymerization
    - conductivity, 181
    - vapor-phase deposition, 148
  - Postpolymerization modification
    - polyaniline synthesis, 154–156
    - polythiophenes, special functional groups, 210–211
  - Printing technologies, 246–249
  - Probes, molecular, 37, 39
  - Processing and device fabrication
    - assembly, in host matrices, 235
    - chemical polymerization, 235
    - deposition, on glass/plastics, 235–238
    - device fabrication, 243
    - electrochemical integration, 239–243
    - fiber-spinning technologies, 243–246
    - fundamentals, 231
    - integration/fabrication after polymerization, 231
    - interfacial polymerization, 238–239
    - melt-processable CEPs, 233–235
    - printing technologies, 246–249
    - solution-processable CEPs, 231–233
  - Proteins
    - chemical sensors, 23
    - electrical stimuli application, 118
  - Pseudodoping, 158
  - PSS (poly(styrenesulfonate)), 148–149
  - pTS (*para*-toluenesulfonic acid), 73
  - PU, *see* Polyurethane (PU) composites
  - Pulsed-potential deposition, 69–70
  - Purification scheme, 233
  - PVA, *see* Poly(vinylalcohol) (PVA)
  - PVC, *see* Poly(vinylchloride) (PVC)
  - PVMK, *see* Poly(vinyl-methylketone) (PVMK) composites
- ## Q
- Quantum Technology (company), 17–18
  - Quartz fibers, 236
- ## R
- Radical-radical coupling, 60
  - Radio-frequency (RF) glow discharges, 150
  - Raman spectroscopy
    - fundamentals, 46, 48–49
    - vapor-phase deposition, 148
  - Redox activity
    - potential, 76
    - supercapacitors, 14
    - switching, 49
  - Regiorandom properties, 204, 206
  - Regioregular properties
    - chiroptical properties, polythiophenes, 222, 224
    - solution-cast polythiophenes, 214
    - substituted polythiophenes, 204, 206–207
  - Regioselective coupling
    - polyaniline chemical polymerization, 147
    - polypyrroles assembly, 77–78
  - Rehabilitation glove, 30–31

Resistometry, 35–36

Rieke synthetic route, 207

## S

Salt solutions, 129, *see also* Emeraldine salt (ES) and salt state

Santa Fe Science and Technology (company), 243

Scanning probe microscopy (SPM), 42–46

Scanning tunneling microscopy (STM), 42–43

Scanning tunneling spectroscopy (STS), 44

Scanning vibrating electrode technique (SVET), 51

Schizophyllan (SPG), 225

Screen-printing technologies, 246, 248

SDS (sodium dodecyl sulfate), 168

Secondary doping, 181

Selective molecular recognition, 21

Self-assembled nanofibers, 169

Self-catalyzing growth, 139

Self-coupling, 201–202

Self-stabilized dispersion polymerization (SSDP), 146–147

SEM, *see* Simple electron microscope (SEM)

Sensing properties, 122

Sensors

application area, 9

biomedical applications, 27

Separation technologies, 18–21

Shirakawa, Hideki, 5, 8

Side-branching, 147

Side-chain-induced solubilization, 81–82

Simple electron microscope (SEM), 126

Single random coil (sSPG), 225

Size, electrode materials, 69

Small organic molecules, 23

Solid polymer electrolyte (SPE), 18

Solid state conformation

electropolymerized polythiophenes, 212–213

polyaniline synthesis, 160–161

Solution-cast, 213–216

Solution-processable CEPs, 231–233

Solvatochromism

organic-solvent-soluble chiral

polythiophenes, 210

polyanilines, 193–194

polythiophene optical properties, 221

Solvents

common interactions, 114

electrochemical conditions, 70–71

polyaniline chemical polymerization, 146

polyaniline electrochemical polymerization, 141–142

polymerization conditions influence, 76

polypyrroles assembly, 70–71

SPE, *see* Solid polymer electrolyte (SPE)

SPG, *see* Schizophyllan (SPG)

SPM, *see* Scanning probe microscopy (SPM)

SSDP, *see* Self-stabilized dispersion polymerization (SSDP)

Steel, corrosion protection, 22

Stiffness, 219

STM, *see* Scanning tunneling microscopy (STM)

Strength, 219

Stretching

conductivity, 105

dry-state mechanical properties, 128

fiber-spinning technologies, 244–245

Structure

polyaniline synthesis, 158

polythiophenes, 1, 211

STS, *see* Scanning tunneling spectroscopy (STS)

Substitution, polyaniline synthesis, 152–154

Sulfonated polyaniline, 1, *see also* Polyanilines

Sulfonic acid substitution, 153–154

Supercapacitors, 13–14

Surface morphology, 89–91

Surfactant-like anions, 77

SVET, *see* Scanning vibrating electrode technique (SVET)

Switching properties and activity

polyanilines, 183–186

polypyrroles, 105–114

polythiophenes, 219–220

repeated, 19–20

Synthetic opals, 94

## T

TBABF<sub>4</sub> (tetrabutylammonium tetrafluoroborate), 73

TBAPF<sub>6</sub> (tetrabutylammonium hexafluorophosphate), 73

TBAP (tetrabutylammonium), 73

TBAP (tetrabutylammonium perchlorate), 73

TCNQ (tetracyanoquinodimethane), 149

TEM, *see* Transmission electron microscopy (TEM)

Temperature

dry-state mechanical properties, 127–128

electrochemically prepared films, 189

electropolymerization, 62–63

obtaining higher conductivity, 87–88

polyaniline chemical polymerization, 144

polyaniline electrochemical polymerization, 142

polymerization conditions influence, 76–77

Template-guided synthesis, 147

Tensile strength, 129, *see also* Young's modulus

Terthiophenes, 199

Thermal analysis, 189

Thermochromism

organic-solvent-soluble chiral

polythiophenes, 210

- polyanilines, 193–194
- polythiophene optical properties, 221
- Thin films, 95
- Thin-layer chromatography (TLC), 40
- Three-electrode potentiostated system, 63
- Tiron, 68
- Tissue-engineering scaffolds, 27
- TLC, *see* Thin-layer chromatography (TLC)
- Toughness, 188
- Transient waveforms, 67–68
- Transition metal (TM) complexes, 157
- Transmission electron microscopy (TEM), 91

## U

- Uniax Corporation, 16
- University of Cambridge, 248
- Unzipping, 208
- UV polymerization, oligothiophenes, 203
- UV-visible-NIR spectra, 120–121
- UV-visible spectra and spectroscopy
  - fundamentals, 46–47
  - polythiophene optical properties, 221
  - solvatochromism, 193

## V

- Valve systems, 31
- Vapor-phase deposition, 148
- Vapor-phase polymerization (VPP)
  - polythiophene synthesis, 202–203
  - vapor-phase deposition, 148

## W

- Water, influence, 166

- Water-soluble properties
  - chiral nanocomposites, 169
  - monomer, 75
  - polythiophenes, special functional groups, 208
- WAXD scattering peaks, 166
- WF, *see* Work function (WF)
- Wilhelmy's plate technique, 41
- Work function (WF), 44–45

## X

- X-ray diffraction (XRD)
  - chiroptical properties, polythiophenes, 224
  - conductivity, 104
  - crystallinity, 166
  - dry-state mechanical properties, 127
  - electrochemically prepared films, 189
  - metallic polyaniline, 183
  - molecular structure, 88–89
  - solution-cast emeraldine base, 161, 163
  - solution-cast polythiophenes, 215
- X-ray photoelectron spectroscopy (XPS)
  - nigraniline oxidation state, 150
  - organic electron acceptors, 158

## Y

- Young's modulus
  - dry-state mechanical properties, 126
  - environmental effects, 129, 132
  - fiber-spinning technologies, 244–245
  - polythiophene properties, 218–219

## Z

- Zeolites, 92





Material Science

THIRD EDITION

# CONDUCTIVE ELECTROACTIVE POLYMERS

## Intelligent Polymer Systems

Gordon G. Wallace • Geoffrey M. Spinks  
Leon A. P. Kane-Maguire • Peter R. Teasdale

Rapid advances in synthetic polymer science and nanotechnology have revealed new avenues of development in conductive electroactive polymers that take greater advantage of this versatile class of materials' unique properties. This third edition of **Conductive Electroactive Polymers: Intelligent Polymer Systems** continues to provide an in-depth understanding of how to engineer dynamic properties in inherently conducting polymers from the molecular level.

### NEW TO THE THIRD EDITION—

- Biomedical, MEMS, and electronic textile applications
- The synthesis and fabrication of nanocomponents and nanostructures
- The energy role of nanotechnology in improving the performance of conducting materials in devices
- Electrochemical Raman, electrochemical ESR, and scanning vibrating reference electrode studies

After establishing the basic principles of polymer chemistry, the book pinpoints the dynamic properties of the more useful conducting polymers, such as polypyrroles, polythiophenes, and polyanilines. It then demonstrates how the control of these properties enables cutting-edge applications in nano, biomedicine, and MEMS as well as sensors and artificial muscles. Subsequent chapters discuss the effect of nanodimensional control on the resultant properties.

Updated to reflect substantial developments and advances that have occurred in the past few years, this third edition unlocks a world of potential for integrating and interfacing conductive polymers.

 **CRC Press**  
Taylor & Francis Group  
an **informa** business

6000 Broken Sound Parkway, NW  
Suite 300, Boca Raton, FL 33487  
270 Madison Avenue  
New York, NY 10016  
2 Park Square, Milton Park  
Abingdon, Oxon OX14 4RN, UK

67095

ISBN: 978-1-4200-6709-5



9 781420 067095

[www.crcpress.com](http://www.crcpress.com)